



Fisheries New Zealand

Tini a Tangaroa

Characterisation and length-based assessment model for scampi (*Metanephrops challenger*) in the Bay of Plenty (SCI 1) and Hawke Bay-Wairarapa (SCI 2)

New Zealand Fisheries Assessment Report 2020/06

I.D. Tuck

ISSN 1179-5352 (online)

ISBN 978-1-99-001738-4 (online)

February 2020



Requests for further copies should be directed to:

Publications Logistics Officer
Ministry for Primary Industries
PO Box 2526
WELLINGTON 6140

Email: brand@mpi.govt.nz
Telephone: 0800 00 83 33
Facsimile: 04-894 0300

This publication is also available on the Ministry for Primary Industries websites at:
<http://www.mpi.govt.nz/news-and-resources/publications>
<http://fs.fish.govt.nz> go to Document library/Research reports

© Crown Copyright – Fisheries New Zealand

TABLE OF CONTENTS

EXECUTIVE SUMMARY	1
1. INTRODUCTION	2
1.1. The Bay of Plenty (SCI 1) and Hawke Bay–Wairarapa (SCI 2) scampi fisheries	2
2. FISHERY CHARACTERISATION AND DATA	5
2.1. Commercial catch and effort data	5
2.1.1. SCI 1 characterisation	5
2.1.2. SCI 2 characterisation	12
2.2. Seasonal patterns in scampi biology	18
2.2.1. Sex ratio	18
2.2.2. Time steps in assessment model	21
2.3. Standardised CPUE indices	21
2.3.1. Core vessel selection for SCI 1	21
2.3.2. Core vessel selection for SCI 2	22
2.3.3. Exclusion of poorly sampled time periods.....	24
2.3.4. Calculation of indices.....	25
2.3.5. SCI 1 indices	27
2.3.6. SCI 2 indices	30
3. MODEL STRUCTURE	33
3.1. Spatial and seasonal structure, and the model partition	33
3.2. Biological inputs	34
3.2.1. Growth	34
3.2.2. Maturity.....	37
3.2.3. Natural mortality	38
3.3. Catch data	38
3.4. CPUE indices	40
3.5. Research survey indices	41
3.5.1. Photographic surveys	41
3.5.2. Trawl surveys.....	42
3.6. Length distributions	43
3.6.1. Commercial catch at length data.....	43
3.6.2. Trawl survey length distributions.....	55
3.6.3. Photo survey length distributions.....	55
3.7. Model assumptions and priors	62
3.7.1. Scampi catchability	62
3.7.2. Priors for qs	65
3.7.3. Estimation of prior distributions	65
3.7.4. Recruitment.....	66

4.	SCI 1 - ASSESSMENT MODEL RESULTS	67
4.1.	Initial models	67
4.2.	Base models for SCI 1	73
4.2.1.	SCI 1 M02CV15 (see Appendix 5).....	73
4.2.2.	SCI 1 M02CV25 (see Appendix 6).....	74
4.2.3.	SCI 1 M025CV15 (see Appendix 7).....	75
4.2.4.	SCI 1 M025CV25 (see Appendix 8).....	76
4.3.	SCI 1 Fishing Pressure	78
5.	SCI 2 - ASSESSMENT MODEL RESULTS	78
5.1.	Initial models	78
5.2.	Base models for SCI 2	87
5.2.1.	SCI 2 M02CV15 (see Appendix 9).....	87
5.2.2.	SCI 2 M02CV25 (see Appendix 10).....	88
5.2.3.	SCI 2 M025CV15 (see Appendix 11).....	90
5.2.4.	SCI 2 M025CV25 (see Appendix 12).....	91
5.3.	SCI 2 Fishing Pressure	92
6.	SHARED PARAMETER (SCI 1 & SCI 2) MODEL	92
6.1.1.	Shared parameter model (Appendix 13)	93
7.	DISCUSSION	95
8.	ACKNOWLEDGEMENTS	96
9.	REFERENCES	97
	APPENDIX 1. CPUE standardisation diagnostics (SCI 1)	100
	APPENDIX 2. CPUE standardisation diagnostics (SCI 2)	107
	APPENDIX 3. Analysis of length composition data (SCI 1)	114
	APPENDIX 4. Analysis of length composition data (SCI 2)	119
	APPENDIX 5. SCI 1 M02CV15 model plots ($M = 0.2$, $CV = 0.15$)	125
	APPENDIX 6. SCI 1 M02CV25 model plots ($M=0.2$, $CV=0.25$)	145
	APPENDIX 7. SCI 1 M025CV15 model plots ($M=0.25$, $CV=0.15$)	165
	APPENDIX 8. SCI 1 M025CV25 model plots ($M=0.25$, $CV=0.25$)	186
	APPENDIX 9. SCI 2 M02CV15 model plots ($M=0.2$, $CV=0.15$)	206
	APPENDIX 10. SCI 2 M02CV25 model plots ($M=0.2$, $CV=0.25$)	228
	APPENDIX 11. SCI 2 M025CV15 model plots ($M=0.25$, $CV=0.15$)	250
	APPENDIX 12. SCI 2 M025CV25 model plots ($M=0.25$, $CV=0.25$)	272
	APPENDIX 13. Shared parameter M025CV15 model plots ($M=0.25$, $CV=0.15$)	294

EXECUTIVE SUMMARY

Tuck, I.D. (2020). Characterisation and length-based population model for scampi (*Metanephrops challengeri*) in the Bay of Plenty (SCI 1) and Hawke Bay–Wairarapa (SCI 2).

New Zealand Fisheries Assessment Report 2020/06. 295 p.

Stock assessments of the Bay of Plenty (SCI 1) and Hawke Bay–Wairarapa (SCI 2) scampi stocks have been undertaken under Fisheries New Zealand project SCI2018-01. This work revised and updated existing models for these stocks. The assessments presented for both stocks were accepted by the Fisheries New Zealand Shellfish Fisheries Working Group (SFWG), but these models were not required to be presented to the Fisheries New Zealand Plenary.

Fishery characterisations were undertaken and a range of Catch per Unit Effort (CPUE) biomass indices were estimated for each stock, based on the spatial and temporal stratification of the previous stock assessment model. Previous stock assessment models have incorporated considerable spatial structure, but, following preliminary investigations, the SFWG recommended only developing single area models for these stocks and fitting an annual CPUE biomass index rather than separate indices for within-year time steps. The sensitivity of the assessment model to the assumed natural mortality rate (M); revised Year Class Strength (YCS) parameterisation; new catchability priors; and data weighting and the exclusion of survey data were investigated, with base models for both stocks taken as those with M fixed at 0.20 and 0.25.

For SCI 1, Spawning Stock Biomass (SSB) was estimated to have increased through the early 1990s, peaking in the mid-1990s, and then declining until the early 2000s. Subsequently, SSB was very stable at around 70% SSB_0 , but increased slightly in the most recent years. SSB_{2018} was estimated to be between 72% and 76% of SSB_0 (median values). MCMC posteriors suggested 0% probability that SSB_{2018} was below 40% SSB_0 . Annual fishing intensity was estimated to consistently be below F 40% B_0 .

For SCI 2, SSB was estimated to have declined slightly through the late 1980s, then increased, peaking around 1993, and then declined to a minimum in 2003, before increasing slightly to 2005. Subsequently, SSB remained stable until about 2008, then increased rapidly to 2013, and declined slightly after this. SSB_{2018} was estimated to be between 73% and 78% of SSB_0 (median values). MCMC posteriors suggested 0% probability that SSB_{2018} was below 40% SSB_0 . Annual fishing intensity (equivalent annual F) peaked in 2002, but declined considerably after this. SSB was at or below 40% SSB_0 between 2002 and 2004, but increased considerably since then.

1. INTRODUCTION

This report provides a fishery characterisation for the Bay of Plenty (SCI 1) and Hawke Bay–Wairarapa (SCI 2) scampi stocks and applies a Bayesian, length-based, two-sex population model to these stocks. Previous characterisations of scampi stocks are described by Tuck (2009; 2014; 2016). The first attempt at developing a length-based population model for any scampi stock was conducted for SCI 1 (Cryer et al. 2005) and this was implemented using the general-purpose stock assessment program CASAL v 2.30 (Bull et al. 2012). This model for SCI 1 was developed further and the same model structure was also applied to SCI 2 in later projects (Tuck & Dunn 2006). The current study used CASAL v 2.30 (Bull et al. 2012). Developments in the model implementation and structure have been largely based on suggestions raised at the MFish funded Scampi Assessment Workshop (Tuck & Dunn 2009), and subsequently at Fisheries New Zealand Shellfish Fisheries Working Group (SFWG) meetings. Assessments for SCI 1 and SCI 2 using this model were accepted in 2011, 2013, and 2016 (Tuck & Dunn 2012; Tuck 2014; Tuck 2016).

We describe the available data and how they were used, the parameterisation of the model, and model fits and sensitivity. This report fulfils Fisheries New Zealand project SCI2018-01 “*Stock assessment of scampi*”, undertaking stock assessments of SCI 1 and SCI 2. The objective of this project was to carry out a stock assessment, including estimating yield, for SCI 1 and SCI 2.

1.1. The Bay of Plenty (SCI 1) and Hawke Bay–Wairarapa (SCI 2) scampi fisheries

Scampi is fished all around New Zealand, in nine fishery management areas (Figure 1). The SCI 1 and SCI 2 fisheries are two of New Zealand’s four main scampi fisheries (the others being SCI 3 and SCI 6A), and over the last 5 years (2013–14 to 2017–18) have contributed an average of 118 and 141 tonnes per annum respectively, with landings from SCI 1 remaining relatively stable while those from SCI 2 have increased in recent years. The Total Allowable Commercial Catch (TACC) for SCI 1 is 120 tonnes, for SCI 2 is 153 tonnes (reduced from 200 tonnes to 100 tonnes in 2011, increased to 133 tonnes in 2014, and increased to 153 tonnes in 2016), and the total TACC for all management areas is 1312 tonnes.

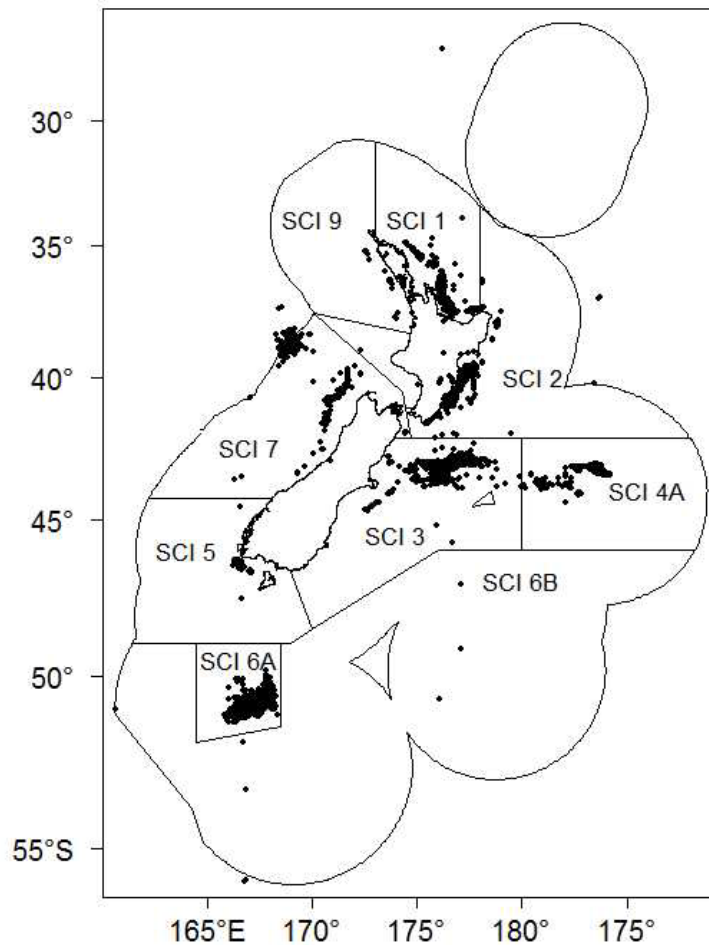


Figure 1: Spatial distribution of the scampi fishery since 1988–89. Each dot shows the mid-point of one or more tows recorded on Trawl Catch Effort Processing Return (TCEPR) forms with scampi as the target species.

The spatial distribution of the targeted scampi fishing within SCI 1 is focussed in a relatively narrow continuous band (interrupted at Mayor Island) within the Bay of Plenty (Figure 2), generally ranging from 300 to 500 m depth. Some isolated areas to the north and east have also been fished in some years, in the same depth range. Targeted scampi fishing in SCI 2 has been focussed in two separate patches, from Hawke Bay to (roughly) Blackhead Point, and from Cape Turnagain to Castlepoint, again generally ranging from 300 to 500 m depth (Figure 3). Smaller isolated patches have also been fished on occasion to the north and south. Surveys in both areas have focussed on the main areas of the fishery, and survey strata coverage is illustrated in the respective figures.

Management areas have remained consistent for SCI 1 and SCI 2 throughout the history of the fishery. Prior to the 1991–92 fishing year there were no limits on scampi catches. Individual Quotas (IQs) were introduced for both areas at the beginning of the 1991–92 fishing year and were allocated on the basis of the catch by permit holders in 1990–91). These IQs were maintained with the introduction of Individual Catch Entitlement (ICE) regulations in 1999 and continued until the Court of Appeal ruled in October 2001 that the scampi ICE regulations were unlawful, after which all scampi stocks were managed under competitive catch limits, until the species was introduced into the QMS (October 2004). Since then all scampi fisheries have been managed with individual quotas.

Previous fishery characterisations have been undertaken for these areas by Cryer & Coburn (2000) and Tuck (2009; 2014; 2016).

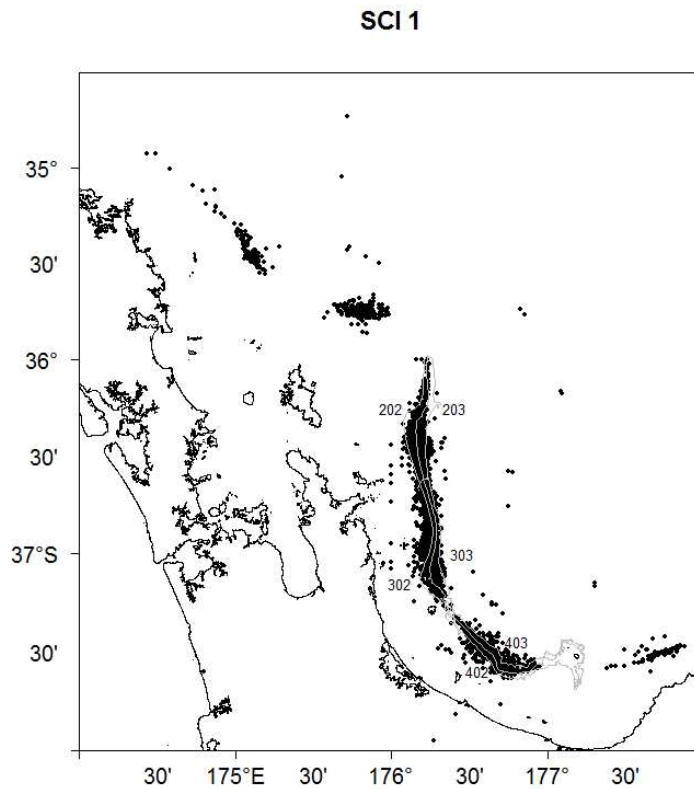


Figure 2: Spatial distribution of the scampi fishery within management area SCI 1 since 1988–89. Each dot shows the mid-point of one or more tows recorded on TCEPR with scampi as the target species. The extents of the six scampi survey strata are shown by grey lines with associated labels.

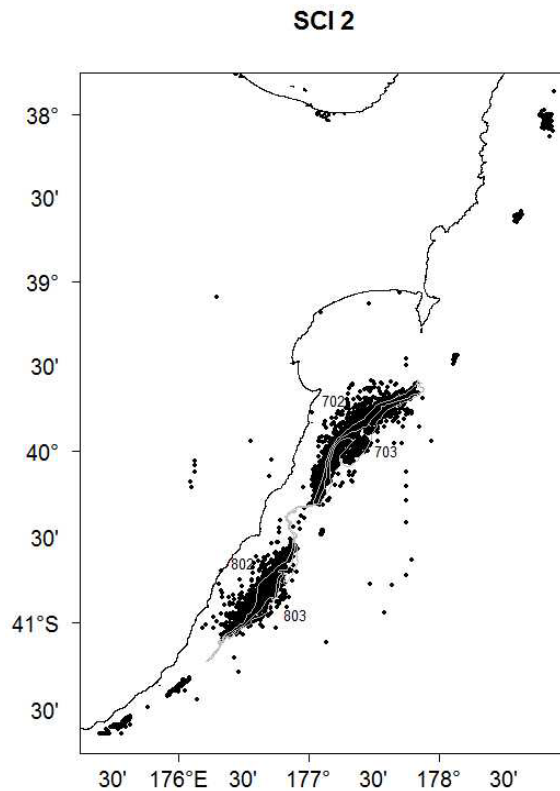


Figure 3: Spatial distribution of the scampi fishery within management area SCI 2 since 1988–89. Each dot shows the mid-point of one or more tows recorded on TCEPR with scampi as the target species. The extents of the four scampi survey strata are shown by grey lines with associated labels.

2. FISHERY CHARACTERISATION AND DATA

2.1. Commercial catch and effort data

Scampi fishers have consistently reported catches on the Trawl Catch, Effort, and Processing Return (TCEPR) form since its introduction in 1989–90, providing a valuable and complete record of catch and effort on a tow by tow basis. Note that references to “year” within this report refer to the modelled or fishing year and are labelled as the most recent calendar year, e.g., the fishing year 1998–99 is referred to as “1999” throughout.

Data were extracted from the MPI *warehou* database, requesting all fishing events (from all areas) where scampi (SCI) was the nominated target species, or was reported in the catch from a trip (rep log 12091). This resulted in an extract of 364 284 fishing events, with scampi target fishing events accounting for 99.9% of estimated scampi catches (130 737 events). Errors in TCEPR records are reducing in frequency, but do occur, and the raw records were groomed in the following manner. For each record, the reported data were used to estimate the duration of the trawl shot, the distance between the start and finish locations, and the midpoint between the start and finish locations. All tows with recorded zero hour tow durations (that caught scampi) were reset to the median tow duration for the trip (184 events). All tows with a tow distance greater than 50 km were reset to the median of the midpoint of tows on the same day, adjacent days, or the trip, depending on available data (2732). These edited events were included in the allocation of catch data to area and time-step analysis, but not included in the CPUE analysis. Where a vessel only reported start position (rather than start and finish position) for a tow (3713 events), this was used instead of the midpoint. Excluding fishing events with no scampi catch and removing additional events where the location could not be determined reduced the data set further, to 127376 events, 2504 of which were those where the original estimated tow distance exceeded 50 km. This groomed dataset accounts for over 99.8% of the estimated scampi catch taken by the New Zealand scampi target fishery. The data for SCI 1 and SCI 2 were then extracted from this full data set on the basis of latitude and longitude.

2.1.1. SCI 1 characterisation

Total annual landings for the fishery are presented in Figure 4, with landings and the percentage by the target scampi fishery also presented in Table 1. Landings have remained stable around the level of the TACC through much of the history of the fishery. The distribution of fishing activity within the SCI 1 area over time is presented in Figure 5 and Figure 6. The area over which the assessment model is applied is defined as the survey strata (300–500 m depth range in the main area of the fishery shown in Figure 2), and over 90% of the targeted scampi catch has been reported from this area in most years (Table 1). The core area has consistently been fished over the history of the fishery, with smaller isolated patches (particularly to the north) fished in some years. Overall, the core (modelled) area has accounted for 92% of scampi targeted catch. Boxplots of the unstandardised Catch per Unit Effort (CPUE) (Figure 7) show catch rates initially increasing in the mid 1990s, peaking in 1996, declining to about 2000, and remaining relatively stable since then, with slightly higher values in the most recent years.

The breakdown of catch by survey strata and fishing year is presented for SCI 1 in Figure 8. In general, more of the catch was taken from the shallower strata (202, 302, and 402, i.e., 300–400 m), and fishing was less consistent (landings have fluctuated more) in the southern area (strata 402 and 403).

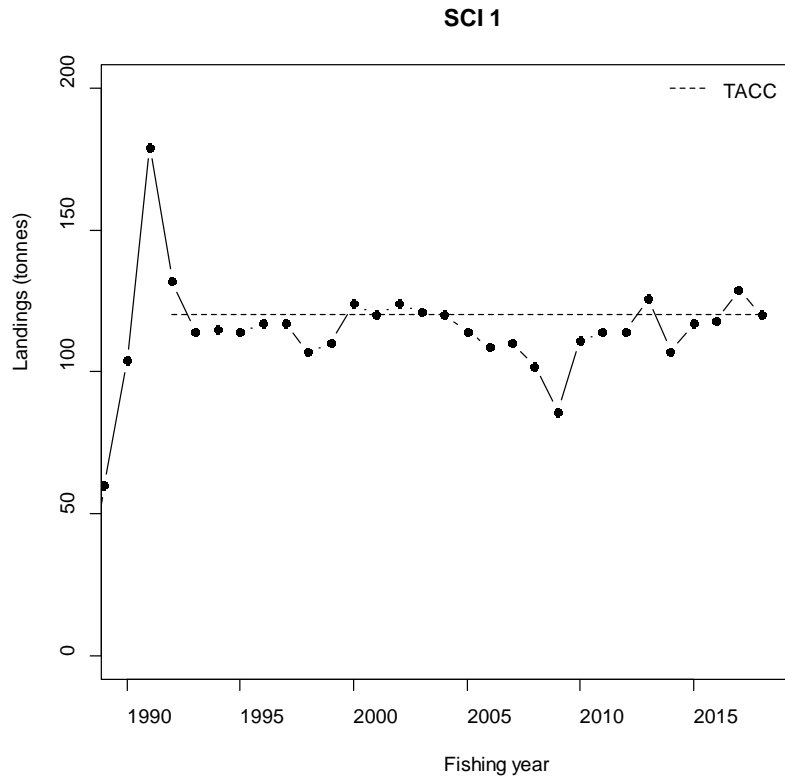


Figure 4: Time series of scampi landings from SCI 1 by fishing year (Monthly Harvest Return data (MHR)). The dashed line indicates the 120 t TACC that was introduced on 1 October 1992.

Table 1: Reported commercial landings (tonnes) from the 1986–87 to 2017–18 fishing years for SCI 1, catch estimated from scampi target fishery, and estimated catch from modelled area (survey strata). MHR is Monthly Harvest Return.

	Landings (MHR)	Target catch (TCEPR)	% SCI target	Estimated catch (modelled area)	% catch (modelled area)
1986–87	5.0				
1987–88	15.0				
1988–89	60.0				
1989–90	104.0	104.3	100%	91.7	88%
1990–91	179.0	163.2	91%	148.5	91%
1991–92	132.0	128.6	97%	122.0	95%
1992–93	114.0	116.0	102%	103.2	89%
1993–94	115.0	111.6	97%	103.3	93%
1994–95	114.0	113.6	100%	97.1	85%
1995–96	117.0	116.4	99%	108.4	93%
1996–97	117.0	114.0	97%	110.2	97%
1997–98	107.0	115.3	108%	89.7	78%
1998–99	110.0	112.4	102%	105.6	94%
1999–00	124.0	116.1	94%	105.3	91%
2000–01	120.0	117.1	98%	103.6	88%
2001–02	124.0	117.3	95%	101.4	86%
2002–03	121.0	113.3	94%	92.9	82%
2003–04	120.0	115.9	97%	114.5	99%
2004–05	114.0	100.1	88%	98.1	98%
2005–06	109.0	93.8	86%	92.3	98%
2006–07	110.0	101.3	92%	100.2	99%
2007–08	102.0	93.1	91%	91.7	99%
2008–09	86.0	81.0	94%	79.8	99%
2009–10	111.4	105.0	94%	99.9	95%
2010–11	113.9	107.9	95%	104.1	97%
2011–12	114.5	107.3	94%	106.3	99%
2012–13	126.1	119.4	95%	111.8	94%
2013–14	106.6	100.3	94%	91.9	92%
2014–15	116.9	107.1	92%	85.4	80%
2015–16	118.9	103.5	87%	88.5	86%
2016–17	128.8	116.0	90%	105.4	91%
2017–18	119.9	113.2	94%	105.4	93%

Monthly patterns of effort and catch are presented in Figure 9 and Figure 10. The fishery was managed with competitive catch limits between 2001–02 and 2003–04. During this period, effort and catches were focussed in the first few months of the fishing year, but prior to and since this time, fishing has been distributed throughout the year (particularly more recently).

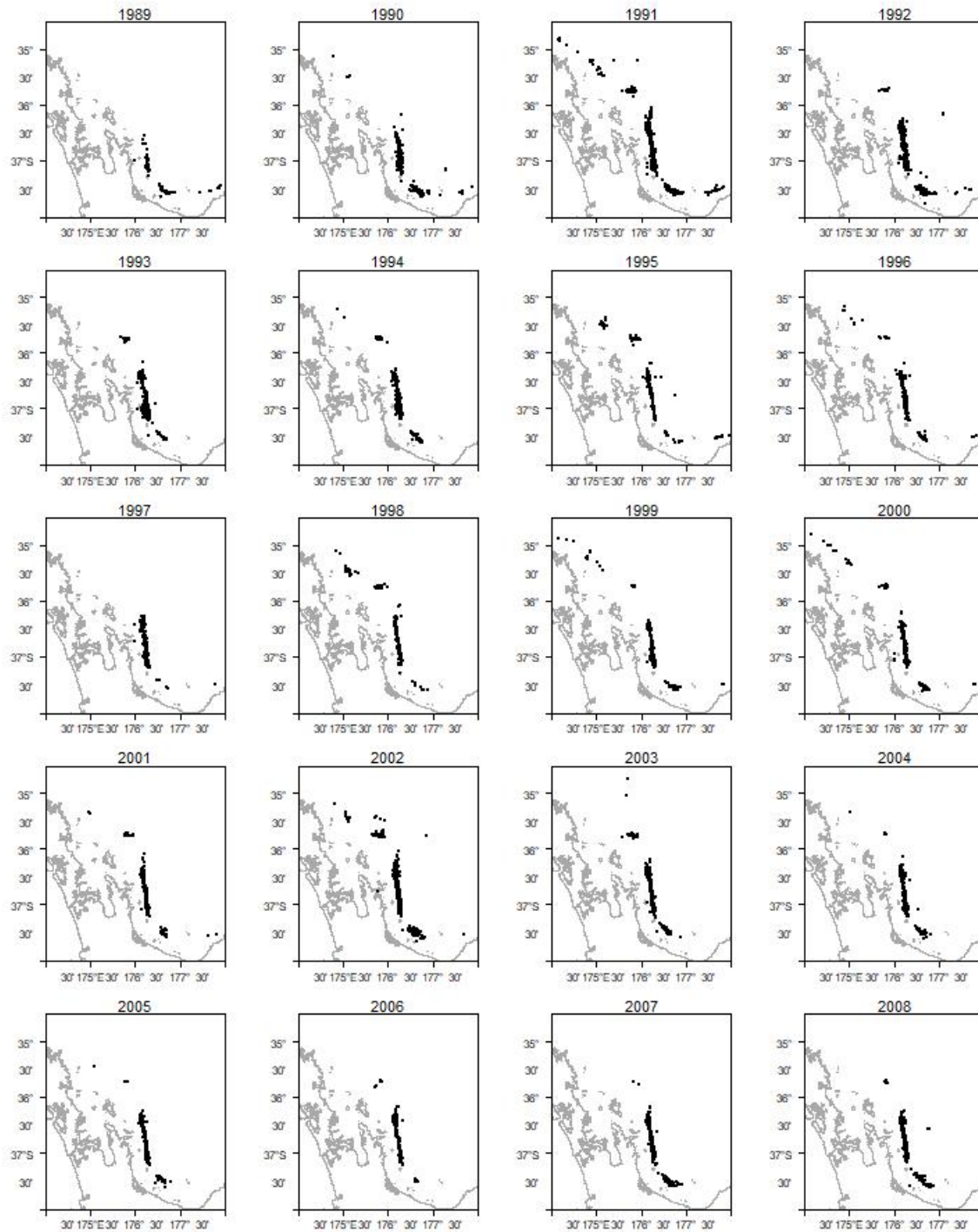


Figure 5: Spatial distribution of the main area of the SCI 1 scampi trawl fishery from 1988–89 to 2007–08. Each dot represents the midpoint of one or more tows reported on TCEPR. The general area covered by the plots is indicated in Figure 6.

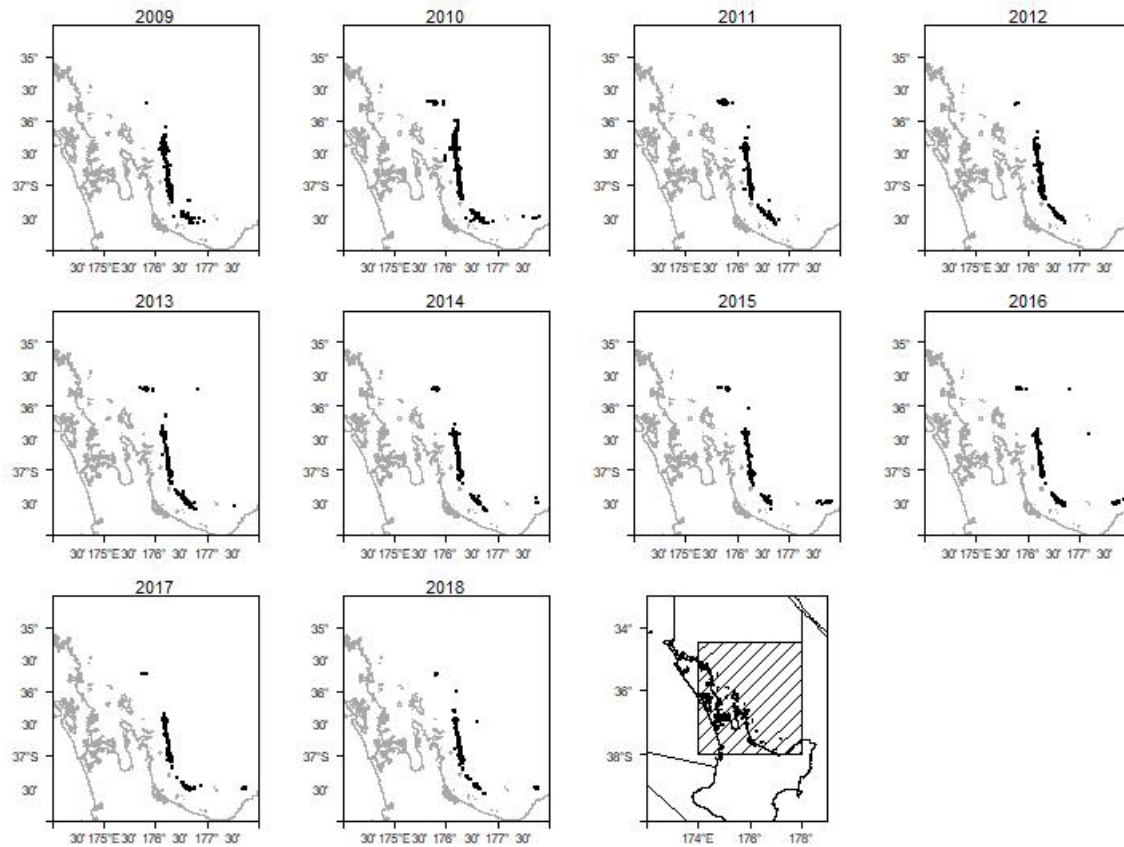


Figure 6: Spatial distribution of the main area of the SCI 1 scampi trawl fishery from 2008–09 to 2017–18. Each dot represents the midpoint of one or more tows reported on TCEPR. The general area covered by the plots is indicated by the shaded box in the bottom right plot.

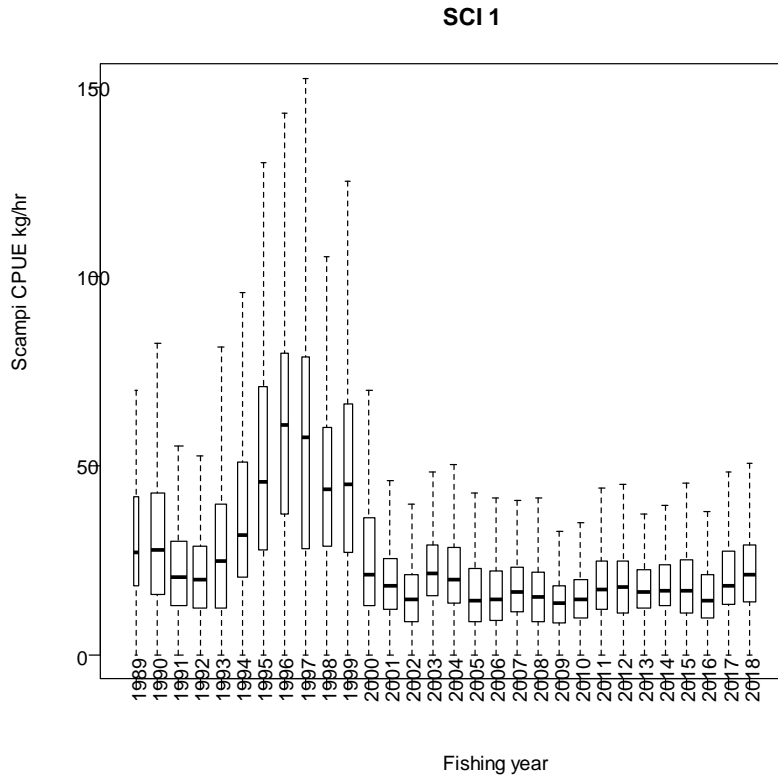


Figure 7: Boxplot (with outliers removed) of individual observations from TCEPR of unstandardised catch rate (catch (kg) divided by tow effort (hours)) with tows of zero scampi catch excluded, by fishing year for the SCI 1 fishery. Box width is proportional to the square root of number of observations.

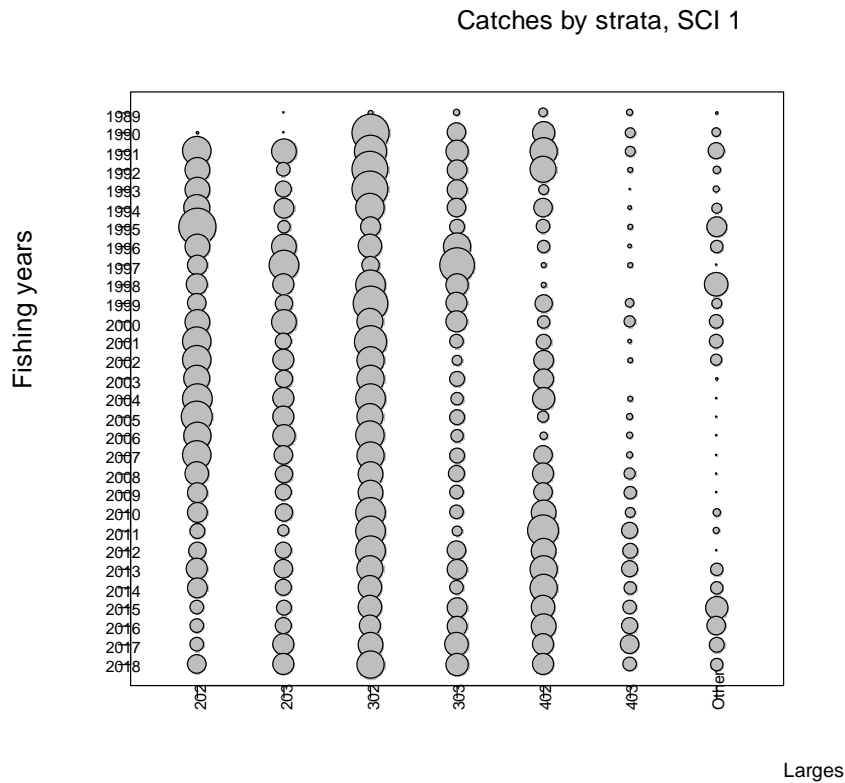


Figure 8: Annual catch breakdown by survey strata (and outside modelled area, 'Other') and fishing year for SCI 1.

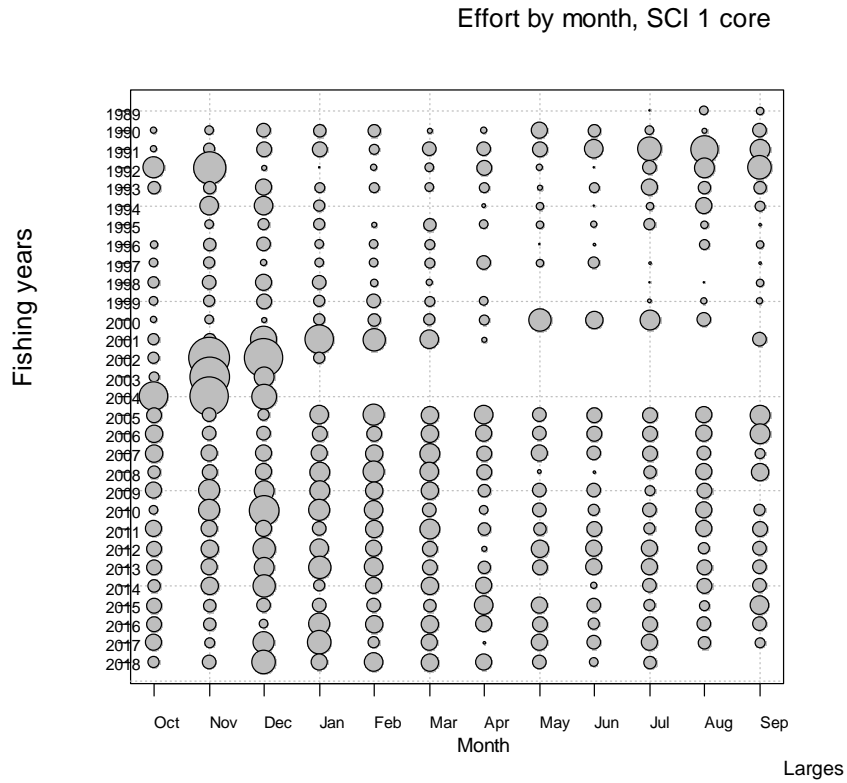


Figure 9: Monthly pattern of fishing effort in the scampi targeted fishery by fishing year for the core (modelled) area of SCI 1.

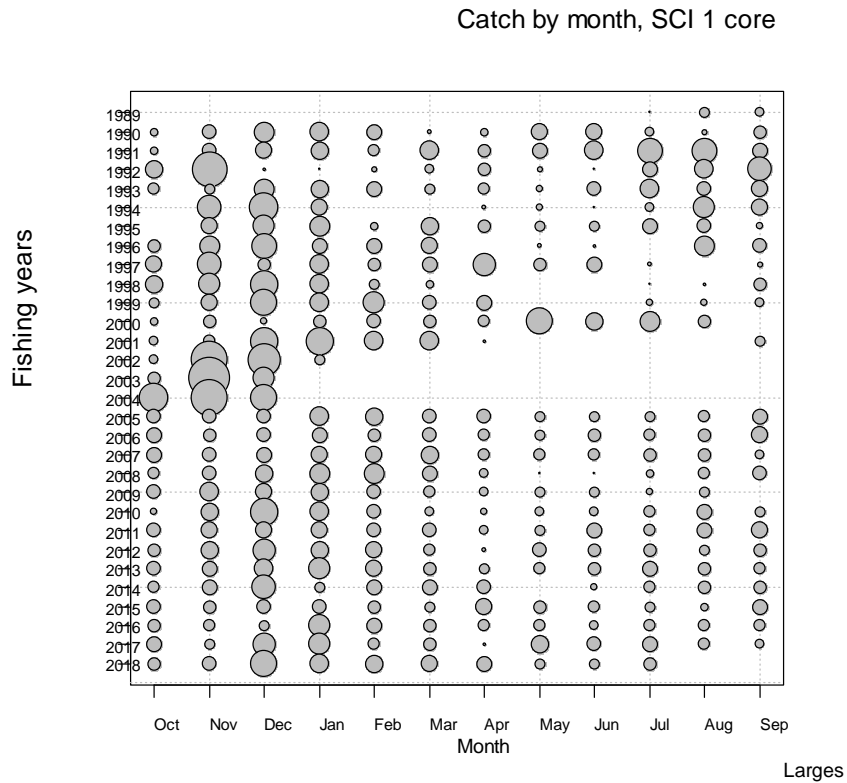


Figure 10: Monthly pattern of scampi catches in the scampi targeted fishery by fishing year for the core (modelled) area of SCI 1.

2.1.2. SCI 2 characterisation

Total annual landings for the SCI 2 fishery are presented in Figure 11, with landings and the percentage by the target scampi fishery presented in Table 2. Landings declined sharply in the early 2000s and remained low until 2010. Since this time landings have recovered and have generally been around the level of the TACC, which was reduced in 2011, but has been incrementally increased since this time. The distribution of fishing activity within the SCI 2 area over time is presented in Figure 12 and 13. The area over which the assessment model is applied is defined by the survey strata (300–500 m depth range in the main area of the fishery shown in Figure 3) with over 99% of the reported targeted scampi catch taken from this area (Table 2). The main fishery comprises two distinct grounds (Hawke Bay and Wairarapa). These core areas have consistently been fished over the history of the fishery, with smaller isolated patches (both to the north and south) fished in some years. A boxplot of the unstandardised CPUE (Figure 14) shows that catch rates were initially stable, increased in 1995, and declined steadily to 2002. This was followed by a slight increase to 2008, and then a rapid increase to a peak in 2014 (at levels similar to those recorded in the early 1990s), before a slight decline to 2016, and stable levels most recently.

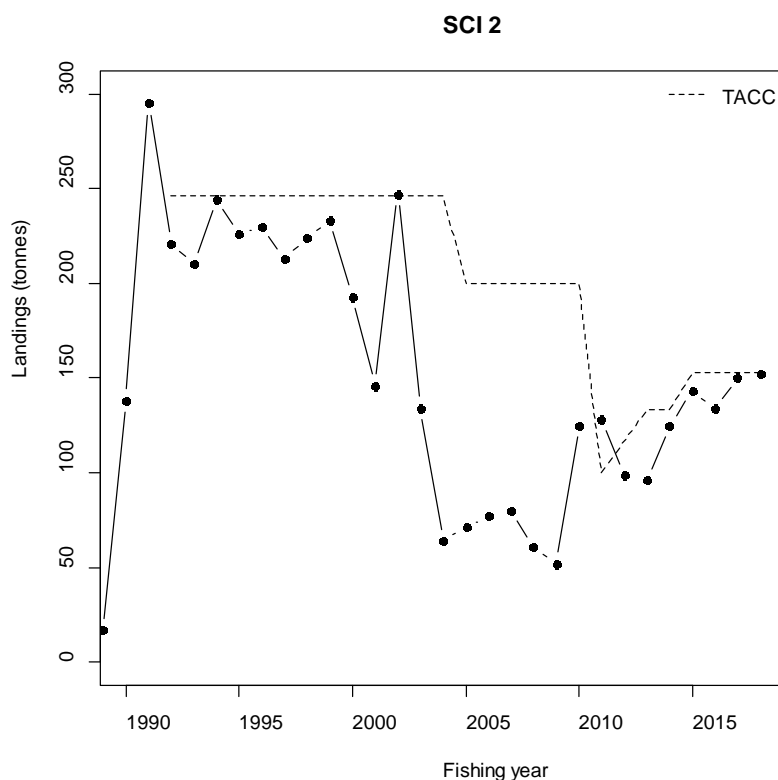


Figure 11: Time series of scampi landings from SCI 2 by fishing year (MHR data). The dashed line indicates the TACC that was introduced on 1 October 1992.

Table 2: Reported commercial landings (tonnes) from the 1986–87 to 2017–18 fishing years for SCI 2, catch estimated from the scampi target fishery, and estimated catch from the modelled area (survey strata).

	Landings (MHR)	Target catch (TCEPR)	% SCI target	Estimated catch (modelled area)	% catch (modelled area)
1986–87	0.0				
1987–88	5.0				
1988–89	17.0				
1989–90	138.0	134.9	98%	134.5	100%
1990–91	295.0	244.4	83%	243.1	99%
1991–92	221.0	187.4	85%	187.0	100%
1992–93	210.0	190.2	91%	189.1	99%
1993–94	244.0	217.1	89%	216.3	100%
1994–95	226.0	226.0	100%	214.7	95%
1995–96	230.0	222.1	97%	221.7	100%
1996–97	213.0	208.2	98%	205.0	98%
1997–98	224.0	219.3	98%	214.3	98%
1998–99	233.0	232.8	100%	230.3	99%
1999–00	193.0	187.0	97%	185.1	99%
2000–01	146.0	187.3	128%	185.1	99%
2001–02	247.0	220.7	89%	215.0	97%
2002–03	134.0	105.7	79%	101.9	96%
2003–04	64.0	52.3	82%	51.8	99%
2004–05	71.0	59.7	84%	48.2	81%
2005–06	77.0	68.5	89%	67.1	98%
2006–07	80.0	71.2	89%	70.4	99%
2007–08	61.0	56.5	93%	55.9	99%
2008–09	52.0	48.4	93%	48.3	100%
2009–10	125.4	118.0	94%	117.8	100%
2010–11	128.2	119.3	93%	119.1	100%
2011–12	98.8	87.8	89%	87.4	100%
2012–13	95.8	89.3	93%	89.3	100%
2013–14	125.4	120.8	96%	120.8	100%
2014–15	142.6	136.1	95%	136.0	100%
2015–16	133.8	128.1	96%	123.5	96%
2016–17	149.9	138.4	92%	138.0	100%
2017–18	152.4	138.7	91%	138.2	100%

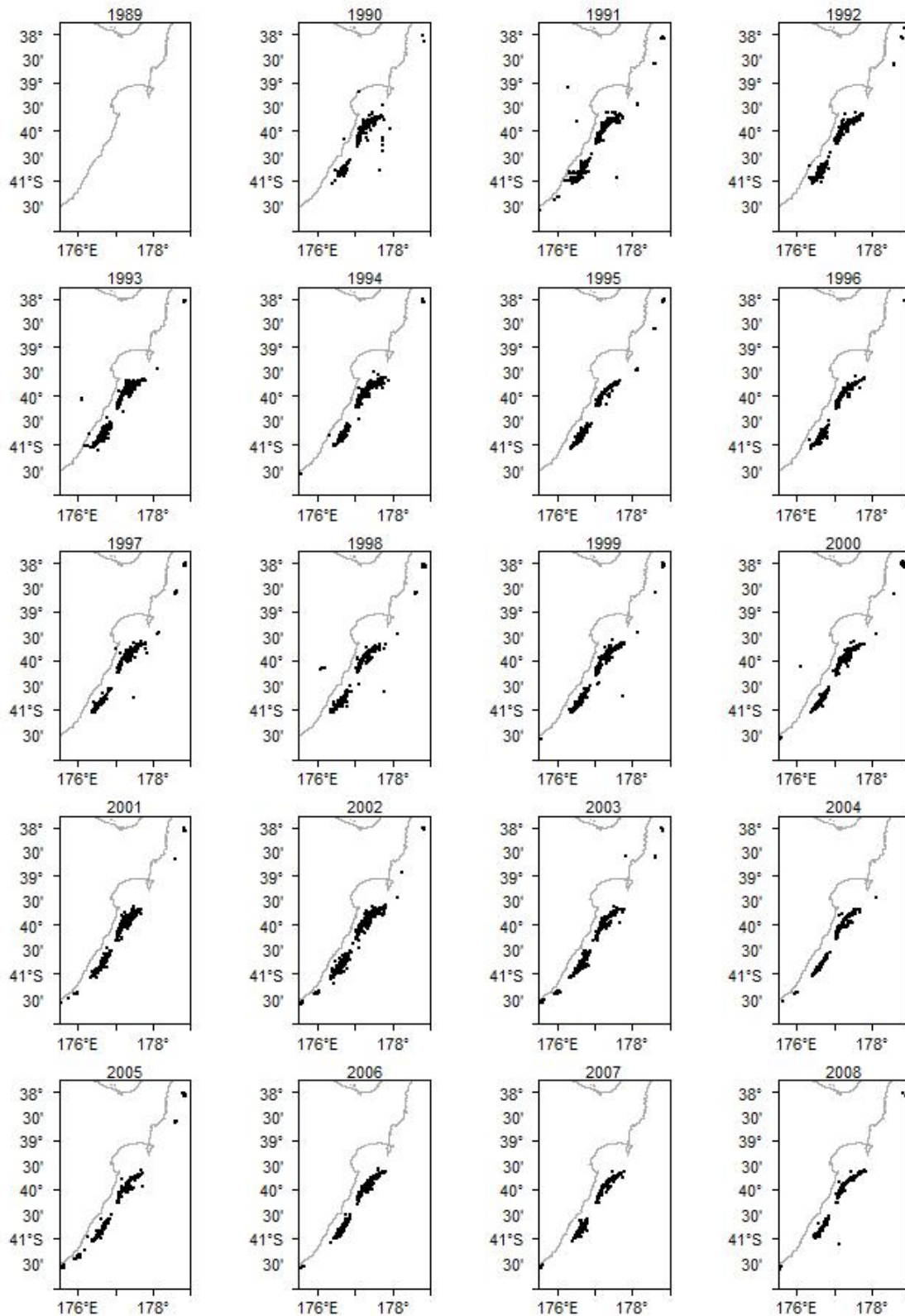


Figure 12: Spatial distribution of the main area of the SCI 2 scampi trawl fishery from 1988–99 to 2007–08. Each dot represents the midpoint of one or more tows reported on TCEPR. The general area covered by the plots is indicated within Figure 13.

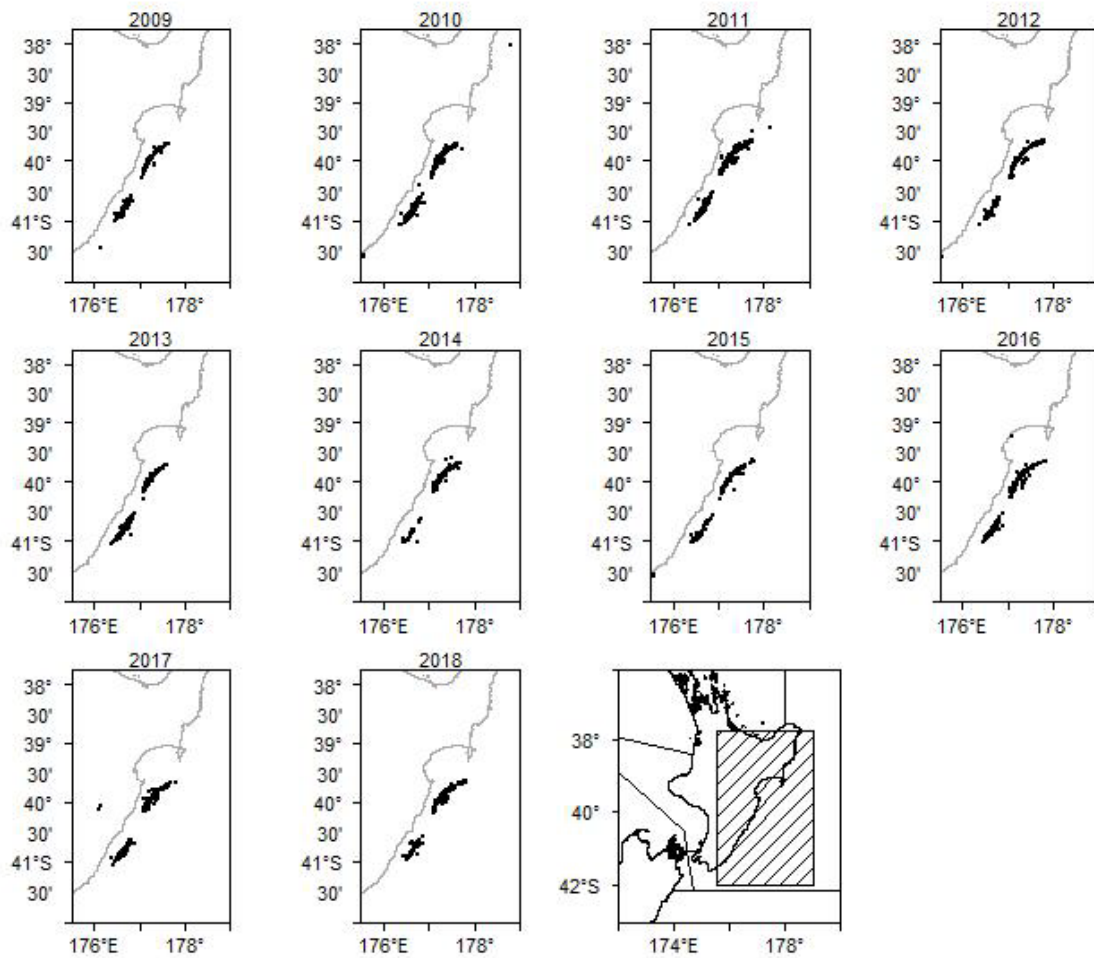


Figure 13: Spatial distribution of the main area of the SCI 2 scampi trawl fishery from 2008–09 to 2017–18. Each dot represents the midpoint of one or more tows reported on TCEPR. The general area covered by the plots is indicated by shaded box in the bottom right plot.

SCI 2

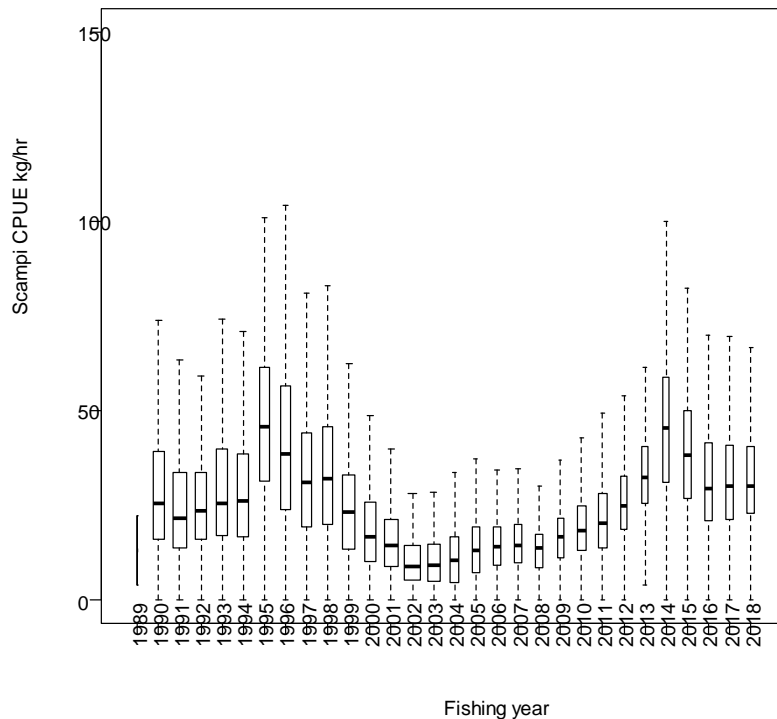


Figure 14: Boxplot (with outliers removed) of individual observations from TCEPR of unstandardised catch rate (catch (kg) divided by tow effort (hours)) with tows of zero scampi catch excluded, by fishing year for the SCI 2 fishery. Box width is proportional to the square root of the number of observations.

The breakdown of catch by survey strata and fishing year is presented for SCI 2 in Figure 15. The two shallower strata (702 and 802, i.e., 300–400 m) contributed far more catch than the deeper strata, with the deeper strata off the Wairarapa coast (strata 803) contributing little in most years.

Monthly patterns of effort and catch are presented in Figure 16 and Figure 17. As with SCI 1, the fishery was managed with competitive catch limits between 2001–02 and 2003–04. During this period, effort and catches were focussed in SCI 2 after the annual catch limit for SCI 1 was reached. Fishing was generally less consistently distributed throughout the year than in SCI 1, and in recent years there was little activity in the fishery between April and August.

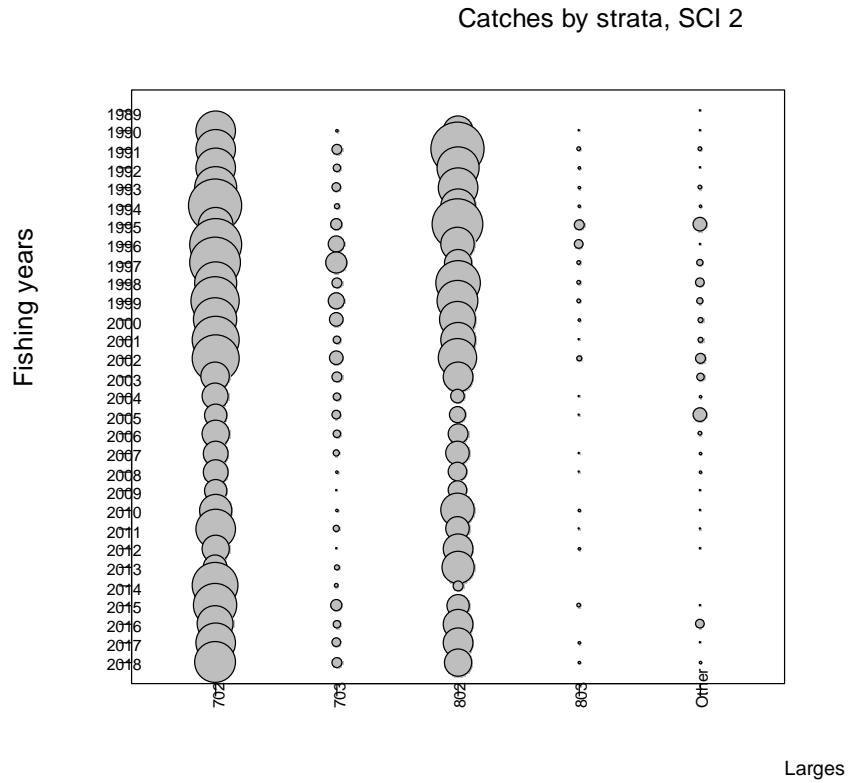


Figure 15: Annual catch breakdown by survey strata (and outside modelled area, 'Other') and fishing year for SCI 2.

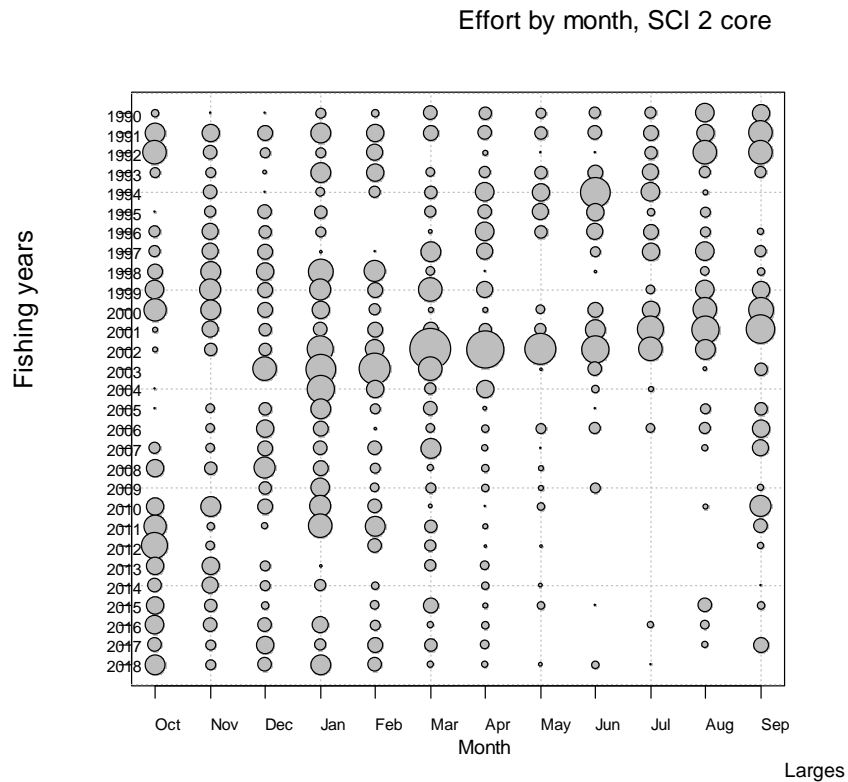


Figure 16: Monthly pattern of fishing effort in the scampi targeted fishery, by fishing year for the core (modelled) area of SCI 2.

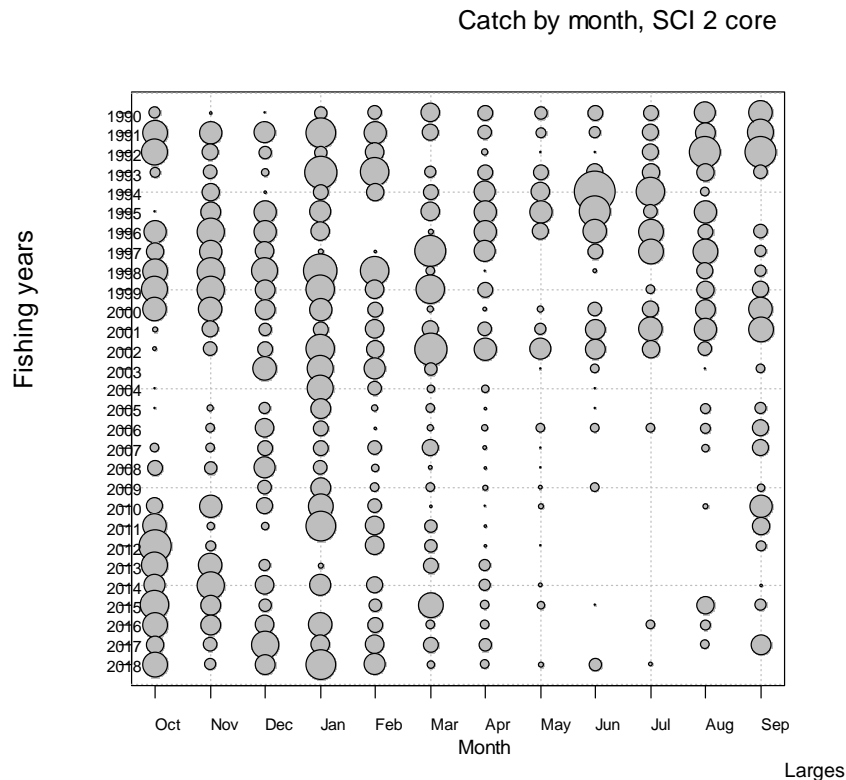


Figure 17: Monthly pattern of scampi catches in the scampi targeted fishery, by fishing year for the core (modelled) area of SCI 2.

2.2. Seasonal patterns in scampi biology

Previous development of the length-based model for scampi has shown that determination of appropriate time steps for the model is important when fitting to length and sex ratio data (Tuck & Dunn 2006; Tuck & Dunn 2009; Tuck & Dunn 2012). Scampi inhabit burrows and are not available to trawling when within a burrow. Catchability varies between the sexes on a seasonal basis in relation to moulting cycles and reproductive behaviour, resulting in seasonal changes in sex ratios in catches.

2.2.1. Sex ratio

The current knowledge of the timing of scampi biological processes in SCI 1 and SCI 2 is summarised in Table 3 (Tuck 2010). From patterns in ovary and egg stage observed from commercial and research trawl sampling, and the proportions of soft animals (Figure 18) and ovigerous females, mature female moulting appears to occur around October and November, just after the hatching period (August and September), with mating occurring at this time and new eggs being spawned onto the pleopods in November–January. The main male moulting period is completed well before the female moult (because mating occurs post moult for females, but the males must have completed the moult to mate), and appears to be concentrated in April and May (Figure 19), but may start as early as February. There is also some evidence of male moulting in September–November, generally for smaller (under 40 mm CL) animals.

The combination of biological processes for males and females lead to different relative availabilities of the two sexes throughout the year, resulting in the sex ratio pattern (displayed as proportion males) shown in Figure 20. Males are markedly less abundant than females in catches between February and

April (male catches being reduced during their moulting period), but females also dominate catches to a lesser extent between May and September.

Table 3: Summary of scampi biological processes for SCI 1. Source: Tuck (2010) and more recent survey data. X, months when the process is known to occur.

	Jan	Feb	Mar	Apr	May	Jun	Jul	Aug	Sep	Oct	Nov	Dec
Male moult		?	?	X	X				?	?	?	
Female moult										X	X	
Mating										X	X	
Eggs spawn	X										X	X
Eggs hatch								X	X			

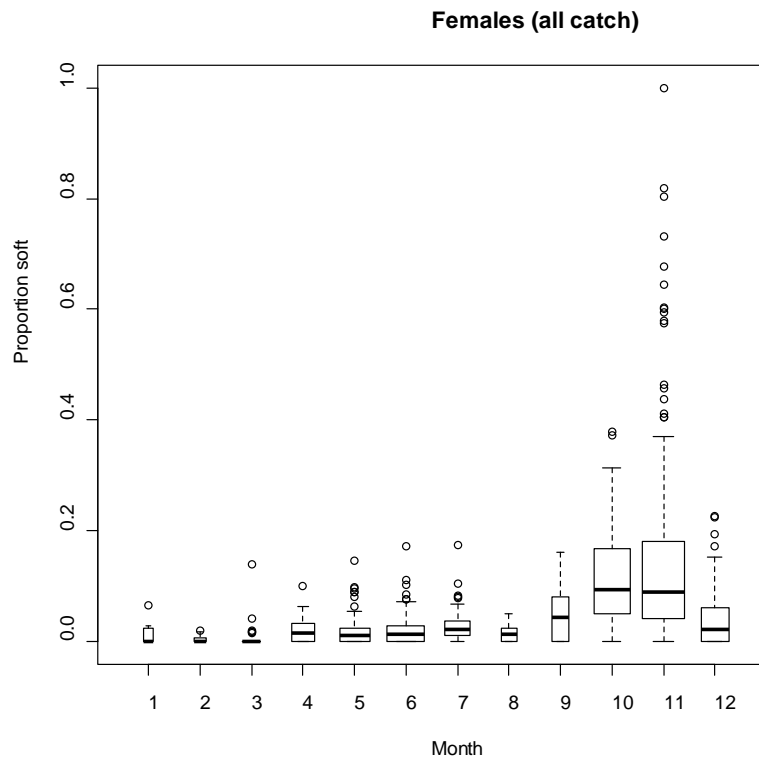


Figure 18: Proportion of females with soft carapace by month, from observer sampling in the SCI 1 and SCI 2 fisheries. Box widths are proportional to the square root of the number of observations.

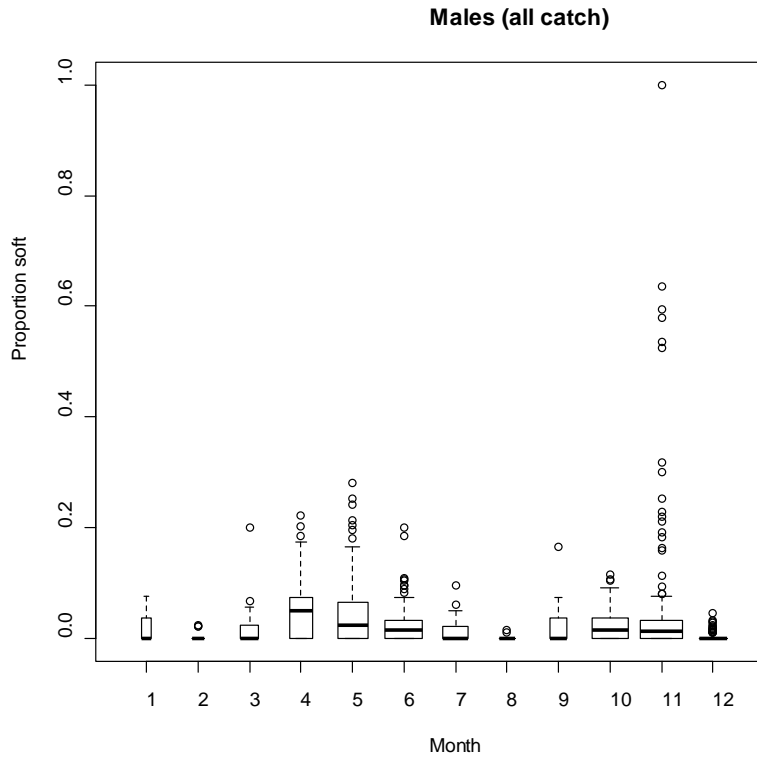


Figure 19: Proportion of males with soft carapace by month, from observer sampling in the SCI 1 and SCI 2 fisheries. Box widths are proportional to the square root of the number of observations.

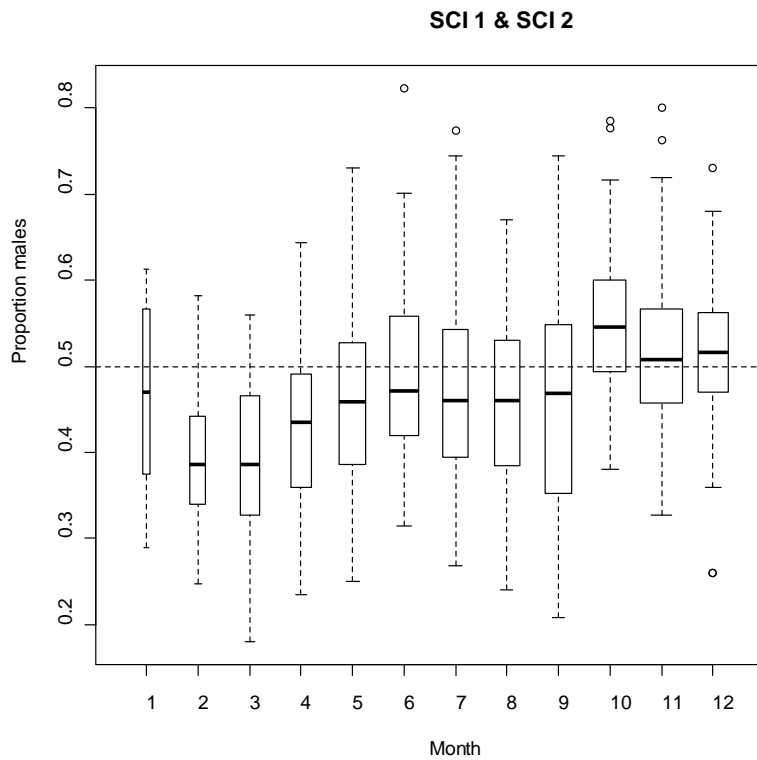


Figure 20: Boxplots of proportion of males in catches by month from observer sampling in the SCI 1 and SCI 2 fisheries. Box widths are proportional to the square root of the number of observations.

2.2.2. Time steps in assessment model

On the basis of our understanding of the timing of biological processes for scampi in this area and the seasonal sex ratio pattern, the assessment model has been partitioned into three time steps, as defined in Table 4. Catch data, stock abundance indices, and length frequency distributions have been collated and estimated in relation to these time steps, for inclusion in the assessment model. This is consistent with previous assessments for these areas (Tuck & Dunn 2012; Tuck 2014; 2016).

Table 4: Annual cycle of the population model for SCI 1 and SCI 2, showing the processes taking place at each time step, and their sequence within each time step. Fishing and natural mortality that occur together within a time step occur after all other processes, with 50% of the natural mortality for that time step occurring before and 50% after the fishing mortality. Natural mortality is apportioned to time steps in relation to their duration (as a fraction of the year). Fishing mortality is apportioned to time steps according to reported landings.

Step	Period	Process
1	October–January	Growth (both sexes) Natural mortality Fishing mortality
2	February–April	Recruitment Maturation Natural mortality Fishing mortality
3	May–September	Natural mortality Fishing mortality

2.3. Standardised CPUE indices

Vessels have been allocated a letter code to maintain confidentiality, with codes applied consistently between the two fisheries.

2.3.1. Core vessel selection for SCI 1

A plot of vessel activity (number of scampi targeted tows recorded) over time is presented for SCI 1 in Figure 21. One vessel (O) has been active and dominant throughout the history of the fishery but stopped fishing in 2017 (being replaced by vessel SS), whereas some others have contributed for a number of years. Some vessels were only active in the fishery during the late 1990s and early 2000s (partly associated with the period of competitive catch limits between 2001–02 and 2003–04). Only three vessels have been routinely active in the fishery in recent years (FF, O, and P).

Figure 22 (upper plot) shows the proportion of the total catch (over the history of the fishery) in relation to number of years vessels contributing that catch have been active in the fishery. Previous characterisations for this and the other main scampi fisheries have taken a default of 10 years activity for inclusion in the core fleet. This approach identified eight core vessels (vessels O, P, FF, S, V, Q, R, and DD) which have contributed over 90% of the targeted scampi catches from SCI 1. These represent vessel DD in addition to the same seven vessels selected as core vessels for SCI 1 in the last assessments (Tuck 2014; Tuck 2016). The lower plot of Figure 22 shows the proportion of catch accounted for each year by vessels active for over 5 or 10 years. Other than the first few years, and 2001–02 and 2002–03, the core vessels (active for over 10 years) accounted for over 90% of annual targeted scampi catches until 2016. Vessel O was replaced in the fishery by vessel SS midway through the 2016–17 fishing year, and so the proportion of annual catch represented by the core vessels drops significantly in 2016–17 and 2017–18. Including vessel SS within the core fleet would increase the proportion of the catch represented to over 90% in the recent years (Figure 22), but mean including a vessel only active for two years.

2.3.2. Core vessel selection for SCI 2

A plot of vessel activity (number of scampi targeted tows recorded) over time is presented for SCI 2 in Figure 23. A number of vessels have been regularly active in the fishery, and none is dominant. A few vessels joined the fishery associated with the period of competitive catch limits between 2001–02 and 2003–04, but to a lesser extent than for SCI 1. Four vessels (DD, P, S, and V) have been routinely active in the fishery in recent years, with other vessels (FF, O, and U) occasionally active, and vessel CC recently starting (at a very low level) in this fishery.

Figure 24 (upper plot) shows the proportion of the total catch (over the history of the fishery) in relation to number of years those vessels contributing that catch have been active in the fishery, and on the basis of this, a cut-off of 10 years of activity has been selected to identify nine core vessels (DD, FF, O, P, Q, R, S, U, and V), which have contributed almost 95% of the targeted scampi catches from SCI 2. These represent the same nine vessels selected as core vessels for SCI 2 in the last assessments (Tuck 2014; Tuck 2016). The same vessel codes have been used for both fisheries, and all the core vessels from SCI 1 are included in the SCI 2 list. The lower plot of Figure 24 shows the proportion of catch accounted for each year by vessels active for over 5 or 10 years (minimal difference between the lines). Other than the first few years, and 2001–02 and 2002–03, and the most recent years, the core vessels (active for over 10 years) have accounted for over 90% of annual targeted scampi catches, and they account for over 80% in all but one year.

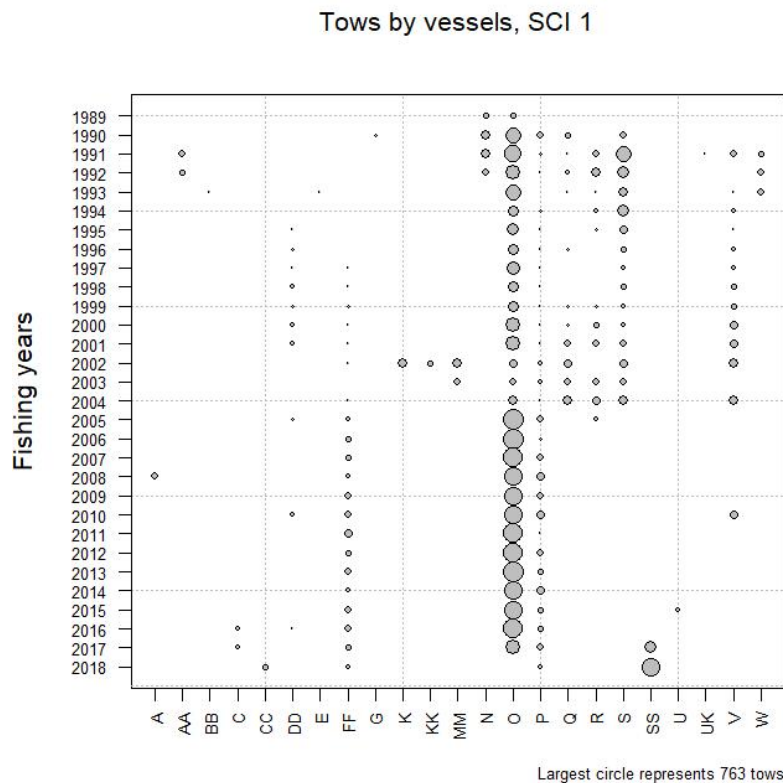


Figure 21: Pattern of fishing activity by vessel and fishing year for SCI 1. The area of the circles is proportional to the number of tows recorded.

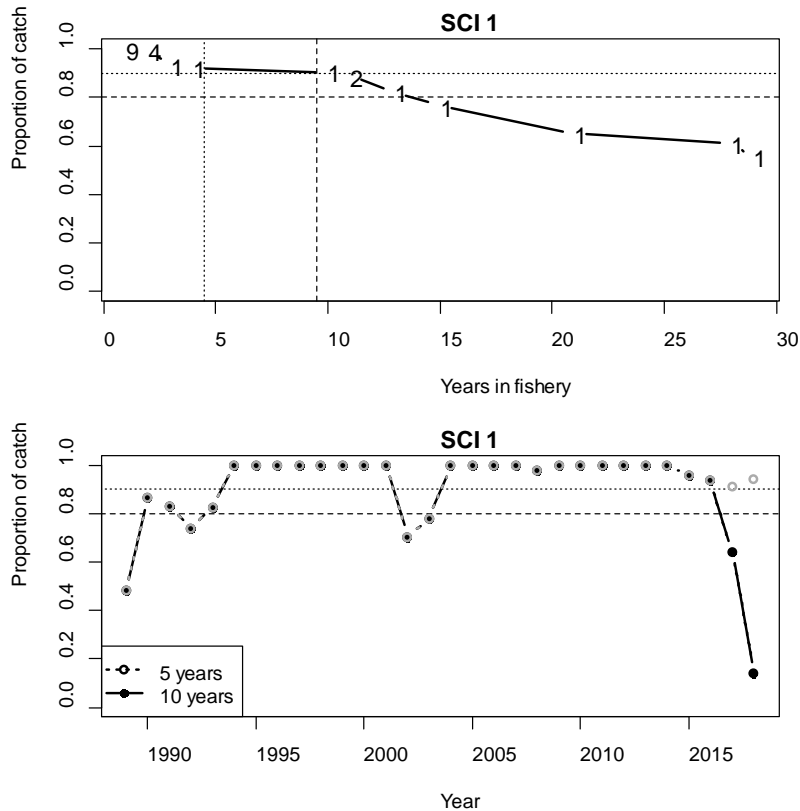


Figure 22: Catch breakdown by vessel. Upper plot: Proportion of total scampi catch (all years) plotted against the number of years the vessels reporting that catch have been active in the fishery. Numbers indicate number of vessels active for that duration. Vertical dotted line represents cut-off for core vessels. Lower plot: Proportion of annual catch reported by vessels active in the fishery for over 5 and 10 years. Grey symbols on lower plot represent proportion of catch reported by vessels active for over 10 years, plus vessel SS.

Tows by vessels, SCI 2

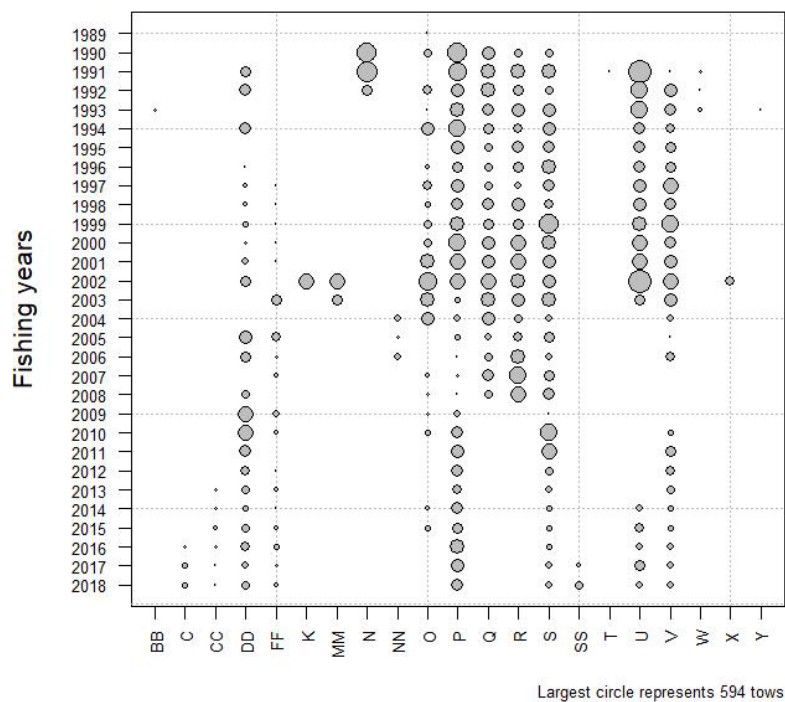


Figure 23: Pattern of fishing activity by vessel and fishing year for SCI 2. The area of the circles is proportional to the number of tows recorded.

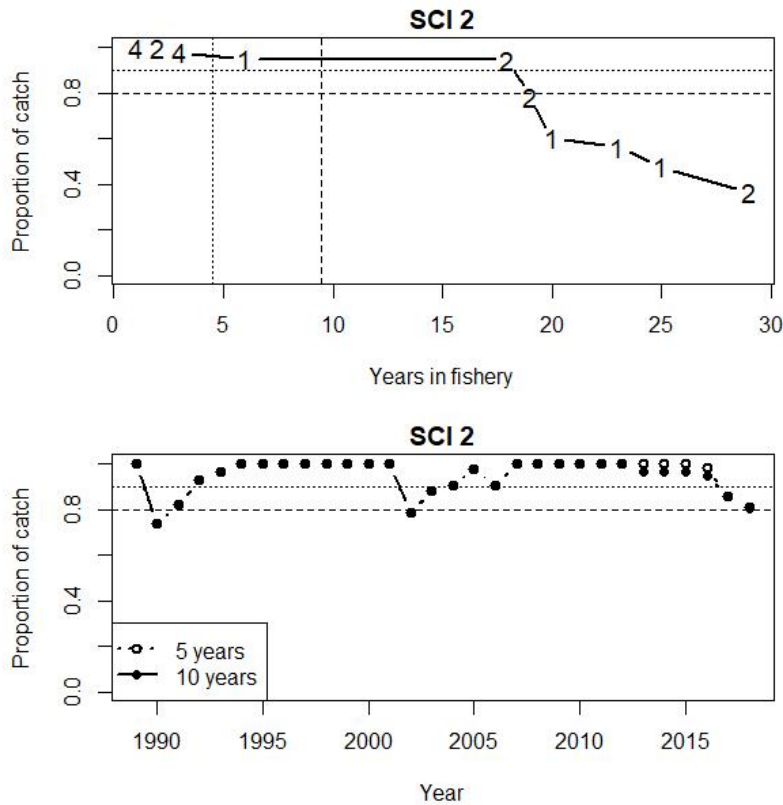


Figure 24: Catch breakdown by vessel. Upper plot: Proportion of total scampi catch (all years) plotted against the number of years the vessels reporting that catch have been active in the fishery. Numbers indicate number of vessels active for that duration. Vertical dotted line represents cut-off for core vessels. Lower plot: Proportion of annual catch reported by vessels active in the fishery for over 5 and 10 years.

2.3.3. Exclusion of poorly sampled time periods

Following the approach developed for SCI 3 (Tuck 2013), time steps that were poorly sampled by the core vessels were excluded from the standardisation of the CPUE, on the basis that a small number of tows in an area, or at a particular time, may not provide a good index of abundance. Records were excluded from the analysis when there were less than 10 tows recorded by core vessels within a time step in a year (Figure 25).

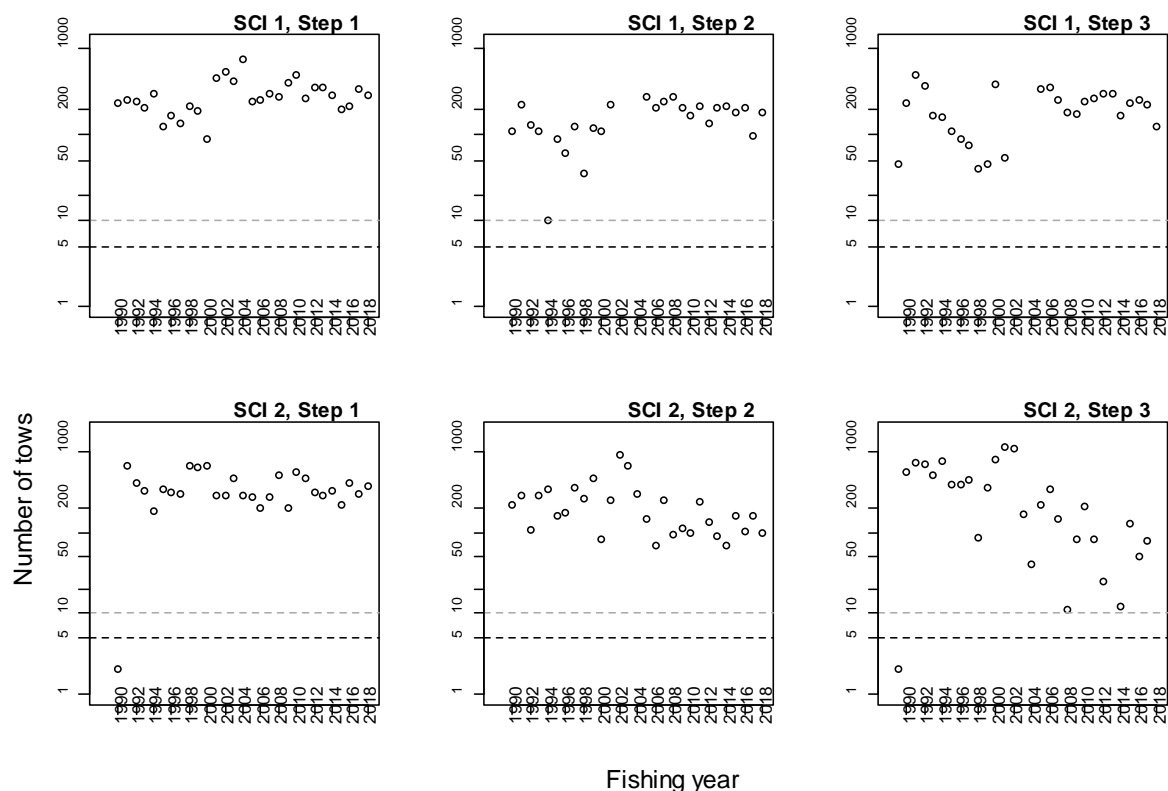


Figure 25: Numbers of commercial tows available within the core vessel dataset by time step and fishing year for SCI 1 (upper row) and SCI 2 (lower row). Dashed lines represent arbitrary cut-offs at 5 and 10 tows.

2.3.4. Calculation of indices

The initial assessments of SCI 1 and SCI 2 fitted separate abundance indices for different survey strata and time steps (Tuck & Dunn 2012), but more recently the SFWG has suggested a simplification of the model structure (Tuck 2014). Therefore, an initial standardisation was conducted to generate an annual index (as applied in Tuck 2014 and subsequent assessments), and this was compared with stratified indices where interaction terms were suggested by the data. For each index, scampi catch rates reported by core vessels within the appropriate area and time step were modelled using combined spatial and time step (forced), vessel, time of day, state of moon, depth, and fishing duration terms. For the three time step indices, the spatial strata variable was included in the model as a term, and for the annual index, spatial strata and time step were included.

The indices were calculated from data for core vessels in the modelled area. Core vessels were selected as described above, by examining the scampi fleet's activity over the history of the fishery and selecting vessels that had consistently contributed over a number of years and, together, had contributed a significant proportion of the overall catches over the whole fishery, and in each year.

Of the core vessels identified, two have changed gear configuration (twin rig to triple rig) in recent years, and two have changed engine power over the history of the fishery. On the basis of previous investigations (Tuck 2013), engine power was fitted within the model (as a factor) and gear configuration as a two-level factor (twin or triple rig). Gear configuration for a particular vessel and date was determined on the basis of information provided by the fishing industry as to when vessels changed from twin to triple, and all tows after this date are defined as triple rig. It is acknowledged that vessels may change configuration within a trip depending on gear damage or fishing conditions, but it is believed that this is not recorded consistently enough over the history of the fishery within the TCEPR records to be useable.

The time of day of each tow was calculated in relation to nautical dawn and dusk (time when the sun is 12 degrees below the horizon in the morning and evening), as calculated by the *crepuscule* function of the *maptools* package in R. Individual tows were categorised on the basis of whether they included dawn (shot before dawn, hauled after dawn and before dusk), day (shot after dawn, hauled before dusk), dusk (shot before dusk, hauled after dusk and before dawn) or night (shot after dusk and hauled before dawn). Longer tows including more than one period (i.e., shot before dusk and hauled after dawn) were excluded from this part of the analysis (excluding 52 records from a total of over 22 300 for SCI 1, and 88 records from a total of over 30 500 for SCI 2).

Individual hauls were also categorised in terms of moon state, on the assumption that tidal current strength at the sea floor will be related to the lunar cycle. Tows were categorised by their date in relation to the lunar cycle, as Full moon (more than 26 days since full moon, or less than 3 days since full moon), Waning (4–11 days since full moon), New moon (12–18 days since full moon), and Waxing (19–26 days since full moon).

In addition, an examination of the data for SCI 3 (Tuck 2013) identified a distinct shift in trawl duration between 2002–03 and 2006–07 (from about 5 hours to 7 hours). This shift (in SCI 3) was fleet-wide and associated with a modification to the top of the trawl to reduce the finfish bycatch (John Finlayson, Sanford Ltd., *pers. comm.*), enabling vessels to fish for longer on each tow. The shift in haul duration is not apparent in data from other scampi management areas, but the vessels use the same trawl gear in all their scampi fishing. For each vessel, the timing of the gear modification was estimated from examination of tow durations in SCI 3 (see Tuck 2014) and fitted as a two-level factor in the catch standardisations of the SCI 1 and SCI 2 data.

Catch indices were derived using generalised linear modelling (GLM) procedures (Vignaux 1994; Francis 1999), using the statistical software package R. The response variable in the GLM was the natural logarithm of scampi catch. The *fishing-year* was entered as a categorical covariate (explanatory) term on the right-hand side of the model. Standardised CPUE abundance indices (canonical) were derived from the exponential of the *fishing-year* covariate terms as described by Francis (1999).

To accommodate a non-linear relationship with the response variable (log catch), the continuous variables (effort and depth) were “offered” to the GLMs as splines. Vessel, time of day, state of tide (i.e., moon state), twin or triple rig, bycatch modification and vessel power were “offered” to the GLMs as factors. A forward-fitting, stepwise, multiple-regression algorithm was used to fit GLMs to groomed catch, effort, and characterisation data. The stepwise algorithm generates a final regression model iteratively and uses a simple model with a single predictor variable, fishing year, as the initial or base model. The reduction in residual deviance relative to the null deviance is calculated for each additional term added to the base model. The term that results in the greatest reduction in residual deviance is added to the base model if this results in an improvement in residual deviance of more than 1%. The algorithm repeats this process, updating the model, until no new terms can be added. Diagnostic plots for the final models are presented in Appendix 1 and 2 (Bentley et al. 2012).

Preliminary investigations into different error distributions (comparing log normal, gamma, and weibull) using a simple standardisation model

$$\text{Log(catch)} \sim \text{fishing_year}$$

identified that the gamma distribution provided a slight improvement in the distribution of residuals, and this error distribution was used for calculation of the indices reported below. Diagnostic plots for the three compared error distributions were examined for both fisheries separately, and for the final standardisation model; these are presented in Appendix 1 and 2.

2.3.5. SCI 1 indices

Single annual index

An initial single annual index was estimated, for consistency with the previous assessment (Tuck 2016) and to provide a baseline for comparison of other indices. Stepwise regression analysis of the dataset to estimate an annual CPUE index for SCI 1 resulted in a final model with fishing year, time of day, effort (tow duration), survey strata, and model time step retained (Table 5). Model diagnostics are presented in Appendix 1. The model explained 42.5% of the variation in the data. Effort was the most influential variable, at 9.9%, with time of day having an influence of 4.4%, and survey strata and time step about 2.5–3.5%. The standardised and unstandardised annual indices are shown in Figure 26. The two indices follow a very similar pattern, although the standardised index is consistently above the unstandardised during the early part of the series (as fishing duration was increasing), and below the unstandardised in later years. The relative effects of the explanatory variables (excluding fishing year) are shown in Figure 27. Expected catch rates are highest during the day and lowest at night, being about half of the daytime rate. Expected catch increases for tow durations up to about 8 hours, but then declines. Catch rates are highest in the southern strata and are highest in time step 1, falling to about 80% of this level in time steps 2 and 3.

Table 5: Analysis of deviance table and overall influence for the standardisation model selected by a stepwise regression for an annual index for SCI 1. TOD is time of day.

	Df	Residual deviance	Deviance explained	Additional deviance explained (%)	Overall influence (%)*
NULL		7124.3			
fishing_year	29	5327.4	1796.9	25.22	
TOD	3	4545.3	782.1	10.98	4.4
bs(fishing duration)	3	4323.7	221.6	3.11	9.9
survstrata	5	4218.7	105.0	1.47	2.5
model_step	2	4096.1	122.6	1.72	3.5

* Overall influence as in table 1 of Bentley et al. (2012)

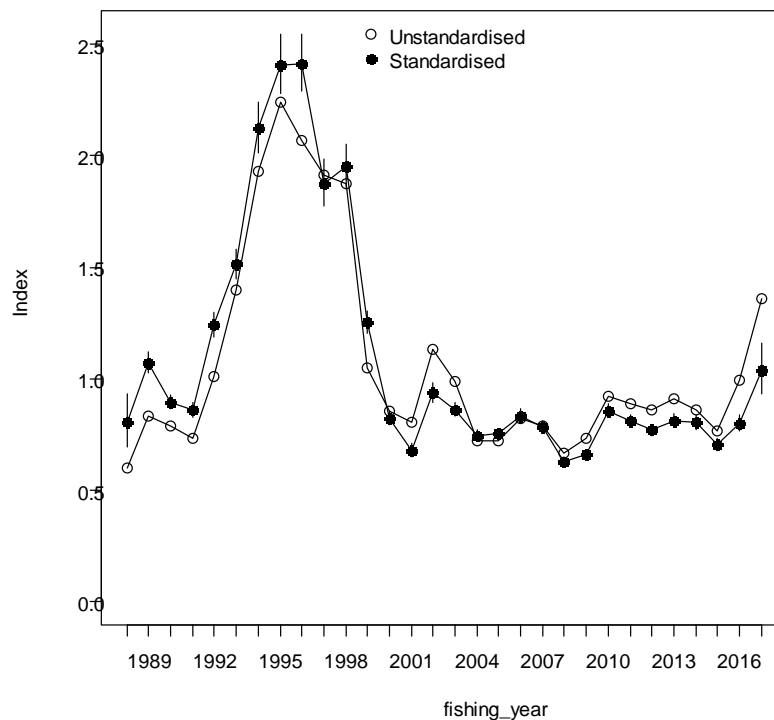


Figure 26: Comparison of standardised (Table 5) and unstandardised annual CPUE index for SCI 1.

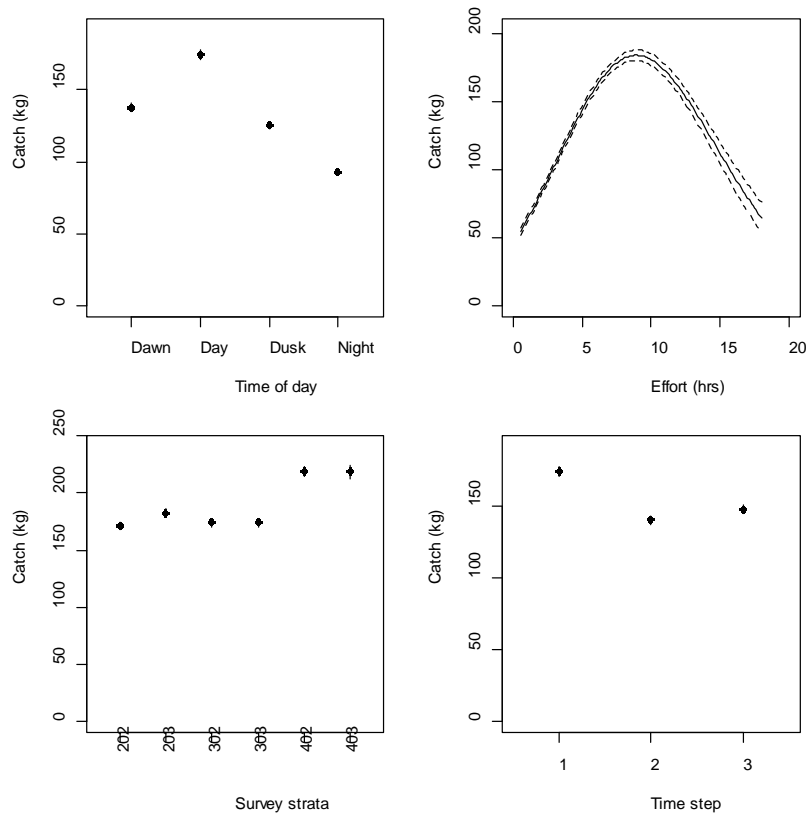


Figure 27: Termplot (in natural space) for annual index standardisation model (Table 5), showing relative effects of time of day, effort (tow duration), survey strata, and time step.

Other indices

The inclusion of interaction terms was explored allowing interactions between fishing year, survey strata and time step, with terms for fishing year (forced), time of day, effort, survey strata, and time step retained, along with interaction terms for fishing year:survey strata and fishing year:time step (Table 6). This model explained 46.3% of the variation in the data.

Table 6: Analysis of deviance table for the standardisation model including interactions selected by stepwise regression for SCI 1. TOD is time of day.

	Df	Residual deviance	Deviance explained	Additional deviance explained (%)
NULL		7124.3		
fishing_year	29	5327.4	1796.9	25.22
TOD	3	4545.3	782.1	10.98
bs(fishing duration)	3	4323.7	221.6	3.11
survstrata	5	4218.7	105.0	1.47
model_step	2	4096.1	122.6	1.72
fishing_year:survstrata	141	3925.6	170.5	2.39
fishing_year:model_step	50	3828.6	97.0	1.36

Given that interaction terms were retained within the initial model, separate stratum time step indices were estimated within a standardisation model including a fishing_year_strata_step term. This model retained terms for fishing_year_strata_step (forced), time of day and effort (Table 7) and explained 48% of the variance in the data. Individual time step indices are plotted for each survey stratum in Figure 28, along with the single annual index (Table 5). In general, the individual strata time step indices are consistent with the single annual index.

Table 7: Analysis of deviance table for the initial standardisation model including a term for fishing_year_strata_time step selected by stepwise regression for SCI 1. TOD is time of day.

	Df	Residual deviance	Deviance explained	Additional deviance explained (%)
NULL		7124.3		
fishing_year_strata_step	433	4446.7	2677.6	37.58
TOD	3	3917.8	528.9	7.42
bs(fishing duration)	3	3688.9	228.9	3.21

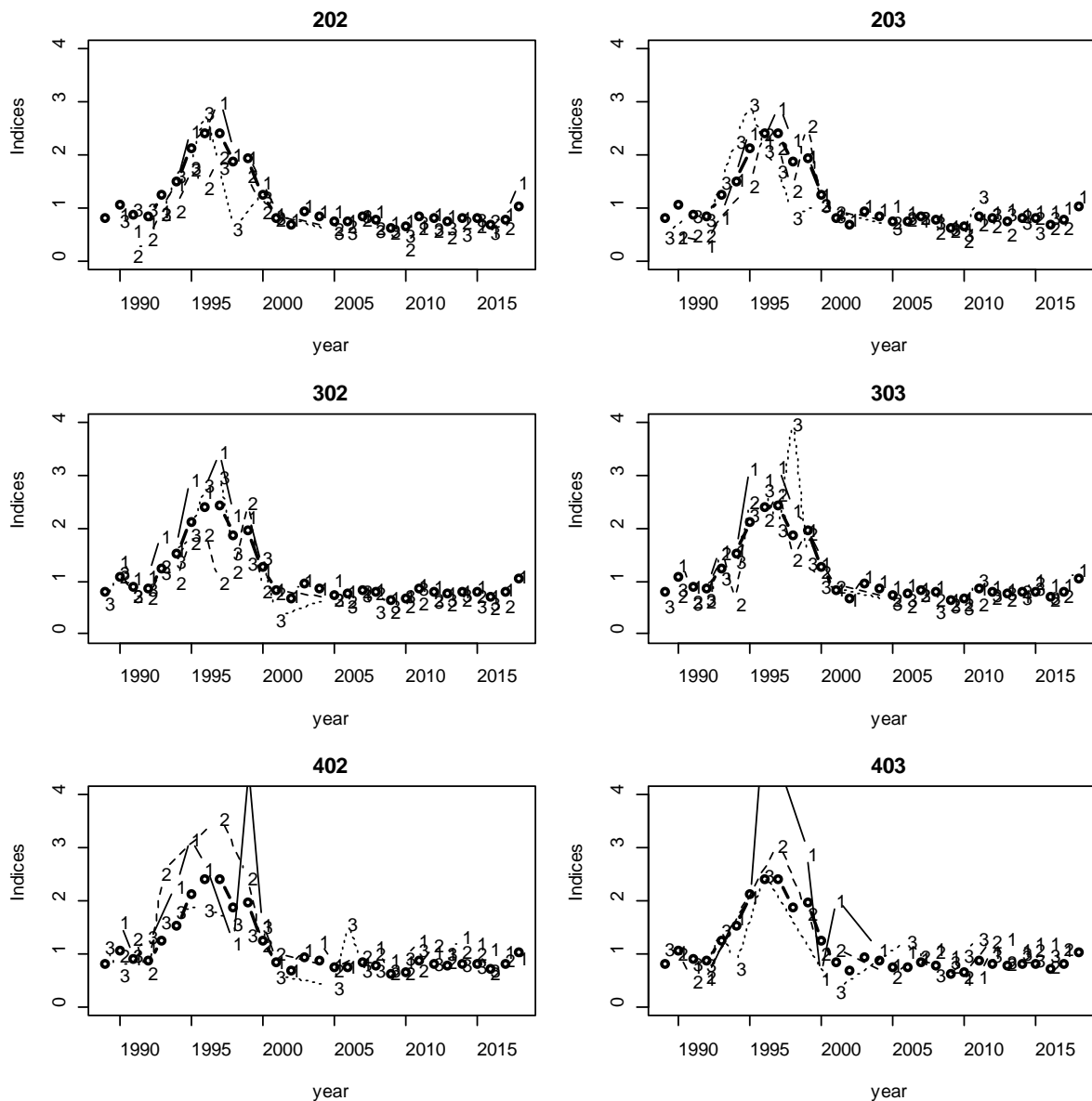


Figure 28: Standardised indices for each time step and strata (Table 7) plotted over the single annual index (Table 5). Annual index is represented by thicker line with open symbols; individual time step indices for each strata are labelled by time step number.

As discussed, previous assessment models for scampi have fitted indices stratified spatially and temporally (Tuck & Dunn 2012), but more recently the SFWG has proposed more simplified model structures (Tuck 2014; Tuck 2016). Given the consistency in the patterns shown in the individual strata time step and single annual index, it was considered that realistic options for weighting individual spatial strata would not generate a composite annual index greatly different from the single

index presented in Figure 26, and the Working Group agreed that the annual index (Table 5, Figure 26) should be used within the models as the index of abundance from the CPUE data.

2.3.6. SCI 2 indices

Single annual index

An initial single annual index was estimated, for consistency with the previous assessment (Tuck 2016) and to provide a baseline for comparison of other indices. Stepwise regression analysis of the dataset to estimate an annual CPUE index for SCI 2 resulted in a final model with fishing year, time of day, effort (tow duration), time step, and vessel code retained (Table 8). Model diagnostics are presented in Appendix 2. The model explained 41.1% of the variation in the data. Effort was the most influential variable, at 8.4%, with time step having about 4% influence, and time of day and vessel about 2%. The standardised and unstandardised annual indices are shown in Figure 29. The two indices follow a very similar pattern, although standardised index is consistently above the unstandardised during the early part of the series (as fishing duration was increasing), and below the unstandardised since this time, when fishing was more focussed in time step 1. The relative effects of the explanatory variables (excluding fishing year) are shown in Figure 30 and these bear a marked similarity to those seen for the same factors selected by the SCI 1 standardisation (see Figure 27). Expected catch rates are highest during the day and lowest at night. Expected catch increases for tow durations up to about 10 hours, but then declines. Catch rates are highest in time step 1, falling to about 80% of this level in time steps 2 and 3, and performance varies between vessels, with one markedly lower than the others.

Table 8: Analysis of deviance table and overall influence for the standardisation model selected by stepwise regression for an annual index for SCI 2. TOD is time of day.

	Df	Residual deviance	Deviance explained	Additional deviance explained (%)	Overall influence (%)*
NULL		11851.5			
fishing_year	28	8376.3	3475.2	29.32	
TOD	3	7835.2	541.1	4.57	1.9
bs(fishing duration)	3	7399.3	435.9	3.68	8.4
model_step	2	7155.4	243.9	2.06	4.1
vessel_code	8	6979.1	176.3	1.49	2.3

* Overall influence as in Table 1 of Bentley et al. (2012)

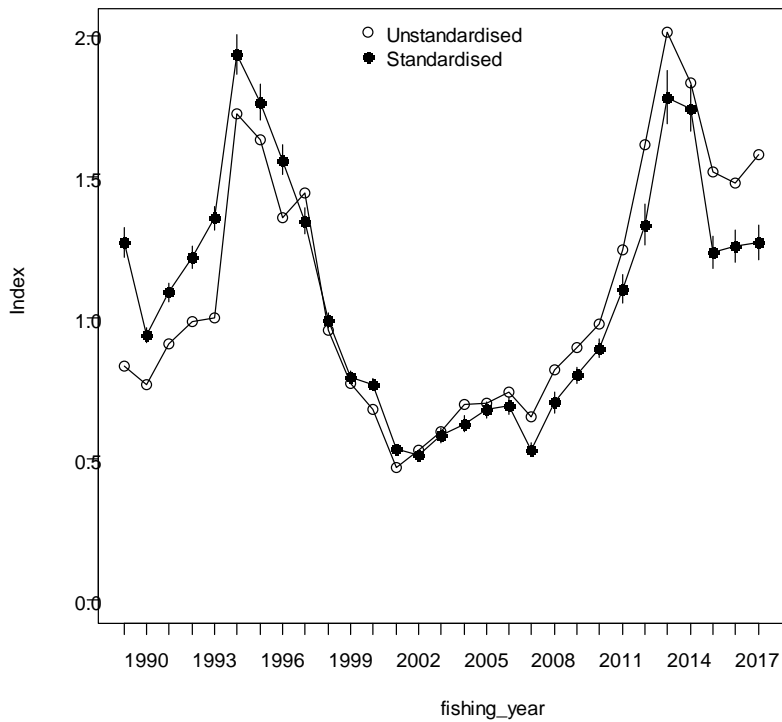


Figure 29: Comparison of standardised (Table 8) and unstandardised annual CPUE index for SCI 2.

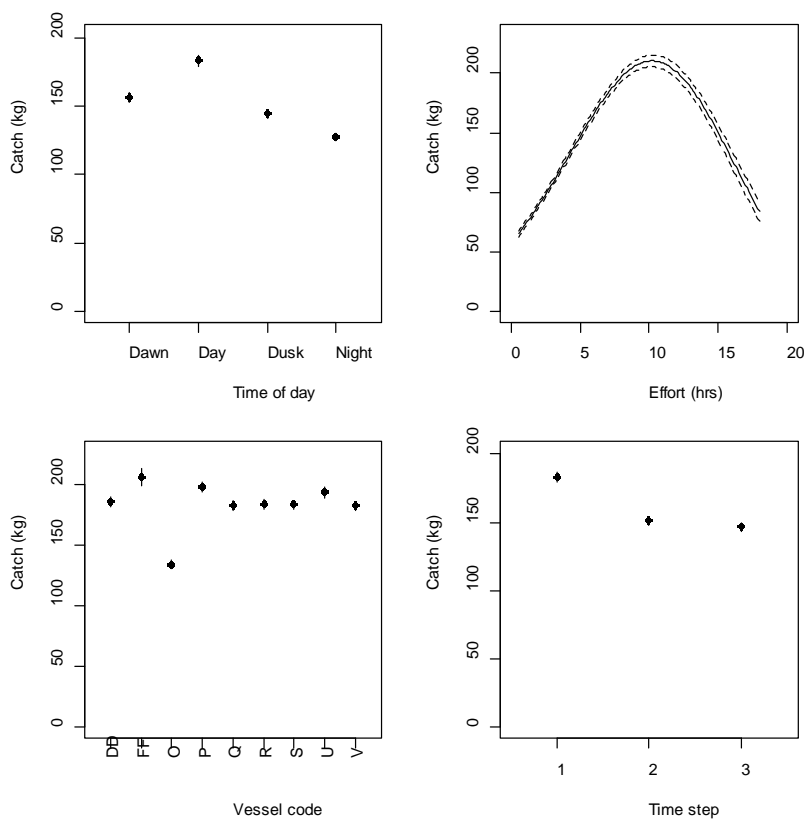


Figure 30: Term plot (in natural space) for annual index standardisation model (Table 8), showing relative effects of time of day, effort (tow duration), vessel, and time step.

Other indices

The inclusion of interaction terms was explored by allowing interactions between fishing year, survey strata, and time step, with terms for fishing year (forced), time of day, effort, and vessel retained, along with an interaction term for fishing_year:model step (Table 9). This model explained 45.3% of the variation in the data.

Table 9: Analysis of deviance table for the standardisation model including interactions selected by stepwise regression for SCI 2. TOD is time of day.

	Df	Residual deviance	Deviance explained	Additional deviance explained (%)
NULL		11851.5		
fishing_year	28	8376.3	3475.2	29.32%
TOD	3	7835.2	541.1	4.57%
bs(fishing duration)	3	7399.3	435.9	3.68%
model_step	2	7155.4	243.9	2.06%
vessel_code	8	6979.1	176.3	1.49%
fishing_year:model_step	54	6488.1	491.0	4.14%

Given that interaction terms were retained within the initial model, separate time step indices were estimated within a standardisation model including a fishing_year_step term. This model retained terms for fishing_year_step (forced), effort, time of day, and vessel code (Table 10) and explained 45.3% of the variance in the data. Individual time step indices are plotted in Figure 31, with the single annual index (Table 8). The individual time step indices are consistent with the single annual index.

Table 10: Analysis of deviance table for the initial standardisation model including a term for fishing_year_step selected by stepwise regression for SCI 2. TOD is time of day.

	Df	Residual deviance	Deviance explained	Additional deviance explained (%)
NULL		11851.5		
fishing_year_step	84	7319.7	4531.8	38.24
bs(fishing duration)	3	6961.6	358.2	3.02
TOD	3	6614.7	346.9	2.93
vessel_code	8	6488.1	126.6	1.07

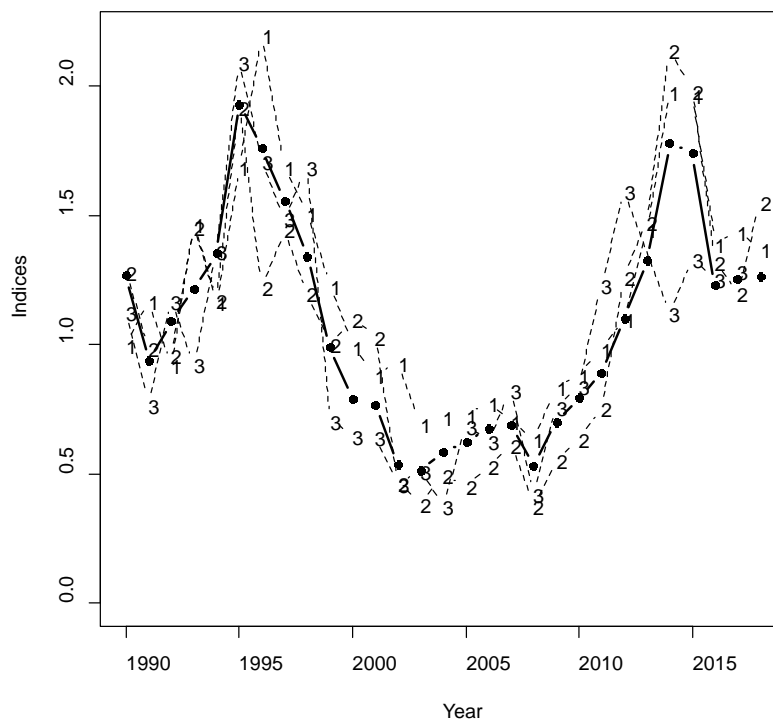


Figure 31: Standardised indices for each time step (Table 10) plotted over the single annual index (Table 8). Annual index is represented by thicker line with open symbols; individual time step indices for each stratum are labelled by time step number.

Given the consistency in the patterns shown in the individual time step and single annual index, it was considered that realistic options for weighting individual time steps would not generate a composite annual index greatly different from the single index presented in Figure 29, and the Working Group agreed that the annual index (Table 8, Figure 29) should be used within the models as the index of abundance from the CPUE data.

3. MODEL STRUCTURE

3.1. Spatial and seasonal structure, and the model partition

The model partitions scampi by sex and length class. Growth between length classes is determined by sex-specific, length-based growth parameters. Individuals enter the partition by recruitment and are removed by natural mortality and fishing mortality. The model's annual cycle is based on the fishing year and is divided into the three time steps described above (Table 4). The choice of three time steps was based on current understanding of scampi biology and sex ratio in catches. Previous models for SCI 1 and SCI 2 have included spatial structure (Tuck & Dunn 2012), but, following the characterisation and preliminary model investigation, the SFWG recommended a single area model for both assessments (Tuck 2014).

The model uses capped logistic length-based selectivity curves for commercial fishing and research trawl surveys, that were assumed to be constant over time, but were allowed to vary with sex and time step (where necessary). Although the sex ratio data suggest that the relative catchability of the sexes varies through the year (hence the model time structure adopted), there is no reason to suggest, that assuming equal availability, selectivity at size would be different between the sexes. Therefore the

two-sex selectivity implementation developed within CASAL for the SCI 1 and SCI 2 assessments (Tuck & Dunn 2012) was applied. This allows the L_{50} (size at which 50% of individuals are retained) and a_{95} (size at which 95% of individuals are retained) selectivity parameters to be estimated as single values shared by both sexes in a particular time step, but allows for different availability between the sexes through estimation of different a_{max} (maximum level of selectivity) values for each sex. Previous assessments have examined using double normal capped selectivity curves for the commercial fishery, to allow domed selectivity (no link between the parameters for each sex) (Tuck 2014), but this had little effect on assessment outputs and has not been repeated here. Photographic survey abundance indices are not sex specific and a standard logistic length-based selectivity curve has been applied.

3.2. Biological inputs

3.2.1. Growth

Scampi growth has been estimated from wild-tagged scampi in SCI 1 (Cryer & Stotter 1997; Cryer & Stotter 1999) and aquarium-reared scampi from SCI 2 (Cryer & Oliver 2001) (Figure 32). The aquarium data have been treated as tag data, with an initial and subsequent length measurement defining a growth increment, over a known time period.

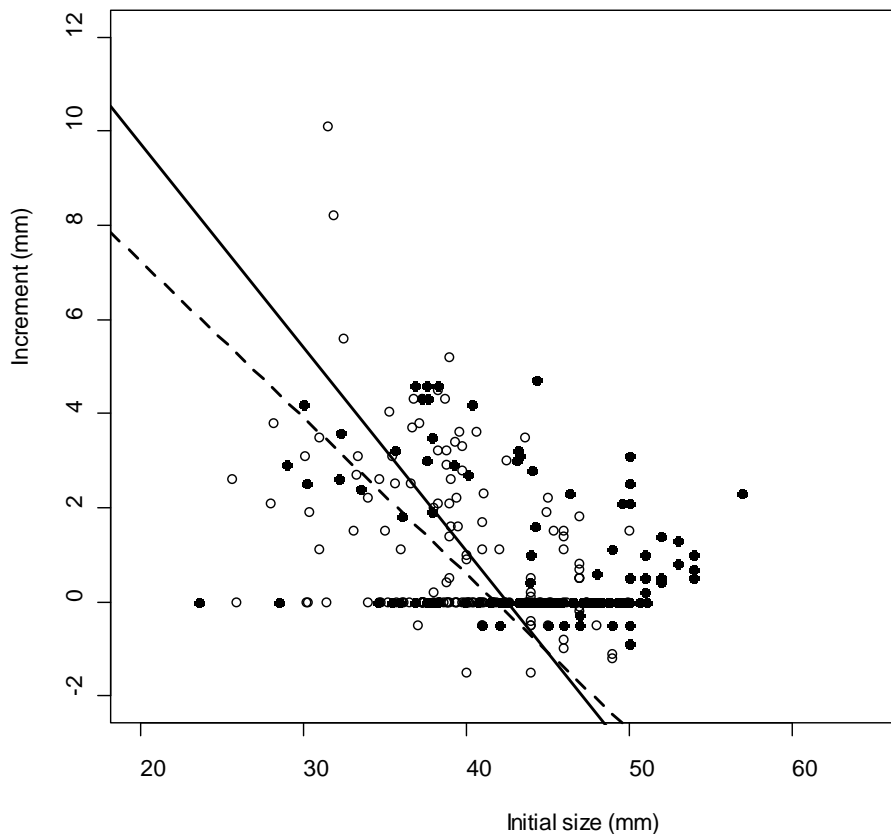


Figure 32: Growth increment data from scampi tagging in SCI 1 and SCI 2 and aquarium studies. Solid and hollow symbols represent males and females, respectively. Solid (males) and dotted (females) lines represent best fits to data from combined growth studies.

In the initial developments of the scampi assessment model (Cryer et al. 2005), the combined data set (SCI 1 field studies and SCI 2 aquarium studies) was analysed externally and the estimated growth parameters for each sex were fixed within the model. However, given the strong influence that growth rate has on length-based models, and the scatter around the externally fitted relationships seen in Figure 32, growth rates are now fitted within the model (Tuck & Dunn 2012). The growth increment

data from SCI 1 and SCI 2 have been combined into a single dataset, but are fitted independently in the two single stock assessment models.

On the basis of the time steps within the model structure, the tag data for which we have recaptures can be split into five release events (labelled year_step; 1996-2, 1996-3, 1997-1, 2012-2, 2015-2). Recaptures of tagged scampi from these releases are tabulated by recapture time step in Table 11. Within the analysis, animals from both wild release and aquarium studies have been combined, although the numbers of animals are provided separately in Table 11.

Table 11: Numbers of scampi recaptured by release and recapture time step (SCI 1 and 2).

Release	Recapture			
	1996-3	1997-1	1997-2	1997-3
1996-2		20	7	13
1996-3*	12	15 (28)	2 (21)	42 (30)
1997-1			15	80
	2012-2	2012-3		
2012-2		2		
	2015-2			
2015-2	10			

* Recapture data from 1996-3 release include 79 animals in aquaria and 71 from wild releases. For recaptures, numbers in parenthesis represent aquarium animals.

For the various combinations of release and recapture, the length increment is plotted by sex against initial length in Figure 33. The model structure has a growth period assigned to the start of time step 1 for both sexes. Therefore no growth would be expected for those animals not at liberty at the start of time step 1. The data available, particularly for males (Figure 19), suggest some evidence of two periods of moulting. The sensitivity of the model to allow two growth periods per year were examined in a previous assessment (Tuck & Dunn 2012).

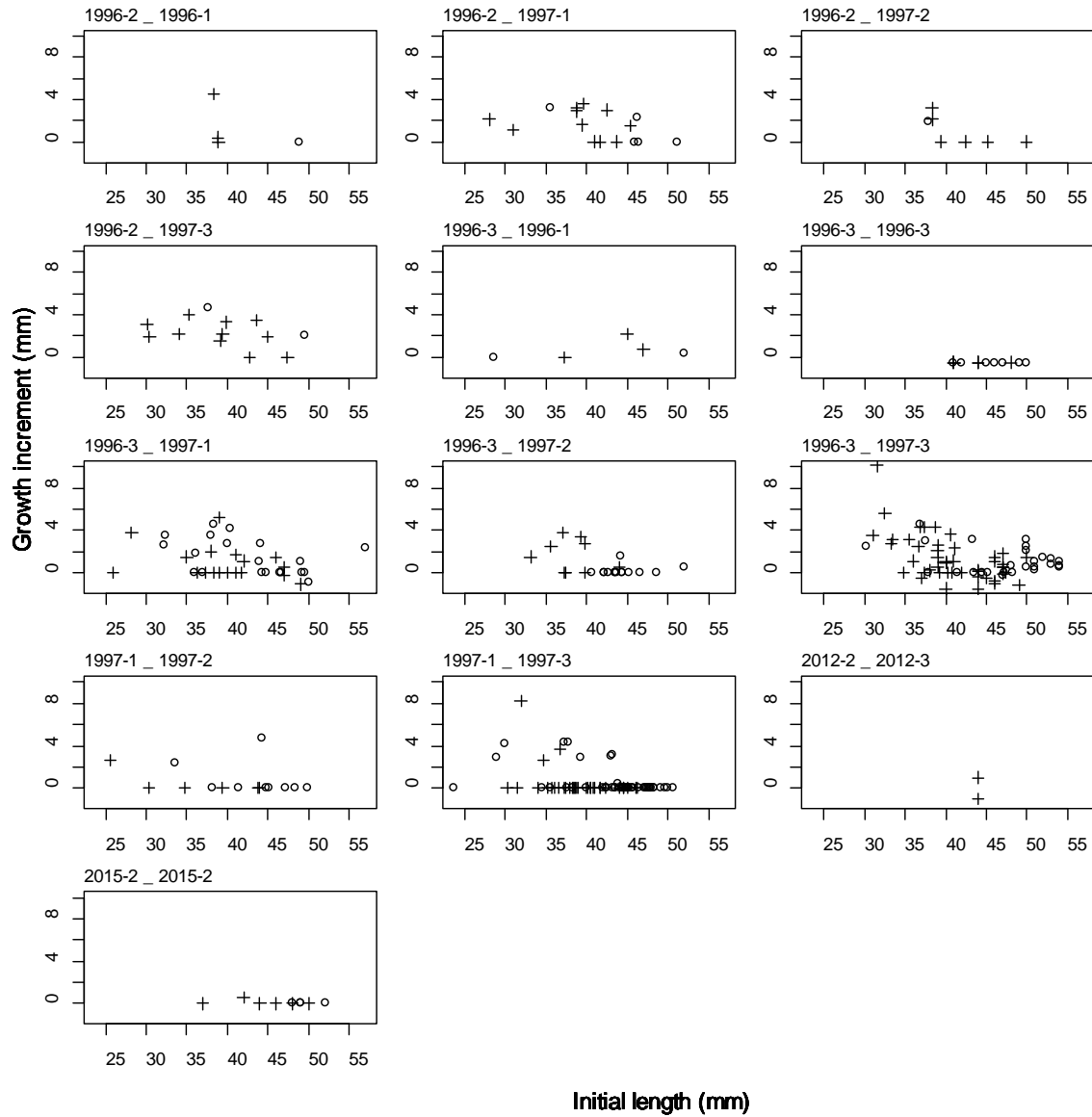


Figure 33: Plot of initial length against growth increment by combination of release and recapture time steps. Males are represented by hollow symbols; females are represented by crosses.

3.2.2. Maturity

The proportion of females mature at each 1 mm size class has been recorded during all research surveys since 1993. These data have been combined for females from SCI 1 and 2, assuming internal gonad stages 2–5 to be mature and stage 1 to be immature. No data are available for the maturity of male scampi, so their maturity ogive was assumed identical to that of females, although studies on *N. norvegicus* have suggested that male maturity may occur at a larger size (though possibly the same age) than females (Tuck et al. 2000). Maturity is not considered to be a part of the model partition, but proportions mature were fitted within the model based on a logistic ogive with a binomial likelihood (Bull et al. 2012).

Analysis of the proportion ovigerous data, modelled as a function of length, was conducted within a GLM framework, with a quasibinomial distribution of errors and a logit link (McCullagh & Nelder 1989),

$$\text{logit}(m) = a + bL$$

where a and b are constants, and L is the orbital carapace length, which equates to the logistic model. The model was weighted by the number measured at each length. After obtaining estimates for the parameters a and b , the length at which 50% are mature (L_{50}) was calculated from:

$$L_{50} = -\frac{a}{b}$$

with selection range (SR, a_{25} to a_{75}) calculated from:

$$SR = \frac{(2 \cdot \ln(3))}{b}$$

Female maturity data for SCI 1 and SCI 2 combined are summarised in Figure 34 (from Tuck & Dunn 2006). The L_{50} estimate for the pooled SCI 1 and SCI 2 data was 29.7 mm, with a selection range of 5.3 mm. The maturity curve fitted to these data is plotted in Figure 35.

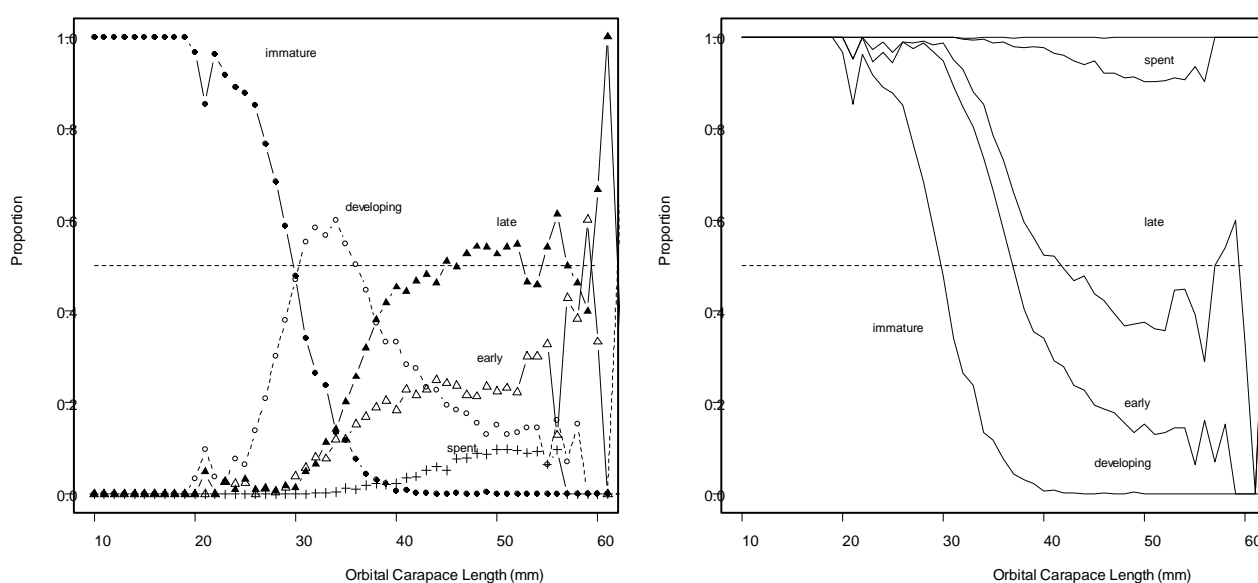


Figure 34: Proportions of female scampi with various developmental stages of internal ovaries. Left panel shows proportions of each stage separately; right panel shows combined proportions. Data are aggregated from research voyages in SCI 1 and SCI 2.

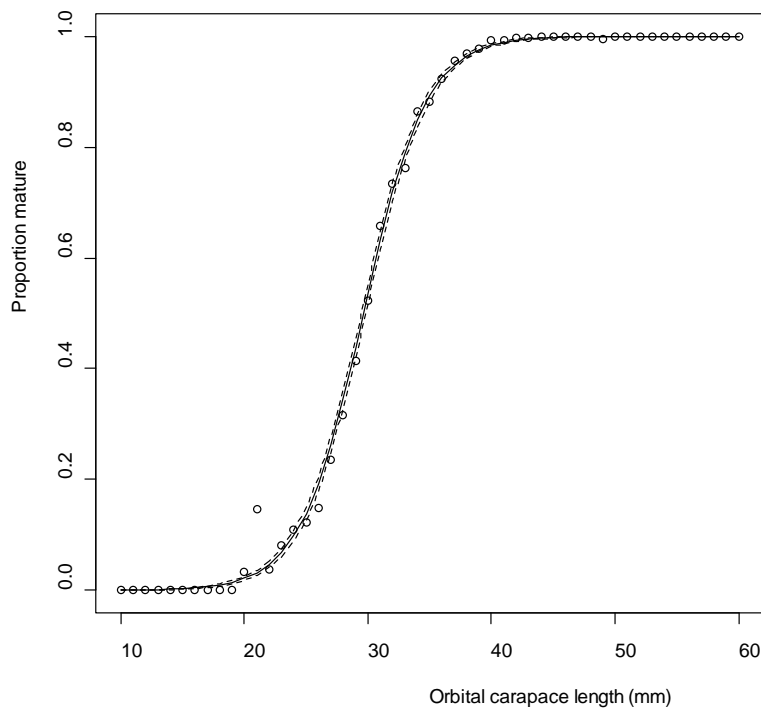


Figure 35: Proportions of female scampi with mature gonad stages at length, from all research trawling in SCI 1 and SCI 2. Solid line represents logistic curve fitted to the data ($L_{50} = 29.7$ mm and selection range = 5.3 mm). Dashed lines represent ± 1 s.e.

3.2.3. Natural mortality

The instantaneous rate of natural mortality (M) has not been estimated directly for any scampi species, but estimates have been made based on the estimate of the K parameter from a von Bertalanffy growth curve (Cryer & Stotter 1999) using a correlative method (Pauly 1980; Charnov et al. 1993). Morizur (1982) used length distributions from ‘quasi-unexploited’ *Nephrops* stocks to obtain estimates for annual M of 0.2–0.3. The values most commonly assumed for assessment of *Nephrops* stocks in the Atlantic are 0.3 for males and immature females and 0.2 for mature females (assumed less vulnerable to predation during the ovigerous period) (Bell et al. 2006). For New Zealand scampi, M has previously been fixed at values between 0.2 and 0.3 (Tuck & Dunn 2012). Within the current assessment, a preliminary attempt was made to estimate M within the model, but this did not provide realistic values. Final model sensitivity analyses were examined with M fixed at 0.2 and 0.25, but an M of 0.3 was also assumed for some initial models.

3.3. Catch data

Data for the model were collated over the spatial and temporal strata as defined in the model structure. Catches in these modelled areas represent over 98% of scampi catches from both SCI 1 and SCI 2. Details of catches by time step, and breakdown by survey strata, are provided for SCI 1 in Table 12 and SCI 2 in Table 13.

Table 12: Catch (in tonnes) and breakdown by survey strata within each time step for each fishing year for SCI 1.

	Step 1					Step 2					Step 3				
	Catch (t)	202	203	3/402	3/403	Catch (t)	202	203	3/402	3/403	Catch (t)	202	203	3/402	3/403
1987	2	1%	0%	70%	29%	1	0%	1%	60%	40%	2	1%	0%	90%	10%
1988	7	1%	0%	70%	29%	3	0%	1%	60%	40%	6	1%	0%	90%	10%
1989	28	1%	0%	70%	29%	10	0%	1%	60%	40%	22	1%	0%	90%	10%
1990	49	1%	0%	71%	28%	15	0%	1%	72%	27%	40	1%	0%	89%	10%
1991	43	0%	0%	75%	25%	34	0%	2%	85%	13%	103	36%	29%	21%	14%
1992	68	12%	4%	68%	15%	13	2%	2%	85%	11%	51	32%	11%	45%	12%
1993	44	42%	5%	48%	5%	22	4%	0%	82%	14%	48	13%	20%	42%	24%
1994	75	32%	4%	53%	11%	1	61%	0%	35%	3%	39	12%	35%	28%	24%
1995	54	56%	3%	29%	11%	26	60%	3%	31%	6%	34	51%	15%	18%	17%
1996	65	39%	17%	21%	22%	23	1%	59%	17%	23%	29	6%	4%	43%	47%
1997	59	5%	28%	16%	51%	38	30%	36%	8%	26%	20	12%	30%	8%	50%
1998	89	22%	23%	36%	19%	9	0%	6%	41%	53%	9	2%	2%	76%	20%
1999	62	17%	12%	57%	14%	39	9%	13%	52%	26%	9	0%	0%	52%	48%
2000	22	17%	36%	17%	30%	24	8%	26%	10%	55%	78	30%	19%	43%	8%
2001	81	32%	12%	47%	10%	34	29%	7%	59%	5%	5	41%	16%	42%	1%
2002	124	32%	17%	45%	6%	0					0				
2003	121	29%	13%	49%	10%	0					0				
2004	120	30%	15%	48%	7%	0					0				
2005	46	41%	22%	27%	9%	34	31%	12%	35%	21%	35	39%	20%	37%	4%
2006	41	25%	6%	53%	16%	25	33%	8%	58%	1%	43	36%	44%	12%	8%
2007	44	33%	10%	44%	13%	34	15%	9%	62%	14%	32	45%	25%	25%	5%
2008	49	29%	3%	49%	19%	34	15%	8%	58%	19%	20	24%	45%	19%	11%
2009	51	21%	11%	47%	21%	18	24%	15%	49%	12%	17	9%	18%	52%	21%
2010	65	26%	21%	47%	6%	15	3%	4%	67%	25%	31	2%	2%	77%	19%
2011	47	5%	6%	87%	3%	23	32%	16%	51%	2%	44	1%	1%	64%	34%
2012	58	14%	9%	63%	14%	19	6%	4%	67%	23%	37	9%	14%	41%	35%
2013	59	25%	13%	48%	14%	25	6%	6%	55%	33%	42	10%	17%	44%	30%
2014	50	27%	17%	51%	6%	32	12%	13%	48%	26%	24	2%	4%	73%	21%
2015	45	8%	7%	64%	21%	31	16%	22%	41%	21%	41	4%	8%	49%	39%
2016	50	12%	13%	47%	28%	31	7%	10%	45%	38%	37	4%	16%	48%	33%
2017	64	10%	11%	52%	27%	16	5%	3%	64%	27%	48	4%	30%	18%	47%
2018	64	21%	21%	40%	18%	36	3%	12%	41%	44%	19	4%	11%	67%	19%

Table 13: Catch (in tonnes) and breakdown by survey strata for each time step for each fishing year for SCI 2.

	Step 1					Step 2					Step 3				
	Catch (t)	702	703	802	803	Catch (t)	702	703	802	803	Catch (t)	702	703	802	803
1987	0					0					0				
1988	1	99%	0%	1%	0%	1	39%	1%	60%	0%	3	70%	1%	29%	0%
1989	2	99%	0%	1%	0%	5	39%	1%	60%	0%	10	70%	1%	29%	0%
1990	17	99%	0%	1%	0%	39	38%	0%	61%	0%	83	70%	1%	30%	0%
1991	142	33%	0%	67%	0%	59	27%	0%	73%	0%	94	44%	9%	46%	1%
1992	73	58%	1%	41%	0%	22	18%	0%	82%	0%	126	45%	3%	52%	1%
1993	77	70%	2%	28%	0%	63	40%	1%	59%	0%	70	41%	5%	53%	1%
1994	31	67%	3%	30%	0%	55	97%	1%	2%	0%	157	59%	1%	39%	1%
1995	71	34%	8%	57%	0%	44	35%	1%	61%	2%	111	25%	2%	67%	6%
1996	107	67%	14%	18%	1%	27	80%	0%	19%	0%	96	56%	2%	38%	4%
1997	61	70%	6%	24%	0%	71	57%	11%	31%	0%	81	73%	18%	8%	1%
1998	157	53%	3%	43%	0%	45	33%	3%	64%	0%	22	15%	1%	80%	3%
1999	130	56%	6%	38%	1%	70	43%	3%	53%	0%	33	64%	15%	21%	0%
2000	103	42%	8%	49%	1%	15	51%	0%	49%	0%	75	73%	6%	20%	0%
2001	29	62%	0%	38%	0%	33	62%	0%	37%	0%	84	63%	3%	34%	0%
2002	69	64%	2%	31%	2%	102	49%	1%	50%	0%	76	59%	14%	26%	1%
2003	82	46%	3%	51%	0%	39	32%	9%	60%	0%	13	75%	24%	1%	0%
2004	42	72%	8%	19%	0%	22	65%	4%	30%	0%	0	100%	0%	0%	0%
2005	42	65%	9%	25%	0%	11	59%	3%	38%	0%	18	44%	16%	39%	2%
2006	37	48%	1%	51%	0%	6	96%	1%	3%	0%	34	69%	13%	18%	0%
2007	36	36%	4%	61%	0%	26	61%	1%	38%	0%	18	66%	11%	23%	0%
2008	55	61%	2%	37%	0%	5	84%	2%	14%	0%	0	74%	0%	26%	0%
2009	32	55%	1%	45%	0%	11	35%	0%	65%	0%	10	93%	0%	7%	0%
2010	86	41%	0%	58%	1%	10	50%	1%	49%	0%	29	62%	3%	36%	0%
2011	82	76%	3%	21%	0%	29	77%	1%	23%	0%	17	45%	1%	54%	0%
2012	61	48%	1%	51%	1%	31	50%	0%	49%	2%	7	3%	0%	97%	0%
2013	75	40%	2%	58%	0%	21	12%	0%	88%	0%	0				
2014	102	93%	1%	6%	0%	21	100%	0%	0%	0%	2	78%	0%	22%	0%
2015	70	63%	0%	35%	2%	46	99%	1%	1%	0%	27	53%	27%	20%	0%
2016	102	52%	3%	44%	0%	21	70%	1%	29%	0%	11	74%	0%	26%	0%
2017	84	51%	1%	47%	1%	41	74%	5%	21%	0%	24	69%	9%	21%	0%
2018	109	56%	6%	38%	1%	32	86%	2%	12%	0%	12	100%	0%	0%	0%

3.4. CPUE indices

The annual CPUE indices estimated within the standardisation (SCI 1, Figure 26; SCI 2, Figure 29) were fitted within the model as abundance indices. There has been considerable discussion on whether CPUE is proportional to abundance for scampi (Tuck 2009), with rapid increases in both CPUE and trawl survey catch rates for a number of stocks in the early to mid 1990s (and changes in sex ratio in trawl survey catches) initially being considered related to changes in catchability. Later analysis (Tuck & Dunn 2009) suggested that the observed changes in sex ratios were related to slight changes in the survey timing in relation to the moult cycle. Similar patterns in CPUE are observed over the same period for rock lobster (Starr 2009; Starr et al. 2009) and scampi in SCI 3 (Tuck 2013), which may suggest broad-scale environmental drivers influencing crustacean recruitment. The CPUE patterns for SCI 1 are mirrored by trawl survey catch rates, suggesting that they do not reflect increases in catchability from fisher learning. Although not considered appropriate for use as an index in the existing assessment model, the middle depths (*R.V. Tangaroa*) trawl survey scampi abundance index shows a very similar temporal pattern to the standardised CPUE indices for SCI 3 (Tuck 2013). The similarity between this trawl survey index and commercial CPUE has also been identified in a recent characterisation of SCI 4A (Tuck 2020), also supporting the suggestion that the increases in scampi catch rates observed during the 1990s reflect scampi abundance rather than changes in catchability.

CPUE standardisation procedures tend to estimate unrealistically low CVs and so we have adopted the approach proposed by Francis (2011), whereby appropriate CVs are estimated by fitting a smoother to the index. The smoothers are presented in Appendices 1 and 2 with the relevant standardisation. On the basis of discussion at the SFWG, initial values for CPUE index CVs were taken as 0.15 for both stocks, and sensitivity analyses to these assumptions were investigated.

3.5. Research survey indices

Trawl surveys were first conducted from the *R.V. Kaharoa* in SCI 1 and SCI 2 in 1993 and have been conducted intermittently (in conjunction with photographic surveys in more recent years). Surveys have been conducted between January and April, but timing within this period has varied between years.

3.5.1. Photographic surveys

Photographic surveys of SCI 1 and SCI 2 (Cryer et al. 2003; Tuck et al. 2006; Tuck et al. 2009; Tuck et al. 2013; Tuck et al. 2016; Tuck et al. 2019) have been used to estimate the absolute abundance (in numbers) of burrows thought to belong to scampi in 1998, 2000–2003, 2008, 2012, 2015, and 2018 (for SCI 1) and 2003–2006, 2012, 2015, and 2018 (for SCI 2). These surveys provide two alternative indices of scampi abundance: one based on major burrow openings and one based on visible scampi. Both indices are subject to uncertainty, either from burrow detection and occupancy rates (for burrow based indices) or emergence patterns (for visible scampi based indices). The burrow index has been used within assessments for SCI 1 and SCI 2 (Tuck & Dunn 2012).

Survey estimates are provided for SCI 1 in Table 14 and SCI 2 in Table 15. Surveys of SCI 1 only covered part of the main fishery area until 2012, and the data are fitted within the model as two separate series, with separate catchability (q) values, with the q for the total area informed by a prior, and the ratio between the qs for the total and part surveys constrained by the @ratio_qs_penalty in CASAL. Details of the estimation of the priors and the ratio are provided in Section 3.7. Although the photographic surveys have occurred in time steps 1 and 2, the survey abundance (based on burrow counts) should be relatively insensitive to moult cycle and reproductive behaviour driving the changes in sex ratio in catches, and therefore the indices are fitted as occurring at the end of time step 1.

Table 14: Time series of photo survey scampi stock estimates (millions) and CV for SCI 1. Estimates are provided for survey combined strata 302, 303, 402, and 403 (areas surveyed in six years during 1998–2008) and the larger area surveyed in 2012, 2015, and 2018 (including survey strata 202 and 203). Time step relates to the assessment model, with surveys in December–January allocated to step 1, and those in February–April allocated to step 2.

	302,303,402,403		Total area		Time step
	Abundance	CV	Abundance	CV	
1998	154.6	0.15			1
2000	96.8	0.13			2
2001	135.9	0.12			1
2002	128.7	0.08			2
2003	101.0	0.12			2
2008	109.8	0.08			2
2012	104.2	0.04	155.9	0.06	2
2015	102.2	0.04	153.0	0.05	2
2018	154.7	0.04	217.0	0.05	2

Table 15: Time series of photo survey scampi stock estimates (millions) and CV for SCI 2. Time step relates to the assessment model, with surveys in December–January allocated to step 1, and those in February–April allocated to step 2.

	Abundance	CV	Time step
2003	93.1	0.16	2
2004	150.2	0.14	1
2005	108.5	0.16	2
2006	111.3	0.11	2
2012	118.7	0.09	2
2015	197.8	0.06	2
2018	167.2	0.07	2

3.5.2. Trawl surveys

Stratified random trawl surveys of scampi in SCI 1 and SCI 2, in 200–600 m depths, were conducted in 1993, 1994, and 1995. Formal trawl surveys to estimate relative abundance were discontinued following this, because it was inferred from the results that catchability had varied among surveys, although it was later concluded that the changes were related to slight differences in survey timing (Tuck & Dunn 2009). Despite these concerns, research trawling continued in both areas for a variety of other purposes (in support of a tagging programme to estimate growth in 1995 and 1996, to assess selectivity of research and commercial mesh sizes in 1996, and in support of photographic surveys since 1998). Identical gear has been used for all of the trawl surveys. Survey coverage in SCI 1 has changed over time, with the early surveys covering the whole modelled area, but surveys in 1998, and from 2001 to 2008 only covered survey strata 302, 303, 402, and 403. Survey estimates (by area) are provided for SCI 1 in Table 16 and SCI 2 in Table 17. As with the photo survey for SCI 1, the trawl survey data were fitted as two indices with separate q_s , with the ratio between the q_s for the total and part surveys constrained by the @ratio_qs_penalty (Section 3.7). Trawl surveys in both fisheries have occurred in time steps 1 and 2. In SCI 1, surveys in time step 2 have generally been early in the time step and, to reduce complexity, because of the two levels of survey coverage, all trawl surveys were assumed to occur at the end of time step 1. In SCI 2, surveys have occurred later in time step 2 and have been fitted as separate indices in each time step.

Table 16: Time series of trawl survey scampi stock estimates (tonnes) by survey strata for SCI 1. Estimates are provided for survey combined strata 302, 303, 402, and 403 (areas surveyed 1998 and between 2001 and 2008) and the larger area surveyed in 1993–1995, 2000, 2012, 2015 and 2018 (including survey strata 202 and 203). Time step relates to the assessment model, with surveys in December–January occurring in step 1 and those in February–April occurring in step 2, although in the model both are allocated to the end of time step 1. N represents number of research tows in each survey.

	<u>302,303,402,403</u>			<u>Total area</u>			Time step
	N	Biomass	CV	N	Biomass	CV	
1993				36	271.6	0.12	1
1994				33	364.0	0.17	1
1995				37	510.4	0.15	1
1998	18	174.0	0.17				1
2000				15	225.1	0.39	2
2001	12	179.5	0.27				1
2002	13	130.6	0.24				2
2008	10	211.9	0.13				2
2012				19	186.6	0.21	2
2015				18	170.6	0.15	2
2018				18	188.6	0.21	2

Table 17: Time series of trawl survey scampi stock estimates (tonnes) by survey strata for SCI 2. Time step relates to the assessment model, with surveys in December–January allocated to step 1 and those in February–April allocated to step 2. N represents number of research tows in each survey.

	N	Biomass	CV	Time step
1993	26	238.2	0.12	1
1994	27	170.0	0.16	1
1995	29	216.2	0.18	1
2003	7	28.0	0.33	2
2004	8	46.9	0.20	1
2005	8	50.8	0.35	2
2006	8	22.9	0.19	2
2012	14	164.2	0.28	2
2015	12	224.5	0.19	2
2018	20	183.3	0.29	2

3.6. Length distributions

3.6.1. Commercial catch at length data

Ministry for Primary Industries observers have collected scampi length frequency data from scampi targeted fishing on commercial vessels in SCI 1 and SCI 2 since 1990–91. The numbers of tows for which length data are available are presented by fishing year and month in Table 18 (SCI 1) and Table 19 (SCI 2).

For both fisheries, levels of sampling, and the pattern of sampling relative to the pattern of catches, vary between years, and the proportion of landings represented by the observer sampling varies considerably (Table 20). There are a number of years when no observer length frequencies were collected. Where size compositions vary markedly between areas, the low proportion of landings being represented by observer sampling in any year may lead to biased estimates of catch composition. For both fisheries, mean orbital carapace length (OCL) and proportion males from observer sampling was modelled for each year individually by survey strata and time step by multivariate tree regression. Very few significant splits were detected, and there was no consistent pattern suggesting length frequencies should be spatially stratified.

Proportional length distributions (and associated CVs) were calculated using CALA (Francis & Bian 2011), using the approaches previously implemented in NIWA’s *Catch-at-Age* software (Bull & Dunn 2002). Plots of the proportional length distribution are shown by year, for SCI 1 by time step in Figure 36 to Figure 38 and for SCI 2 by time step in Figure 39 to Figure 41.

Table 18: Number of commercial tows for which length distributions are available for SCI 1, by fishing year, time step, and survey strata.

	Step 1				Step 2				Step 3			
	202	203	3/402	3/403	202	203	3/402	3/403	202	203	3/402	3/403
1991									9	59	27	6
1992		1	14	1					16			
1993	2		1									
1994											1	
1995									3			
1996	1		4						1			
1997						7	2	6				
1998												
1999					1	3	9	1				
2000									4	16	9	2
2001												
2002		2	1									
2003												
2004	2											
2005									6	7	2	1
2006	3	1	4	5					10	14		1
2007	4	2	13	1					12	1	4	2
2008	1	4	9	10			24	8				
2009	2	5	12	8								
2010	9		1	3	2		9	4	1	5	11	12
2011	1	3	19	3							37	8
2012			3	2			16	11				
2013												
2014	14	10	7	4								
2015												
2016					1	3	40	24				
2017												
2018	5	14	13	23								

Table 19: Number of commercial tows for which length distributions are available for SCI 2, by fishing year, time step, and survey strata.

	Step 1				Step 2				Step 3			
	702	703	802	803	702	703	802	803	702	703	802	803
1991									35	15	12	
1992	9		5									
1993	1		2						8	1	18	
1994						1			32	2	25	
1995					4	2	17	1	7	24	6	
1996	13								4	11		
1997	27	1	6		1				5			
1998	3	1			1	1						
1999	54	6	23		21	4						
2000	24	22	29						1			
2001	37	1	16						7	1		
2002	25		13									
2003	11	2										
2004												
2005			6									
2006												
2007					3	1			1			
2008	11	1	8		7	3			2	1		
2009					6	7						
2010									10	3	10	
2011	9	2	31	1					6	6		
2012	45		64	1		2						
2013			11									
2014	1											
2015												
2016												
2017												
2018												

Table 20: Proportion of landings represented by observer catch sampling (proportion of catch by survey strata and time step in each fishing year represented by at least 1 observer sample). Blank cells represent periods with no fishing activity.

	SCI 1			SCI 2		
	Step 1	Step 2	Step 3	Step 1	Step 2	Step 3
1991	0%	0%	64%	0%	0%	99%
1992	88%	0%	11%	99%	0%	0%
1993	90%	0%	0%	98%	0%	99%
1994	0%	0%	24%	0%	1%	99%
1995	0%	0%	15%	0%	100%	98%
1996	60%	0%	4%	67%	0%	94%
1997	0%	34%	0%	100%	57%	73%
1998	0%	0%	0%	57%	36%	0%
1999	0%	91%	0%	99%	46%	0%
2000	0%	0%	70%	99%	0%	73%
2001	0%	0%	0%	100%	0%	66%
2002	62%			96%	0%	0%
2003	0%			49%	0%	0%
2004	30%			0%	0%	0%
2005	0%	0%	61%	25%	0%	0%
2006	100%	0%	56%	0%	0%	0%
2007	100%	0%	55%	0%	99%	66%
2008	100%	19%	0%	100%	98%	100%
2009	100%	0%	0%	0%	100%	0%
2010	79%	30%	98%	0%	0%	100%
2011	100%	0%	34%	100%	0%	99%
2012	77%	23%	0%	99%	49%	0%
2013	0%	0%	0%	58%	0%	
2014	100%	0%	0%	93%	0%	0%
2015	0%	0%	0%	0%	0%	0%
2016	0%	93%	0%	0%	0%	0%
2017	0%	0%	0%	0%	0%	0%
2018	100%	0%	0%	0%	0%	0%

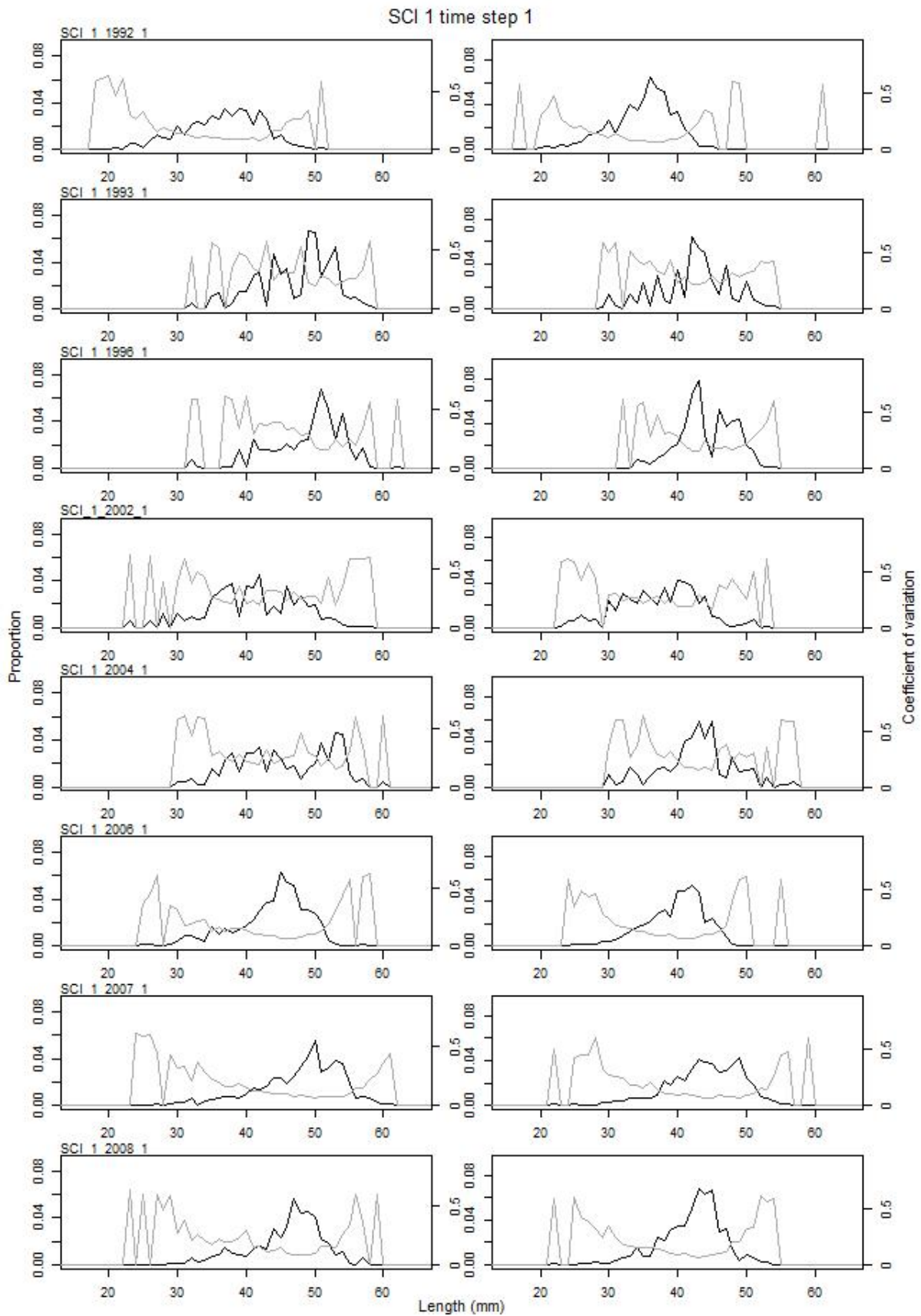


Figure 36: Proportional length frequency distributions (black line) and CVs (grey line) for commercial catches by model year and time step 1 for SCI 1. Males are plotted on the left, females on the right.

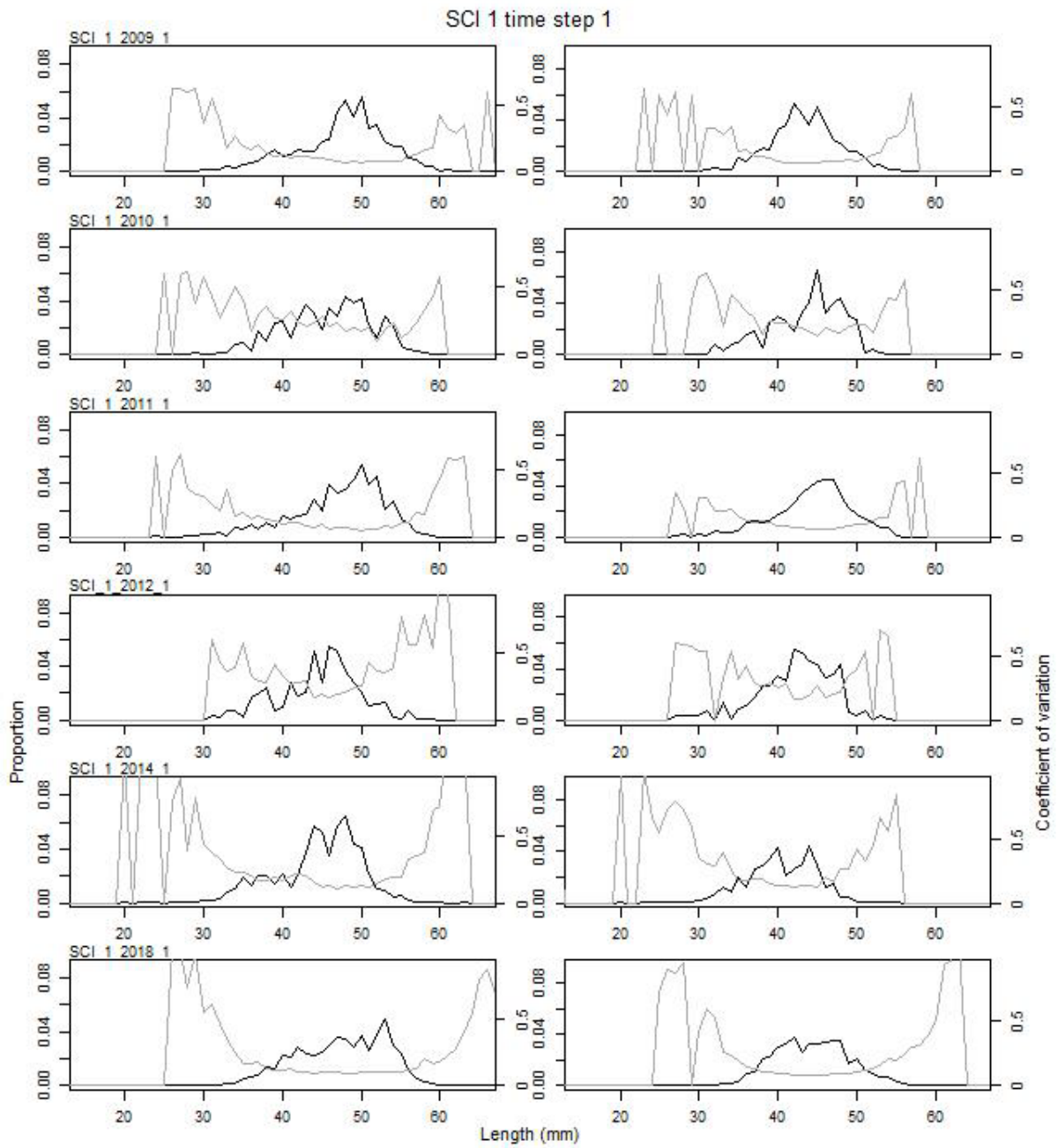


Figure 36 (continued): Proportional length frequency distributions (black line) and CVs (grey line) for commercial catches by model year and time step 1 for SCI 1. Males are plotted on the left, females on the right.

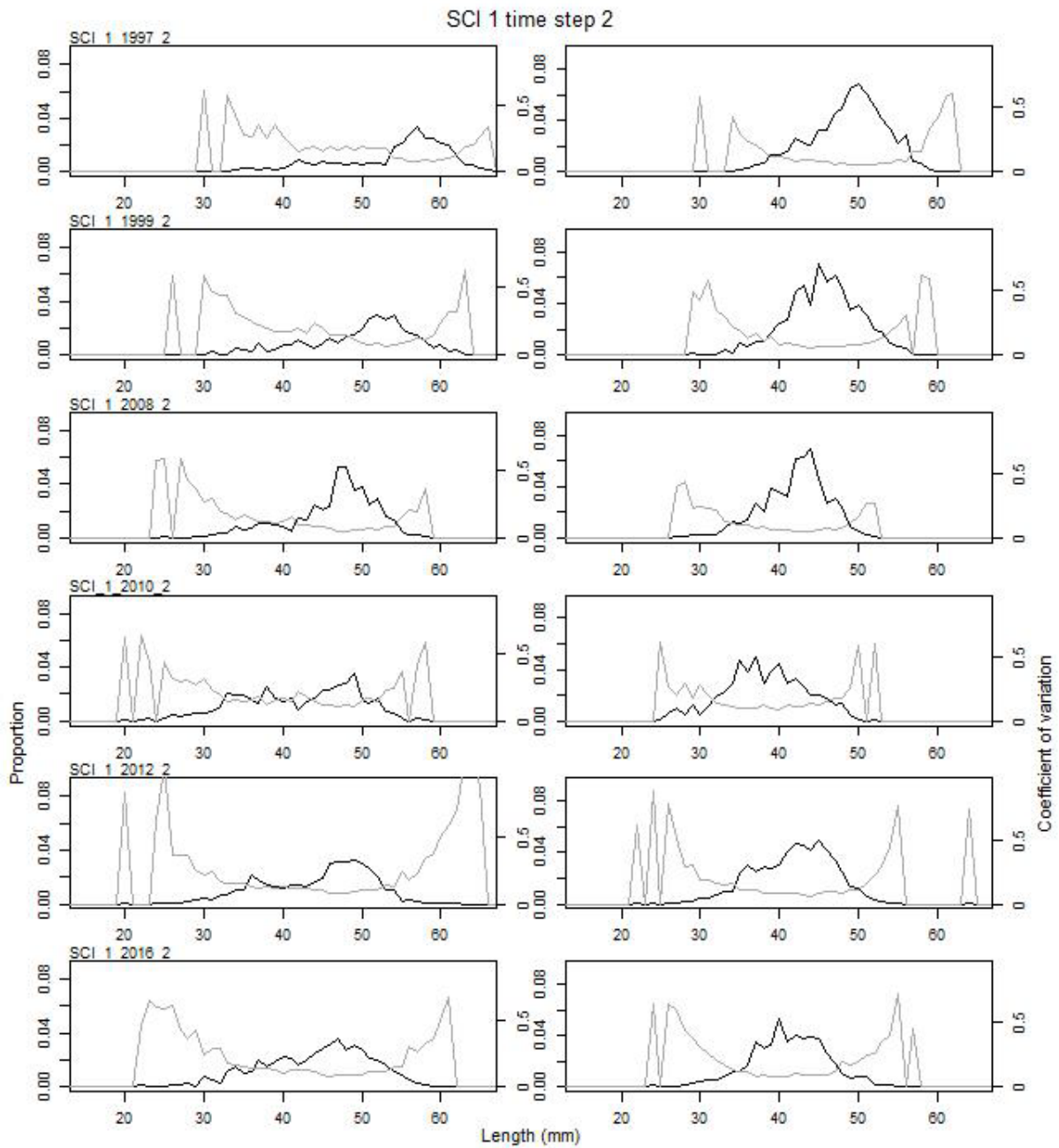


Figure 37: Proportional length frequency distributions (black line) and CVs (grey line) for commercial catches by model year and time step 2 for SCI 1. Males are plotted on the left, females on the right.

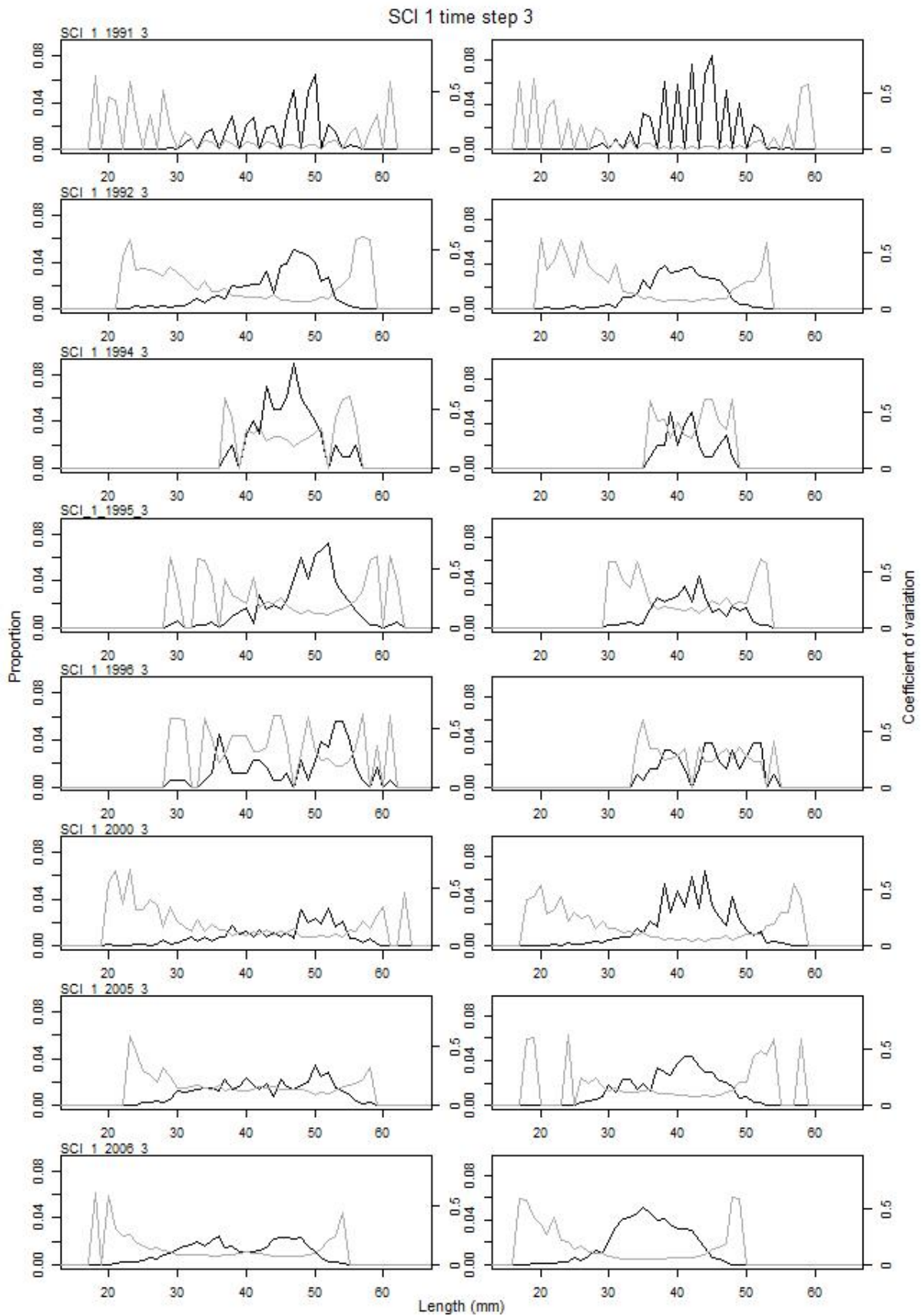


Figure 38: Proportional length frequency distributions (black line) and CVs (grey line) for commercial catches by model year and time step 3 for SCI 1. Males are plotted on the left, females on the right.

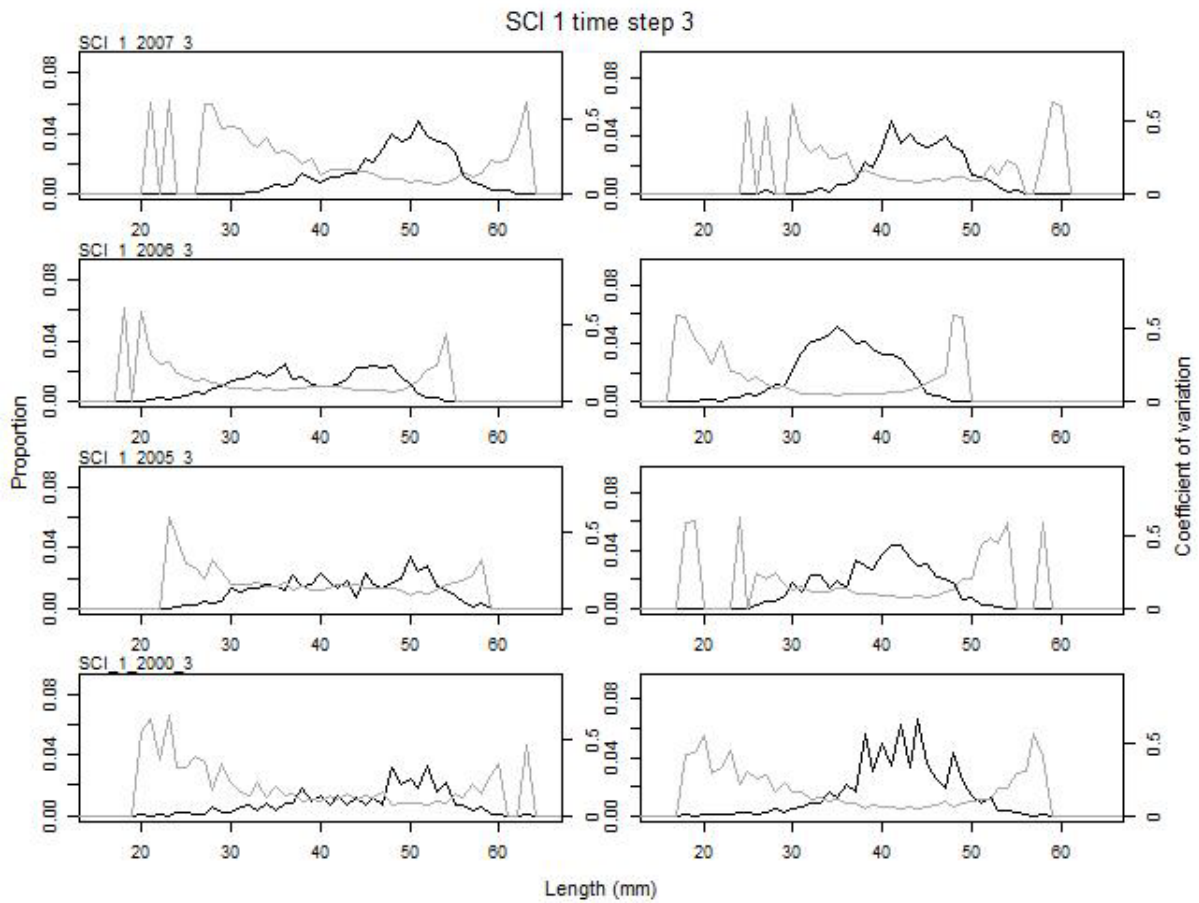


Figure 38 (continued): Proportional length frequency distributions (black line) and CVs (grey line) for commercial catches by model year and time step 3 for SCI 1. Males are plotted on the left, females on the right.

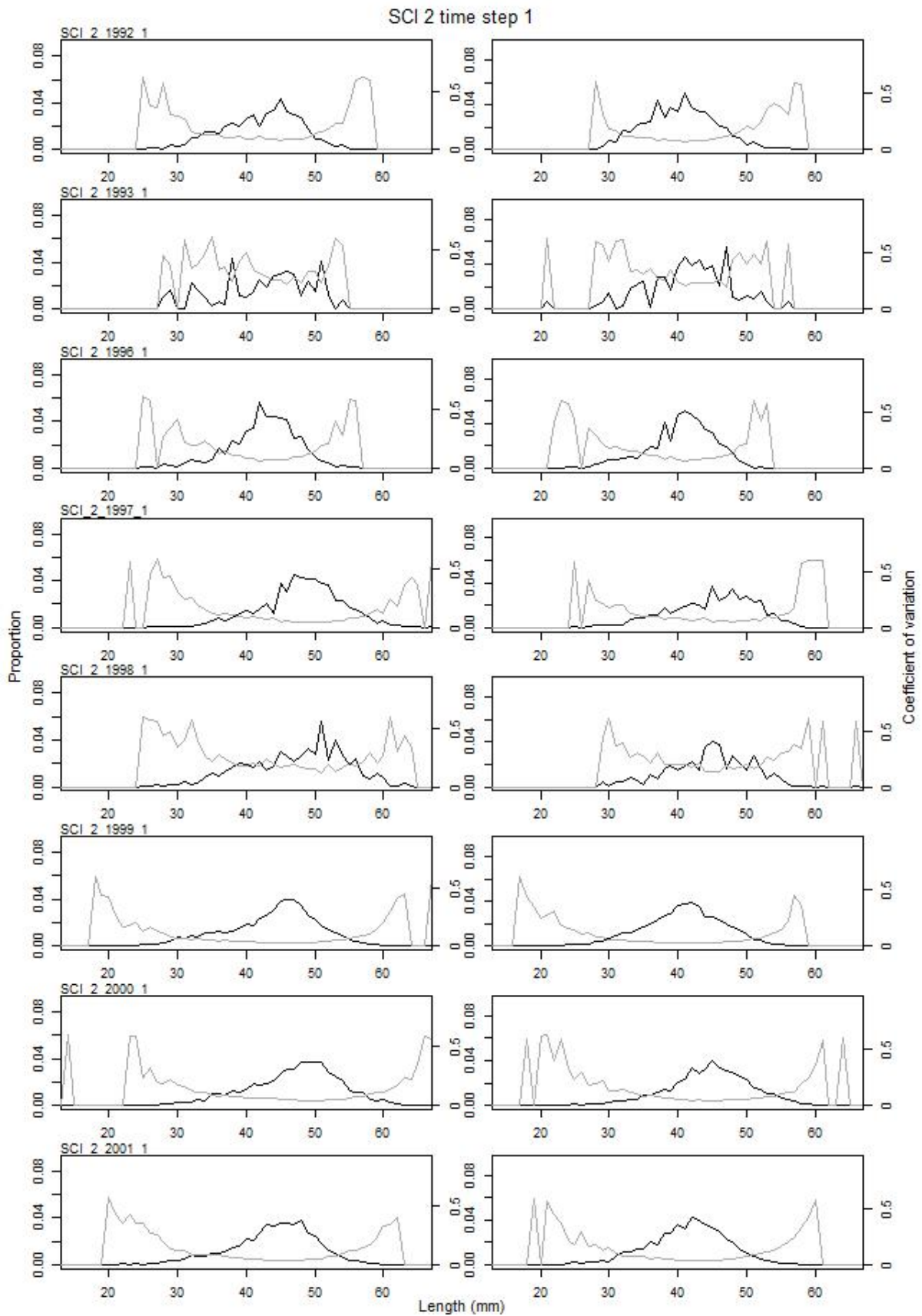


Figure 39: Proportional length frequency distributions (black line) and CVs (grey line) for commercial catches by model year and time step 1 for SCI 2. Males are plotted on the left, females on the right.

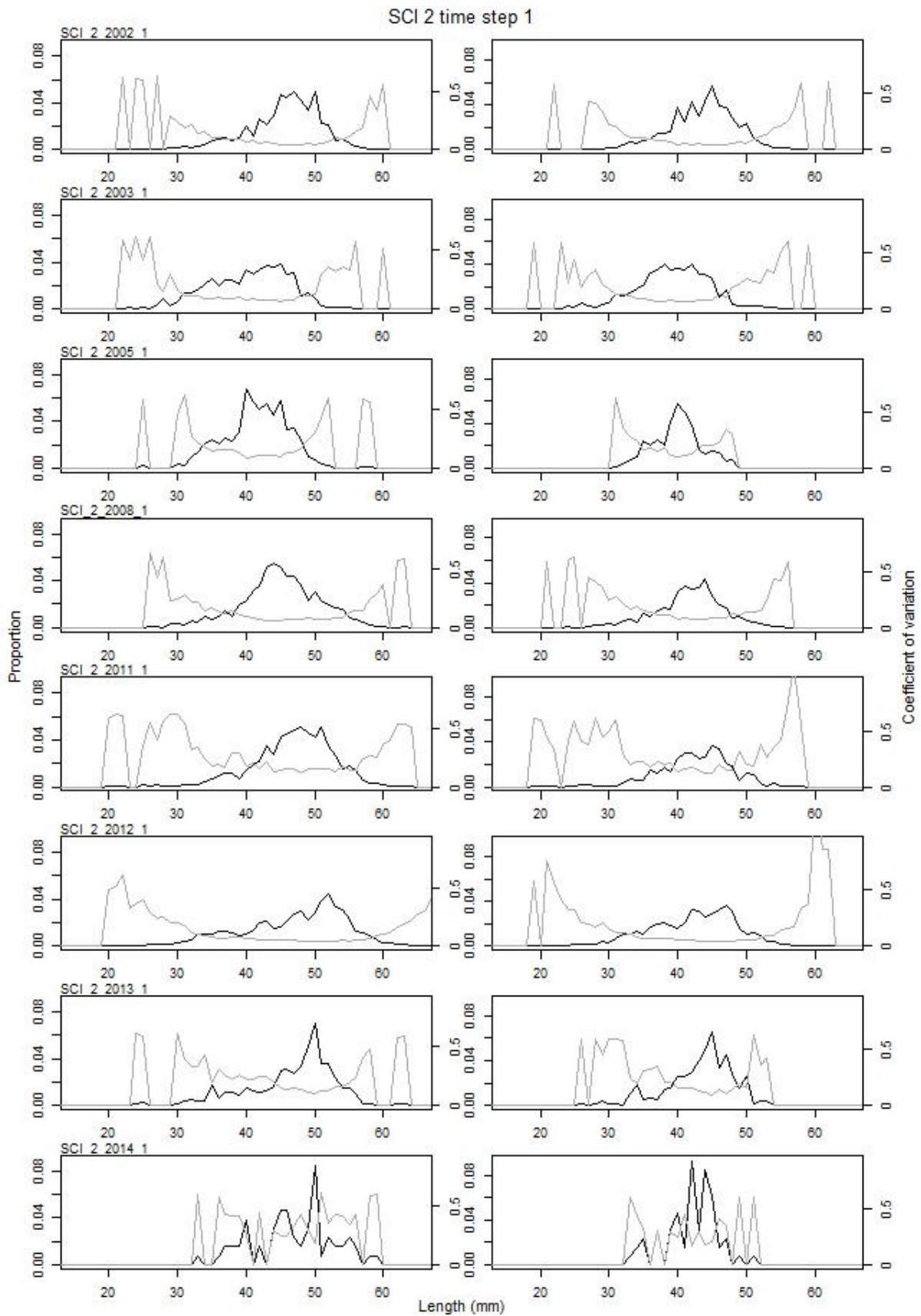


Figure 39 (continued): Proportional length frequency distributions (black line) and CVs (grey line) for commercial catches by model year and time step 1 for SCI 2. Males are plotted on the left, females on the right.

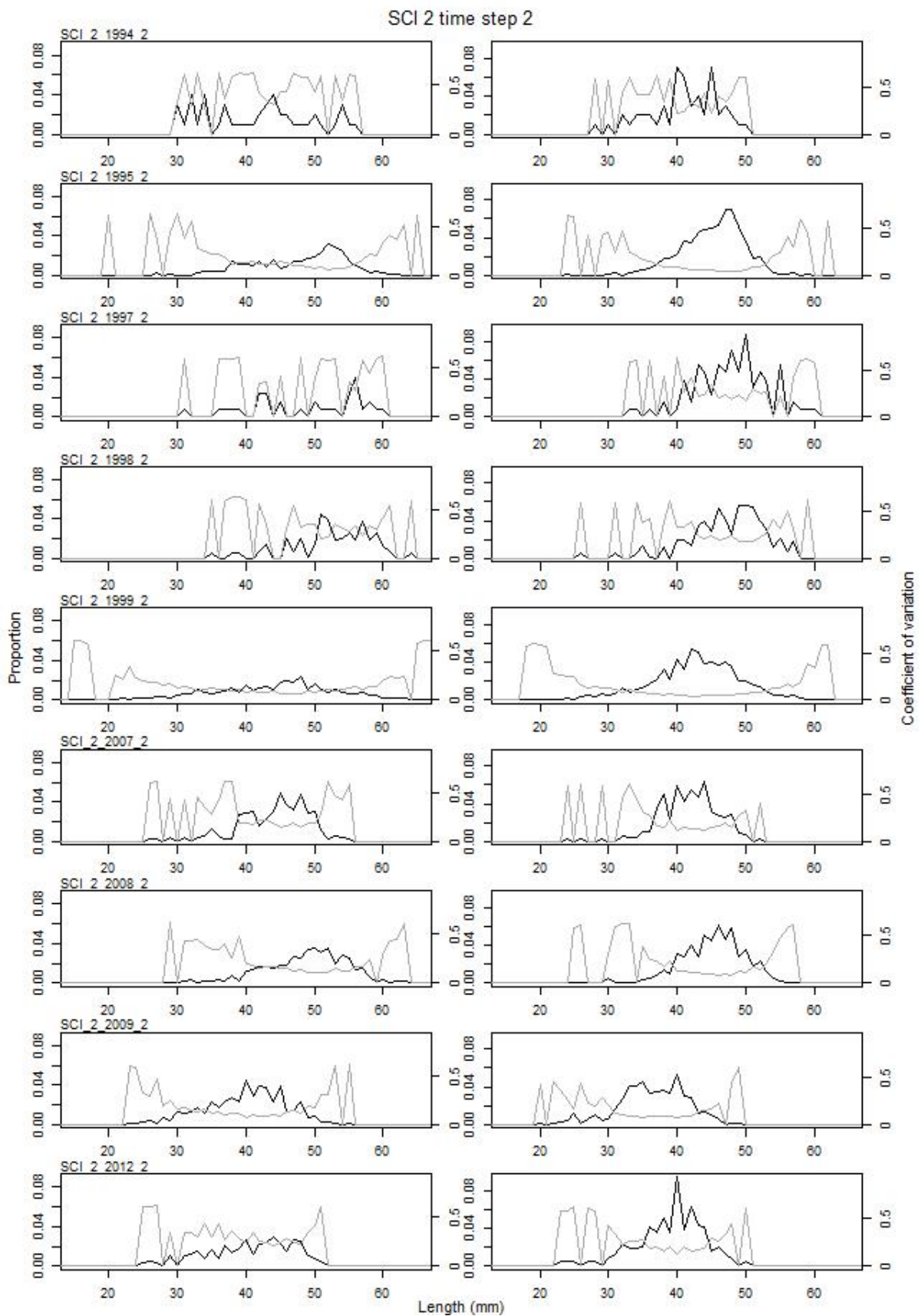


Figure 40: Proportional length frequency distributions (black line) and CVs (grey line) for commercial catches by model year and time step 2 for SCI 2. Males are plotted on the left, females on the right.

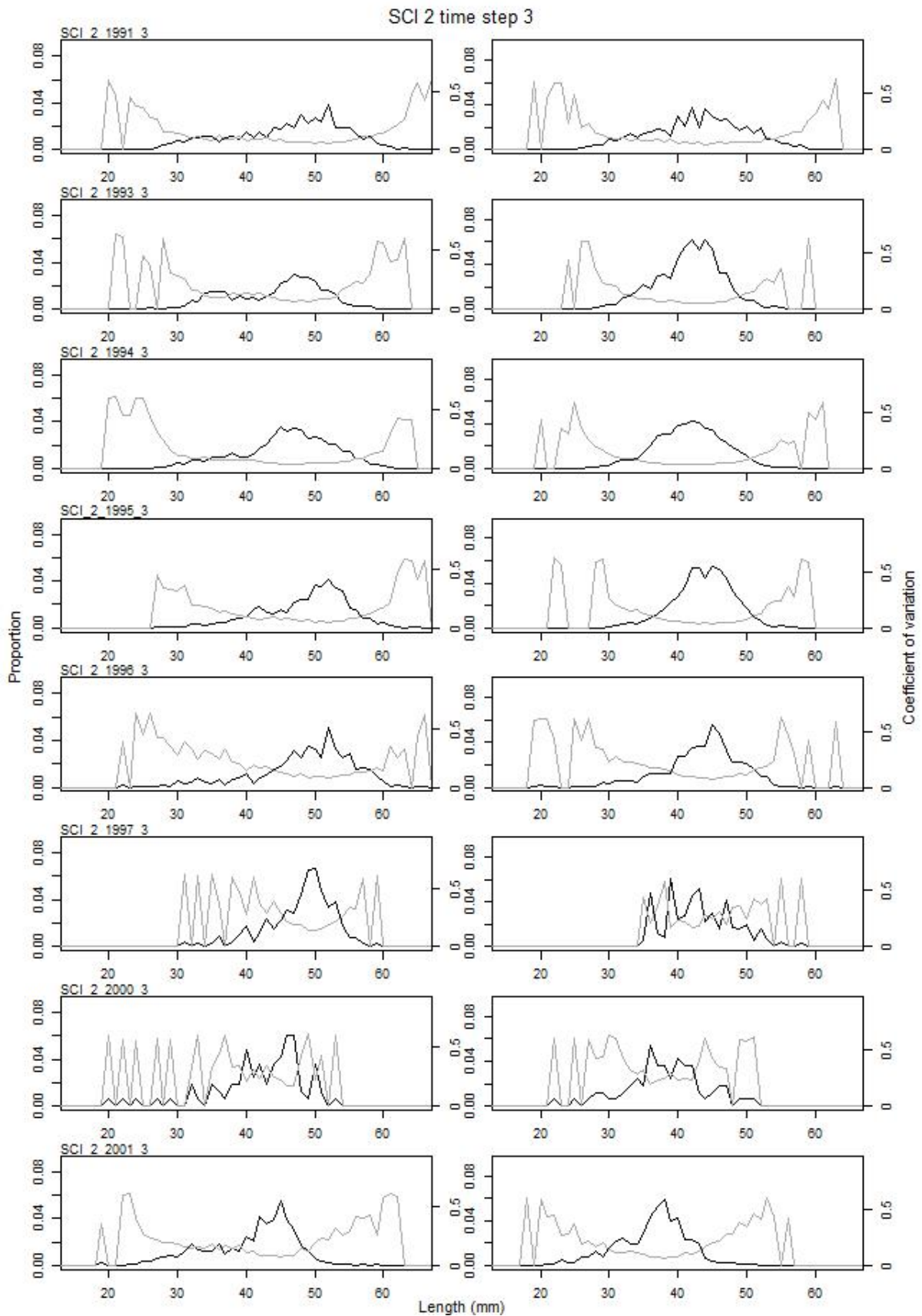


Figure 41: Proportional length frequency distributions (black line) and CVs (grey line) for commercial catches by model year and time step 3 for SCI 2. Males are plotted on the left, females on the right.

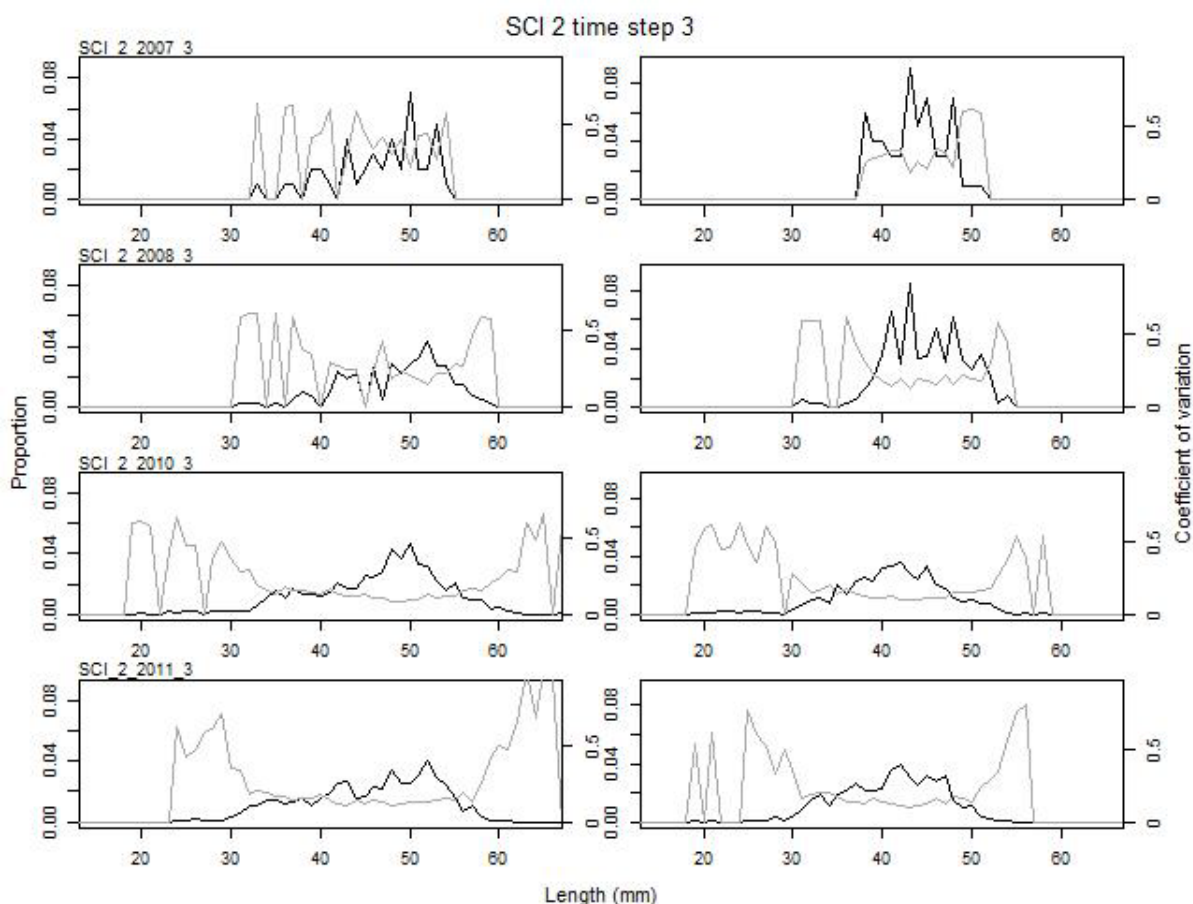


Figure 41 (continued): Proportional length frequency distributions (black line) and CVs (grey line) for commercial catches by model year and time step 3 for SCI 2. Males are plotted on the left, females on the right.

3.6.2. Trawl survey length distributions

Length frequency samples from research trawling in both fisheries have been collected by scientific staff since 1993 (Table 16 and Table 17). Estimates of the length frequency distributions (with associated CVs) were derived using the NIWA CALA software (Francis & Bian 2011), using 1 mm OCL (Orbital Carapace Length) length classes by sex, and are presented in Figure 42 and Figure 43 (SCI 1) and Figure 44 and Figure 45 (SCI 2).

3.6.3. Photo survey length distributions

Length frequency distributions were estimated for the relative photographic abundance series, by measuring the widths of a large sample of major burrow openings in the images and converting these to orbital carapace lengths using a regression of OCL on major opening width (Cryer et al. 2005), augmented with additional data collected from more recent surveys. To estimate the CVs at length for each year, we used a bootstrap procedure to resample with replacement from the original observations of burrow width and convert each observation to an estimated scampi size (in OCL), using an error term sampled from a normal distribution fitted to the regression residuals. Compared with the length frequency distributions from trawl catches, this procedure gave very large CVs which are considered to be realistic given the uncertainties involved in generating a length frequency distribution from burrow sizes. Estimates of the length frequency distributions (with associated CVs) for scampi generating burrows are presented for SCI 1 in Figure 46 and for SCI 2 in Figure 47.

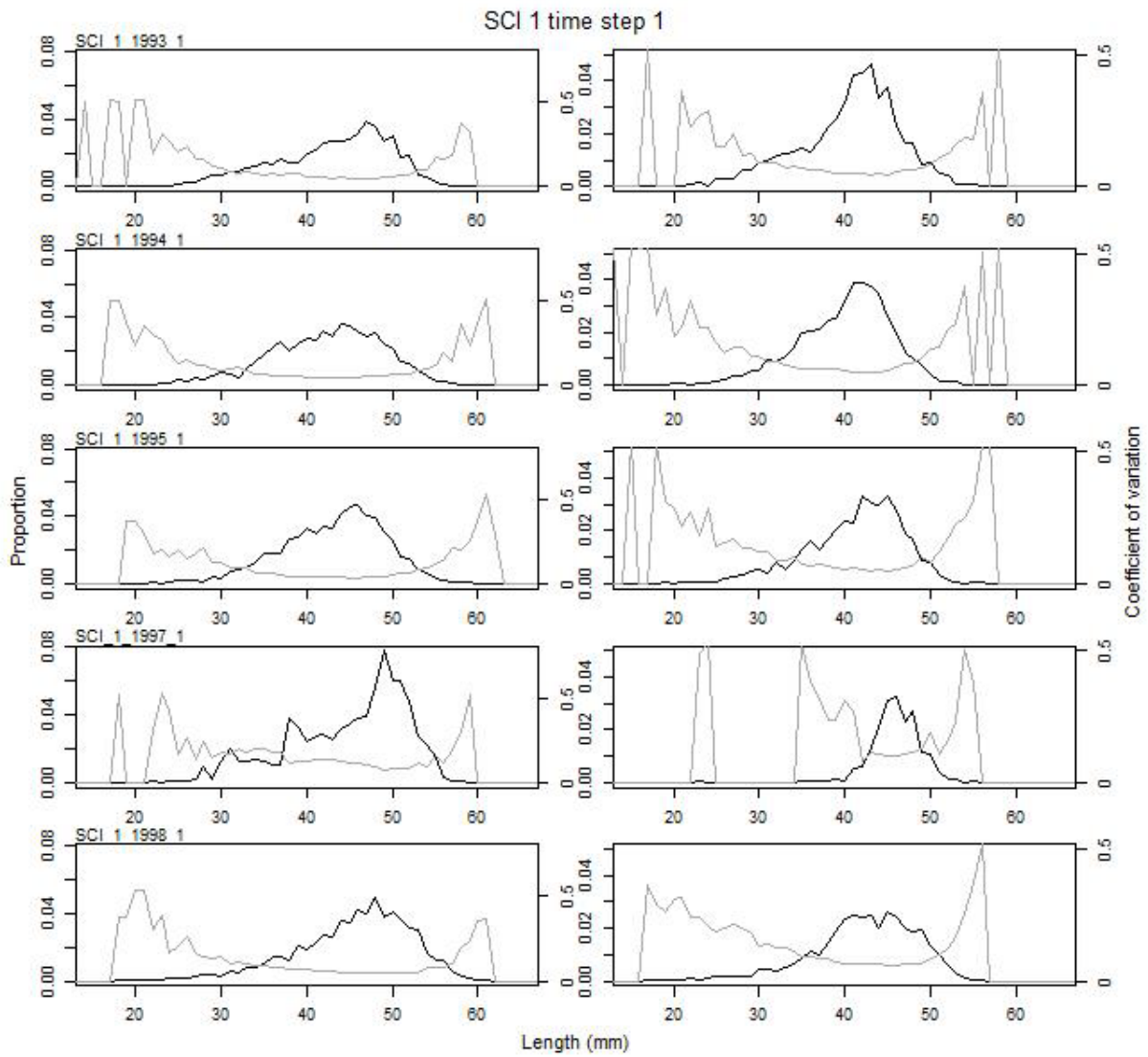


Figure 42: Proportional length frequency distributions (black line) and CVs (grey line) for research survey catches by model year for SCI 1, step 2. Males are plotted on the left, females on the right.

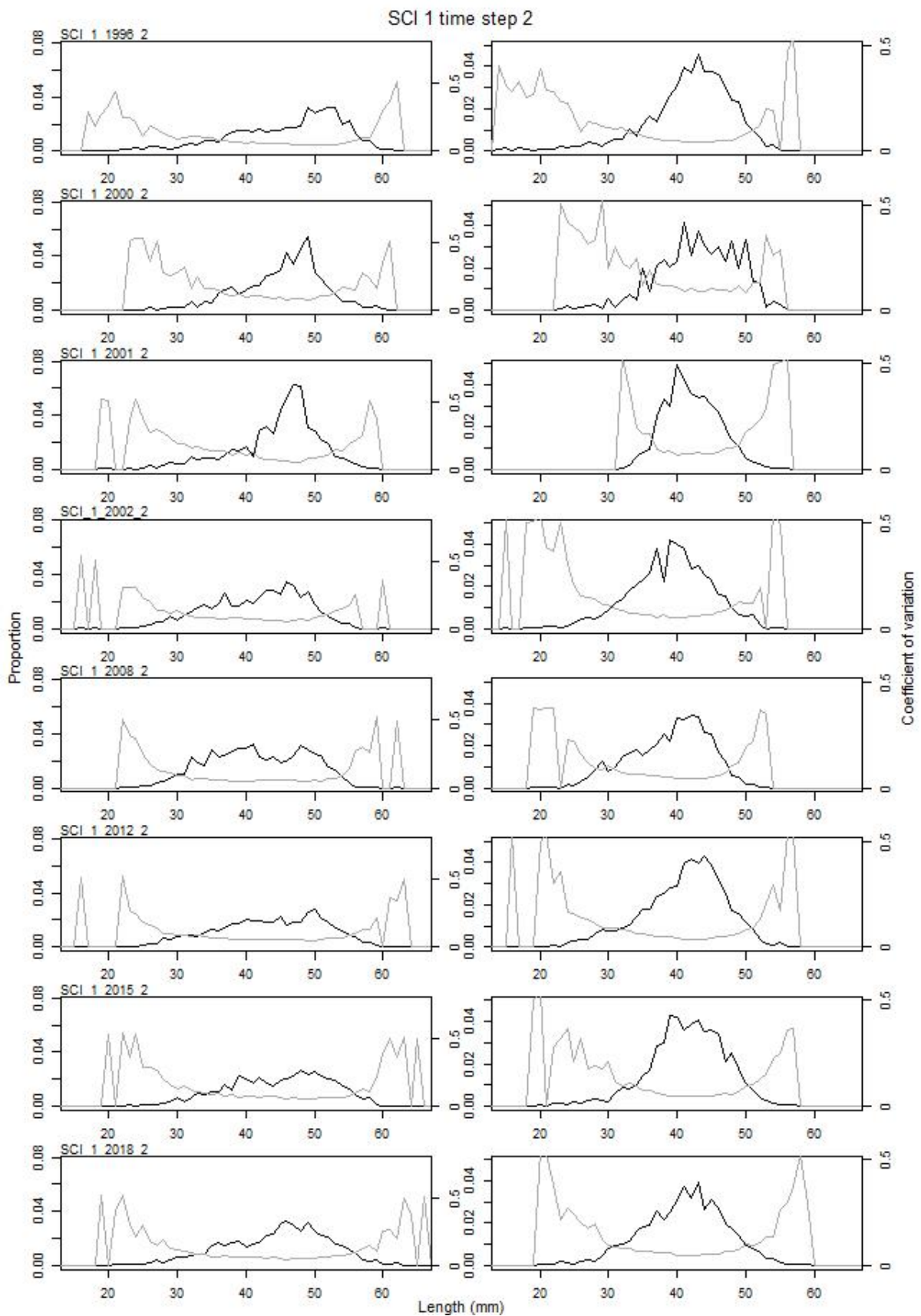


Figure 43: Proportional length frequency distributions (black line) and CVs (grey line) for research survey catches by model year for SCI 1, step 2. Males are plotted on the left, females on the right.

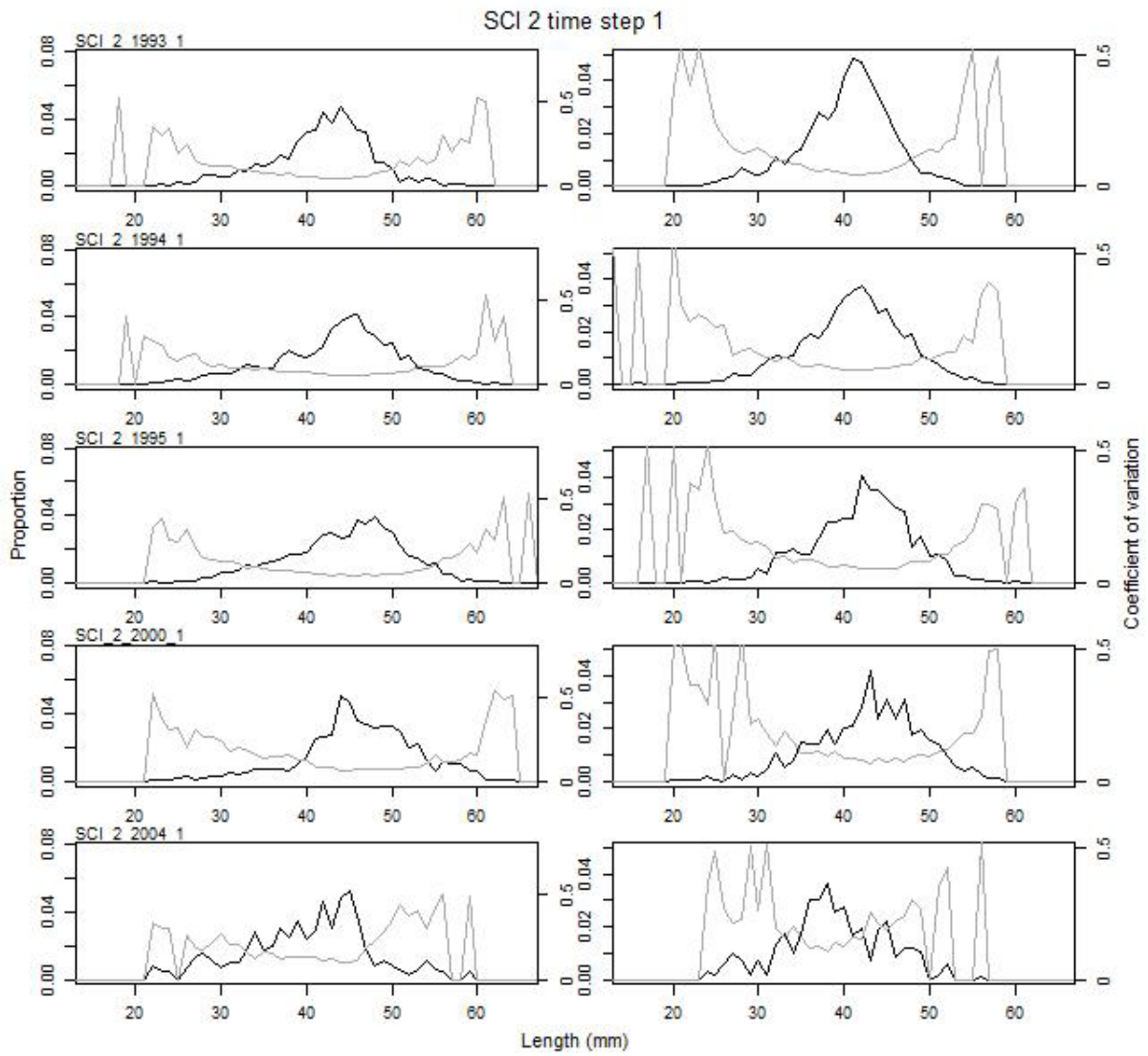


Figure 44: Proportional length frequency distributions (black line) and CVs (grey line) for research survey catches by model year for SCI 2, time step 1. Males are plotted on the left, females on the right.

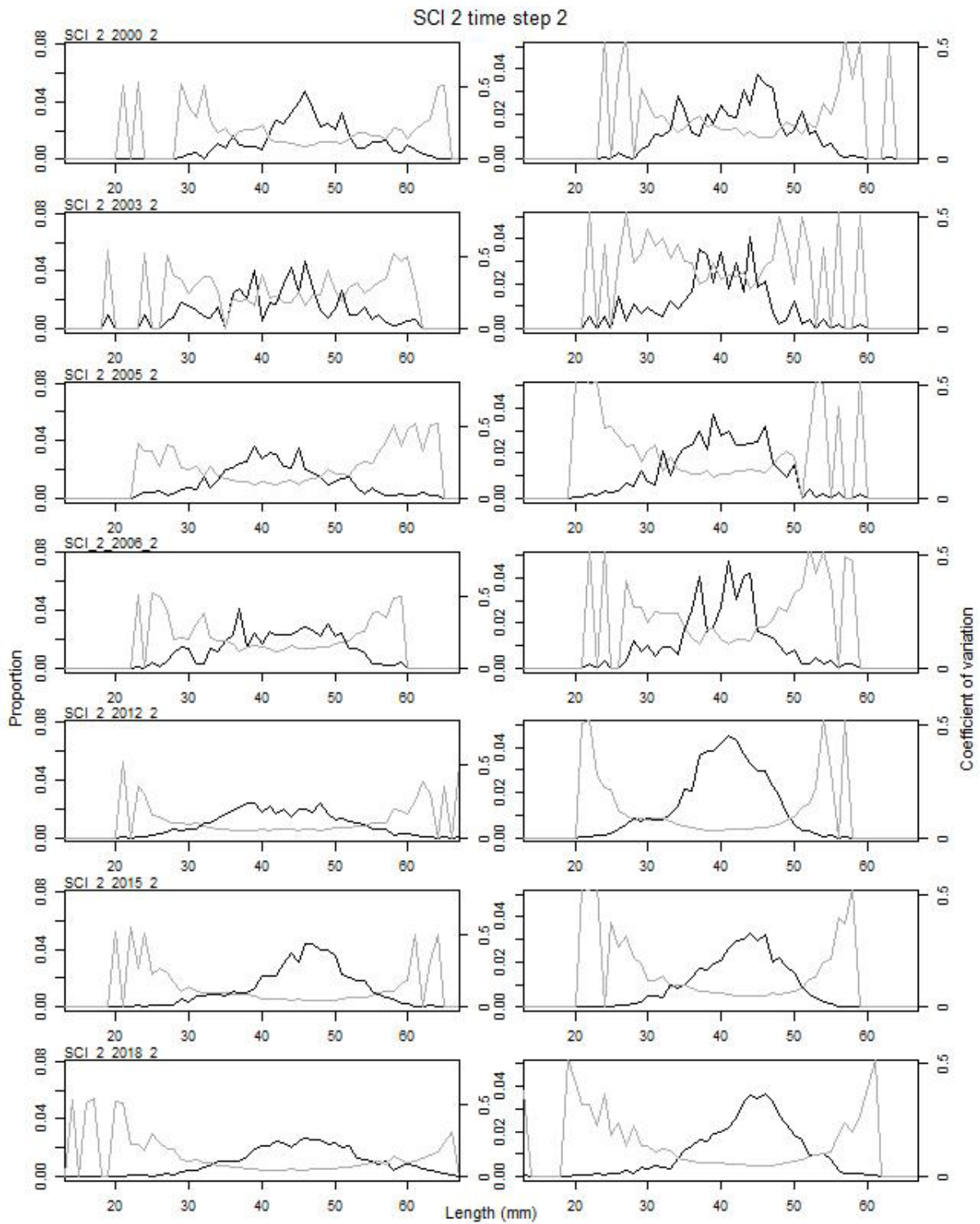


Figure 45: Proportional length frequency distributions (black line) and CVs (grey line) for research survey catches by model year for SCI 2, time step 2. Males are plotted on the left, females on the right.

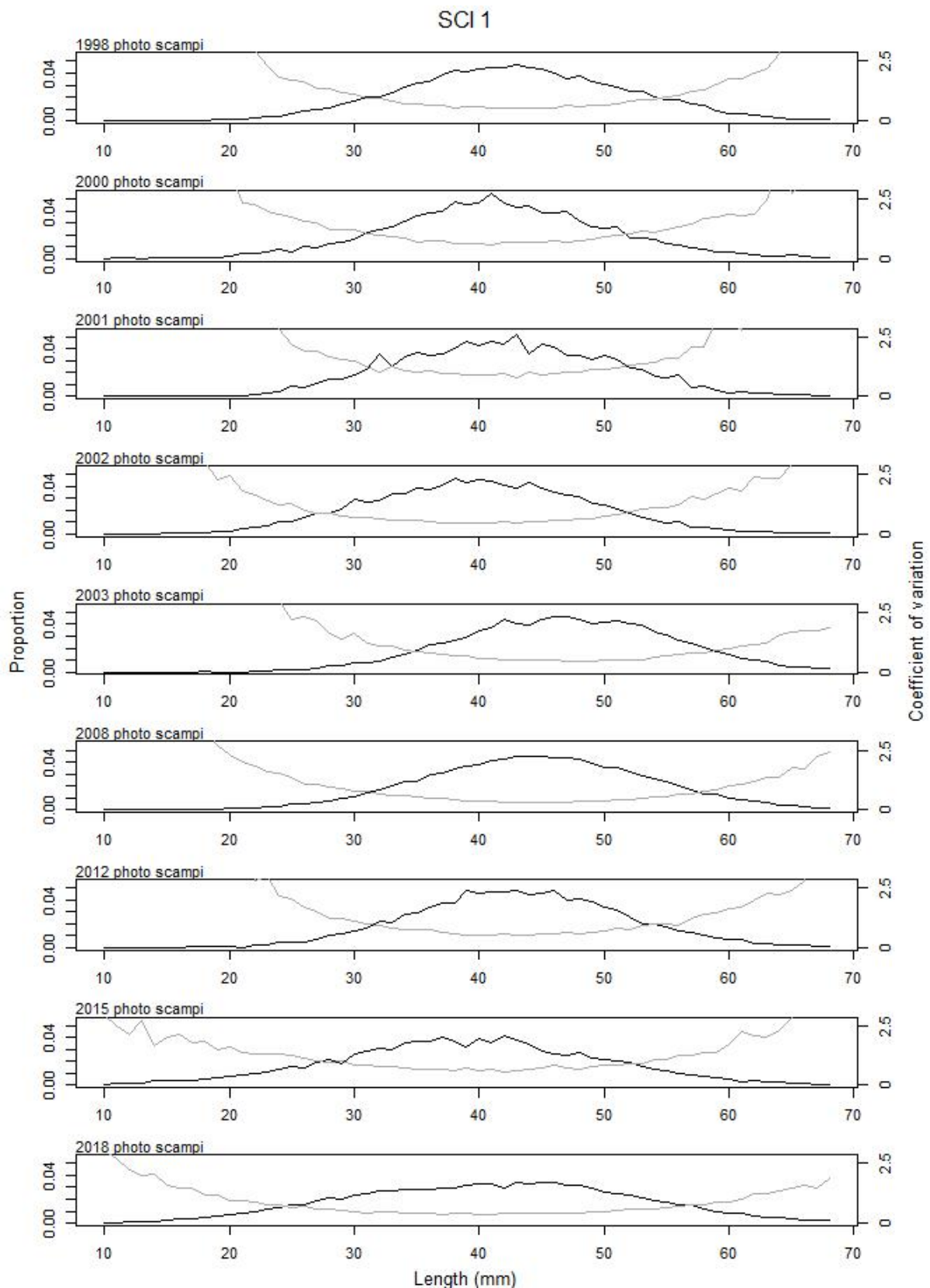


Figure 46: Proportional length frequency distributions (black line) and CVs (grey line) for scampi responsible for burrows counted within photo survey for SCI 1.

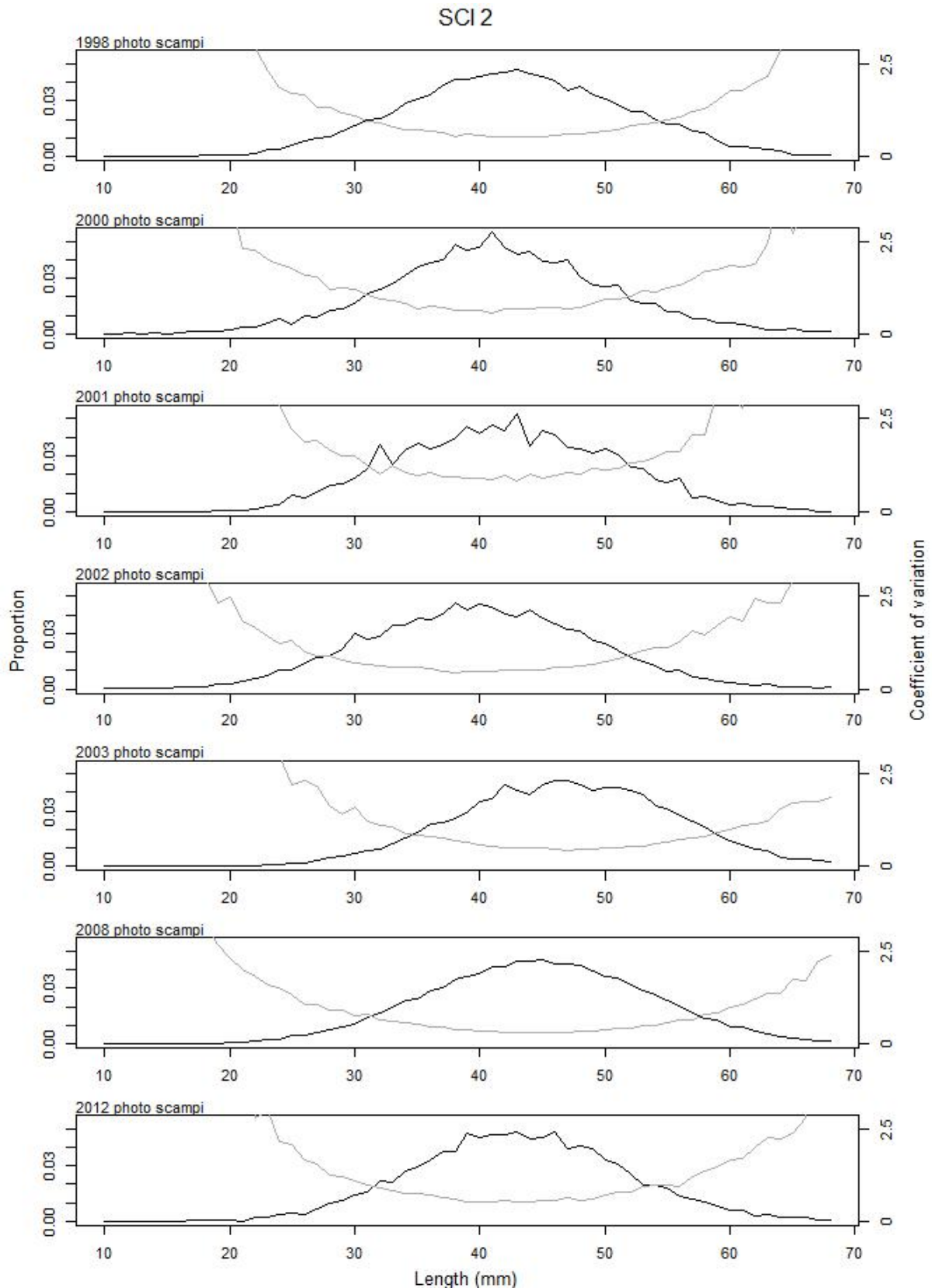


Figure 47: Proportional length frequency distributions (black line) and CVs (grey line) for scampi responsible for burrows counted within photo survey for SCI 2.

3.7. Model assumptions and priors

Maximum Posterior Density (MPD) fits were found within CASAL using a quasi-Newton optimiser and the BETADIFF automatic differentiation package (Bull et al. 2012). Fitting was done inside the model except for the weighting of the CPUE indices and length frequency data. For the length frequency data, observation-error CVs were estimated using CALA, converted to equivalent observation-error multinomial N s, and used within the model. The appropriate multinomial N s to account for both observation and process error were then calculated from the model residuals (method TA1.8 by (Francis 2011), and these final N s were used in all models reported. Generally this process resulted in small N s for the commercial length frequency data in particular and were, therefore, given relatively low weighting within the model. For the CPUE indices, the approach proposed by Francis (2011) was initially investigated (estimate appropriate CVs by fitting a smoother to the index), although sensitivity analyses were examined, and in the final models CVs were fixed at the lower range of the sensitivity runs, with additional process error estimated within the model. CASAL was also used to run Markov chain Monte Carlo (MCMC) on the base models. MPD output was analysed using the extract and plot utilities in the CASAL library running under the general analytical package R.

For all final models documented in this report, three independent MCMC chains were started a random step away from the MPD for each model and run for 2 million simulations, with every one thousandth sample saved, to give a set of 2000 samples. The three chains were examined for evidence of lack of convergence (trace plots are provided in relevant Appendices) and concatenated and systematically thinned to produce a 2000 sample chain. Posterior distributions of trawl survey and photo survey catchability were examined in relation to the prior distribution, and posterior trajectories of SSB, stock status, and YCS were provided.

The initial model was based on that described by Tuck (2016). The model inputs include catch data, abundance indices (CPUE, trawl surveys, and photo surveys), and associated length frequency distributions. The parameters estimated by the model include SSB_0 and R_0 , a time series of SSBs and year class strengths, selectivity parameters for commercial and research trawling and the photo survey, and associated catchability coefficients. Catchability coefficients (q s) for commercial fishing, research trawling, and photographic surveys were estimated as nuisance parameters. The only informative priors used in the initial model were for q -Photo, q -Trawl, the ratio of q values for q -Photo and q -Trawl for the whole and part areas of SCI 1, and the YCS vector (to constrain recruitment variability).

3.7.1. Scampi catchability

Previous priors for scampi catchability have been largely based on information on *Nephrops* emergence and occupancy rates from European studies conducted in far shallower waters than *Metanephrops* populations inhabit (Tuck & Dunn 2012), but the acoustic tagging pilot study conducted at the Mernoo Bank in October 2010 offered an opportunity to estimate priors for occupancy and emergence from New Zealand data (Tuck et al. 2011; Tuck 2013). Acoustic tagging experiments were repeated successfully during the SCI 1 and SCI 2 surveys in 2012 (Tuck et al. 2013) and were also conducted within the SCI 6A and SCI 3 surveys in 2013 (although less successfully). The data collected within these studies have been used to estimate catchability priors (Tuck et al. 2015).

Acoustic tags were fitted to scampi released with a moored hydrophone, to record tag detections and hence when animals were emerged from burrows. The tag detection hydrophones were deployed over a period of up to 46 days (Tuck et al. 2013). Some tag detections showed distinct cyclical patterns (12.6 hour cycle), but most animals showed no clear behavioural pattern, and the proportion of scampi detectable during the daytime over the duration of the studies varied from 41 to 51% (95% confidence interval), with a median detection of 46%.

In previous analysis, the density of all visible scampi (ranging from those walking free on the surface to those within burrows, where only the tips of claws can be seen) is scaled by emergence. Before conducting emergence trials with live scampi, scuba divers activated and placed tags in burrows in shallow waters to confirm whether they became undetectable when they were acoustically obscured by the burrow. This showed that tags were detected on the surface of the seabed and in the entrance to burrows, but not within a burrow.

Scampi are thought to spend a considerable amount of time within their burrow entrances, “door keeping”, and classification of these individuals as visible scampi to be scaled up by the emergence rate is likely to overestimate the population density. When “door keeping”, a scampi’s position (and the likelihood of it being acoustically detectable if it carried a tag) can range from only just in the burrow (Figure 48, left, very likely to be detected), to about half in (Figure 48, centre, as likely or not to be detected), or almost fully in, with only the claws visible (Figure 48, right, very unlikely to be detected). Therefore, scampi considered to be acoustically detectable scampi are those walking free on the surface (emerged) and a proportion of door keepers.

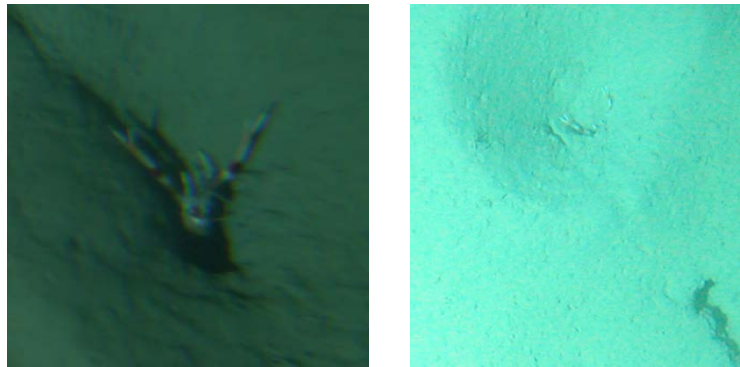


Figure 48: Examples of scampi within the entrance to burrows (door keeping).

From the 2018 survey, the 388 scampi observed in the photographic component were re-examined, to determine whether it was considered they would have been acoustically detectable, had they been acoustically tagged. It was estimated that 33% of the scampi would have been detectable, with a 95% confidence interval (estimated by resampling from the original data with replacement) of 28% – 37%.

The process of using the emergence and photo survey data to estimate priors for *q-Photo* (the proportion of the scampi population represented by the count of major burrow openings) is summarised in Table 21. For each term in the process, a distribution was estimated by resampling from the original data with replacement. The density of detectable scampi was estimated by summing the density of emerged scampi with the density of door keepers multiplied by the proportion of detectable door keepers. The density of all scampi was estimated by dividing the density of detectable scampi by the emergence rate. The *q-Photo* term was estimated by dividing the density of major burrow openings by the density of all scampi. While expressed as densities (for convenience), the catchabilities are estimated on the basis of the ratio between scampi and burrow counts, with the area viewed cancelled out.

Table 21: Estimation of *qPhoto* prior for SCI 1 & 2 from emergence and photo data.

		Percentile			Source
		2.5%	50%	97.5%	
Door keeper detectability	(1)	28.3%	32.7%	37.4%	Seabed images
Daytime emergence	(2)	41.7%	46.1%	50.7%	Acoustic tagging (2012)
Major opening density (m ⁻²)	(3)	0.0680	0.0772	0.0858	Photo survey (2012)
Door keeper density (m ⁻²)	(4)	0.0113	0.0138	0.0166	Photo survey (2012)
Emerged scampi density (m ⁻²)	(5)	0.0022	0.0035	0.0050	Photo survey (2012)
Detectable scampi density (m ⁻²)	(6)	0.0065	0.0081	0.0100	(5) + (4) * (1)
Estimated scampi density (m ⁻²)	(7)	0.0111	0.0178	0.0365	(6) / (2)
<i>q-Photo</i>		2.233	4.365	6.829	(3) / (7)

Having used the emergence rate and acoustically detectable scampi density to estimate scampi population density, the density of scampi seen that are likely to be caught in a trawl is then used to estimate trawl catchability. In previous analyses, the density of all scampi out of burrows was divided by the estimated scampi population density. However, examination of the relationship between estimates of scampi abundance (animals out of burrows) from photographic surveys and trawl sampling at a later date during the same survey, suggests that although there is a noisy positive relationship ($r^2=0.22$), it is not a 1:1 slope, and, on average, the trawl catch estimates are a half to a third of the emerged scampi estimates. The pattern appears reasonably consistent between stocks.

Therefore, trawl survey catchability (*q-Trawl*) varies with both the percentage of door keepers that are acoustically detectable and the percentage of emerged scampi that would be caught if within the path of a trawl (Table 22). On the basis of Table 22, a distribution for *q-Trawl* has been assumed, with a median of 0.0788 (33% door keepers detectable, 40% of emerged scampi caught) and with 95% confidence intervals bounded by 37% door keepers detectable, 10% of emerged scampi caught and 28% door keepers detectable, 70% of emerged scampi caught.

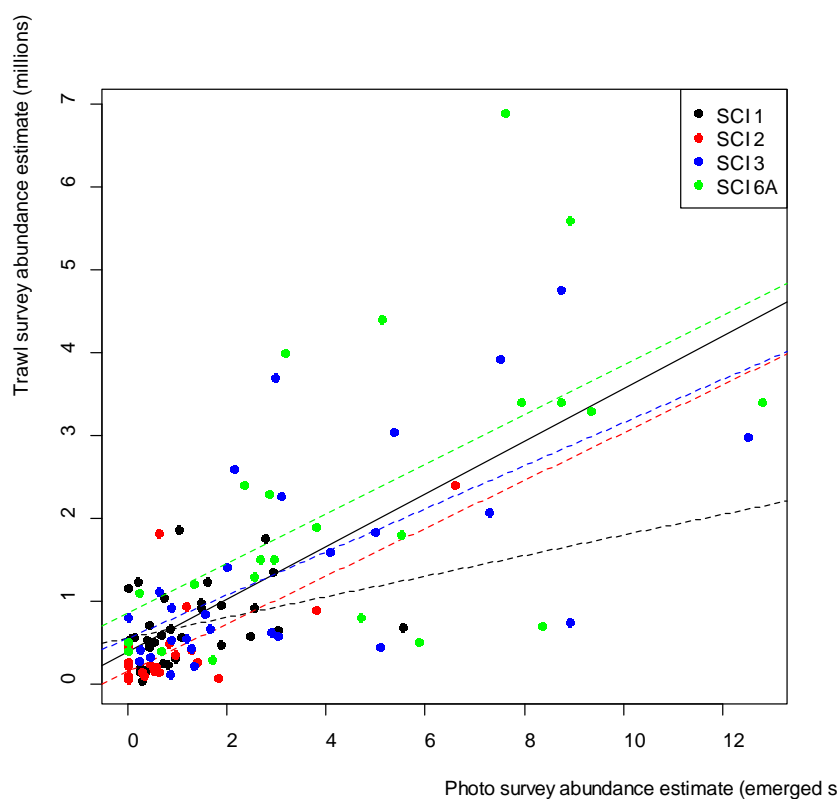


Figure 49: Relationship between strata level photographic survey estimates of emerged scampi density and trawl survey scampi density. Solid line represents best linear fit through all data ($r^2=0.22$). Dashed lines represent best linear fit through data from each management area.

Table 22: Estimated scampi density (on the basis of observed data and assumptions on detectability of door keepers), the density of available scampi, and implied *q-Trawl*, on basis of assumptions on percentage of emerged scampi caught. Bold value represents assumed median *q-Trawl*, with 95% confidence interval bounded by italicised values.

% of emerged scampi likely to be caught	Density of available scampi (m ⁻²)	% of door keepers detectable acoustically		
		28%	33%	37%
Estimated density (m ⁻²)		0.0111	0.0178	0.0365
10%	0.00035	0.0314	0.0197	<i>0.0096</i>
30%	0.00105	0.0943	0.0591	0.0288
40%	0.00140	0.1258	0.0788	0.0384
50%	0.00175	0.1572	0.0984	0.0480
70%	0.00245	<i>0.2201</i>	0.1378	0.0672
100%	0.00350	0.3144	0.1969	0.0959

3.7.2. Priors for *qs*

q-Photo

This is the proportion of the scampi population represented by the count of major burrow openings. The best estimate is 4.365 (major burrow openings divided by estimated scampi density; Table 21). Lower (2.233) and upper (6.829) estimates are taken as the 2.5th and 97.5th percentiles of the distribution.

q-Trawl

This is the proportion of the scampi population represented by the trawl survey catches. The best estimate is 0.0788 (Table 22). Lower (0.0096) and upper (0.2201) estimates are taken as the 2.5th and 97.5th percentiles of the distribution.

Ratio of *q*, part: whole survey (SCI 1)

As discussed above (Section 3.5), some surveys in SCI 1 have only covered four of the six survey strata that comprise the modelled area. These limited area surveys have been fitted as a separate index, with *q* constrained as a proportion of *q-Trawl* or *q-Photo* for the whole area survey, using the @ratio_qs_penalty command. The prior distribution for this ratio was estimated from the distribution of relative catch rates in the two areas by all scampi targeting commercial trips fishing in both areas, scaled by the relative size of the areas. The best estimate was that 80% of the biomass was within the limited survey area, with lower and upper 95% confidence limits of 65% and 94%.

3.7.3. Estimation of prior distributions

The bounds and best estimate were assumed to represent the 2.5th, 50th, and 97.5th percentiles of the prior distribution. These values were fitted within a binomial GLM (probit link) to estimate the slope and intercept of the cumulative frequency distribution, which in turn were used to estimate the mean and standard deviation of the lognormal distribution of the prior. The distributions of the priors are presented in Figure 50. Because not all visible scampi would be acoustically detectable, and not all emerged scampi would be caught in a trawl, we have modified the priors from those applied in previous assessments (Tuck 2016).

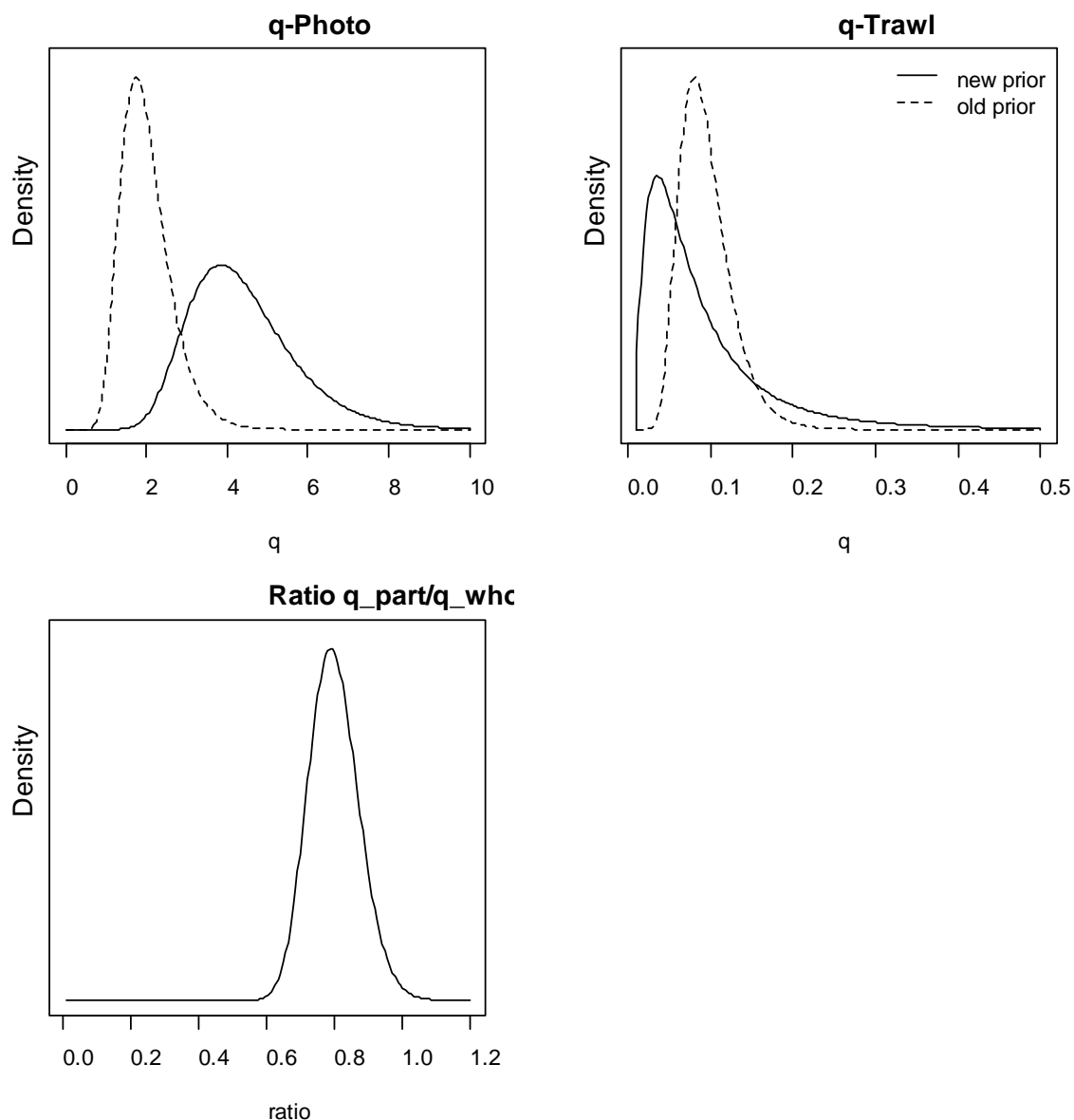


Figure 50: Estimated distribution of *q-Photo*, *q-Trawl*, and the ratio of *q_part/q_whc* for SCI 1. Dashed lines represent the prior distributions used in the previous assessments (Tuck 2016) .

3.7.4. Recruitment

Few data are available on scampi recruitment. Relative year class strengths were fixed at 1 for the two most recent years and were assumed to average 1.0 over all other years. In the initial model development (Cryer et al. 2005) lognormal priors on relative year class strengths were assumed, with mean 1.0 and CV of 0.2. The sensitivity of year class strength (YCS) variation was examined in further developments (Tuck & Dunn 2006), and later increased to a CV of 1 (Tuck & Dunn 2012). Model explorations within the recent SCI 6A assessment (Tuck 2017) suggested that extreme YCS values estimated by the model were related to model structure rather than data. The preliminary model, and those applied to other scampi stocks, used the Haist parameterisation of YCS (Bull et al. 2012) where

$$YCS_i = \frac{y_i}{\bar{y}}$$

with a lognormal prior on y_i with mean of 1 and CV of 1, and a small penalty to ensure that the mean of YCS does not drift away from 1 (“a YCS average to 1 penalty”). Sensitivity trials (Tuck 2017) with the Haist parameterisation showed that both individually removing the penalty, and tightening the CV on the YCS prior, reduced the final YCS estimated by the model, but only removing the penalty and tightening the CV (to 0.7) generated a final YCS estimate of similar magnitude to previous good years. Further investigations examined the sensitivity to the CV on the YCS prior for models with the Haist parameterisation without a penalty on YCS averaging to 1 and a YCS average to 1 penalty, and also without the Haist parameterisation but with a YCS average to 1 penalty (Tuck 2017).

On the basis of these sensitivity analyses, the SFWG agreed to proceed with a model structure implementing the Haist parameterisation, without the YCS average to 1 penalty and with tighter CVs on the YCS prior. Preliminary examination of the implications of this parameterisation change to previously accepted stock assessment models for SCI 1 and SCI 2 did not suggest that any change in perceived stock status, although this will be further examined as these assessments are updated.

The relationship between stock size and recruitment for scampi is unknown, and a Beverton-Holt relationship with a steepness of 0.8 has been assumed. New Zealand scampi have very low fecundity (Wear 1976; Fenaughty 1989) (in the order of tens to hundreds of eggs carried by each female), so high levels of recruitment are unlikely at low abundance. Recruitment enters the model partition as a year class, with a normally distributed OCL of mean 10 mm and CV of 0.4.

4. SCI 1 - ASSESSMENT MODEL RESULTS

4.1. Initial models

As described in Section 3.1, a single area model was applied, with an annual CPUE index, and the photo and trawl survey data were fitted as separate indices, both in time step 1, but with different areas covered. Model developments since the last assessment have introduced a new year class strength parameterisation and new catchability priors, and, so as a first step, the influence of these on the previous assessment, and the influence of three years additional data, were examined (Table 23). Key parameter and quantity estimates from the MPD fits for the models are presented in Table 24, with stock and recruitment trajectories for the models presented in Figure 51 and catchabilities in relation to the informed prior distributions in Figure 52.

Table 23: General details of initial models examined within sensitivity analyses for SCI 1.

Model name	Final year	YCS	q priors	M	CPUE CV	Survey process error
2015	2015	Old	Old	0.3	0.1	estimated
YC	2015	New	Old	0.3	0.1	estimated
new q	2015	New	New	0.3	0.1	estimated
2018	2018	New	New	0.3	0.1	estimated

The revised parameterisation of the YCS reduced the magnitude of the peak recruitments estimated at the beginning of the time series (Figure 51), but still estimated YCSs well above average in the early 1990s. The magnitude of stock increase associated with this period of high recruitment was slightly lower with the revised parameterisation, but there was minimal effect on estimates of B_0 or stock trajectory and status (relative to B_0) since 2000. The revised catchability priors reduced the estimate of B_0 , but did not affect the YCS of stock trajectory patterns. The new priors resulted in slightly larger estimated q values for q -Trawl, but markedly greater estimated values for q -Photo (Figure 52). Updating the model data up to the 2018 fishing year (new survey and length frequency data) resulted in slightly lower catchability estimates, and a slightly increased estimate of B_0 , but did not affect YCS or stock trajectory patterns. The previous assessments (Tuck 2016) and these updates were unable to

provide plausible estimates for photo survey selectivity parameters, or L_{50} for commercial selectivity in time step 2, and so these were fixed (based on values estimated previously).

Table 24: Estimated key parameters and quantities from MPD fits for SCI 1 initial sensitivity model runs. Italicised values indicate parameters that were fixed rather than estimated.

	2015	YC	new q	2018
SSB ₀	5660	5578	4243	4781
SSB ₂₀₁₅	4207	4284	3126	3250
SSB ₂₀₁₅ /SSB ₀	0.74	0.77	0.74	0.68
<i>q-Photo</i>	2.2798	2.3366	3.2805	3.0704
<i>q-Trawl</i>	0.0546	0.0517	0.0637	0.0587
Growth				
Male g20	11.57	12.98	13.73	12.43
Male g40	2.57	2.71	2.81	2.74
Female g20	10.78	12.15	12.90	11.75
Female g40	0.00	0.00	0.00	0.00
min_sigma	4.21	4.31	4.45	4.43
Selectivity				
step1 L ₅₀	39.12	38.18	37.99	38.80
step1 a ₉₅	11.16	12.30	12.68	11.37
step1 a _{max}	0.85	0.87	0.88	0.83
step2 L ₅₀	<i>37.00</i>	<i>37.00</i>	<i>37.00</i>	<i>37.00</i>
step2 a ₉₅	10.69	10.86	11.32	9.66
step2 a _{max}	0.59	0.59	0.60	0.61
trawl L ₅₀	37.07	35.63	34.73	35.50
trawl a ₉₅	12.42	12.89	12.53	12.22
trawl a _{max}	0.99	1.03	1.08	1.08
photo L ₅₀	<i>35.00</i>	<i>35.00</i>	<i>35.00</i>	<i>35.00</i>
photo a ₉₅	<i>25.00</i>	<i>25.00</i>	<i>25.00</i>	<i>25.00</i>
Process error				
CPUE	0.12	0.17	0.16	0.16
Trawl_1	0.00	0.00	0.00	0.00
Trawl_2	0.30	0.26	0.26	0.26
Photo all	0.00	0.00	0.00	0.00
Photo part	0.00	0.00	0.00	0.00

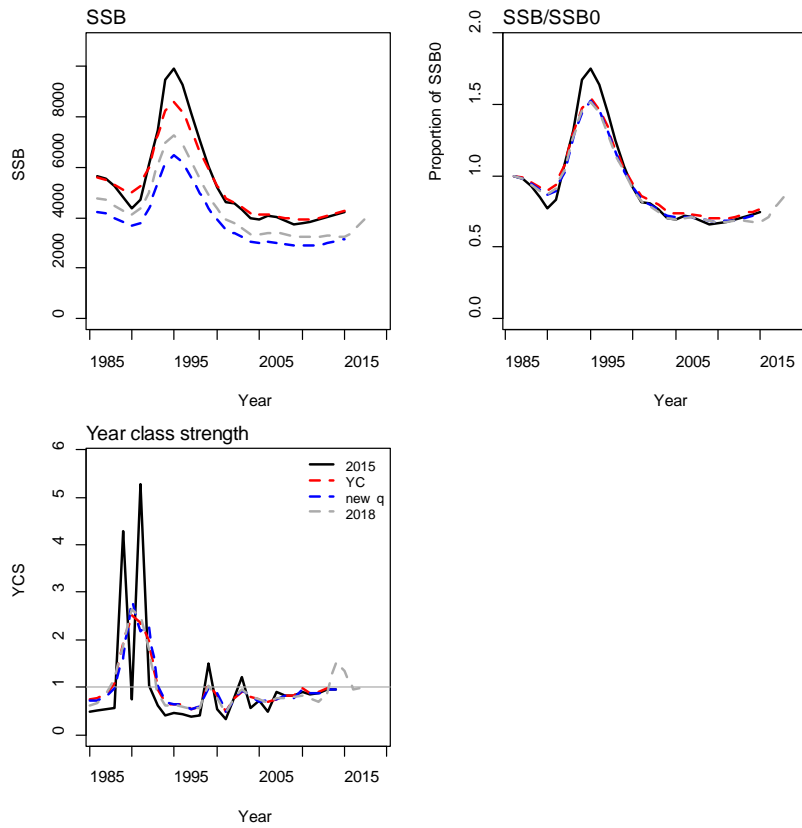


Figure 51: Plots of absolute SSB, SSB as a proportion of SSB₀, and year class strength (YCS) for MPD fits to the initial SCI 1 sensitivity runs.

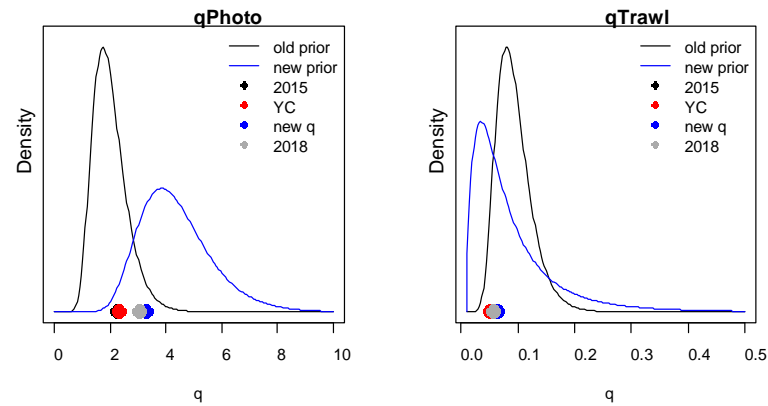


Figure 52: Prior distributions for the informed q terms (old and new versions) and estimated for MPD fits to the initial SCI 1 sensitivity runs.

Attempts to estimate natural mortality within the model were not considered reliable, and therefore M was fixed at 0.3, with sensitivity runs. Sensitivity analyses were also run in relation to the CPUE process error (CV), the estimation of photo survey selectivity, and the exclusion of survey time series. Details of differences between models examined within these further sensitivity analyses are presented in Table 25.

Table 25: General details of models examined within further sensitivity analyses for SCI 1. All models used the new YCS parameterisation and new q priors and included data to the 2018 fishing year. PE is CPUE process error.

Model name	M	CPUE CV	Survey process error	Photo selectivity	Survey data
PE est	0.3	estimated	estimated	fixed	all
PE 10%	0.3	0.10	estimated	fixed	all
PE 20%	0.3	0.20	estimated	fixed	all
PE 25%	0.3	0.25	estimated	fixed	all
$M=0.2$	0.2	0.15	estimated	fixed	all
$M=0.25$	0.25	0.15	estimated	fixed	all
$M=0.3$	0.3	0.15	estimated	fixed	all
Drop photo	0.25	0.15	estimated	fixed	photo excluded
Drop trawl	0.25	0.15	estimated	fixed	trawl excluded

Exploration of the effect of process error on the CPUE series (Figure 53; Table 26) estimated process error at 0.16 and found that estimated B_0 showed little sensitivity, other than for the lowest process error considered (10%). This model also showed marked effects on YCS. Fits to the CPUE series improved as process error was reduced, but fits to observer length frequency distributions worsened, although differences were small. The largest process error considered (0.25) estimated lower peak YCS values in the early 1990s, but within the process error range 0.15 (not included in Figure 53) to 0.25, estimates of B_0 and stock trajectories were very consistent.

Estimates of B_0 were sensitive to the assumed natural mortality rate (Figure 54; Table 26), with B_0 decreasing as M increases, and the magnitude of the population increase and decline in the mid 1990s also increased with increasing M . However, overall stock trajectory in recent years was far less sensitive, and, other than a slight shift in the timing of peak YCS (associated with slight changes in growth parameters), the patterns in YCS appear very similar between models.

The estimate of B_0 was very sensitive to the exclusion of the photographic survey data (along with the q -Photo prior and length composition data), but showed only slight differences when the trawl survey data were excluded (Figure 55; Table 26). Excluding the photographic data from the model results in the estimation of a significantly larger B_0 and a slightly higher stock trajectory from the mid 1990s until about 2016. This model estimated a slowly increasing stock status since about 2010, whereas both the models that were fitted to the photographic survey (including or excluding the trawl survey data) estimated a more stable stock status between 2010 and 2016, with an increase in the most recent years. This difference is reflected in above average YCS estimates in 2014 and 2015 in models including the photographic data. The model excluding the trawl survey data estimated a slightly lower B_0 than the full model, but the stock trajectory was very similar. The working group's conclusion that the SCI 1 model is heavily influenced by the q -Photo prior was confirmed by later examination of likelihood profiles.

As in previous assessments for SCI 1 (Tuck 2016), photo survey selectivity was fixed because attempts to estimate L_{50} in particular, resulted in values considered implausibly small (e.g., 17 mm), given the estimated size distributions. The size distribution of scampi associated with the major burrow openings recorded in the surveys is estimated from the width of the burrows, and a carapace length burrow width relationship generated from images collected in early surveys (see Section 3.6.3). This process incorporates considerable uncertainty, because the CVs on the length compositions are high, and the iterative weighting of data sets (following Francis 2011) downweights these data further. It is unclear whether generation of the carapace length-burrow width relationship accounted for potential foreshortening effects of measuring scampi carapace length from images when the animals may not be perpendicular to the plane of the image. This has been accounted for in estimation of the carapace length of visible scampi in SCI 6A surveys by estimation from carapace width (Tuck 2017),

but could result in an underestimation of scampi size, and hence an underestimation in photo selectivity L_{50} . This has been explored further for SCI 2 (see Section 5.1).

Table 26: Estimated key parameters and quantities from MPD fits for SCI 1 sensitivity model runs described in Table 25. Italicised values indicate parameters that were fixed rather than estimated.

	PE est	PE 10%	PE 20%	PE 25%	$M=0.2$	$M=0.25$	$M=0.3$	Drop photo	Drop trawl
SSB ₀	4781	4463	4816	4901	5090	4822	4691	6315	4586
SSB ₂₀₁₈	4141	3722	4184	4308	4044	3991	4008	4756	3719
SSB ₂₀₁₈ /SSB ₀	0.87	0.83	0.87	0.88	0.79	0.83	0.85	0.75	0.81
<i>q-Photo</i>	3.0704	3.4917	3.0360	2.9398	3.1493	3.2154	3.1883		3.4409
<i>q-Trawl</i>	0.0587	0.0624	0.0583	0.0573	0.0534	0.0568	0.0598	0.0388	
Growth									
Male g ₂₀	12.43	13.28	12.38	12.29	10.32	11.63	12.58	14.15	11.34
Male g ₄₀	2.74	2.88	2.73	2.70	2.15	2.51	2.78	2.45	2.88
Female g ₂₀	11.75	12.21	11.73	11.68	10.25	11.23	11.83	13.17	9.96
Female g ₄₀	0.00	0.00	0.00	0.00	0.00	0.00	0.00	0.00	0.00
min_sigma	4.43	4.61	4.42	4.38	3.82	4.21	4.48	4.33	4.18
Selectivity									
step1 L_{50}	38.80				36.55	37.15	38.34	35.67	37.17
step1 a ₉₅	11.37	9.30	11.52	12.11	9.23	9.81	10.67	10.25	9.17
step1 a _{max}	0.83	0.85	0.83	0.82	0.89	0.87	0.84	0.91	0.80
step2 L_{50}	<i>37.00</i>	37.00	37.00						
step2 a ₉₅	9.66	10.40	9.63	9.54	10.58	10.28	9.83	13.45	9.63
step2 a _{max}	0.61	0.60	0.62	0.62	0.61	0.62	0.61	0.63	0.57
trawl L_{50}	35.50	35.11	35.45	35.29	33.11	34.51	35.54	32.47	
trawl a ₉₅	12.22	11.85	12.23	12.23	11.28	11.89	12.18	12.57	
trawl a _{max}	1.08	1.08	1.08	1.08	1.13	1.11	1.08	1.12	
photo L_{50}	<i>35.00</i>		35.00						
photo a ₉₅	<i>25.00</i>		25.00						
Process error									
CPUE	0.16	<i>0.10</i>	<i>0.20</i>	<i>0.25</i>	<i>0.15</i>	<i>0.15</i>	<i>0.15</i>	<i>0.15</i>	<i>0.15</i>
Trawl_1	0.00	0.00	0.05	0.09	0.11	0.00	0.00	0.00	
Trawl_2	0.26	0.33	0.25	0.23	0.26	0.28	0.28	0.31	
Photo all	0.00	0.00	0.00	0.00	0.00	0.00	0.00		0.00
Photo part	0.00	0.08	0.00	0.00	0.00	0.00	0.00		0.00

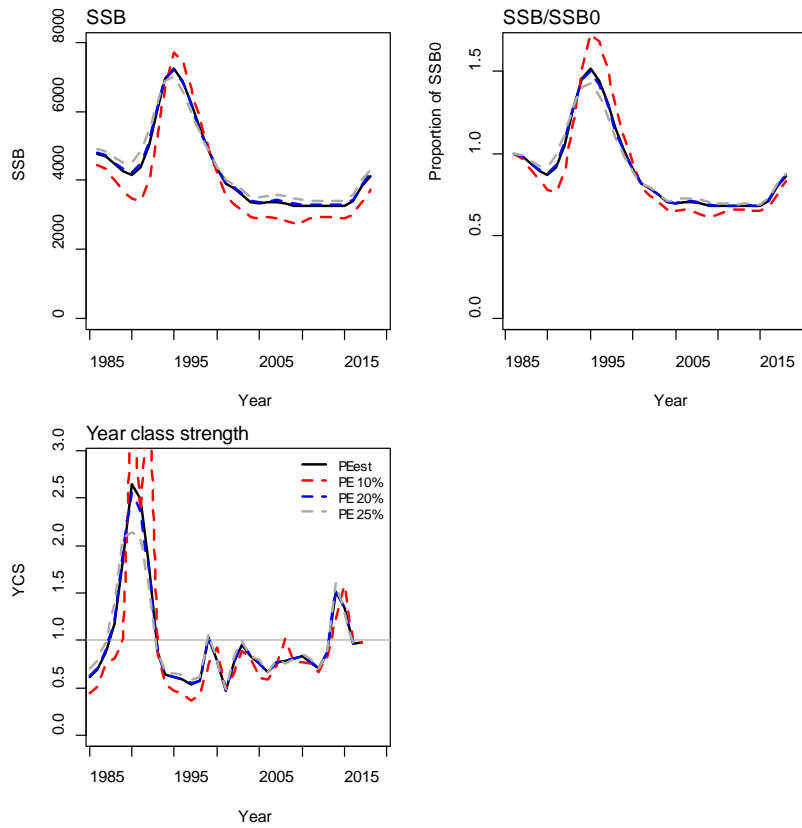


Figure 53: Plots of absolute SSB, SSB as a proportion of SSB_0 , and year class strength (YCS) for MPD fits to the SCI 1 sensitivity runs to CPUE process error.

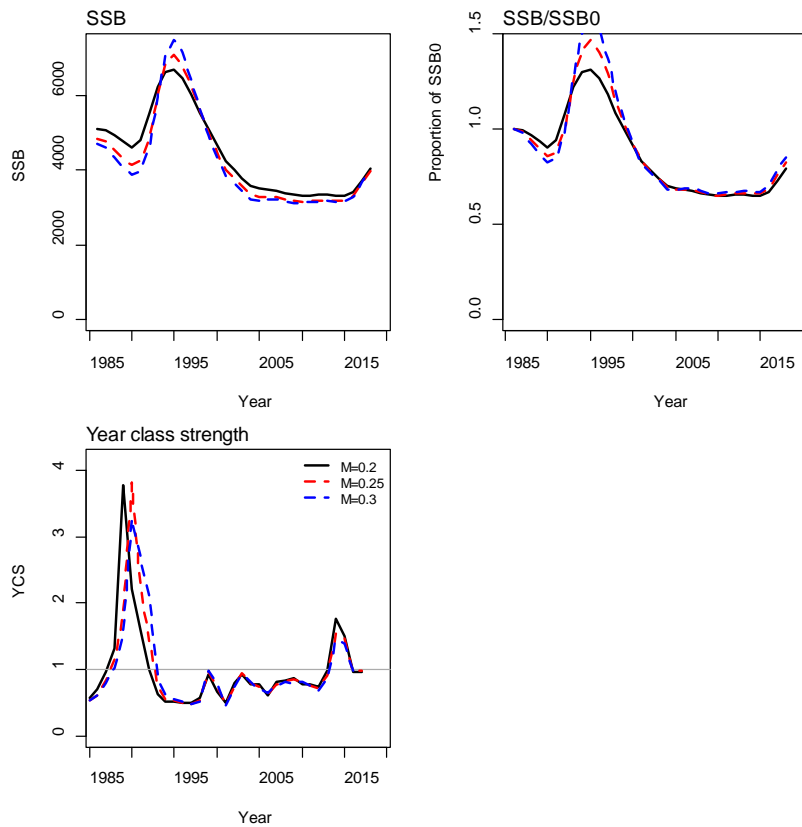


Figure 54: Plots of absolute SSB, SSB as a proportion of SSB_0 , and year class strength (YCS) for MPD fits to the SCI 1 sensitivity runs to natural mortality.

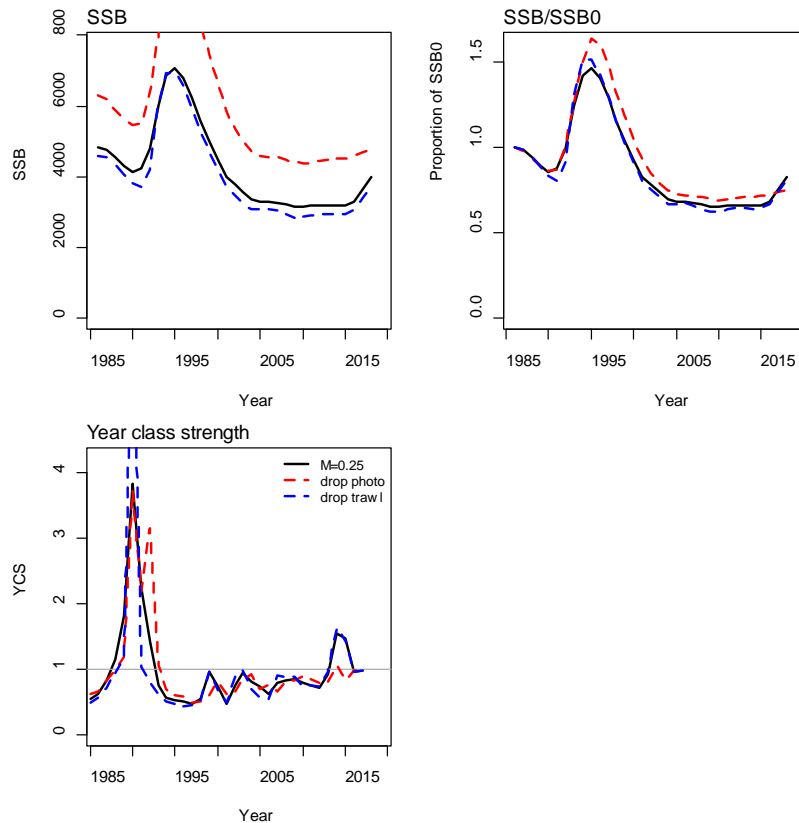


Figure 55: Plots of absolute SSB, SSB as a proportion of SSB_0 , and year class strength (YCS) for MPD fits to the SCI 1 sensitivity runs to exclusion of trawl or photographic surveys.

4.2. Base models for SCI 1

On the basis of presentation of the sensitivity runs to the SFWG, base models with M fixed at 0.2 and 0.25 were examined further, with process error for CPUE fixed at 0.15 and 0.25. Various model output plots and diagnostics are presented as an Appendix for each model (as indicated in the headings below).

4.2.1. SCI 1 M02CV15 (see Appendix 5)

The M02CV15 model ($M = 0.2$, $CV = 0.15$) estimated a SSB_0 of 4183 t, with SSB_{2018} of 2990 t, 71% of SSB_0 . Fits to the abundance indices and normalised residuals (A5. 1) show that the model did not match the observed increase and decline in CPUE in the mid 1990s, but fits to the trawl and photographic surveys (particularly over more recent years) were better. SSB is estimated to have declined slightly to the late 1980s, increased rapidly to 1995, declined through the later 1990s until about 2003, and then increased slightly (A5. 2). Strong year class strengths were estimated around 1990, but have been lower and since increased to average levels. Estimated selectivity curves matched observed changes in sex ratio between time steps, with males less available to trawling during time step 2 (A5. 3). Both parameters for the photo selectivity were fixed because estimated values were considered unrealistic. MPD estimates of trawl and photo survey catchability were within the prior distributions. Individual fits to the observer length frequency distributions were variable (A5. 5, A5. 8, A5. 11) There is some evidence across all time steps of a slight undulating pattern in the residuals from the fits to the length frequency distributions (A5.6, A5.9, A5.12), which may suggest behavioural effects on availability, in addition to the size-based logistic selectivity applied in the model, but the magnitude of the pattern is small (less than half a standard deviation), and there was no

pattern in the residuals in relation to year. Fits to the trawl survey length frequency distributions were generally better (A5.14), but the fits showed a similar pattern in the residuals (A5.15). Fits to the photo length frequencies varied (A5.17), but as discussed above, these had little weight in the model and residuals were acceptable (A5. 18).

The overall likelihood profile when B_0 is fixed was relatively U shaped (A5. 19), but the majority of the signal appears to come from the priors rather than the data.

MCMC runs

MCMC diagnostics provided reasonable evidence the model converged (A5. 20–A5. 24). The posterior trajectory of SSB (Figure 56) suggests an increase in biomass between 1990 and 1994, followed by a decline to about 2004, with the stock increasing slightly after this. The median estimate of current status (SSB_{2018}/SSB_0) is 76% (95% confidence interval 65%–87%), with 0% probability that SSB_{2018} is below 40% SSB_0 .

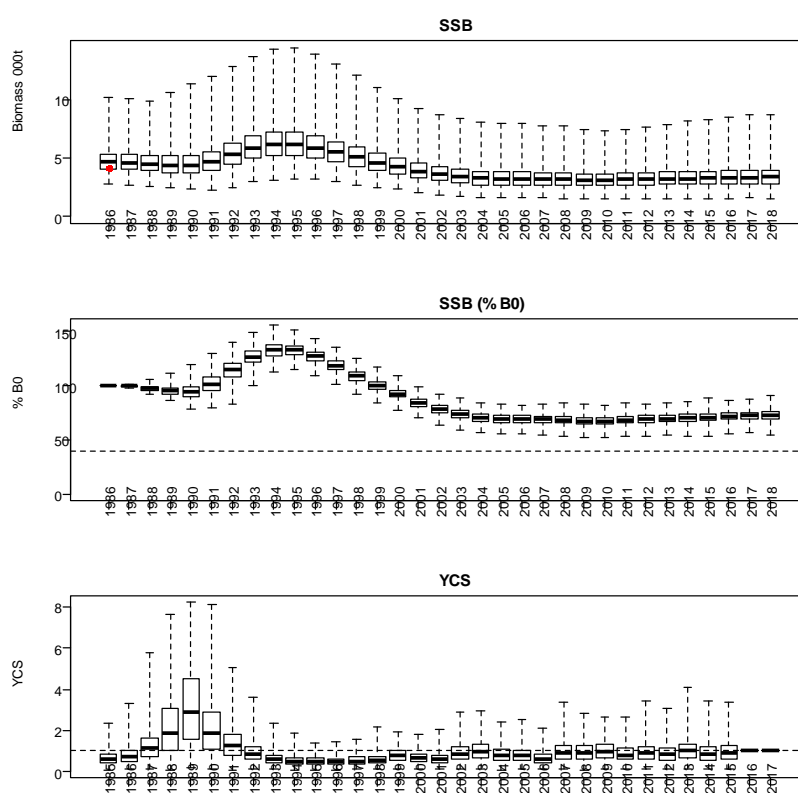


Figure 56: Posterior trajectories of SSB, SSB_{2018}/B_0 , and YCS from the MCMC run for the SCI 1 M02CV15 model. Red dot represents MPD estimate of B_0 .

4.2.2. SCI 1 M02CV25 (see Appendix 6)

The M02CV25 model ($M = 0.2$, $CV = 0.25$) estimated a SSB_0 at 4049 t, with SSB_{2018} of 3012 t, 74% of SSB_0 . Fits to the abundance indices and normalised residuals (A6. 1), show that the model did not fit the observed increase and decline in CPUE in the mid 1990s well, although fits to the trawl and photographic surveys (particularly over recent years) were reasonable. SSB is estimated to have increased from 1990 to 1995, declined through the later 1990s until about 2004, and then remained relatively stable (A6. 2). Strong year class strengths were estimated for the late 1980s and early 1990s, followed by a period of consistently below average recruitment until the early 2000s, and then a period of more variable but below average recruitment (A6. 2). Estimated selectivity curves (A6. 3) were similar to those for the M02CV15 model, in that they matched observed changes in sex ratio between

time steps, but also that some estimates had to be fixed because estimated values were considered unrealistic. MPD estimates of trawl and photo survey catchability were within the prior distribution (A6. 4). As with the previous model, fits to the observer length frequency distributions were variable (A6. 5, A6. 8, A6. 11), and there was slight evidence of a pattern in the residuals with length (A6.6, A6.9, A6.12). Fits to the trawl survey length data appeared better (A6.14), but the pattern in the residuals appeared stronger (A6.15). Fits to the photo length frequencies varied (A6.17).

The overall likelihood profile when B_0 is fixed was strongly U shaped (A6.19), but as with the previous model, the majority of the signal appears to come from the priors (and particularly $q-Photo$) rather than the data.

MCMC runs

MCMC diagnostics provided reasonable evidence the model converged (A6. 20–A6. 24). The posterior trajectory of SSB (Figure 57) suggests an increase in biomass between 1990 and 1994, followed by a decline to about 2004, with the stock remaining stable after this. The median estimate of current status (SSB_{2018}/SSB_0) is 74% (95% confidence interval 63%–85%), with 0% probability that SSB_{2018} is below 40% SSB_0 .

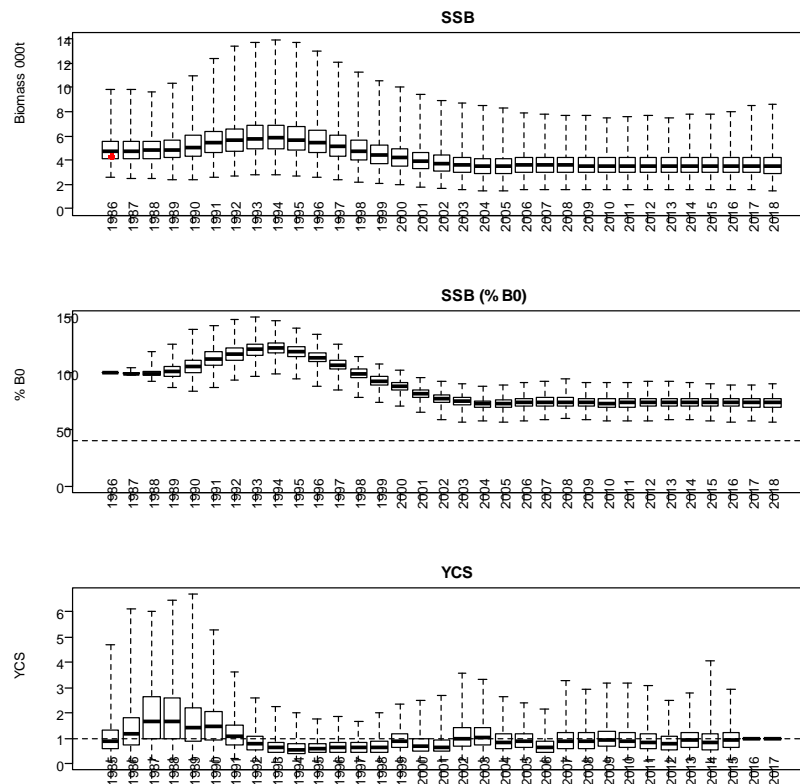


Figure 57: Posterior trajectories of SSB, SSB_{2018}/B_0 , and YCS from the MCMC run for the SCI 1 M02CV25 model. Red dot represents MPD estimate of B_0 .

4.2.3. SCI 1 M025CV15 (see Appendix 7)

The M025CV15 model ($M = 0.25$, $CV = 0.15$) estimated a SSB_0 at 4049 t, with SSB_{2018} at 2867 t, 71% of SSB_0 . Fits to the abundance indices and normalised residuals (A7. 1), show that the model fitted the observed increase and decline in CPUE in the mid 1990s slightly better than the M02CV15 model, which was in turn better than the fits to the M02CV025 model. Fits to the trawl and photographic surveys (particularly over recent years) were similar to previous models, and reasonable. SSB is estimated to have increased rapidly from 1990 to 1995, declined to about 2004, remained relatively stable until about 2010, and increased slightly in recent years (A7. 2). Strong year class strengths are evident around 1990, followed by a period of below average but increasing recruitment (A7. 2).

Estimated selectivity curves (A7. 3) were similar to those for the other models, in that they matched observed changes in sex ratio between time steps. MPD estimates of trawl and photo survey catchability were within the prior distribution (A7. 4). As with the other models, fits to the observer length frequency distributions were variable (e.g., A7. 5), and fits to the trawl length frequencies were better (A7. 14), but both showed evidence of a pattern in the residuals in relation to length, which was more apparent in the trawl survey data (A7. 15).

As with the other SCI 1 models, the overall likelihood profile when B_0 is fixed was strongly U shaped (A7. 19), with the majority of the signal appearing to come from the priors (and particularly q -Photo) rather than the data.

MCMC runs

MCMC diagnostics provided reasonable evidence the model converged (A7. 20–A7. 24). The posterior trajectory of SSB (Figure 58) suggests an increase in biomass between 1991 and 1995, followed by a decline to about 2004, with the stock remaining stable until about 2010, and increasing slightly after this. The median estimate of current status (SSB_{2018}/SSB_0) is 76% (95% confidence interval 65%–87%), with 0% probability that SSB_{2018} is below 40% SSB_0 .

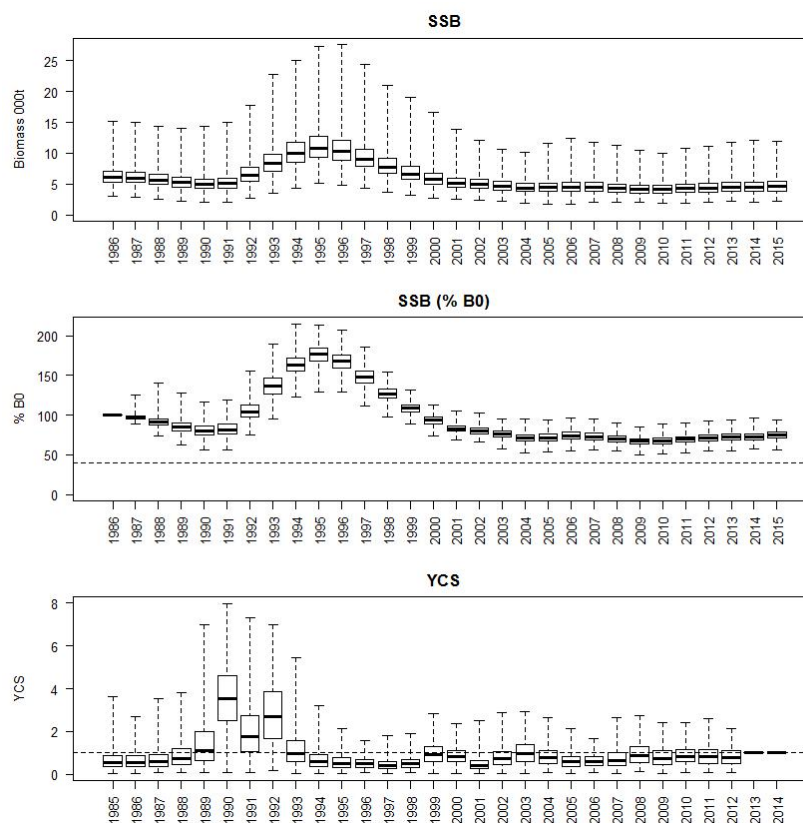


Figure 58: Posterior trajectories of SSB, SSB_{2018}/B_0 , and YCS from the MCMC run for the SCI 1 M025CV15 model.

4.2.4. SCI 1 M025CV25 (see Appendix 8)

The M025CV25 model ($M = 0.25$, $CV = 0.25$) estimated a SSB_0 at 4238 t, with SSB_{2018} at 3180 t, 75% of SSB_0 . Fits to the abundance indices and normalised residuals (A8. 1), show that as with the other higher CV model (M02CV25), the estimated trend in abundance did not match the observed increase and decrease in CPUE in the mid 1990s. Fits to the other series were similar to previous models. SSB is estimated to have increased rapidly from 1990 to 1995, declined to about 2004, and then increased

slightly in recent years (A8. 2). Overall patterns in YCS were very similar to previous models, but the magnitude of the peak recruitment in the early 1990s was lower. Estimated selectivity curves (A8. 3) were also very similar to those for the other models, as were the estimates of trawl and photo survey catchability (A8. 4). Fits to the observer length frequencies were variable (e.g., A8. 5), and fits to the trawl length frequencies were better (A8. 14), but both showed evidence of the same pattern in the residuals in relation to length observed in other models (A8. 15).

As with the other SCI 1 models, the overall likelihood profile when B_0 is fixed was strongly U shaped (A8. 19), with the majority of the signal appearing to come from the priors (and particularly q -Photo), and little signal coming from the data.

MCMC runs

MCMC diagnostics provided reasonable evidence the model converged (A8. 20 – A8. 24). As with the previous models, the posterior trajectory of SSB (Figure 59) suggests an increase in biomass between 1990 and 1994, followed by a decline to about 2004. For this model, SSB increases slightly in the mid2000s, and then again in more recent years. The median estimate of current status (SSB_{2018}/SSB_0) is 76% (95% confidence interval 64%–88%), with 0% probability that SSB_{2018} is below 40% SSB_0 .

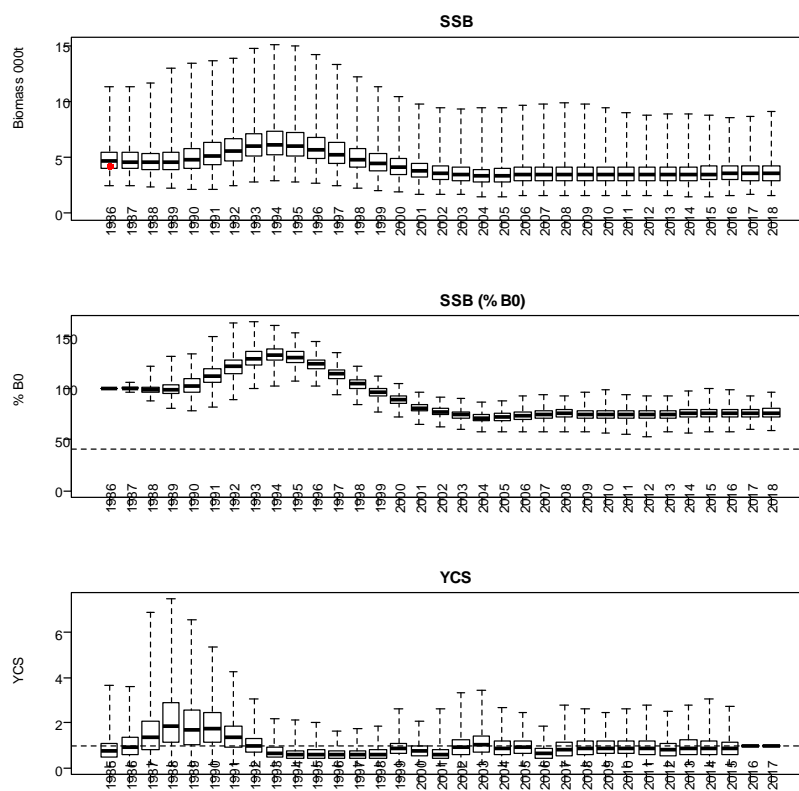


Figure 59: Posterior trajectories of SSB, SSB_{2018}/B_0 , and YCS from the MCMC run for the SCI 1 M025CV25 model. Red dot represents MPD estimate of B_0 .

4.3. SCI 1 Fishing Pressure

Model outputs were very similar across the sensitivity runs, and only the phase plot for the M025CV15 model is presented. Annual fishing intensity (equivalent annual F) and the level of fishing, that if applied for ever would result in an equilibrium biomass of 40% SSB_0 (F 40% B_0), were calculated using methods described by Cordue (2012). Plots of annual fishing intensity against proportion SSB_0 (presented for the M025CV15 model in Figure 60) show that although SSB has declined since the mid 1990s with the development of the fishery, it remains well above the 40% SSB_0 target, and annual fishing intensity remains well below F 40% B_0 . Annual catches of 100–120 tonnes throughout much of the history of the fishery are low relative to the current estimated biomass of around 4000 tonnes, and so estimates of F are low.

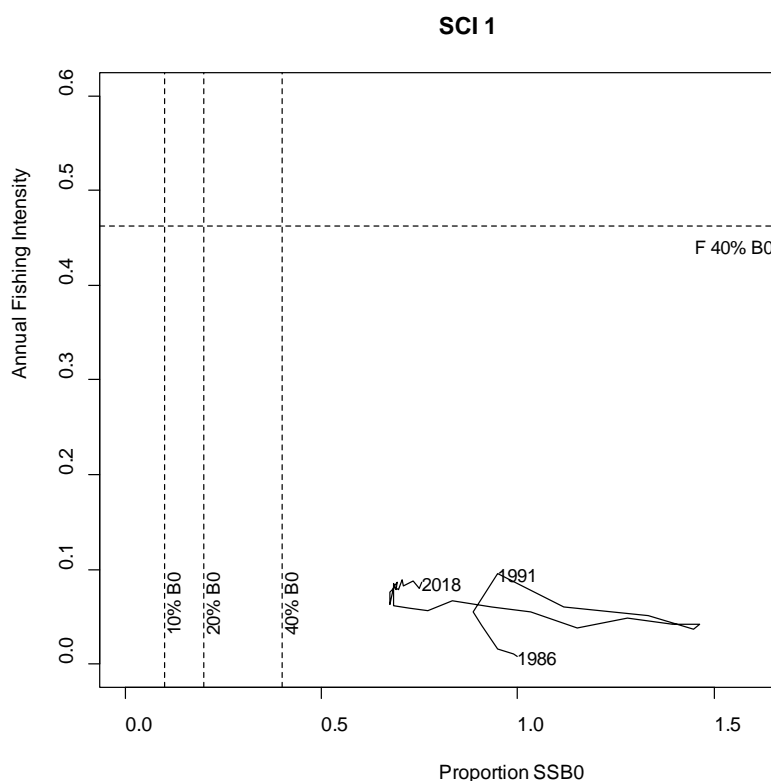


Figure 60: Trajectory of annual fishing intensity (equivalent annual F) plotted against proportion SSB_0 for the SCI 1 M025CV15 model, in relation to Harvest Strategy Standard target and limit reference points.

5. SCI 2 - ASSESSMENT MODEL RESULTS

5.1. Initial models

As with SCI 1, a single area model was applied, with an annual CPUE index, but for this stock the trawl survey data was fitted as two separate indices in different time steps. The same model developments since the last assessment were applied to the SCI 2 model (Table 27), and sensitivity analyses were run. Key parameter and quantity estimates from the MPD fits for the models are presented in Table 28, with stock and recruitment trajectories for the models presented in Figure 61 and catchabilities in relation to the informed prior distributions in Figure 62.

Table 27: General details of initial models examined within sensitivity analyses for SCI 2.

Model name	Final year	YCS	q priors	M	CPUE CV	Survey process error
2015	2015	Old	Old	0.3	0.1	estimated
YC	2015	New	Old	0.3	0.1	estimated
new q	2015	New	New	0.3	0.1	estimated
2018	2018	New	New	0.3	0.1	estimated

The revised parameterisation of the YCS slightly reduced the magnitude of the peak recruitments estimated at the beginning and towards the end of the time series (Figure 61), but the overall YCS pattern remained very similar. The magnitude of stock increases associated with these peak recruitments was slightly lower with the revised parameterisation, and both B_0 and B_{2018} relative to B_0 were slightly reduced compared with the 2015 model, although the stock trajectory up to about 2012 appeared unaffected. The revised catchability priors reduced the estimate of B_0 , and also B_{2018}/B_0 , but did not affect YCS or the earlier stock trajectory. The new priors resulted in larger estimated q values for q -Photo, but did not appear to affect q -Trawl (Figure 62). Updating the model data up to the 2018 fishing year (new survey and length frequency data) resulted in a further increase in catchability estimates, and a reduced estimate of B_0 , but did not affect YCS. The most recent survey and CPUE data suggest a decline in abundance since 2015, and this is also reflected in stock trajectory patterns for the most recent years. The previous assessments (Tuck 2016) and these updates were unable to provide plausible estimates for photo survey selectivity parameters, and so these were fixed.

Table 28: Estimated key parameters and quantities from MPD fits for SCI 2 initial sensitivity model runs. Italicised values indicate parameters that were fixed rather than estimated.

	2015	YC	new q	2018
SSB ₀	2749	2687	2376	2075
SSB ₂₀₁₅	2779	2606	2147	1723
SSB ₂₀₁₅ /SSB ₀	1.01	0.97	0.90	0.83
q -Photo	3.8353	3.9789	5.5026	7.0015
q -Trawl	0.0758	0.0723	0.0744	0.0823
Growth				
Male g ₂₀	12.09	12.20	12.66	12.49
Male g ₄₀	2.55	2.63	3.01	3.38
Female g ₂₀	12.54	12.45	12.68	12.77
Female g ₄₀	0.00	0.13	0.57	1.15
min_sigma	4.58	4.51	4.37	4.23
Selectivity				
step1 L ₅₀	44.32	43.28	42.80	41.68
step1 a ₉₅	14.53	14.53	14.47	13.30
step1 a _{max}	0.87	0.86	0.86	0.88
step2 L ₅₀	46.62	47.02	45.29	42.87
step2 a ₉₅	19.40	19.74	18.77	17.25
step2 a _{max}	0.50	0.50	0.50	0.51
trawl 1 L ₅₀	37.59	36.02	34.11	33.11
trawl 1 a ₉₅	16.88	15.51	14.06	12.69
trawl 1 a _{max}	1.09	1.09	1.11	1.13
trawl 2 L ₅₀	37.59	36.02	34.11	33.11
trawl 2 a ₉₅	16.88	15.51	14.06	12.69
trawl 2 a _{max}	1.09	1.09	1.11	1.13
photo L ₅₀	35.00	35.00	35.00	35.00
photo a ₉₅	25.00	25.00	25.00	25.00
Process error				
CPUE	0.10	0.14	0.15	0.14
Trawl_1	0.00	0.00	0.00	0.00
Trawl_2	0.56	0.59	0.58	0.58
Photo all	0.41	0.39	0.36	0.29

As with the SCI 1 models, attempts to estimate natural mortality within the model were not considered reliable, and therefore M was fixed at 0.3, and sensitivity analyses were run. Sensitivity analyses were also run in relation to the CPUE process error (CV), the estimation of photo survey selectivity, and the exclusion of survey time series. Details of differences between models examined within these further sensitivity analyses are presented in Table 29.

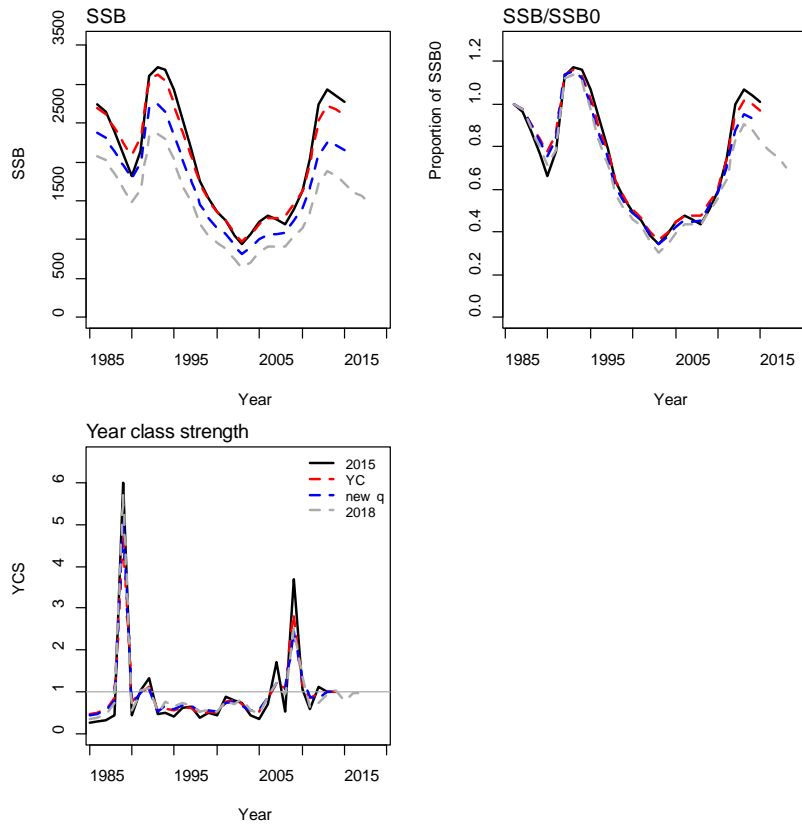


Figure 61: Plots of absolute SSB, SSB as a proportion of SSB₀, and year class strength (YCS) for MPD fits to the initial SCI 2 sensitivity runs.

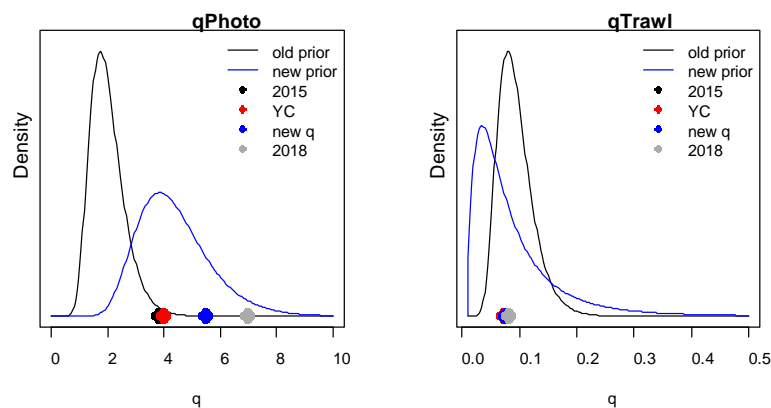


Figure 62: Prior distributions for the informed q terms (old and new versions) and estimated for MPD fits to the initial SCI 2 sensitivity runs.

Table 29: General details of models examined within further sensitivity analyses for SCI 2. All models used the new YCS parameterisation and new q priors and included data to the 2018 fishing year. PE is CPUE process error.

Model name	M	CPUE CV	Survey process error	Photo selectivity	Survey data
PE est	0.3	estimated	estimated	fixed	all
PE 10%	0.3	0.10	estimated	estimated	all
PE 20%	0.3	0.20	estimated	estimated	all
PE 25%	0.3	0.25	estimated	estimated	all
$M=0.2$	0.2	0.15	estimated	estimated	all
$M=0.25$	0.25	0.15	estimated	estimated	all
$M=0.3$	0.3	0.15	estimated	estimated	all
$M=0.25p$	0.25	0.15	estimated	fixed	all
Drop photo	0.25	0.15	estimated		photo excluded
Drop trawl	0.25	0.15	estimated	fixed	trawl excluded

Exploration of the effect of process error on the CPUE series (Figure 63; Table 30) estimated process error at 0.14, and identified that estimated B_0 showed little sensitivity, other than for the higher process error considered (25%). Changing the process error slightly shifted the timing of the peak YCS in the early 1990s (and growth parameters), but not the overall pattern. The process error on CPUE affected the model's ability to match the magnitude of the fluctuation in CPUE in the early 1990s, but had minimal effect on the estimate of stock trajectory after about 1995 (Figure 63).

As with the SCI 1 models, estimates of B_0 were sensitive to natural mortality assumptions (Figure 64; Table 30), with B_0 decreasing as M increased, and the magnitude of the population increase and decline in the mid 1990s and around 2014 also increased with increasing M . Overall stock trajectory in recent years was far less sensitive, and, other than a slight shift in the timing of peak YCS (associated with slight changes in growth parameters), the patterns in YCS appear very similar between models.

The estimate of B_0 was sensitive to the exclusion of either survey data series (along with the associated catchability prior and length composition data), but showed only slight differences when the trawl survey data were excluded (Figure 65; Table 30), although the stock trajectory was relatively less sensitive. Excluding the photographic data from the model results in the estimation of a smaller B_0 , and a slightly lower stock trajectory from the mid 1990s, but has minimal effect on the YCS pattern. Excluding the trawl survey data results in the estimation of a larger B_0 , but a smaller relative increase in the mid 1990s. Stock trajectory is higher than the base (both surveys) model between about 1997 and 2010, but falls below the other models between 2010 and 2015, exceeding them after this, because the estimated improvement in recruitment occurs later in this model.

Photo selectivity was estimated in some sensitivity runs, but was only constrained to plausible values by the parameter bounds. As discussed above, the size distribution of scampi generating the major burrow openings recorded in the surveys was estimated from the width of the burrows and a carapace length to burrow width relationship generated from images collected in early surveys (see Section 3.6.3). It is currently unclear whether generation of the carapace length-burrow width relationship accounted for potential foreshortening effects of measuring scampi carapace length from images, when the animals may not be perpendicular to the plane of the image. The potential implications of such a foreshortening effect were explored by running sensitivity analyses (Table 31) assuming scampi were on average at 15° or 25° from the horizontal, and recalculating the length frequency on the basis of this (Figure 66), incorporating the revised data into the assessment model. The effect of increasing the assumed angle from the horizontal is to increase the overall length distribution (Figure 66).

Table 30: Estimated key parameters and quantities from MPD fits for SCI 2 sensitivity model runs described in Table 29. Italicised values indicate parameters that were fixed rather than estimated.

	PE est	PE 10%	PE 20%	PE 25%	<i>M=0.2</i>	<i>M=0.25</i>	<i>M=0.3</i>	<i>M=0.25p</i>	Drop photo	Drop trawl
SSB ₀	2075	1984	2090	2435	2989	2378	2109	2411	2077	2589
SSB ₂₀₁₈	1461	1385	1446	1709	2140	1660	1478	1696	1254	1861
SSB ₂₀₁₈ /SSB ₀	0.70	0.70	0.69	0.70	0.72	0.70	0.70	0.70	0.60	0.77
<i>q-Photo</i>	7.0015	6.6325	6.0168	4.6339	4.5762	5.7044	5.9512	6.3366		5.4094
<i>q-Trawl</i>	0.0823	0.1197	0.0811	0.0661	0.0610	0.0769	0.0834	0.0770	0.0885	
Growth										
Male g ₂₀	12.49	14.13	12.92	10.39	10.67	12.70	12.84	12.38	13.01	11.87
Male g ₄₀	3.38	2.92	3.38	3.19	2.02	2.68	3.42	2.65	3.23	2.33
Female g ₂₀	12.77	14.09	12.80	10.38	10.90	12.77	12.74	12.49	13.01	11.32
Female g ₄₀	1.15	0.00	1.08	1.38	0.00	0.24	1.11	0.23	0.91	0.00
min_sigma	4.23	5.21	4.34	3.67	4.28	4.67	4.32	4.64	4.39	4.64
Selectivity										
step1 L ₅₀	41.68	40.79	40.73	41.78	38.80	39.91	41.05	39.71	40.03	38.58
step1 a ₉₅	13.30	13.95	13.00	13.03	12.71	13.10	12.96	12.70	12.82	12.07
step1 a _{max}	0.88	0.91	0.89	0.86	0.89	0.91	0.90	0.91	0.91	0.86
step2 L ₅₀	42.87	43.54	42.16	42.58	40.77	43.04	43.25	40.76	41.75	42.61
step2 a ₉₅	17.25	19.29	16.79	14.95	17.41	19.76	18.01	16.90	17.59	17.71
step2 a _{max}	0.51	0.54	0.53	0.51	0.52	0.53	0.52	0.54	0.53	0.49
trawl 1 L ₅₀	33.11	39.21	32.77	32.94	31.38	32.68	33.67	33.23	31.58	
trawl 1 a ₉₅	12.69	16.98	13.05	10.95	10.92	13.84	13.52	13.87	12.61	
trawl 1 a _{max}	1.13	1.06	1.11	1.11	1.12	1.11	1.10	1.11	1.12	
trawl 2 L ₅₀	33.11	39.21	32.77	32.94	31.38	32.68	33.67	33.23	31.58	
trawl 2 a ₉₅	12.69	16.98	13.05	10.95	10.92	13.84	13.52	13.87	12.61	
trawl 2 a _{max}	1.13	1.06	1.11	1.11	1.12	1.11	1.10	1.11	1.12	
photo L ₅₀	<i>35.00</i>	30.00	30.00	31.42	30.00	30.01	30.04	<i>35.00</i>		<i>35.00</i>
photo a ₉₅	<i>25.00</i>	29.04	28.45	18.30	29.95	29.95	28.85	<i>25.00</i>		<i>25.00</i>
Process error										
CPUE	0.14	<i>0.10</i>	<i>0.20</i>	<i>0.25</i>	<i>0.15</i>	<i>0.15</i>	<i>0.15</i>	<i>0.15</i>	<i>0.15</i>	<i>0.15</i>
Trawl_1	0.00	0.20	0.00	0.00	0.00	0.00	0.00	0.00	0.00	
Trawl_2	0.58	0.57	0.58	0.61	0.62	0.59	0.58	0.59	0.57	
Photo all	0.29	0.25	0.26	0.26	0.24	0.27	0.27	0.27		0.00

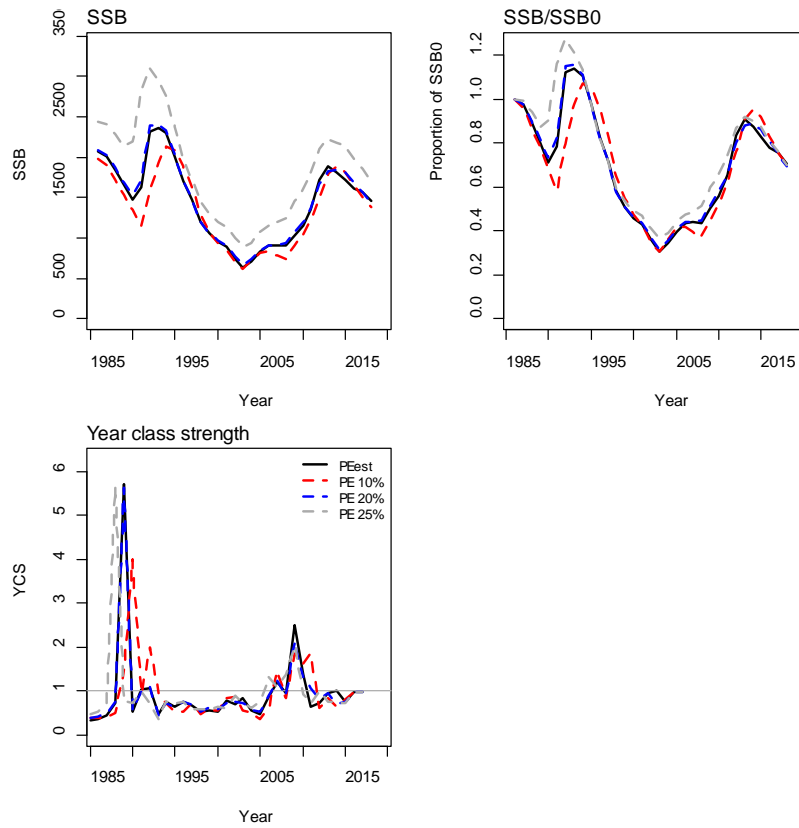


Figure 63: Plots of absolute SSB, SSB as a proportion of SSB₀, and year class strength (YCS) for MPD fits to the SCI 2 sensitivity runs to CPUE process error.

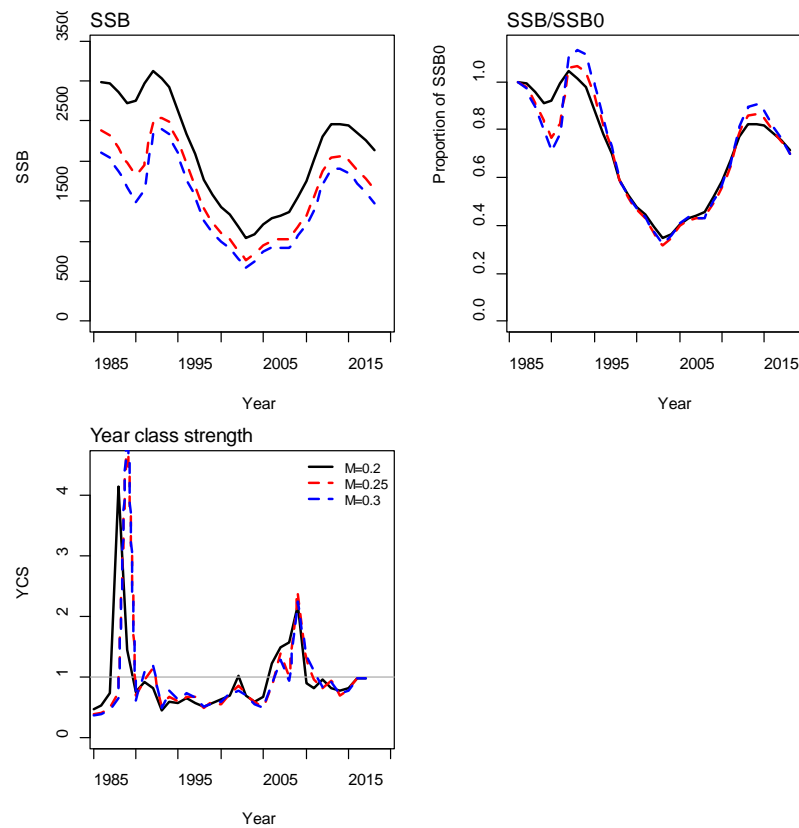


Figure 64: Plots of absolute SSB, SSB as a proportion of SSB₀, and year class strength (YCS) for MPD fits to the SCI 2 sensitivity runs to natural mortality.

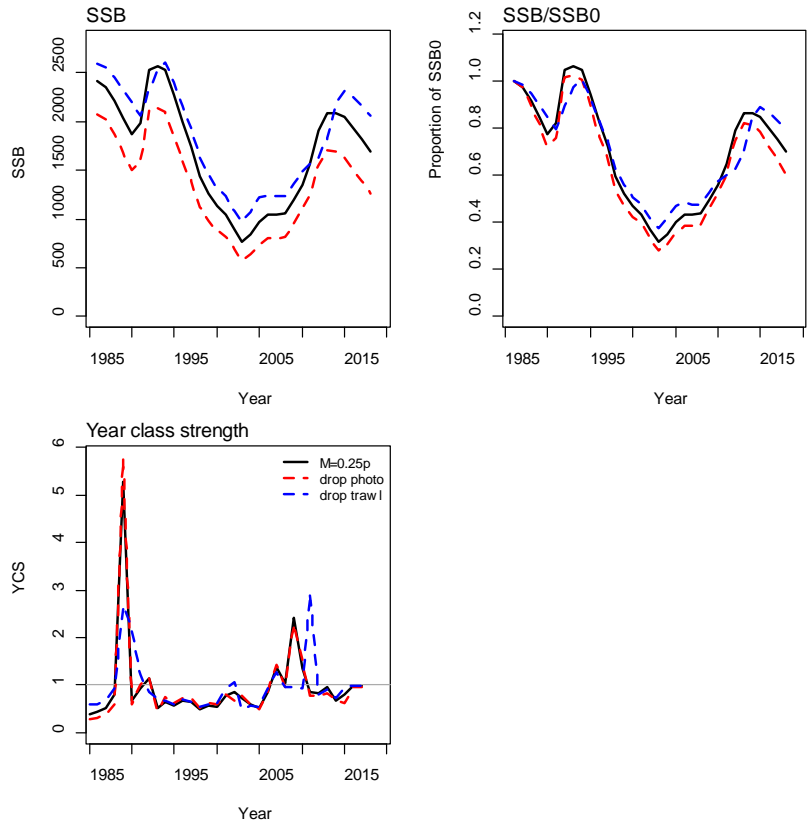


Figure 65: Plots of absolute SSB, SSB as a proportion of SSB₀, and year class strength (YCS) for MPD fits to the SCI 2 sensitivity runs to exclusion of trawl or photographic surveys.

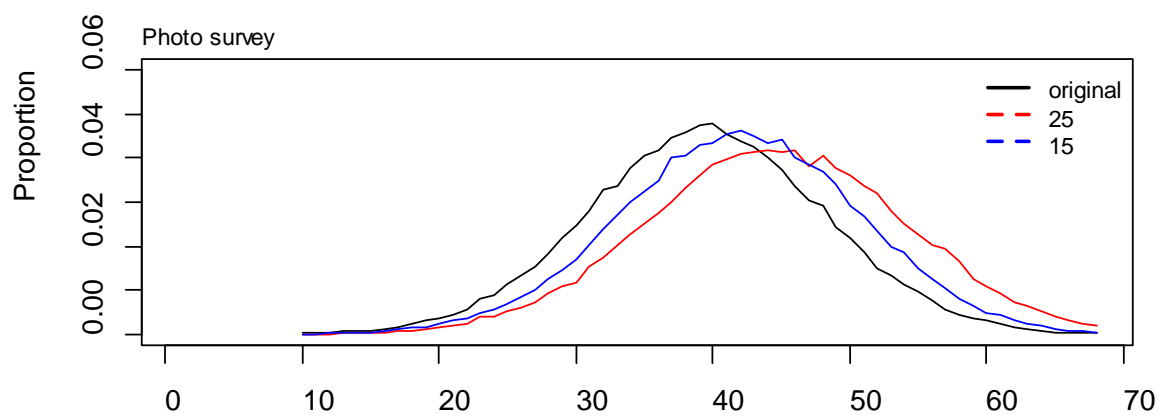


Figure 66: Average estimated length composition (mm) from photo survey, from the original estimation and adjusting the measurements allowing for animals being 15° or 25° from the horizontal

Table 31: General details of models examined within photo length frequency sensitivity analyses for SCI 2. All models used the new YCS parameterisation and new q priors and included data to the 2018 fishing year.

Model name	M	CPUE CV	Survey process error	Photo selectivity	Survey data
original	0.25	0.15	fixed	fixed	all
25	0.25	0.15	fixed	estimated	all
15	0.25	0.15	fixed	estimated	all

Model outputs were sensitive to the shift in the photo survey length composition associated with foreshortening assumptions (Figure 67, Table 32). As the potential foreshortening increased the estimated length of scampi creating the observed burrows, the L_{50} of the estimated selectivity increased (Figure 68). Estimated B_0 and current stock status (B_{2018}/B_0) also increased, but the overall pattern of stock trajectory remained similar, and YCS patterns were not affected. Fits to the photo survey length frequency data varied between the models (Figure 69), but none was consistently better across the time series of available data.

The working group agreed that although the model was sensitive to any potential foreshortening effect, it would be unlikely to change the perception of current stock status in a way that would raise concerns over current sustainability. Photographic survey length composition data should be re-examined prior to future assessments using data in this way, to clarify the foreshortening issue.

Table 32: Estimated key parameters and quantities from MPD fits for SCI 2 sensitivity model runs described in Table 31. Italicised values indicate parameters that were fixed rather than estimated.

	original	15	25
SSB ₀	2796	3030	3508
SSB ₂₀₁₈	2128	2384	2833
SSB ₂₀₁₈ /SSB ₀	0.76	0.79	0.81
<i>q-Photo</i>	4.9492	5.3593	6.7695
<i>q-Trawl</i>	0.0648	0.0547	0.0422
Growth			
Male g ₂₀	10.05	10.80	10.38
Male g ₄₀	2.50	2.61	2.87
Female g ₂₀	10.36	10.95	10.46
Female g ₄₀	0.53	0.50	0.94
min_sigma	4.07	4.18	3.77
Selectivity			
step1 L_{50}	40.91	40.14	39.89
step1 a ₉₅	12.77	12.84	12.55
step1 a _{max}	0.89	0.88	0.86
step2 L_{50}	41.56	39.79	38.24
step2 a ₉₅	15.20	14.69	13.41
step2 a _{max}	0.53	0.53	0.53
trawl 1 L_{50}	34.21	32.67	30.89
trawl 1 a ₉₅	12.32	11.55	9.66
trawl 1 a _{max}	1.11	1.12	1.13
trawl 2 L_{50}	34.21	32.67	30.89
trawl 2 a ₉₅	12.32	11.55	9.66
trawl 2 a _{max}	1.11	1.12	1.13
photo L_{50}	<i>35.00</i>	38.51	45.72
photo a ₉₅	<i>25.00</i>	24.73	23.10
Process error			
CPUE	<i>0.15</i>	<i>0.15</i>	<i>0.15</i>
Trawl_1	<i>0.20</i>	<i>0.20</i>	<i>0.20</i>
Trawl_2	<i>0.20</i>	<i>0.20</i>	<i>0.20</i>
Photo all	<i>0.20</i>	<i>0.20</i>	<i>0.20</i>

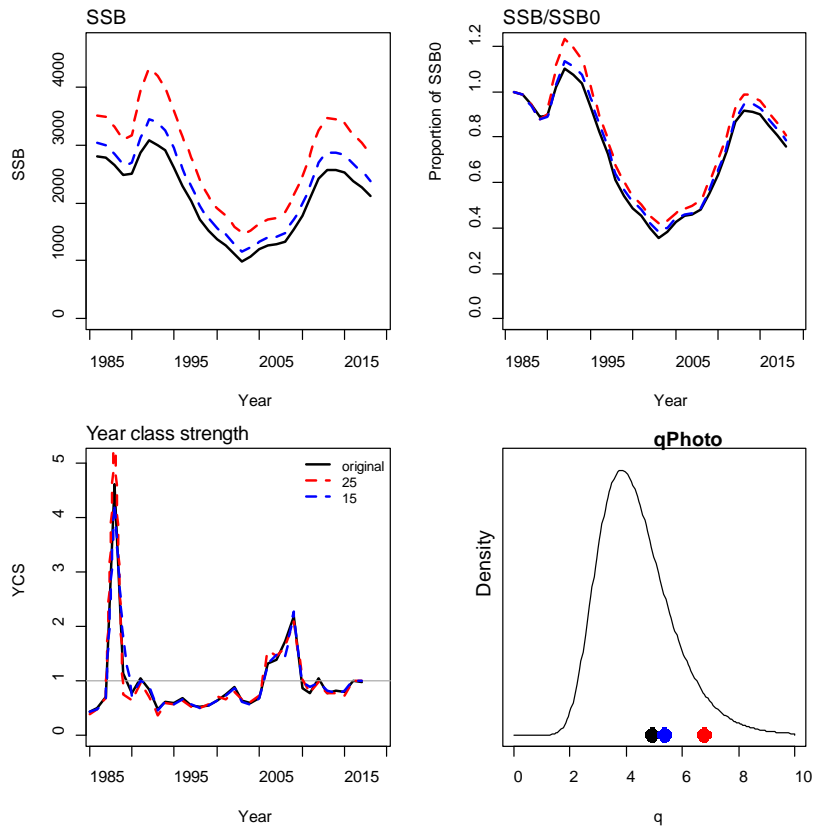


Figure 67: Plots of absolute SSB, SSB as a proportion of SSB_0 , and year class strength (YCS) and estimates of q -Photo in relation to the prior distribution for MPD fits to the SCI 2 sensitivity runs to the photographic survey length frequency distribution data.

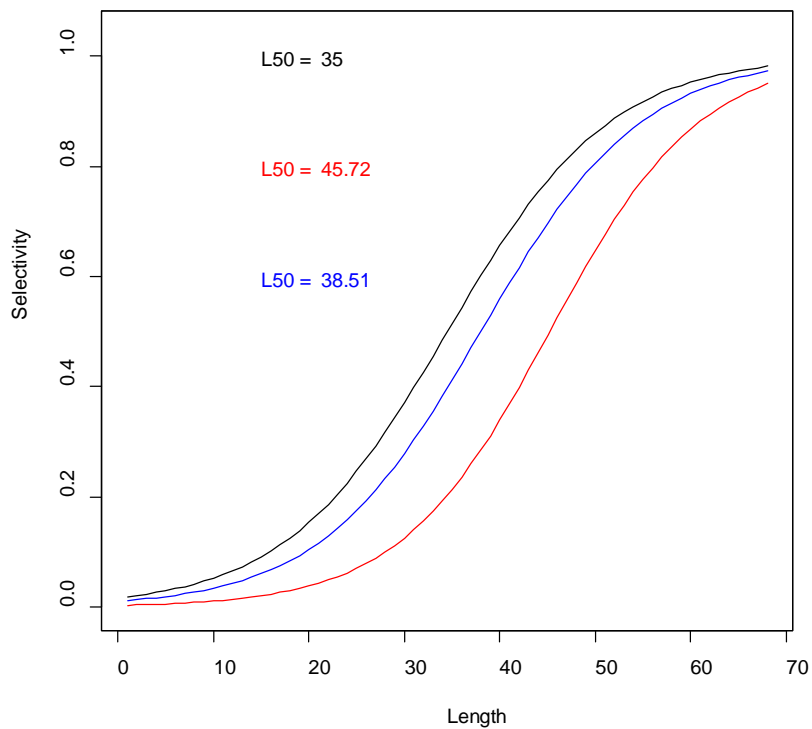


Figure 68: Selectivity ogives for the photo selectivity for models presented above (Figure 67), for length (mm).

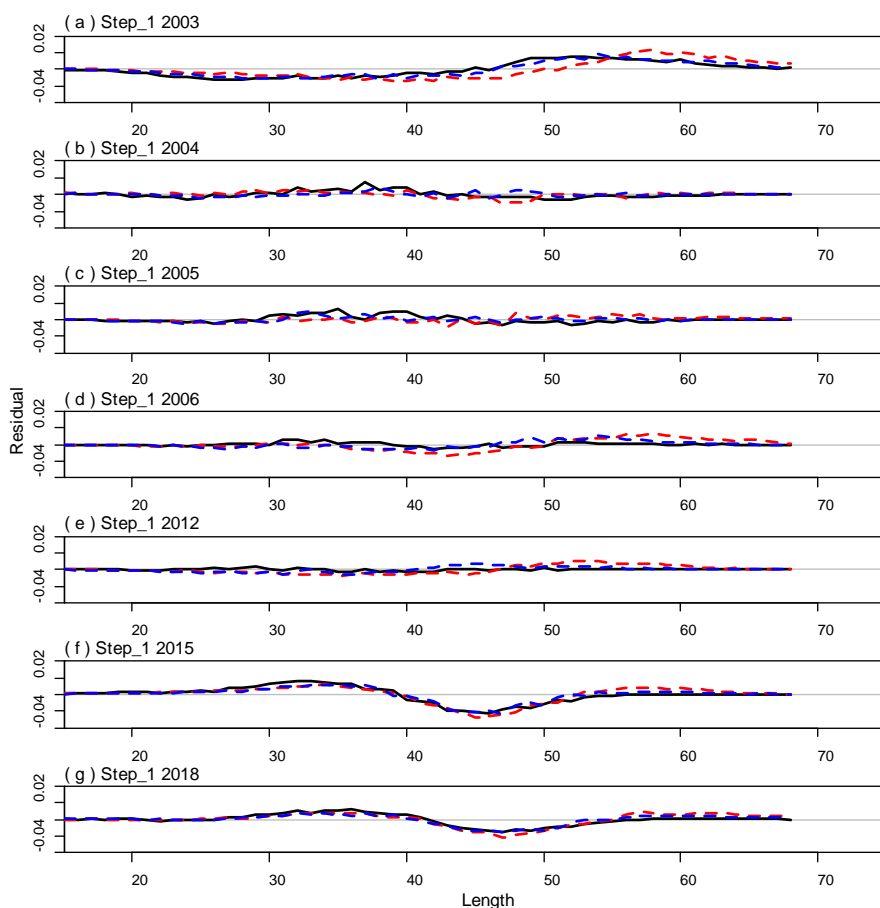


Figure 69 Residuals to fits of photo survey length (mm) composition data for 3 models presented above (Figure 67).

5.2. Base models for SCI 2

On the basis of presentation of the sensitivity runs to the SFWG, base models with M fixed at 0.2 and 0.25 were examined further, with process error for CPUE fixed at 0.15 and 0.25. Various model output plots and diagnostics are presented as an Appendix for each model.

5.2.1. SCI 2 M02CV15 (see Appendix 9)

The M02CV15 model ($M = 0.2$, $CV = 0.15$) estimated a SSB_0 of 3069 t, with SSB_{2018} of 2273 t, 74% of SSB_0 . Fits to the abundance indices and normalised residuals (A9. 1) show that the model estimated a stable abundance in the early 1990s followed by a decline, rather than the observed initial decline, followed by an increase to a peak CPUE in the mid 1990s and a subsequent sharper decline. The model also did not match the increase in CPUE observed in 2014 and 2015. Fits to the declining trawl survey abundance between the early 1990s and 2005 were good, but the model did not match the magnitude of the increase in catch rates observed in recent years. The overall fit to the photo survey was good, but the model underestimated the abundance in 2004 and overestimated abundance in 2012. SSB is estimated to have remained relatively stable until the early 1990s, then declined steadily until about 2003 (to just below 40% B_0), but recovered to levels approaching those of the early 1990s by 2014 before declining slightly in the most recent years (A9. 2). Particularly strong year class strengths were estimated in 1988 and (to a lesser extent) in 2008 and 2009, with a period of below average recruitment in the intervening period. Estimated selectivity curves matched observed changes in sex ratio between time steps, with males less available to trawling during time step 2 (A9. 3). As with the SCI 1 models, L_{50} for the photo selectivity was fixed because estimated values were considered

unrealistic. MPD estimates of trawl and photo survey catchability were within the prior distributions (A9. 4). Fits to the observer length frequency distributions were variable (e.g., A9. 5), and as with the SCI 1 models, although fits to the trawl length frequencies were better (e.g., A9. 17), both showed evidence of the same undulating pattern in the residuals in relation to length observed in other models (e.g., A9. 18).

The overall likelihood profile when B_0 is fixed was U shaped (A9. 22), with overall contributions from the abundance indices, proportions, and priors suggesting a reasonably consistent B_0 , although there were some differences between individual data sets. The priors suggest a larger biomass than the data, but appear far less influential than for the SCI 1 models.

MCMC runs

MCMC diagnostics provided reasonable evidence the model converged (A9. 23–A9. 27). The posterior trajectory of SSB (Figure 70) suggests a stable biomass (around B_0) until around 1994, followed by a decline to just below 40% B_0 by 2003. Biomass increased slowly after this until higher than average YCSs between 2007 and 2009 led to an increase in biomass, which peaked around 2014 (around 80% B_0), but has declined since this time. The median estimate of current status (SSB_{2018}/SSB_0) is 75% (95% confidence interval 64%–87%), with 0% probability that SSB_{2018} is below 40% SSB_0 .

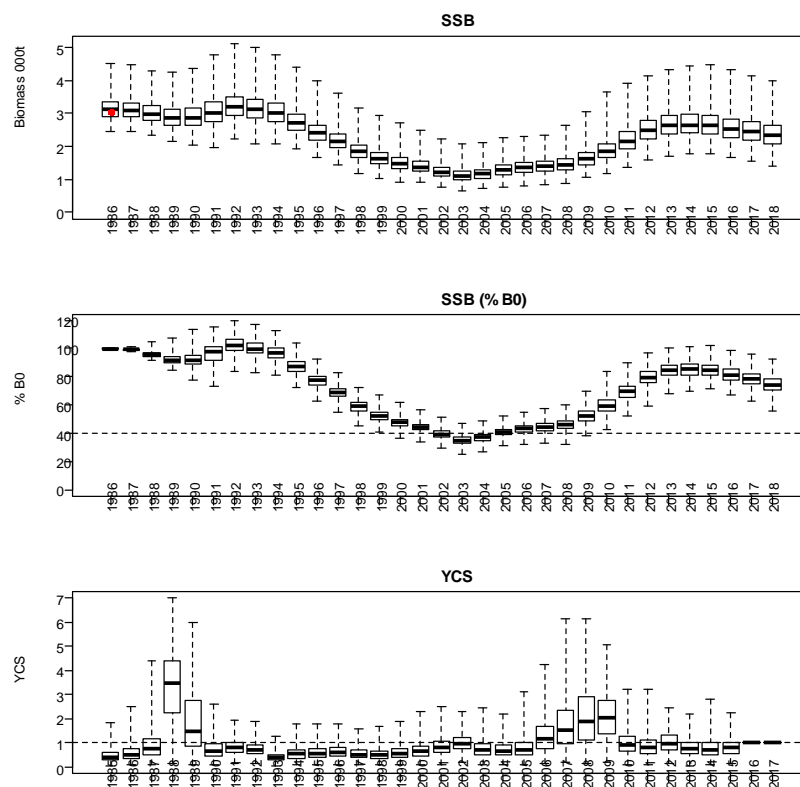


Figure 70: Posterior trajectory of SSB, SSB/ SSB_0 , and YCS for the SCI 2 M02CV15 model. Red dot represents MPD estimate of B_0 .

5.2.2. SCI 2 M02CV25 (see Appendix 10)

The M02CV25 model ($M = 0.2$, $CV = 0.25$) estimated a SSB_0 of 2918 t, with SSB_{2018} of 2100 t, 72% of SSB_0 . Fits to the abundance indices and normalised residuals (A10. 1), show that the model estimated a slowly declining abundance in the early 1990s followed by a steeper decline to 2004,

rather than the observed increase to a peak CPUE in the mid 1990s. The model also did not match the increase in CPUE observed in 2014 and 2015. As with the previous model, fits to the declining trawl survey abundance between the early 1990s and 2005 were good, but the model did not match the magnitude of the increase in catch rates observed in more recent years. Again, the overall fit to the photo survey was good, but the model underestimated the abundance in 2004, and overestimated abundance in 2012. SSB is estimated to have remained relatively stable until the early 1990s, then declined steadily until about 2003 (to just below 40% B_0), but recovered to levels approaching those of the early 1990s by 2014, before declining slightly in the most recent years (A10. 2). Particularly strong year class strengths were estimated in 1988 and (to a lesser extent) in 2008 and 2009, with a period of below average recruitment in the intervening period. Estimated selectivity curves were similar to the previous model and matched observed changes in sex ratio between time steps (A10. 3). MPD estimates of trawl and photo survey catchability were within the prior distributions (A10. 4). Fits to the length frequencies were similar to the previous model, with fits to the observer data variable (e.g., A10. 5), and better fits to the trawl length frequencies (e.g., A10. 17), with both showing evidence of a pattern in the residuals (e.g., A10. 18).

The overall likelihood profile when B_0 is fixed was U shaped (A10. 22), with individual data sets showing a similar pattern to the previous model.

MCMC runs

MCMC diagnostics provided reasonable evidence the model converged (A10. 23–A10. 27). The posterior trajectory of SSB (Figure 71) was very similar to the previous model, suggesting a stable biomass (around B_0) until around 1994, followed by a decline to just below 40% B_0 by 2003. Biomass increased slowly after this until higher than average YCSs between 2007 and 2009 led to an increase in biomass, which peaked around 2014 (around 80% B_0), but has declined since this time. The median estimate of current status (SSB_{2018}/SSB_0) is 73% (95% confidence interval 60%–88%), with 0% probability that SSB_{2018} is below 40% SSB_0 .

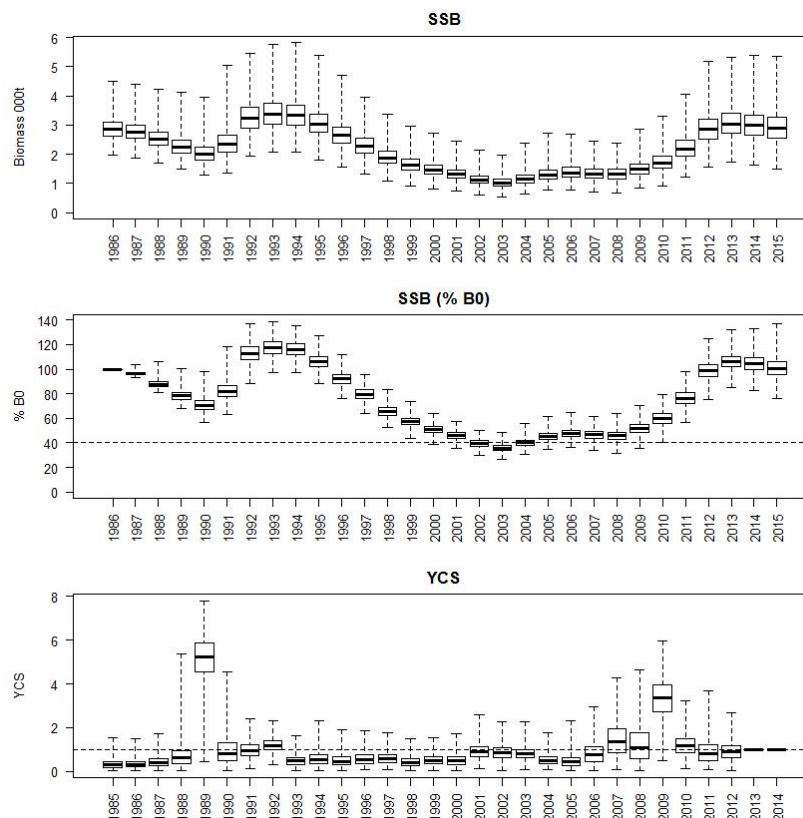


Figure 71: Posterior trajectory of SSB, SSB/SSB_0 , and YCS for the SCI 2 M02CV25 model.

5.2.3. SCI 2 M025CV15 (see Appendix 11)

The M025CV15 model ($M = 0.25$, $CV = 0.15$) estimated a SSB_0 of 2796 t, with SSB_{2018} of 2127 t, 76% of SSB_0 . Fits to the abundance indices (A11. 1) followed the general trends in the observed data, but did not match the CPUE peaks in the mid 1990s and 2010s, or the magnitude of the increase in trawl survey catch rates observed in more recent years. SSB appears more variable in the early 1990s than estimated in previous models, but the overall pattern was very similar, with a decline to just below 40% B_0 by 2003, an increase to 2014, and then a more recent decline (A11. 2). As with previous models, a particularly strong year class strength was estimated in 1988 and above average recruitment in 2008 and 2009. Estimated selectivity curves were similar to the previous model and matched observed changes in sex ratio between time steps (A11. 3). MPD estimates of trawl and photo survey catchability were also similar to previous models (A11. 4). Again, fits to the length frequency distributions were very similar to the previous model, with fits to the trawl survey data (e.g., A11. 17) generally less variable than those to the observer data (e.g., A11. 5), and both showing evidence of a pattern in the residuals (e.g., A11. 18).

The overall likelihood profile when B_0 is fixed was U shaped (A11. 22) and was similar to the previous models.

MCMC runs

MCMC diagnostics provided reasonable evidence the model converged (A11. 23–A11. 27). The posterior trajectory of SSB (Figure 72) suggested a slight increase in the early 1990s, but a very similar pattern to the previous models after this: biomass declining to just below 40% B_0 by 2003, increasing following higher than average YCSs between 2007 and 2009, and then declining after 2014. The median estimate of current status (SSB_{2018}/SSB_0) is 78% (95% confidence interval 66%–91%), with 0% probability that SSB_{2018} is below 40% SSB_0 .

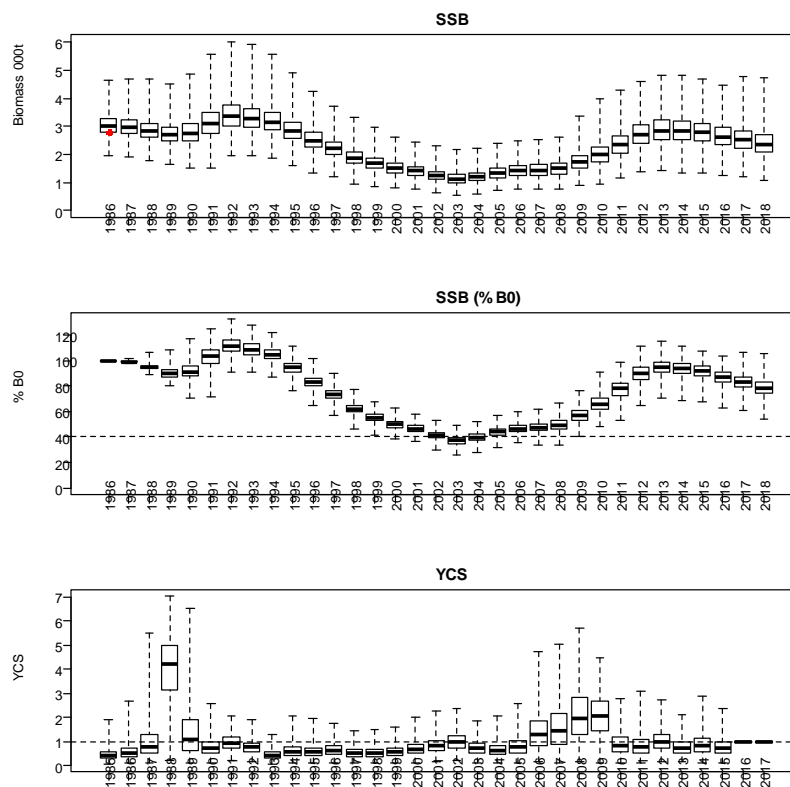


Figure 72: Posterior trajectory of SSB , SSB/SSB_0 , and YCS for the SCI 2 M025CV15 model. Red dot represents MPD estimate of B_0 .

5.2.4. SCI 2 M025CV25 (see Appendix 12)

The M025CV25 model ($M = 0.25$, $CV = 0.25$) estimated a SSB_0 of 2668 t, with SSB_{2018} of 2002 t, 75% of SSB_0 . Fits to the abundance indices (A12. 1) followed the general trends in the observed data, but did not match the CPUE peaks in the mid 1990s and 2010s, or the magnitude of the increase in trawl survey catch rates observed in more recent years. SSB followed the same general pattern as previous models, initially declining and then increasing in the early 1990s, then declining to just below 40% B_0 by 2003, increasing to 2014, and then declining in the most recent years (A12. 2). As with previous models, a particularly strong year class strength was estimated in 1988 and above average recruitment in 2008 and 2009. Estimated selectivity curves matched observed changes in sex ratio between time steps (A12. 3), and MPD estimates of trawl and photo survey catchability were similar to previous models (A12. 4). As with the previous model, fits to the trawl survey length frequency data (e.g., A12. 17) were generally less variable than those to the observer data (e.g., A12. 5), but both show evidence of a pattern in the residuals (e.g., A12. 18).

The overall likelihood profile when B_0 is fixed was U shaped (A12. 22) and is generally similar to the previous models, although the CPUE data provide less contrast across the B_0 range examined. Other data sets show similar patterns to previous models.

MCMC runs

MCMC diagnostics provided reasonable evidence the model converged (A12. 23–A12. 27). The posterior trajectory of SSB (Figure 73) suggested a very similar pattern to the M025CV15 model, with a slight increase in the early 1990s, a decline to just below 40% B_0 by 2003, an increase following higher than average YCSs between 2007 and 2009, and a decline after 2014. The median estimate of current status (SSB_{2018}/SSB_0) is 78% (95% confidence interval 64%–93%), with 0% probability that SSB_{2018} is below 40% SSB_0 .

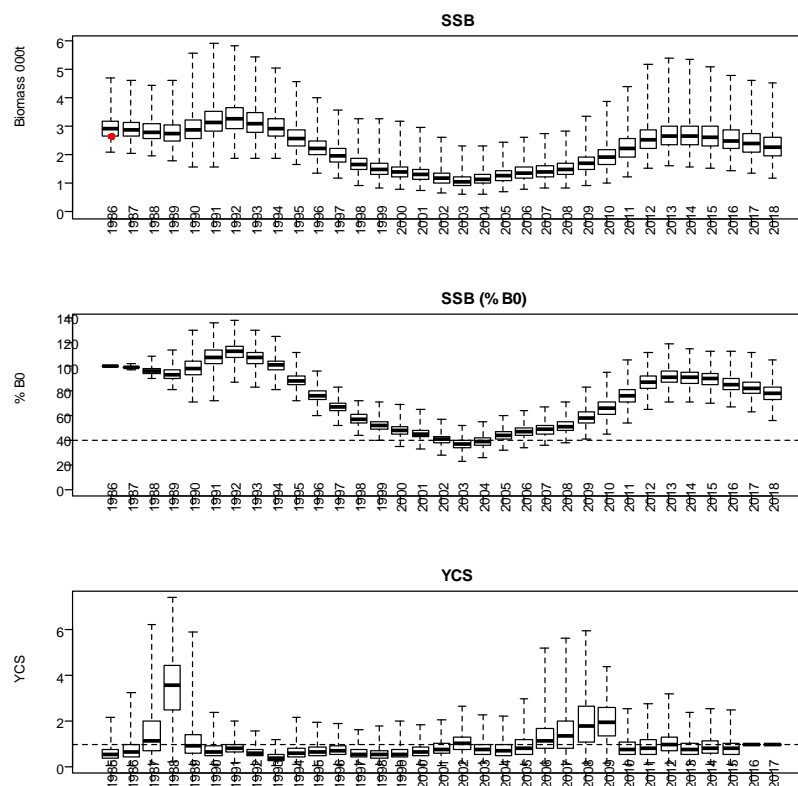


Figure 73: Posterior trajectory of SSB , SSB/SSB_0 , and YCS for the SCI 2 M025CV25 model. Red dot represents MPD estimate of B_0 .

5.3. SCI 2 Fishing Pressure

Model outputs were very similar across the sensitivity runs, and only the phase plot for the M025CV15 model is presented. Annual fishing intensity (equivalent annual F) and the level of fishing, that if applied for ever would result in an equilibrium biomass of 40% SSB_0 (F 40% B_0), were calculated using methods described by Cordue (2012). Plots of annual fishing intensity against proportion SSB_0 (presented for the M025CV15 model in Figure 74) show that fishing intensity increased from very low levels throughout the late 1980s while biomass increased overall, but after the early 1990s biomass declined and fishing intensity increased, so that by 2002 fishing intensity was almost at F 40% B_0 . After this fishing intensity declined rapidly, but biomass declined below 40% B_0 in 2003. Since 2004 fishing intensity has remained at about a quarter of F 40% B_0 , and biomass has increased.

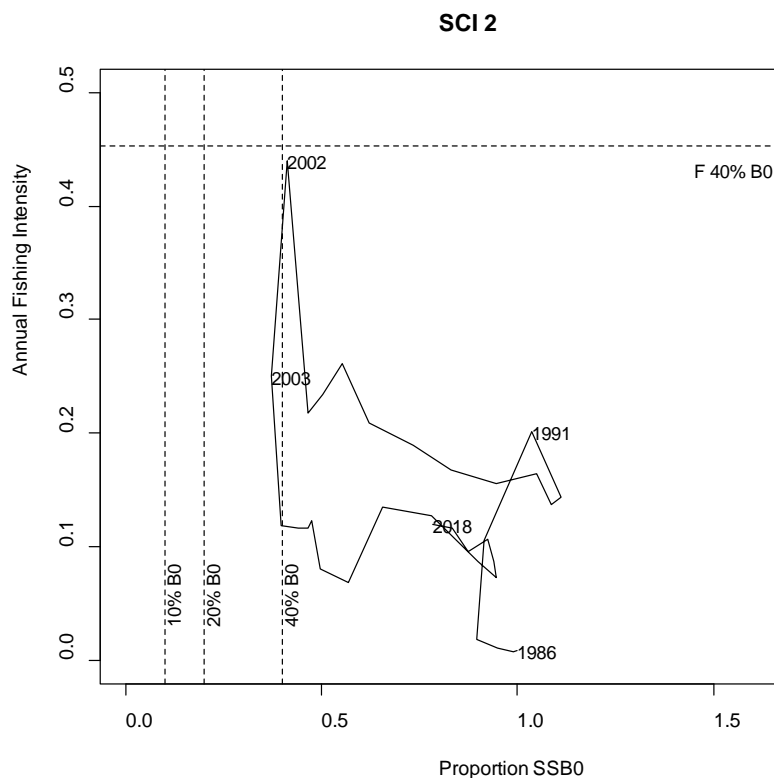


Figure 74: Trajectory of annual fishing intensity (equivalent annual F) plotted against proportion SSB_0 for the SCI 2 M025CV15 model, in relation to Harvest Strategy Standard target and limit reference points.

6. SHARED PARAMETER (SCI 1 & SCI 2) MODEL

The SCI 1 and SCI 2 stocks are reasonably geographically adjacent on the east coast of North Island (Figure 1), but have experienced quite different fishing histories (Section 2.1) and apparent recruitment patterns (e.g., Figure 58 and Figure 72). Within the individual area models, some data are already shared (e.g., pooled SCI 1 and SCI 2 growth increment data, although growth is estimated in each model independently), and although it is not appropriate to pool the assessments into a single area model, previous assessments have explored the potential to conduct the assessment as a two area model (with no migration), sharing parameters for growth and selectivity. It was hoped that by combining and fitting to the two area data sets in a single model that more realistic estimates for some of the parameters (particularly for some selectivity terms) would be provided. A single shared parameter model ($M = 0.25$, $CV = 0.25$) was explored.

6.1.1. Shared parameter model (Appendix 13)

The shared parameter model ($M = 0.25$, $CV = 0.25$) estimated SCI 1 SSB_0 at 3527 t, with SSB_{2018} at 2677 t, 73% of SSB_0 , and SCI 2 SSB_0 at 2639 t, with SSB_{2018} at 2122 t, 79% of SSB_0 . Fits to the abundance indices (A13. 1) followed the general trends in the observed data, but did not match the CPUE peaks in the mid 1990s and 2010s, or the magnitude of the increase in trawl survey catch rates observed in more recent years. SSB followed the same general pattern as previous models, initially declining and then increasing in the early 1990s, then declining to just below 40% B_0 by 2003, increasing to 2014, and then declining in the most recent years (A12. 2). As with previous models, a particularly strong year class strength was estimated in 1988 and above average recruitment in 2008 and 2009. Estimated selectivity curves matched observed changes in sex ratio between time steps (A12. 3), and MPD estimates of trawl and photo survey catchability were similar to previous models (A12. 4). As with the previous model, fits to the trawl survey length frequency distributions (e.g., A12. 17) were generally less variable than those to the observer data (e.g., A12. 5), but both show evidence of a pattern in the residuals (e.g., A12. 18).

The shared parameter model ($M = 0.25$, $CV = 0.25$) estimated SCI 1 SSB_0 at 3527 t, with SSB_{2018} at 2677 t, 73% of SSB_0 , and SCI 2 SSB_0 at 2639 t, with SSB_{2018} at 2122 t, 79% of SSB_0 . Fits to the abundance indices and normalised residuals (A13. 1 and A13. 2) show that for both areas the model fits were very similar to the equivalent single area models, with the most apparent but still minor differences relating to the photo survey. For SCI 1, SSB followed a very similar trajectory to the equivalent single area model (Figure 75), but a shift in catchability estimates (Figure 76) resulted in a lower estimated B_0 . Although the magnitude of the peak YCS around 1990 was higher in the shared parameter model, the overall pattern in YCSs was very similar to the single area model. For SCI 2, the shared parameter model estimated a slightly lower B_0 , but also a slightly different trajectory to the single area model, with the strong YCS years and increases in abundance occurring slightly later. Estimated selectivity curves (Figure 77) were updated by estimation across both data sets, particularly so for relatively poorly sampled sets (e.g., fishery selectivity, time step 2), and the shared parameter estimates appear more consistent across time steps and gear (research and commercial). Photo selectivity was not estimated, but following clarification of the potential issues with these length composition data estimation of a shared selectivity may be valuable. These preliminary investigations (and others not presented) have assumed q -Photo and q -Trawl would differ between regions and have not been estimated as shared parameters. The two areas are anecdotally reported by the fishing industry to “fish differently”, but, if considered appropriate, sharing some of the catchability terms between areas would provide additional advantages for a shared parameter model.

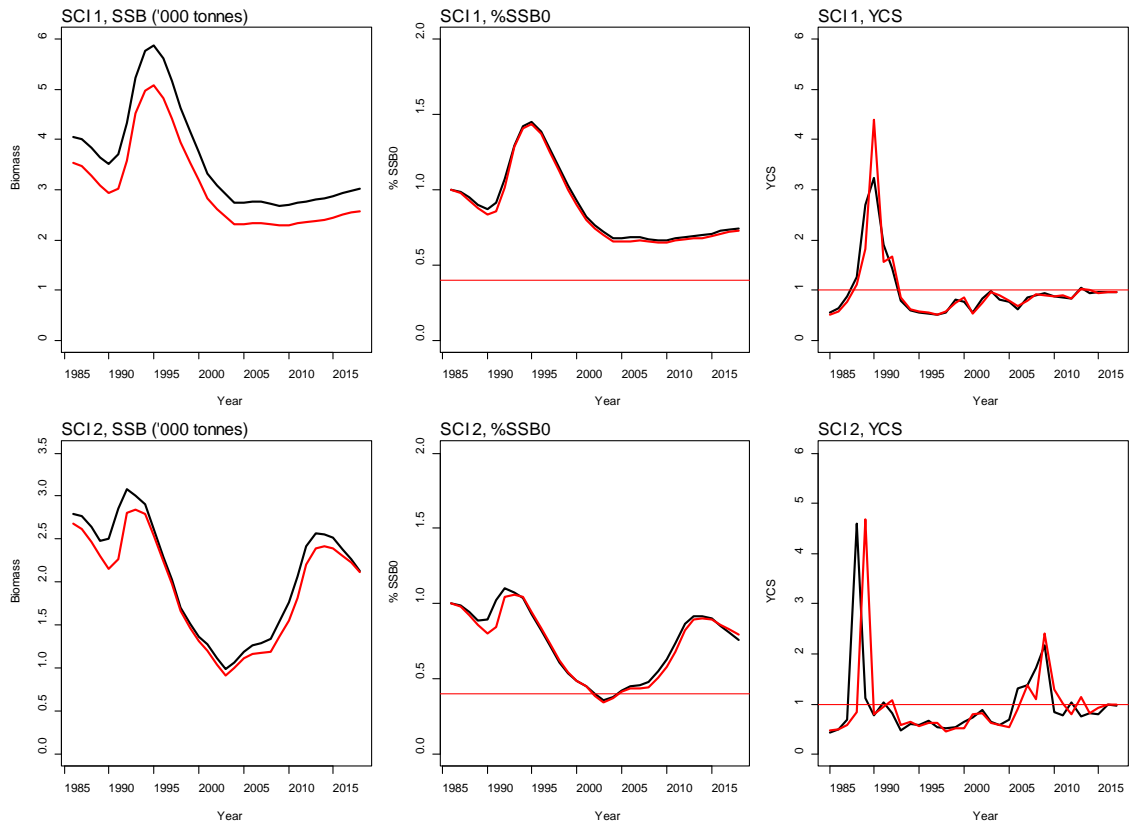


Figure 75: Spawning stock biomass trajectory (left), stock status (middle), and year class strength (right) for SCI 1 (top) and SCI 2 (bottom) from the shared parameter (red) and single area (black) M025CV15 models.

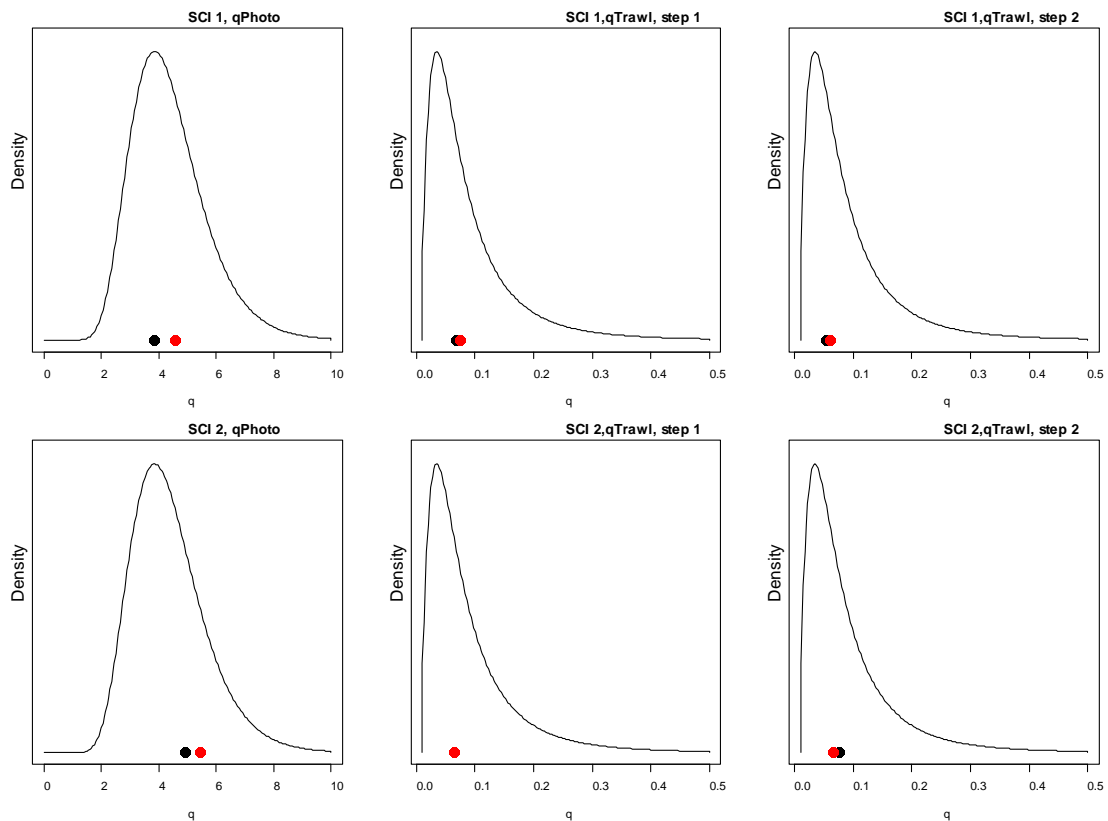


Figure 76: Catchability estimates from MPD model run, plotted in relation to prior distribution for the shared parameter (red) and single area (black) M025CV15 models.

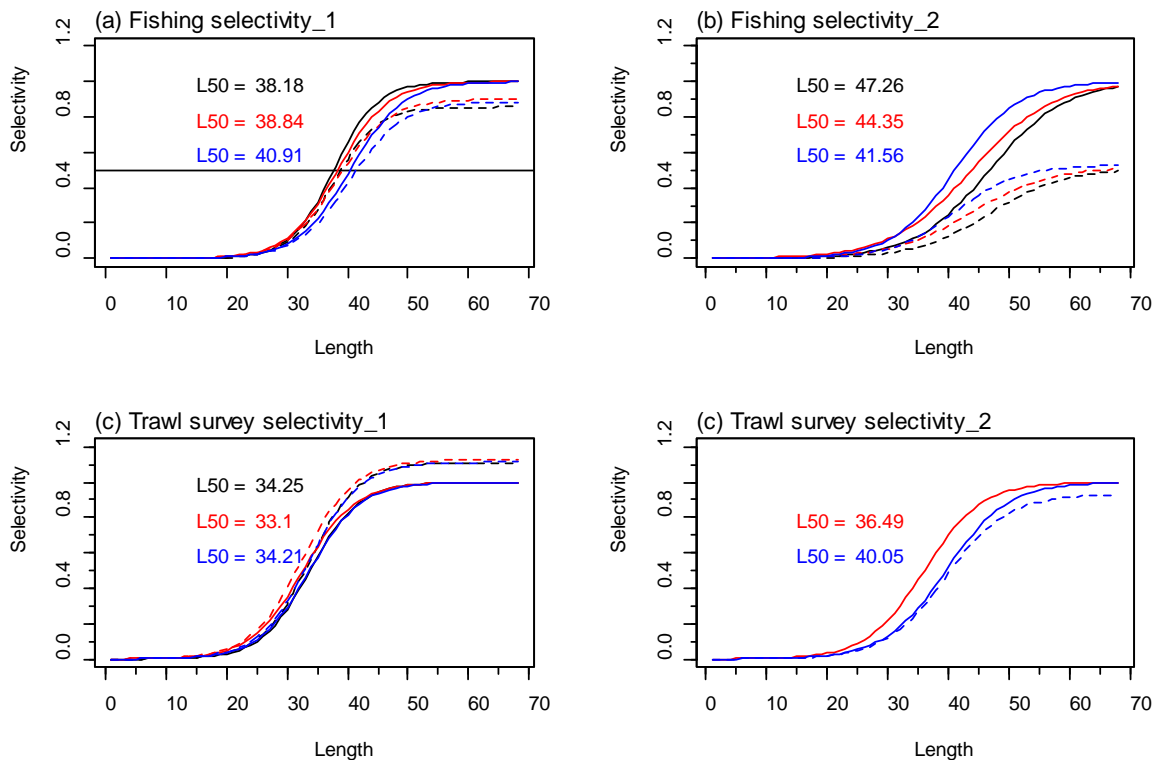


Figure 77: Fishery and trawl survey selectivity curves for the shared parameter (red) and single area SCI 1 (black) and SCI 2 (blue) M025CV15 models. Solid line – females, dotted line – males. The scampi burrow index is not sexed, and a single selectivity applies.

7. DISCUSSION

Assessments of the SCI 1 and SCI 2 stocks were last conducted in 2013 (Tuck 2016), building on the previous investigations developing the model structure (Tuck & Dunn 2012; Tuck 2014) and revised parameterisation and catchabilities (Tuck 2017; Tuck in press). In the 2016 assessment, SCI 1 was estimated to be between 59% and 86% SSB_0 , and SCI 2 was estimated to be between 74% and 103% SSB_0 .

The first accepted models for SCI 1 and SCI 2 included spatial structure, based on survey strata (Tuck & Dunn 2012), but the revised assessment in 2013 adopted a simpler spatial structure (Tuck 2014), and the SFWG agreed a single area model was appropriate for both separate assessments, although a combined area model was also examined. Models estimating M were not considered to generate realistic outputs, and base models were developed for both areas with M fixed at 0.2 and 0.25. For each area, single annual standardised CPUE indices were calculated, and, with trawl survey and photo survey data using updated priors for catchability (further developing the approach recently applied in SCI 3; Tuck in press), were fitted as abundance indices, with associated length frequency distributions. The updated catchability priors were estimated with greater uncertainty than the previous parameters and, accounting for the assumption that not all visible scampi would be acoustically detectable and not all emerged scampi would be caught, resulted in a higher q -Photo and lower q -Trawl distribution. Updates to the parameterisation of YCS within the model had minimal effect, but the updated catchability priors resulted in lower B_0 estimates (but no change to stock trajectory).

Neither assessment was considered to estimate photo selectivity parameters plausibly, and concerns were raised that the size of scampi generating photo burrows has been underestimated owing to the

foreshortening effect of measuring scampi from above when they are not orientated at an angle to the plane of the image. There is generally very little evidence of recruitment variability in the trawl survey and observer length frequency data, and YCS patterns estimated within the model appear to be driven by CPUE.

Likelihood profiles suggest that the abundance indices data provide little information on biomass for SCI 1, and B_0 is strongly influenced by the priors. Catches have been very stable throughout the history of the fishery, and do not appear to have had an effect on abundance. In SCI 2, both catches and abundance indices have changed markedly throughout the history of the fishery, and likelihood profiles suggest that the abundance indices data provide a reasonably consistent signal on biomass.

For SCI 1, the MPD estimate of SSB_0 was about 4100 t, but although the likelihood profiles were somewhat U shaped, most of the signal appears to come from the priors rather than the data. The estimated stock trajectory was sensitive to the value of M (higher M allowing the model to better fit rapid changes in CPUE), but all models showed an increase in biomass up to the mid 1990s (associated with very high recruitment a few years earlier) and a decline to the early 2000s, followed by a very stable period where SSB was around 70% SSB_0 , but increasing slightly in the most recent years. The MCMC estimate of SSB_0 was between 4600 and 4800 t. SSB_{2018} was estimated to be between 3300 and 3600 t, and MCMC posteriors suggest a 0% probability that SSB_{2018} is below 40% SSB_0 . Annual fishing intensity (equivalent annual F) has consistently been estimated to be below F 40% B_0 .

For SCI 2, the MPD estimate of SSB_0 was about 2800 t, with the likelihood profiles indicating more signal from the abundance data than was apparent for SCI 1. The models were sensitive to M , with a higher value resulting in a lower estimate of SSB_0 , and a stock trajectory more able to match the magnitude of the CPUE patterns but not influence current stock status. SSB is estimated to have declined (the extent to which depends on the model examined) through the late 1980s, but increased to a peak around 1993 following very strong recruitment in the late 1980s. SSB then declined to a minimum (just below 40% B_0) in 2003, increased slightly and stabilised just above 40% B_0 until 2008, and then increased to a peak in 2013 (following a strong recruitment in 2009), declining slightly since then. The MCMC estimate of SSB_0 was between 2900 and 3100 t. SSB_{2018} was estimated to be between 2180 and 2360 t, and MCMC posteriors suggest a 0% probability that SSB_{2018} is below 40% SSB_0 . Annual fishing intensity (equivalent annual F) peaked in 2002, but declined considerably after this. SSB was at or below 40% SSB_0 between 2002 and 2004, but has increased considerably since this time.

A shared parameter (SCI 1 and SCI 2) model was examined. Sharing growth and selectivity parameters resulted in some shifts in catchability estimates and lower B_0 . Stock trajectories (relative to SSB_0) were similar between the combined and single area models, particularly for SCI 1. Sharing these parameters offers some advantages, but a model sharing survey catchability terms is likely to be more useful, if this is considered appropriate.

8. ACKNOWLEDGEMENTS

This work was funded by the Ministry for Primary Industries under project SCI2018-01 and builds on a series of scampi assessment projects funded by the Ministry. I thank the many NIWA and Ministry of Fisheries staff who measured scampi over the years, and the members of the NIWA scampi image reading team. Development of the model structure benefitted greatly from comments members of the Shellfish Fisheries Assessment Working Group. This report was reviewed by Bruce Hartill (NIWA, Auckland).

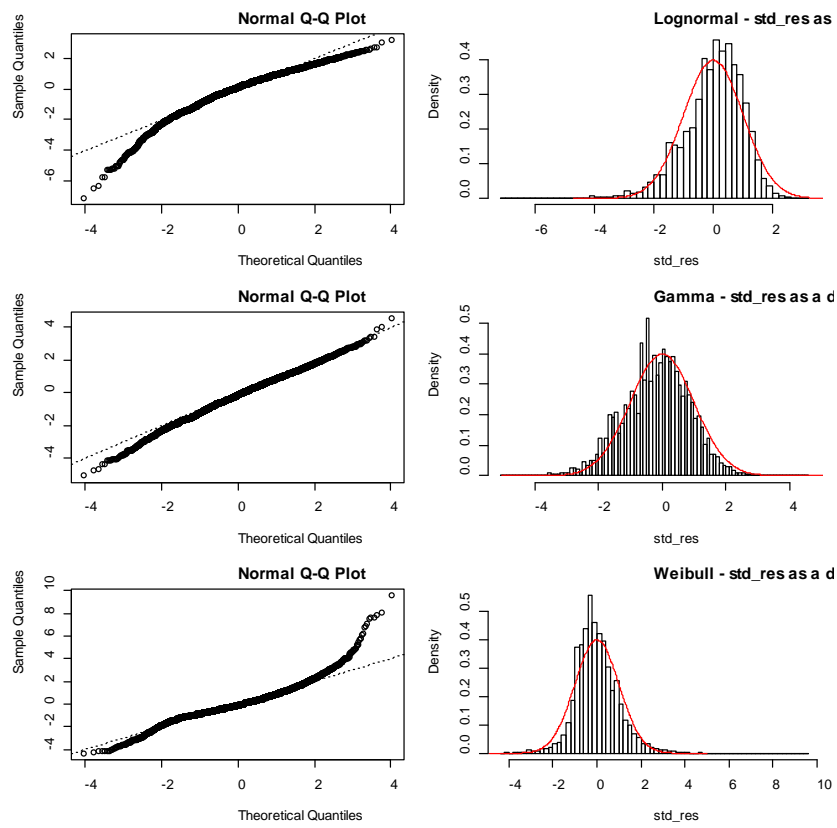
9. REFERENCES

- Bell, M.C.; Redant, F.; Tuck, I.D. (2006). Nephrops species. In: B. Phillips (Ed). *Lobsters: Biology, management, Aquaculture and Fisheries*. Blackwell Publishing, Oxford, pp. 412–461.
- Bentley, N.; Kendrick, T.H.; Starr, P.J.; Breen, P.A. (2012). Influence plots and metrics: tools for better understanding fisheries catch-per-unit-effort standardisations. *ICES Journal of Marine Science* 69: 84–88.
- Bull, B.; Dunn, A. (2002). Catch-at-age: User manual v 1.06.2002/09/12. NIWA Internal Report No. 114. 23 p.
- Bull, B.; Francis, R.I.C.C.; Dunn, A.; McKenzie, A.; Gilbert, D.J.; Smith, M.H.; Bian, R.; Fu, D. (2012). CASAL (C++ algorithmic stock assessment laboratory): CASAL user manual v2.30-2012/03/21. *NIWA Technical Report No. 135*. 280 p.
- Charnov, E.L.; Berrigan, D.; Shine, R. (1993). The M/k ratio is the same for fish and reptiles. *Amer Naturalist* 142: 707–711.
- Cordue, P.L. (2012). Fishing intensity metrics for use in overfishing determination. *ICES Journal of Marine Science: Journal du Conseil* 69(4): 615–623. 10.1093/icesjms/fss036
- Cryer, M.; Coburn, R. (2000). Scampi stock assessment for 1999. *New Zealand Fisheries Assessment Report 2000/07*. 61 p.
- Cryer, M.; Dunn, A.; Hartill, B. (2005). Length-based population model for scampi (*Metanephrops challengeri*) in the Bay of Plenty (QMA 1). *New Zealand Fisheries Assessment Report 2005/27*. 56 p.
- Cryer, M.; Hartill, B.; Drury, J.; Armiger, H.; M.D, S.; Middleton, C. (2003). Indices of relative abundance for scampi, *Metanephrops challengeri*, based on photographic surveys in QMA 1 (1998–2003) and QMA 2 (2003). Final Research Report for Ministry of Fisheries Research Project SCI2002/01 Objectives 1–3. 18 p.
- Cryer, M.; Oliver, M. (2001). Estimating age and growth in New Zealand scampi, *Metanephrops challengeri*. Final Research Report for Ministry of Research Project, SCI9802(Objective 2). 50 p.
- Cryer, M.; Stotter, D.R. (1997). Trawling and tagging of scampi off the Alderman Islands, western Bay of Plenty, September 1995 (KAH9511). *New Zealand Fisheries Data Report No. 84*. 29 p.
- Cryer, M.; Stotter, D.R. (1999). Movement and growth rates of scampi inferred from tagging, Alderman Islands, western Bay of Plenty. *NIWA Technical Report No. 49*. 36 p.
- Fenaughty, C. (1989). Reproduction in *Metanephrops challengeri*. Unpubl. Rep. MAF Fisheries, Wellington. 46 p.
- Francis, R.I.C.C. (1999). The impact of correlations in standardised CPUE indices. *New Zealand Fisheries Assessment Research Document 99/42*. 31 p.
- Francis, R.I.C.C. (2011). Data weighting in statistical fisheries stock assessment models. *Canadian Journal Fisheries and Aquatic Science* 68: 1124–1138.
- Francis, R.I.C.C.; Bian, R. (2011). Catch-at-length and -age (CALA) User Manual. 83 p.
- McCullagh, P.; Nelder, J.A. (1989). *Generalised Linear Models*. Chapman and Hall, London. 511 p.
- Morizur, Y. (1982). Estimation de la mortalité pour quelques stocks de langoustine, *Nephrops norvegicus*. *ICES-CM-1982/K:10*.
- Pauly, D. (1980). On the interrelationships between natural mortality, growth parameters, and mean environmental temperature in 175 fish stocks. *Journal du Conseil International pour l'Exploration du Mer* 39: 175–192.

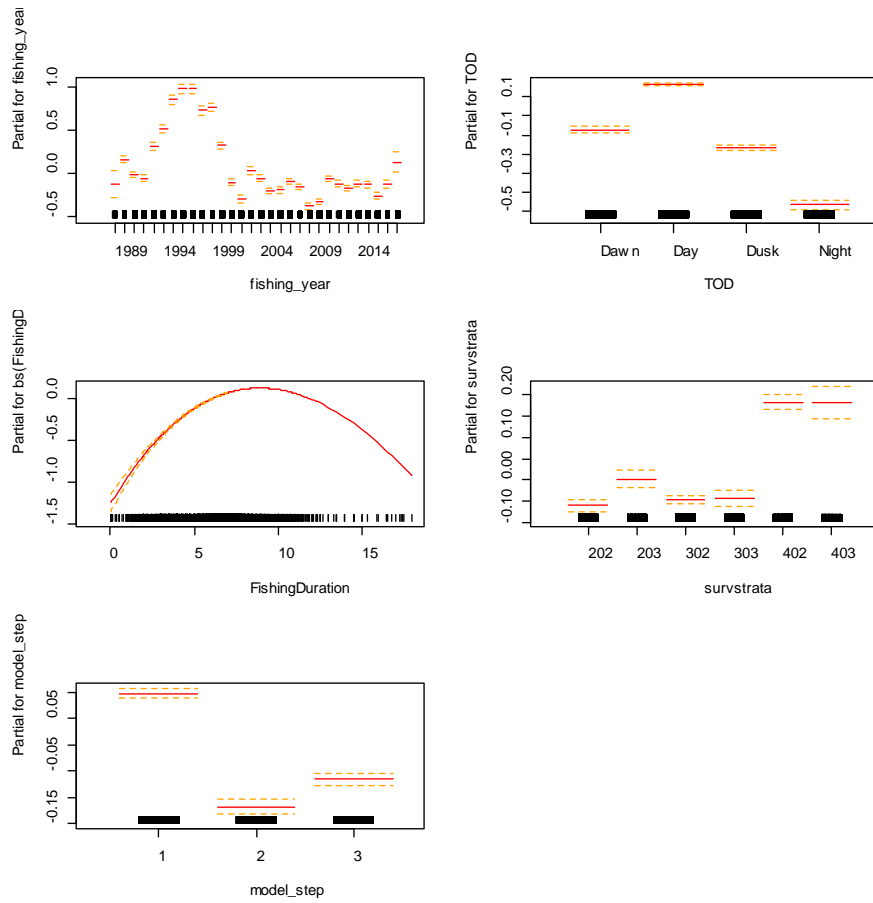
- Starr, P.J. (2009). Rock lobster catch and effort data: summaries and CPUE standardisations, 1979–80 to 2007–08. *New Zealand Fisheries Assessment Report 2009/38*. 73 p.
- Starr, P.J.; Breen, P.A.; Kendrick, T.H.; Haist, V. (2009). Model and data used for the 2008 stock assessment of rock lobsters (*Jasus edwardsii*) in CRA 3. *New Zealand Fisheries Assessment Report 2009/22*. 62 p.
- Tuck, I.D. (2009). Characterisation of scampi fisheries and the examination of catch at length and spatial distribution of scampi in SCI 1, 2, 3, 4A and 6A. *New Zealand Fisheries Assessment Report 2009/27*. 102 p.
- Tuck, I.D. (2010). Scampi burrow occupancy, burrow emergence and catchability. *New Zealand Fisheries Assessment Report 2010/13*. 58 p.
- Tuck, I.D. (2013). Characterisation and length-based population model for scampi (*Metanephrops challengeri*) on the Mernoo Bank (SCI 3). *New Zealand Fisheries Assessment Report 2013/24*. 165 p.
- Tuck, I.D. (2014). Characterisation and length-based population model for scampi (*Metanephrops challengeri*) in the Bay of Plenty (SCI 1) and Hawke Bay/Wairarapa (SCI 2). *New Zealand Fisheries Assessment Report 2014/33*. 172 p.
- Tuck, I.D. (2016). Characterisation and length-based assessment model for scampi (*Metanephrops challengeri*) in the Bay of Plenty (SCI 1) and Hawke Bay– Wairarapa (SCI 2). *New Zealand Fisheries Assessment Report 2016/51*. 194 p.
- Tuck, I.D. (2017). Characterisation and length-based population model for scampi (*Metanephrops challengeri*) at the Auckland Islands (SCI 6A). *New Zealand Fisheries Assessment Report 2017/56*. 180 p.
- Tuck, I.D. (2020). Characterisation and CPUE standardisation of scampi in SCI 4A. *New Zealand Fisheries Assessment Report 2020/04*. 49 p.
- Tuck, I.D. (in press). Characterisation and a length-based assessment model for scampi (*Metanephrops challengeri*) on the Mernoo Bank (SCI 3). *New Zealand Fisheries Assessment Report*: 246 p.
- Tuck, I.D.; Atkinson, R.J.A.; Chapman, C.J. (2000). Population biology of the Norway lobster, *Nephrops norvegicus* (L.) in the Firth of Clyde, Scotland. II. Fecundity and size at onset of maturity. *ICES Journal of Marine Science* 57. 1222–1237.
- Tuck, I.D.; Dunn, A. (2006). Length based population model for scampi (*Metanephrops challengeri*) in the Bay of Plenty (SCI 1) and Wairarapa / Hawke Bay (SCI 2). Final Research Report for Ministry of Research Project SCI200501 (Objectives 2 & 3). 42 p.
- Tuck, I.D.; Dunn, A. (2009). Length-based population model for scampi (*Metanephrops challengeri*) in the Bay of Plenty (SCI 1) and Wairarapa / Hawke Bay (SCI 2). Final Research Report for Ministry of Fisheries Research Projects SCI2006-01 & SCI2008-03W Obj 1. 30 p.
- Tuck, I.D.; Dunn, A. (2012). Length-based population model for scampi (*Metanephrops challengeri*) in the Bay of Plenty (SCI 1), Wairarapa / Hawke Bay (SCI 2) and Auckland Islands (SCI 6A). *New Zealand Fisheries Assessment Report 2012/01*. 125 p.
- Tuck, I.D.; Hartill, B.; Drury, J.; Armiger, H.; Smith, M.; Parkinson, D. (2006). Measuring the abundance of scampi - Indices of abundance for scampi, *Metanephrops challengeri*, based on photographic surveys in SCI 2 (2003-2006). Final Research Report for Ministry of Research Project SCI200501 Objective 1. 21 p.
- Tuck, I.D.; Hartill, B.; Parkinson, D.; Harper, S.; Drury, J.; Smith, M.; Armiger, H. (2009). Estimating the abundance of scampi - Relative abundance of scampi, *Metanephrops challengeri*, from a photographic survey in SCI 1 and SCI 6A (2008). Final Research Report for Ministry of Fisheries Research Project SCI2007-02 Objectives 1 & 2. 37 p.
- Tuck, I.D.; Hartill, B.; Parkinson, D.; Smith, M.; Armiger, H.; Rush, N.; Drury, J. (2011). Estimating the abundance of scampi – Relative abundance of scampi, *Metanephrops challengeri*, from photographic surveys in SCI 3 (2009 & 2010). Final Research Report for Ministry of Fisheries research projects SCI2009-01 & SCI2010-01. 29 p.

- Tuck, I.D.; Parkinson, D.; Armiger, H.; Smith, M.; Miller, A.; Rush, N.; Spong, K. (2016). Estimating the abundance of scampi in SCI 1 (Bay of Plenty) and SCI 2 (Wairarapa / Hawke Bay) in 2015. *New Zealand Fisheries Assessment Report 2016/17*. 60 p.
- Tuck, I.D.; Parkinson, D.; Armiger, H.; Smith, M.; Miller, A.; Rush, N.; Spong, K. (2019). Estimating the abundance of scampi in SCI 1 (Bay of Plenty) and SCI 2 (Wairarapa / Hawke Bay) in 2018. *New Zealand Fisheries Assessment Report 2019/18*. 52 p.
- Tuck, I.D.; Parkinson, D.; Drury, J.; Armiger, H.; Miller, A.; Rush, N.; Smith, M.; Hartill, B. (2013). Estimating the abundance of scampi - Relative abundance of scampi, *Metanephrops challengeri*, from a photographic survey in SCI 1 and SCI 2 (2012). Final Research Report for Ministry of Fisheries Research Project SCI201002A. 54 p.
- Tuck, I.D.; Parsons, D.M.; Hartill, B.W.; Chiswell, S.M. (2015). Scampi (*Metanephrops challengeri*) emergence patterns and catchability. *ICES Journal of Marine Science* 72 (Supplement 1): i199–i210.
<http://icesjms.oxfordjournals.org/content/early/2015/01/08/icesjms.fsu244.abstract>
- Vignaux, M. (1994). Catch per unit effort (CPUE) analysis of west coast South Island and Cook Strait spawning hoki fisheries, 1987–93. New Zealand Fisheries Assessment Research Document 94/11. 29 p.
- Wear, R.G. (1976). Studies on the larval development of *Metanephrops challengeri* (Balss, 1914) (Decapoda, Nephropidae). *Crustaceana* 30: 113–122.

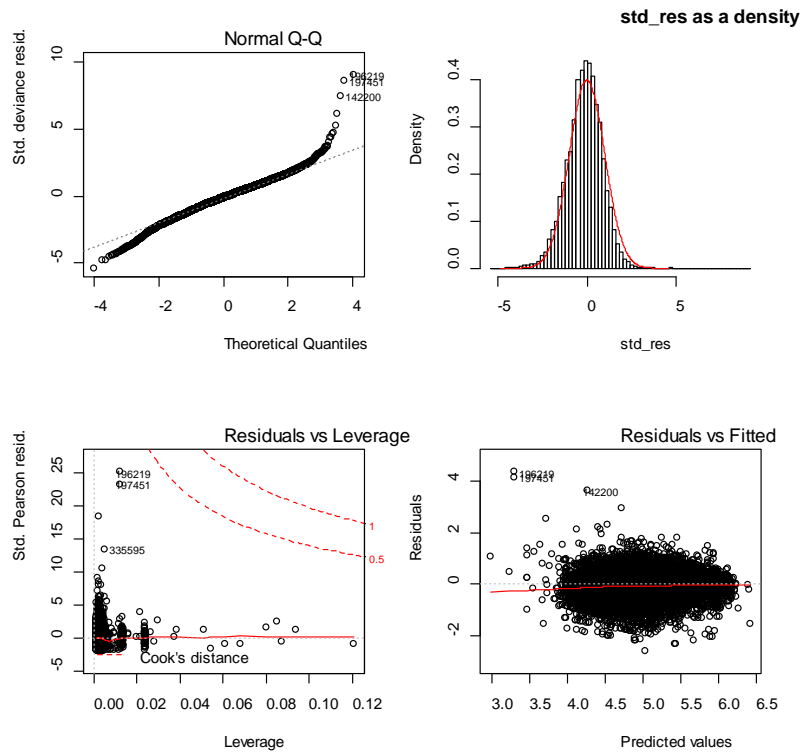
APPENDIX 1. CPUE standardisation diagnostics (SCI 1)



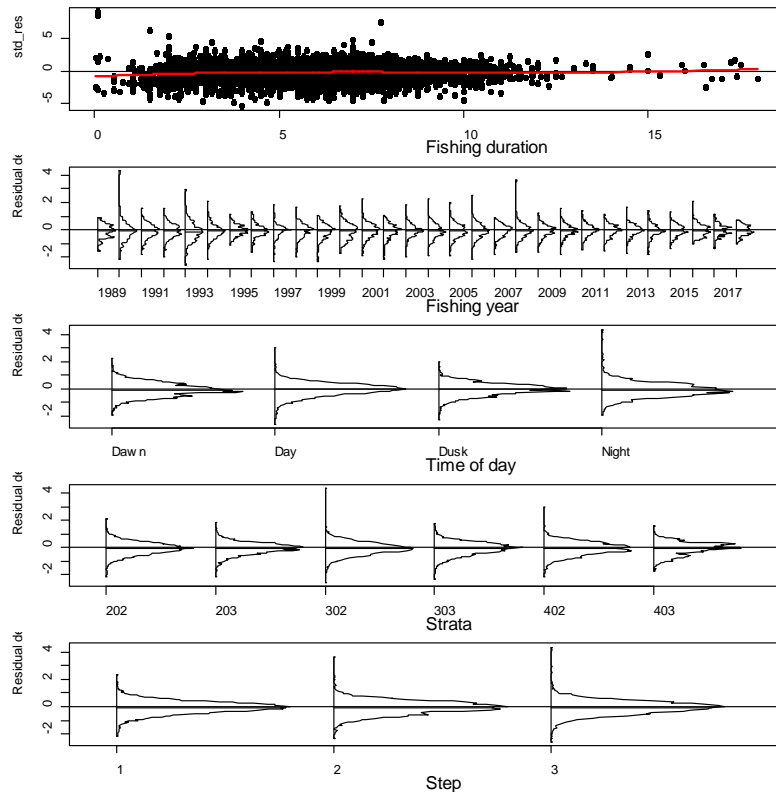
A1. 1: Plots of the distributions of standardised residuals for simple standardised CPUE models for SCI 1 with log normal (top panel), gamma (middle panel), and weibull (bottom panel) error distributions.



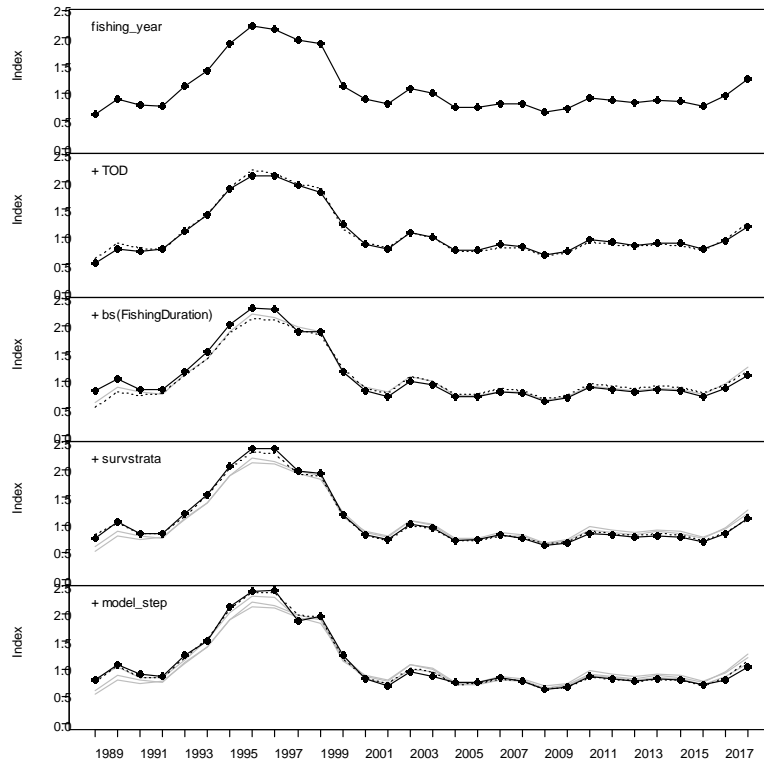
A1. 2: Termplot for final SCI 1 CPUE standardisation model (Table 5).



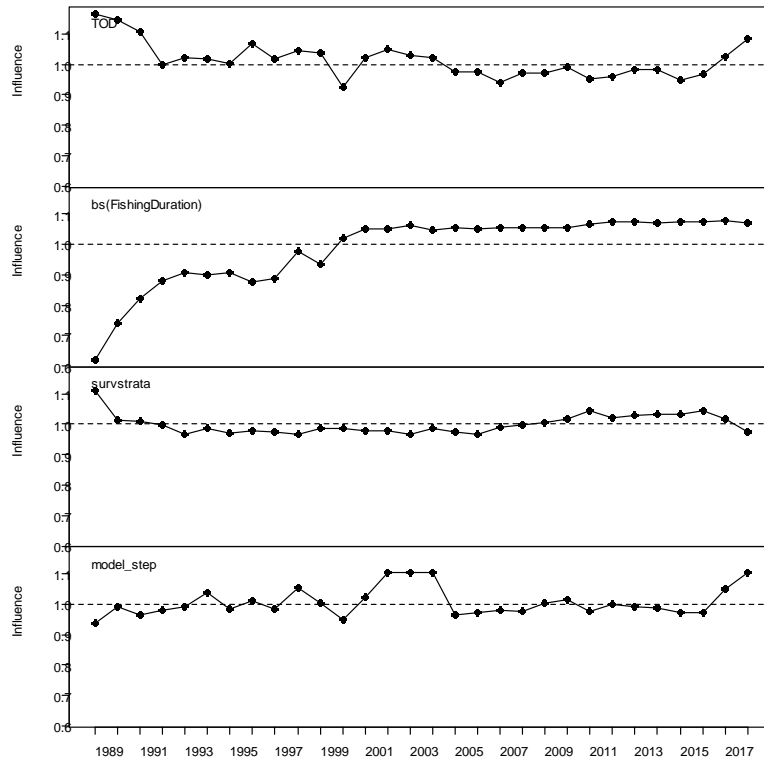
A1. 3: Diagnostic plots for final SCI 1 CPUE standardisation model (Table 5).



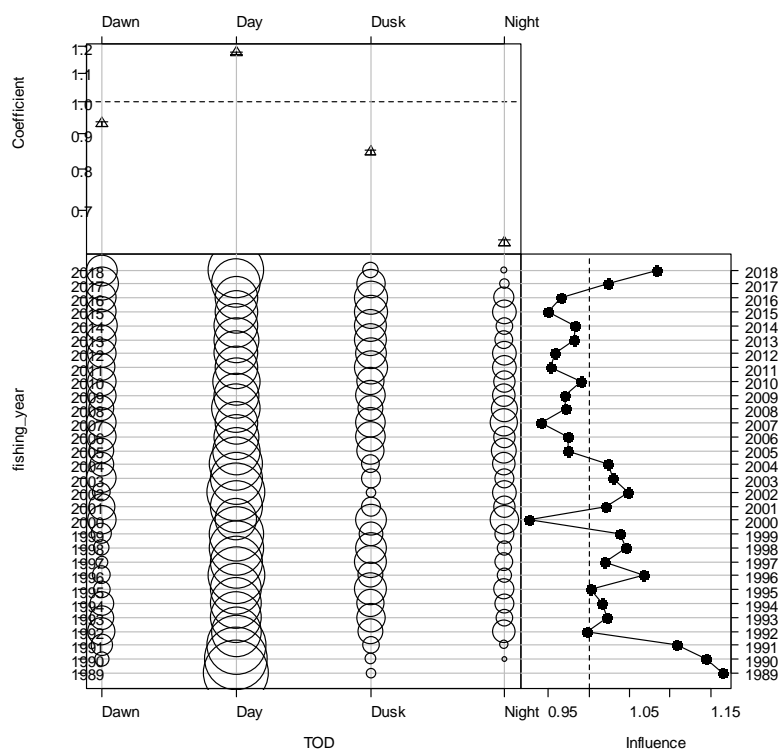
A1. 4: Distributions of residuals for final SCI 1 CPUE standardisation model (Table 5).



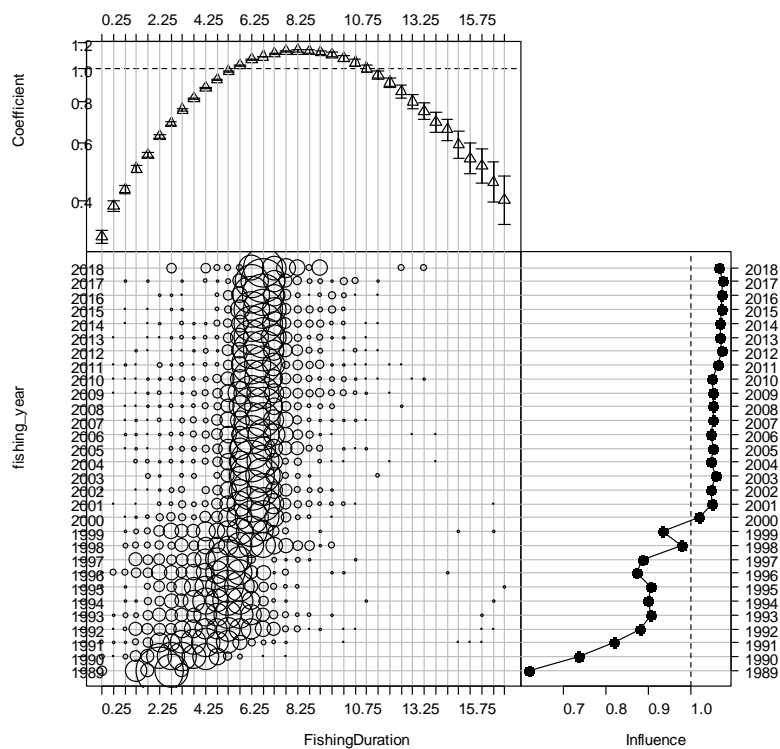
A1. 5: Step influence plot for final SCI 1 CPUE standardisation model (Table 5).



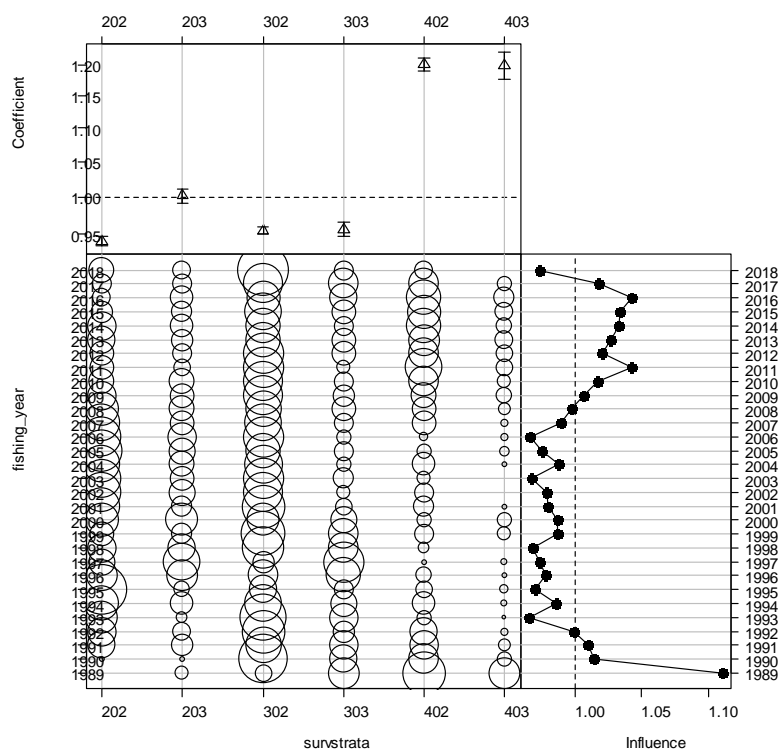
A1. 6: Year influence plots for each explanatory variable for final SCI 1 CPUE standardisation model (Table 5).



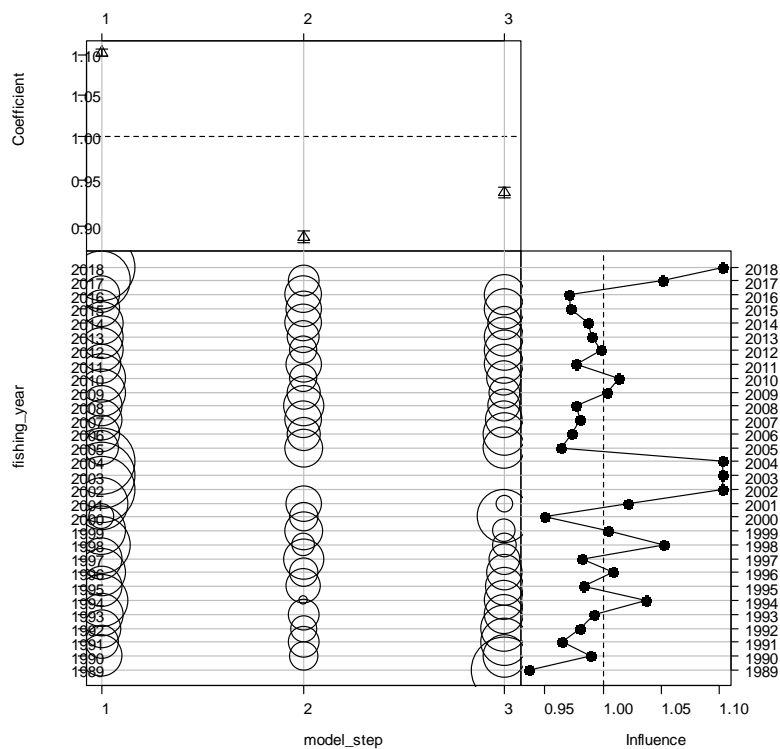
A1. 7: Coefficient-distribution influence plot for time of day for final SCI 1 CPUE standardisation model (Table 5).



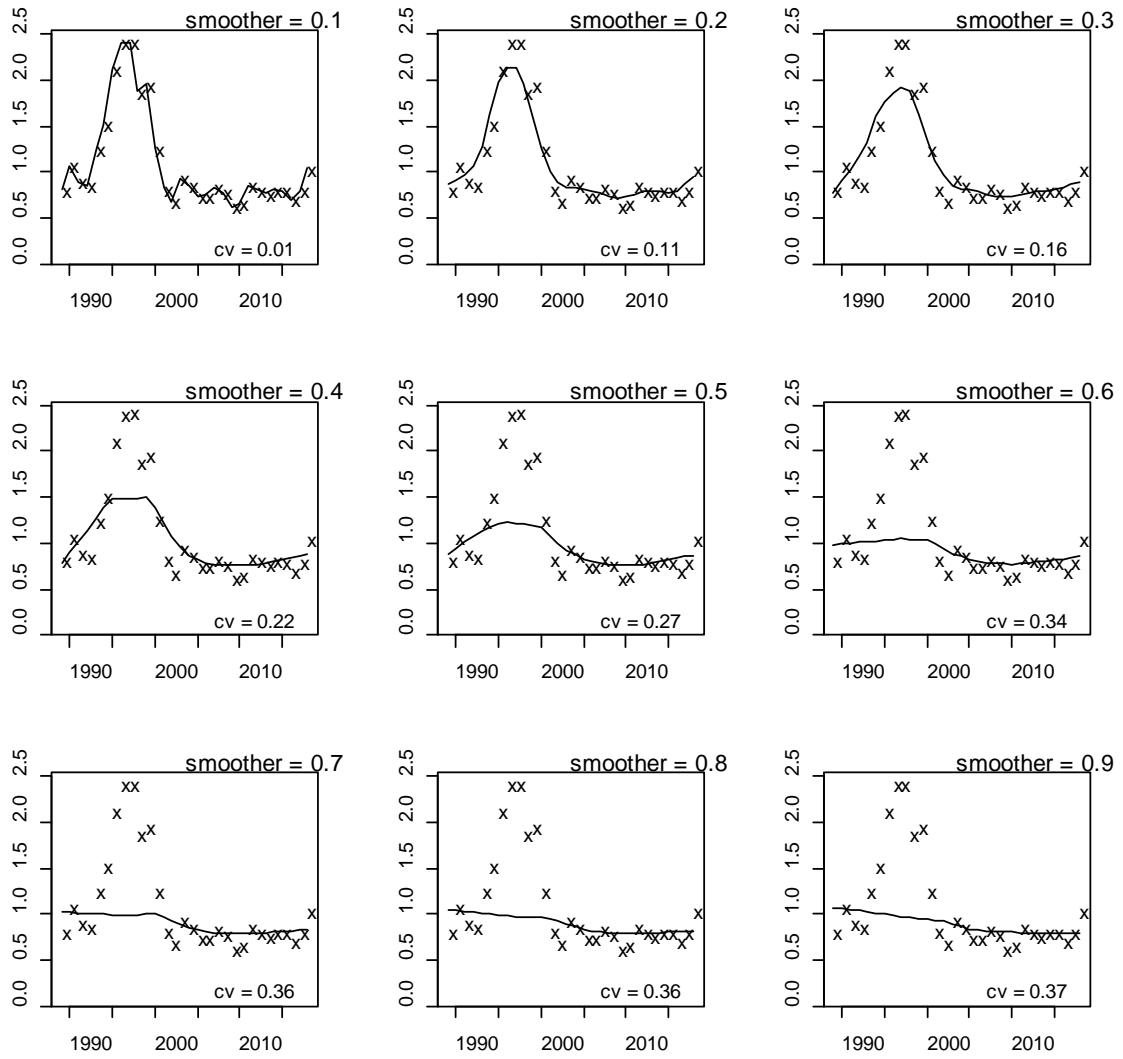
A1. 8: Coefficient-distribution influence plot for effort (fishing duration) for final SCI 1 CPUE standardisation model (Table 5).



A1. 9: Coefficient-distribution influence plot for survstrata (survey strata) for final SCI 1 CPUE standardisation model (Table 5).

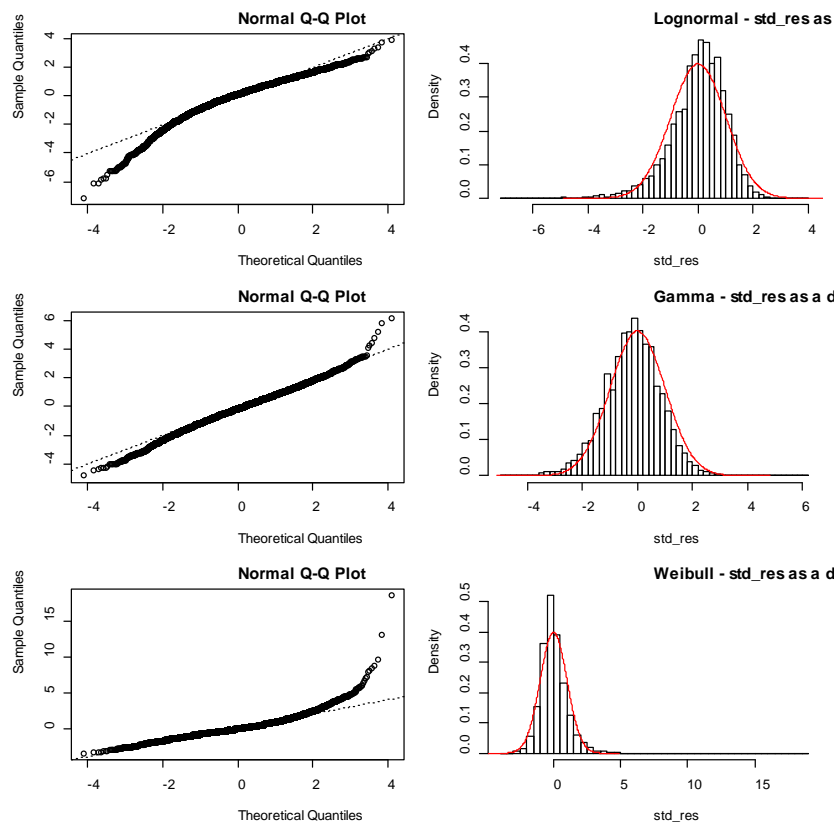


A1. 10: Coefficient-distribution influence plot for timestep for final SCI 1 CPUE standardisation model (Table 5).

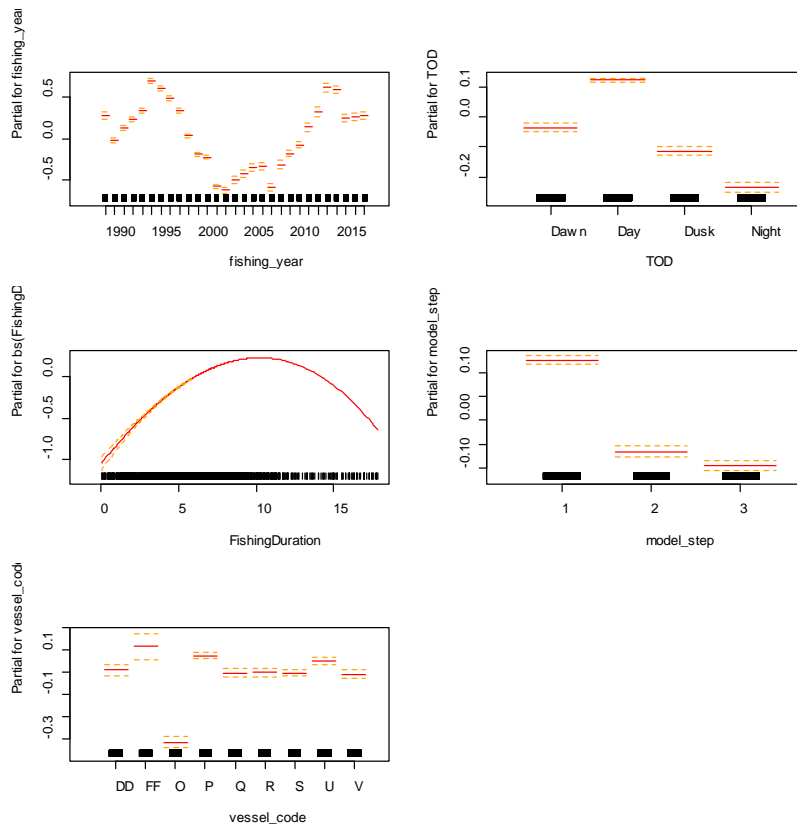


A1. 11: Range of smoothers fitted to index from the final SCI 1 CPUE standardisation model (Table 5).

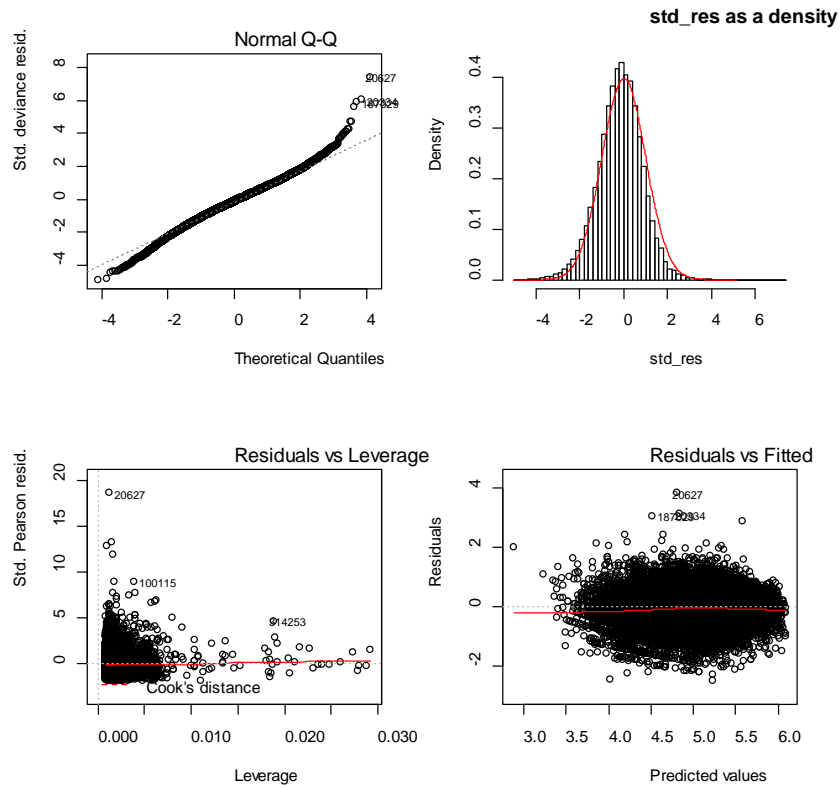
APPENDIX 2. CPUE standardisation diagnostics (SCI 2)



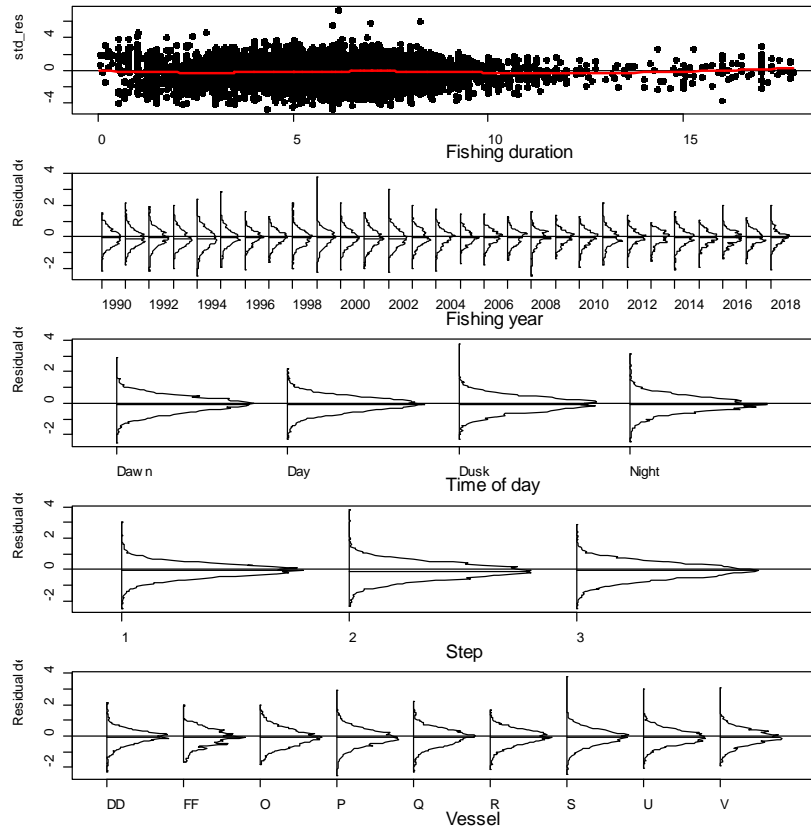
A2. 1: Plots of the distributions of standardised residuals for simple standardised CPUE models for SCI 2 with log normal (top panel), gamma (middle panel), and weibull (bottom panel) error distributions.



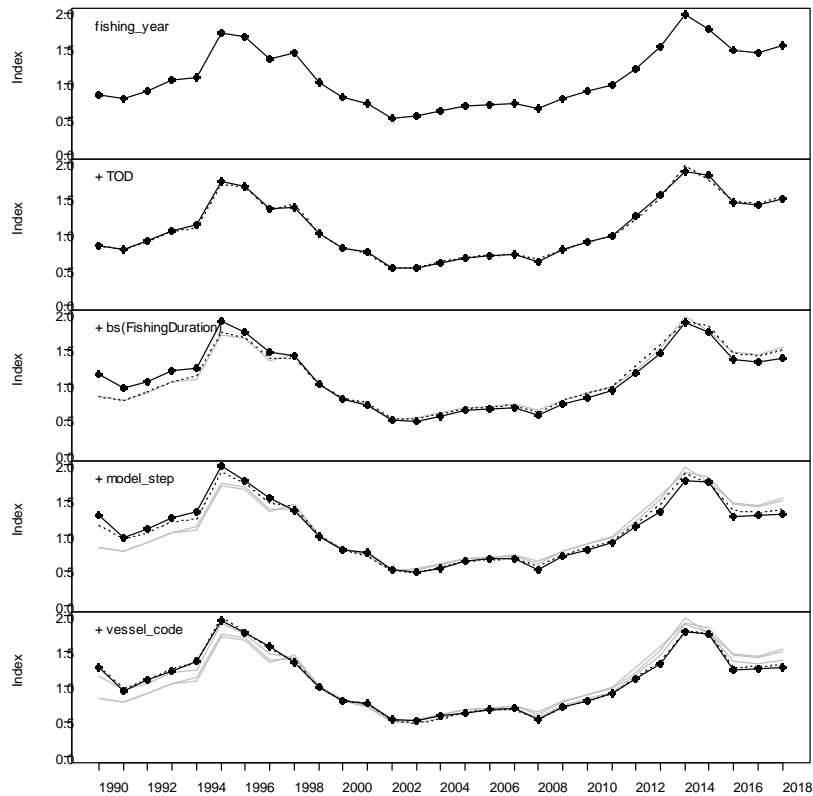
A2. 2: Termplot for final SCI 2 CPUE standardisation model (Table 8).



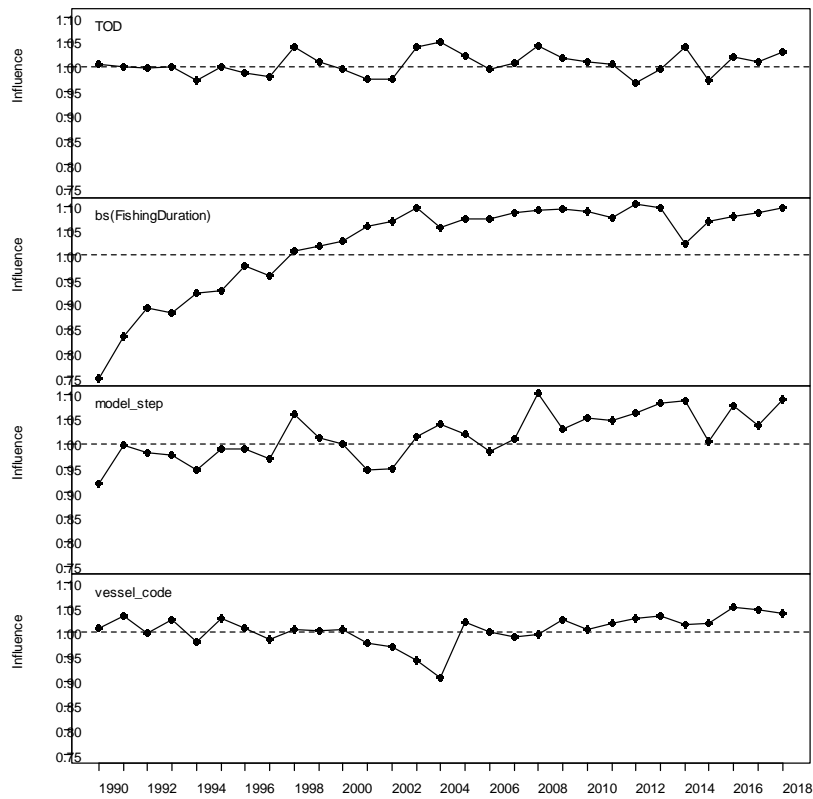
A2. 3: Diagnostic plots for final SCI 2 CPUE standardisation model (Table 8).



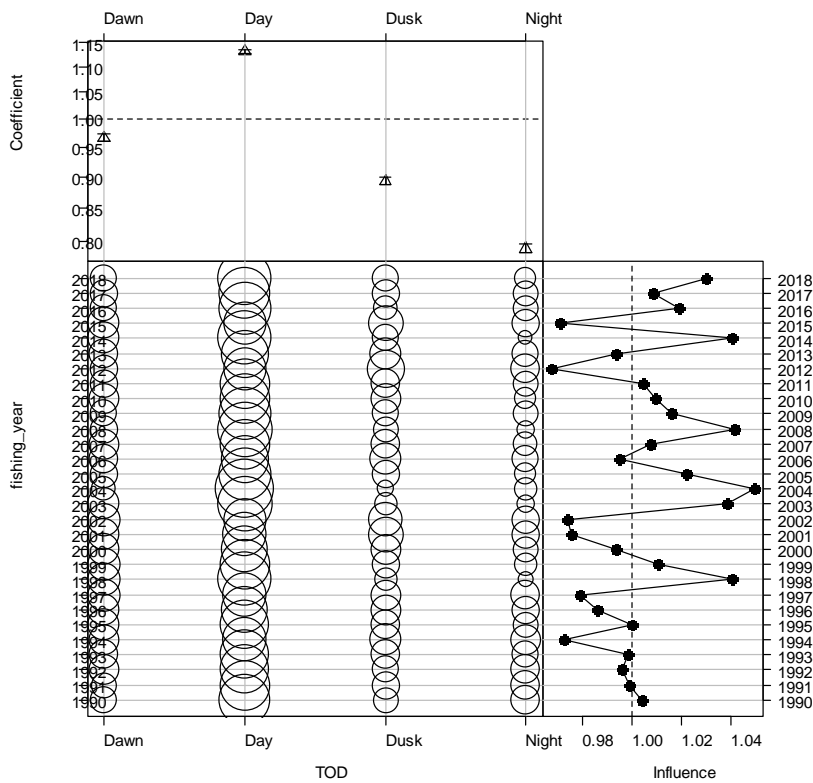
A2. 4: Distributions of residuals for final SCI 2 CPUE standardisation model (Table 8).



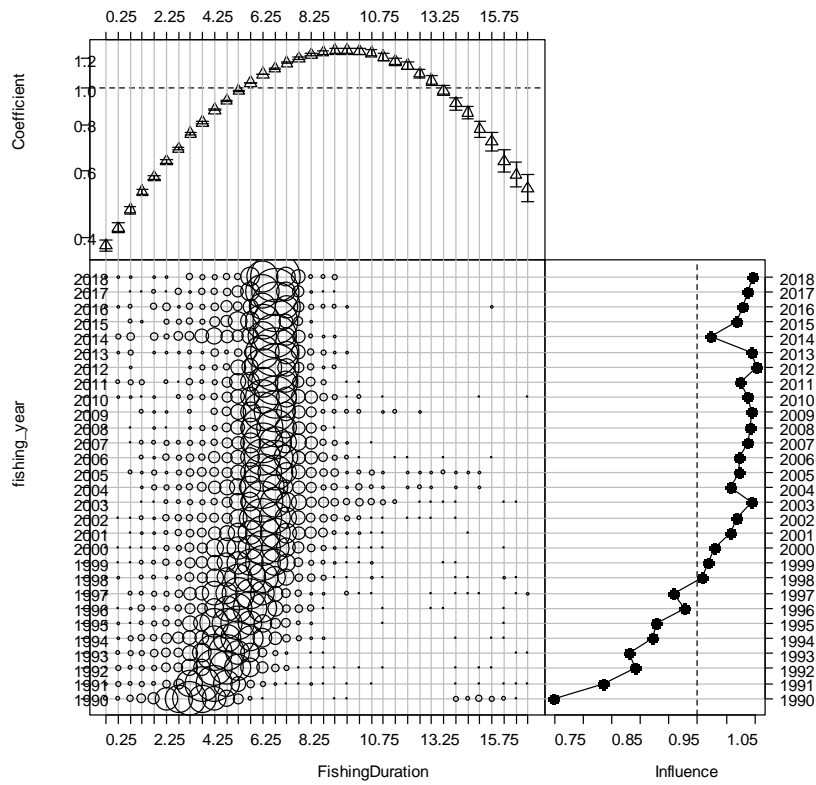
A2. 5: Step influence plot for final SCI 2 CPUE standardisation model (Table 8).



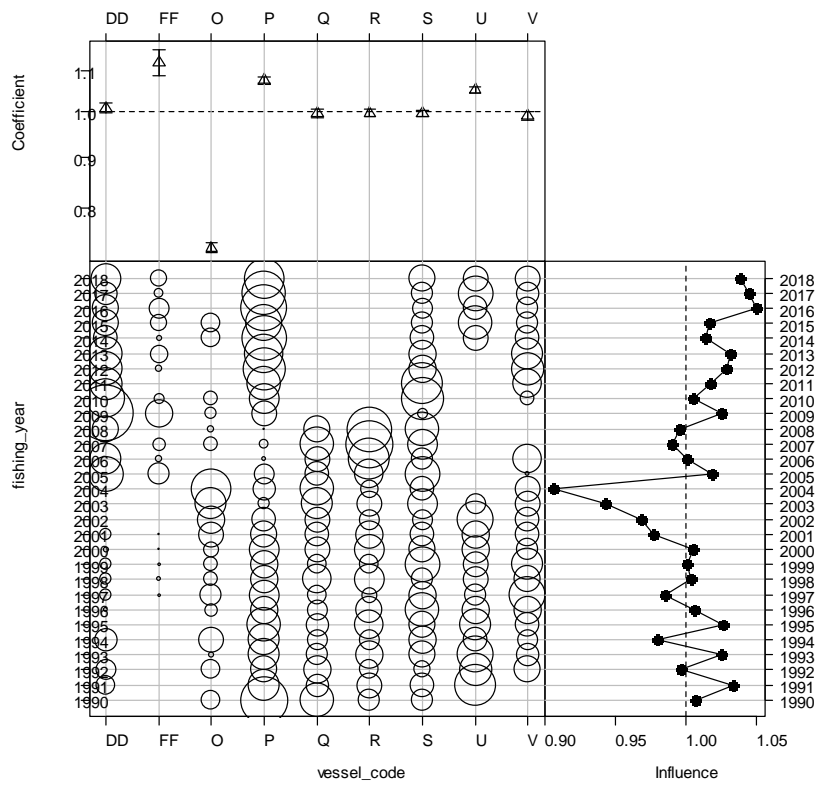
A2. 6: Year influence plots for each explanatory variable for final SCI 2 CPUE standardisation model (Table 8).



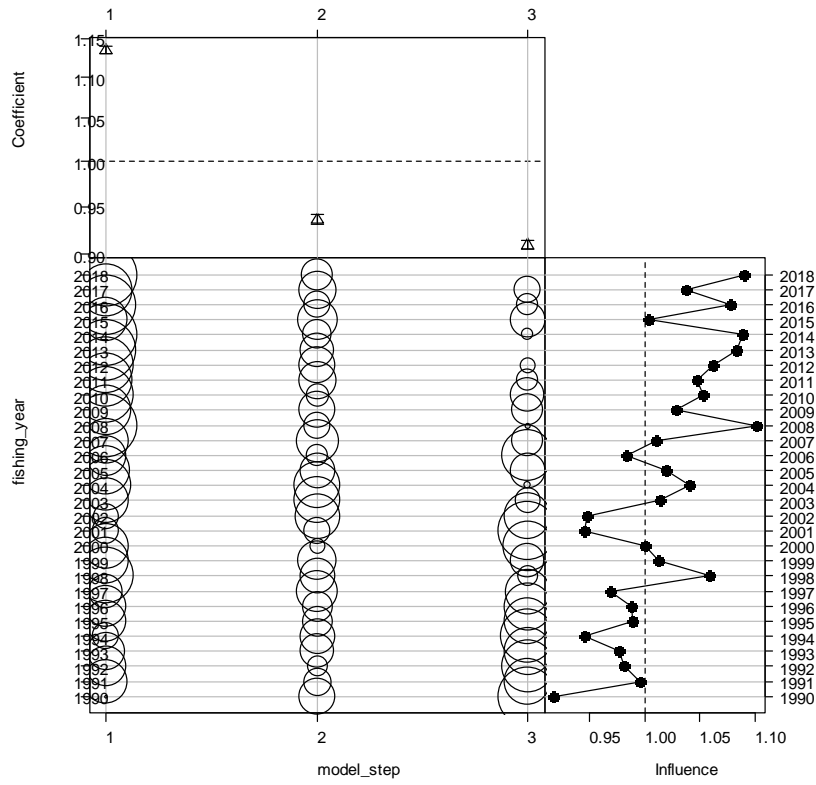
A2. 7: Coefficient-distribution influence plot for time of day for final SCI 2 CPUE standardisation model (Table 8).



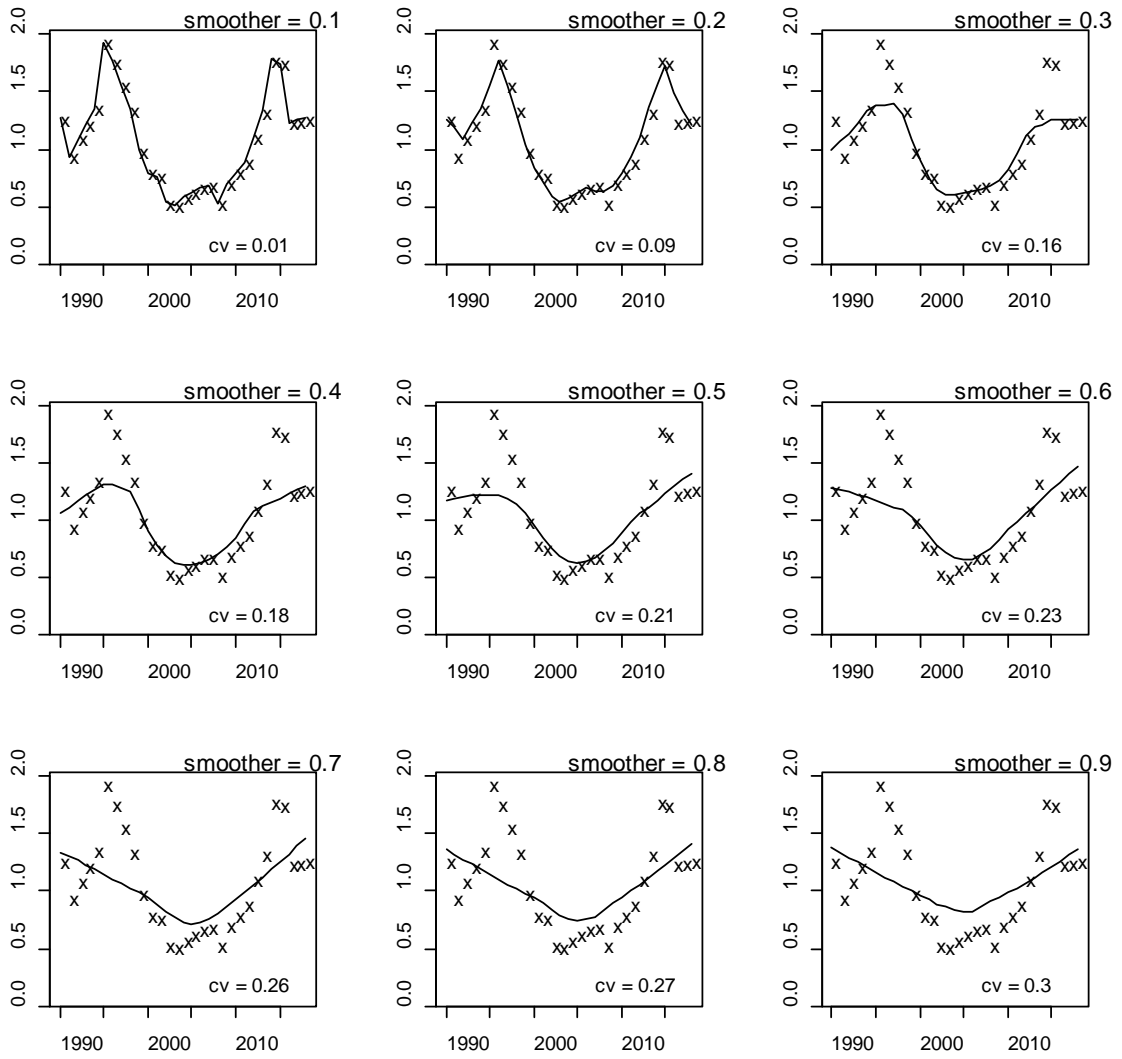
A2. 8: Coefficient-distribution influence plot for effort (fishing duration) for final SCI 2 CPUE standardisation model (Table 8).



A2. 9: Coefficient-distribution influence plot for vessel for final SCI 2 CPUE standardisation model (Table 8).



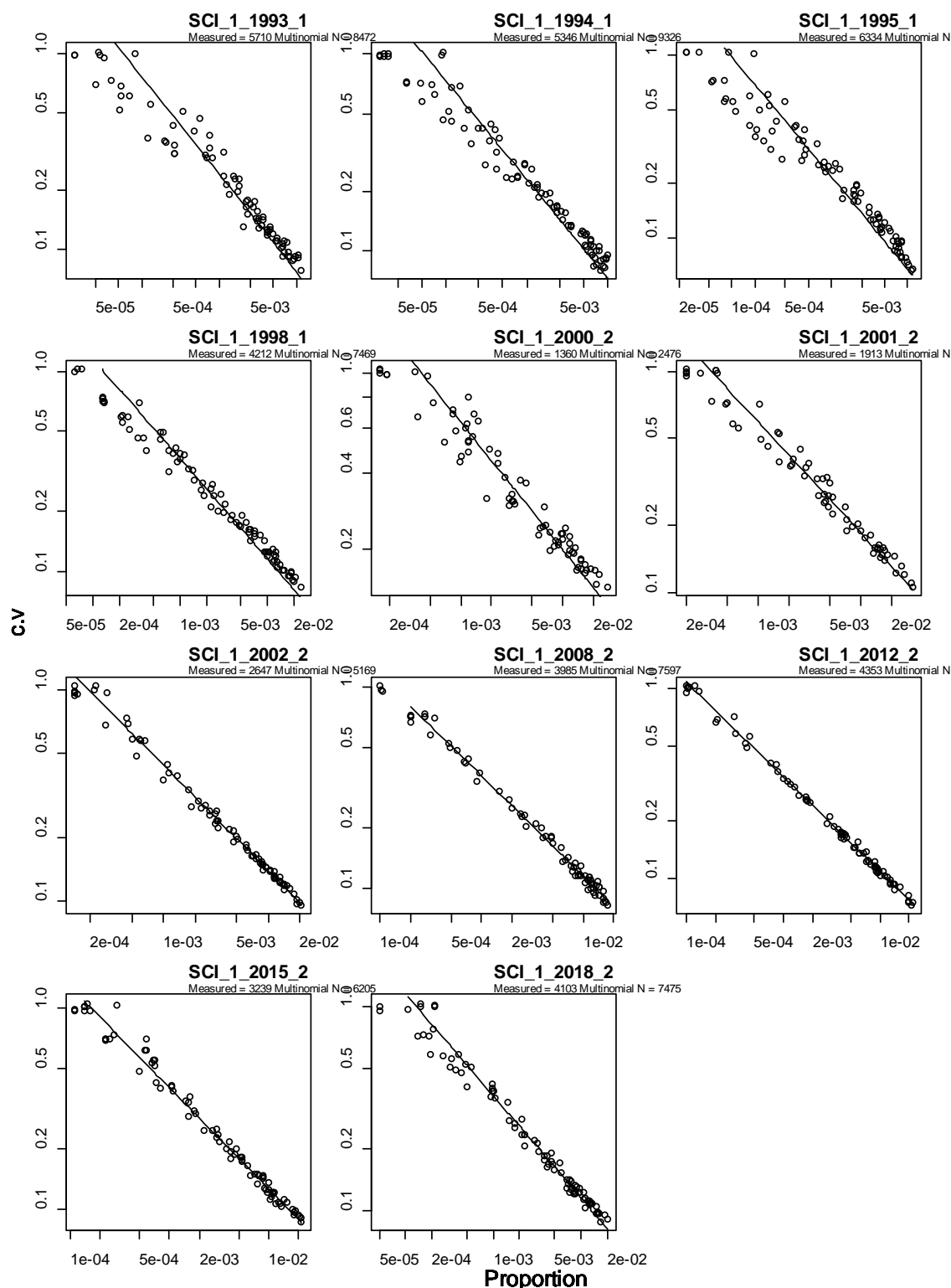
A2. 10: Coefficient-distribution influence plot for time step for final SCI 2 CPUE standardisation model (Table 8).



A2. 11: Range of smoothers fitted to the index from the final SCI 2 CPUE standardisation model (Table 8).

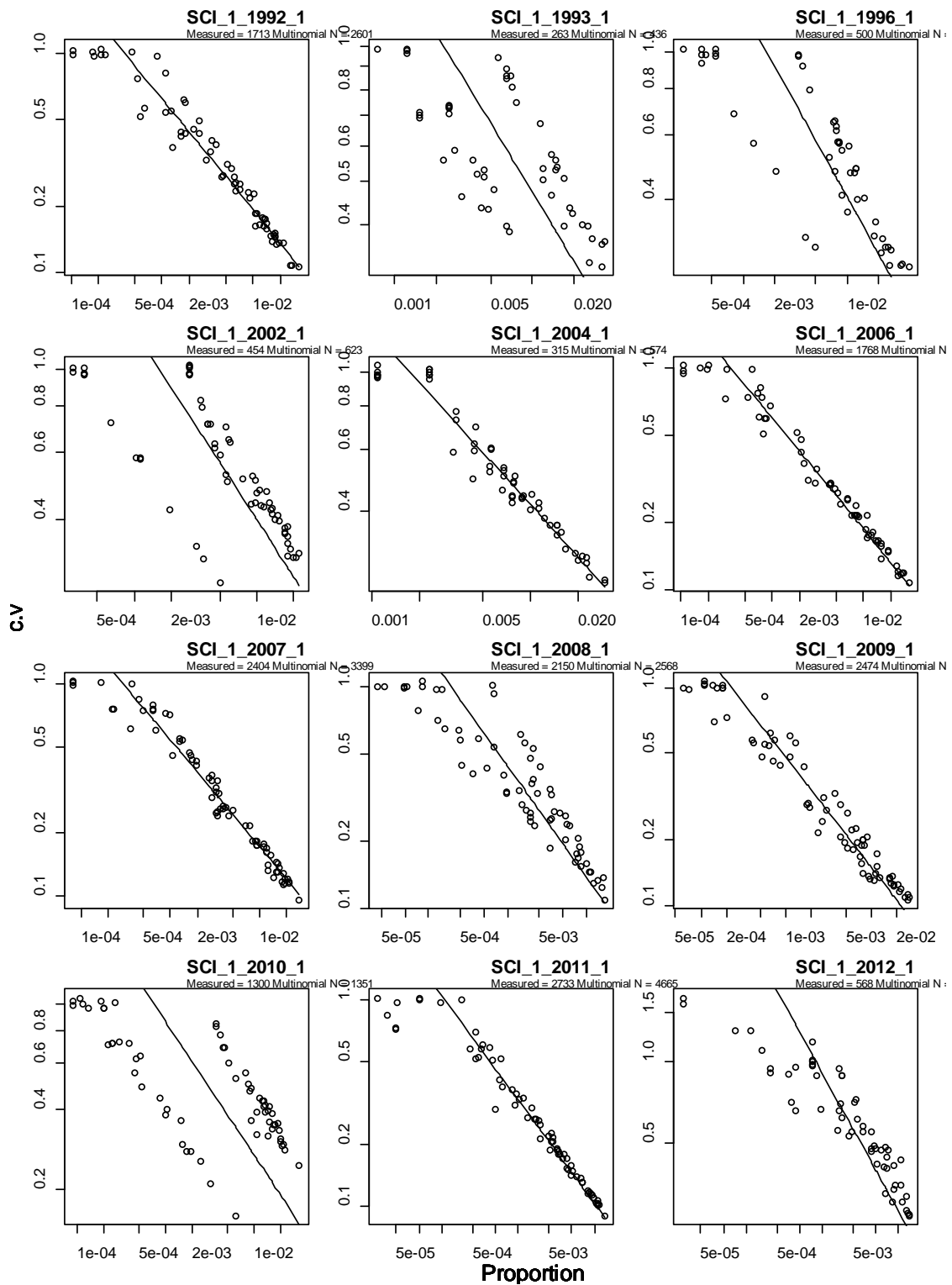
APPENDIX 3. Analysis of length composition data (SCI 1)

Trawl survey length frequency

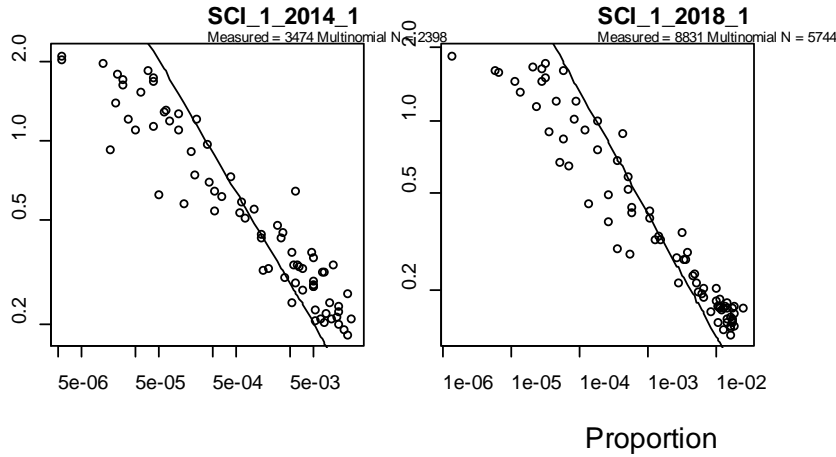


A3. 1: Observation-error CVs for the SCI 1 trawl survey proportions-at-length data sets. Each point represents a proportion at a specific length and sex for a given year. The diagonal line, which is the same in each panel, is added to aid comparison between panels; it shows the relationship between proportion and CV that would hold with simple multinomial sampling with sample size 500.

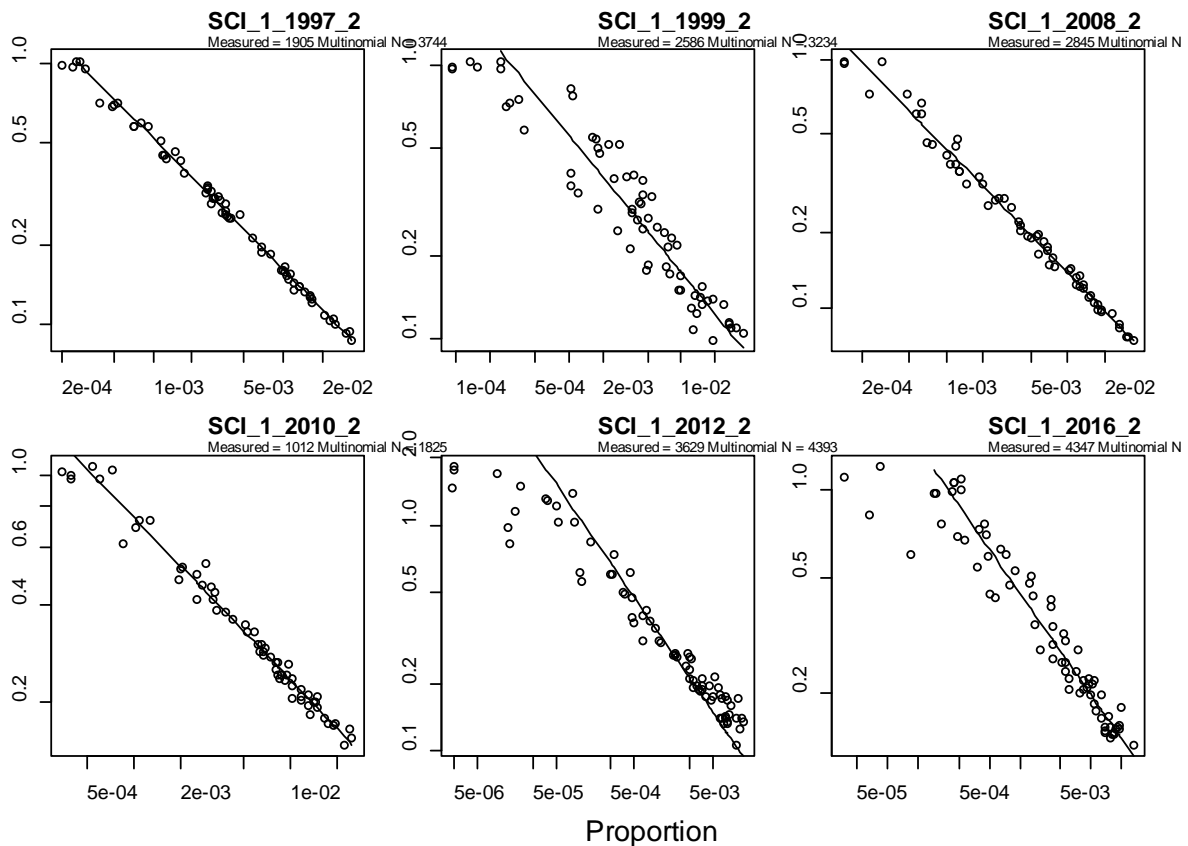
Observer length frequency



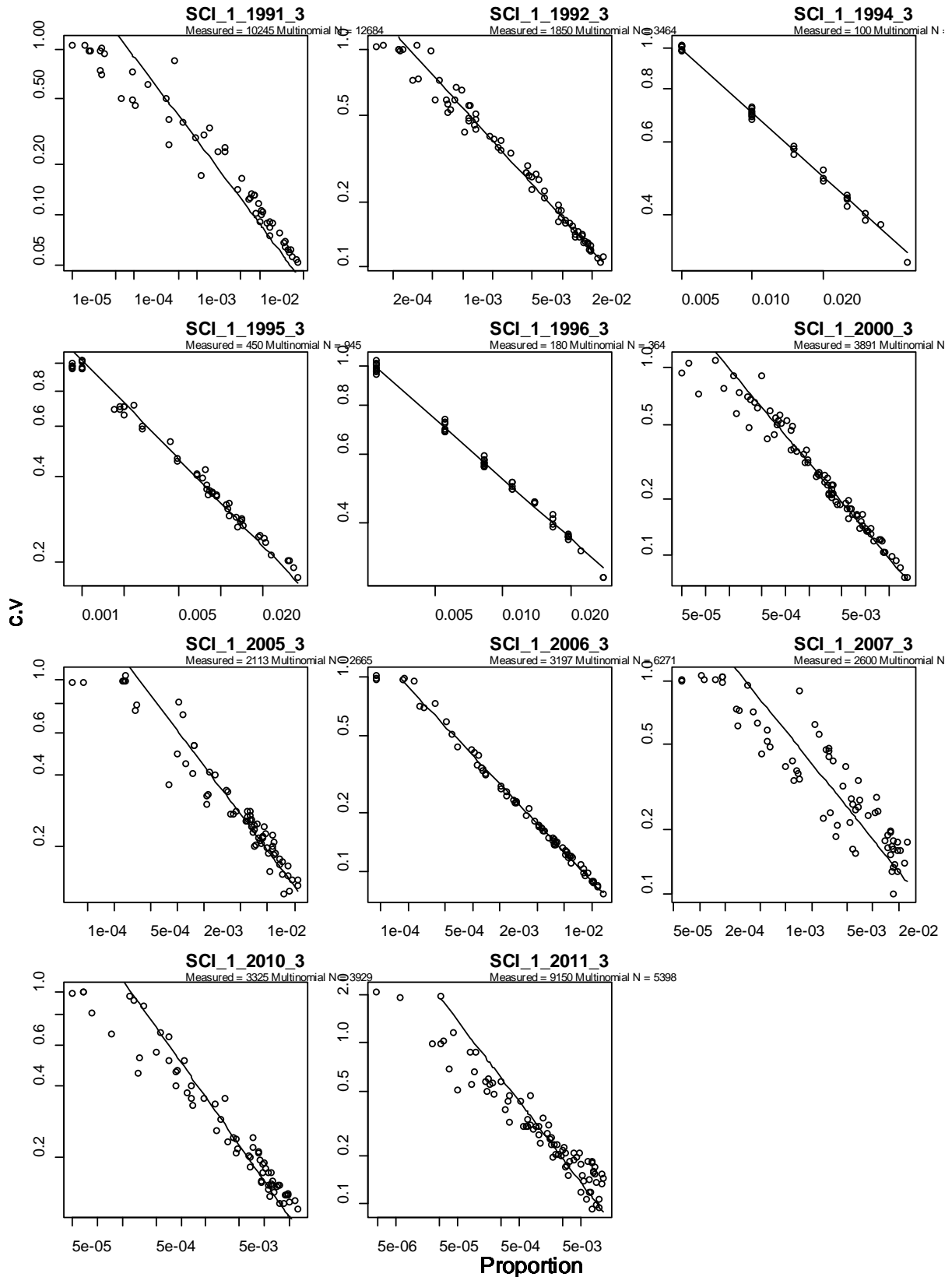
A3. 2: Observation-error CVs for the SCI 1 step 1 observer proportions-at-length data sets. Each point represents a proportion at a specific length and sex for a given year. The diagonal line, which is the same in each panel, is added to aid comparison between panels; it shows the relationship between proportion and CV that would hold with simple multinomial sampling with sample size 500.



A3.2 (continued): Observation-error CVs for the SCI 1 step 1 observer proportions-at-length data sets. Each point represents a proportion at a specific length and sex for a given year. The diagonal line, which is the same in each panel, is added to aid comparison between panels; it shows the relationship between proportion and CV that would hold with simple multinomial sampling with sample size 500.

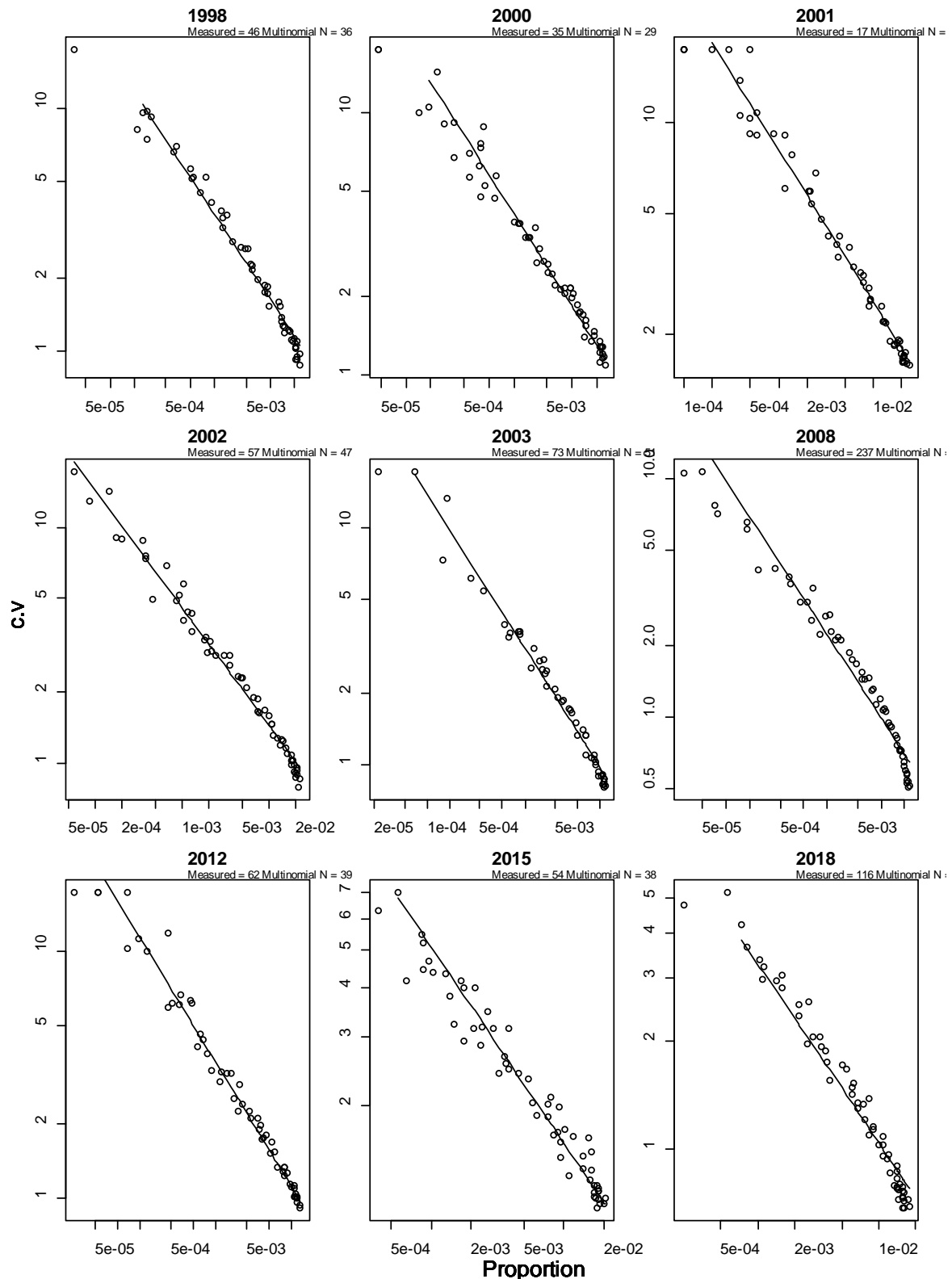


A3.3: Observation-error CVs for the SCI 1 step 2 observer proportions-at-length data sets. Each point represents a proportion at a specific length and sex for a given year. The diagonal line, which is the same in each panel, is added to aid comparison between panels; it shows the relationship between proportion and CV that would hold with simple multinomial sampling with sample size 500.



A3. 4: Observation-error CVs for the SCI 1 step 3 observer proportions-at-length data sets. Each point represents a proportion at a specific length and sex for a given year. The diagonal line, which is the same in each panel, is added to aid comparison between panels; it shows the relationship between proportion and CV that would hold with simple multinomial sampling with sample size 500.

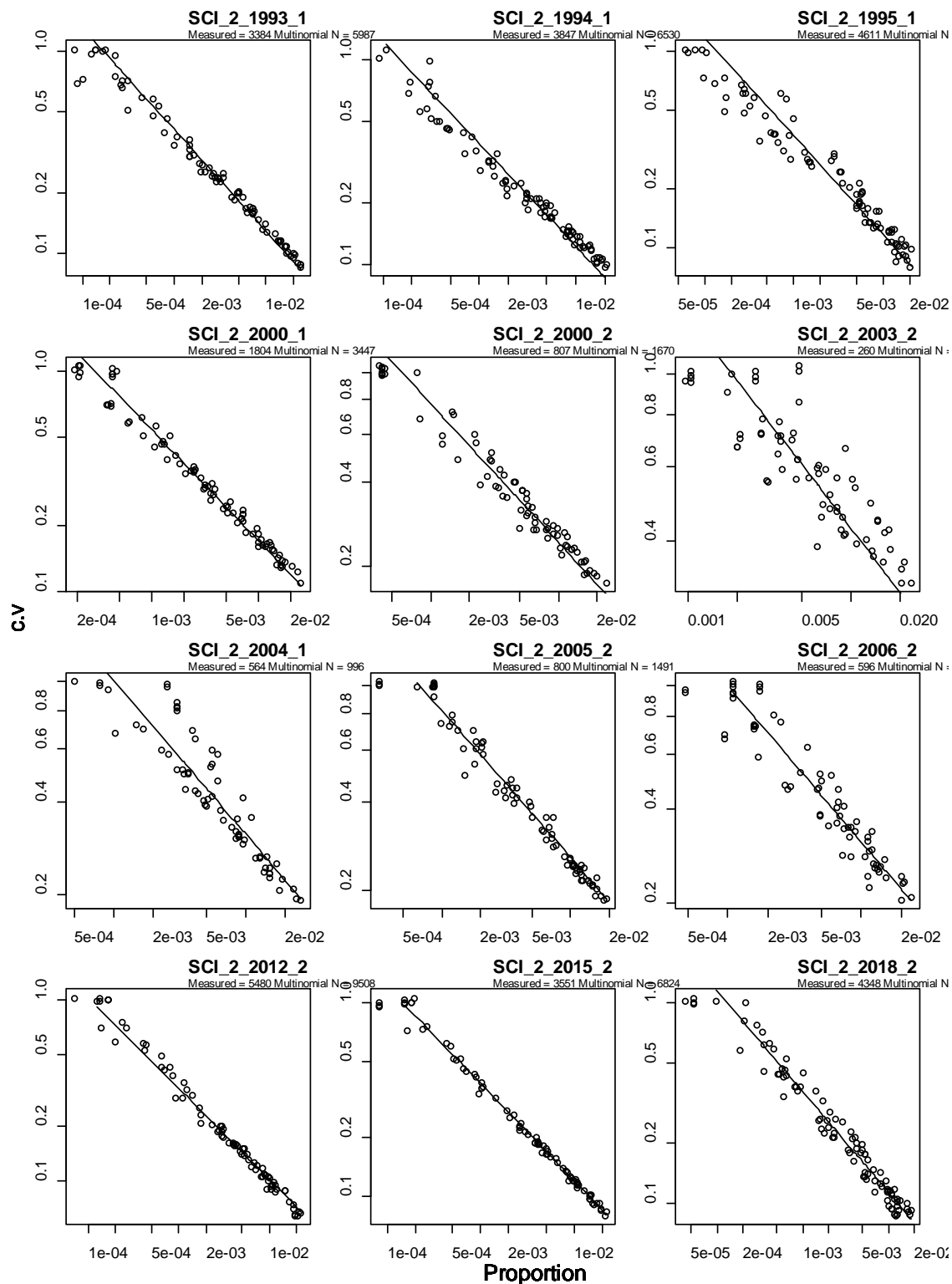
Photo Survey



A3. 5: Observation-error CVs for the SCI 1 photo survey proportions-at-length data sets. Each point represents a proportion at a specific length and sex for a given year. The diagonal line, which is the same in each panel, is added to aid comparison between panels; it shows the relationship between proportion and CV that would hold with simple multinomial sampling with sample size 500.

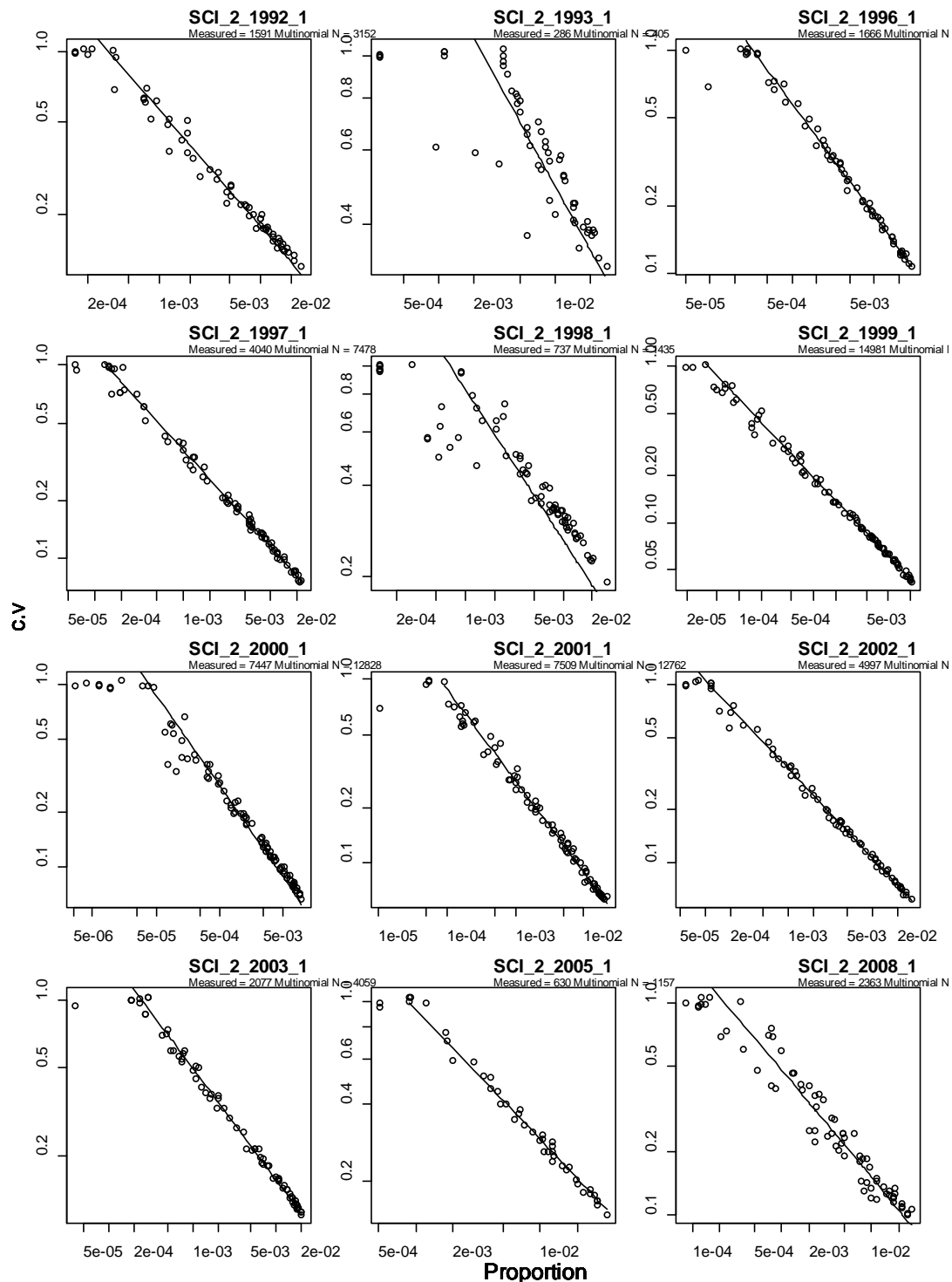
APPENDIX 4. Analysis of length composition data (SCI 2)

Trawl survey length frequency



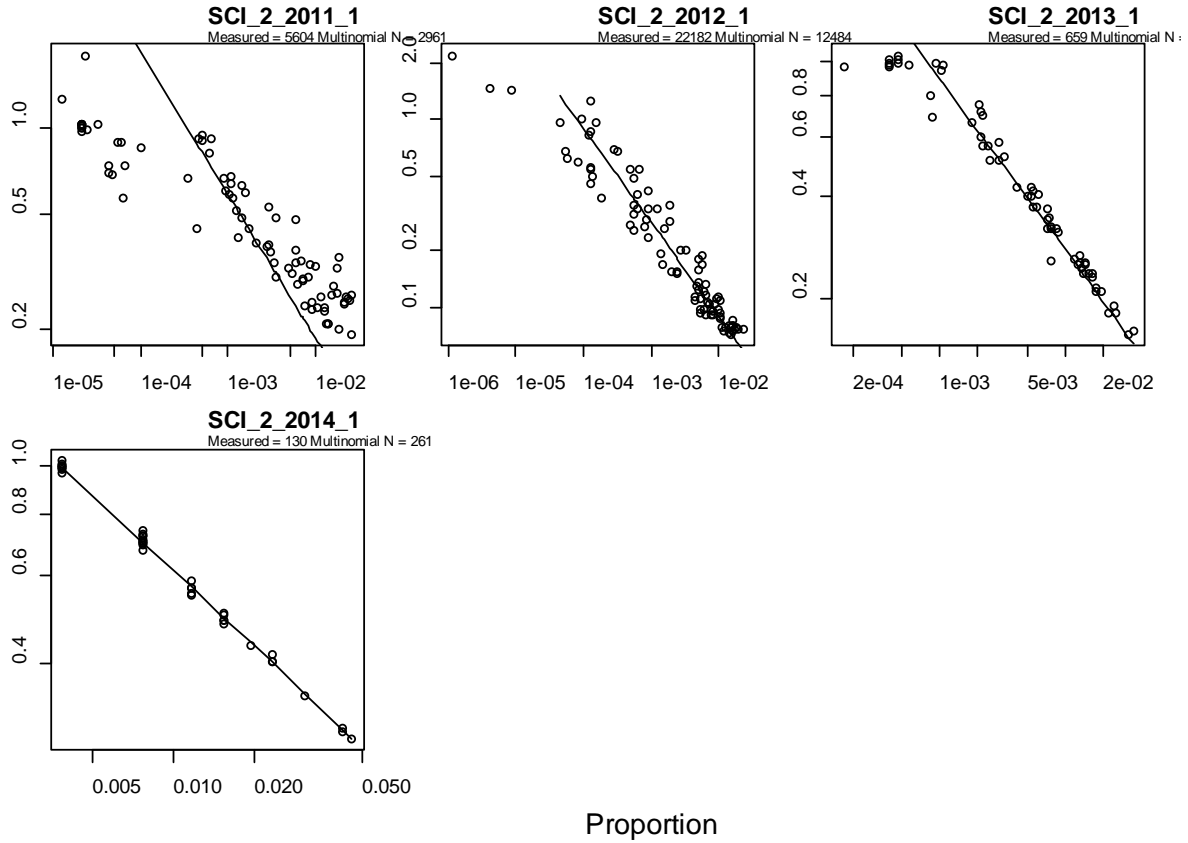
A4. 1: Observation-error CVs for the SCI 2 trawl survey proportions-at-length data sets. Each point represents a proportion at a specific length and sex for a given year. The diagonal line, which is the same in each panel, is added to aid comparison between panels; it shows the relationship between proportion and CV that would hold with simple multinomial sampling with sample size 500.

Observer length frequency

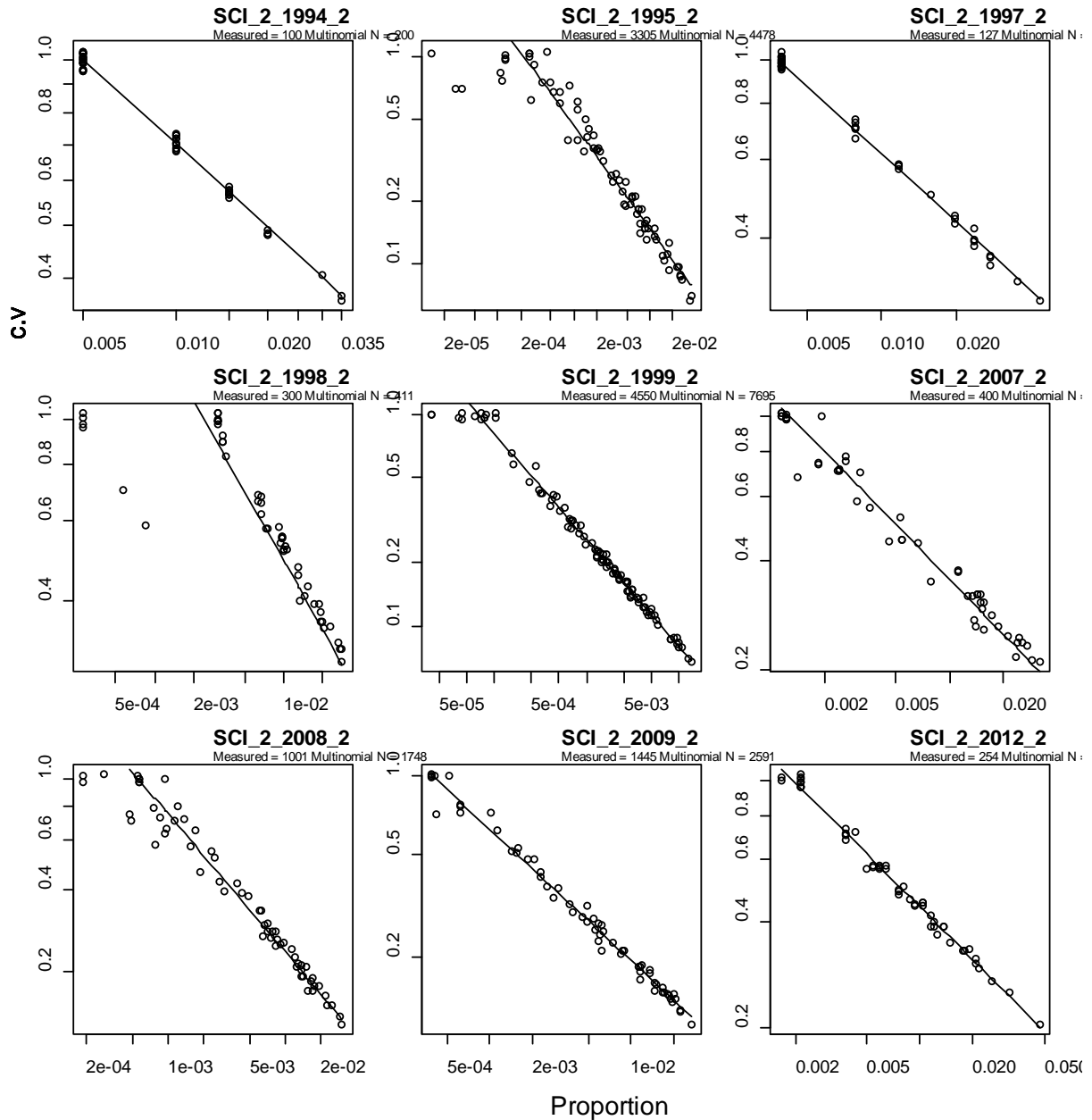


A4. 2: Observation-error CVs for the SCI 2 step 1 observer proportions-at-length data sets. Each point represents a proportion at a specific length and sex for a given year. The diagonal line, which is the same in each panel, is added to aid comparison between panels; it shows the relationship between proportion and CV that would hold with simple multinomial sampling with sample size 500.

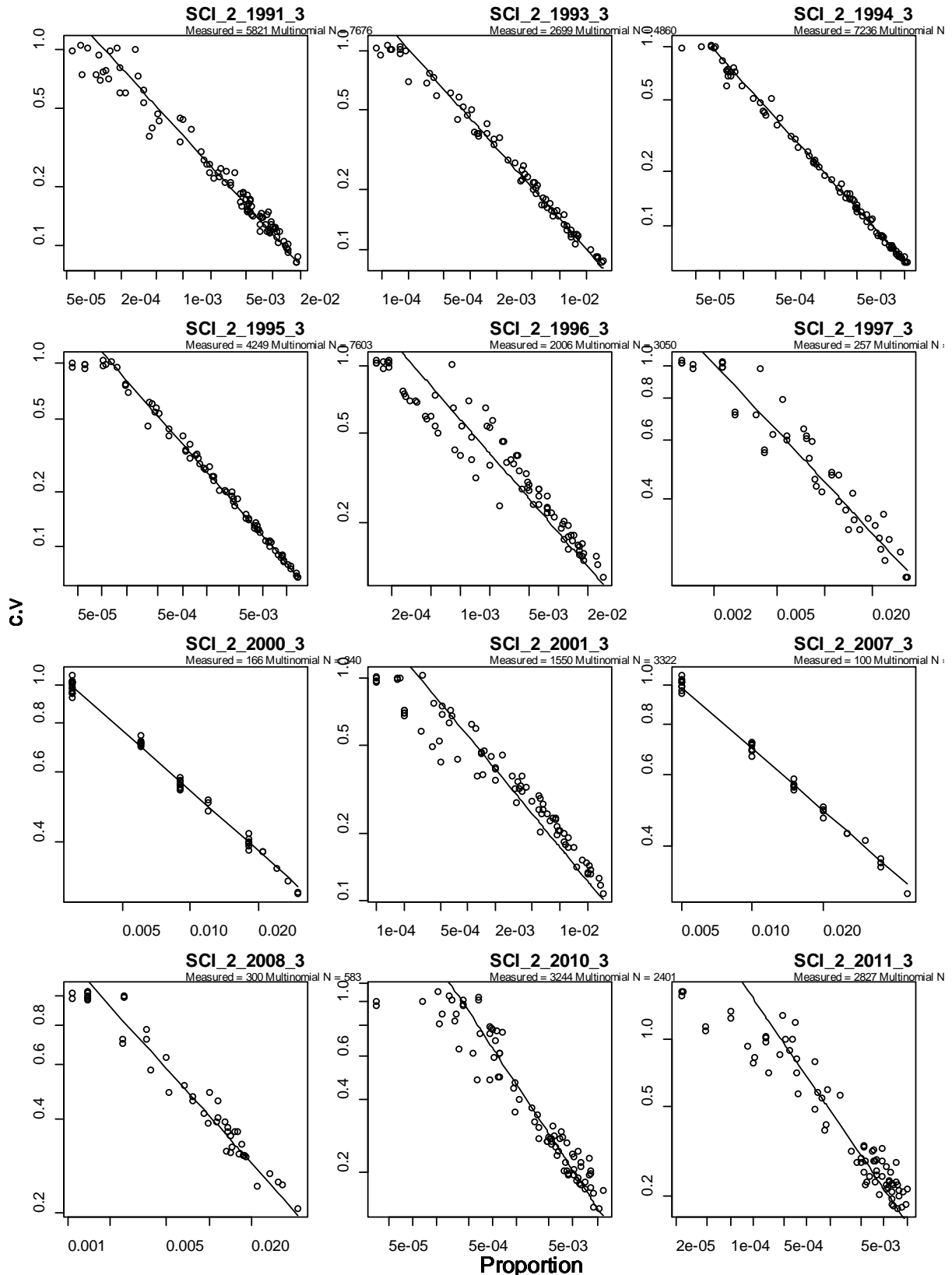
C.



A4. 2 (continued): Observation-error CVs for the SCI 2 step 1 observer proportions-at-length data sets. Each point represents a proportion at a specific length and sex for a given year. The diagonal line, which is the same in each panel, is added to aid comparison between panels; it shows the relationship between proportion and CV that would hold with simple multinomial sampling with sample size 500.

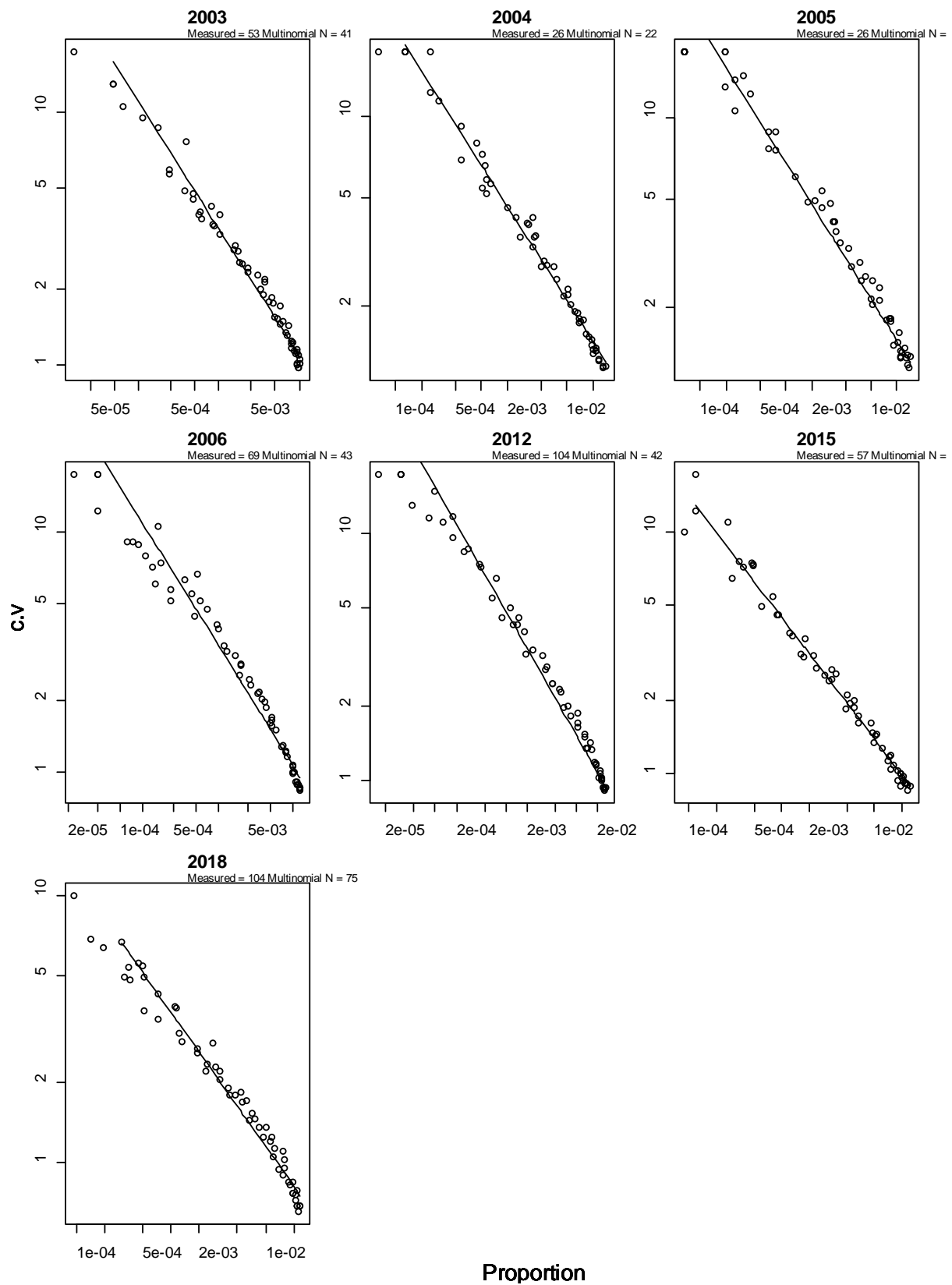


A4. 3: Observation-error CVs for the SCI 2 step 2 observer proportions-at-length data sets. Each point represents a proportion at a specific length and sex for a given year. The diagonal line, which is the same in each panel, is added to aid comparison between panels; it shows the relationship between proportion and CV that would hold with simple multinomial sampling with sample size 500.



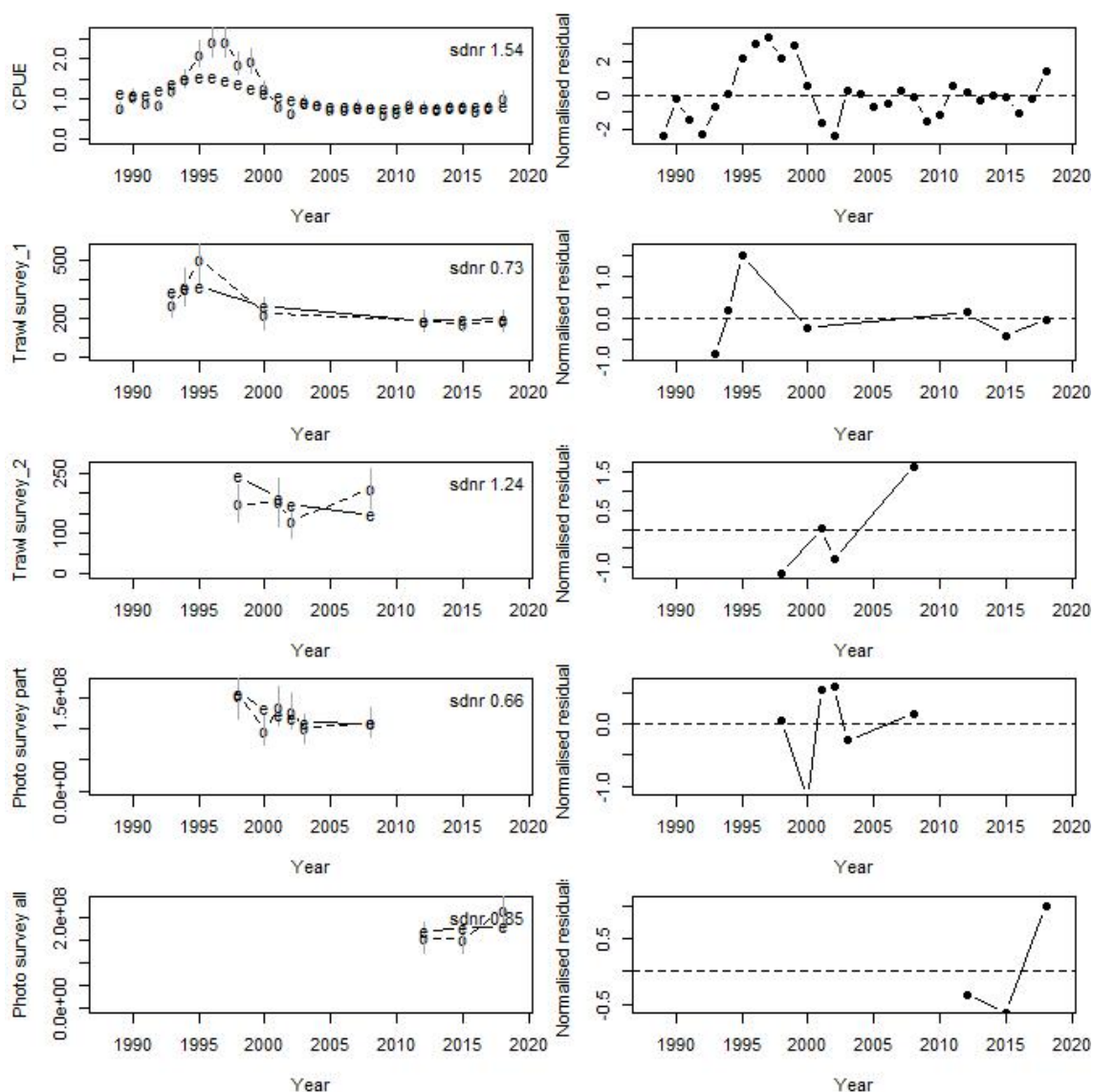
A4. 4: Observation-error CVs for the SCI 2 step 3 observer proportions-at-length data sets. Each point represents a proportion at a specific length and sex for a given year. The diagonal line, which is the same in each panel, is added to aid comparison between panels; it shows the relationship between proportion and CV that would hold with simple multinomial sampling with sample size 500.

Photo survey

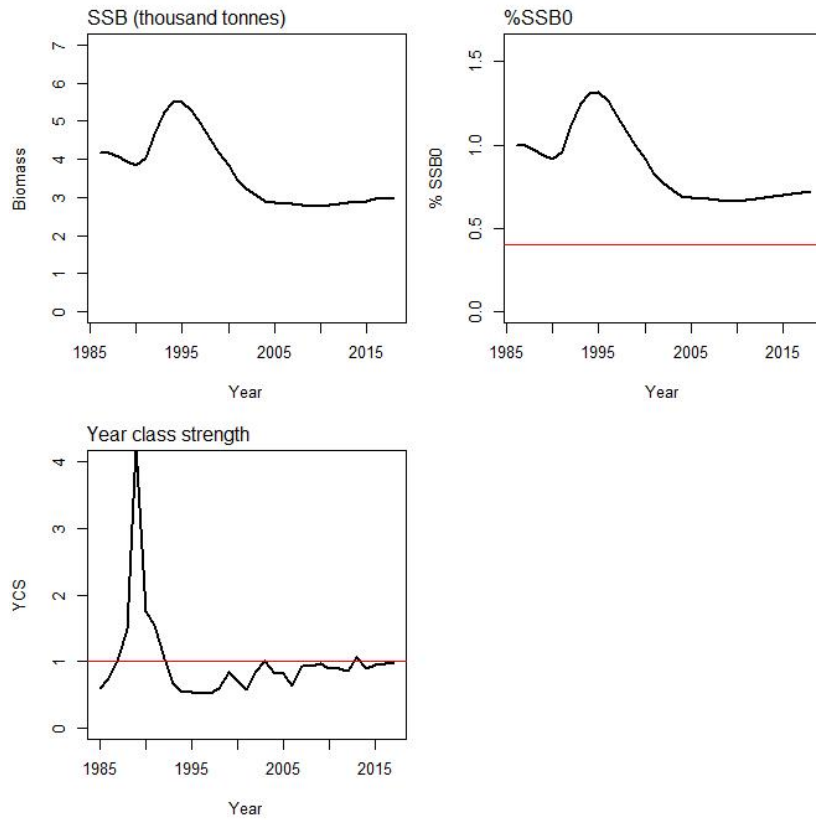


A4. 5: Observation-error CVs for the SCI 2 photo survey proportions-at-length data sets. Each point represents a proportion at a specific length and sex for a given year. The diagonal line, which is the same in each panel, is added to aid comparison between panels; it shows the relationship between proportion and CV that would hold with simple multinomial sampling with sample size 500.

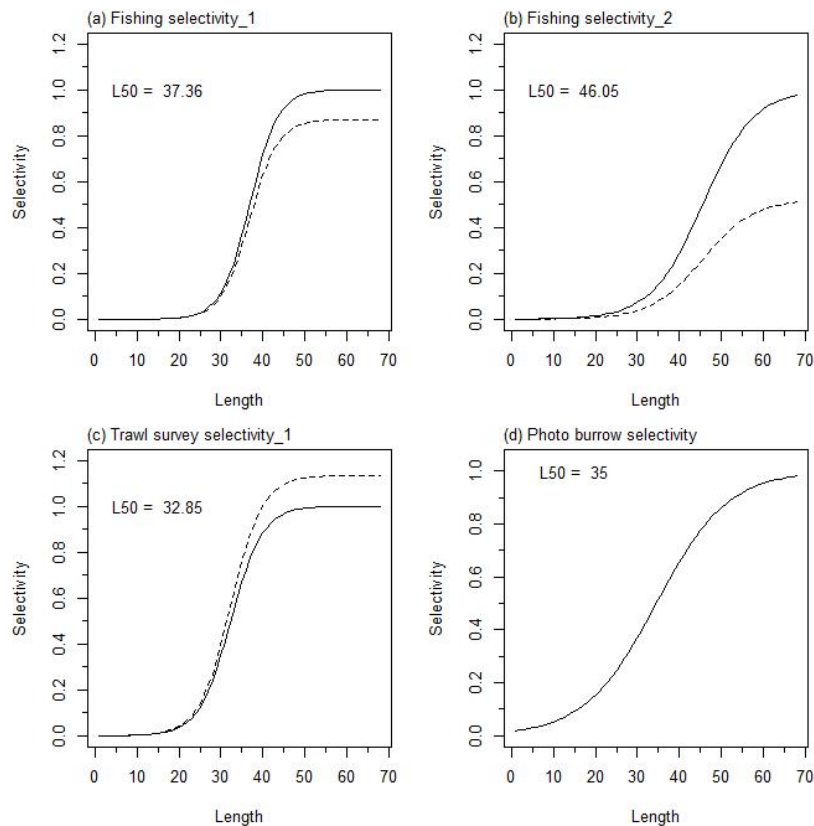
APPENDIX 5. SCI 1 M02CV15 model plots ($M=0.2$, $CV=0.15$)



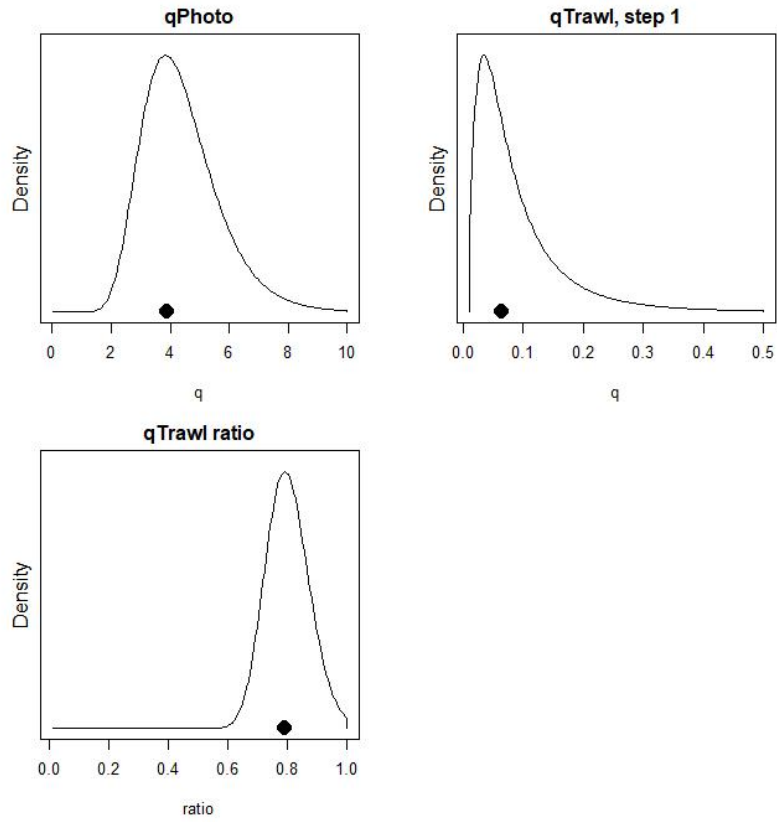
A5. 1: Fits to abundance indices (left column) and normalised residuals (right column) for standardised CPUE index (top row) trawl survey biomass index covering whole area (second row), trawl survey biomass index covering limited area (third row), photo survey abundance index covering limited area (fourth row), and photo survey abundance index covering whole area (fifth row) for SCI 1 M02CV15 model.



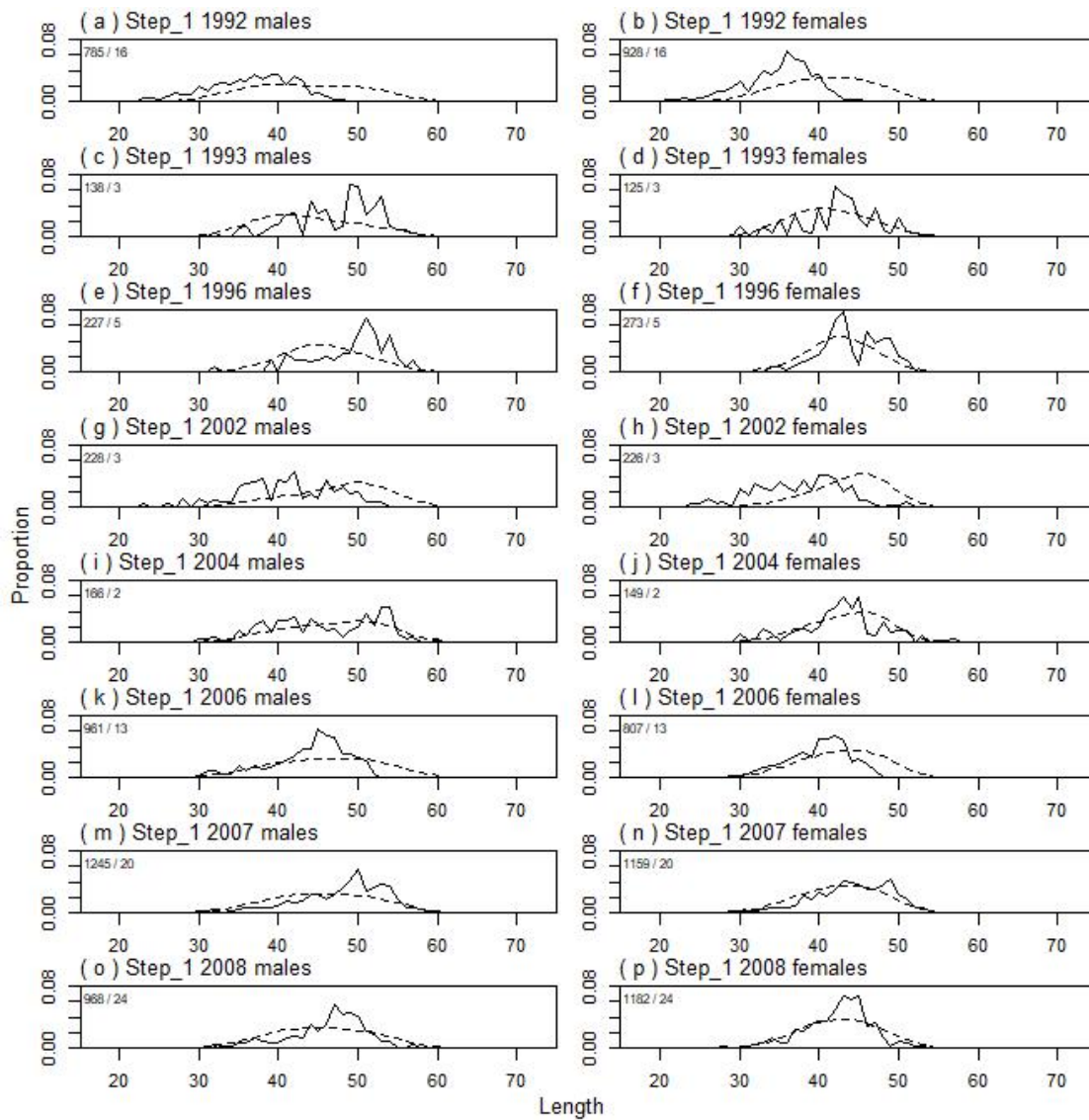
A5. 2: Spawning stock biomass trajectory (upper left), stock status (upper right), and year class strength (lower left) for SCI 1 M02CV15 model.



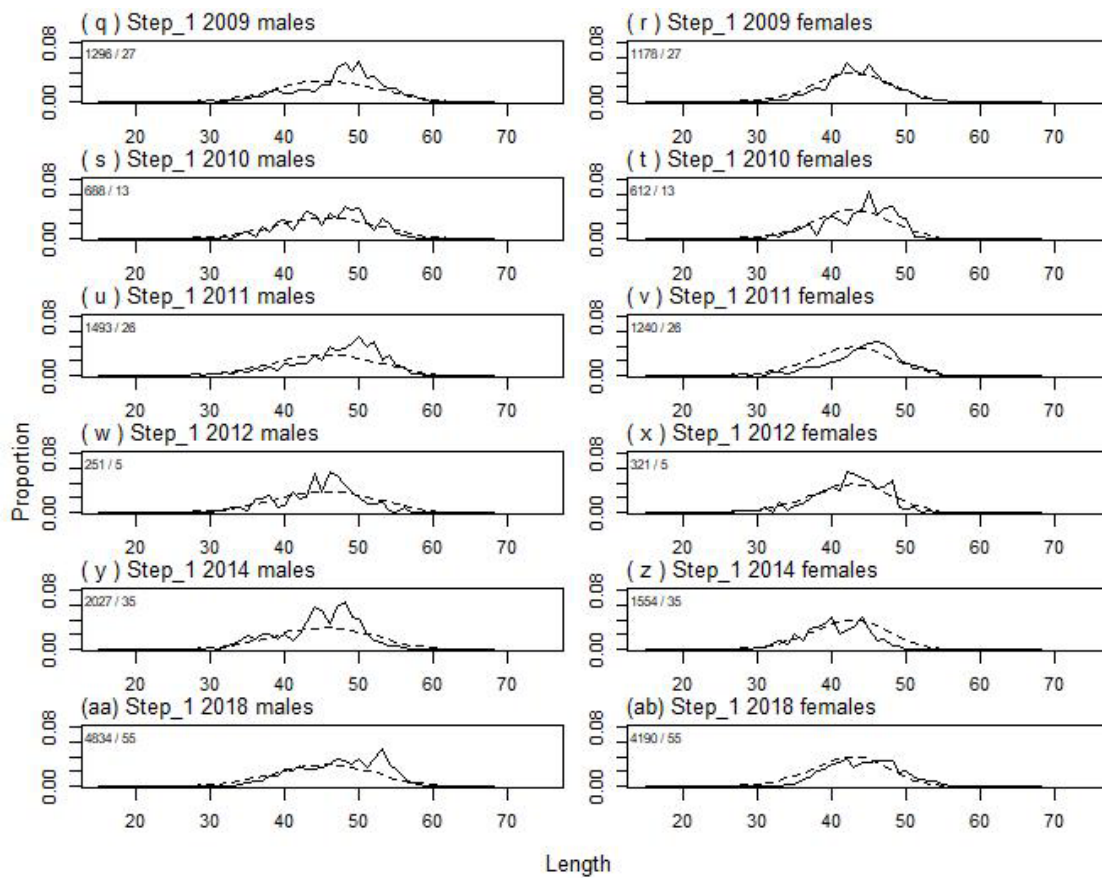
A5. 3: Fishery and survey selectivity curves for SCI 1 M02CV15 model. Solid line – females, dotted line – males. The scampi burrow index is not sexed, and a single selectivity applies.



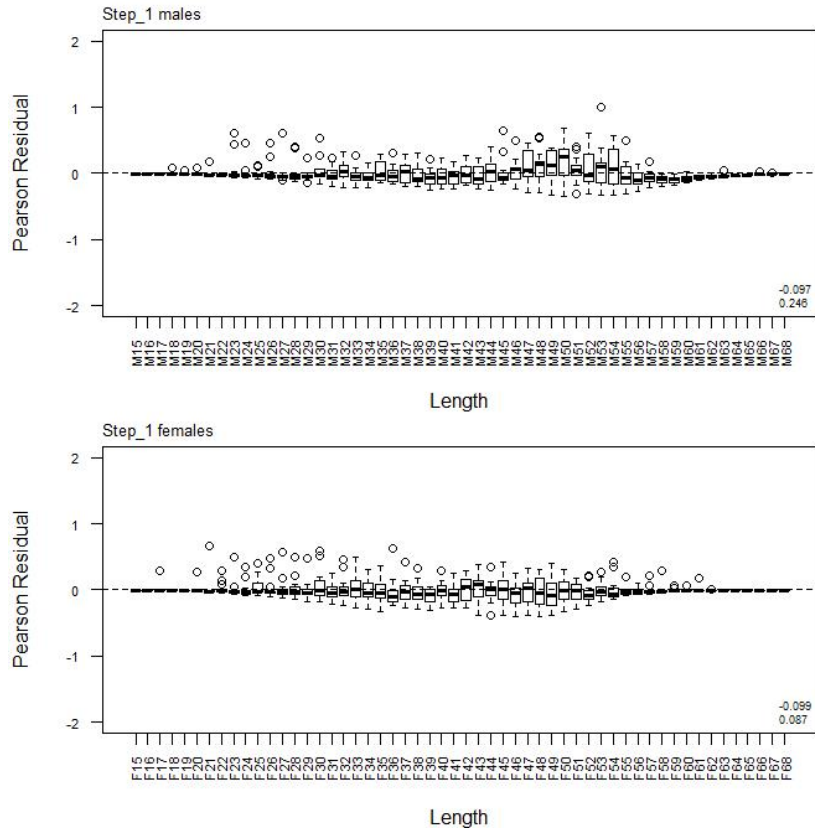
A5. 4: Catchability estimates from MPD model run, plotted in relation to prior distribution for SCI 1 M02CV15 model.



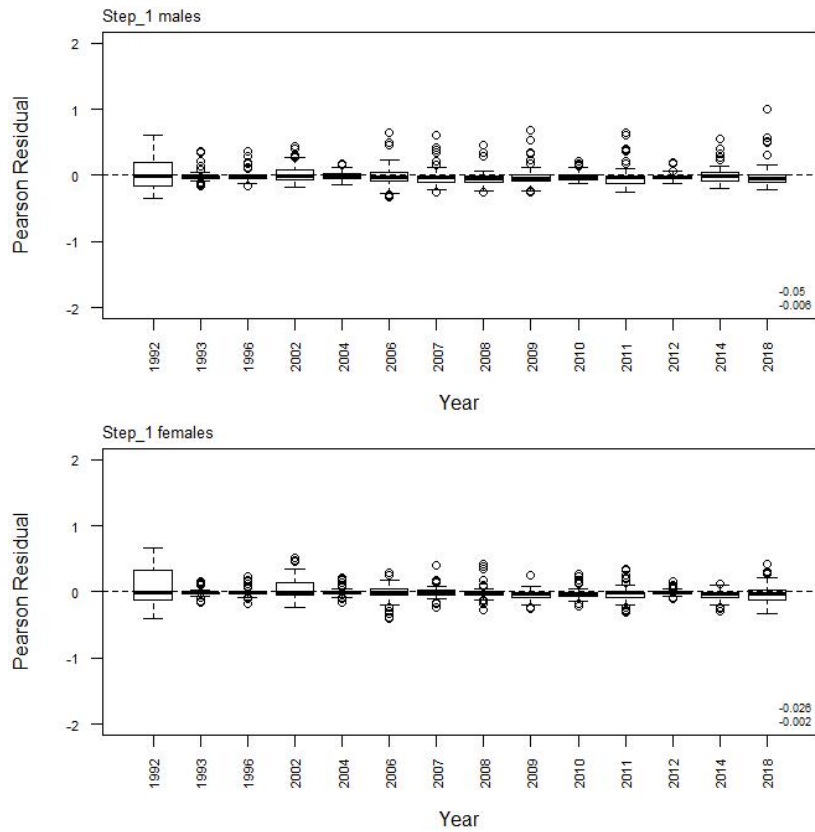
A5. 5: Observed (solid line) and fitted (dashed line) length frequency distributions from observer samples, time step 1 for SCI 1 M02CV15 model. Numbers in top left corner of each plot represent number of scampi measured / number of events sampled.



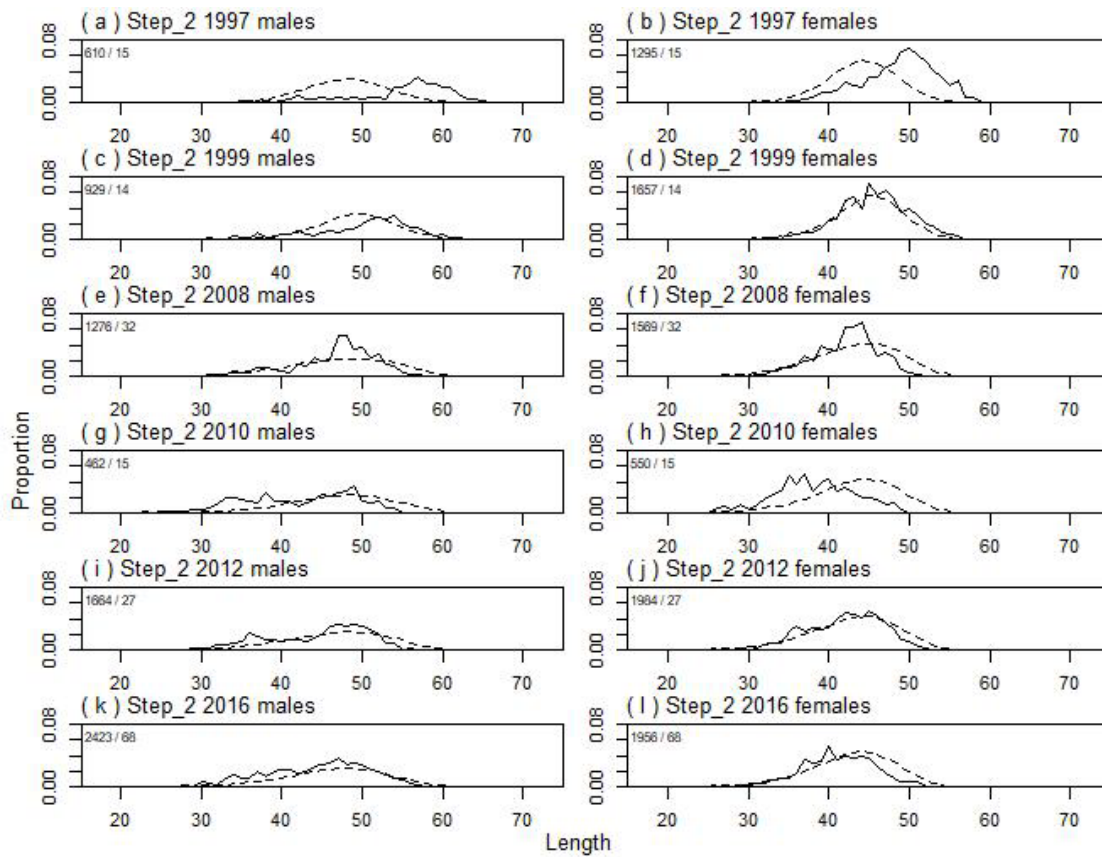
A5. 5 (continued): Observed (solid line) and fitted (dashed line) length frequency distributions from observer samples, time step 1 for SCI 1 M02CV15 model. Numbers in top left corner of each plot represent number of scampi measured / number of events sampled.



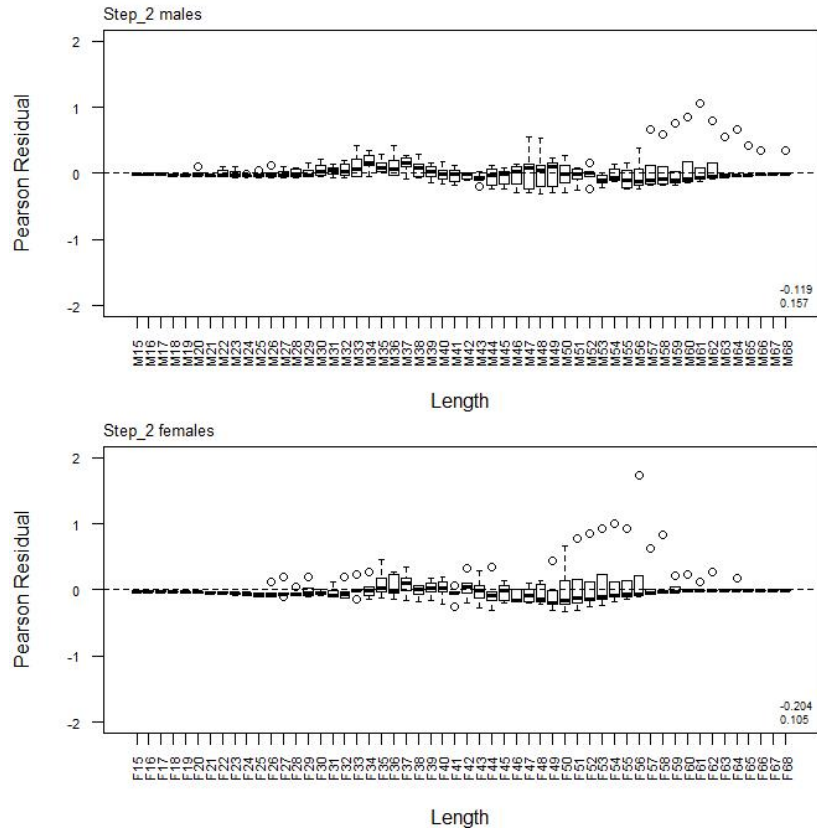
A5. 6: Box plots of Pearson residuals from the fit to length frequency distributions by length from observer sampling by sex for time step 1 for SCI 1 M02CV15 model.



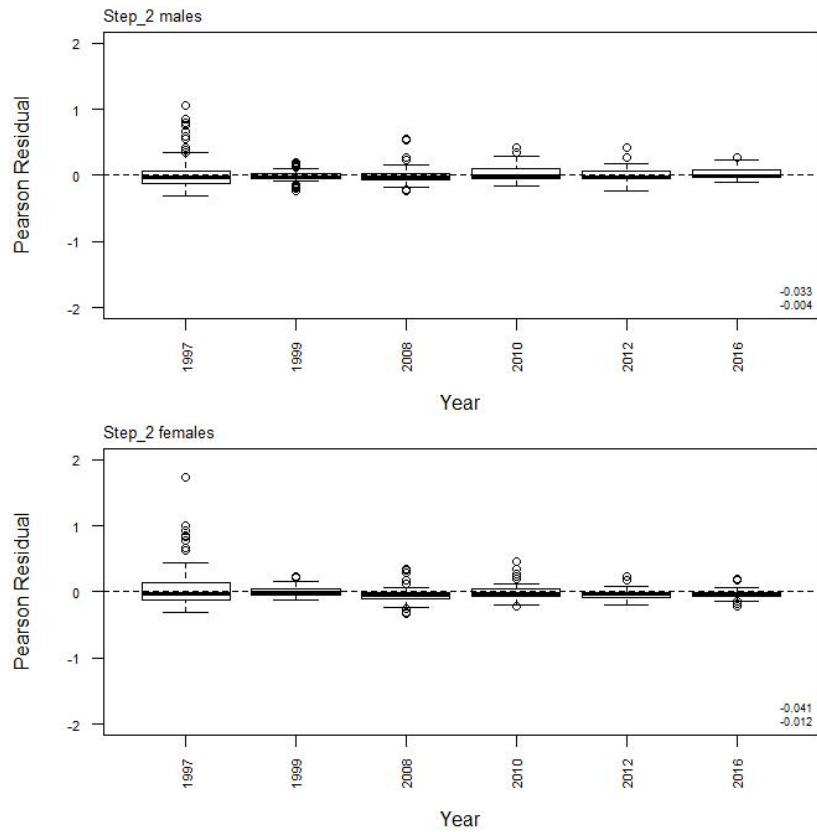
A5. 7: Box plots of Pearson residuals from the fit to length frequency distributions by year from observer sampling by sex for time step 1 for SCI 1 M02CV15 model.



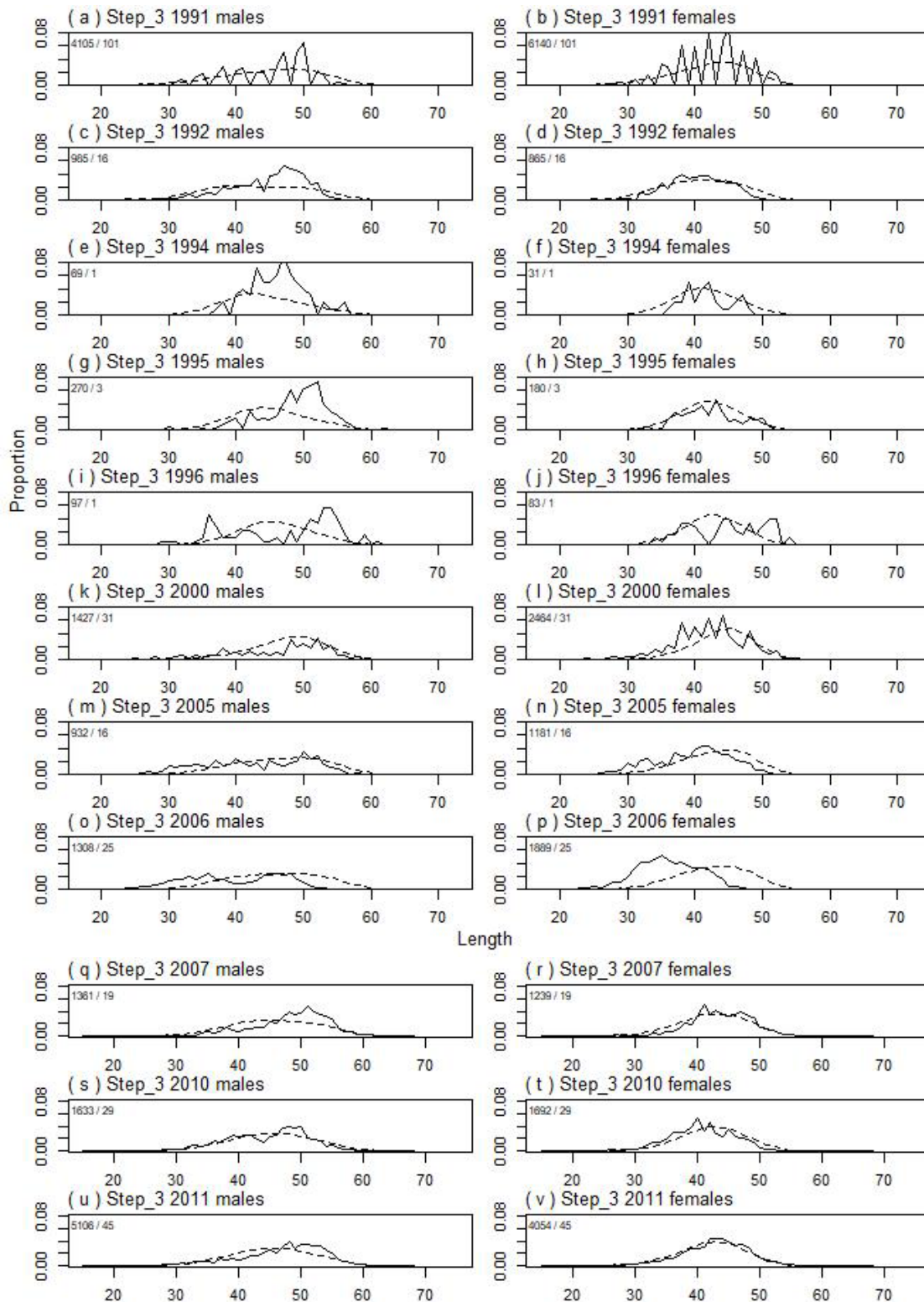
A5. 8: Observed (solid line) and fitted (dashed line) length frequency distributions from observer samples, time step 2 for SCI 1 M02CV15 model. Numbers in top left corner of each plot represent number of scampi measured / number of events sampled.



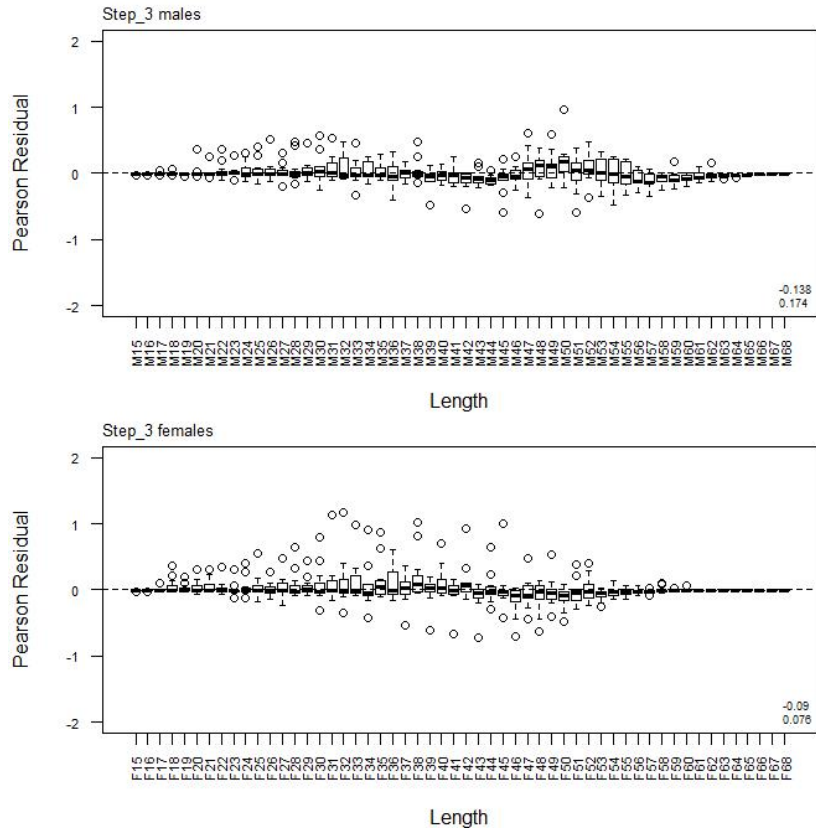
A5. 9: Box plots of Pearson residuals from the fit to length frequency distributions by length from observer sampling by sex for time step 2 for SCI 1 M02CV15 model.



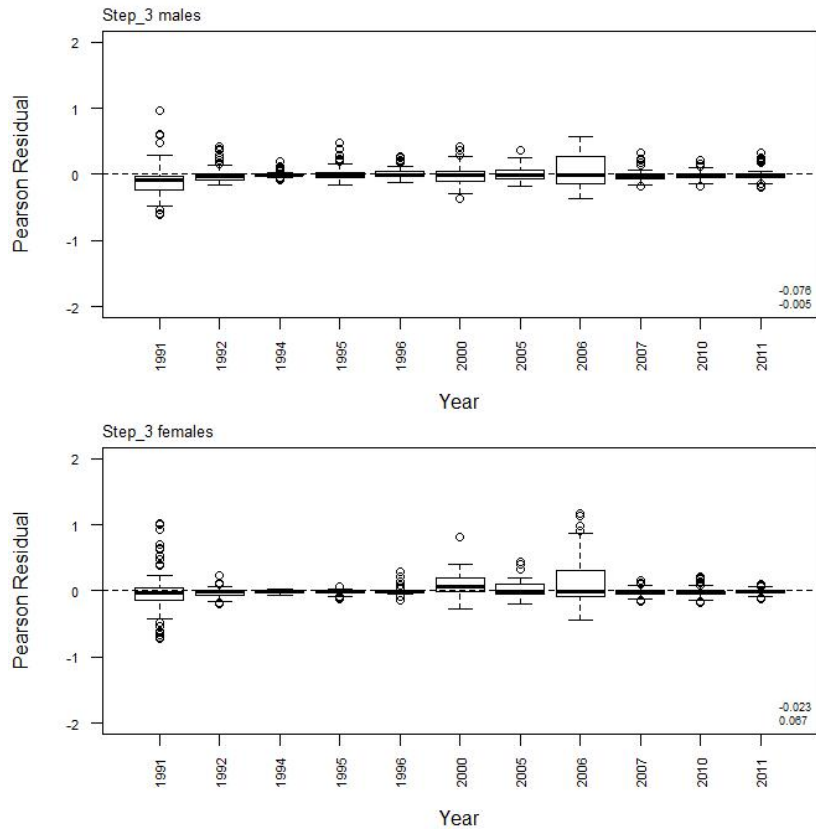
A5. 10: Box plots of Pearson residuals from the fit to length frequency distributions by year from observer sampling by sex for time step 2 for SCI 1 M02CV15 model.



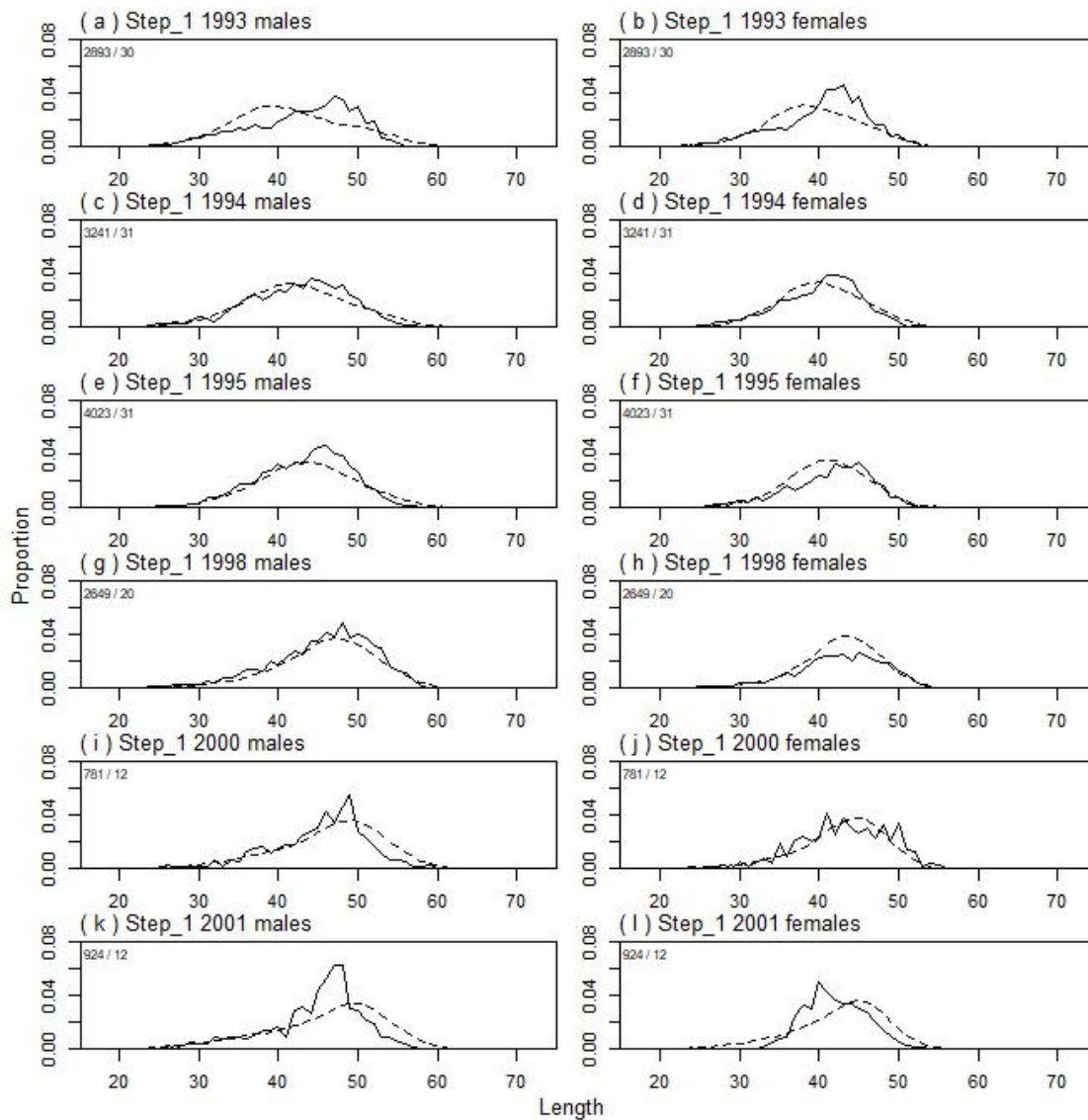
A5. 11: Observed (solid line) and fitted (dashed line) length frequency distributions from observer samples, time step 3 for SCI 1 M02CV15 model. Numbers in top left corner of each plot represent number of scampi measured / number of events sampled.



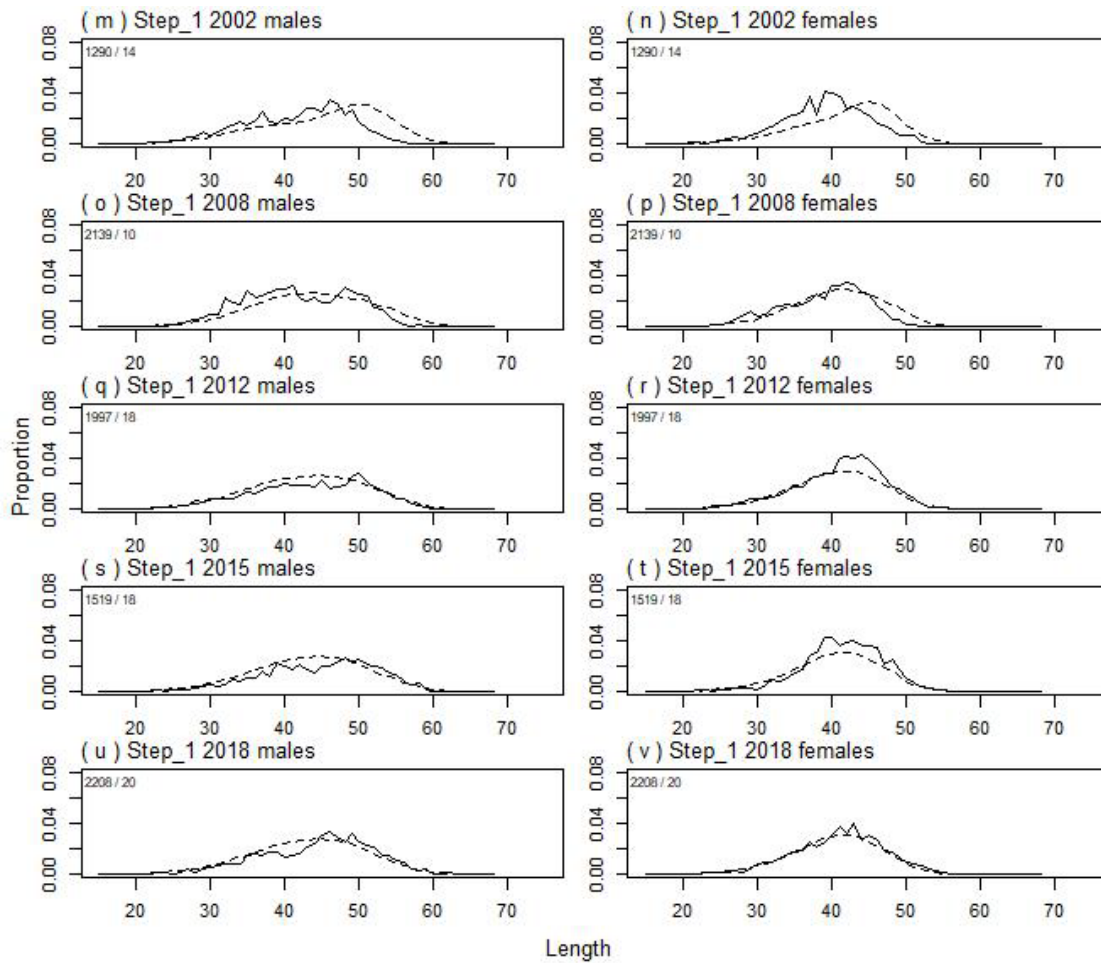
A5. 12: Box plots of Pearson residuals from the fit to length frequency distributions by length from observer sampling by sex for time step 3 for SCI 1 M02CV15 model.



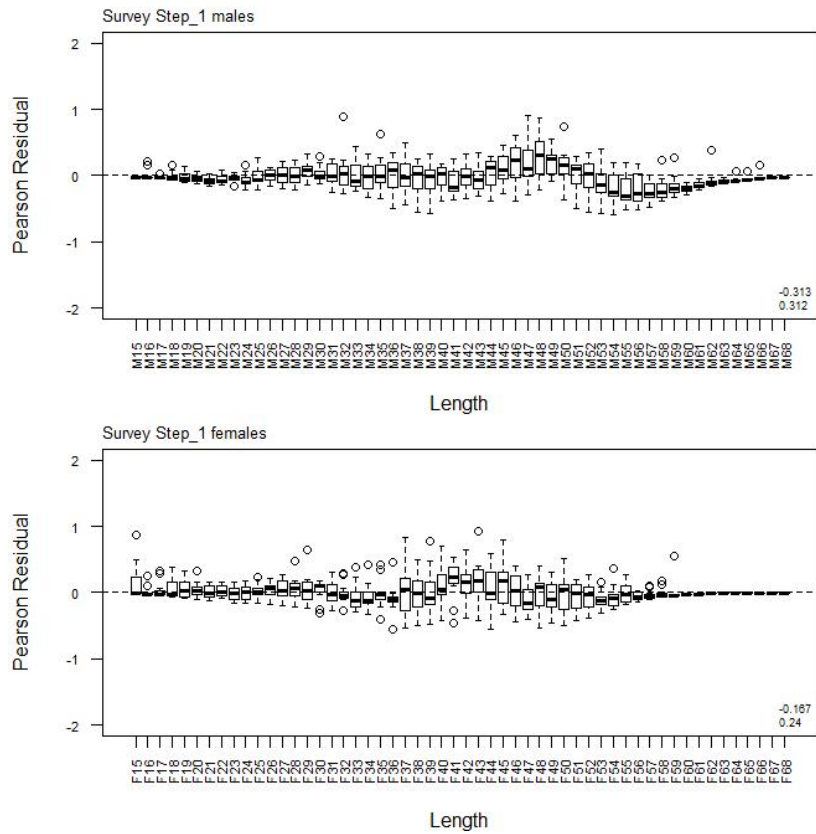
A5. 13: Box plots of Pearson residuals from the fit to length frequency distributions by year from observer sampling by sex for time step 3 for SCI 1 M02CV15 model.



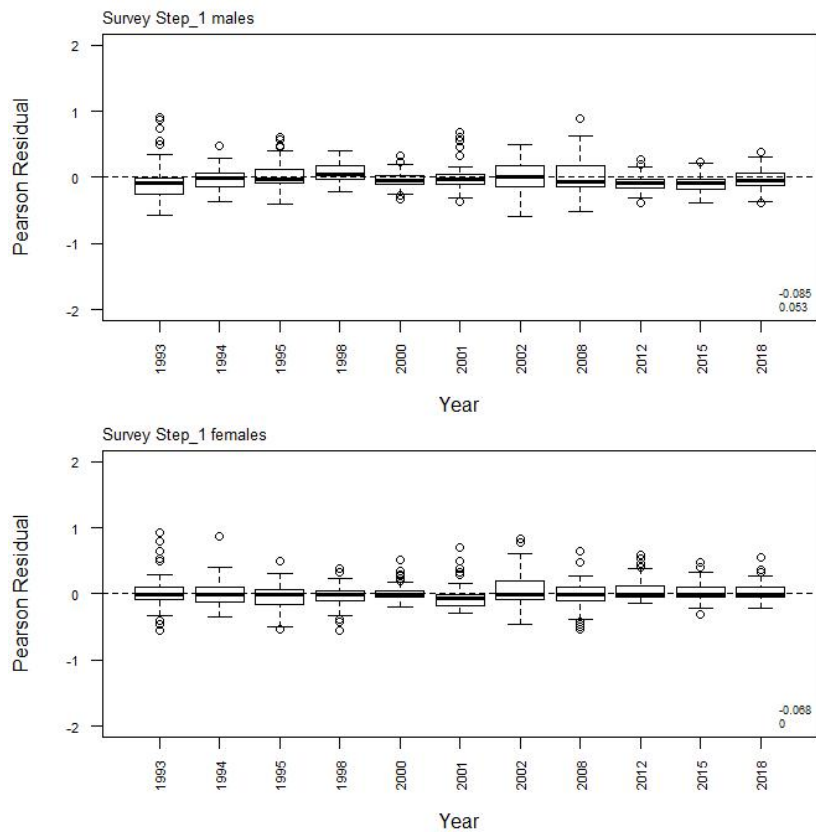
A5. 14: Observed (solid line) and fitted (dashed line) length frequency distributions from trawl survey samples for SCI 1 M02CV15 model. Numbers in top left corner of each plot represent number of scampi measured / number of events sampled.



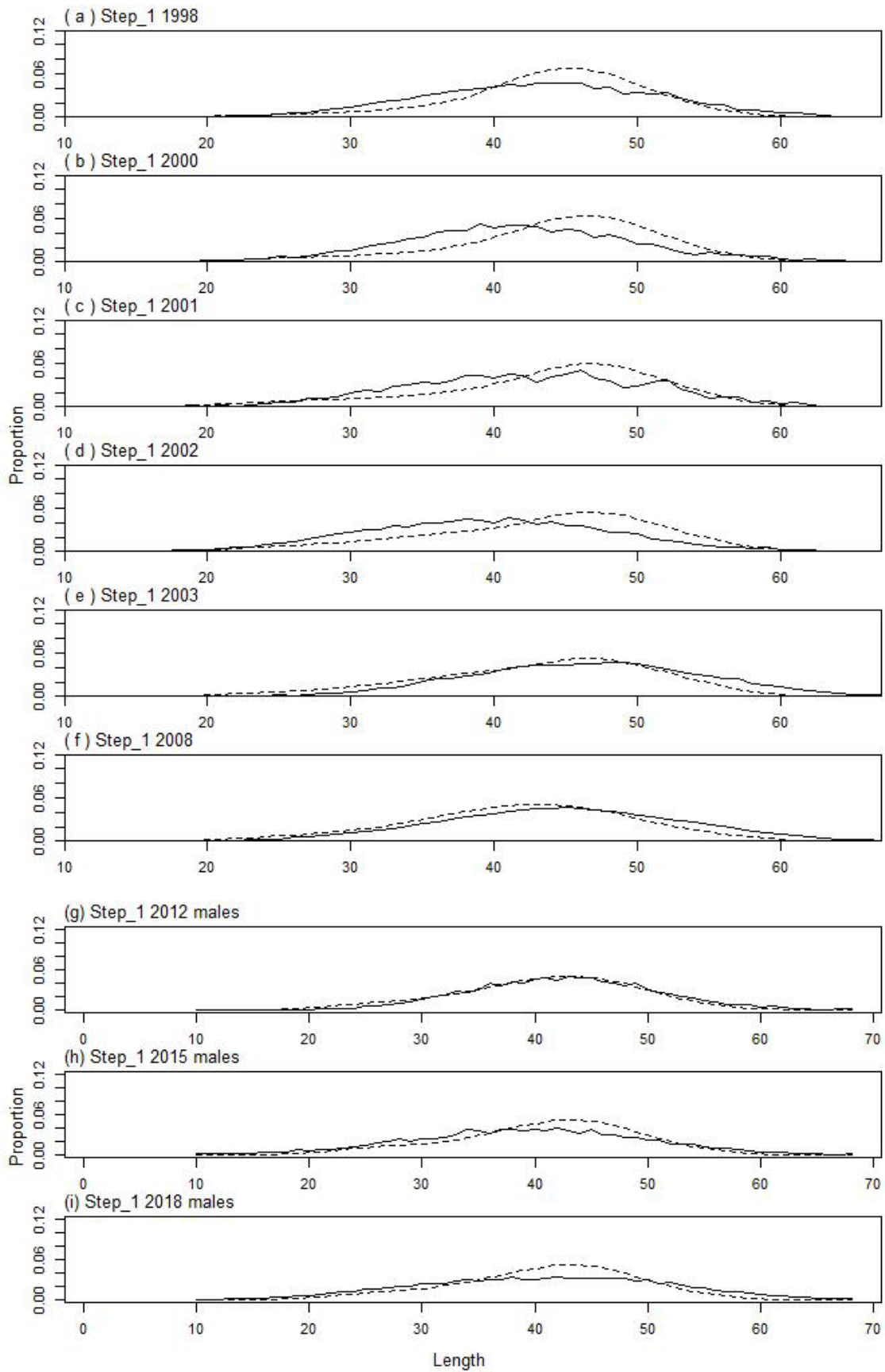
A5. 14(continued): Observed (solid line) and fitted (dashed line) length frequency distributions from trawl survey samples for SCI 1 M02CV15 model. Numbers in top left corner of each plot represent number of scampi measured / number of events sampled.



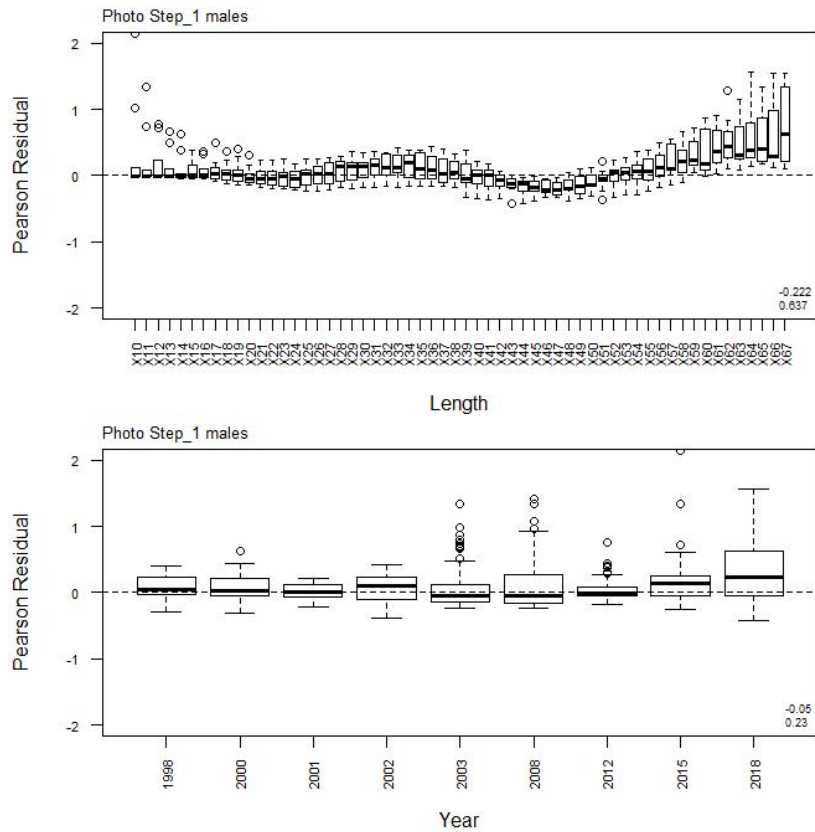
A5. 15: Box plots of Pearson residuals from the fit to length frequency distributions by length from trawl survey sampling by sex for SCI 1 M02CV15 model.



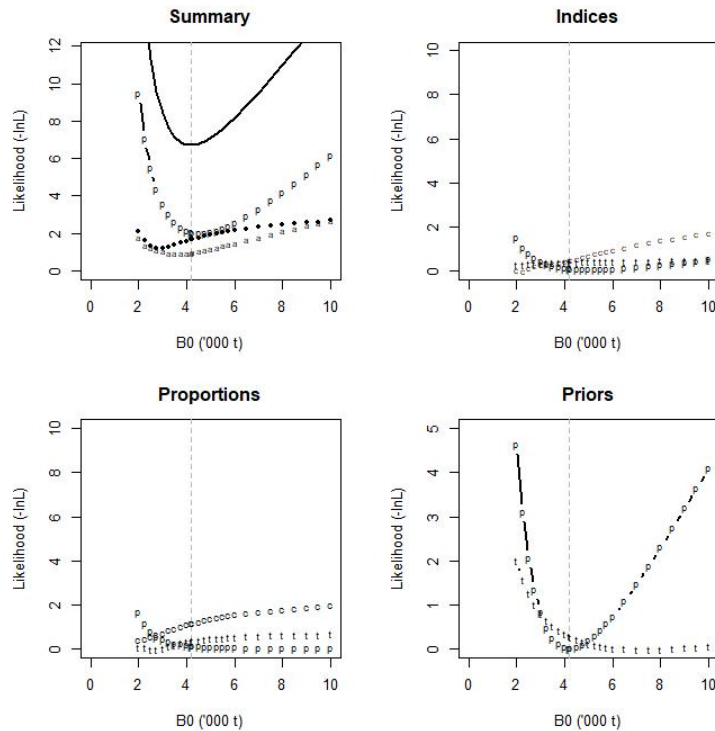
A5. 16: Box plots of Pearson residuals from the fit to length frequency distributions by year from trawl survey sampling by sex for SCI 1 M02CV15 model.



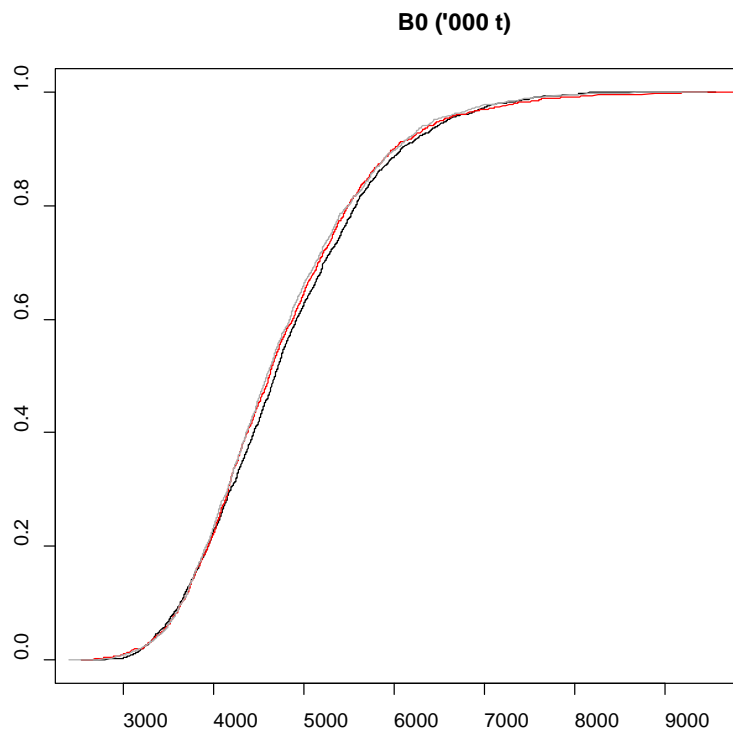
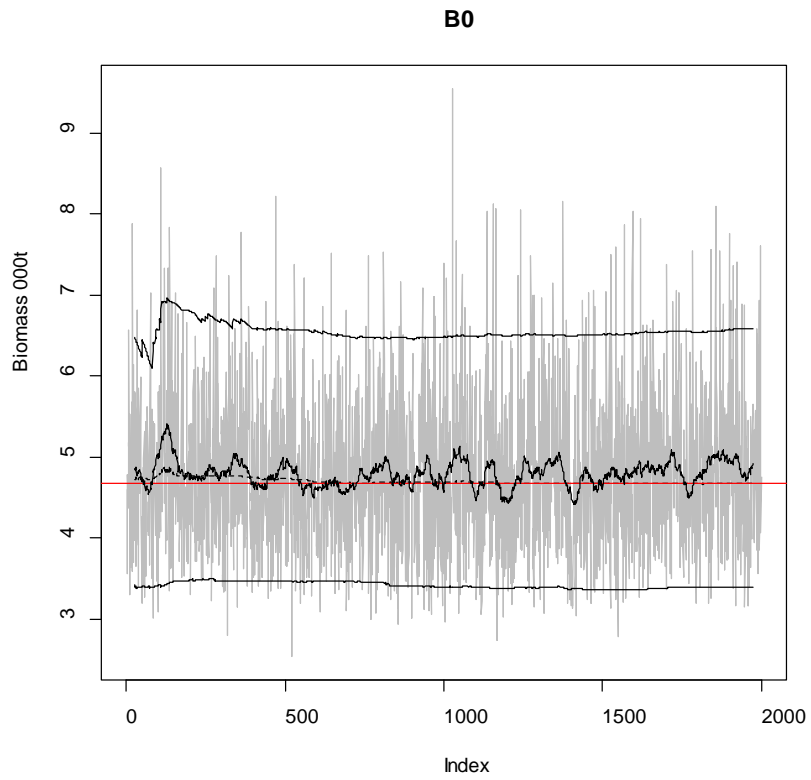
A5. 17: Observed (solid line) and fitted (dashed line) length frequency distributions from photo survey samples for SCI 1 M02CV15 model.



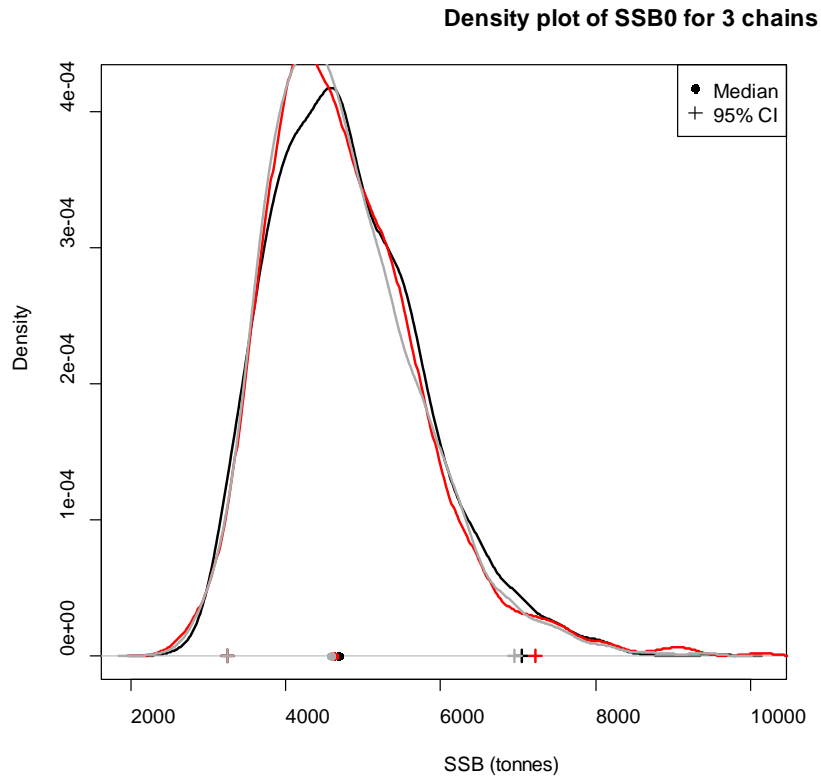
A5. 18: Box plots of Pearson residuals from the fit to length frequency distributions by length (top plot) and year (bottom plot) from photo survey sampling by sex for SCI 1 M02CV15 model.



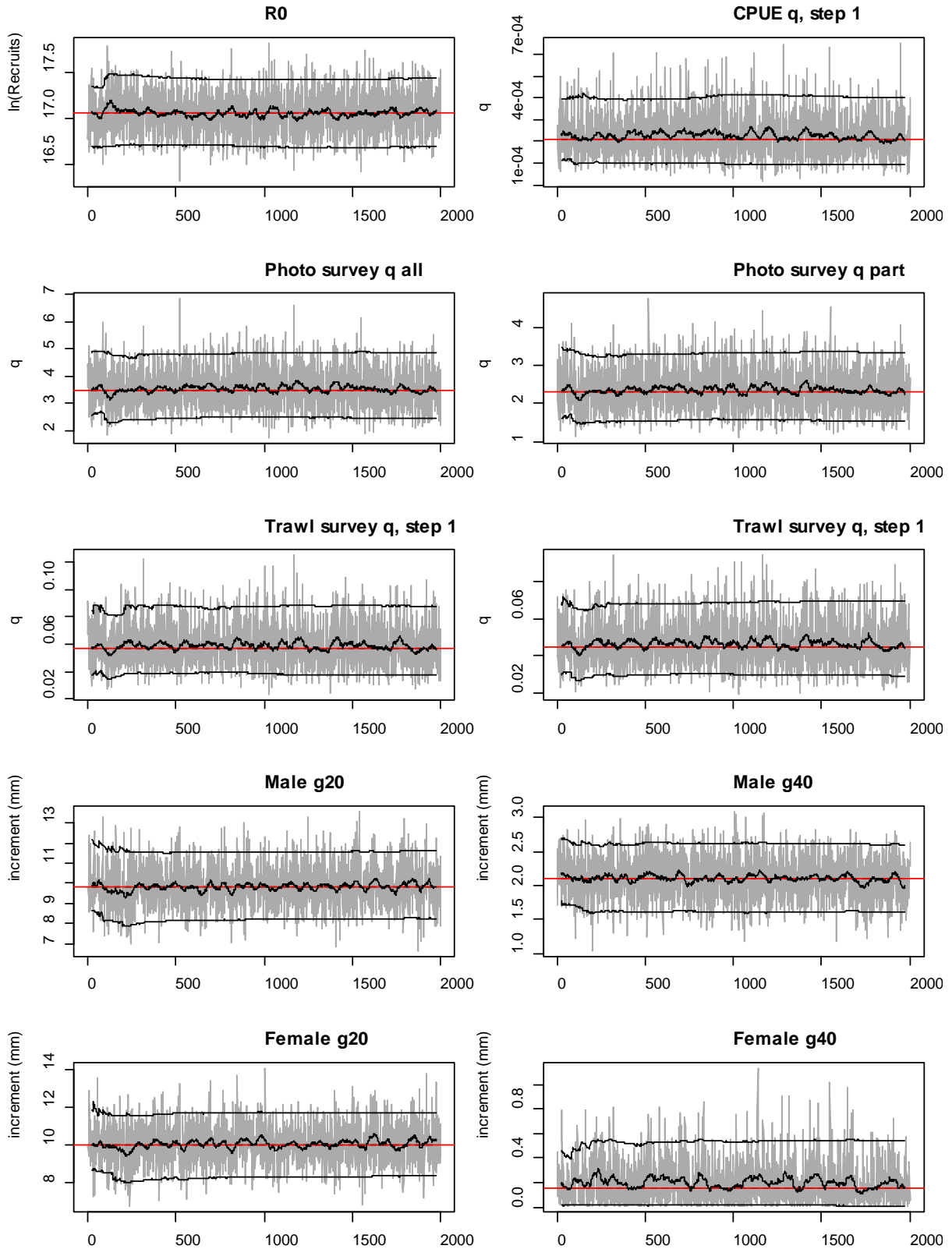
A5. 19: Likelihood profiles for model M02CV15 for SCI 1 when B_0 is fixed in the model. Figures show profiles for main priors (top left, p – priors, a – abundance indices, • – proportions at length), abundance indices (top right, t – trawl survey step, c – CPUE, p – photo survey), proportion at length data (bottom left, p – photo, t – trawl, c – observer) and priors (bottom right, p – *q-Photo*, t – *q-Trawl*).



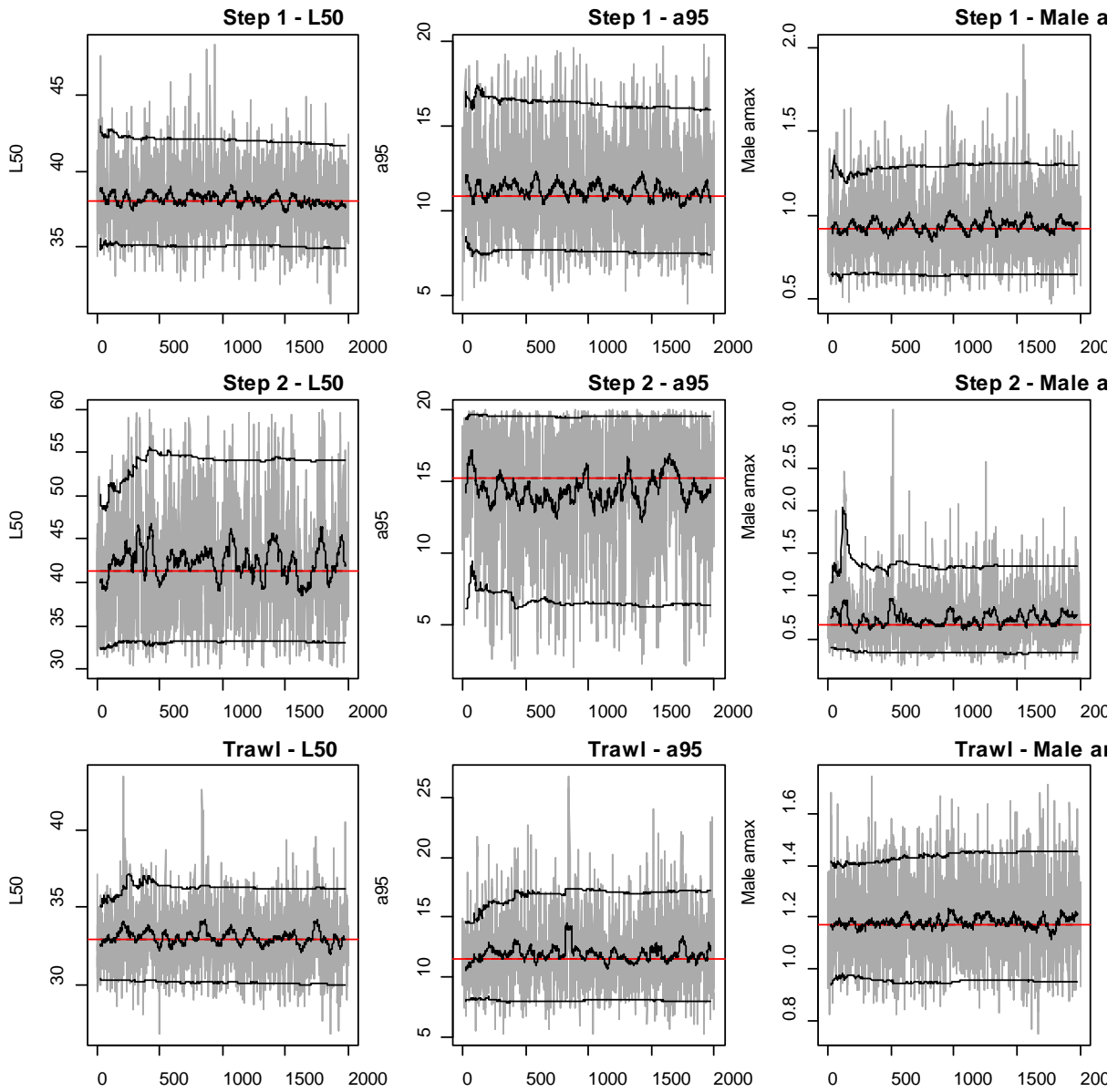
A5. 20: MCMC traces for B_0 and cumulative frequency distributions for three independent MCMC chains for the SCI 1 M02CV15 model.



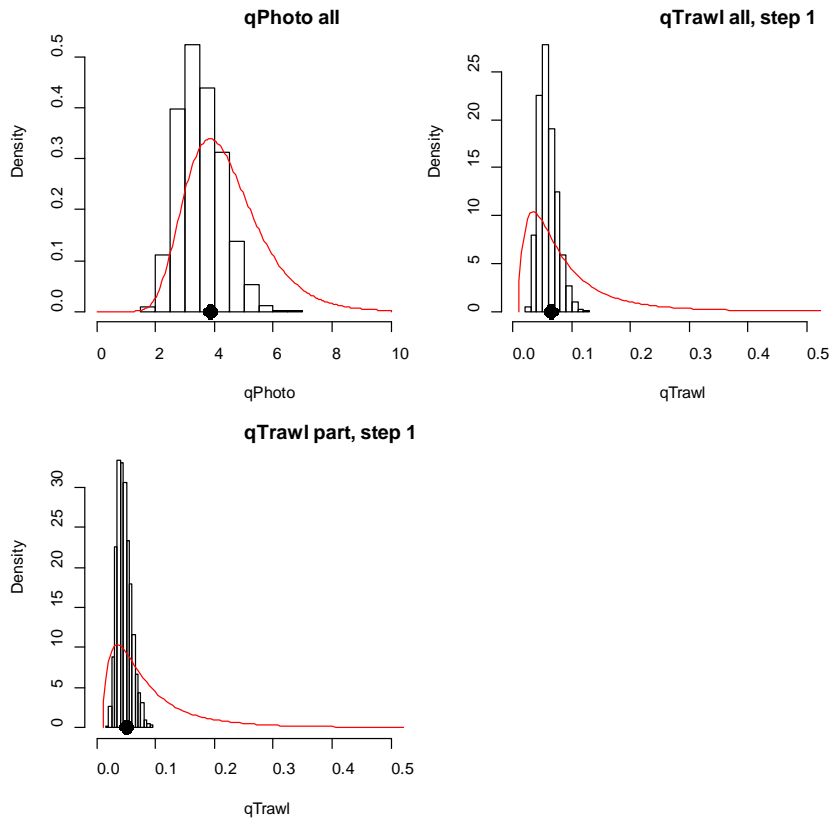
A5. 21: Density plots for B_0 for the SCI 1 M02CV15 model for three independent MCMC chains, with median and 95% confidence intervals.



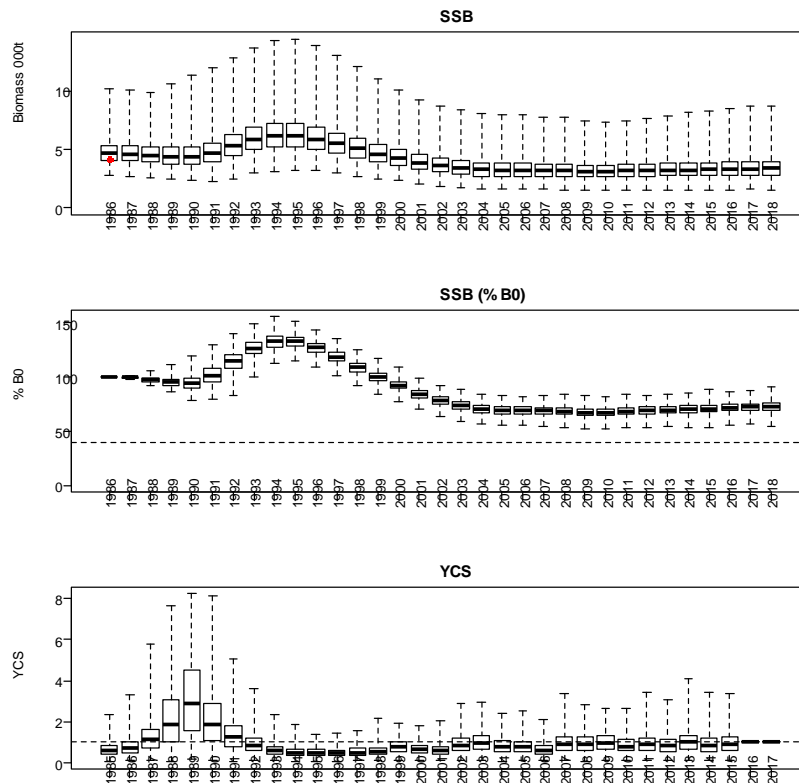
A5. 22: MCMC traces for R_0 , catchability, and growth terms for the SCI 1 M02CV15 model.



A5. 23: MCMC traces for selectivity terms for the SCI 1 M02CV15 model.

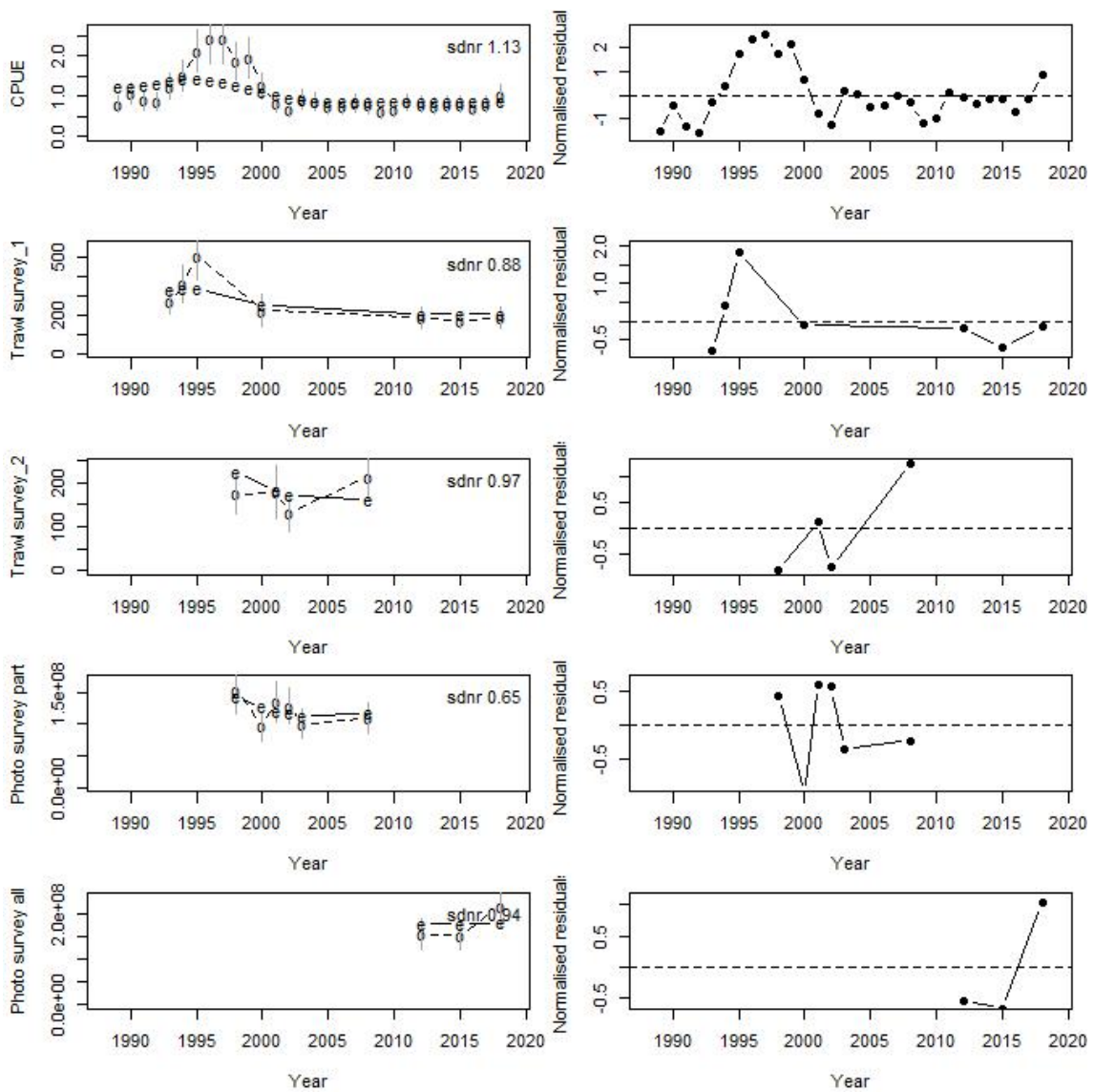


A5. 24: Marginal posterior distributions (histograms), MPD estimates (solid symbols) and distributions of priors (lines) for catchability terms for the SCI 1 M02CV15 model.

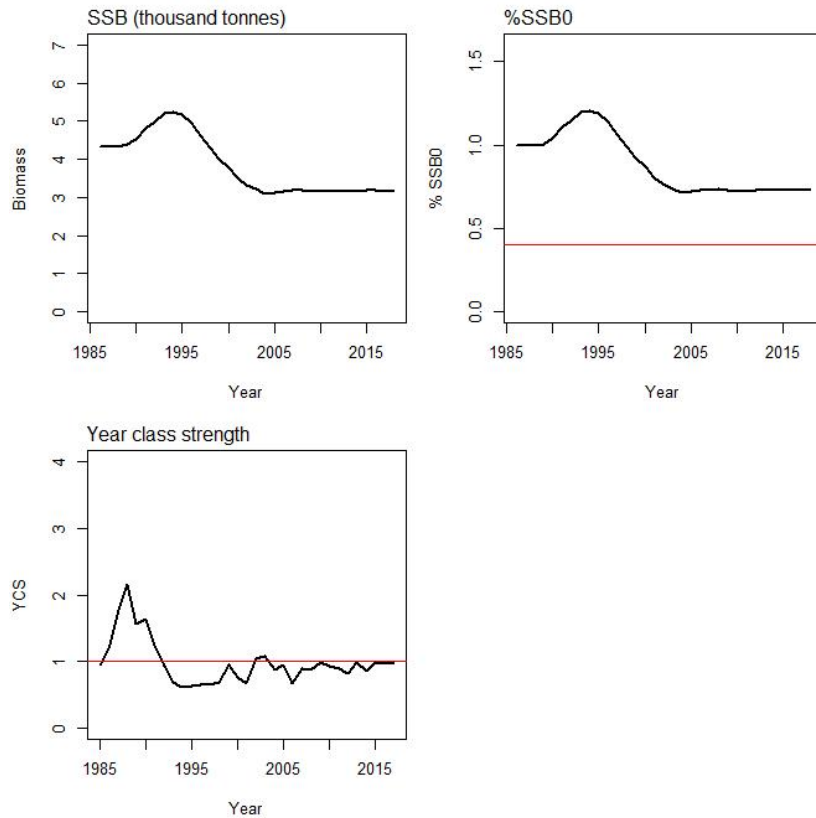


A5. 25: Posterior trajectory of SSB, SSB/SSB₀, and YCS for the SCI 1 M02CV15 model. Red dot represents MPD estimate of B₀.

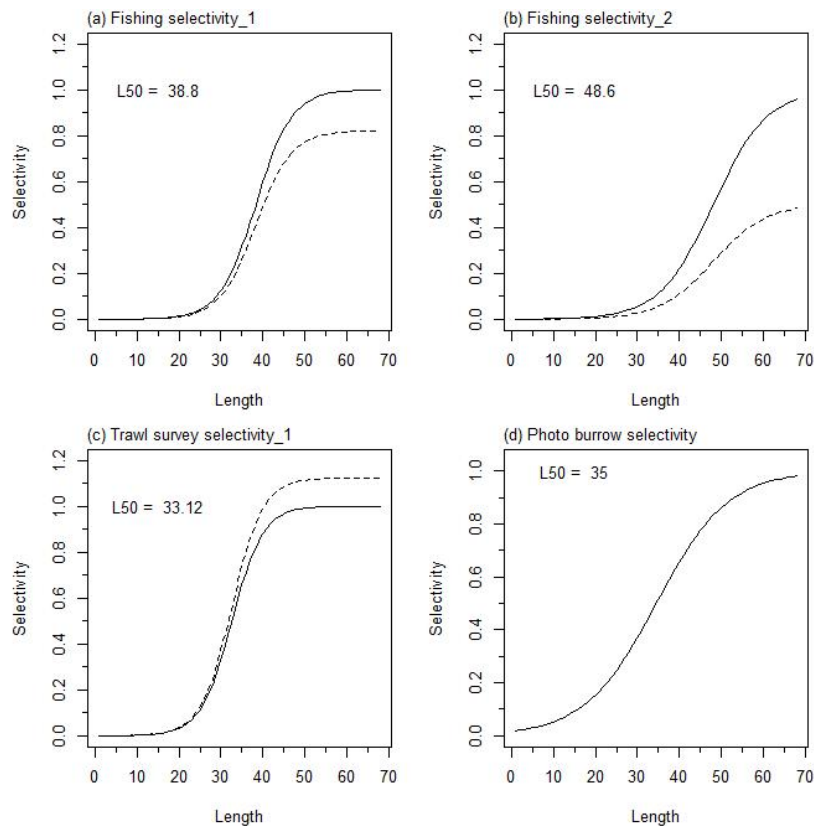
APPENDIX 6. SCI 1 M02CV25 model plots ($M=0.2$, $CV=0.25$)



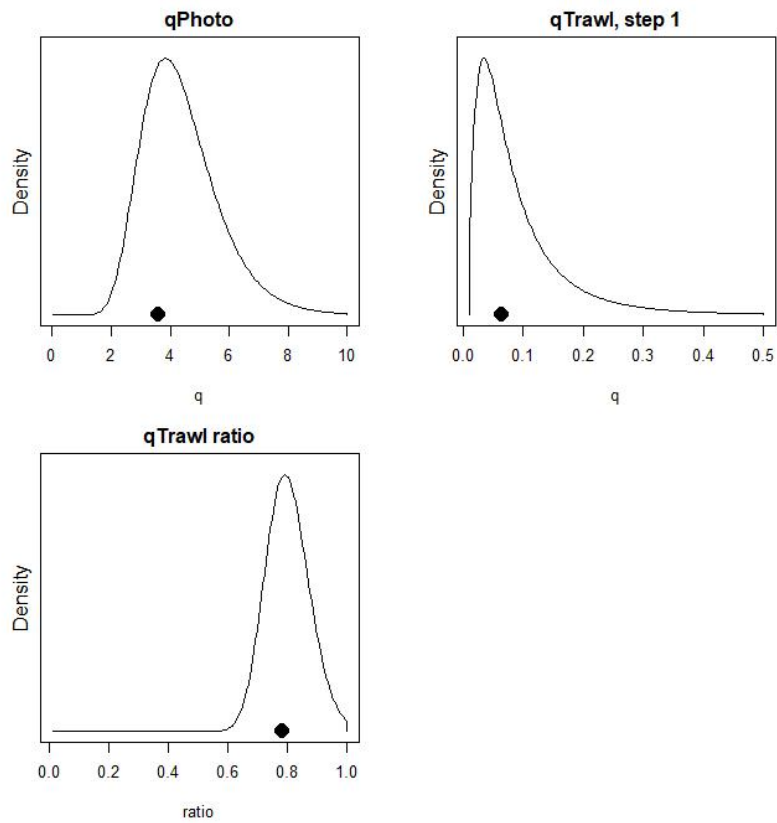
A6. 1: Fits to abundance indices (left column) and normalised residuals (right column) for standardised CPUE index (top row) trawl survey biomass index covering whole area (second row), trawl survey biomass index covering limited area (third row), photo survey abundance index covering limited area (fourth row), and photo survey abundance index covering whole area (fifth row) for the SCI 1 M02CV25 model.



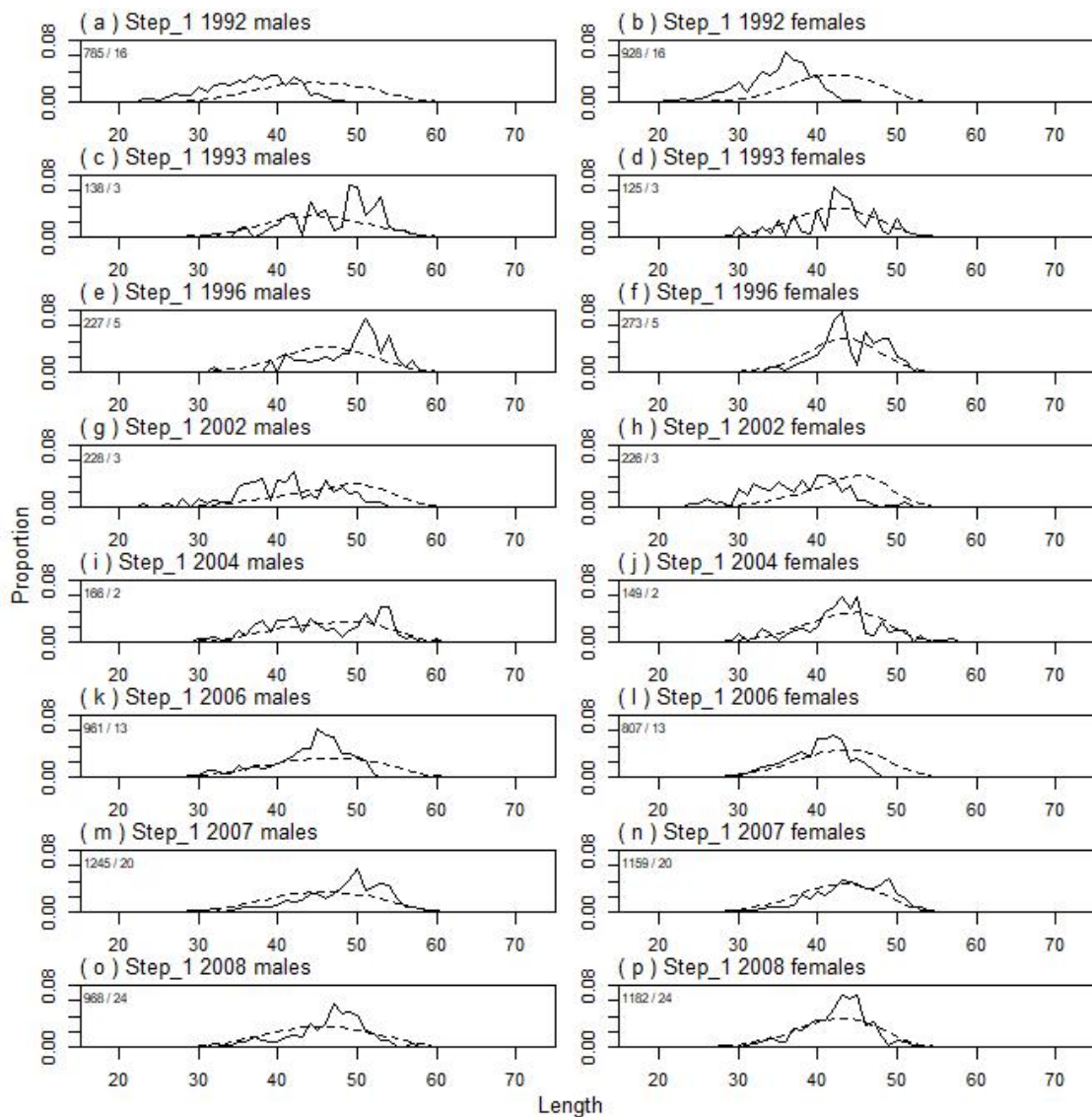
A6. 2: Spawning stock biomass trajectory (upper left), stock status (upper right), and year class strength (lower left) for the SCI 1 M02CV25 model.



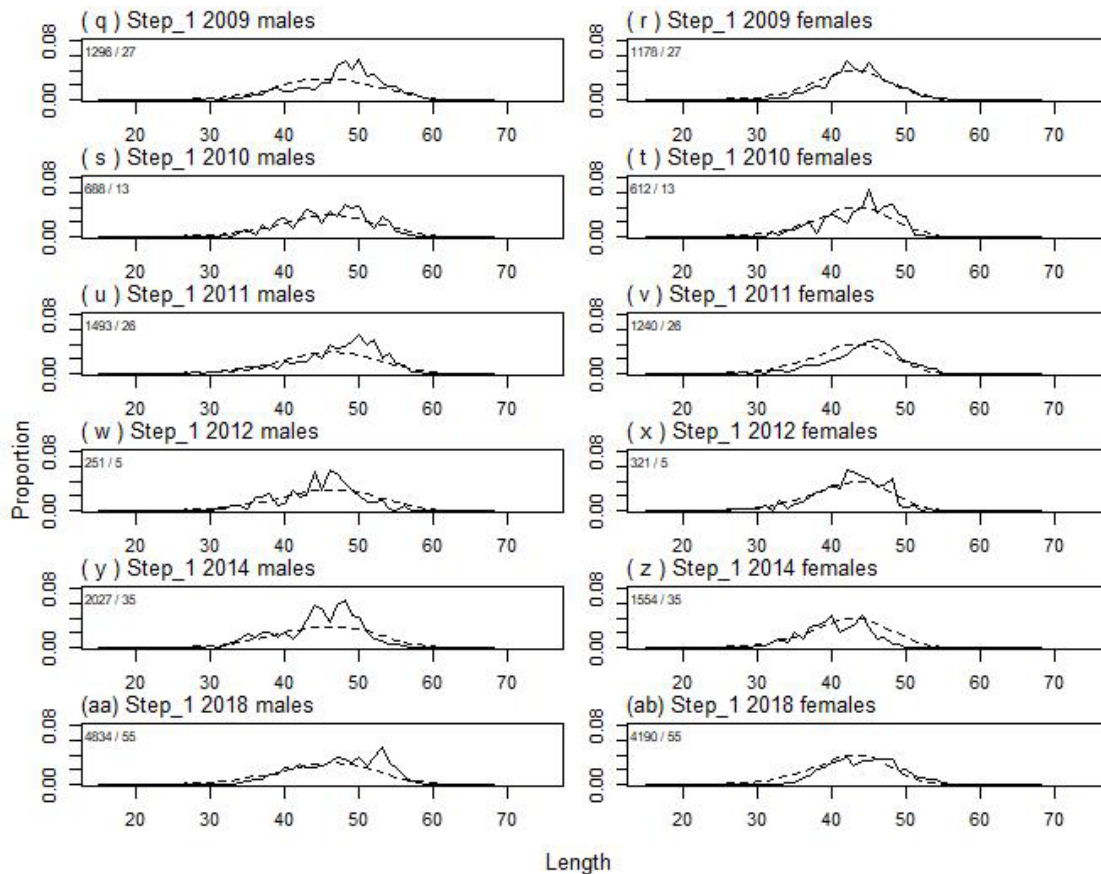
A6. 3: Fishery and survey selectivity curves for the SCI 1 M02CV25 model. Solid line – females, dotted line – males. The scampi burrow index is not sexed, and a single selectivity applies.



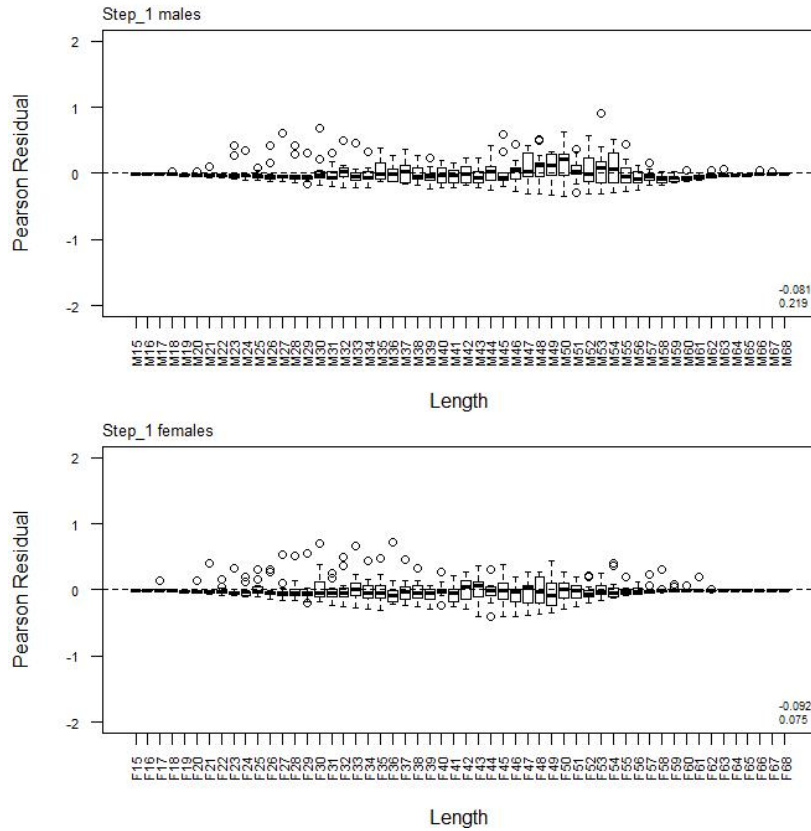
A6. 4: Catchability estimates from MPD model run, plotted in relation to prior distribution for the SCI 1 M02CV25 model.



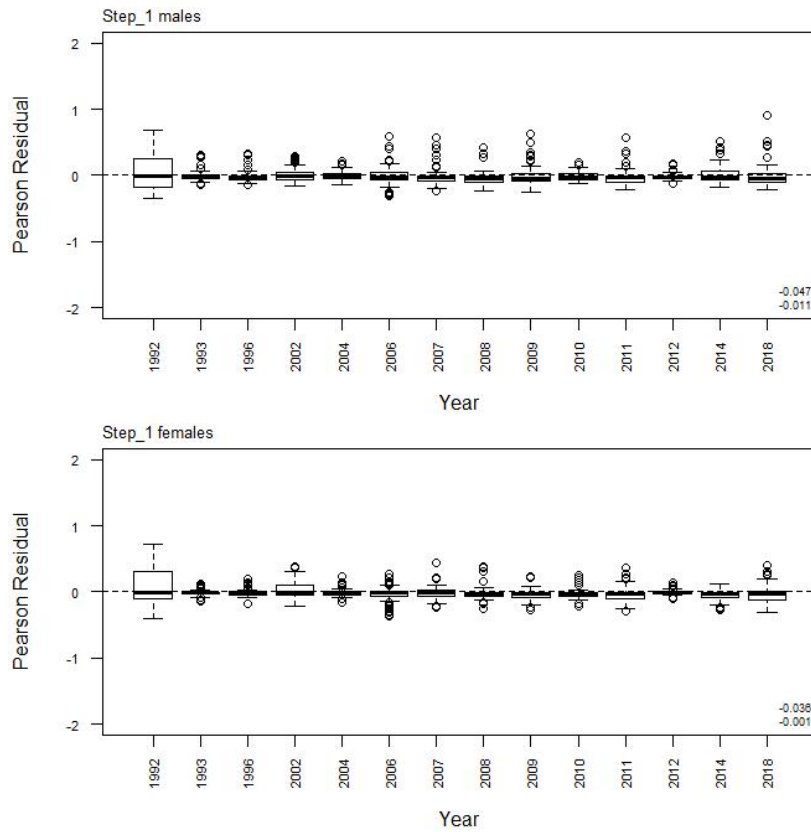
A6. 5: Observed (solid line) and fitted (dashed line) length frequency distributions from observer samples, time step 1 for SCI 1 M02CV25 model. Numbers in top left corner of each plot represent number of scampi measured / number of events sampled.



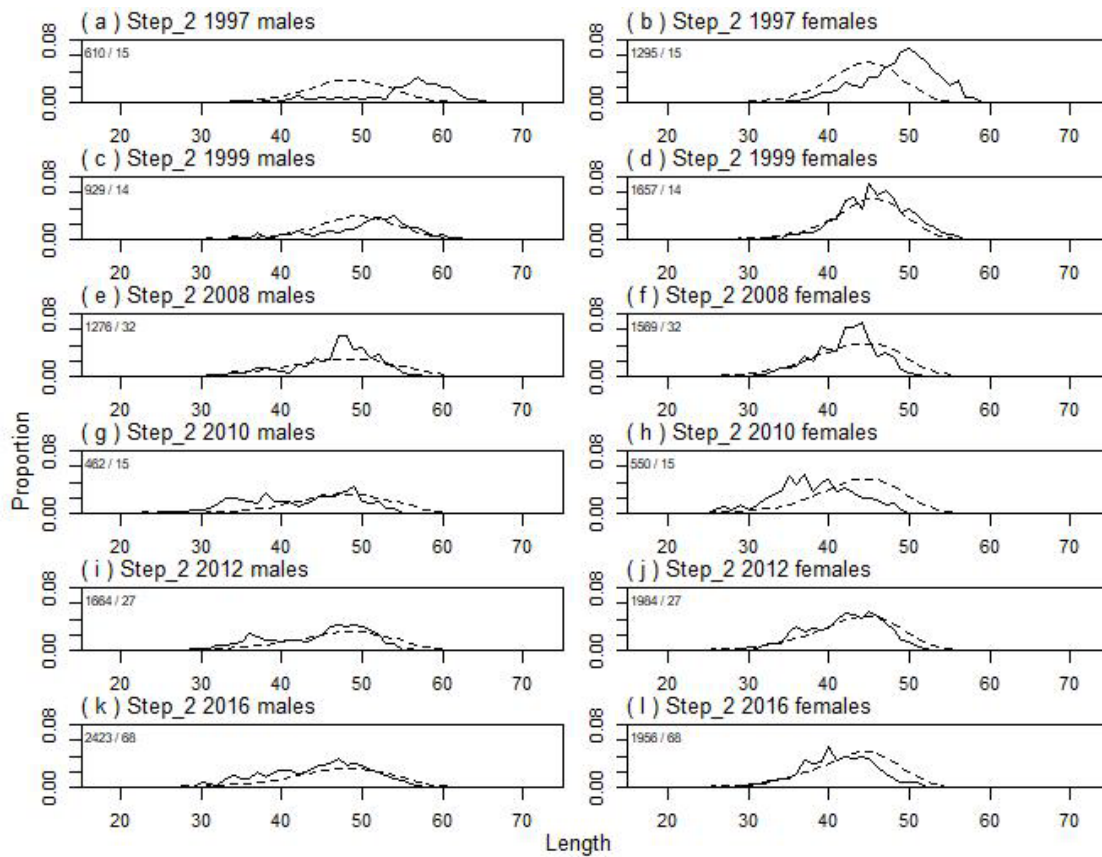
A6.5 (continued): Observed (solid line) and fitted (dashed line) length frequency distributions from observer samples, time step 1 for SCI 1 M02CV25 model. Numbers in top left corner of each plot represent number of scampi measured / number of events sampled.



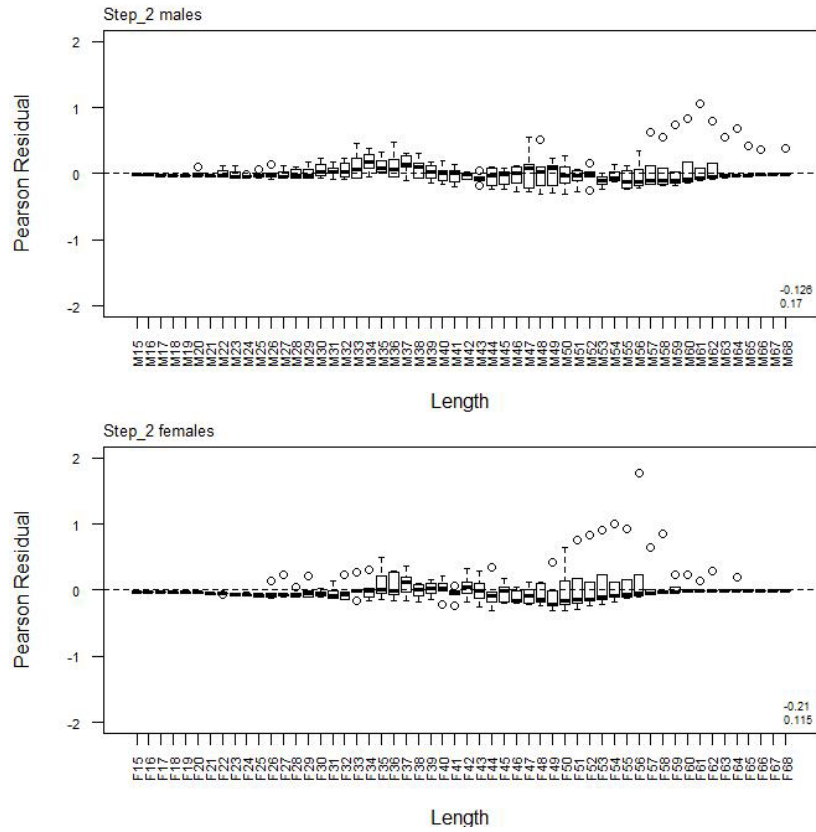
A6. 6: Box plots of Pearson residuals from the fit to length frequency distributions by length from observer sampling by sex for time step 1 for SCI 1 M02CV25 model.



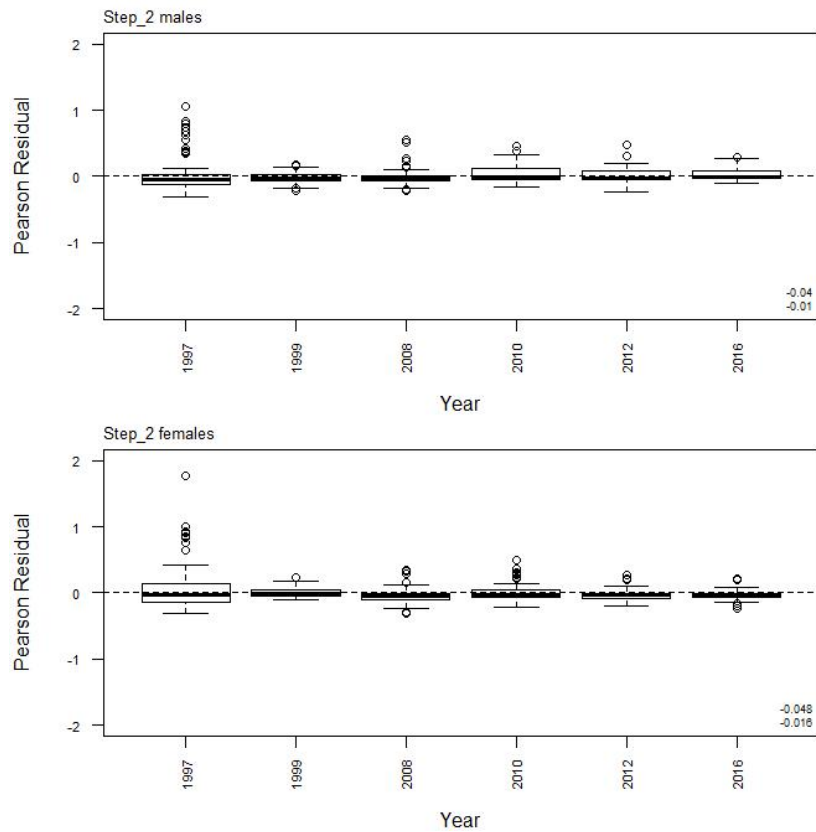
A6. 7: Box plots of Pearson residuals from the fit to length frequency distributions by year from observer sampling by sex for time step 1 for SCI 1 M02CV25 model.



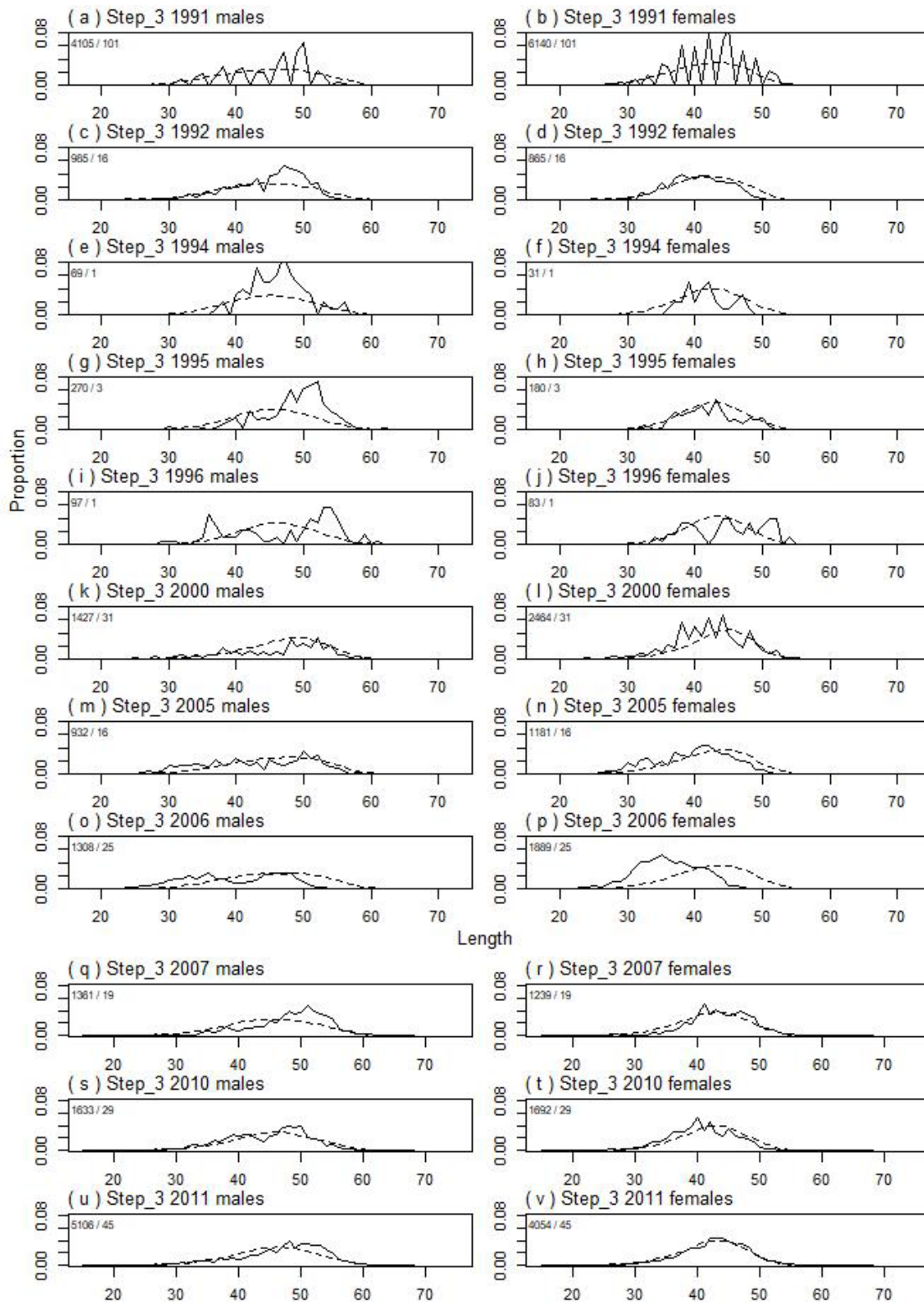
A6. 8: Observed (solid line) and fitted (dashed line) length frequency distributions from observer samples, time step 2 for SCI 1 M02CV25 model. Numbers in top left corner of each plot represent number of scampi measured / number of events sampled.



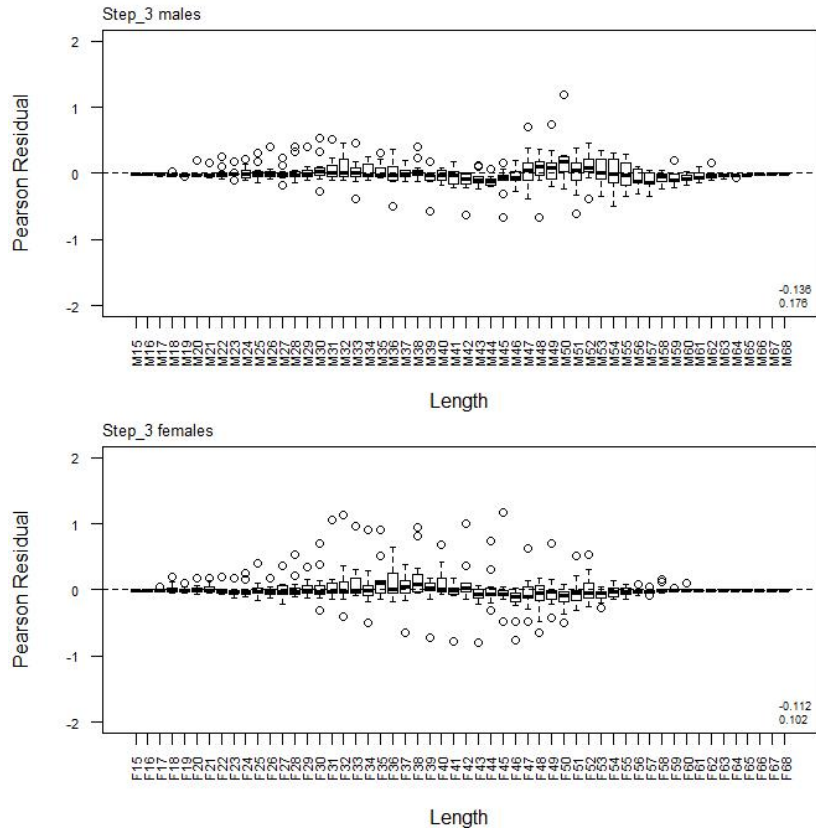
A6. 9: Box plots of Pearson residuals from the fit to length frequency distributions by length from observer sampling by sex for time step 2 for SCI 1 M02CV25 model.



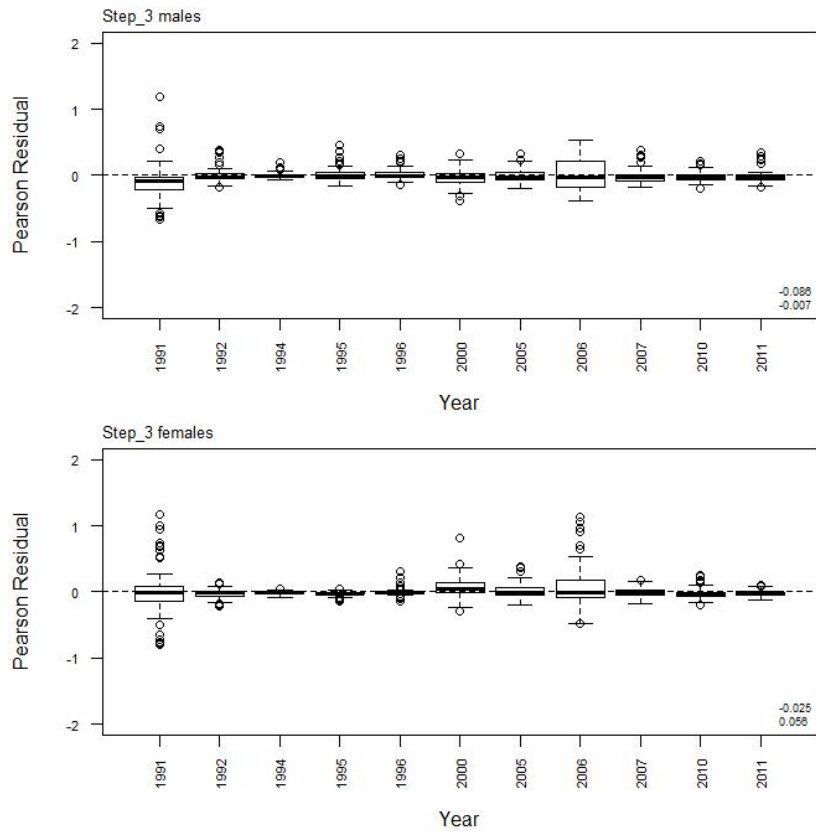
A6. 10: Box plots of Pearson residuals from the fit to length frequency distributions by year from observer sampling by sex for time step 2 for SCI 1 M02CV25 model.



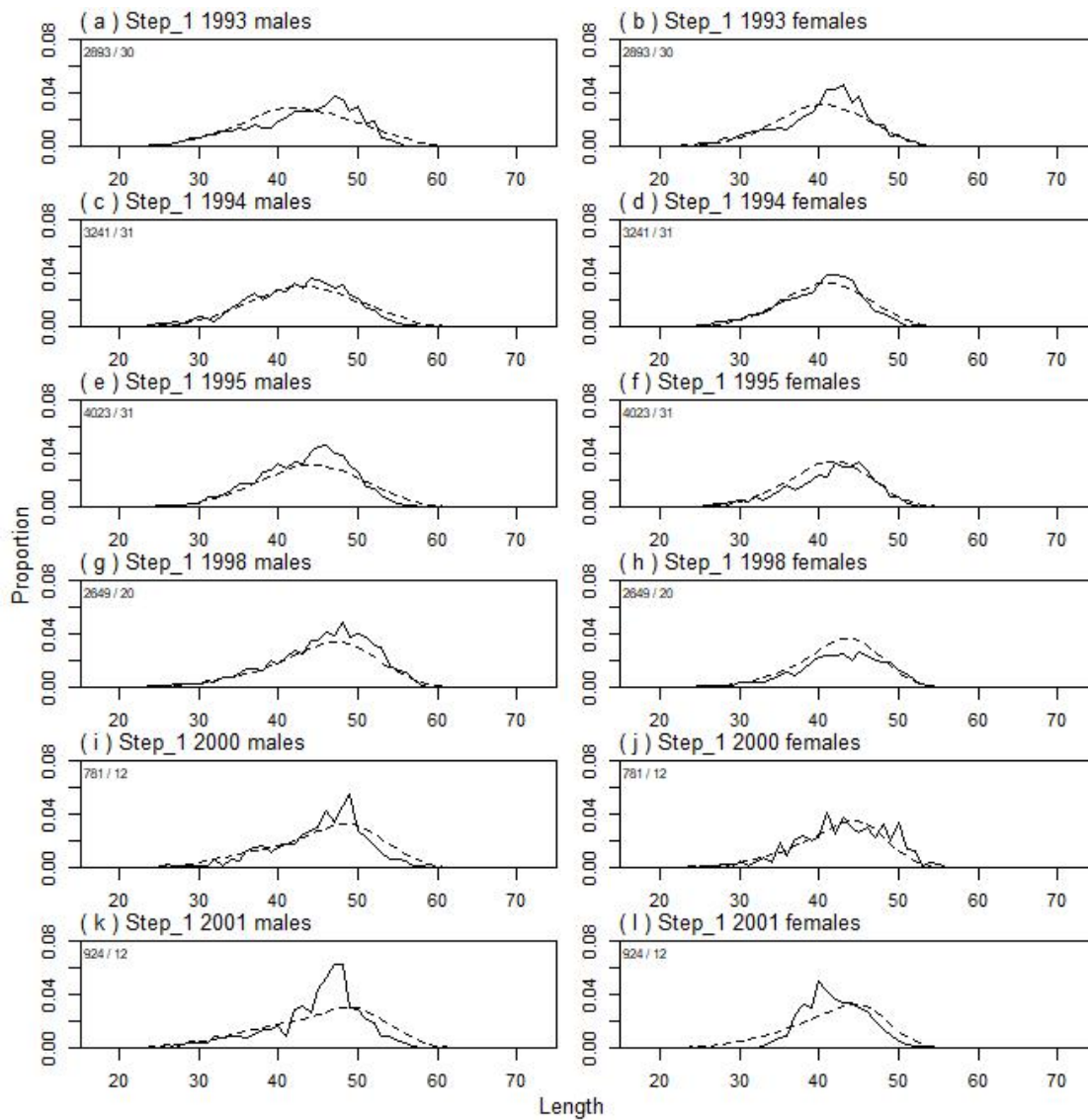
A6. 11: Observed (solid line) and fitted (dashed line) length frequency distributions from observer samples, time step 3 for SCI 1 M02CV25 model. Numbers in top left corner of each plot represent number of scampi measured / number of events sampled.



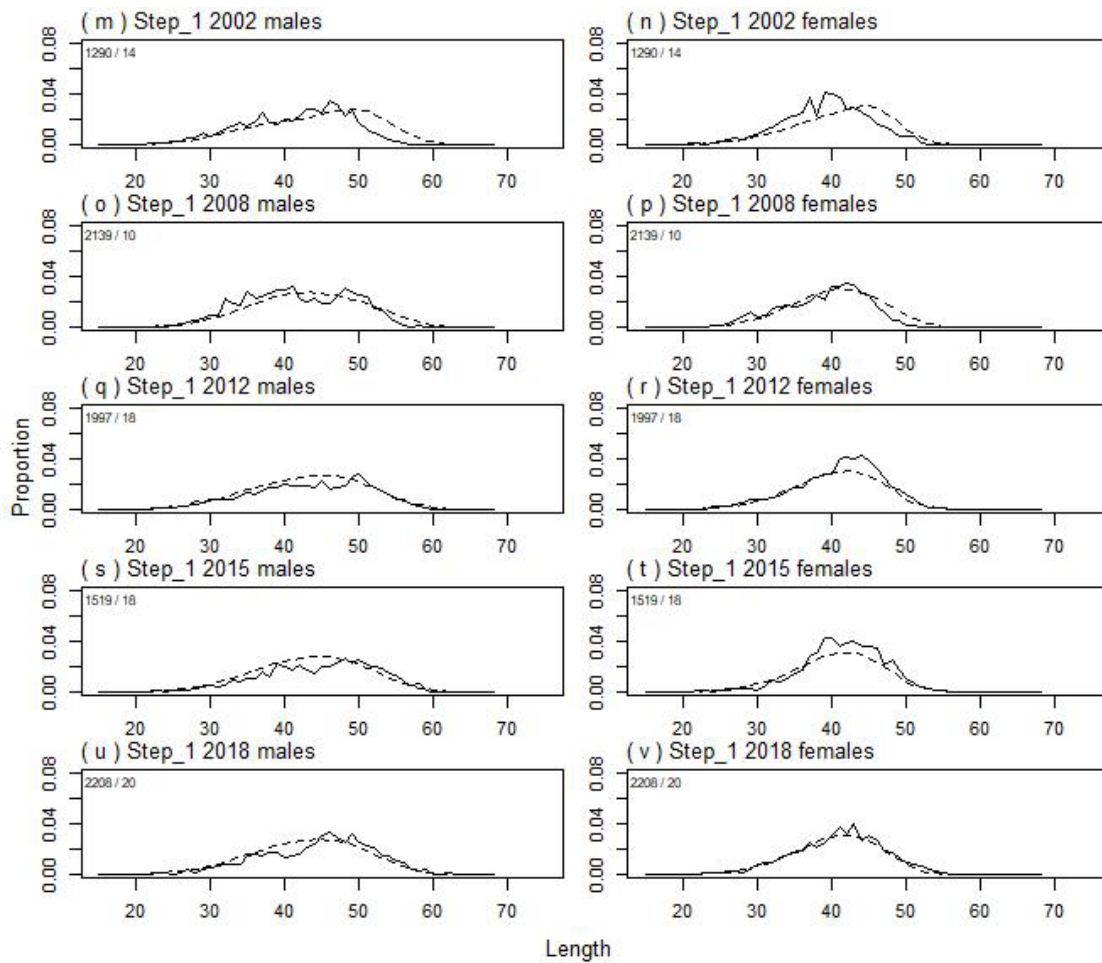
A6. 12: Box plots of Pearson residuals from the fit to length frequency distributions by length from observer sampling by sex for time step 3 for SCI 1 M02CV25 model.



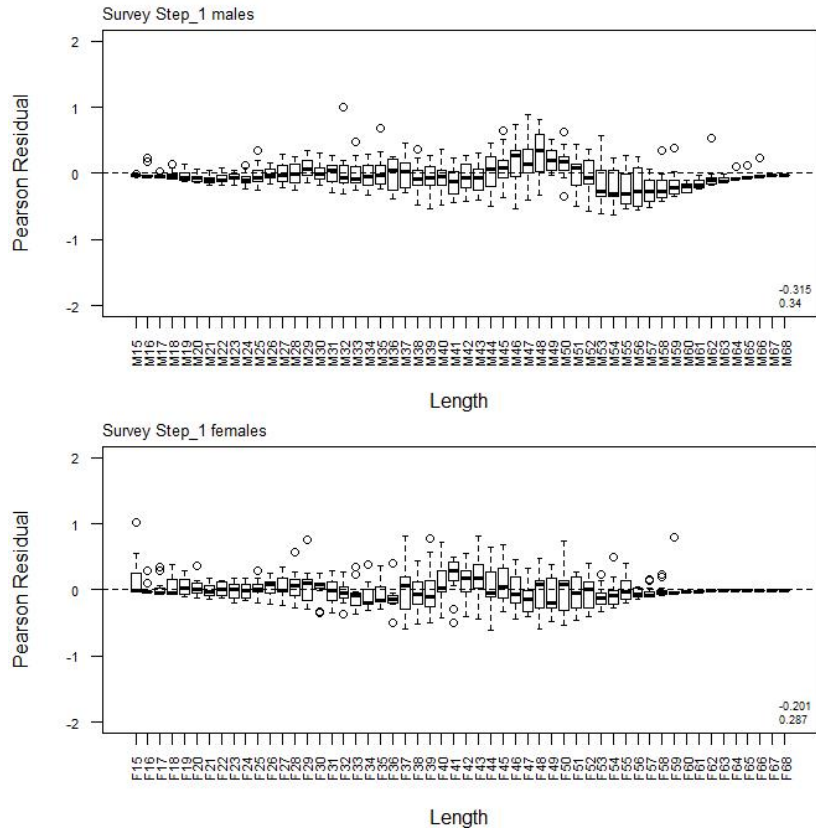
A6. 13: Box plots of Pearson residuals from the fit to length frequency distributions by year from observer sampling by sex for time step 3 for SCI 1 M02CV25 model.



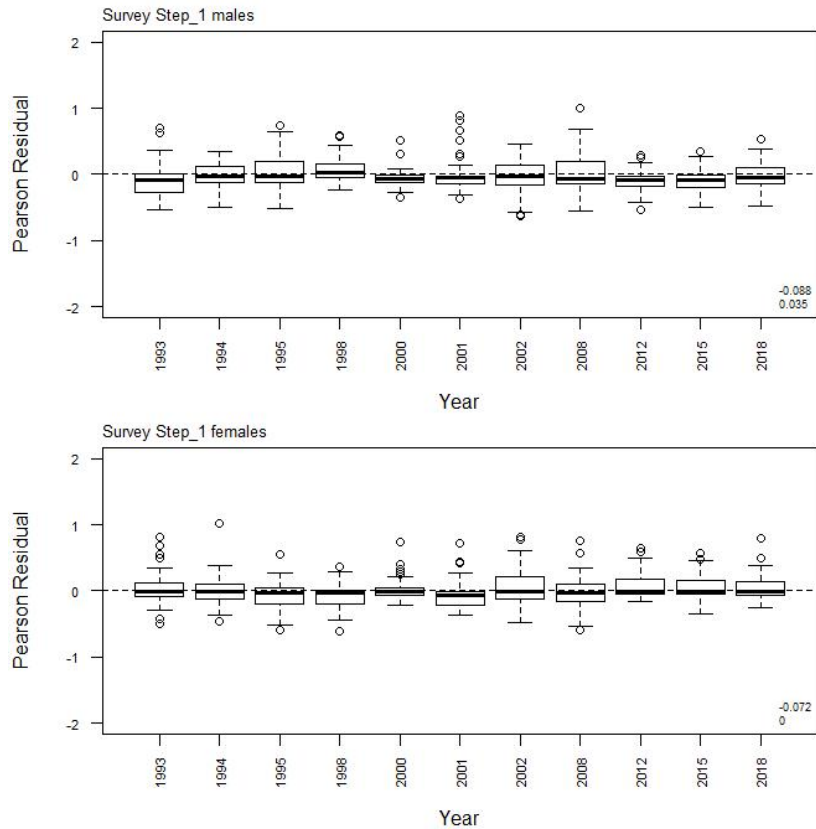
A6. 14: Observed (solid line) and fitted (dashed line) length frequency distributions from trawl samples for SCI 1 M02CV25 model. Numbers in top left corner of each plot represent number of scampi measured / number of events sampled.



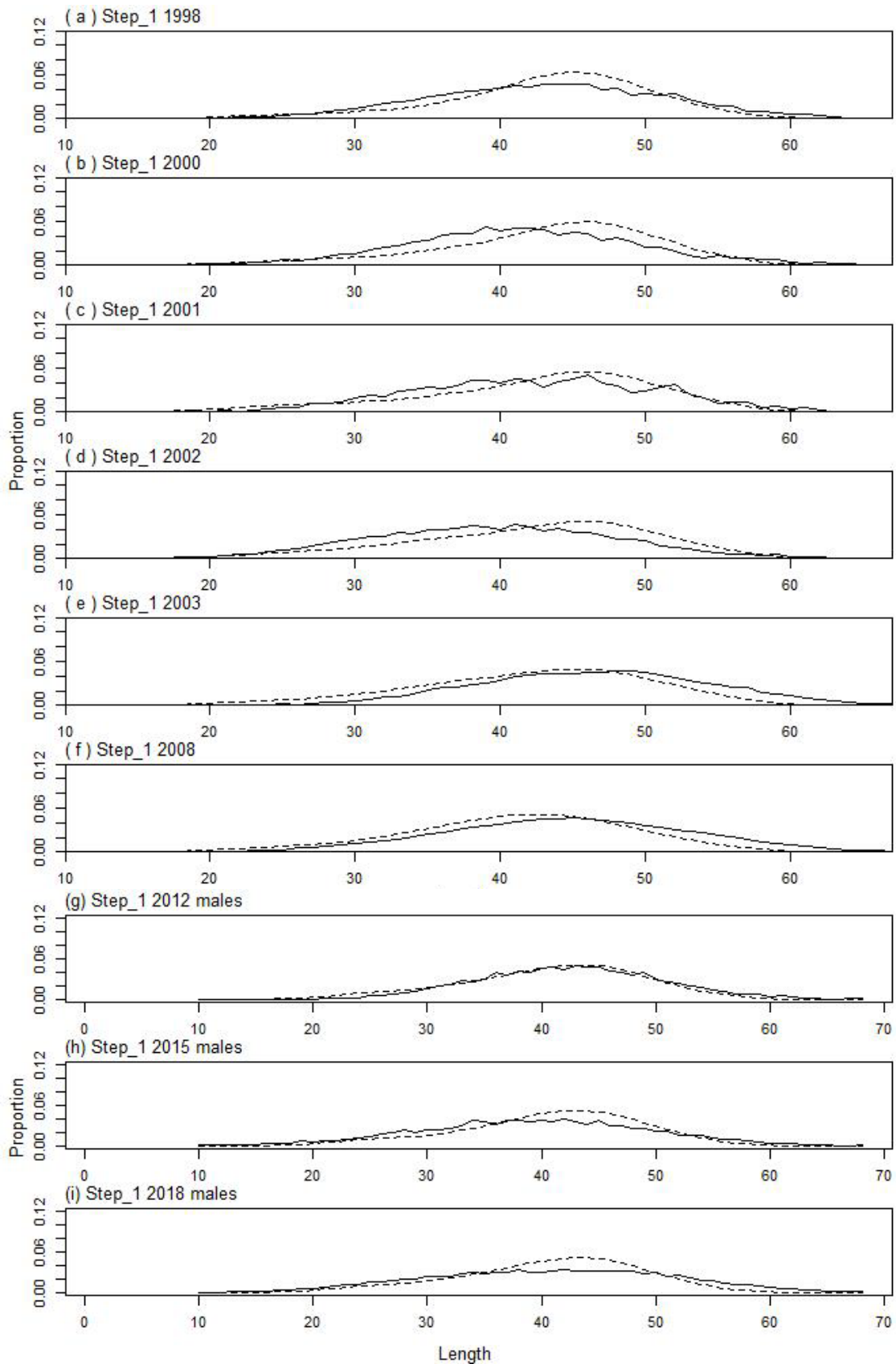
A6. 14(continued): Observed (solid line) and fitted (dashed line) length frequency distributions from trawl samples for SCI 1 M02CV25 model. Numbers in top left corner of each plot represent number of scampi measured / number of events sampled.



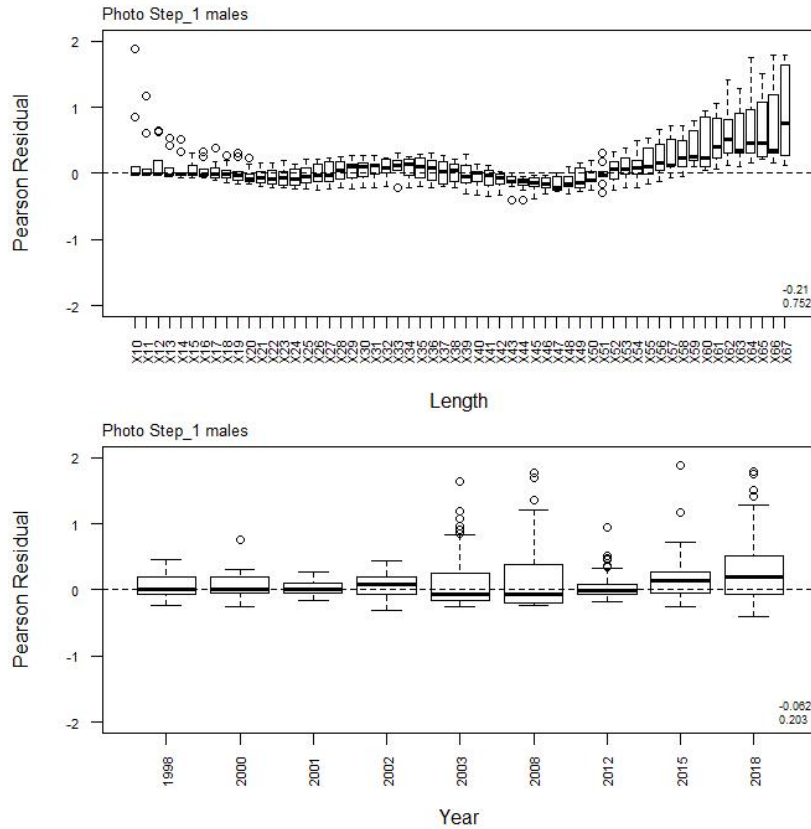
A6. 15: Box plots of Pearson residuals from the fit to length frequency distributions by length from trawl survey sampling by sex for SCI 1 M02CV25 model.



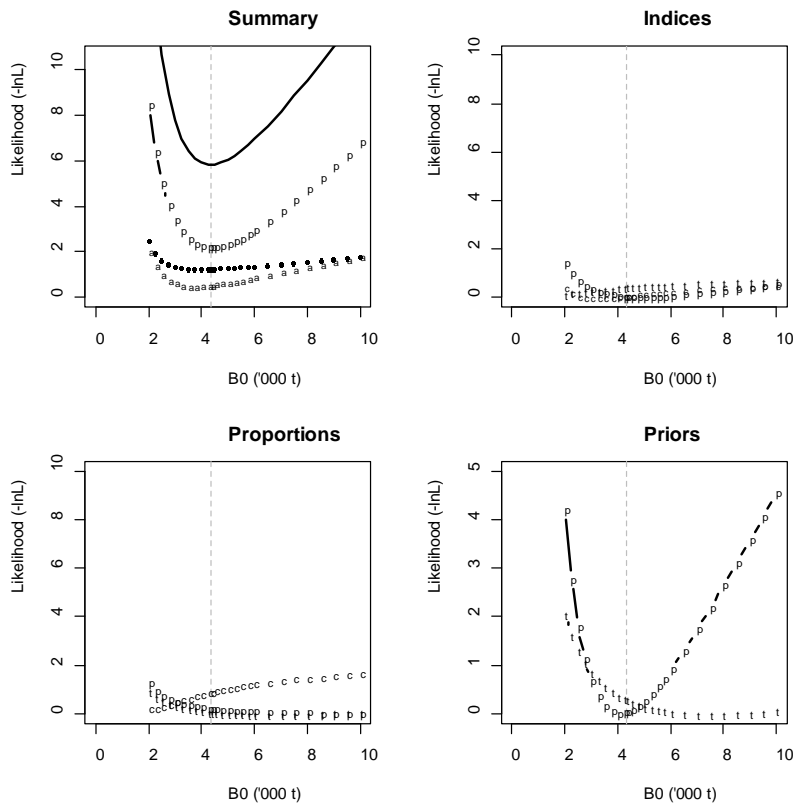
A6. 16: Box plots of Pearson residuals from the fit to length frequency distributions by year from trawl survey sampling by sex for SCI 1 M02CV25 model.



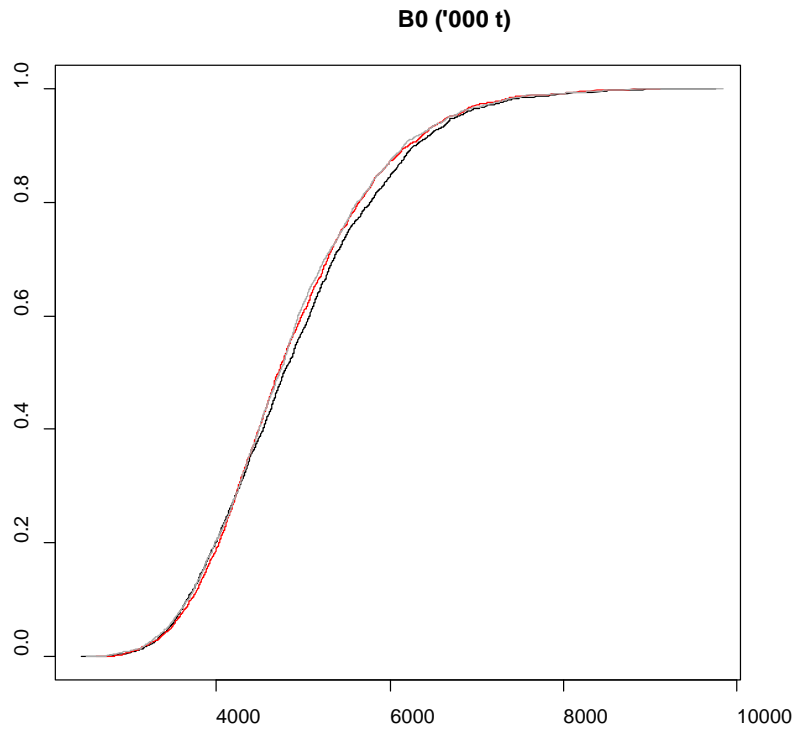
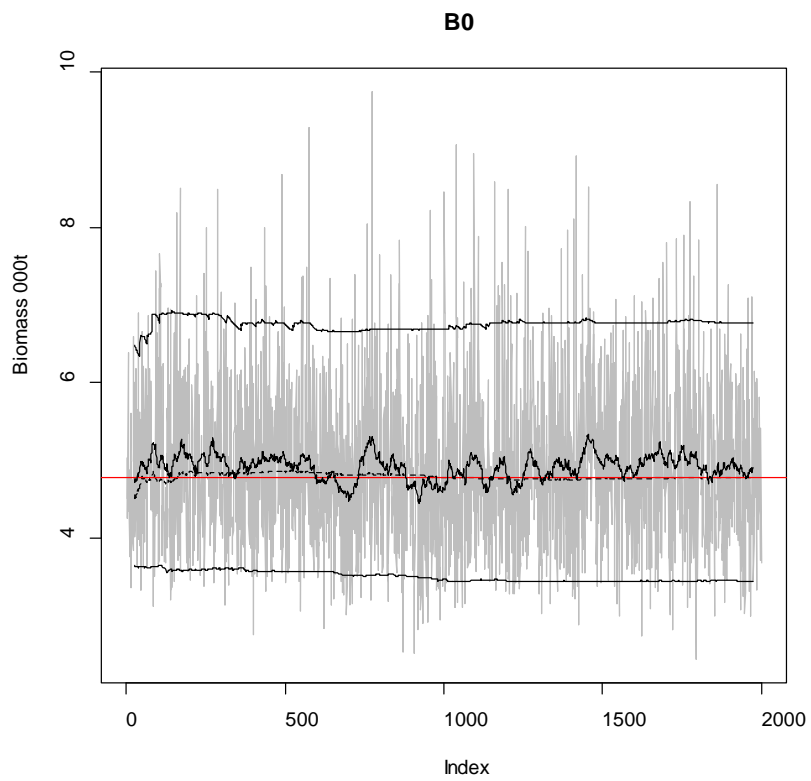
A6. 17: Observed (solid line) and fitted (dashed line) length frequency distributions from photo survey samples for SCI 1 M02CV25 model.



A6. 18: Box plots of Pearson residuals from the fit to length frequency distributions by length (top plot) and year (bottom plot) from photo survey sampling by sex for SCI 1 M02CV25 model.

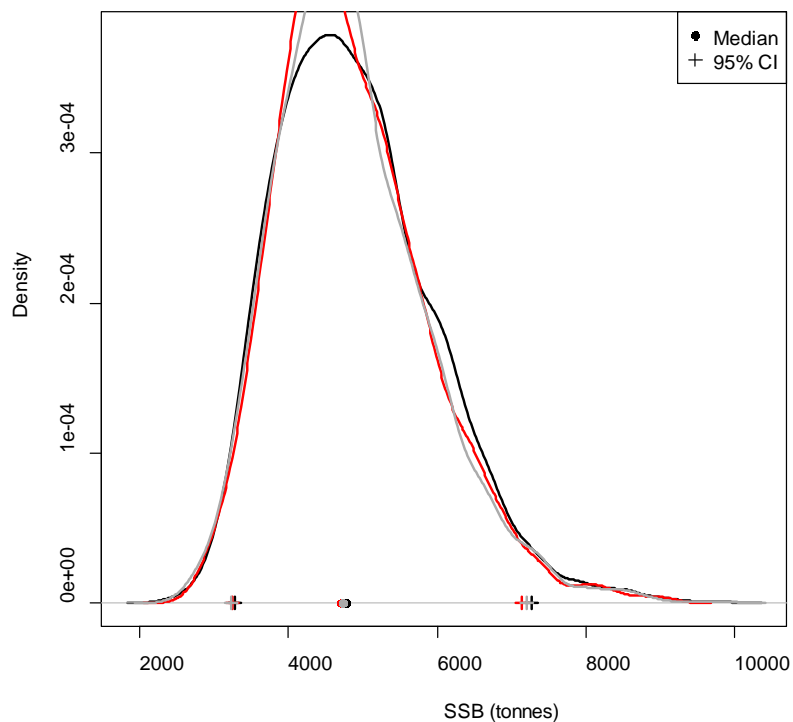


A6. 19: Likelihood profiles for model M02CV25 for SCI 1 when B_0 is fixed in the model. Figures show profiles for main priors (top left, p – priors, a – abundance indices, • – proportions at length), abundance indices (top right, t – trawl survey step, c – CPUE, p – photo survey), proportion at length data (bottom left, p – photo, t – trawl, 1 – observer) and priors (bottom right, p – q-Photo, t – q-Trawl).

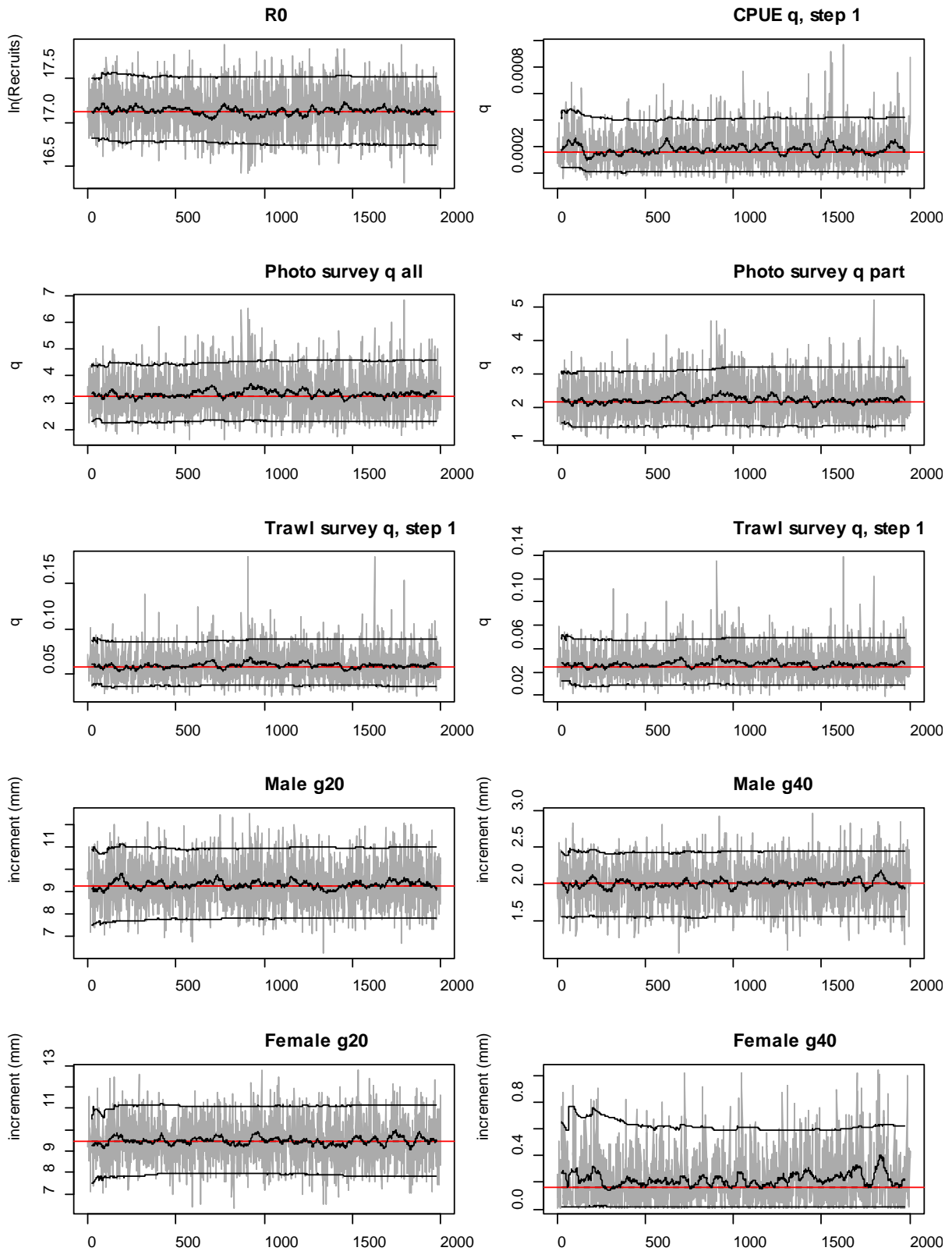


A6. 20: MCMC traces for B_0 and cumulative frequency distributions for three independent MCMC chains for the SCI 1 M02CV25 model.

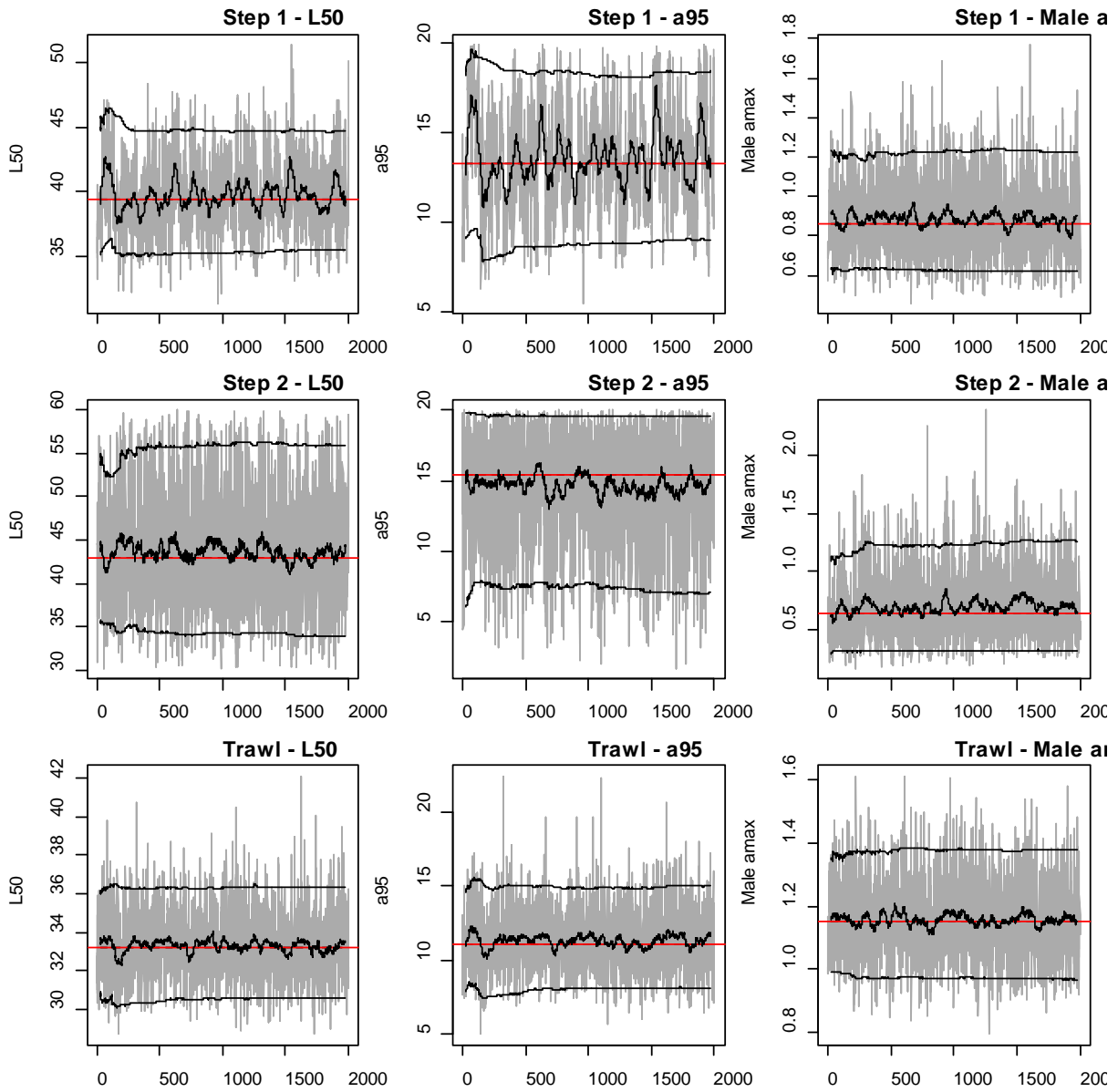
Density plot of SSB0 for 3 chains



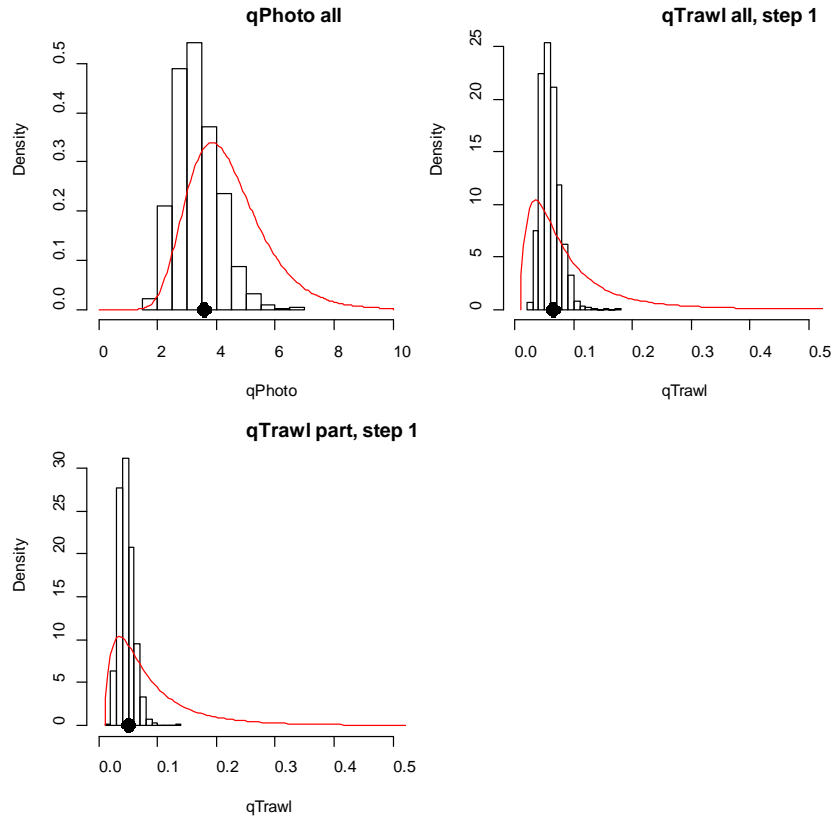
A6. 21: Density plots for B_0 for the SCI 1 M02CV25 model for three independent MCMC chains, with median and 95% confidence intervals.



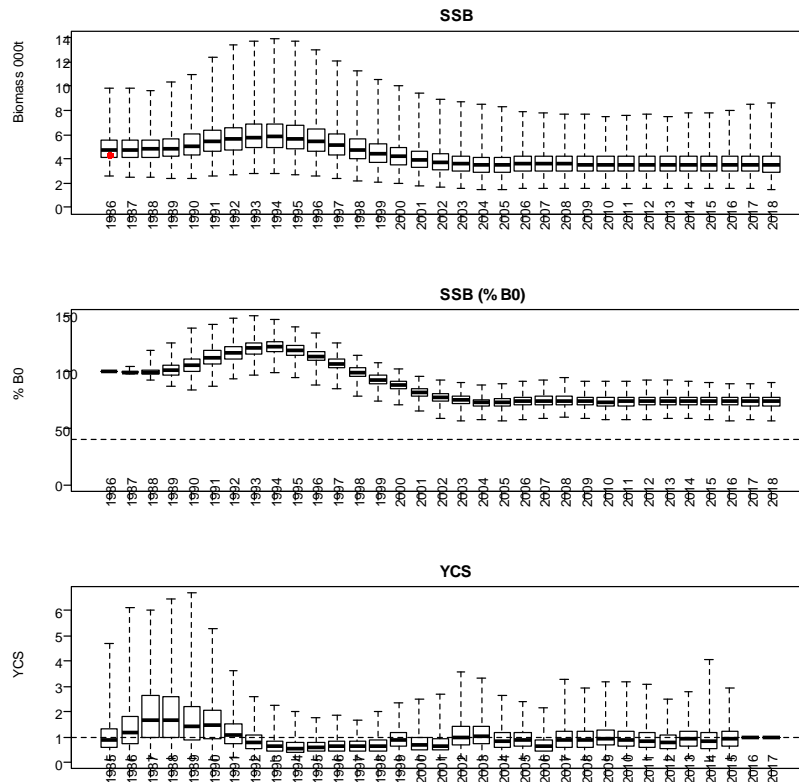
A6. 22: MCMC traces for R_0 , catchability, and growth terms for the SCI 1 M02CV25 model.



A6. 23: MCMC traces for selectivity terms for the SCI 1 M02CV25 model.

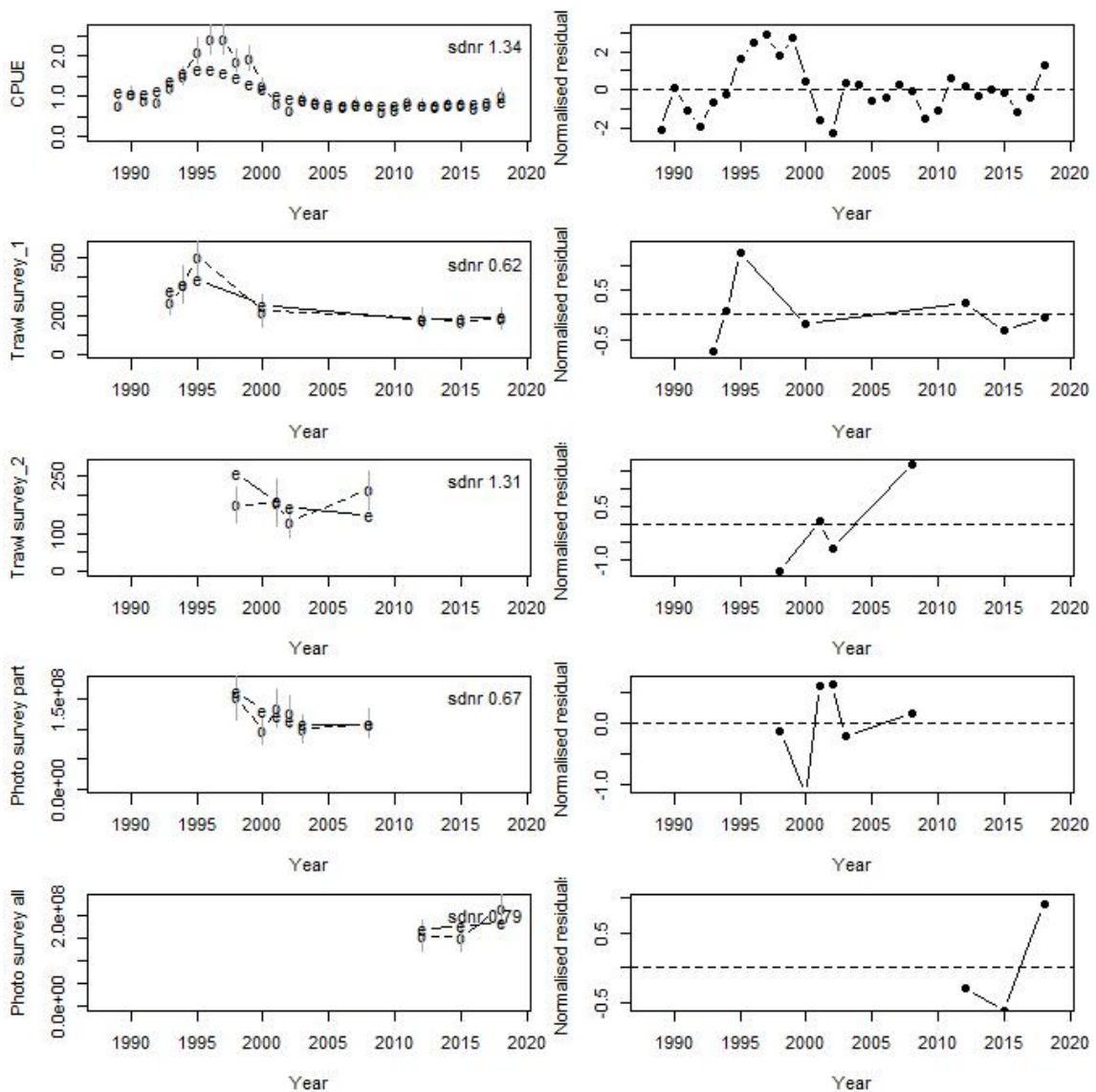


A6. 24: Marginal posterior distributions (histograms), MPD estimates (solid symbols), and distributions of priors (lines) for catchability terms for the SCI 1 M02CV25 model.

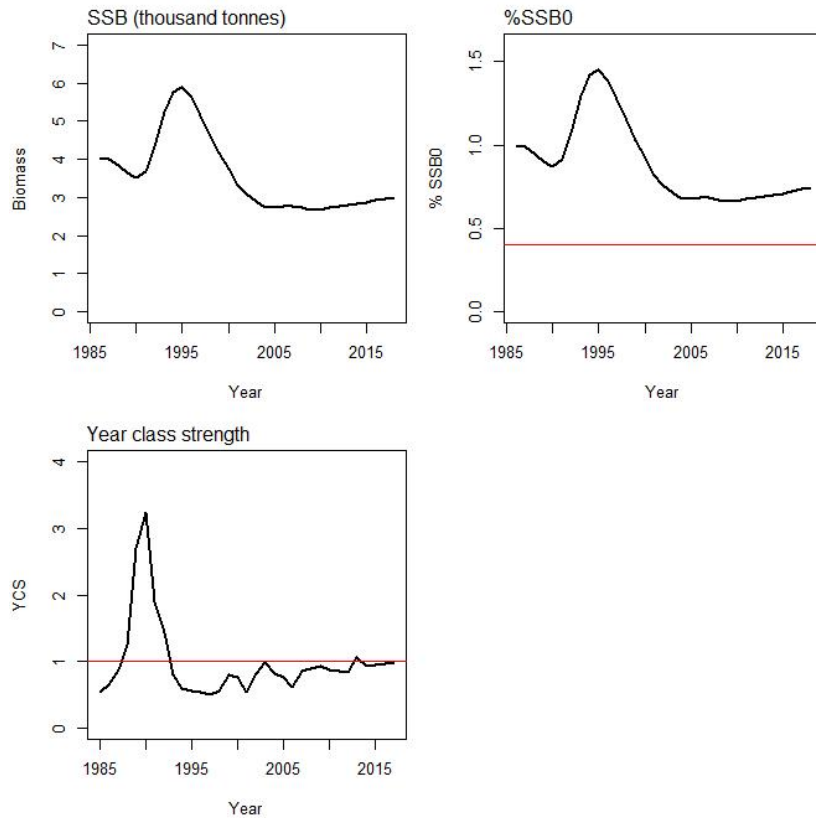


A6. 25: Posterior trajectory of SSB, SSB/SSB₀, and YCS for the SCI 1 M02CV25 model. Red dot represents MPD estimate of B₀.

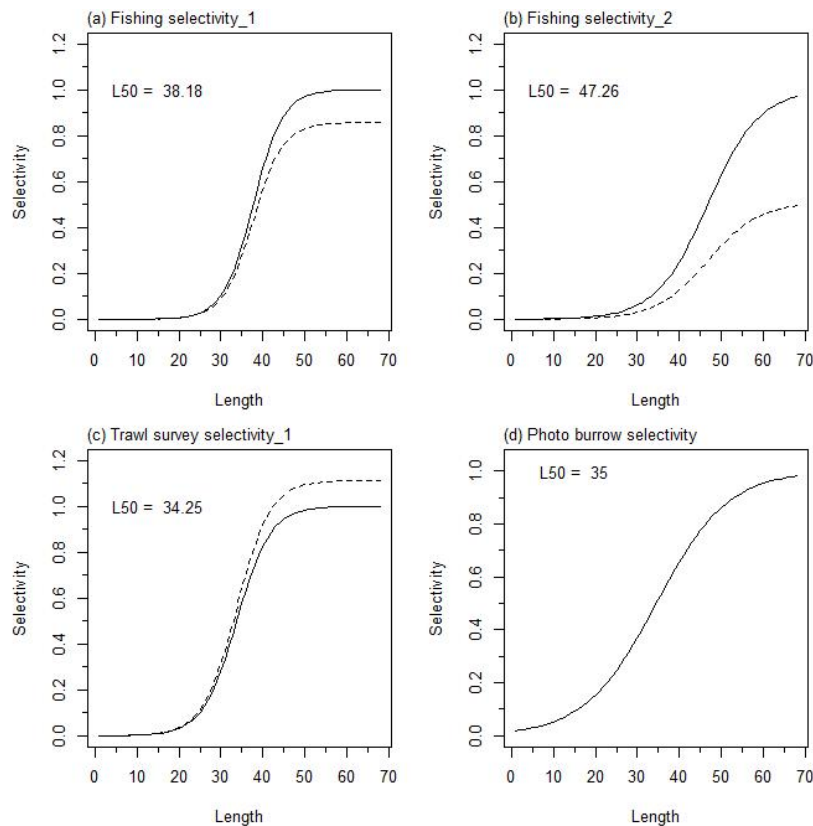
APPENDIX 7. SCI 1 M025CV15 model plots ($M=0.25$, $CV=0.15$)



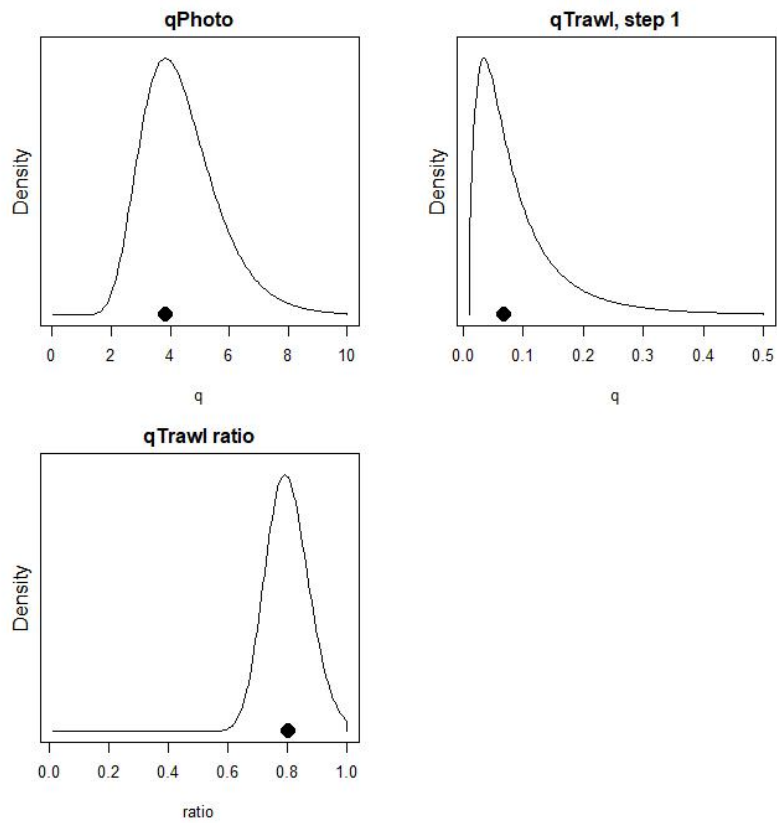
A7. 1: Fits to abundance indices (left column) and normalised residuals (right column) for standardised CPUE index (top row) trawl survey biomass index covering whole area (second row), trawl survey biomass index covering limited area (third row), photo survey abundance index covering limited area (fourth row), and photo survey abundance index covering whole area (fifth row) for SCI 1 M025CV15 model.



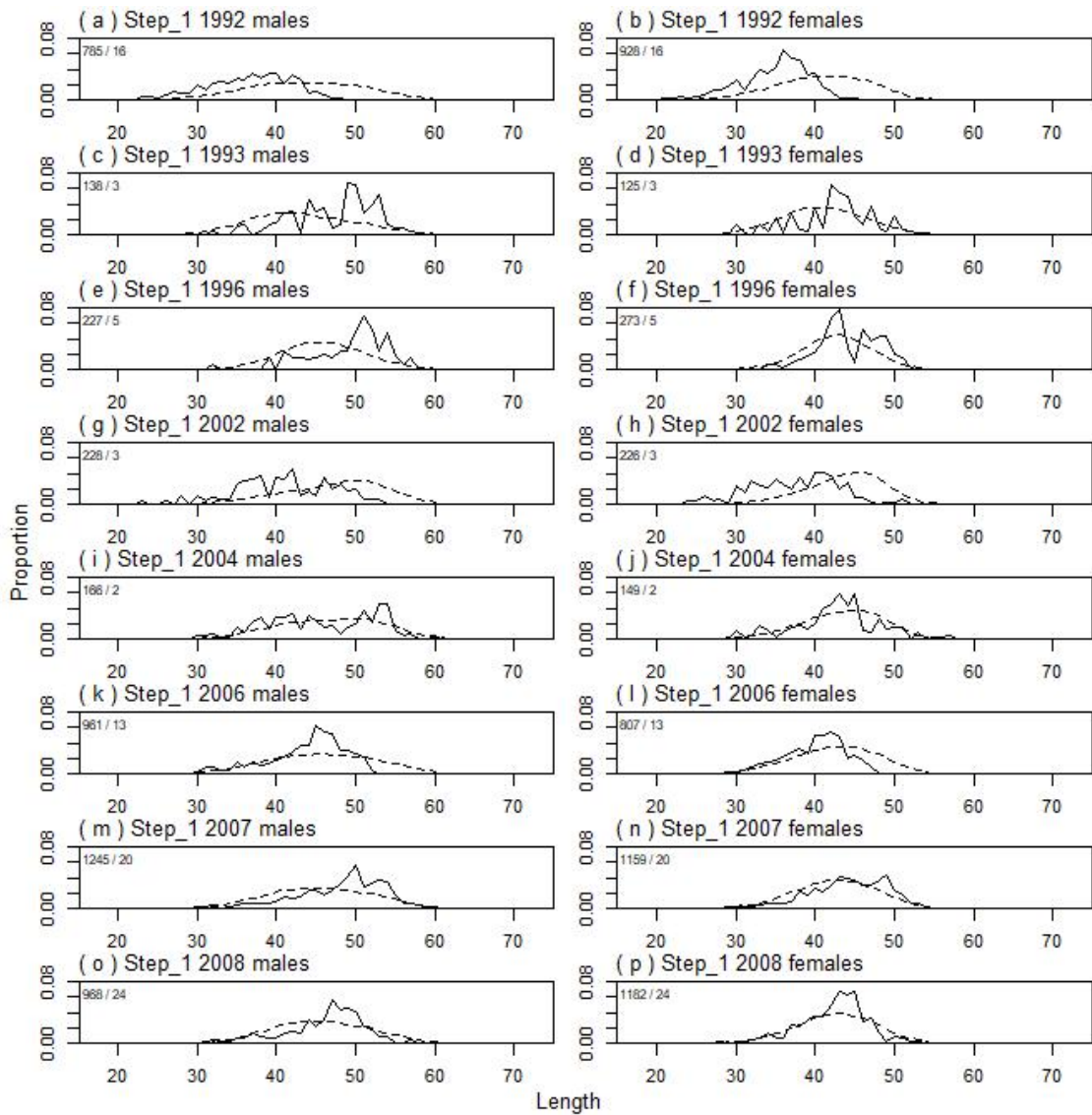
A7. 2: Spawning stock biomass trajectory (upper left), stock status (upper right), and year class strength (lower left) for SCI 1 M025CV15 model.



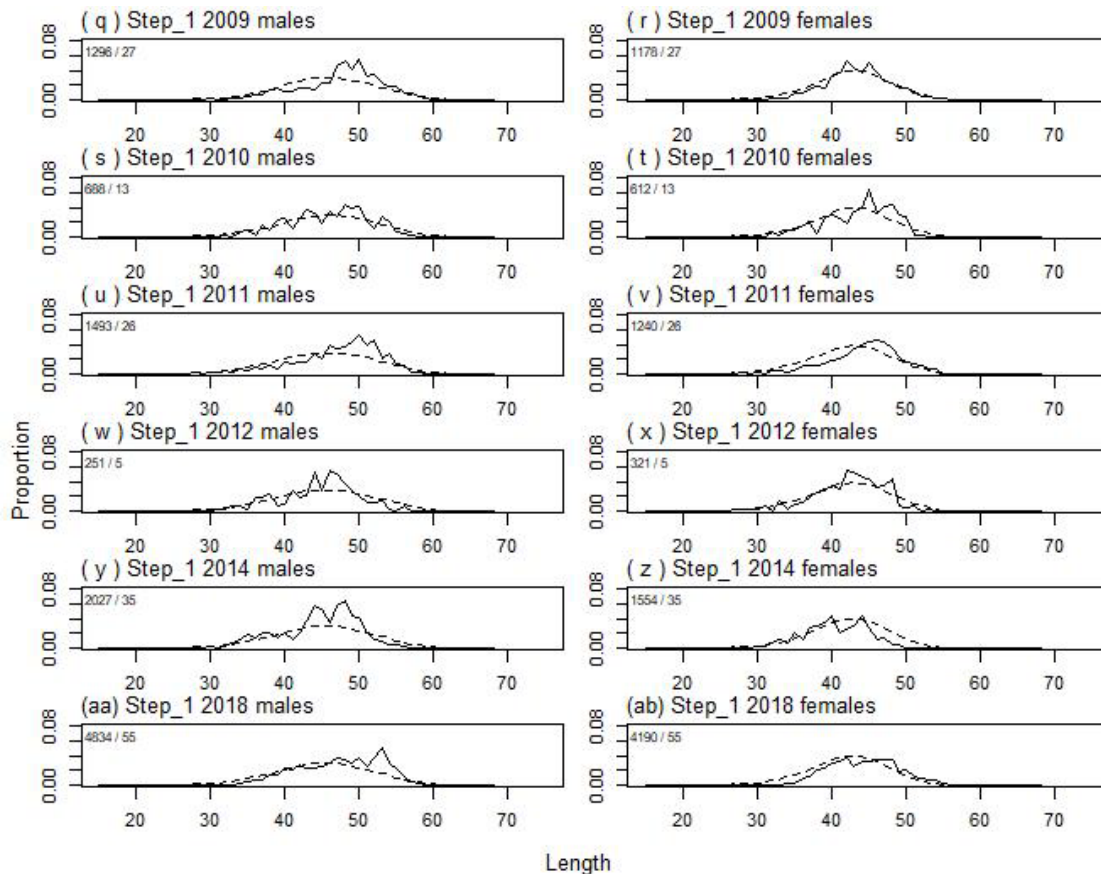
A7. 3: Fishery and survey selectivity curves for SCI 1 M025CV15 model. Solid line – females, dotted line – males. The scampi burrow index is not sexed, and a single selectivity applies.



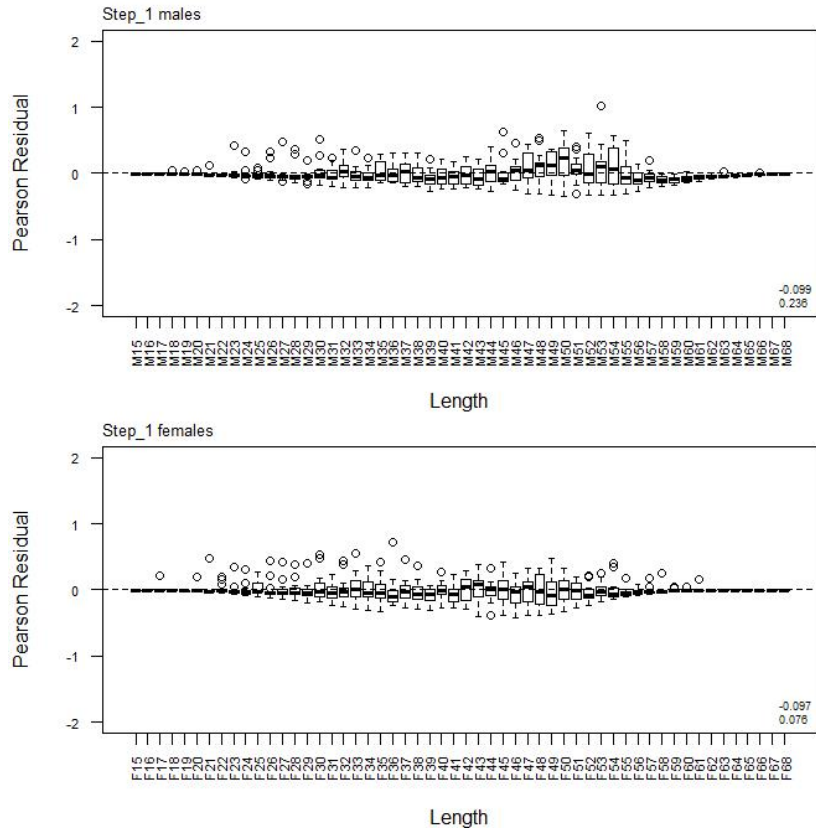
A7. 4: Catchability estimates from MPD model run, plotted in relation to prior distribution for SCI 1 M025CV15 model.



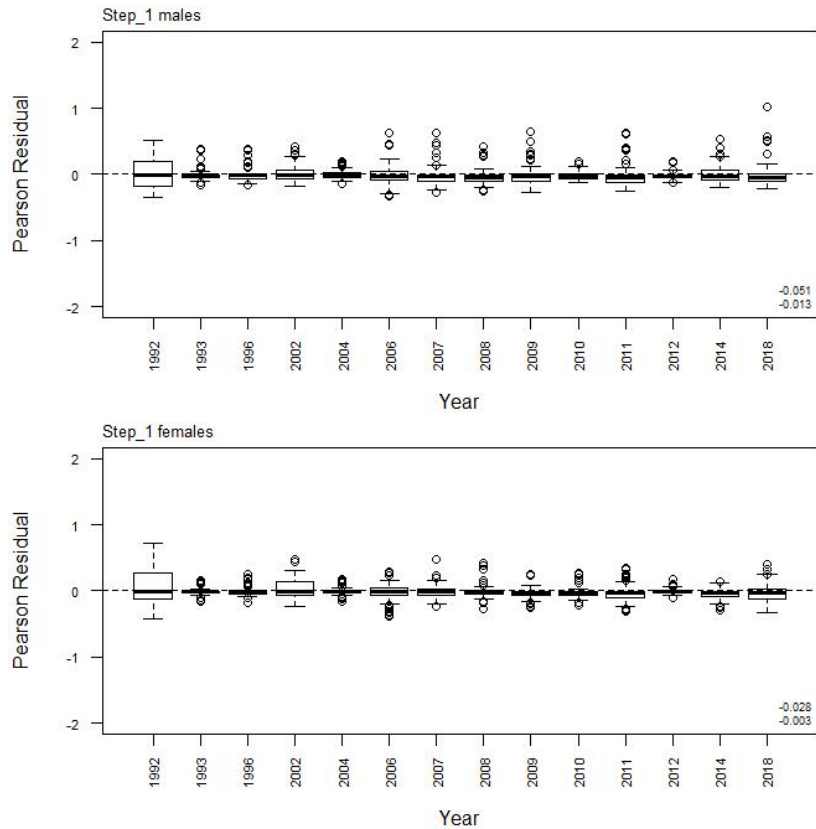
A7. 5: Observed (solid line) and fitted (dashed line) length frequency distributions from observer samples, time step 1 for SCI 1 M025CV15 model. Numbers in top left corner of each plot represent number of scampi measured / number of events sampled.



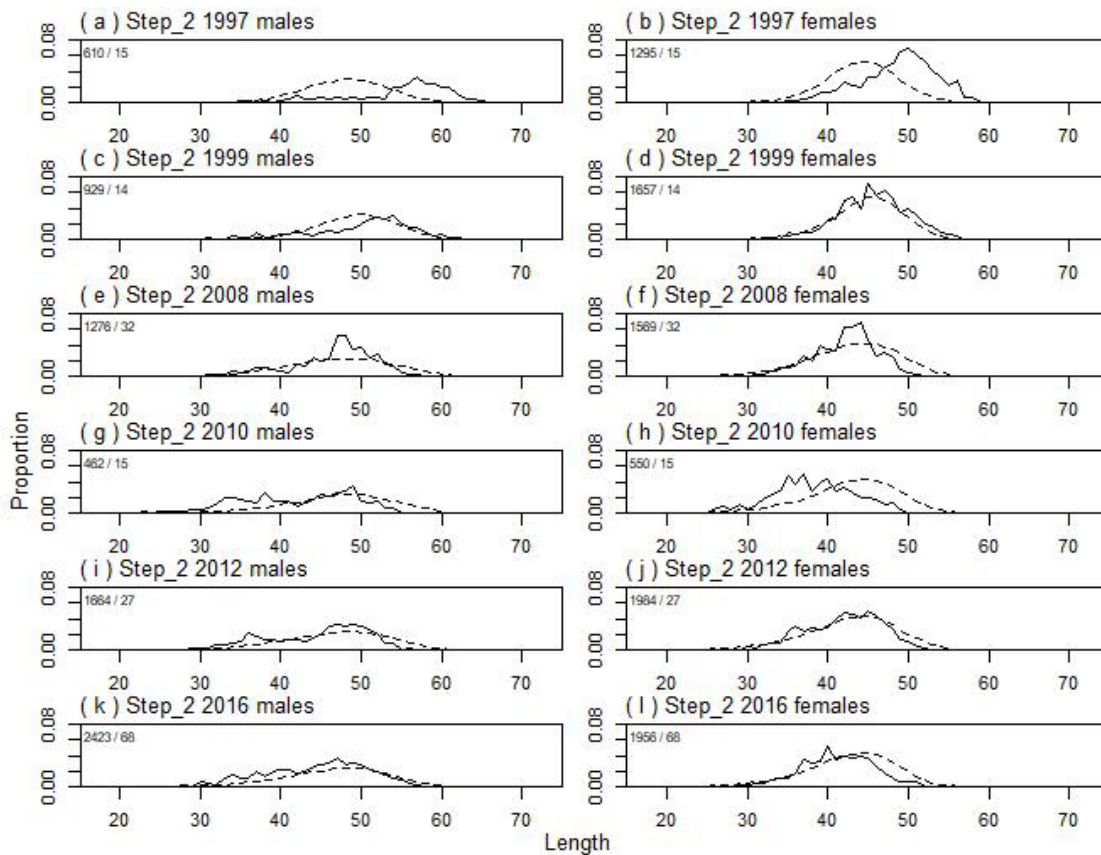
A7. 5(continued): Observed (solid line) and fitted (dashed line) length frequency distributions from observer samples, time step 1 for SCI 1 M025CV15 model. Numbers in top left corner of each plot represent number of scampi measured / number of events sampled.



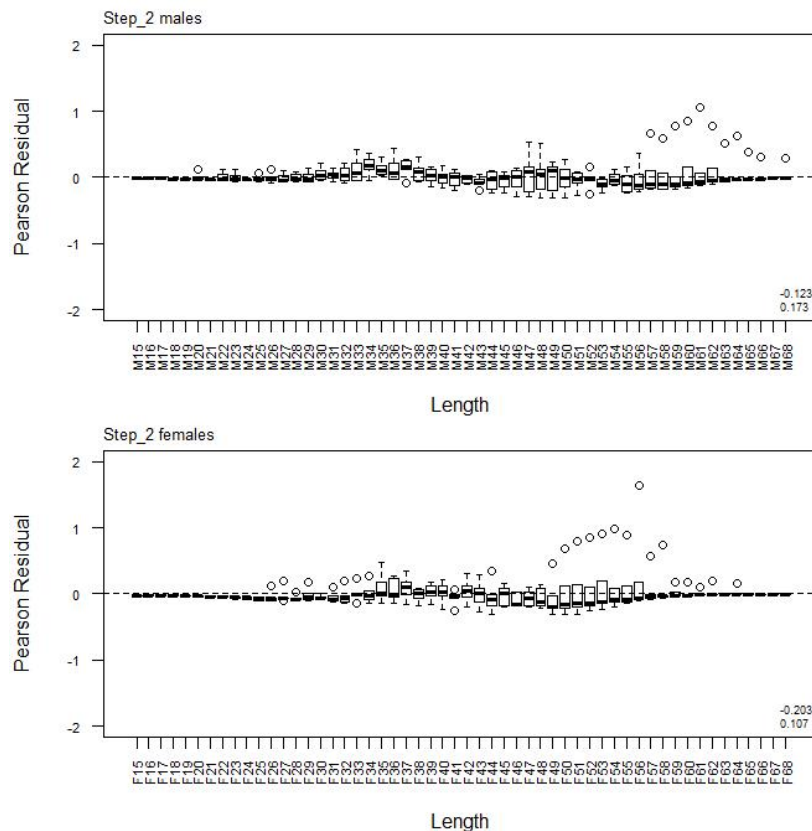
A7. 6: Box plots of Pearson residuals from the fit to length frequency distributions by length from observer sampling by sex for time step 1 for SCI 1 M025CV15 model.



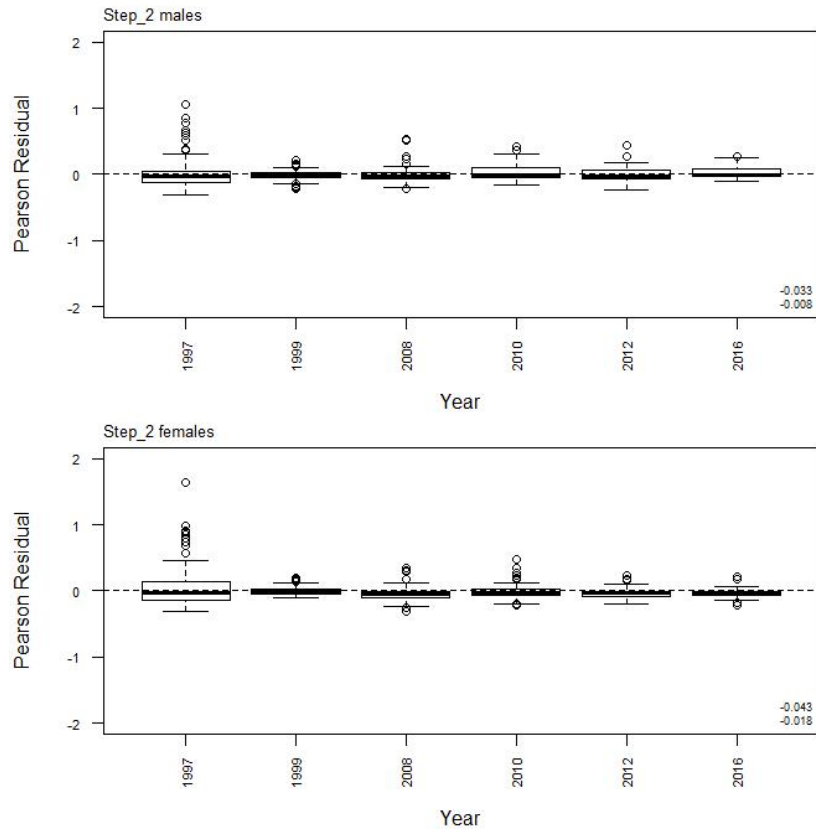
A7. 7: Box plots of Pearson residuals from the fit to length frequency distributions by year from observer sampling by sex for time step 1 for SCI 1 M025CV15 model.



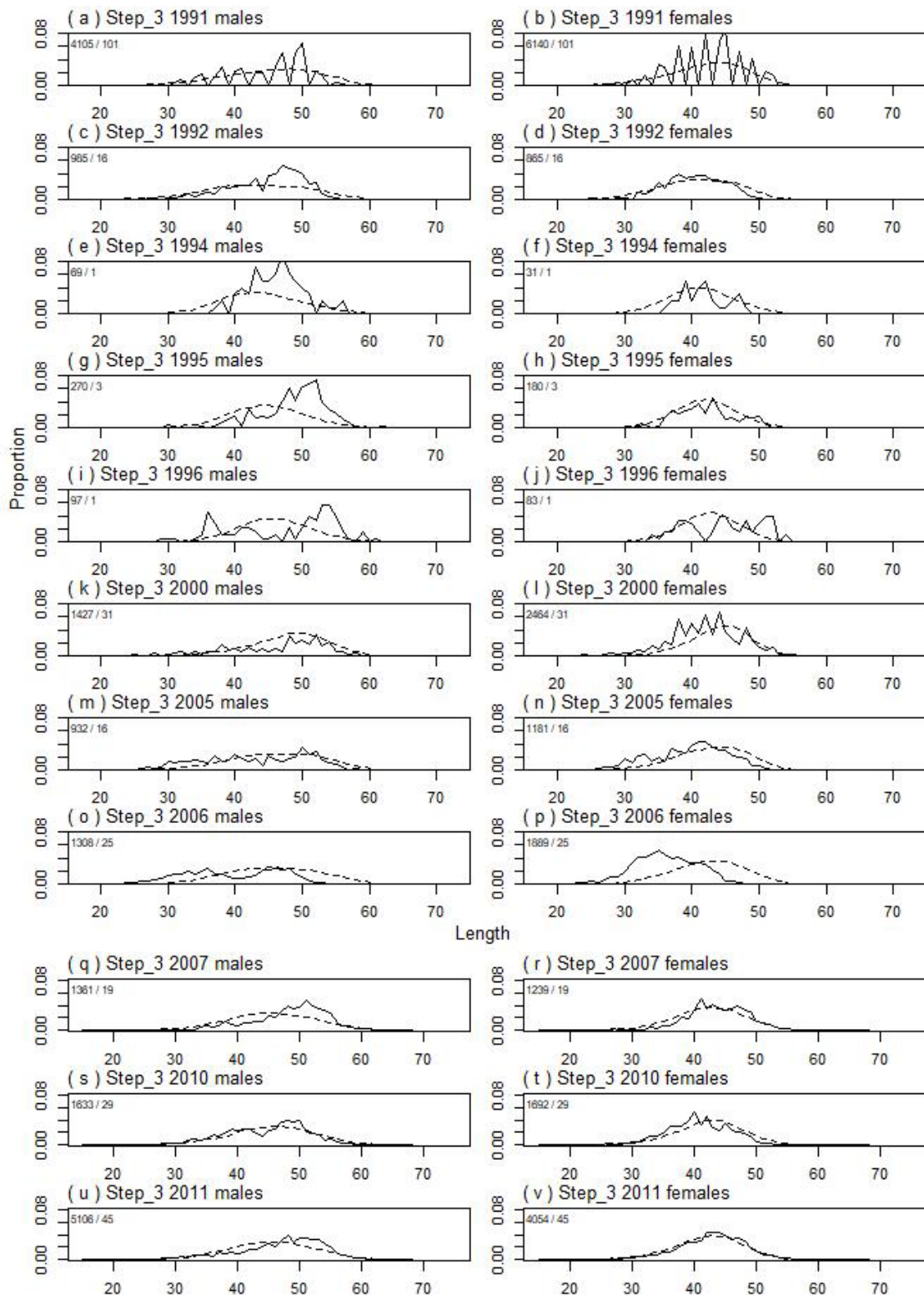
A7. 8: Observed (solid line) and fitted (dashed line) length frequency distributions from observer samples, time step 2 for SCI 1 M025CV15 model. Numbers in top left corner of each plot represent number of scampi measured / number of events sampled.



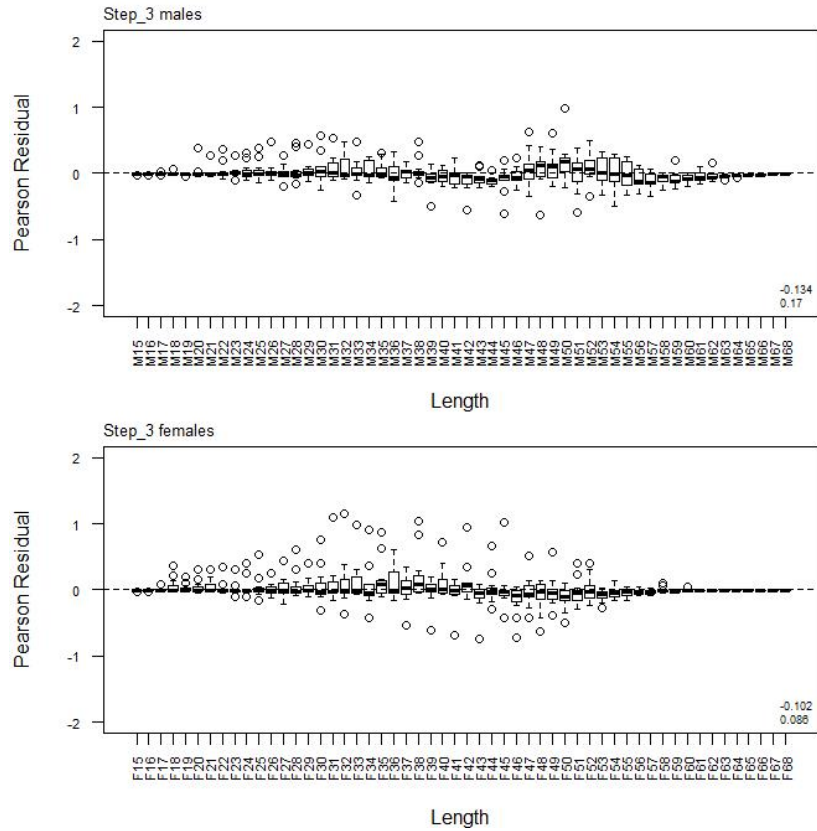
A7. 9: Box plots of Pearson residuals from the fit to length frequency distributions by length from observer sampling by sex for time step 2 for SCI 1 M025CV15 model.



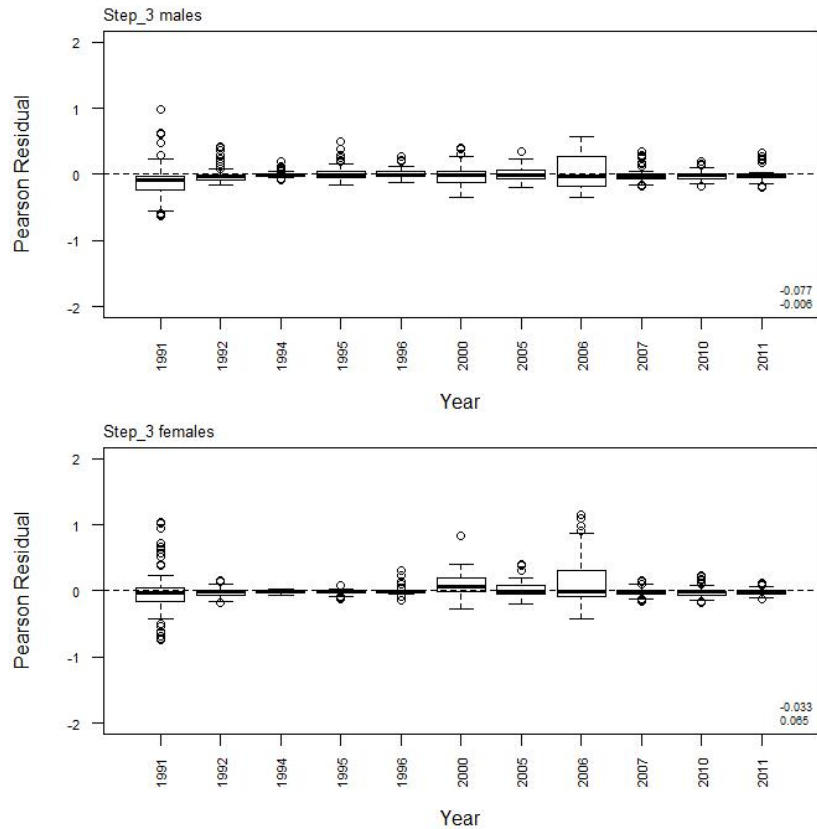
A7. 10: Box plots of Pearson residuals from the fit to length frequency distributions by year from observer sampling by sex for time step 2 for SCI 1 M025CV15 model.



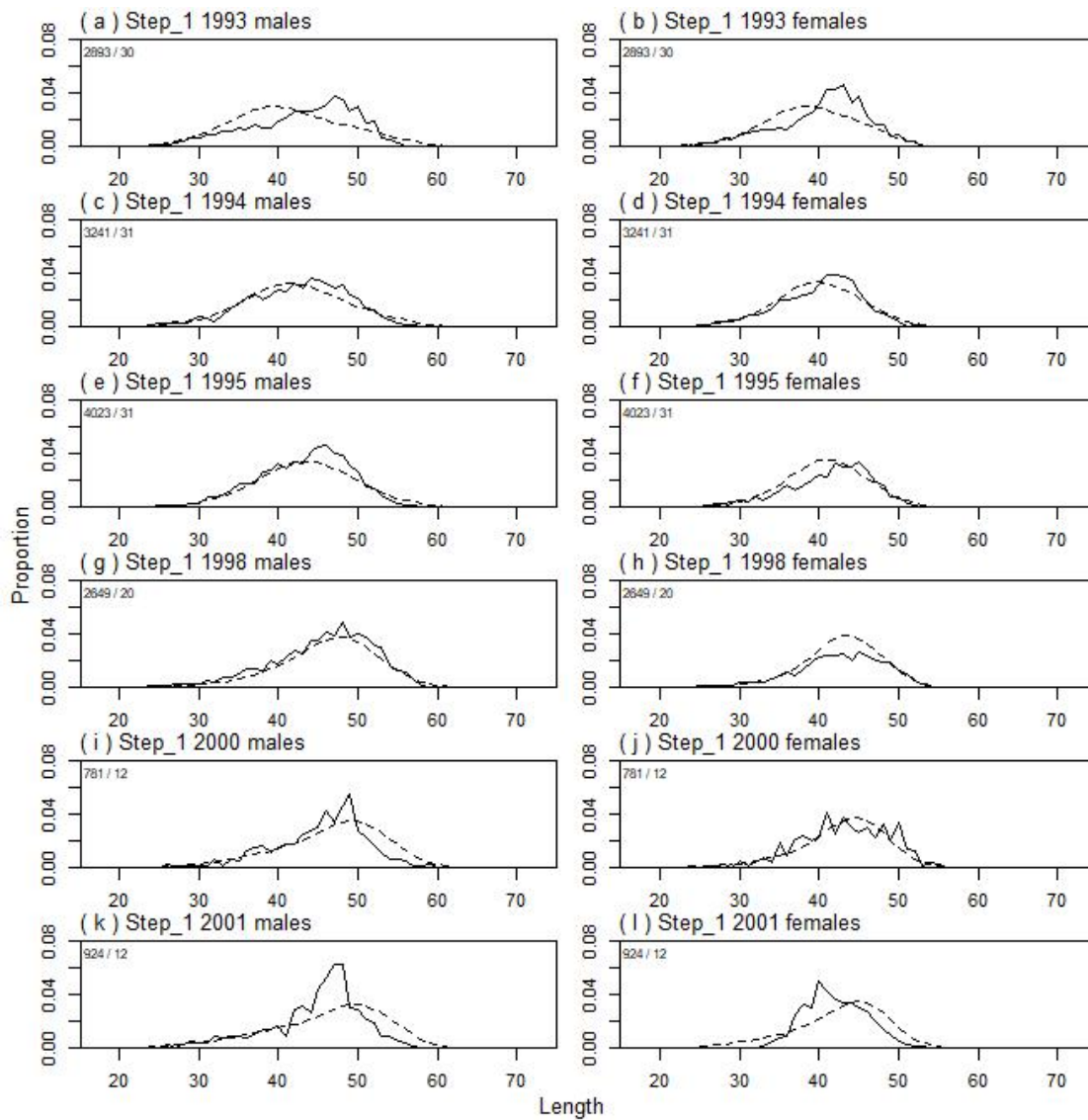
A7. 11: Observed (solid line) and fitted (dashed line) length frequency distributions from observer samples, time step 3 for SCI 1 M025CV15 model. Numbers in top left corner of each plot represent number of scampi measured / number of events sampled.



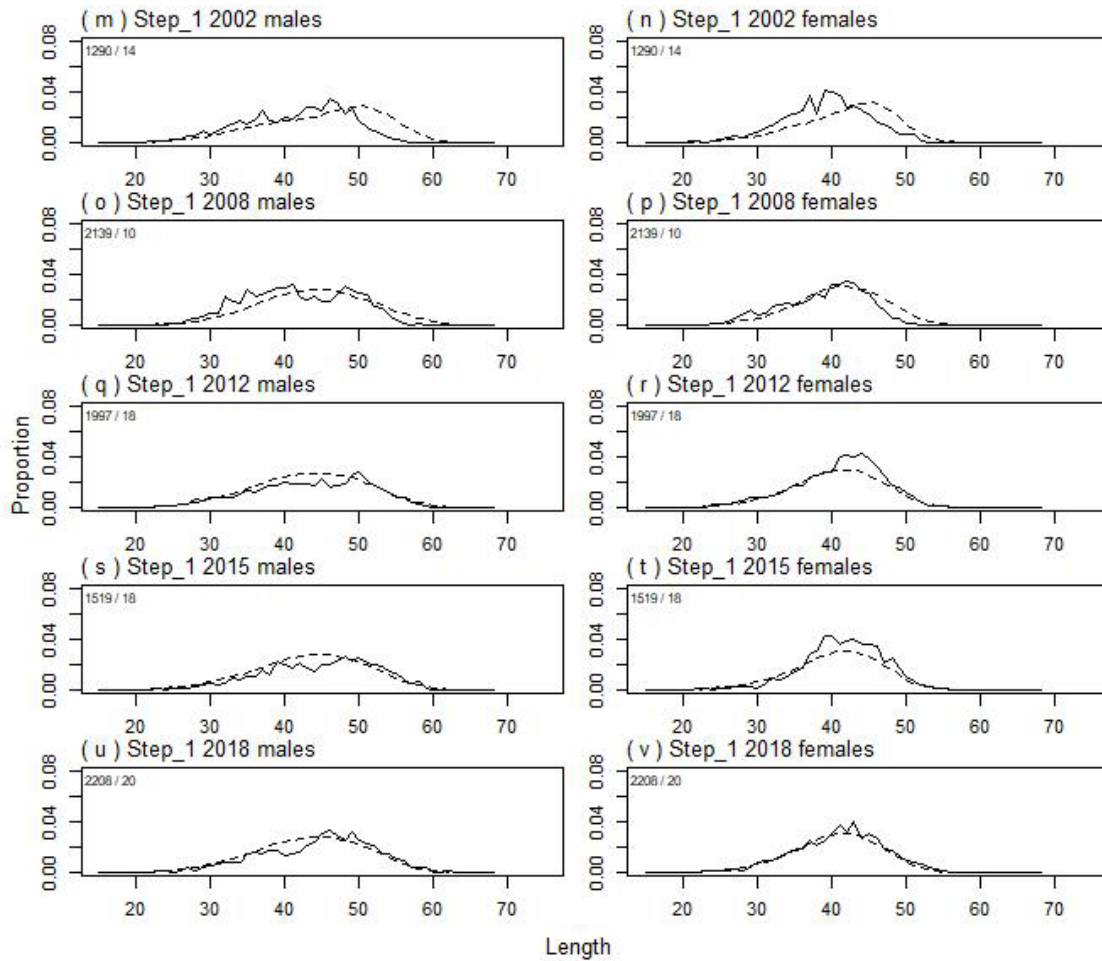
A7. 12: Box plots of Pearson residuals from the fit to length frequency distributions by length from observer sampling by sex for time step 3 for SCI 1 M025CV15 model.



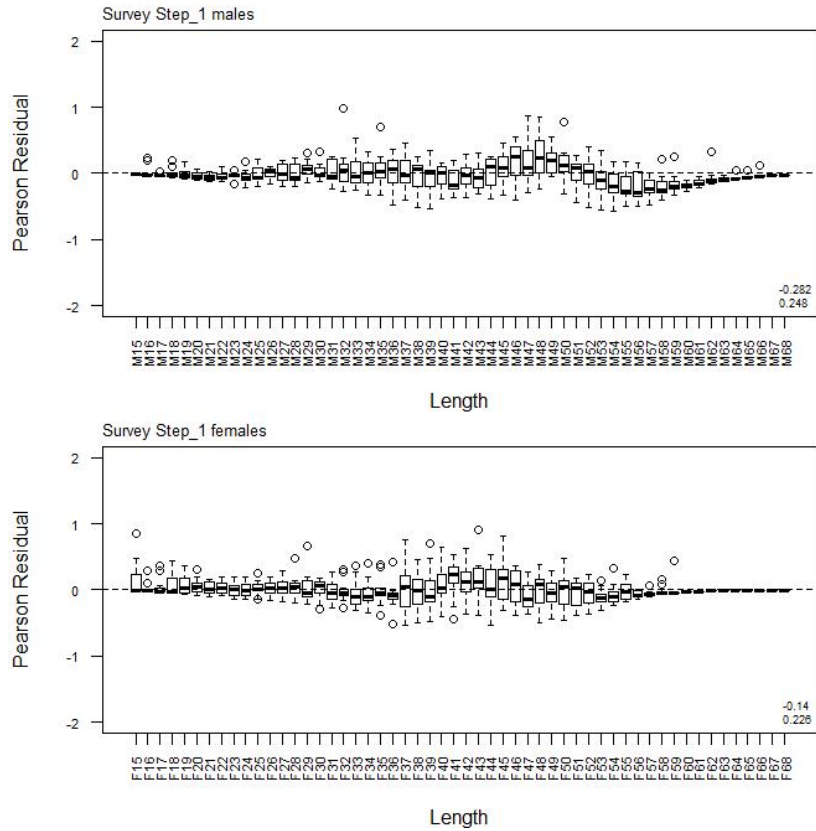
A7. 13: Box plots of Pearson residuals from the fit to length frequency distributions by year from observer sampling by sex for time step 3 for SCI 1 M025CV15 model.



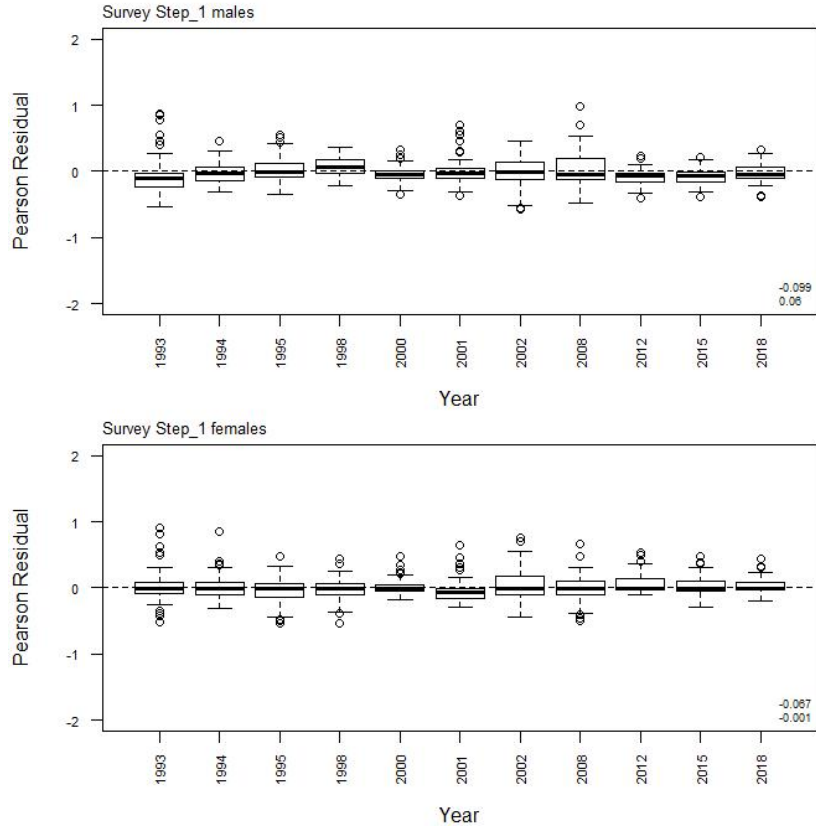
A7. 14: Observed (solid line) and fitted (dashed line) length frequency distributions from trawl survey samples for SCI 1 M025CV15 model. Numbers in top left corner of each plot represent number of scampi measured / number of events sampled.



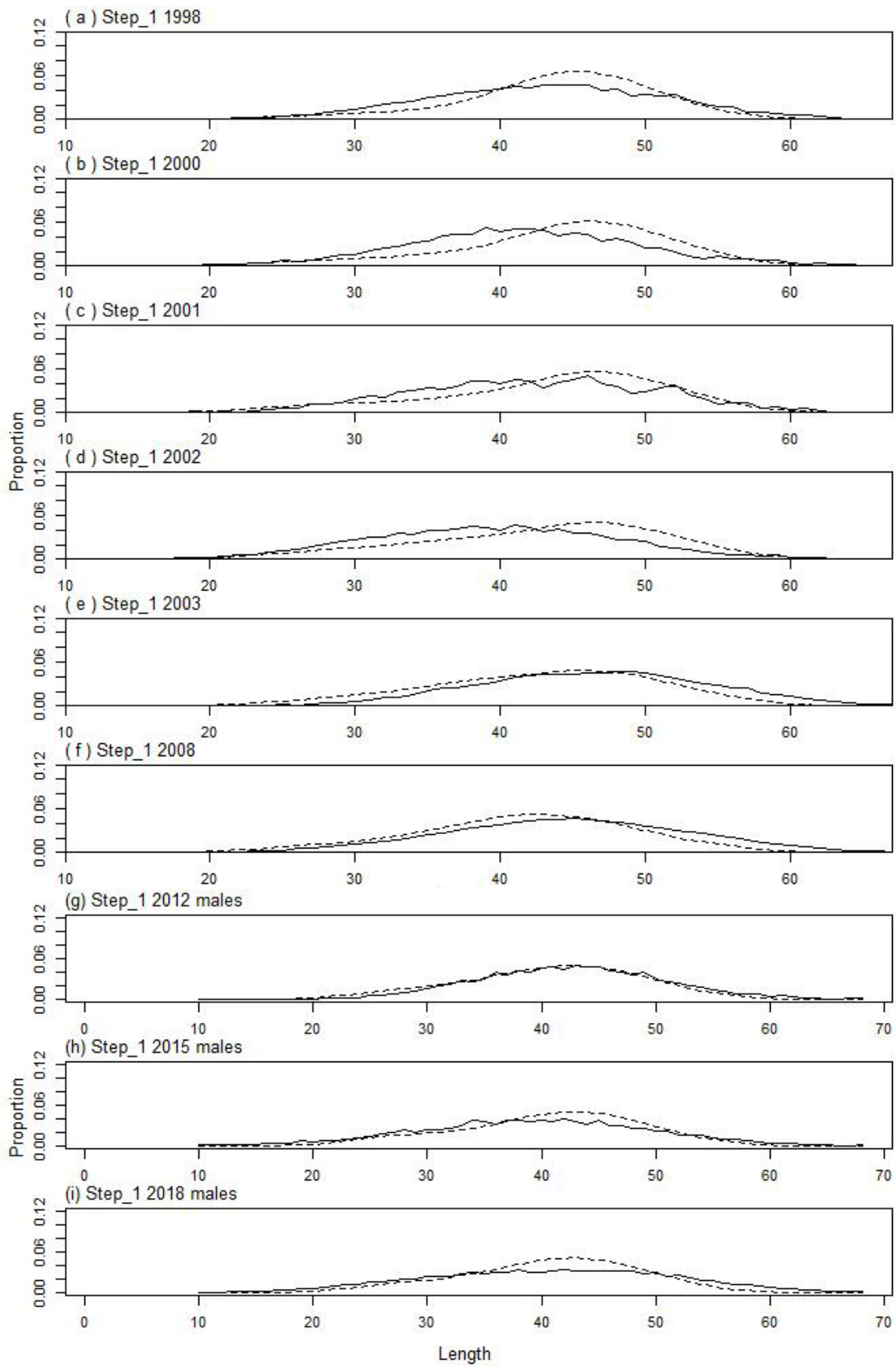
A7. 14(continued): Observed (solid line) and fitted (dashed line) length frequency distributions from trawl survey samples for SCI 1 M025CV15 model. Numbers in top left corner of each plot represent number of scampi measured / number of events sampled.



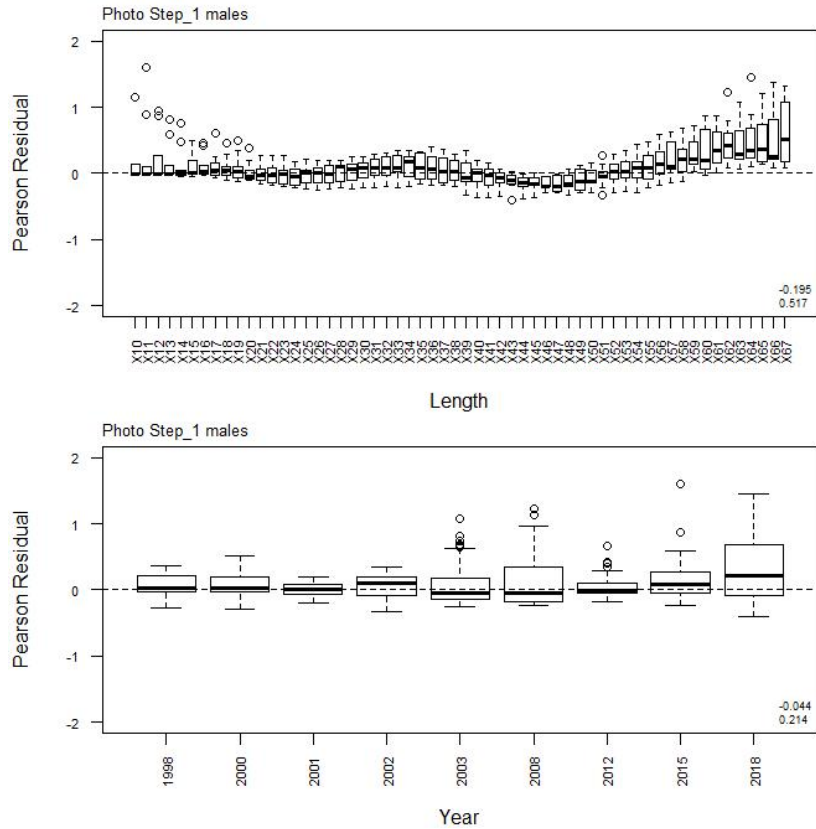
A7. 15: Box plots of Pearson residuals from the fit to length frequency distributions by length from trawl survey sampling by sex for SCI 1 M025CV15 model.



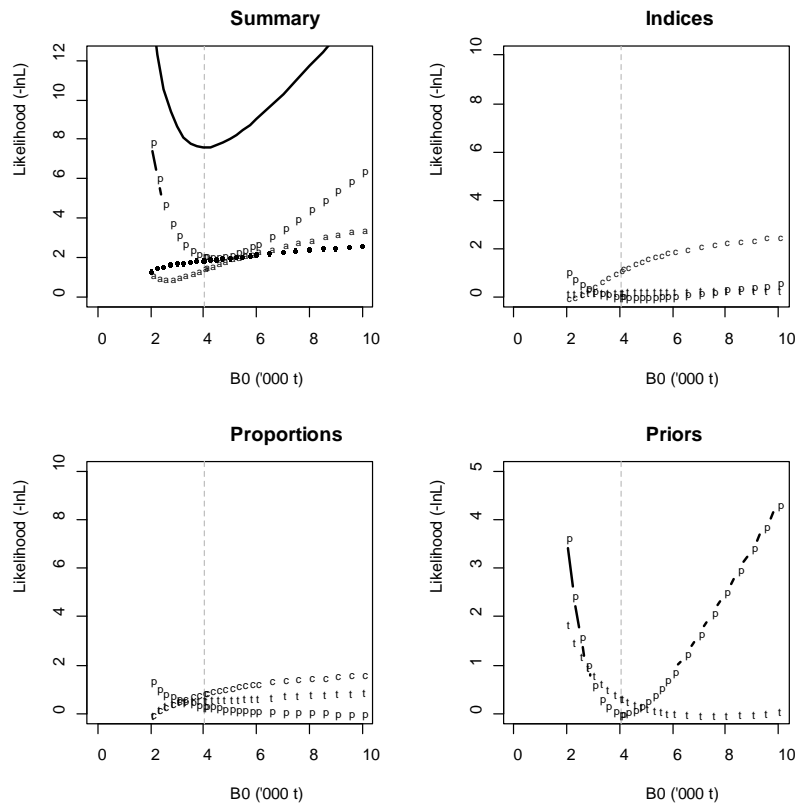
A7. 16: Box plots of Pearson residuals from the fit to length frequency distributions by year from trawl survey sampling by sex for SCI 1 M025CV15 model.



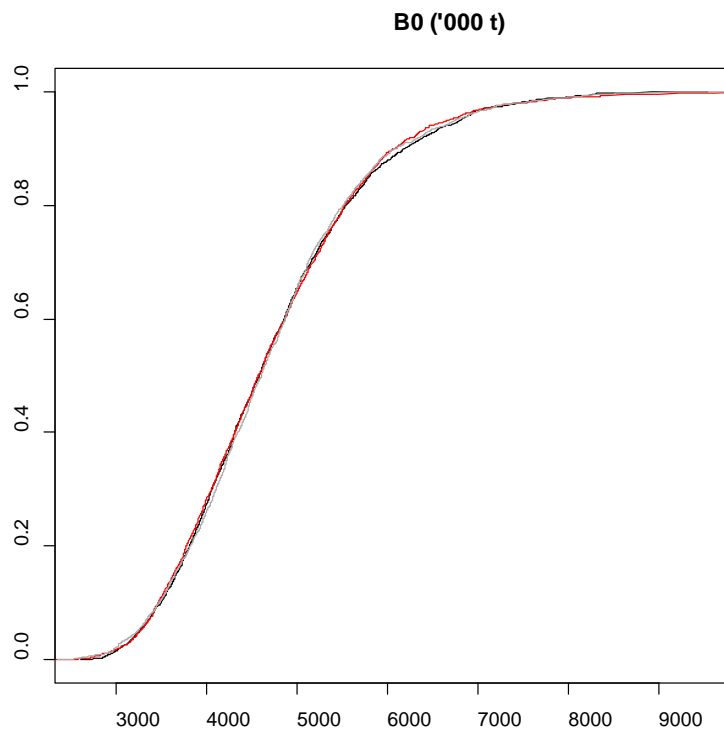
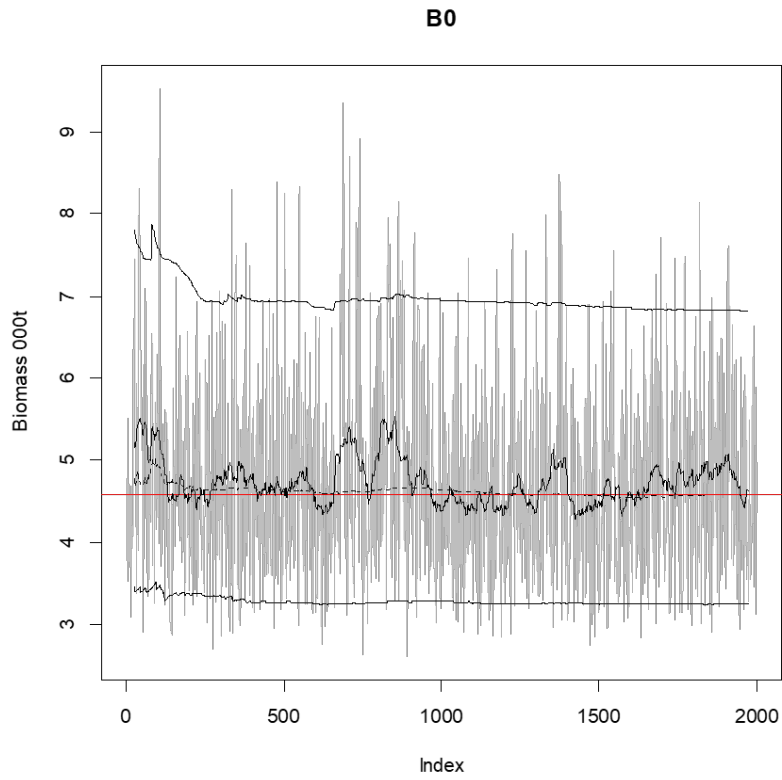
A7. 17: Observed (solid line) and fitted (dashed line) length frequency distributions from photo survey samples for SCI 1 M025CV15 model.



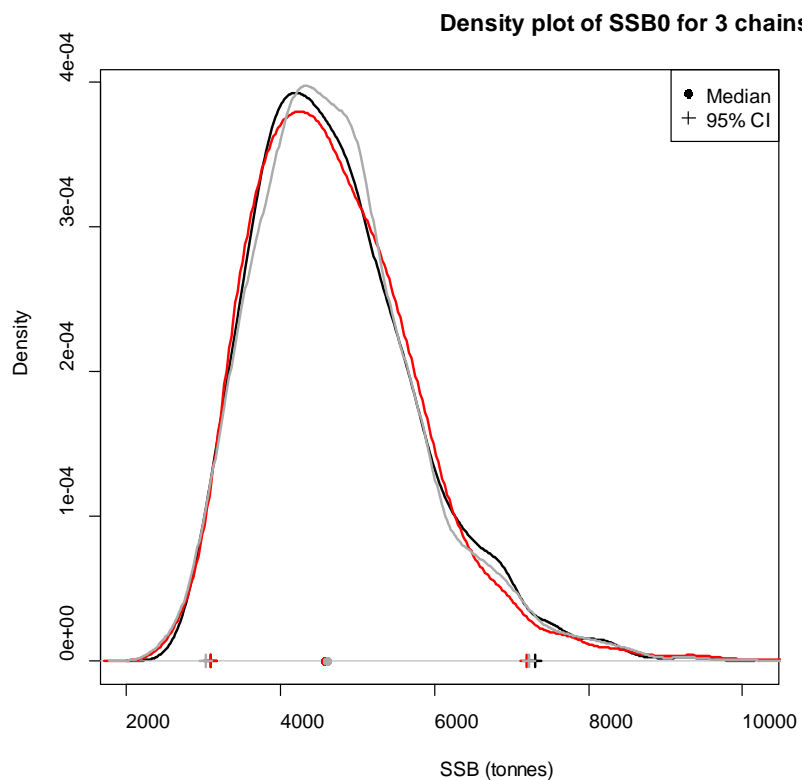
A7. 18: Box plots of Pearson residuals from the fit to length frequency distributions by length (top plot) and year (bottom plot) from photo survey sampling by sex for SCI 1 M025CV15 model.



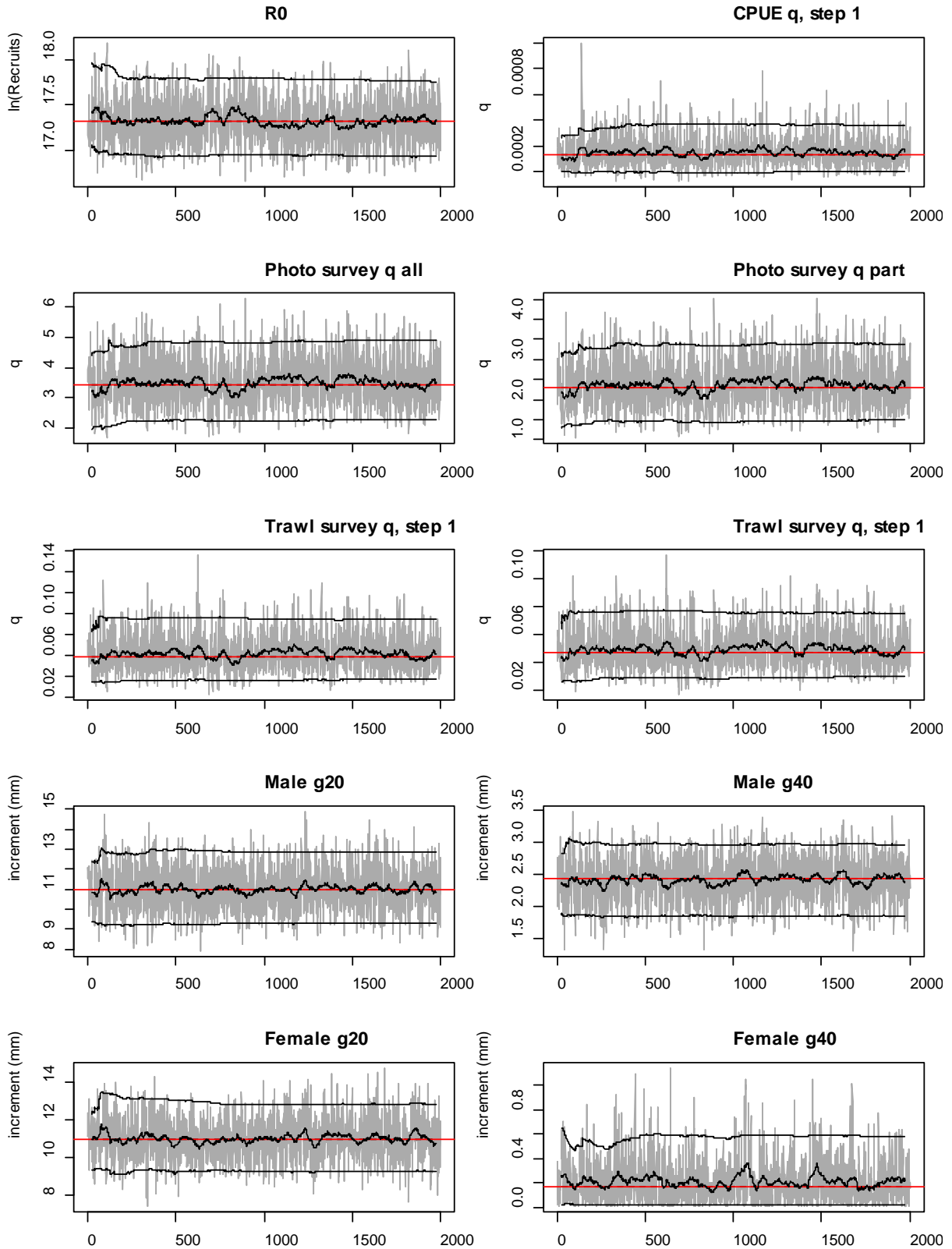
A7. 19: Likelihood profiles for model M025CV15 for SCI 1 when B_0 is fixed in the model. Figures show profiles for main priors (top left, p – priors, a – abundance indices, • – proportions at length), abundance indices (top right, t – trawl survey step, c – CPUE, p – photo survey), proportion at length data (bottom left, p-photo, t – trawl, c – observer) and priors (bottom right, p – q-Photo, t – q-Trawl).



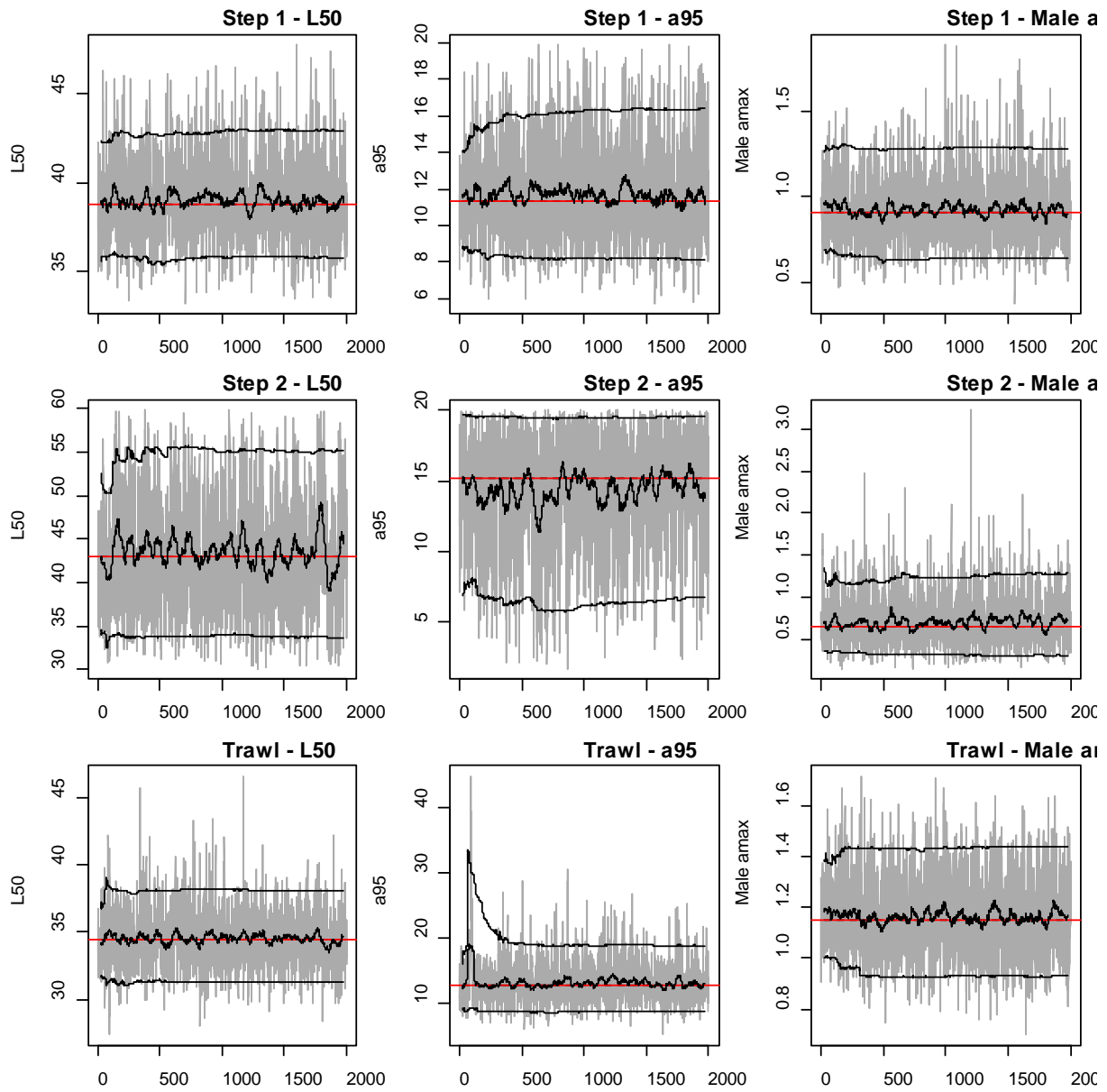
A7. 20: MCMC traces for B_0 and cumulative frequency distributions for three independent MCMC chains for the SCI 1 M025CV15 model.



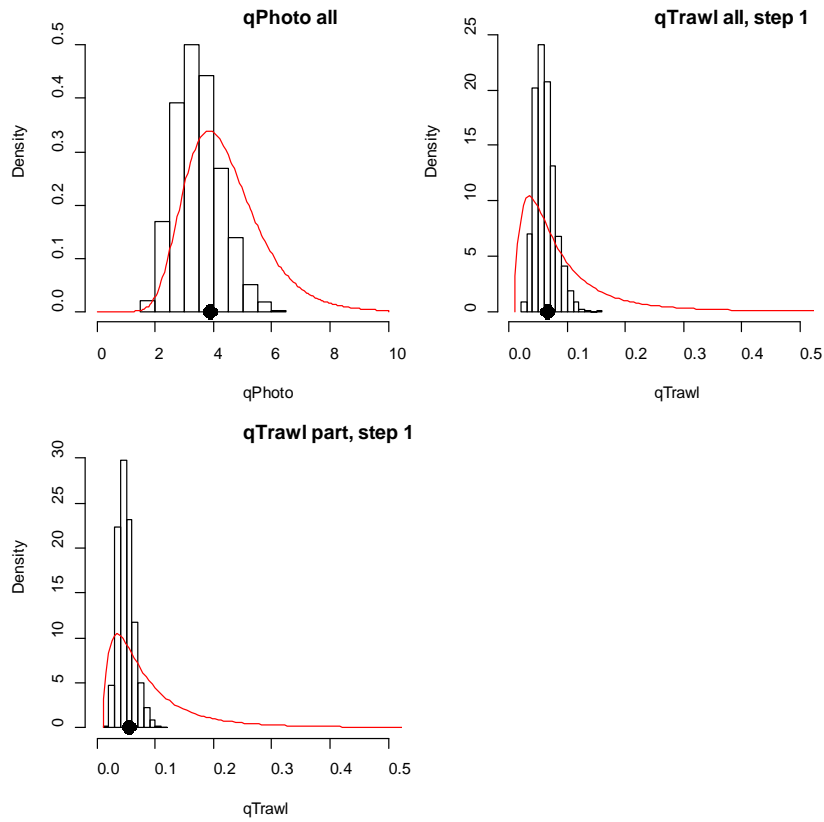
A7. 21: Density plots for B_0 for the SCI 1 M025CV15 model for three independent MCMC chains, with median and 95% confidence intervals.



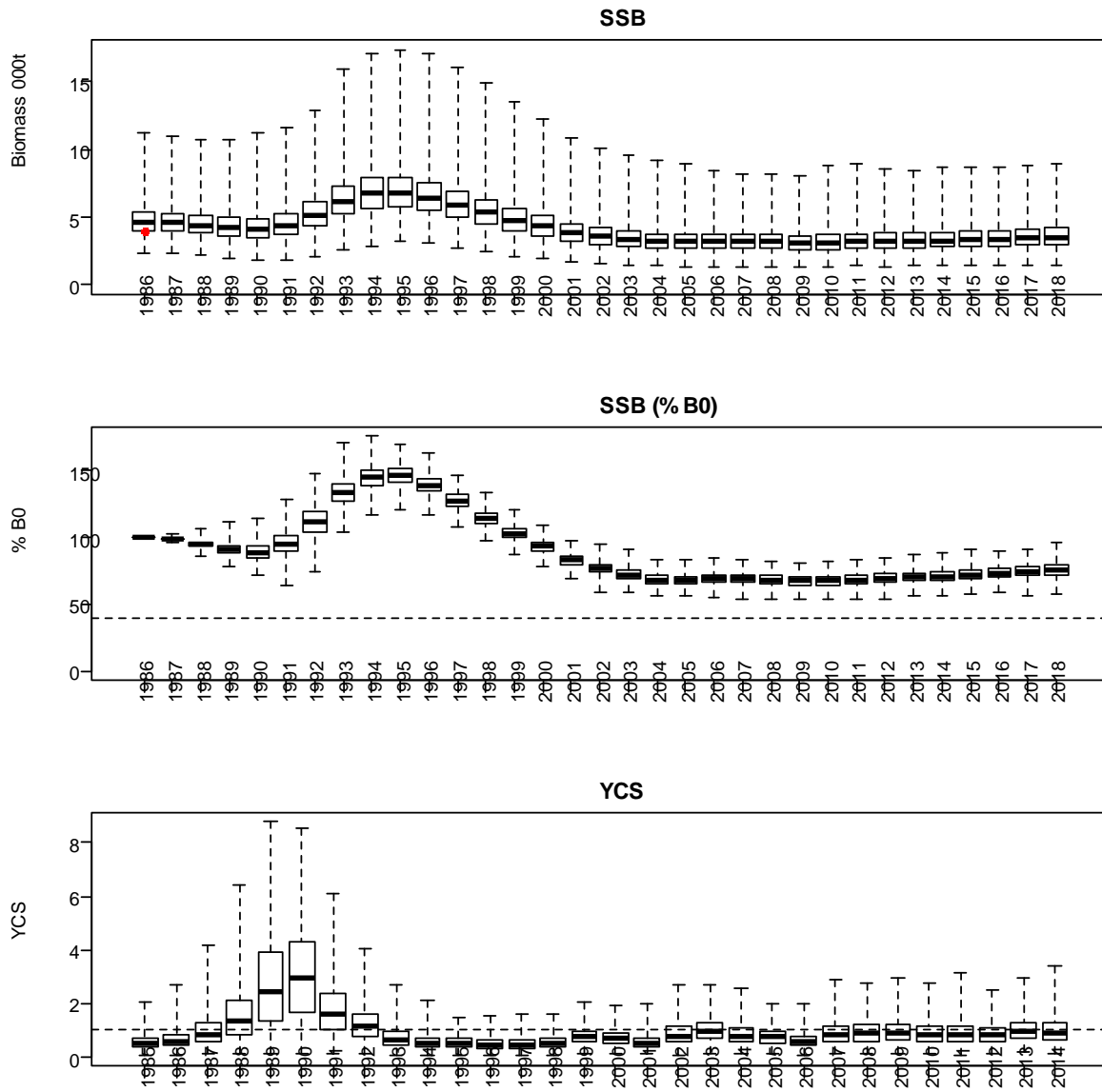
A7. 22: MCMC traces for R_0 , catchability, and growth terms for the SCI 1 M025CV15 model.



A7. 23: MCMC traces for selectivity terms for the SCI 1 M025CV15 model.

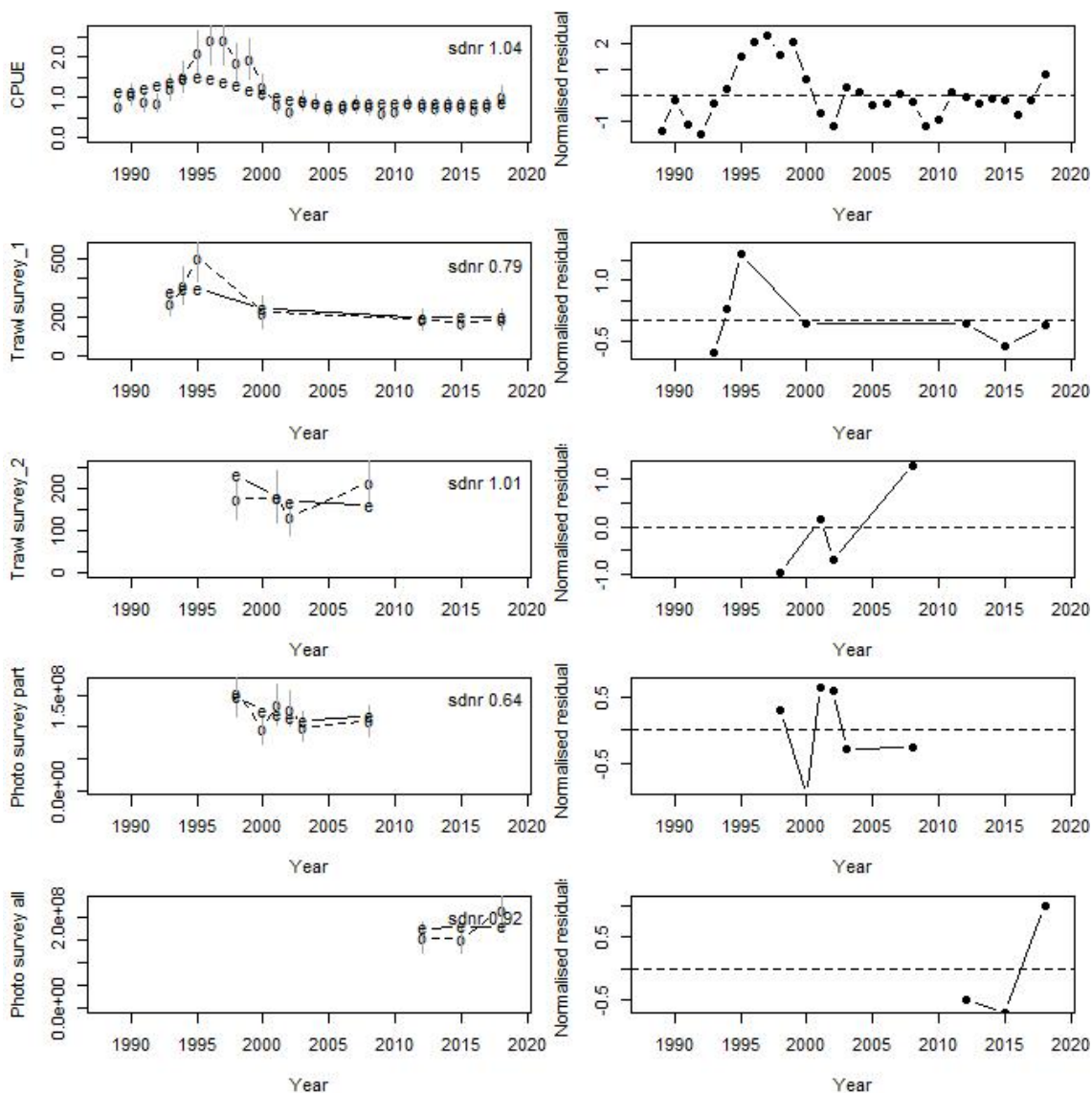


A7. 24: Marginal posterior distributions (histograms), MPD estimates (solid symbols), and distributions of priors (lines) for catchability terms for the SCI 1 M025CV15 model.

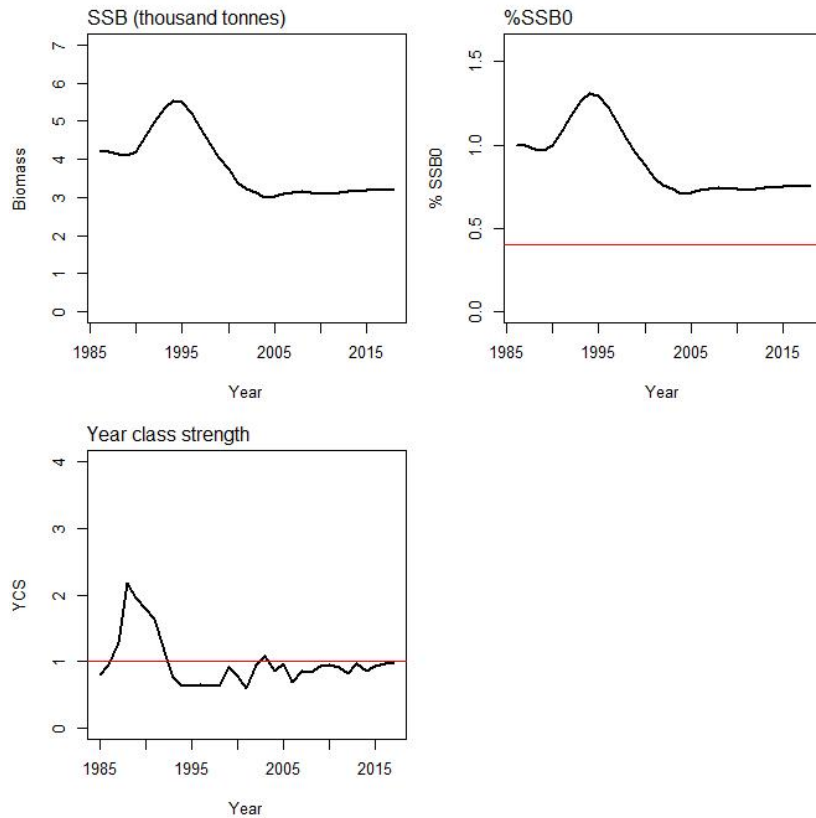


A7. 25: Posterior trajectory of SSB, SSB/SSB₀ and YCS for the SCI 1 M025CV15 model. Red dot represents MPD estimate of B₀.

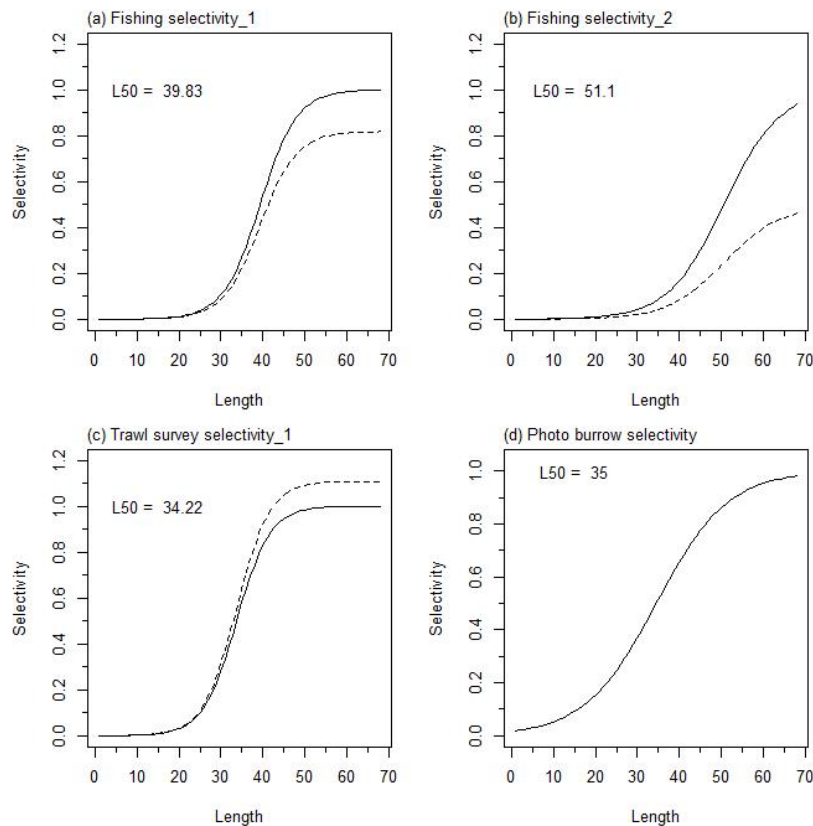
APPENDIX 8. SCI 1 M025CV25 model plots ($M=0.25$, $CV=0.25$)



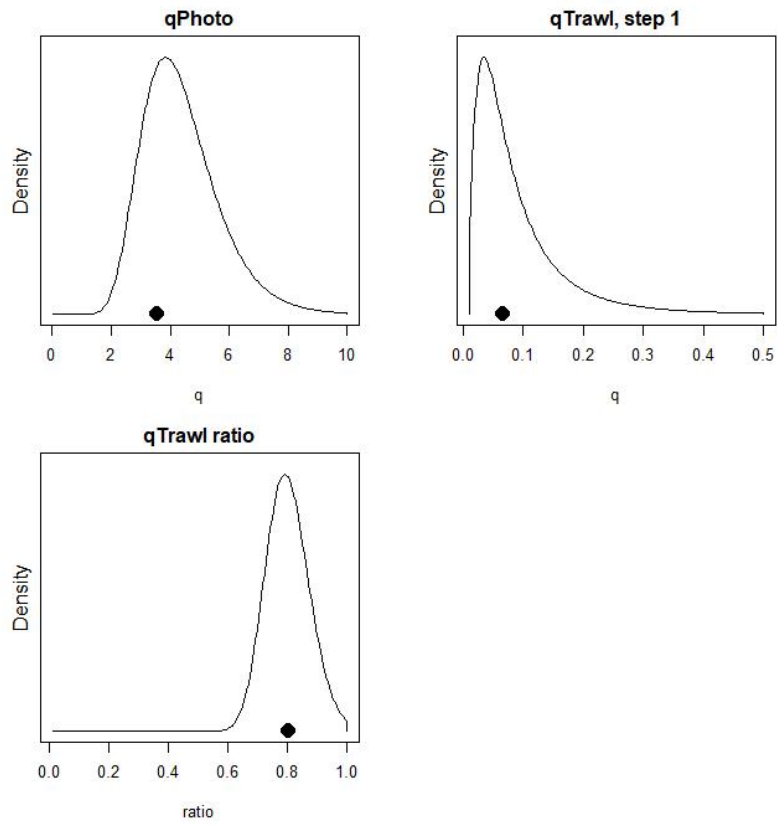
A8. 1: Fits to abundance indices (left column) and normalised residuals (right column) for standardised CPUE index (top row) trawl survey biomass index covering whole area (second row), trawl survey biomass index covering limited area (third row), photo survey abundance index covering limited area (fourth row), and photo survey abundance index covering whole area (fifth row) for the SCI 1 M025CV25 model.



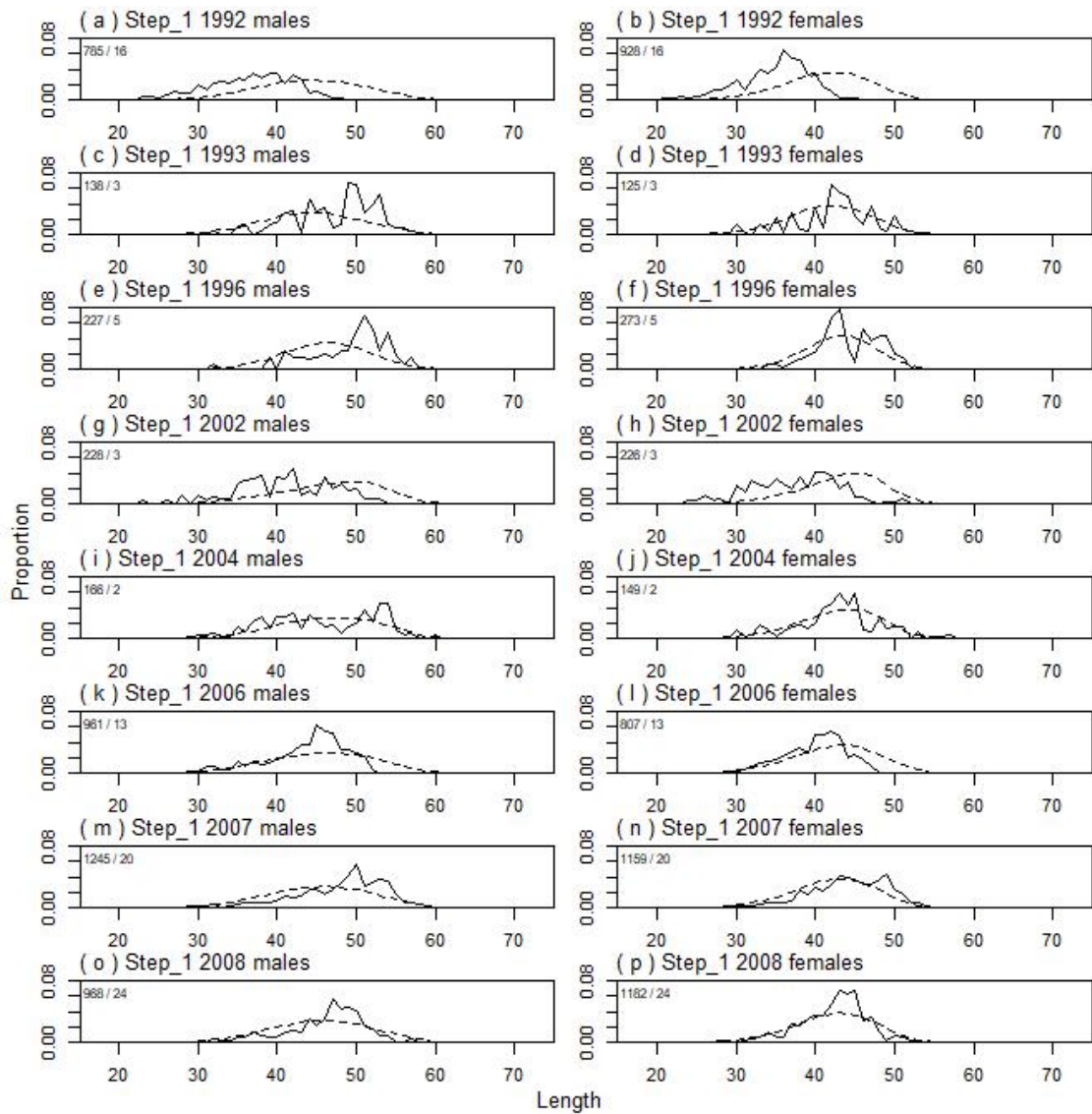
A8. 2: Spawning stock biomass trajectory (upper left), stock status (upper right), and year class strength (lower left) for the SCI 1 M025CV25 model.



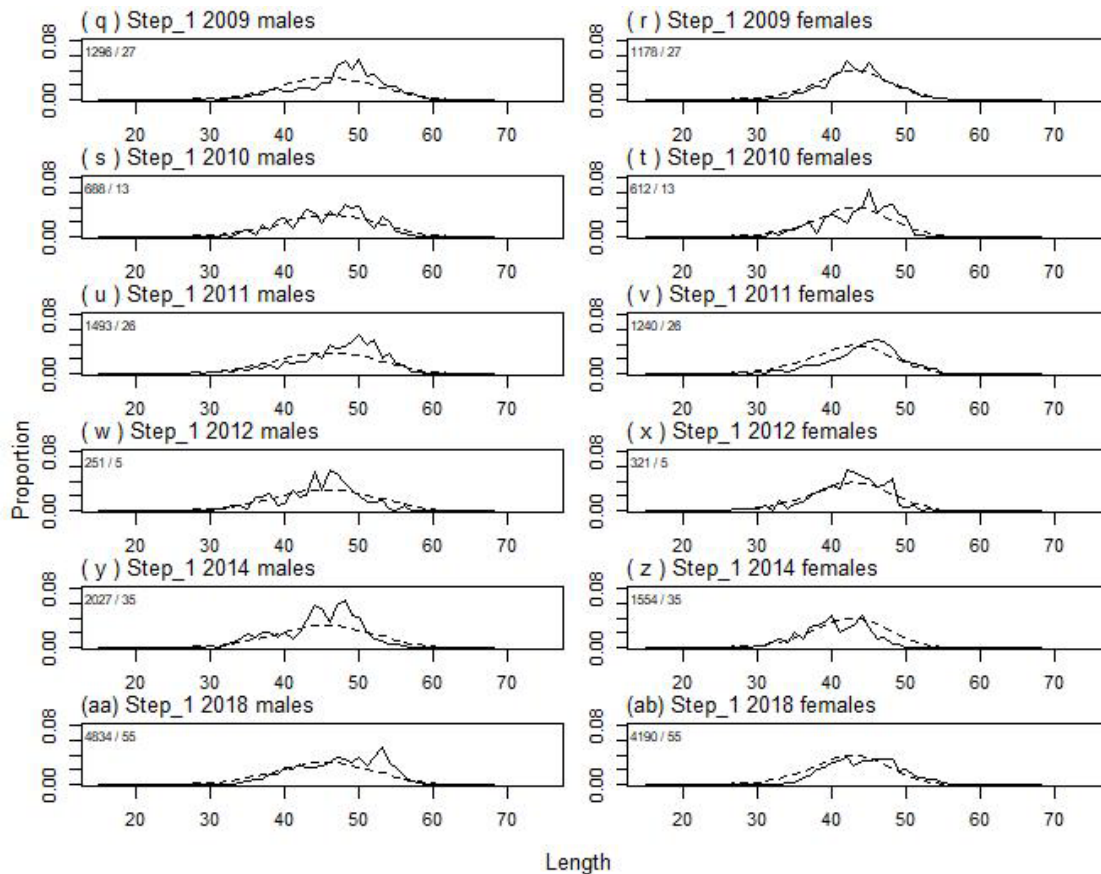
A8. 3: Fishery and survey selectivity curves for the SCI 1 M025CV25 model. Solid line – females, dotted line – males. The scampi burrow index is not sexed, and a single selectivity applies.



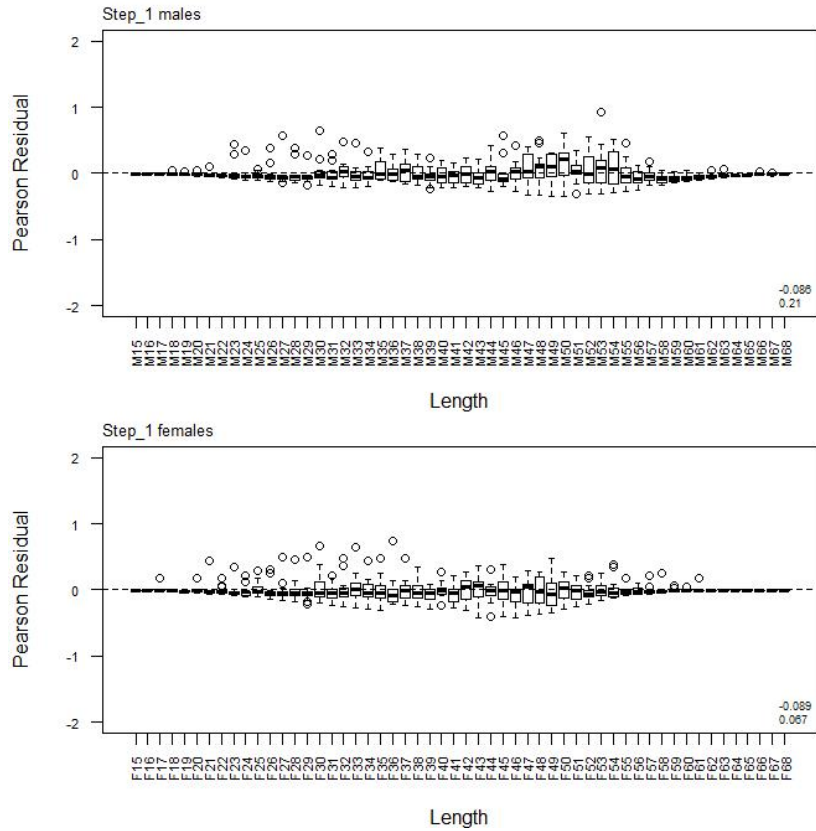
A8. 4: Catchability estimates from MPD model run, plotted in relation to prior distribution for the SCI 1 M025CV25 model.



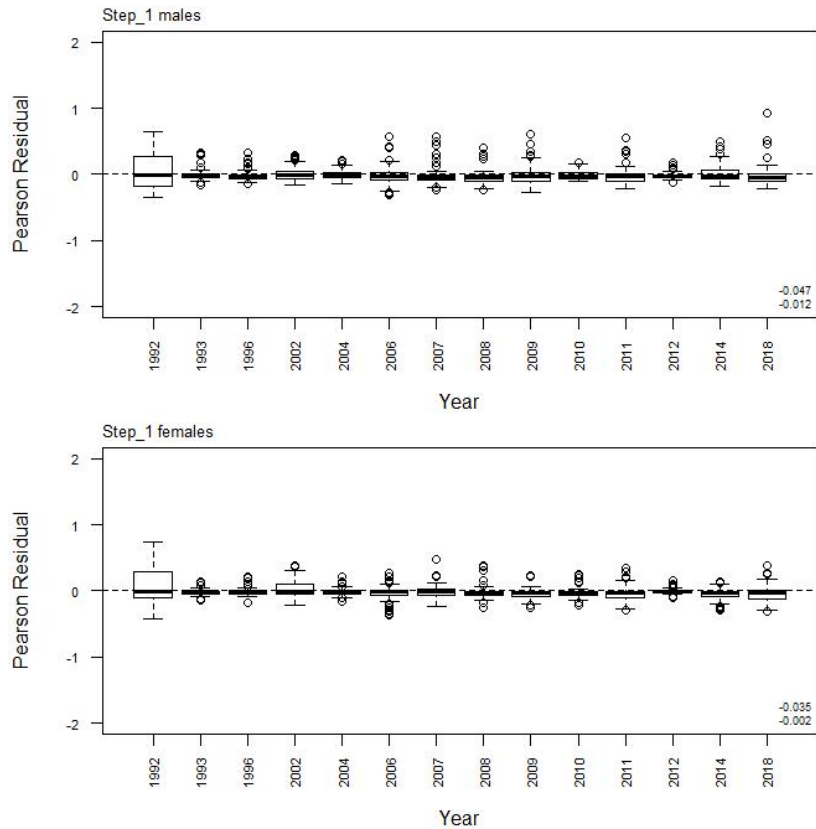
A8. 5: Observed (solid line) and fitted (dashed line) length frequency distributions from observer samples, time step 1 for SCI 1 M025CV25 model. Numbers in top left corner of each plot represent number of scampi measured / number of events sampled.



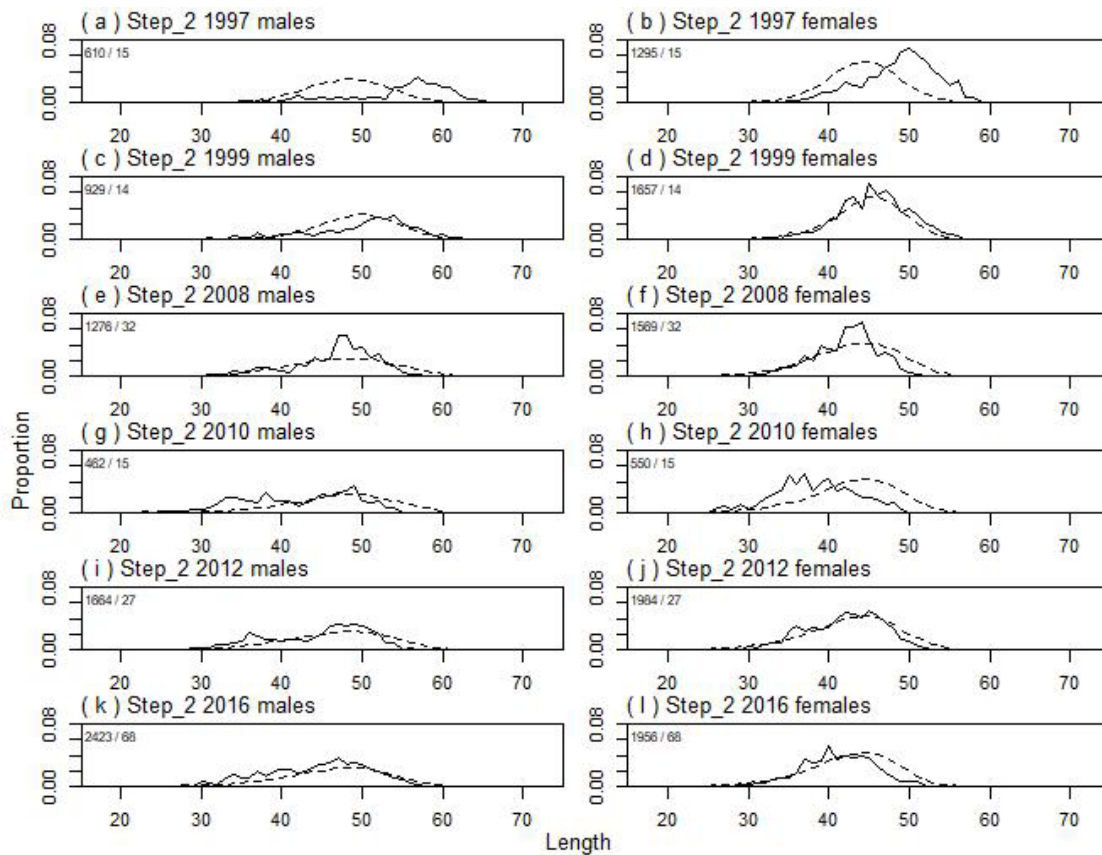
A8. 5(continued): Observed (solid line) and fitted (dashed line) length frequency distributions from observer samples, time step 1 for SCI 1 M025CV25 model. Numbers in top left corner of each plot represent number of scampi measured / number of events sampled.



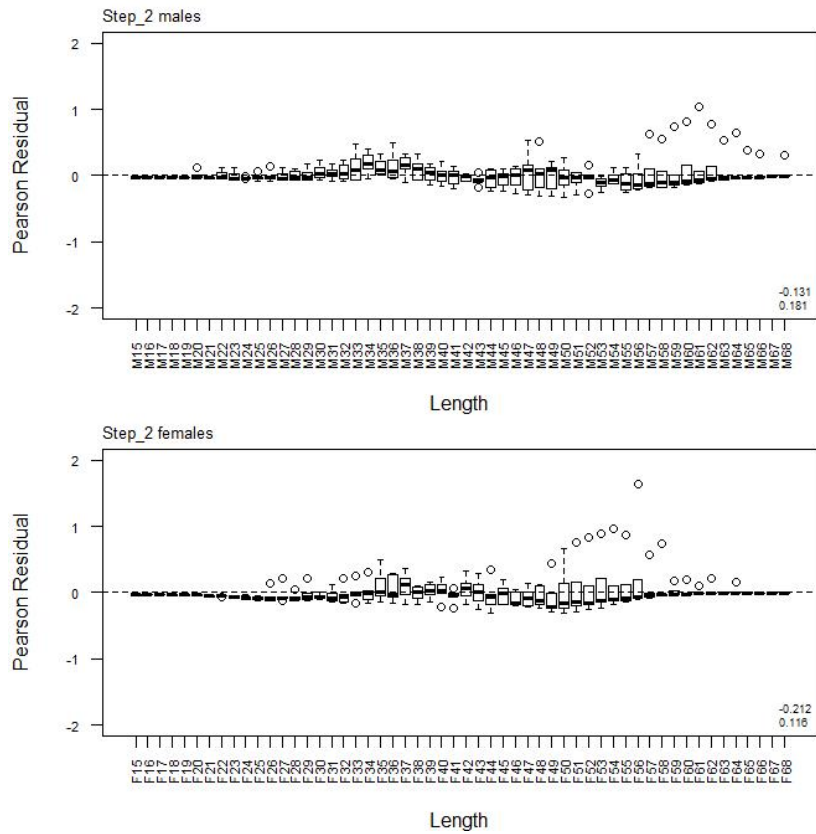
A8. 6: Box plots of Pearson residuals from the fit to length frequency distributions by length from observer sampling by sex for time step 1 for SCI 1 M025CV25 model.



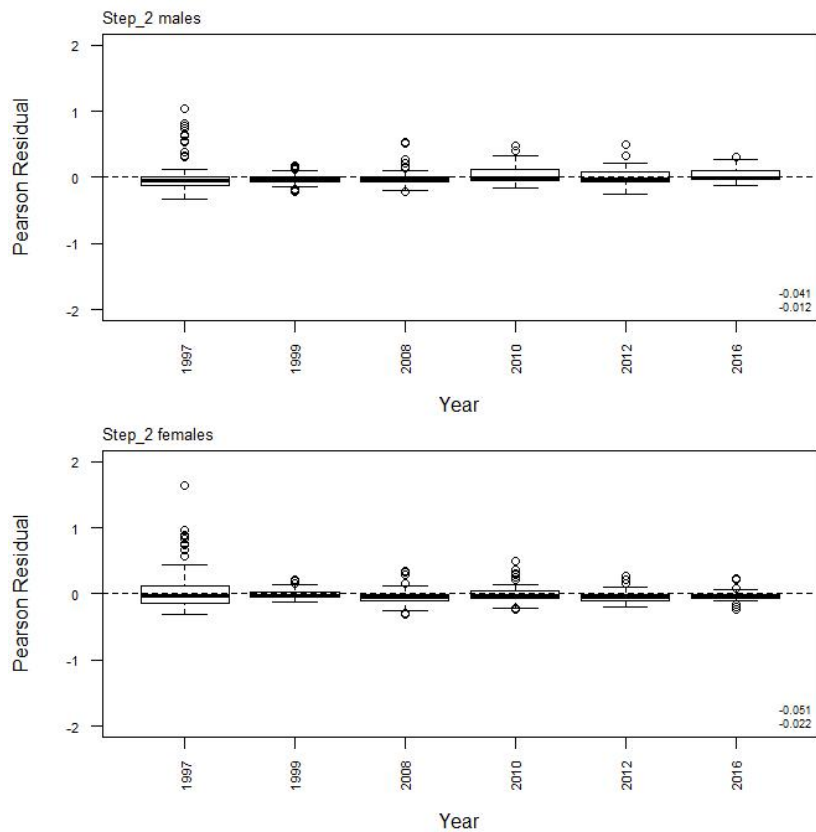
A8. 7: Box plots of Pearson residuals from the fit to length frequency distributions by year from observer sampling by sex for time step 1 for SCI 1 M025CV25 model.



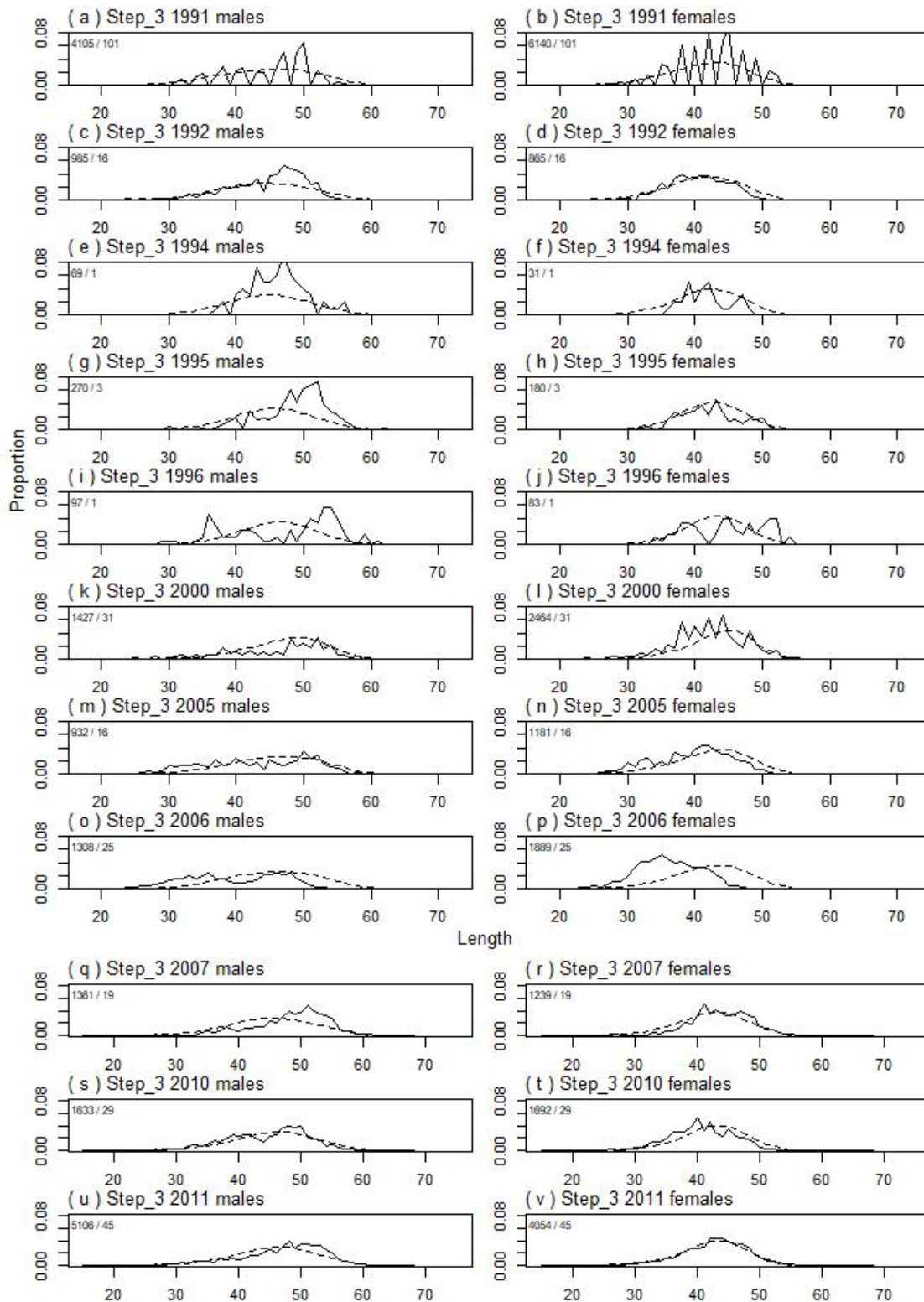
A8. 8: Observed (solid line) and fitted (dashed line) length frequency distributions from observer samples, time step 2 for SCI 1 M025CV25 model. Numbers in top left corner of each plot represent number of samplings measured / number of events sampled.



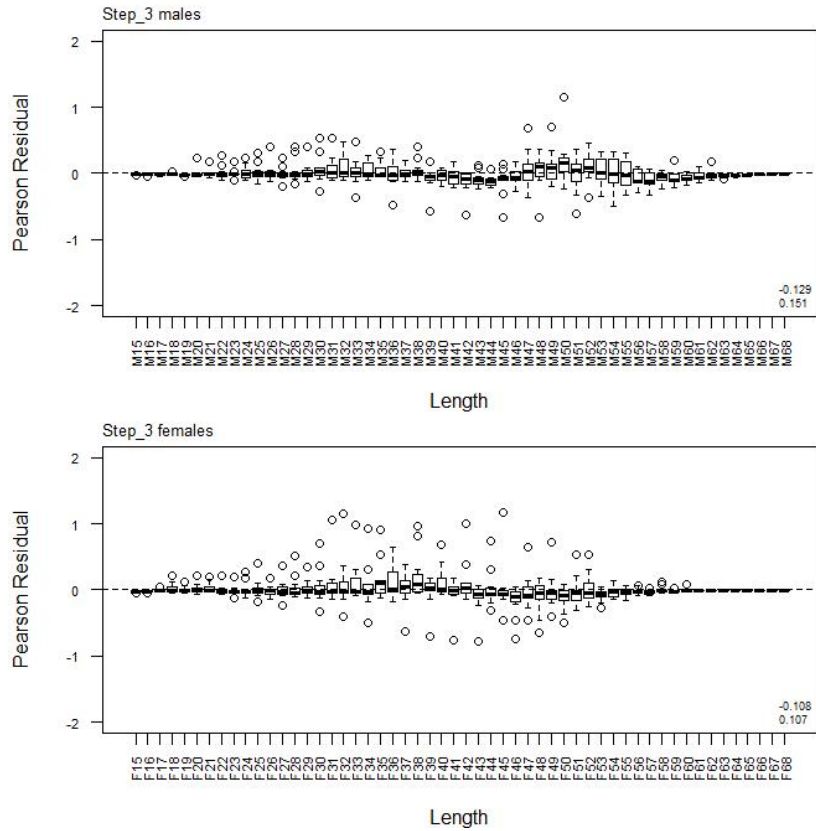
A8. 9: Box plots of Pearson residuals from the fit to length frequency distributions by length from observer sampling by sex for time step 2 for SCI 1 M025CV25 model.



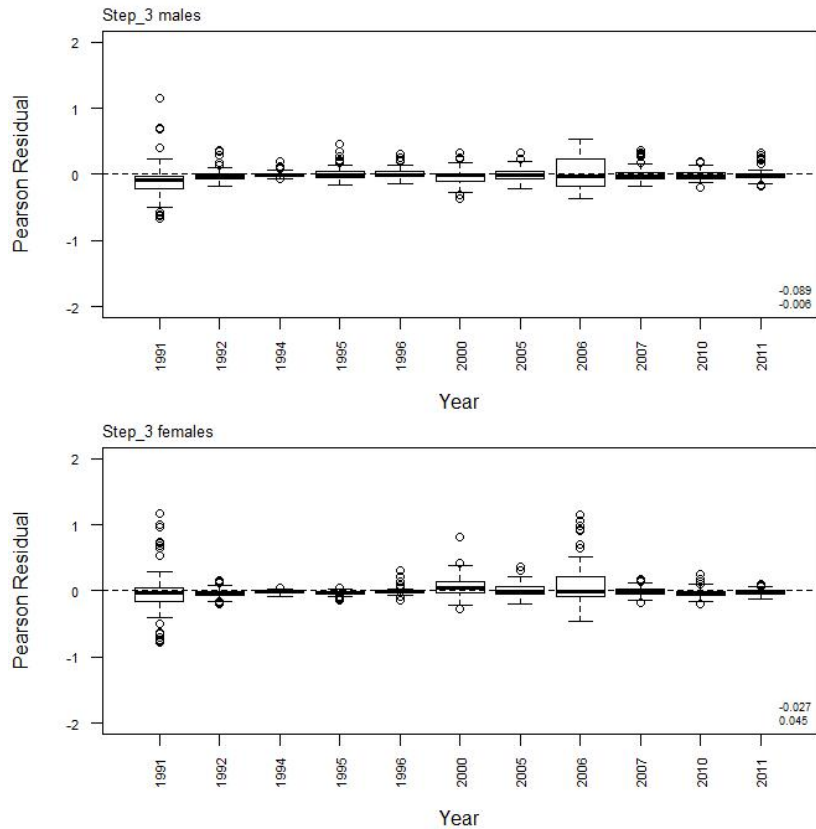
A8. 10: Box plots of Pearson residuals from the fit to length frequency distributions by year from observer sampling by sex for time step 2 for SCI 1 M025CV25 model.



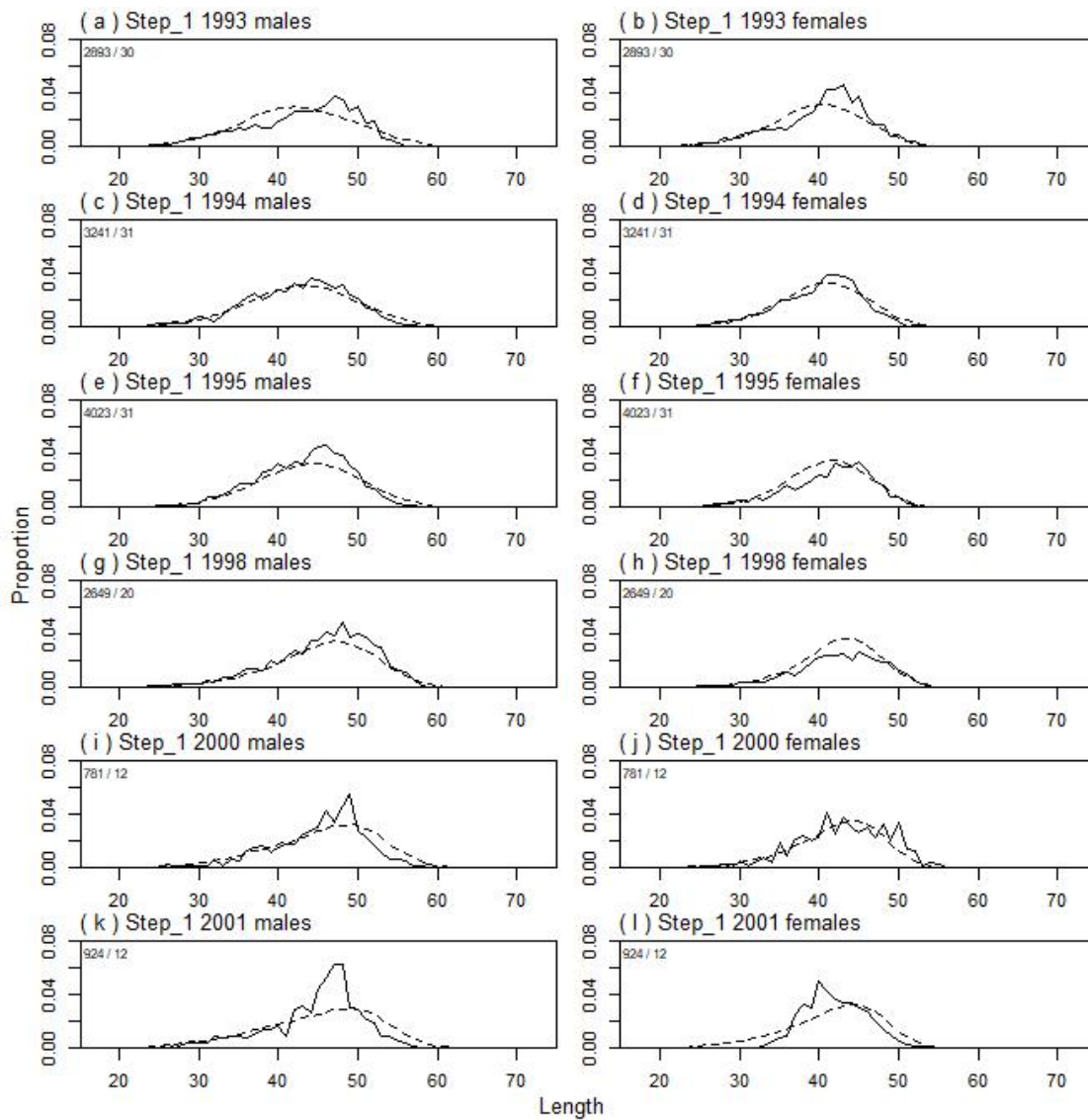
A8. 11: Observed (solid line) and fitted (dashed line) length frequency distributions from observer samples, time step 3 for SCI 1 M025CV25 model. Numbers in top left corner of each plot represent number of scampi measured / number of events sampled.



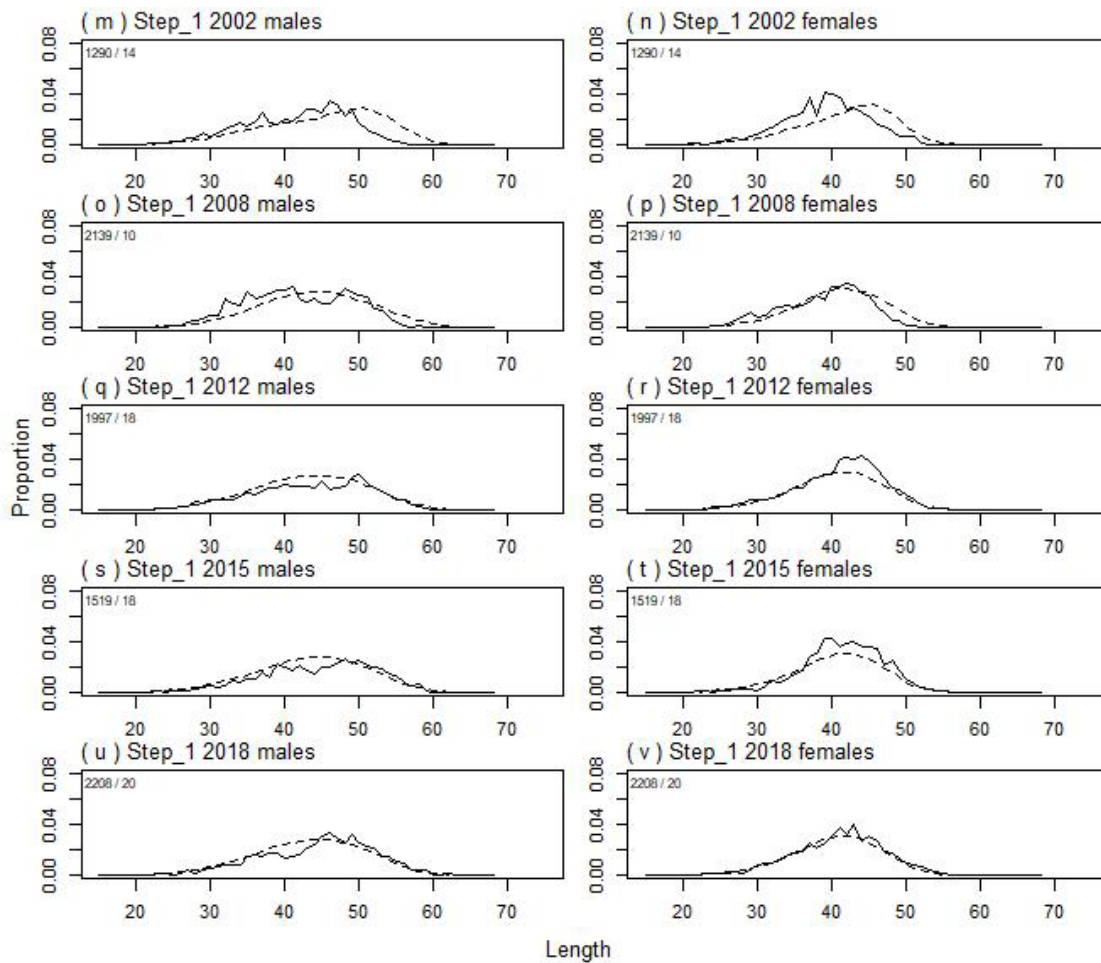
A8. 12: Box plots of Pearson residuals from the fit to length frequency distributions by length from observer sampling by sex for time step 3 for SCI 1 M025CV25 model.



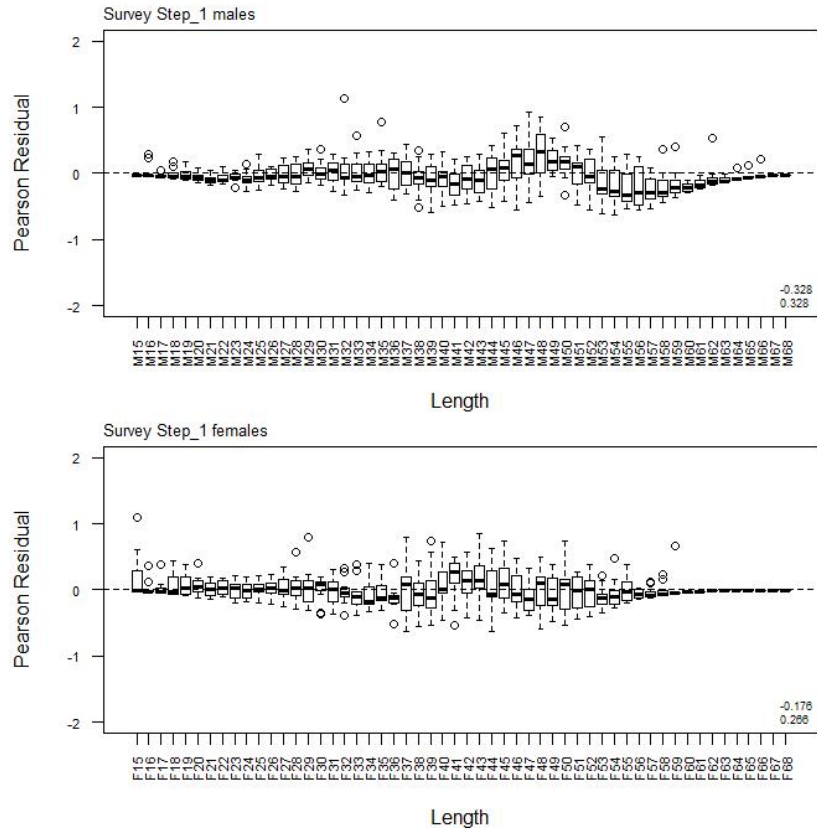
A8. 13: Box plots of Pearson residuals from the fit to length frequency distributions by year from observer sampling by sex for time step 3 for SCI 1 M025CV25 model.



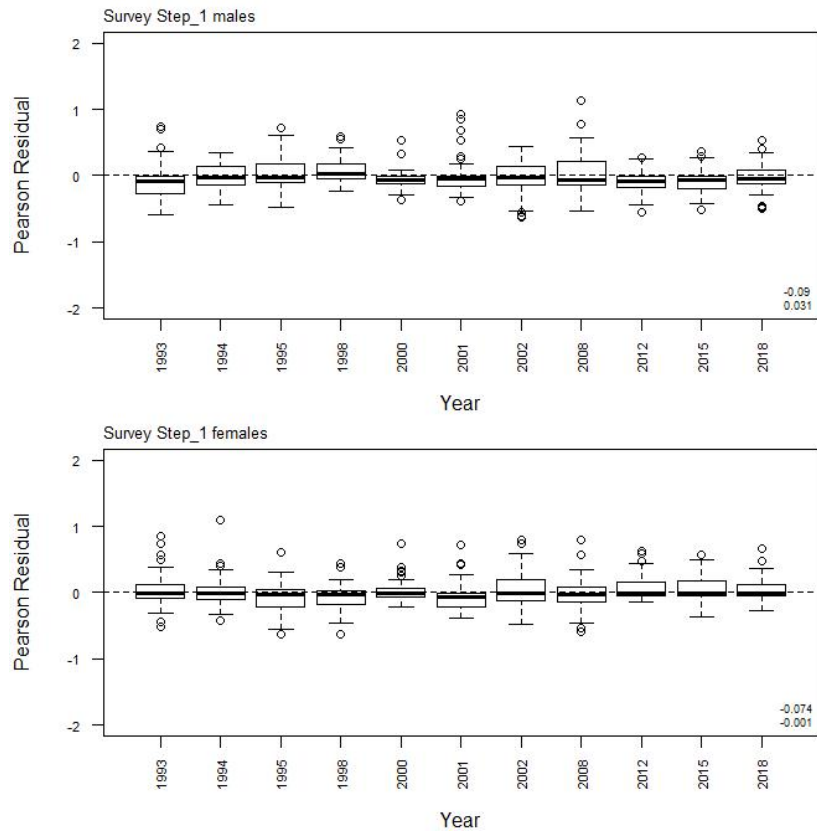
A8. 14: Observed (solid line) and fitted (dashed line) length frequency distributions from trawl samples for SCI 1 M025CV25 model. Numbers in top left corner of each plot represent number of scampi measured / number of events sampled.



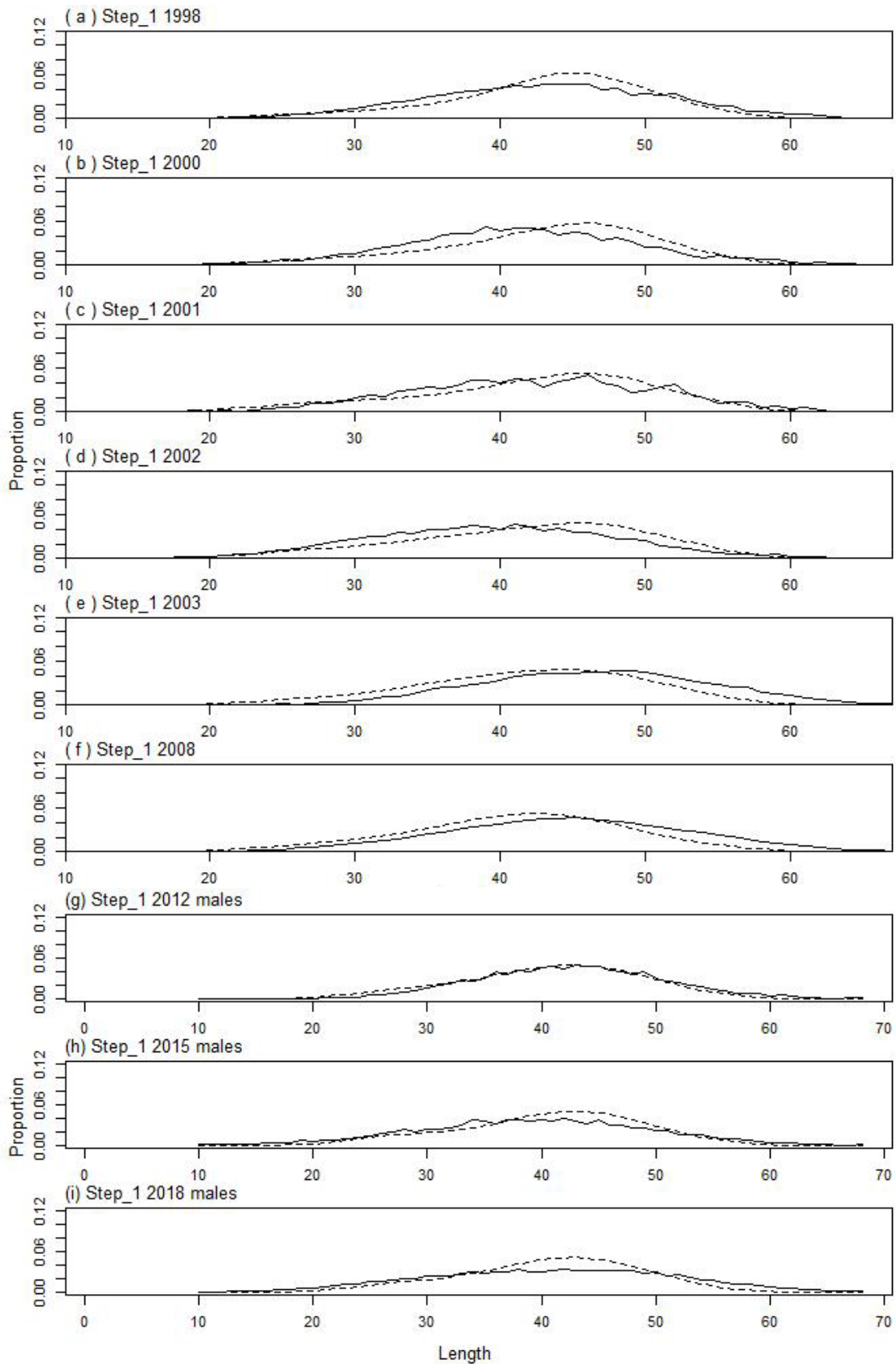
A8. 14(continued): Observed (solid line) and fitted (dashed line) length frequency distributions from trawl samples for SCI 1 M025CV25 model. Numbers in top left corner of each plot represent number of scampi measured / number of events sampled.



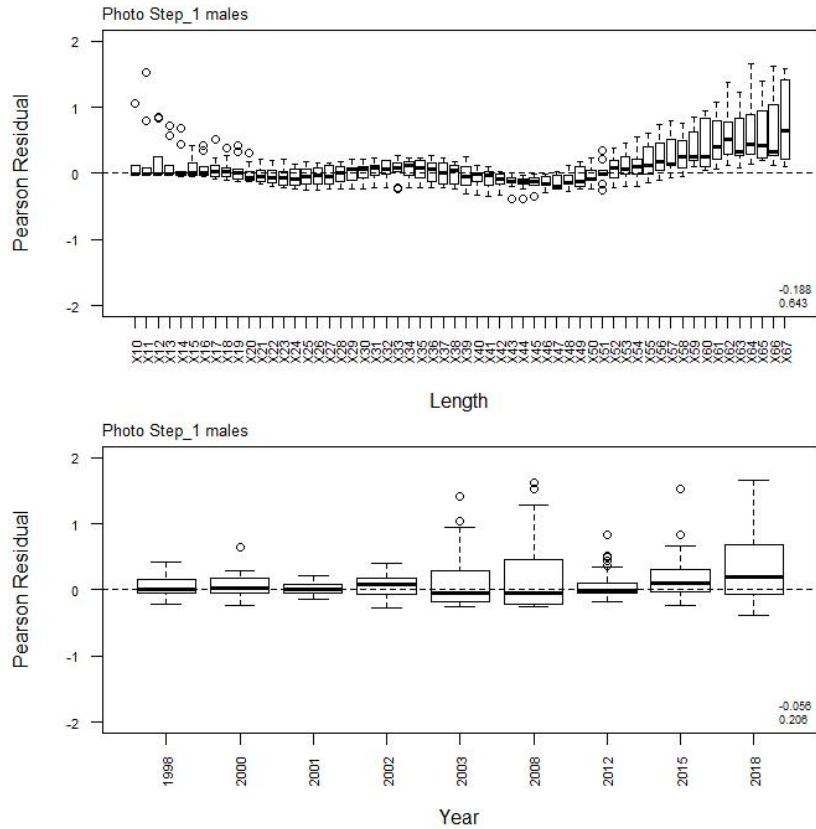
A8. 15: Box plots of Pearson residuals from the fit to length frequency distributions by length from trawl survey sampling by sex for SCI 1 M025CV25 model.



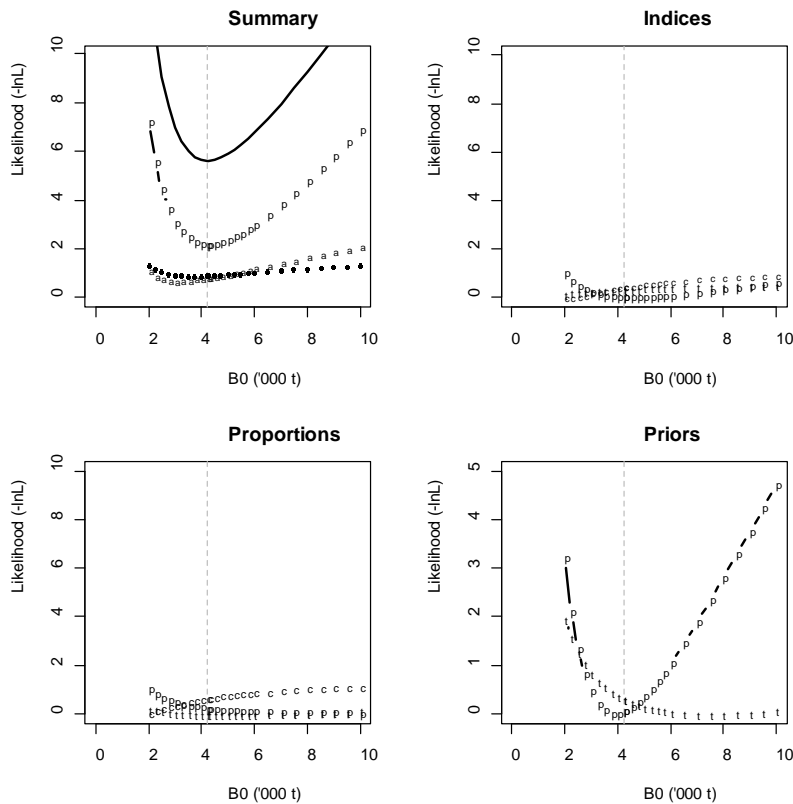
A8. 16: Box plots of Pearson residuals from the fit to length frequency distributions by year from trawl survey sampling by sex for SCI 1 M025CV25 model.



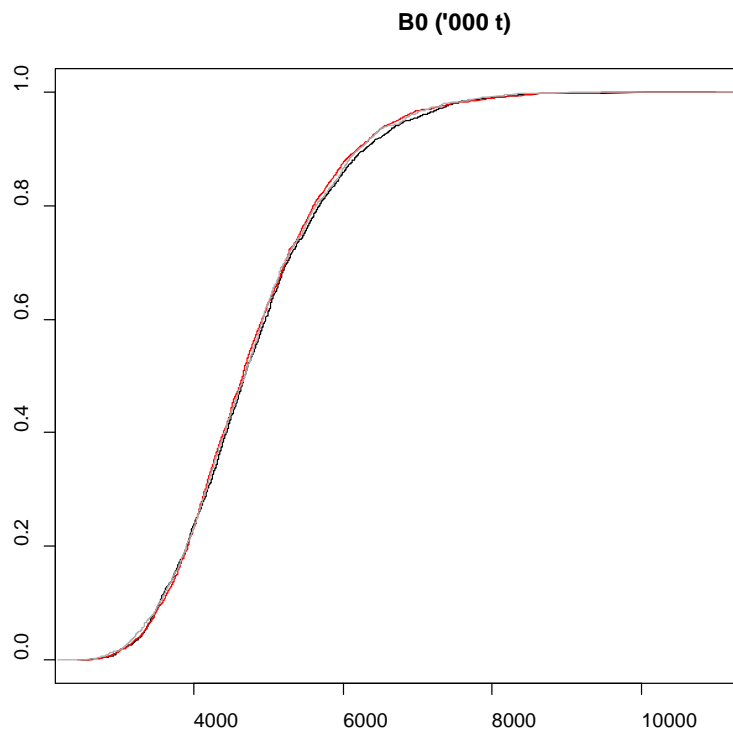
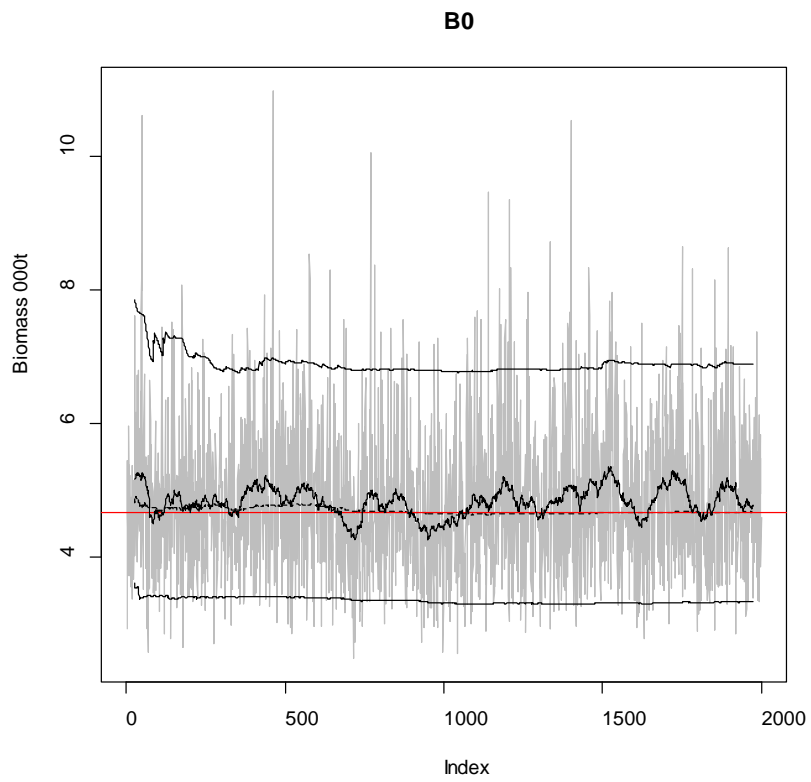
A8. 17: Observed (solid line) and fitted (dashed line) length frequency distributions from photo survey samples for SCI 1 M025CV25 model.



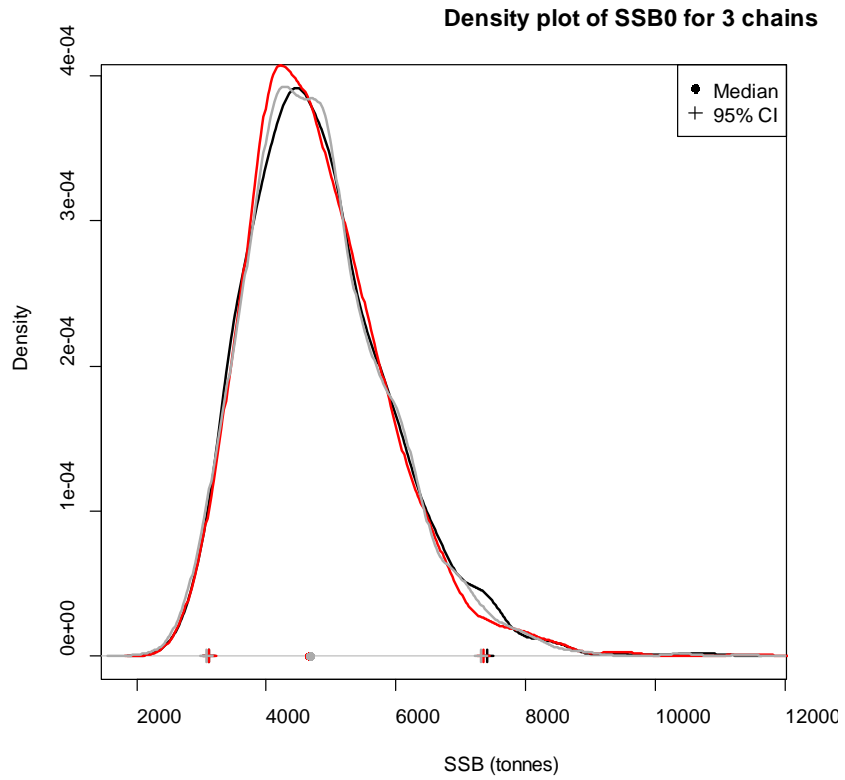
A8. 18: Box plots of Pearson residuals from the fit to length frequency distributions by length (top plot) and year (bottom plot) from photo survey sampling by sex for SCI 1 M025CV25 model.



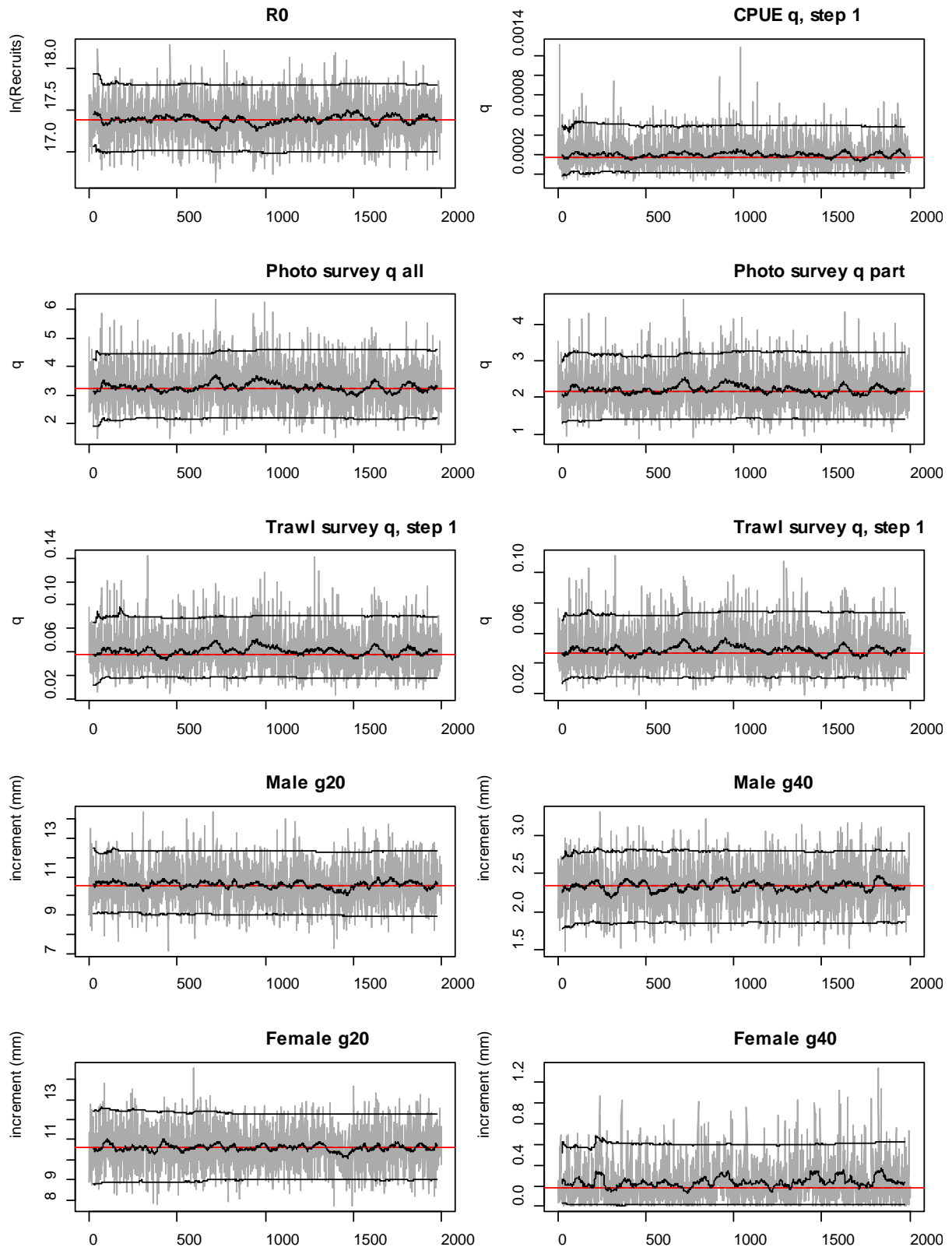
A8. 19: Likelihood profiles for model M025CV25 for SCI 1 when B_0 is fixed in the model. Figures show profiles for main priors (top left, p – priors, a – abundance indices, • – proportions at length), abundance indices (top right, t – trawl survey step, c – CPUE, p – photo survey), proportion at length data (bottom left, p – photo, t – trawl, 1 – observer) and priors (bottom right, p – q-Photo, t – q-Trawl).



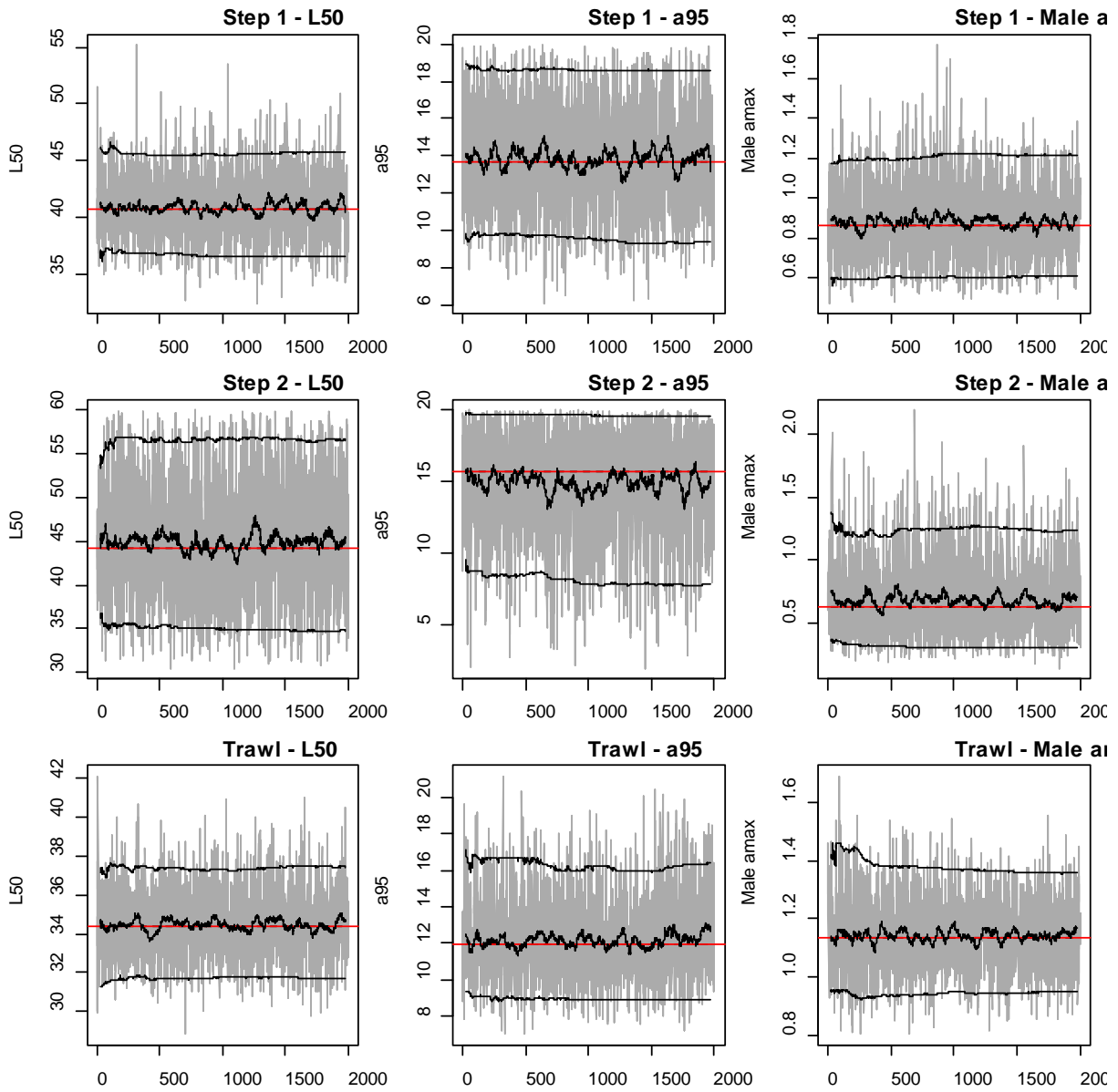
A8. 20: MCMC traces for B_0 and cumulative frequency distributions for three independent MCMC chains for the SCI 1 M025CV25 model.



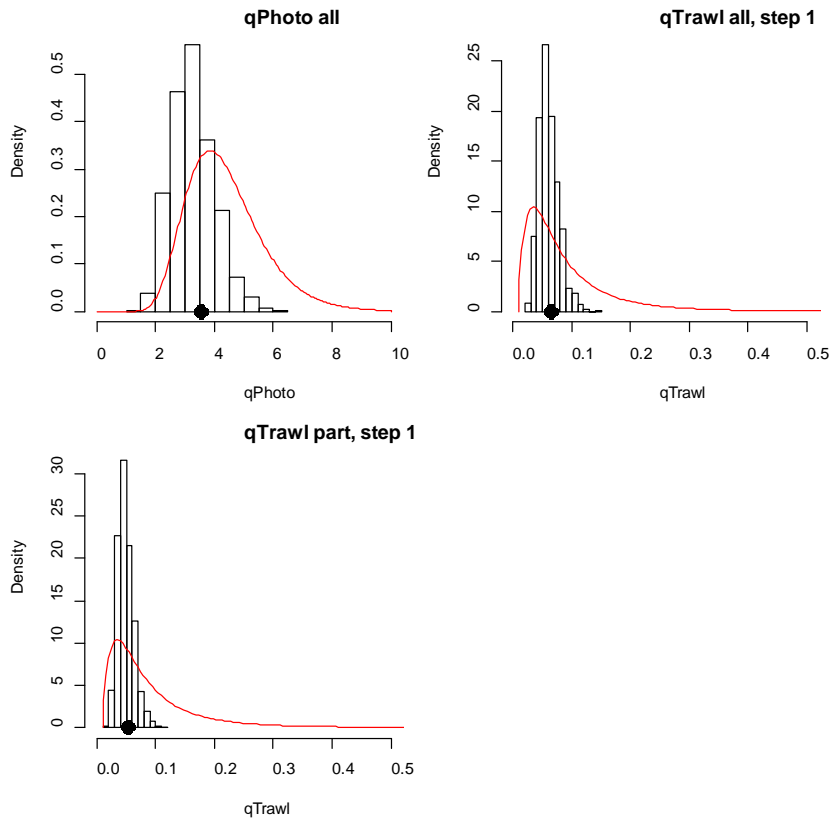
A8. 21: Density plots for B_0 for the SCI 1 M025CV25 model for three independent MCMC chains, with median and 95% confidence intervals.



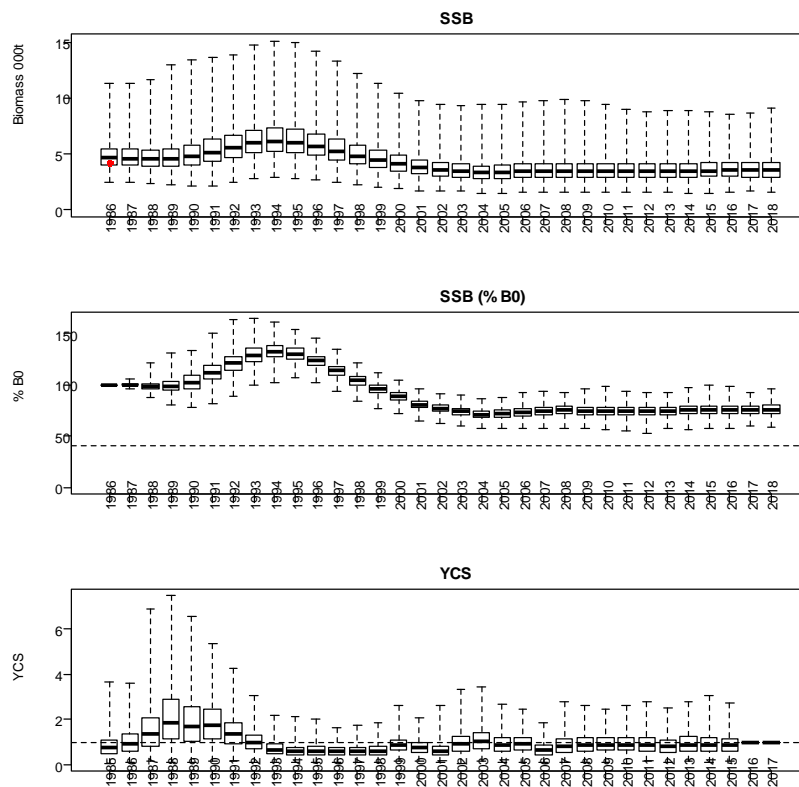
A8. 22: MCMC traces for R_0 , catchability, and growth terms for the SCI 1 M025CV25 model.



A8. 23: MCMC traces for selectivity terms for the SCI 1 M025CV25 model.

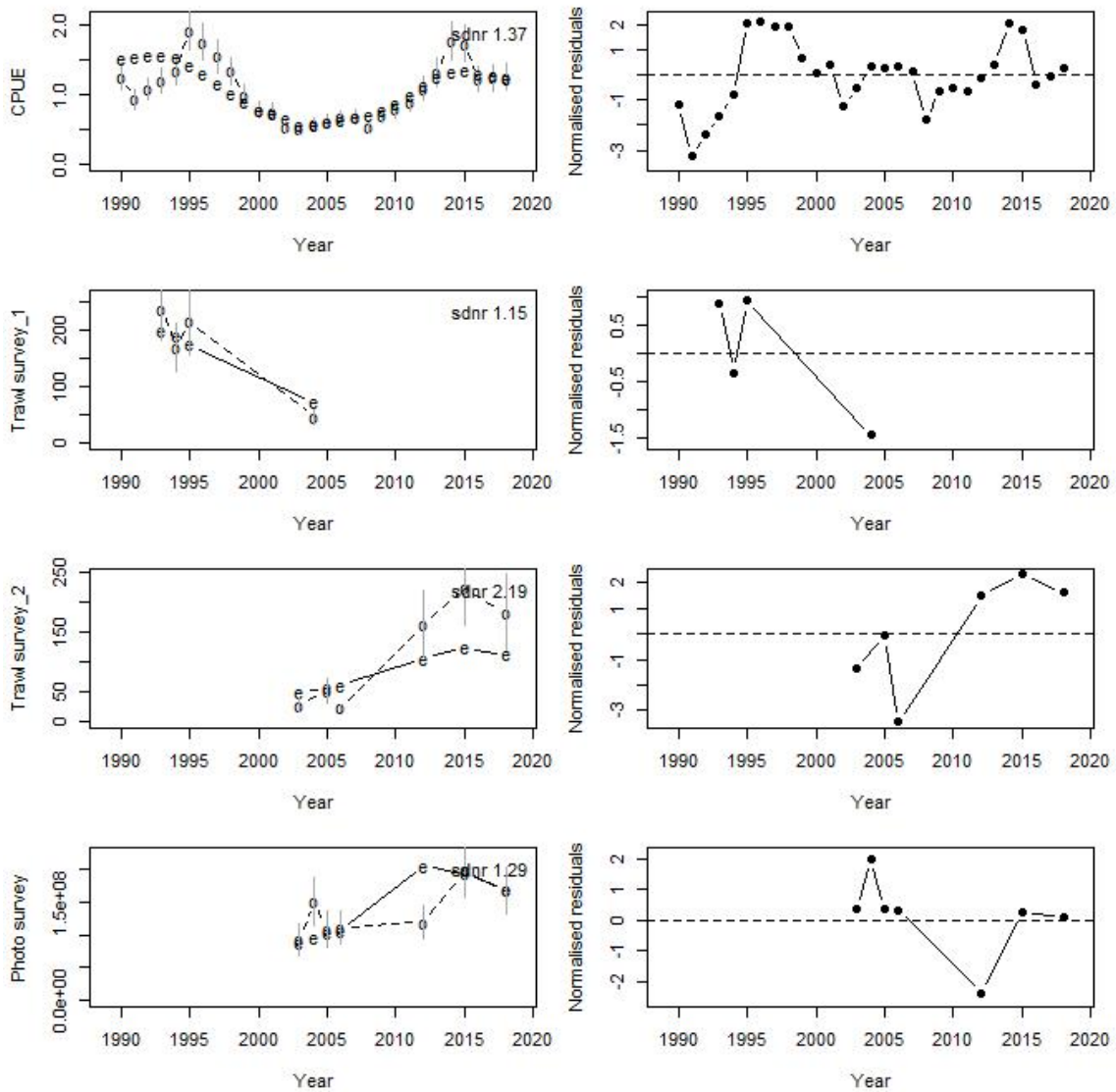


A8. 24: Marginal posterior distributions (histograms), MPD estimates (solid symbols), and distributions of priors (lines) for catchability terms for the SCI 1 M025CV25 model.

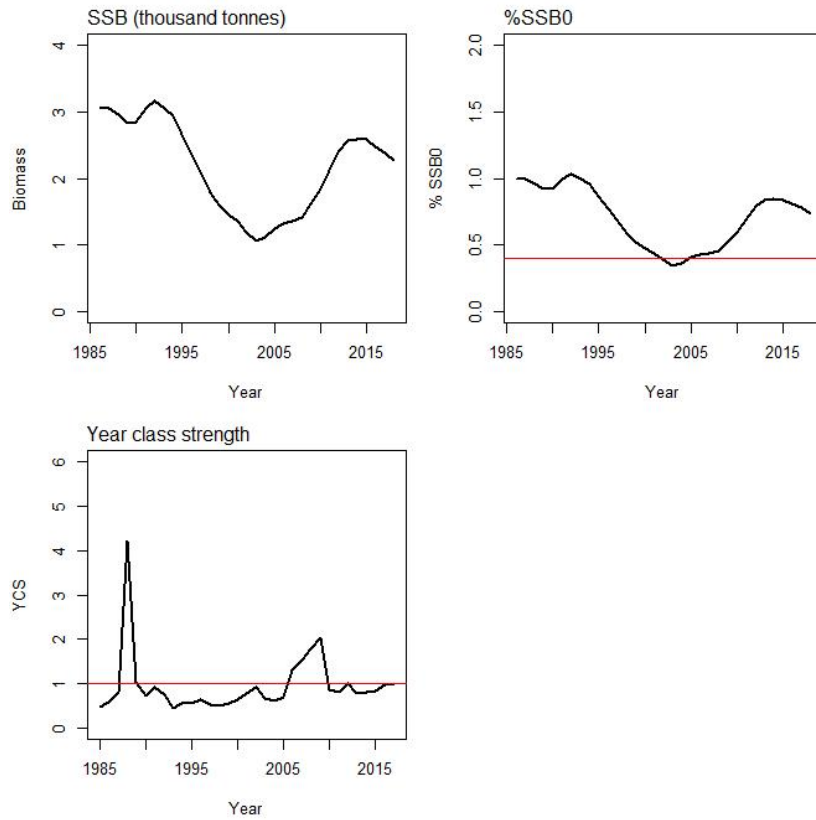


A8. 25: Posterior trajectory of SSB, SSB/SSB₀, and YCS for the SCI 1 M025CV25 model. Red dot represents MPD estimate of B₀.

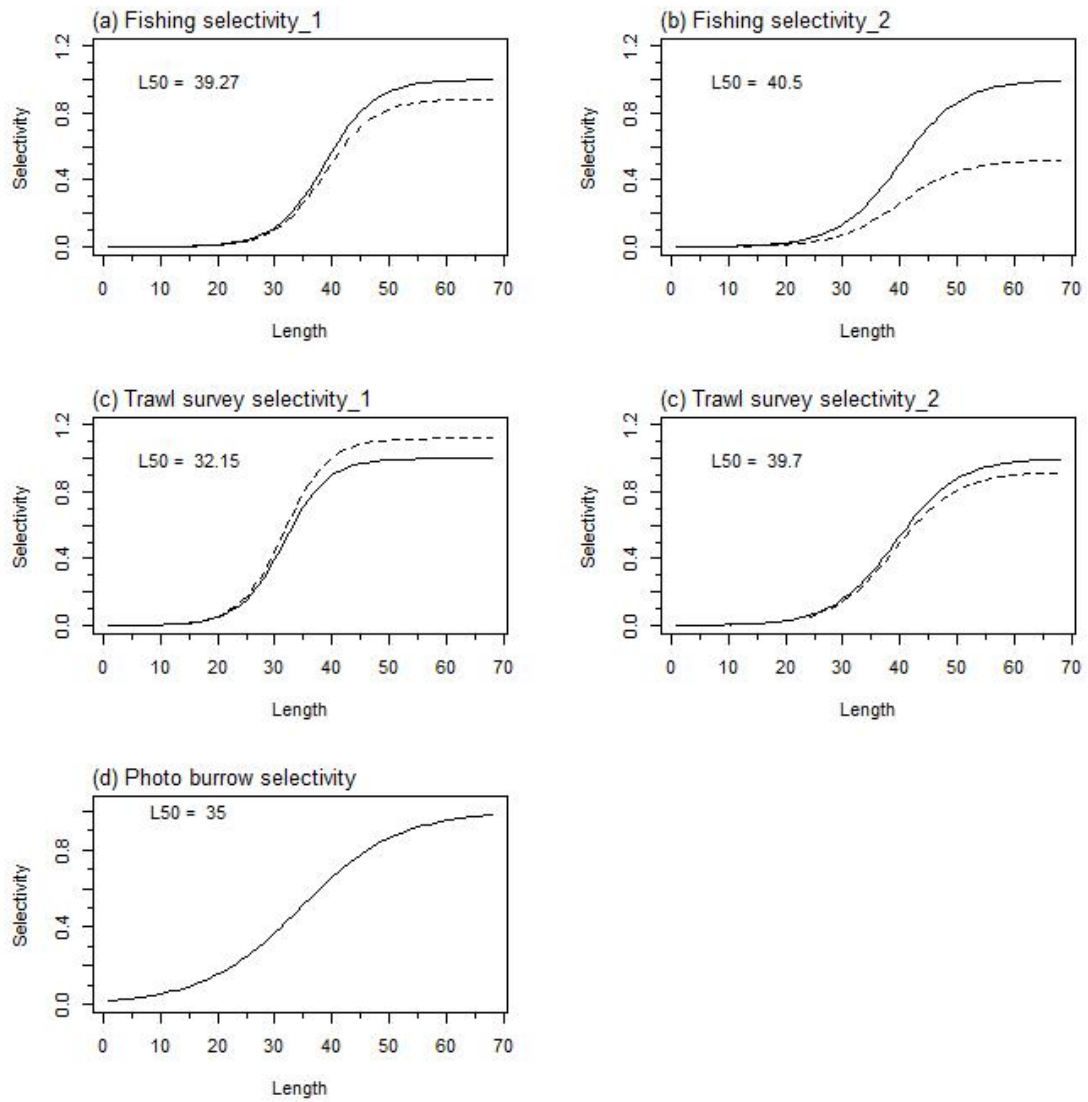
APPENDIX 9. SCI 2 M02CV15 model plots ($M=0.2$, $CV=0.15$)



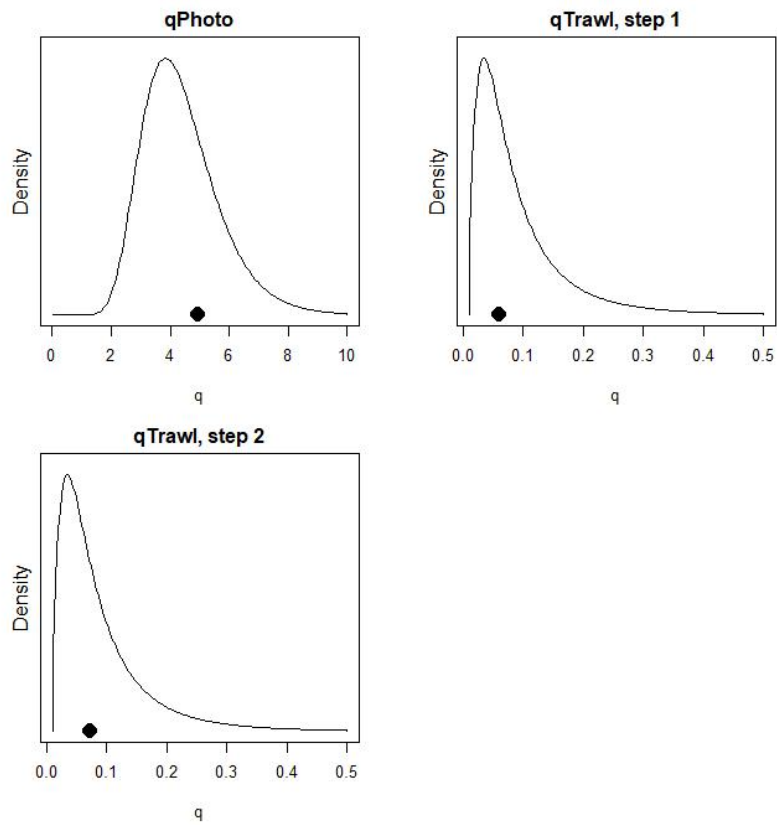
A9. 1: Fits to abundance indices (left column) and normalised residuals (right column) for standardised CPUE index (top row) trawl survey biomass index time step 1 (second row), trawl survey biomass index time step 2 (third row), and photo survey abundance index (fourth row) for the SCI 2 M02CV15 model.



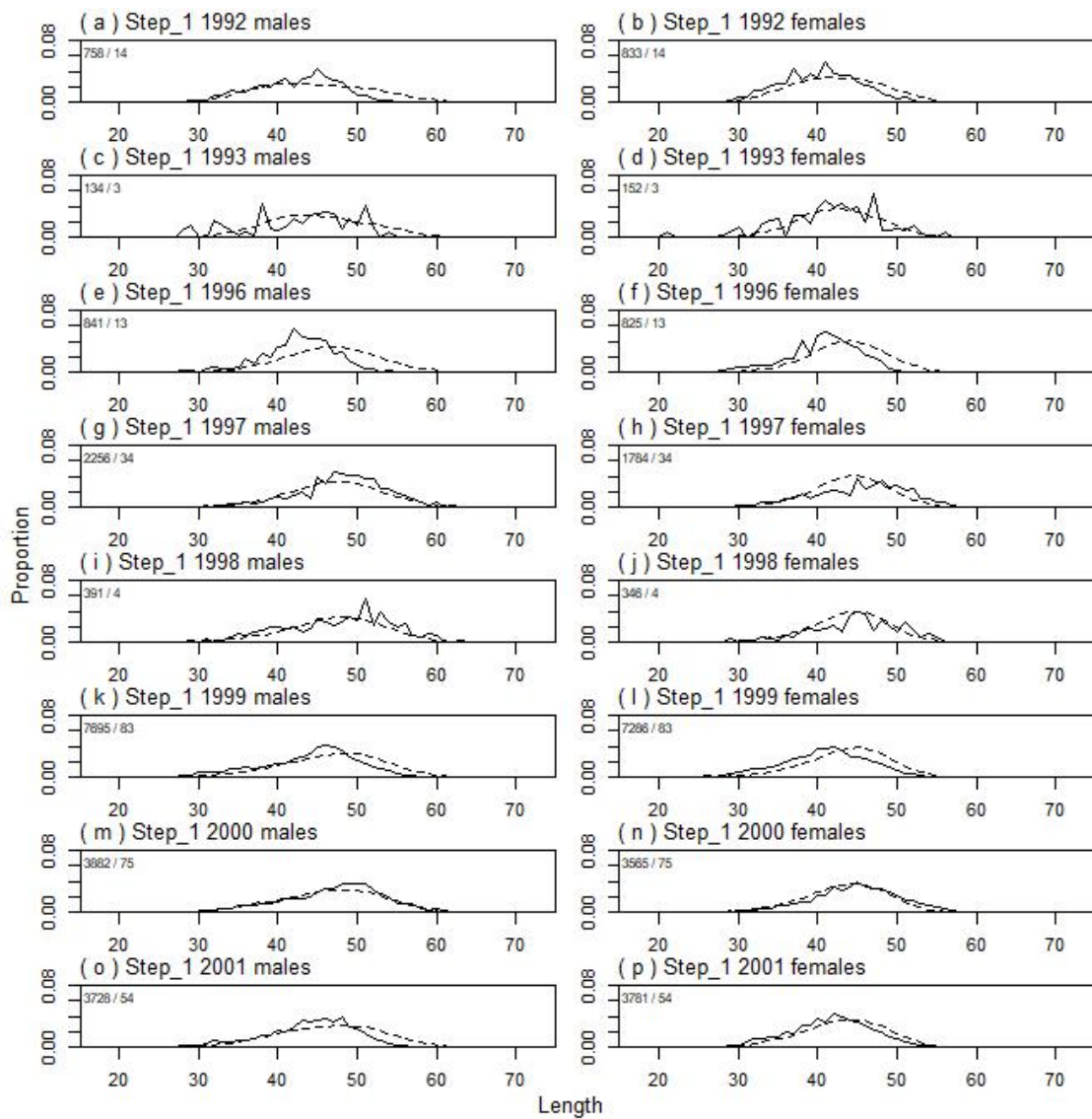
A9. 2: Spawning stock biomass trajectory (upper left), stock status (upper right), and year class strength (lower left) for the SCI 2 M02CV15 model.



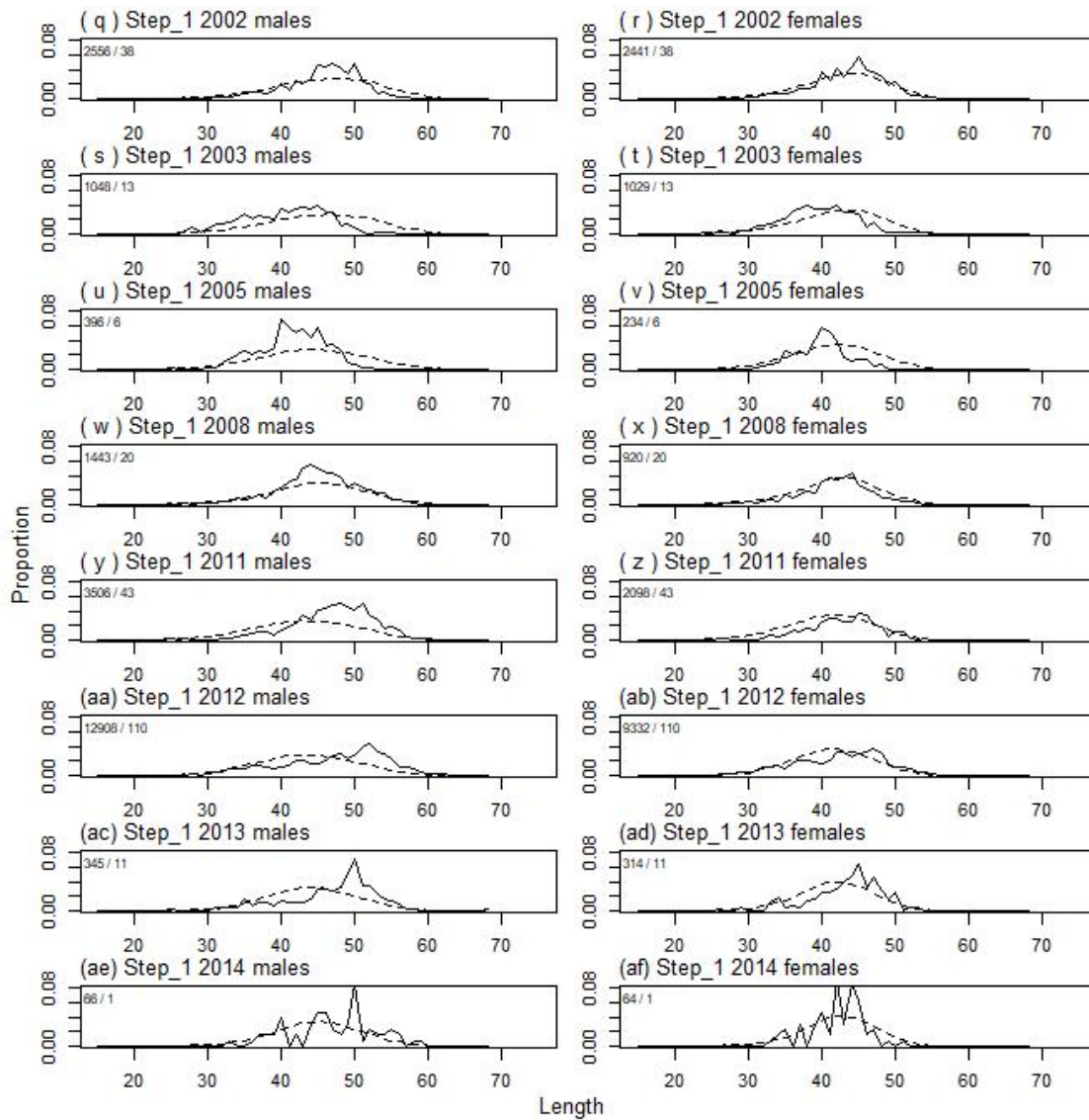
A9. 3: Fishery and survey selectivity curves for the SCI 2 M02CV15 model. Solid line – females, dotted line – males. The scampi burrow index is not sexed, and a single selectivity applies.



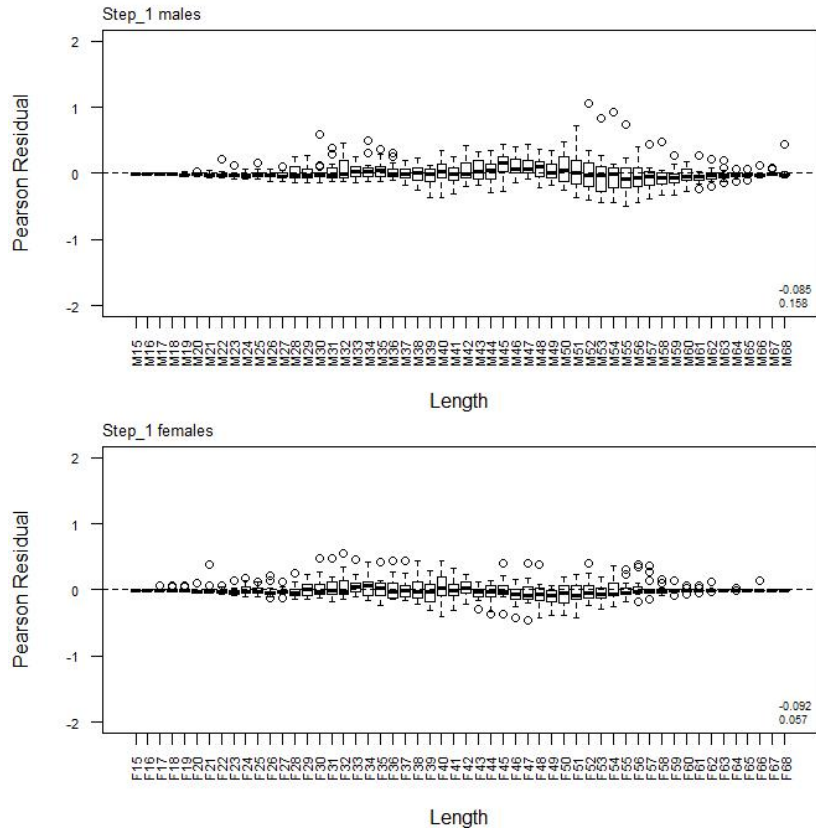
A9. 4: Catchability estimates from MPD model run, plotted in relation to prior distribution for the SCI 2 M02CV15 model.



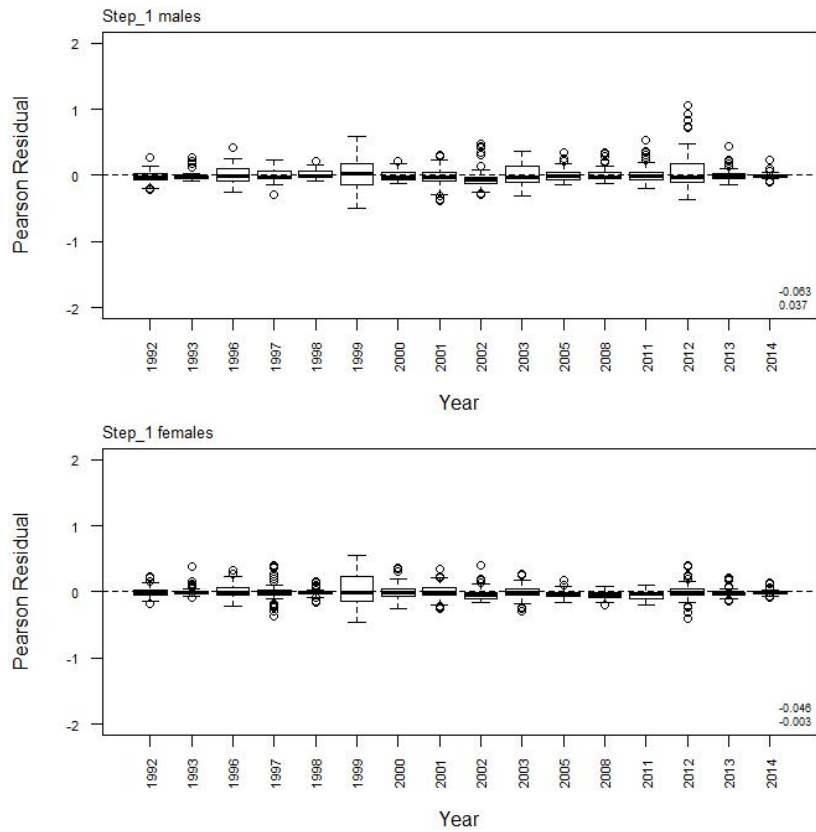
A9. 5: Observed (solid line) and fitted (dashed line) length frequency distributions from observer samples, time step 1 for SCI 2 M02CV15 model. Numbers in top left corner of each plot represent number of scampi measured / number of events sampled.



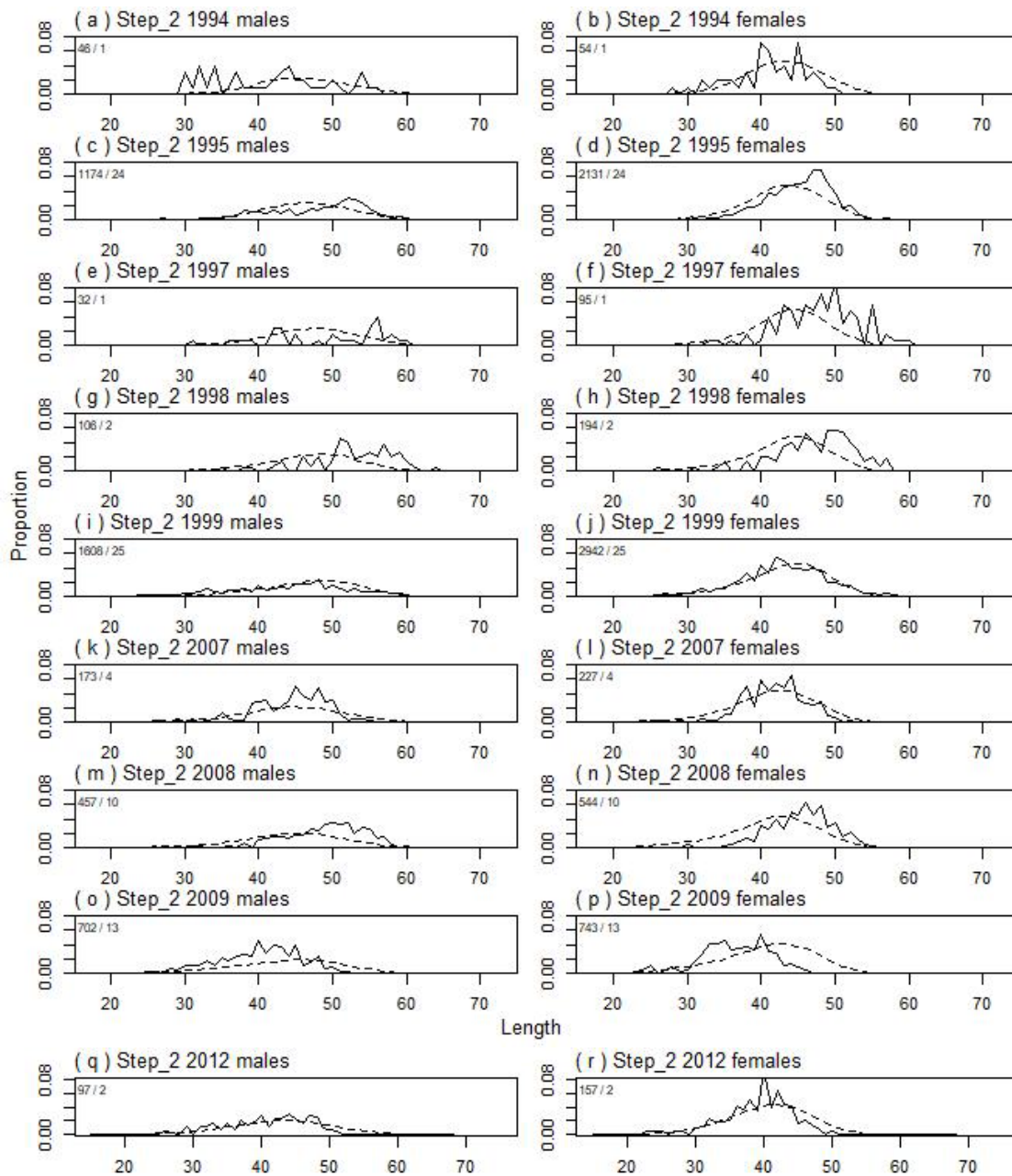
A9. 5(continued): Observed (solid line) and fitted (dashed line) length frequency distributions from observer samples, time step 1 for SCI 2 M02CV15 model. Numbers in top left corner of each plot represent number of scampi measured / number of events sampled.



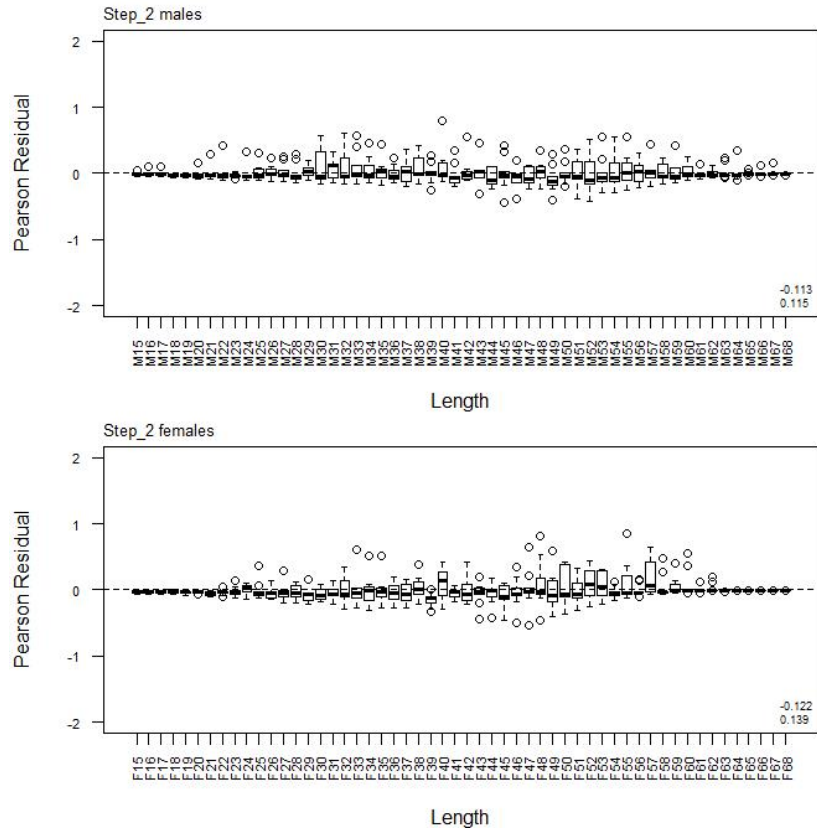
A9. 6: Box plots of Pearson residuals from the fit to length frequency distributions by length from observer sampling by sex for time step 1 for SCI 2 M02CV15 model.



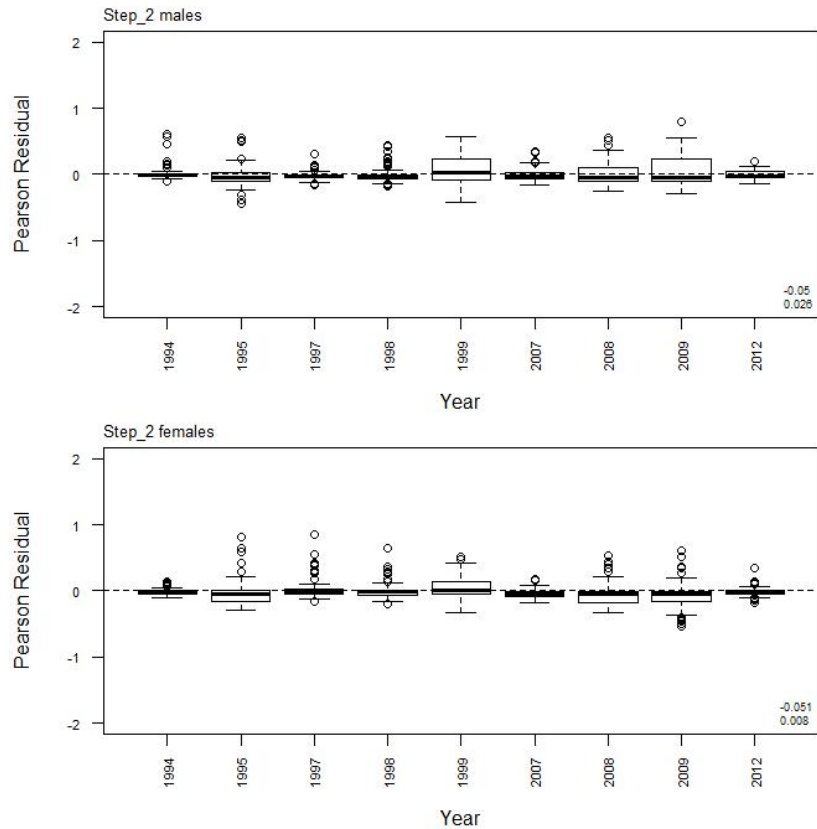
A9. 7: Box plots of Pearson residuals from the fit to length frequency distributions by year from observer sampling by sex for time step 1 for SCI 2 M02CV15 model.



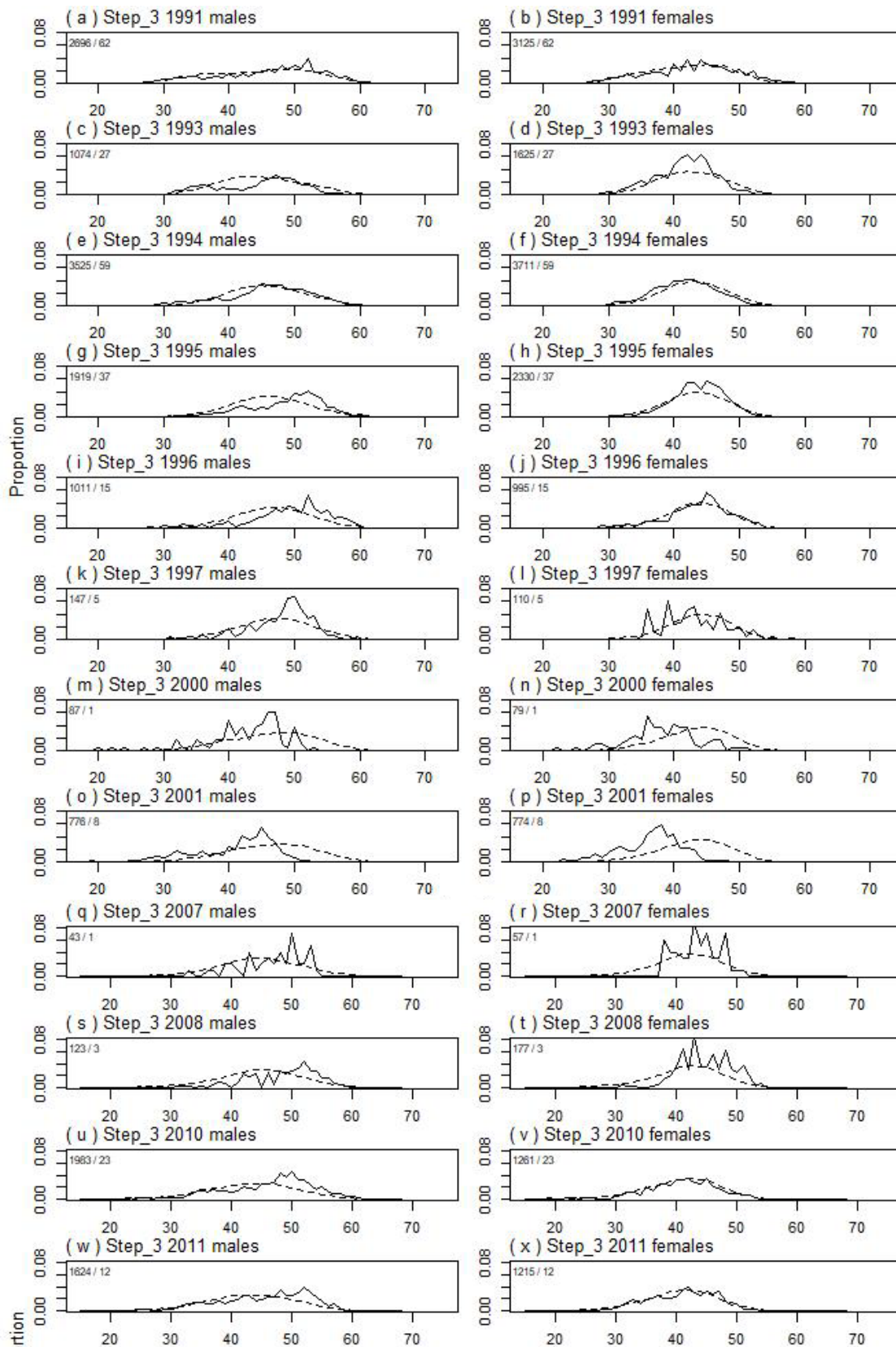
A9. 8: Observed (solid line) and fitted (dashed line) length frequency distributions from observer samples, time step 2 for SCI 2 M02CV15 model. Numbers in top left corner of each plot represent number of scampi measured / number of events sampled.



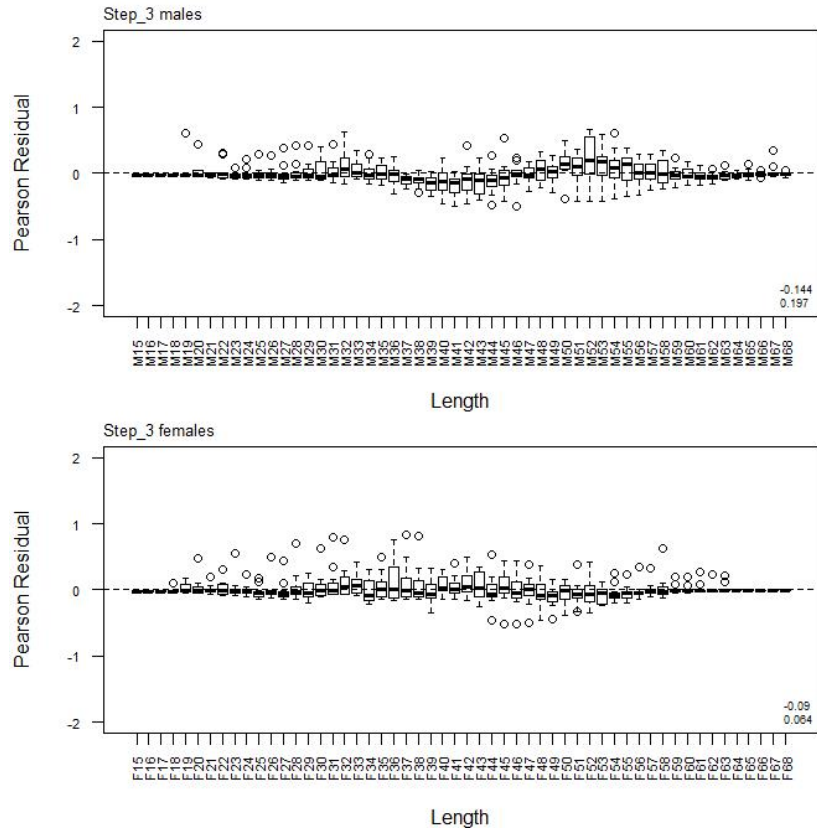
A9. 9: Box plots of Pearson residuals from the fit to length frequency distributions by length from observer sampling by sex for time step 2 for SCI 2 M02CV15 model.



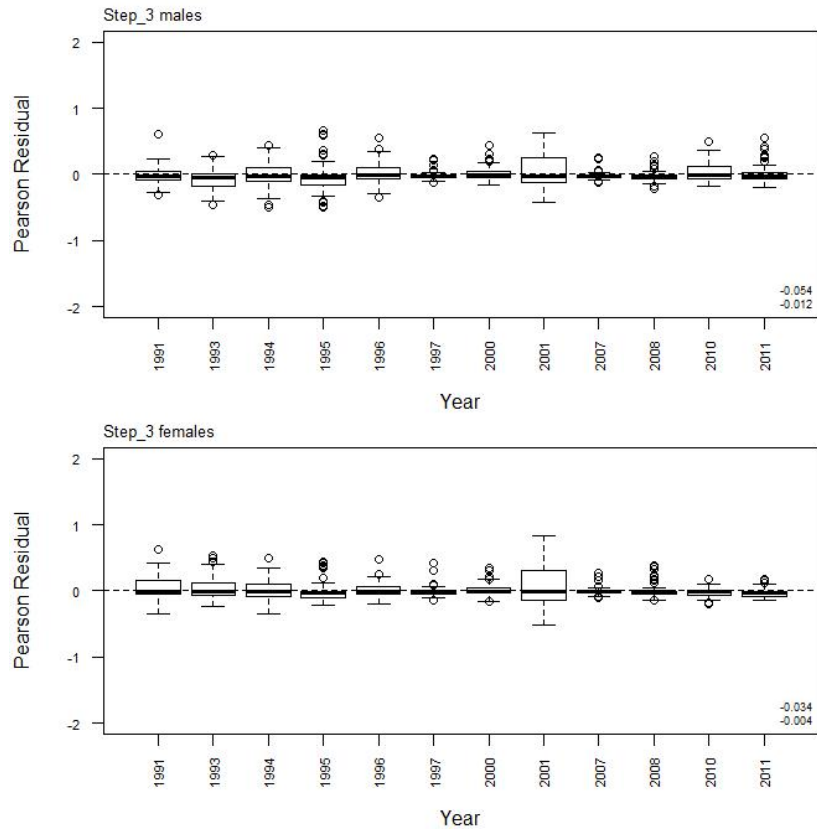
A9. 10: Box plots of Pearson residuals from the fit to length frequency distributions by year from observer sampling by sex for time step 2 for SCI 1 M02CV15 model.



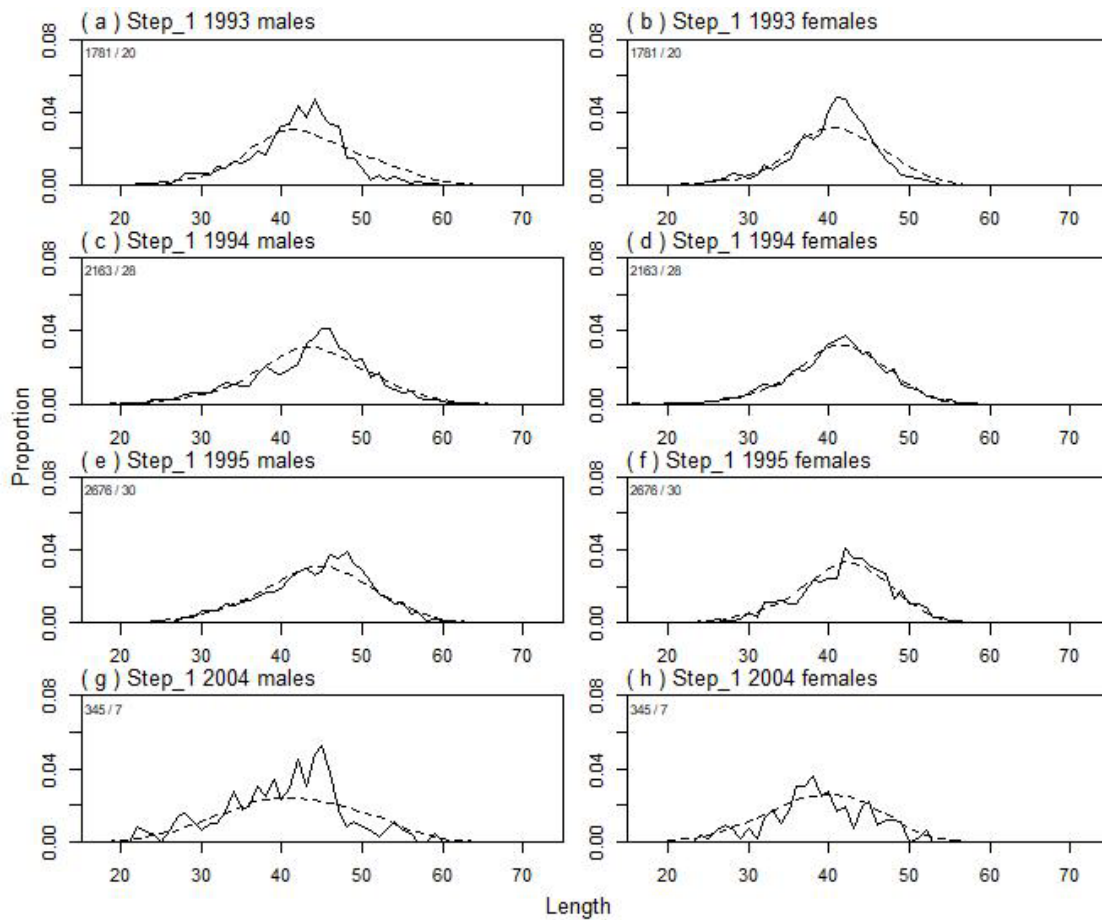
A9. 11: Observed (solid line) and fitted (dashed line) length frequency distributions from observer samples, time step 3 for SCI 2 M02CV15 model. Numbers in top left corner of each plot represent number of scampi measured / number of events sampled.



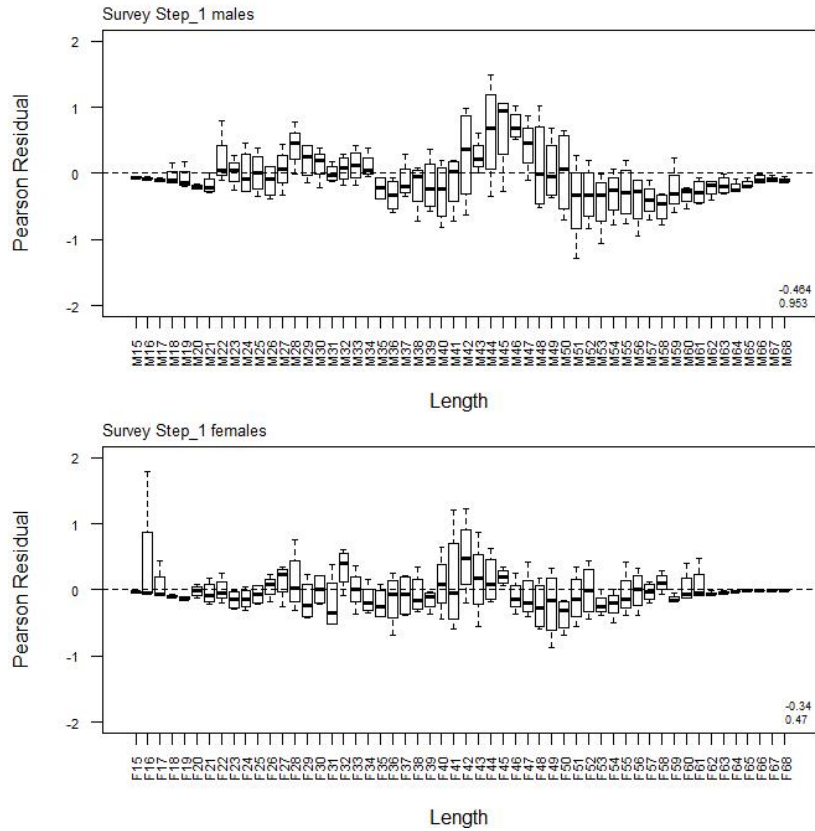
A9. 12: Box plots of Pearson residuals from the fit to length frequency distributions by length from observer sampling by sex for time step 3 for SCI 2 M02CV15 model.



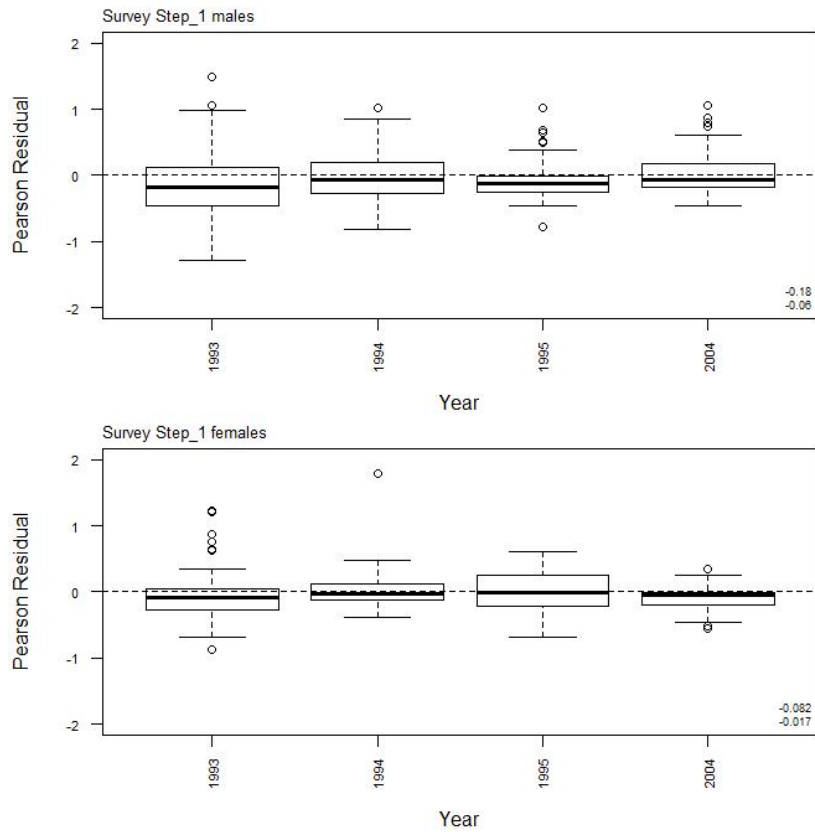
A9. 13: Box plots of Pearson residuals from the fit to length frequency distributions by year from observer sampling by sex for time step 3 for SCI 2 M02CV15 model.



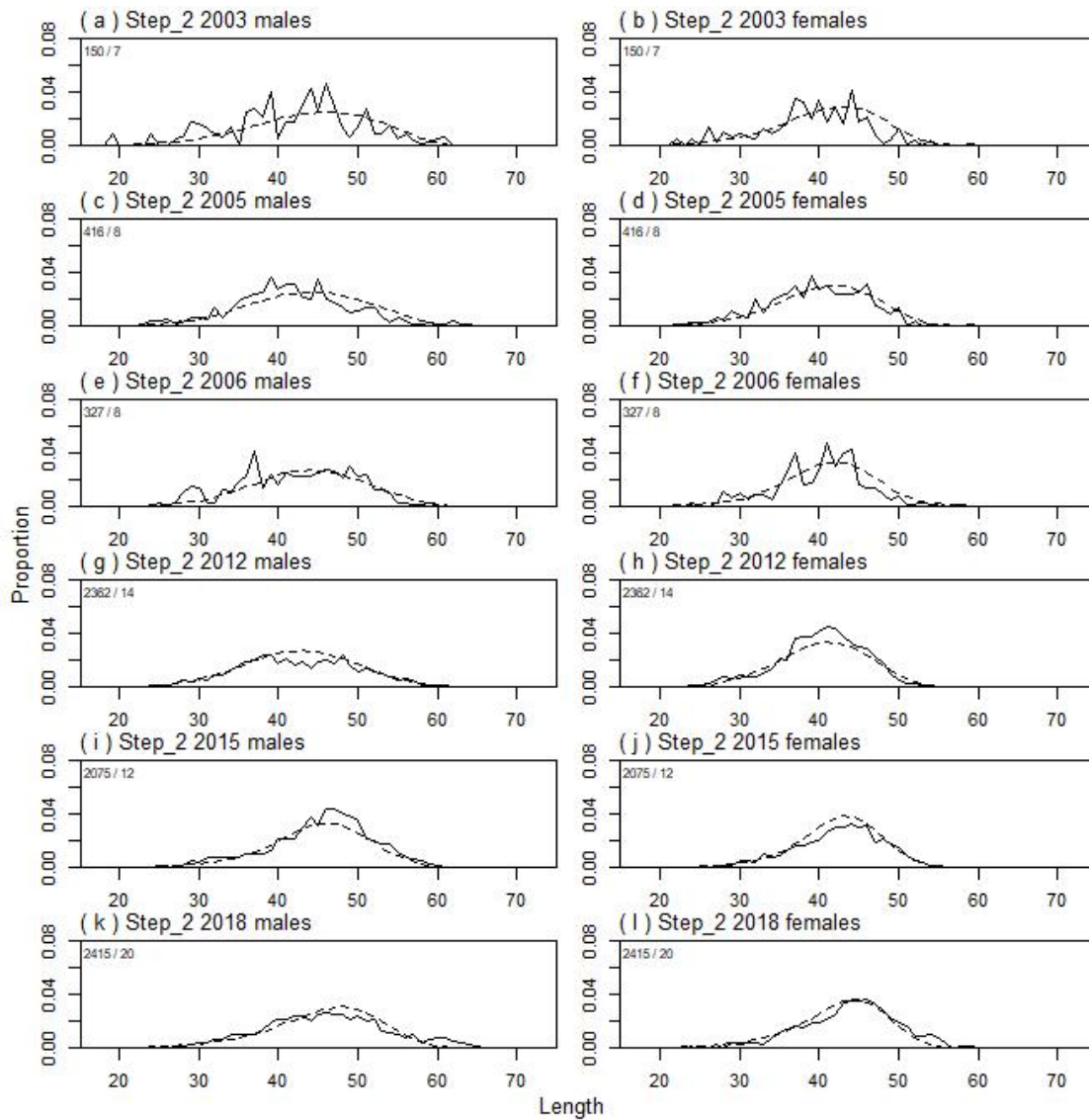
A9. 14: Observed (solid line) and fitted (dashed line) length frequency distributions from trawl survey samples for time step 1, SCI 2 M02CV15 model. Numbers in top left corner of each plot represent number of scampi measured / number of events sampled.



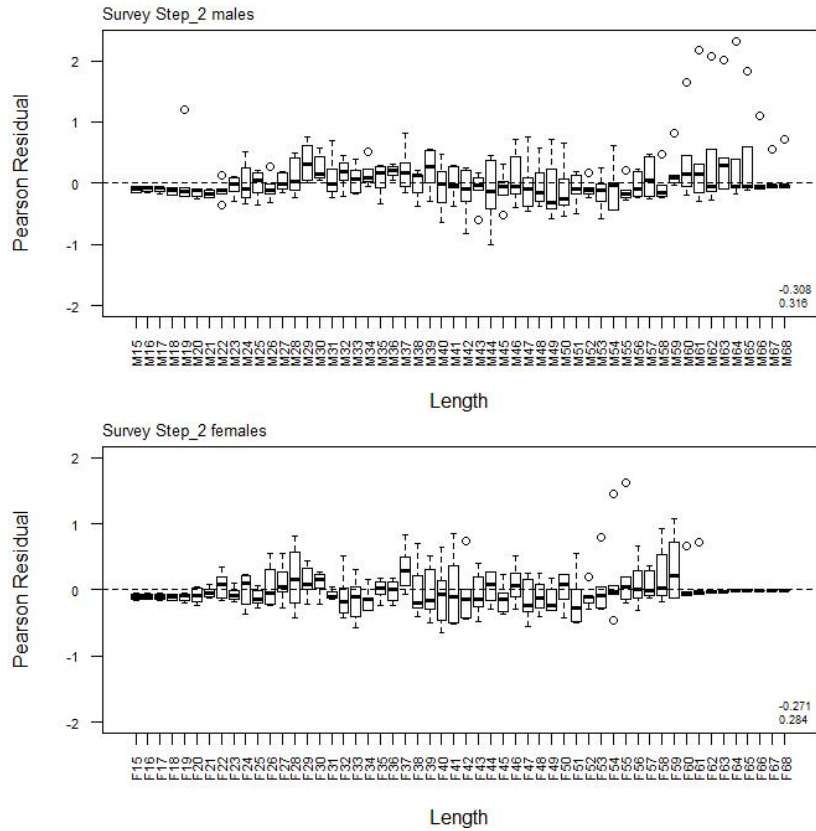
A9. 15: Box plots of Pearson residuals from the fit to length frequency distributions by length from trawl survey sampling by sex for time step 1, SCI 2 M02CV15 model.



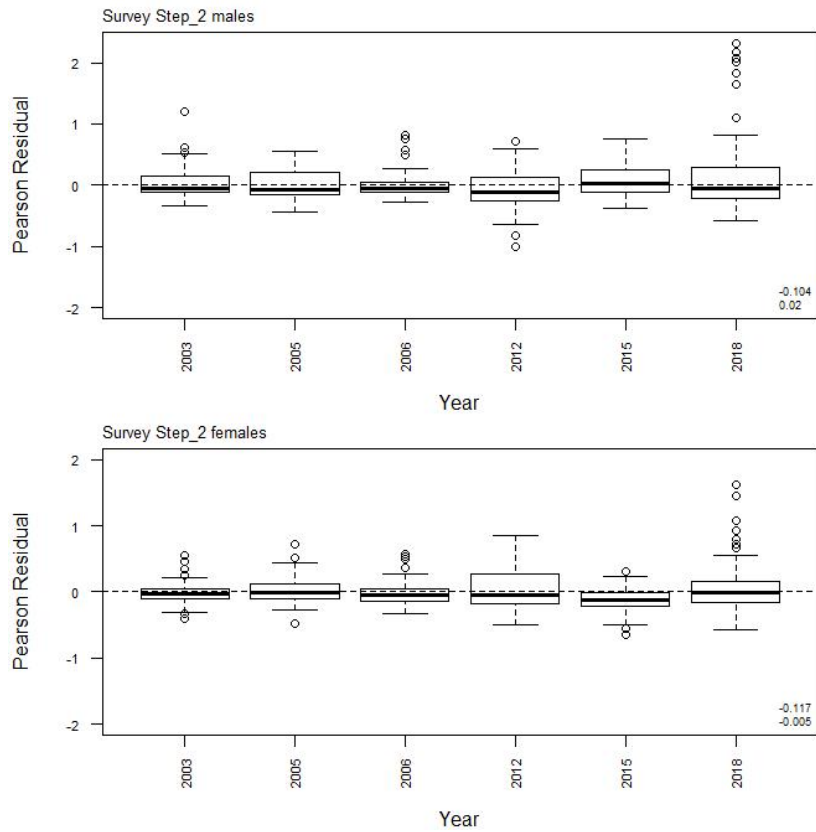
A9. 16: Box plots of Pearson residuals from the fit to length frequency distributions by year from trawl survey sampling by sex for time step 1, SCI 2 M02CV15 model.



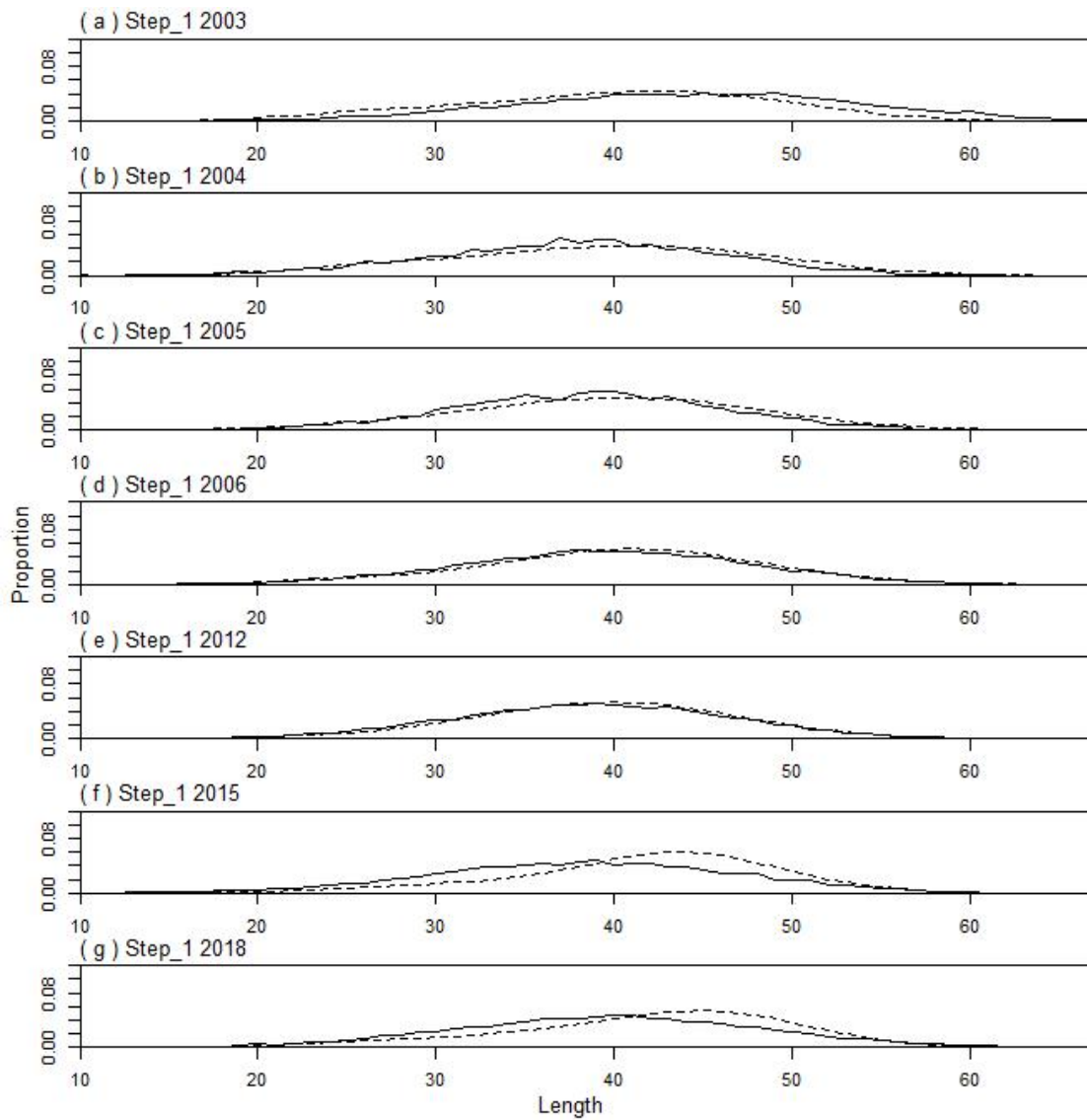
A9. 17: Observed (solid line) and fitted (dashed line) length frequency distributions from trawl survey samples for time step 2, SCI 2 M02CV15 model. Numbers in top left corner of each plot represent number of scampi measured / number of events sampled.



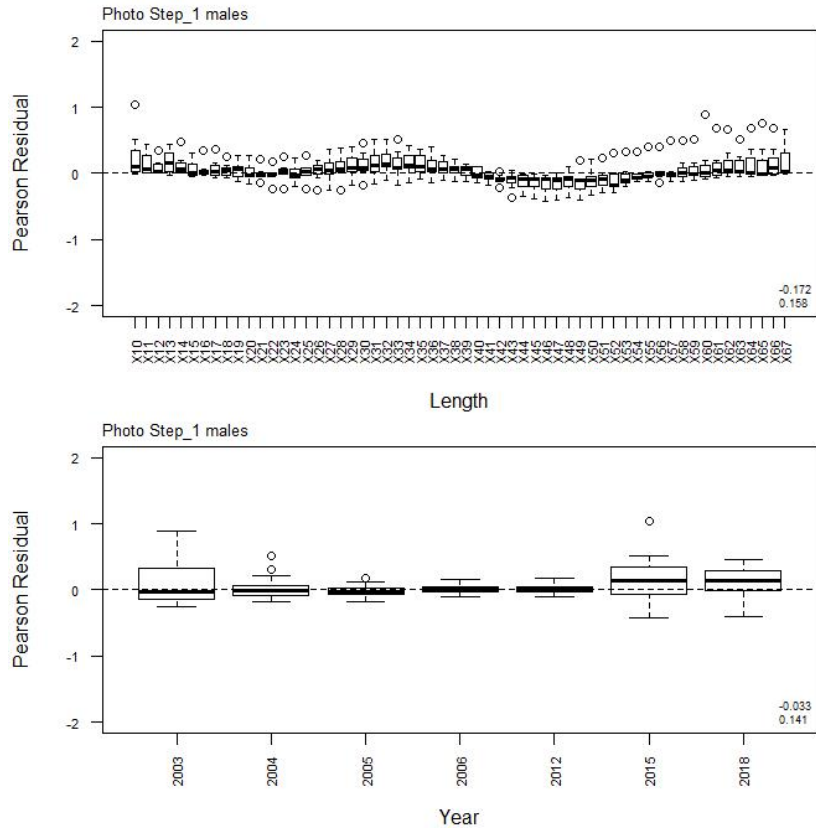
A9. 18: Box plots of Pearson residuals from the fit to length frequency distributions by length from trawl survey sampling by sex for time step 2, SCI 2 M02CV15 model.



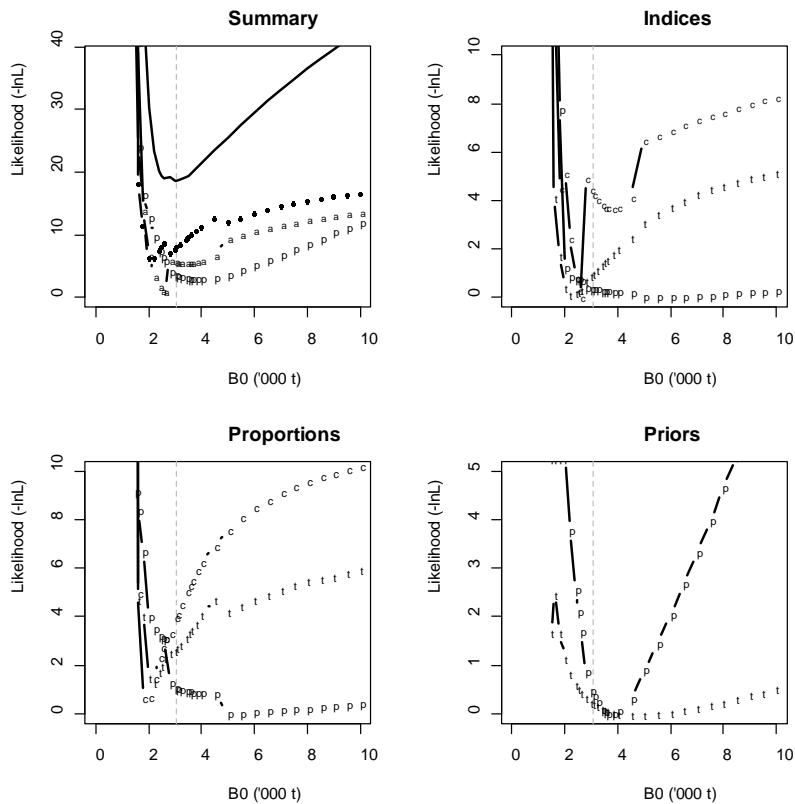
A9. 19: Box plots of Pearson residuals from the fit to length frequency distributions by year from trawl survey sampling by sex for time step 2, SCI 2 M02CV15 model.



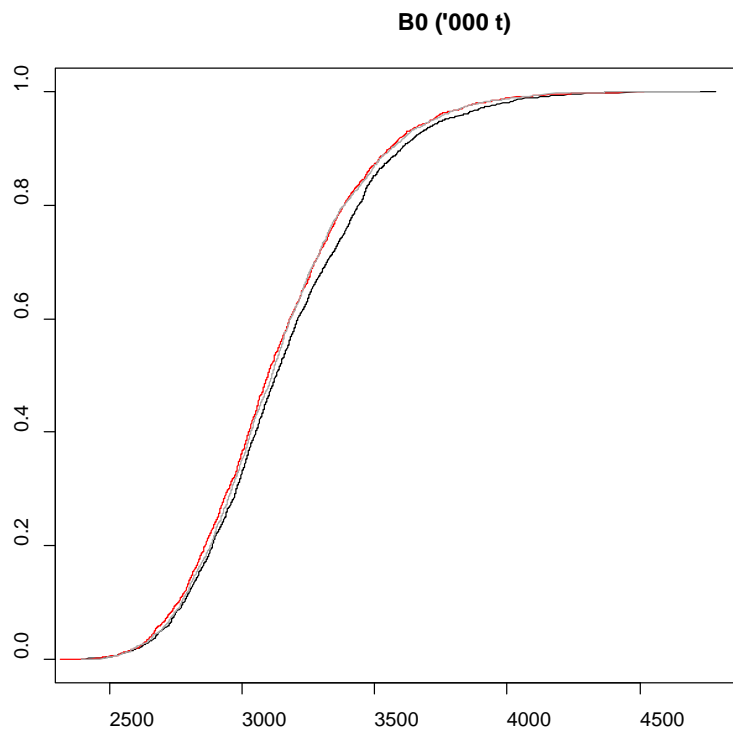
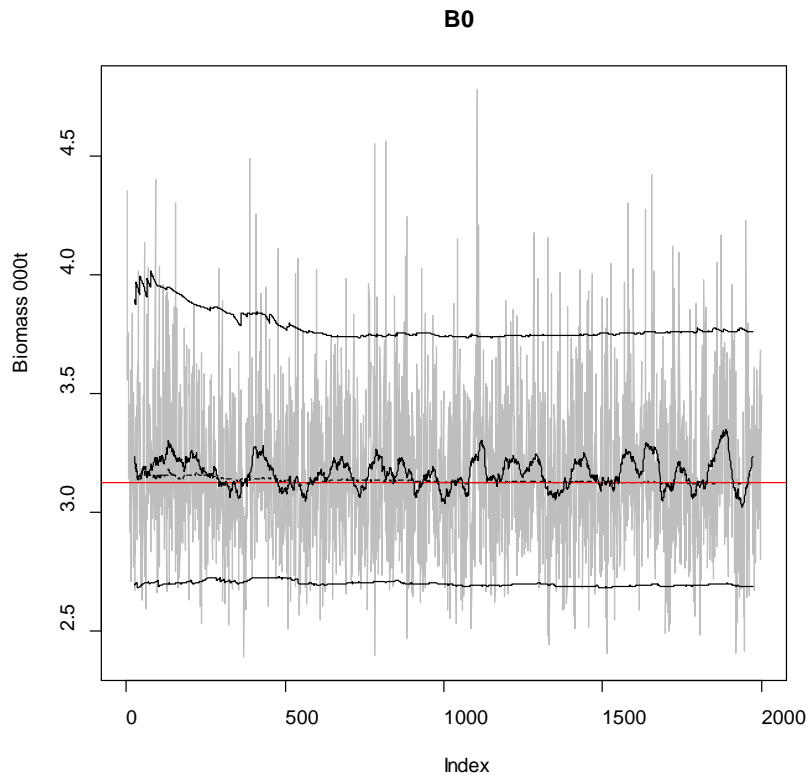
A9. 20: Observed (solid line) and fitted (dashed line) length frequency distributions from photo survey samples for SCI 2 M02CV15 model.



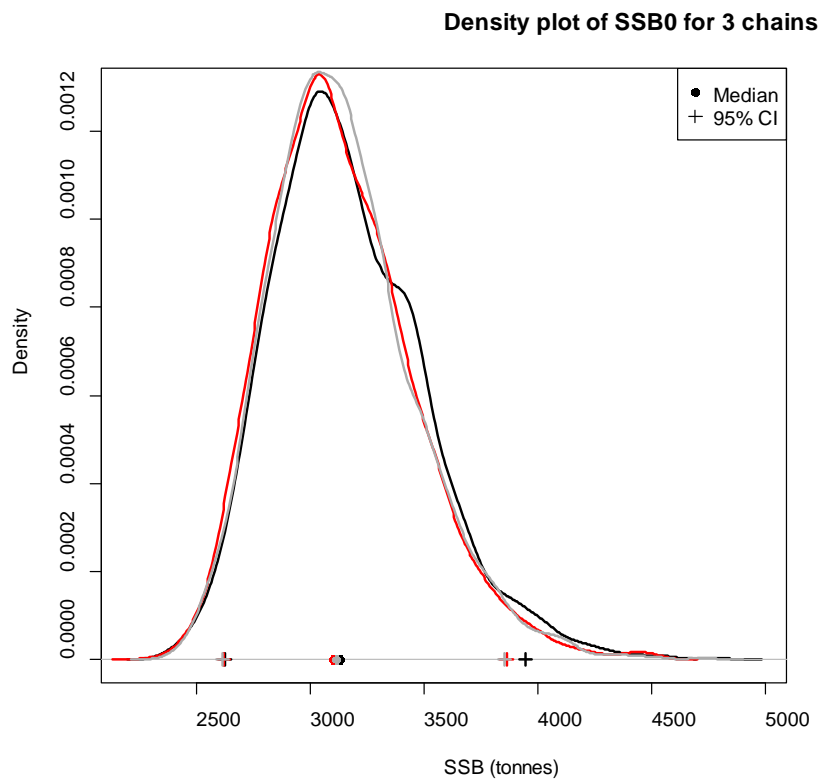
A9. 21: Box plots of Pearson residuals from the fit to length frequency distributions by length (top plot) and year (bottom plot) from photo survey sampling by sex for SCI 2 M02CV15 model.



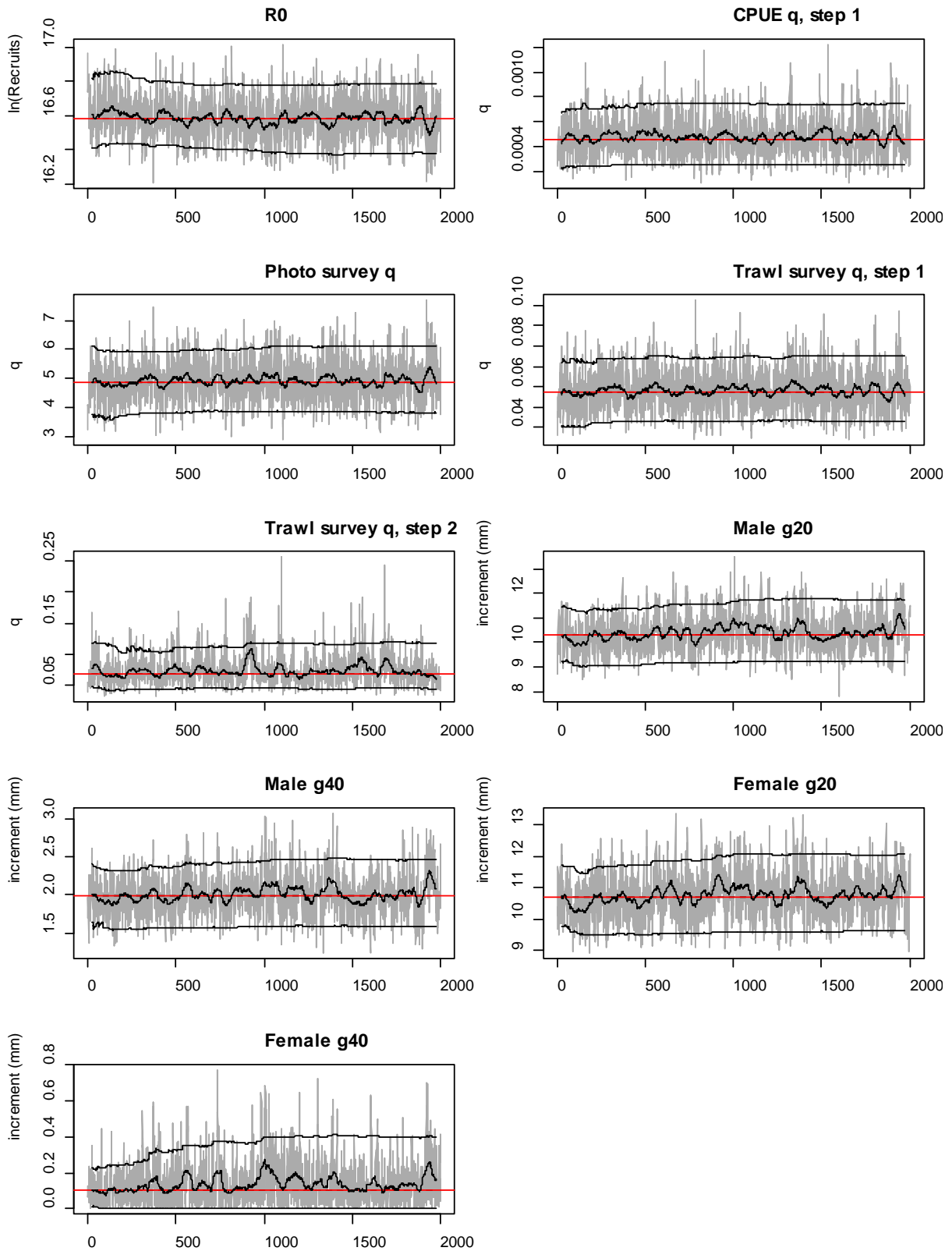
A9. 22: Likelihood profiles for model M02CV15 for SCI 2 when B_0 is fixed in the model. Figures show profiles for main priors (top left, p – priors, a – abundance indices, • – proportions at length), abundance indices (top right, t – trawl survey step, c – CPUE, p – photo survey), proportion at length data (bottom left, p – photo, t – trawl, c – observer) and priors (bottom right, p – q-Photo, t – q-Trawl).



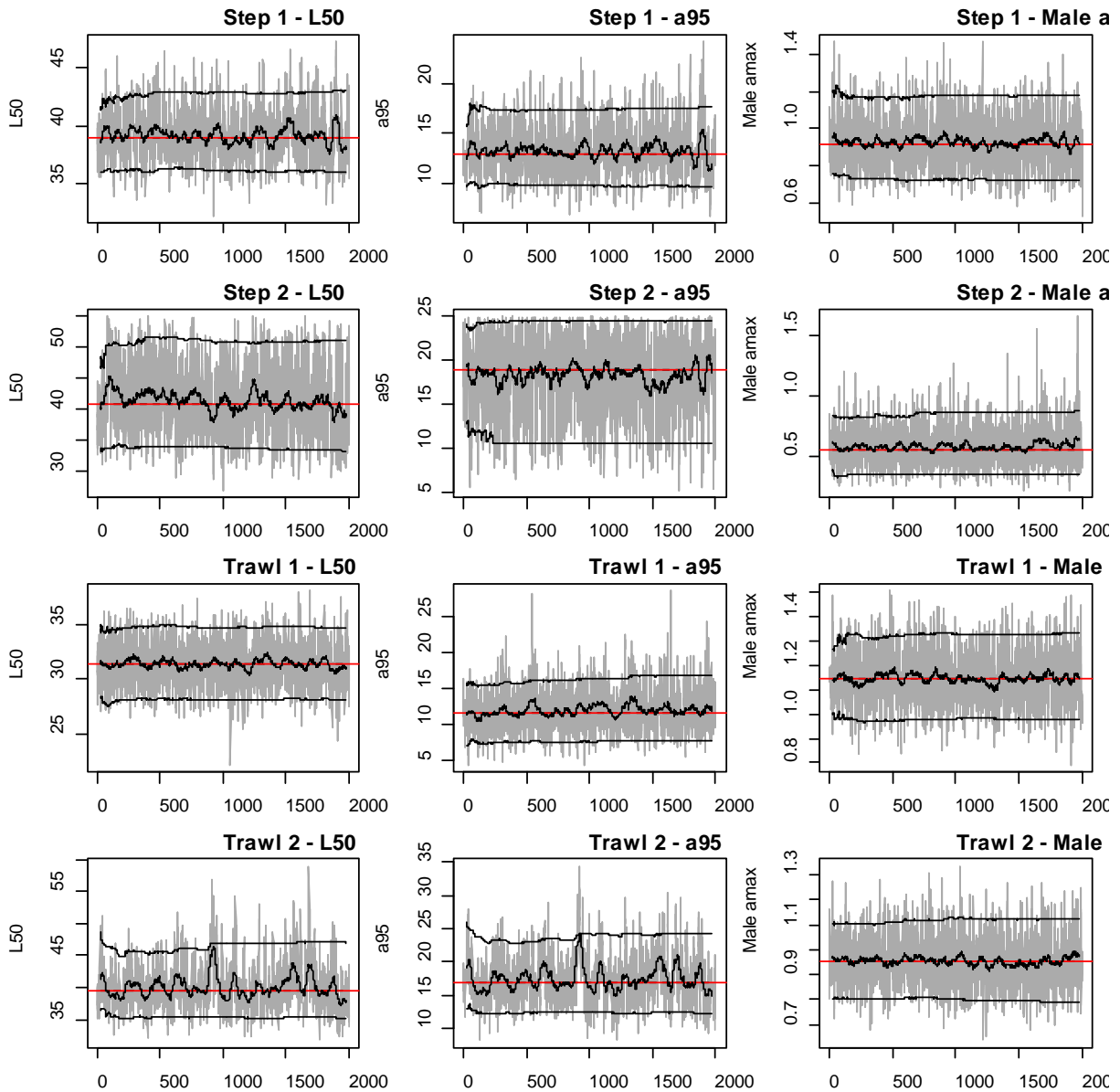
A9. 23: MCMC traces for B_0 and cumulative frequency distributions for three independent MCMC chains for the SCI 2 M02CV15 model.



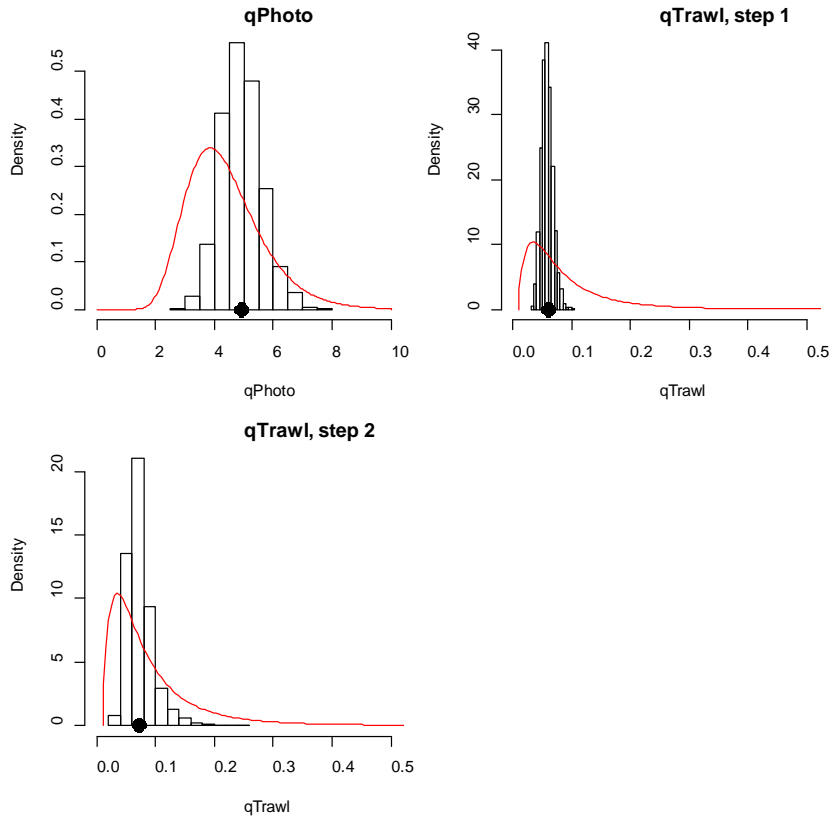
A9. 24: Density plots for B_0 for the SCI 2 M02CV15 model for three independent MCMC chains, with median and 95% confidence intervals.



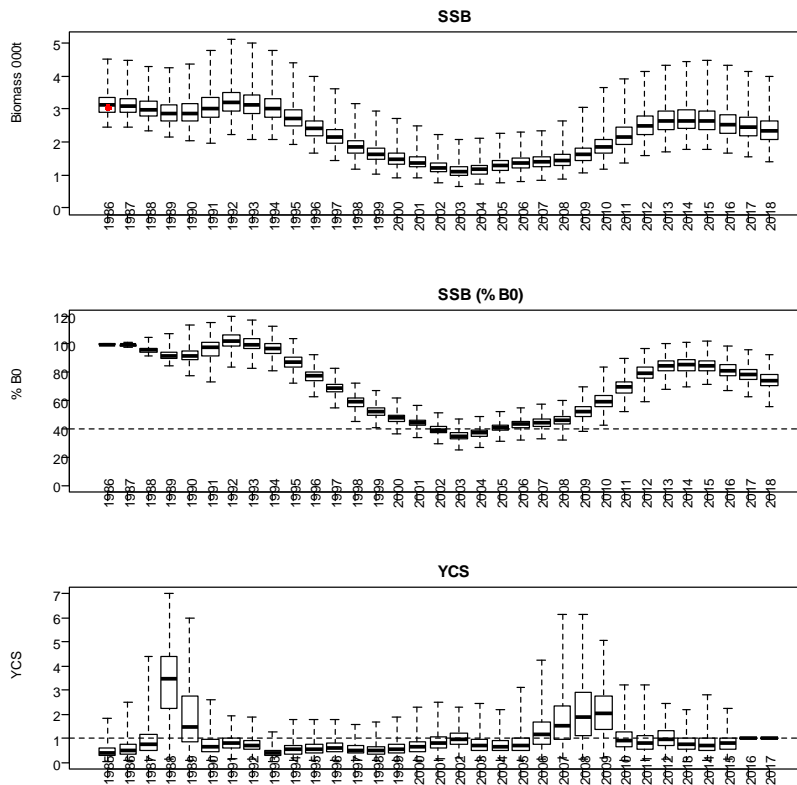
A9. 25: MCMC traces for R_0 , catchability, and growth terms for the SCI 2 M02CV15 model.



A9. 26: MCMC traces for selectivity terms for the SCI 2 M02CV15 model.

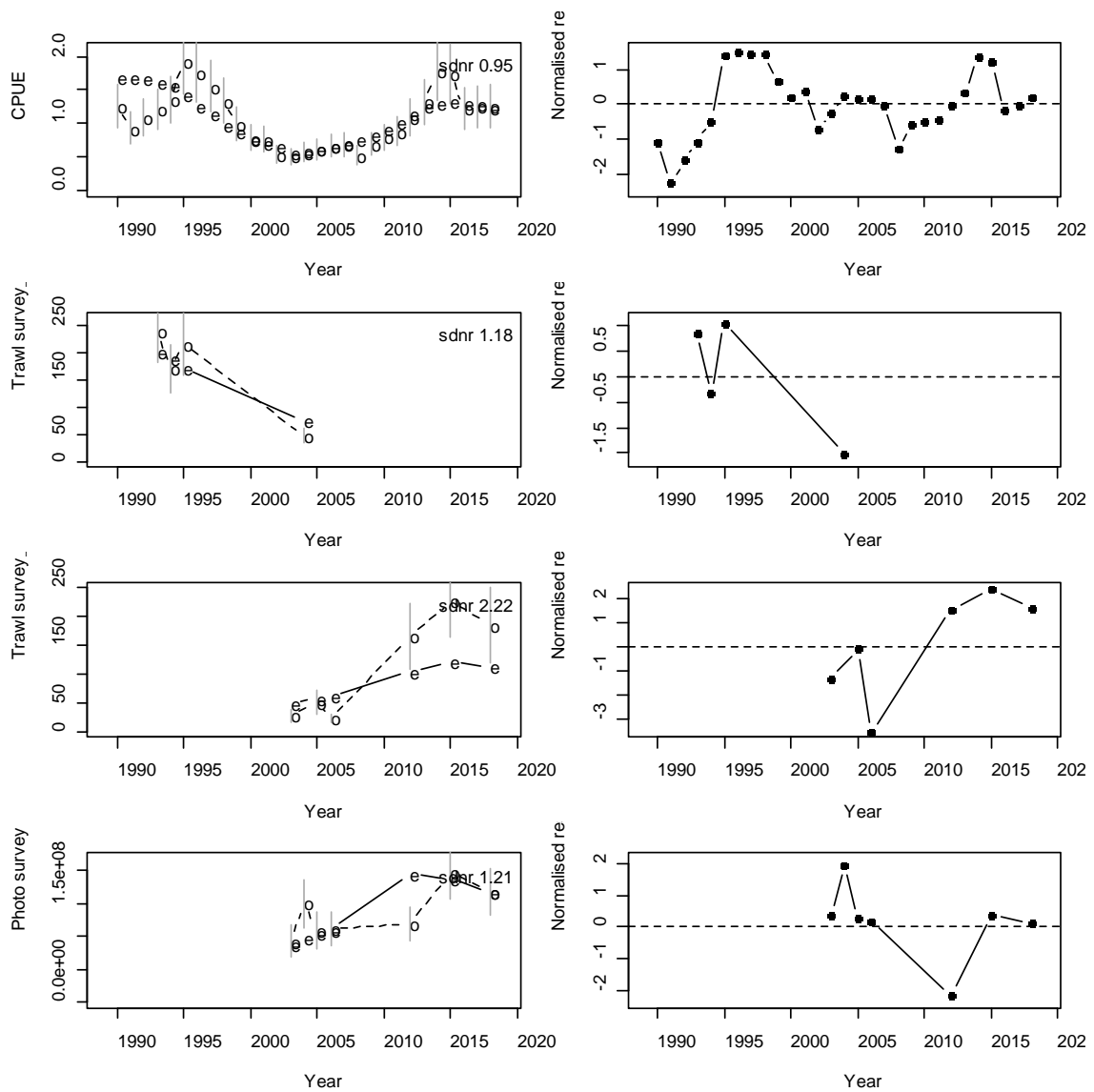


A9. 27: Marginal posterior distributions (histograms), MPD estimates (solid symbols), and distributions of priors (lines) for catchability terms for the SCI 2 M02CV15 model.

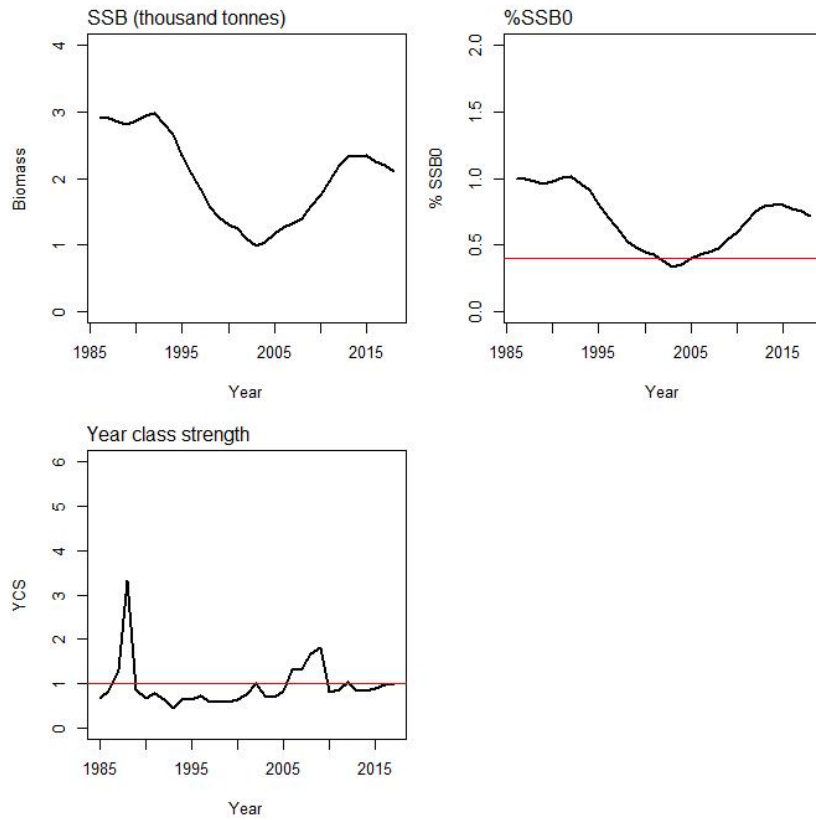


A9. 28: Posterior trajectory of SSB, SSB/SSB₀, and YCS for the SCI 2 M02CV15 model. Red dot represents MPD estimate of B₀.

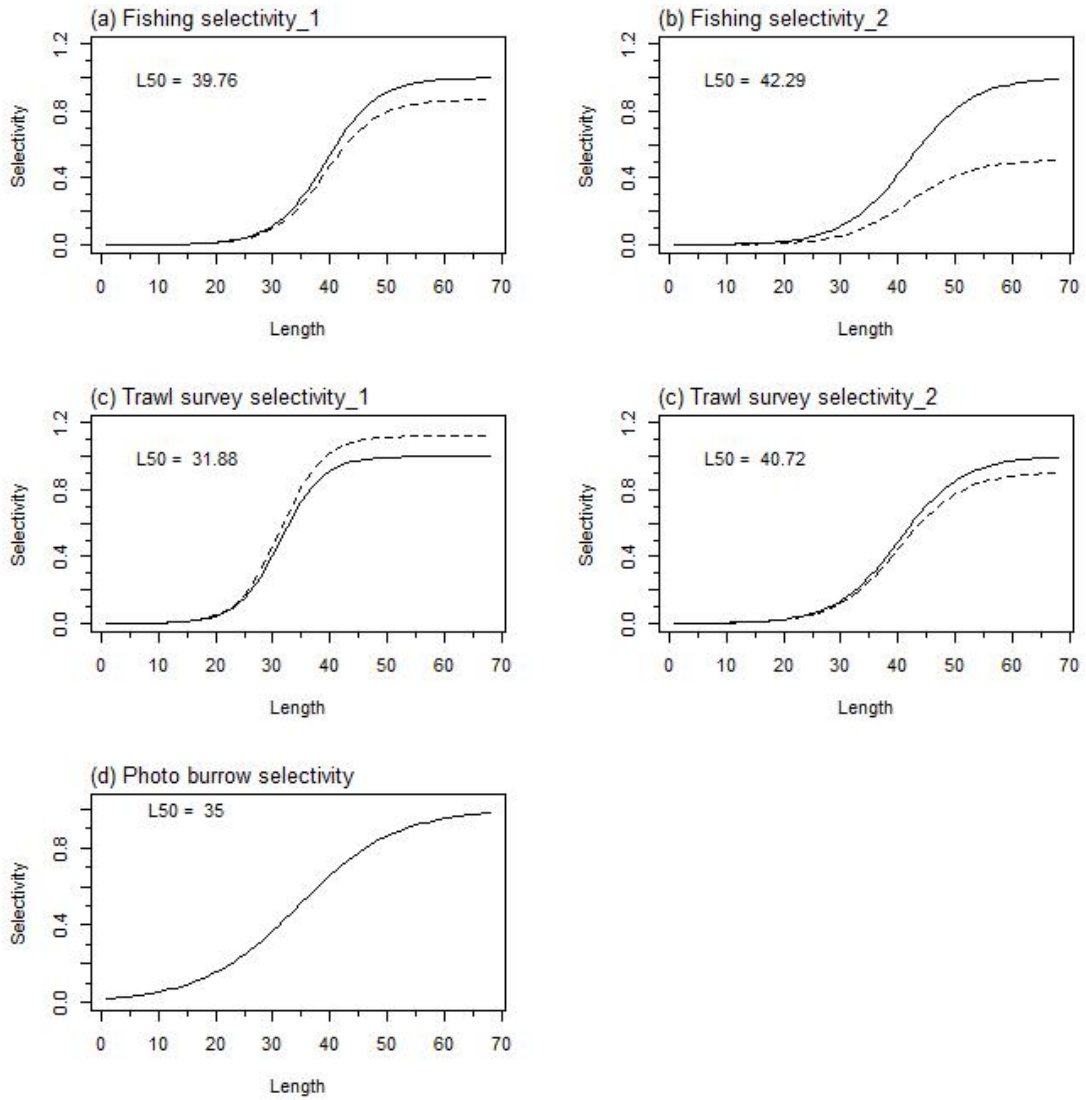
APPENDIX 10. SCI 2 M02CV25 model plots ($M=0.2$, $CV=0.25$)



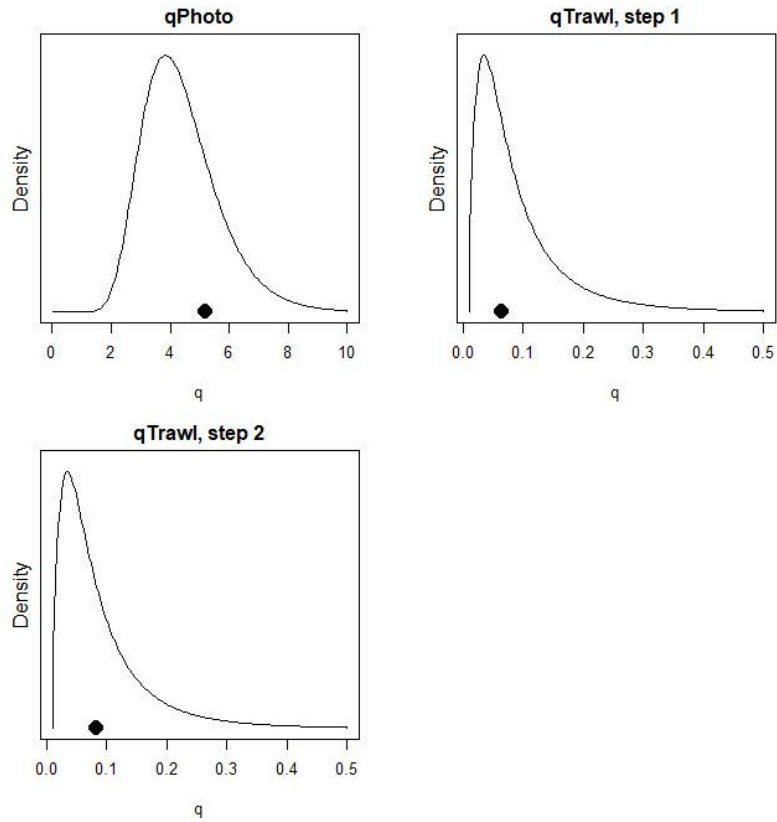
A10. 1: Fits to abundance indices (left column) and normalised residuals (right column) for standardised CPUE index (top row) trawl survey biomass index time step 1 (second row), trawl survey biomass index time step 2 (third row), and photo survey abundance index (fourth row) for the SCI 2 M02CV25 model.



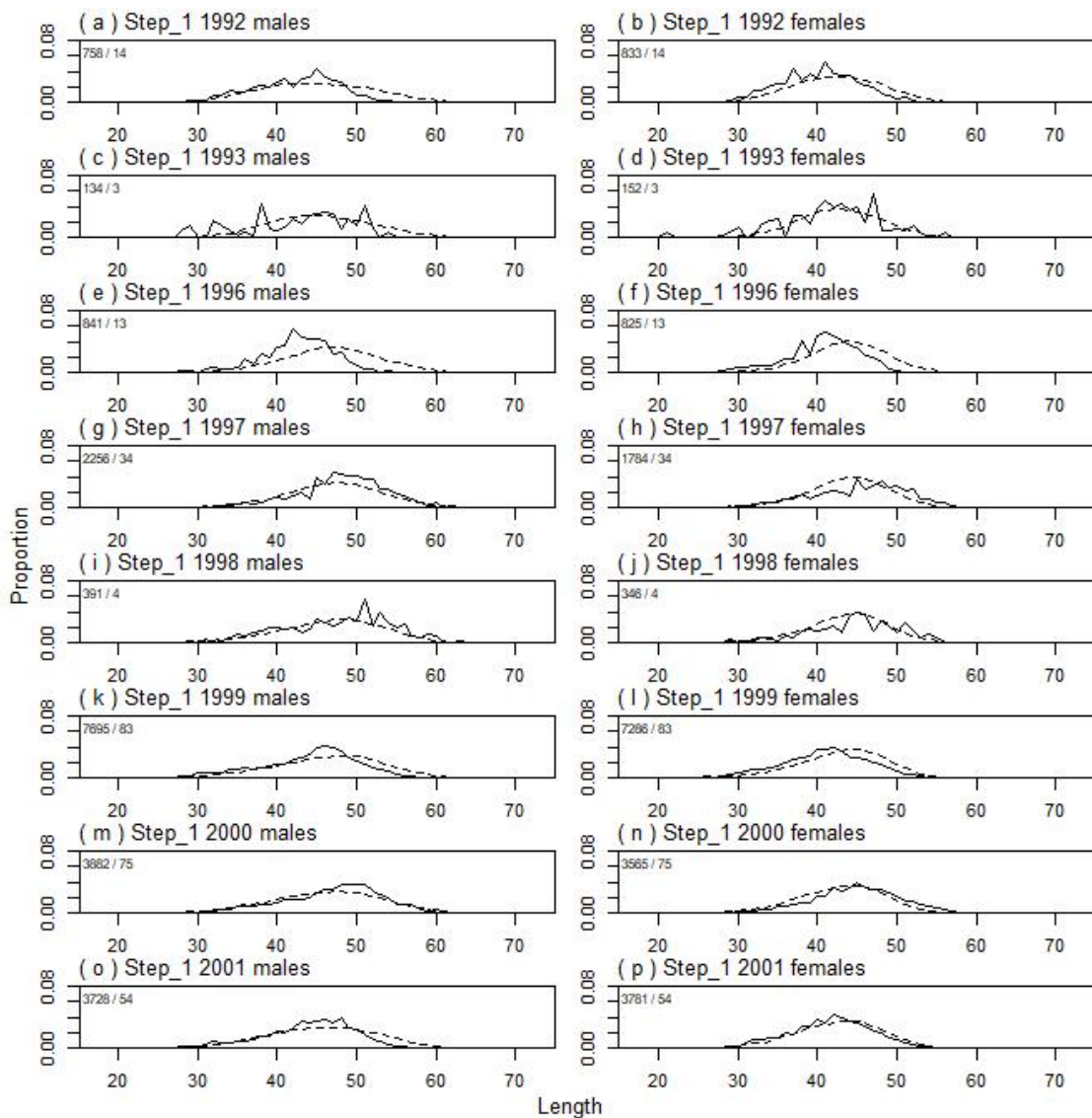
A10. 2: Spawning stock biomass trajectory (upper left), stock status (upper right), and year class strength (lower left) for the SCI 2 M02CV25 model.



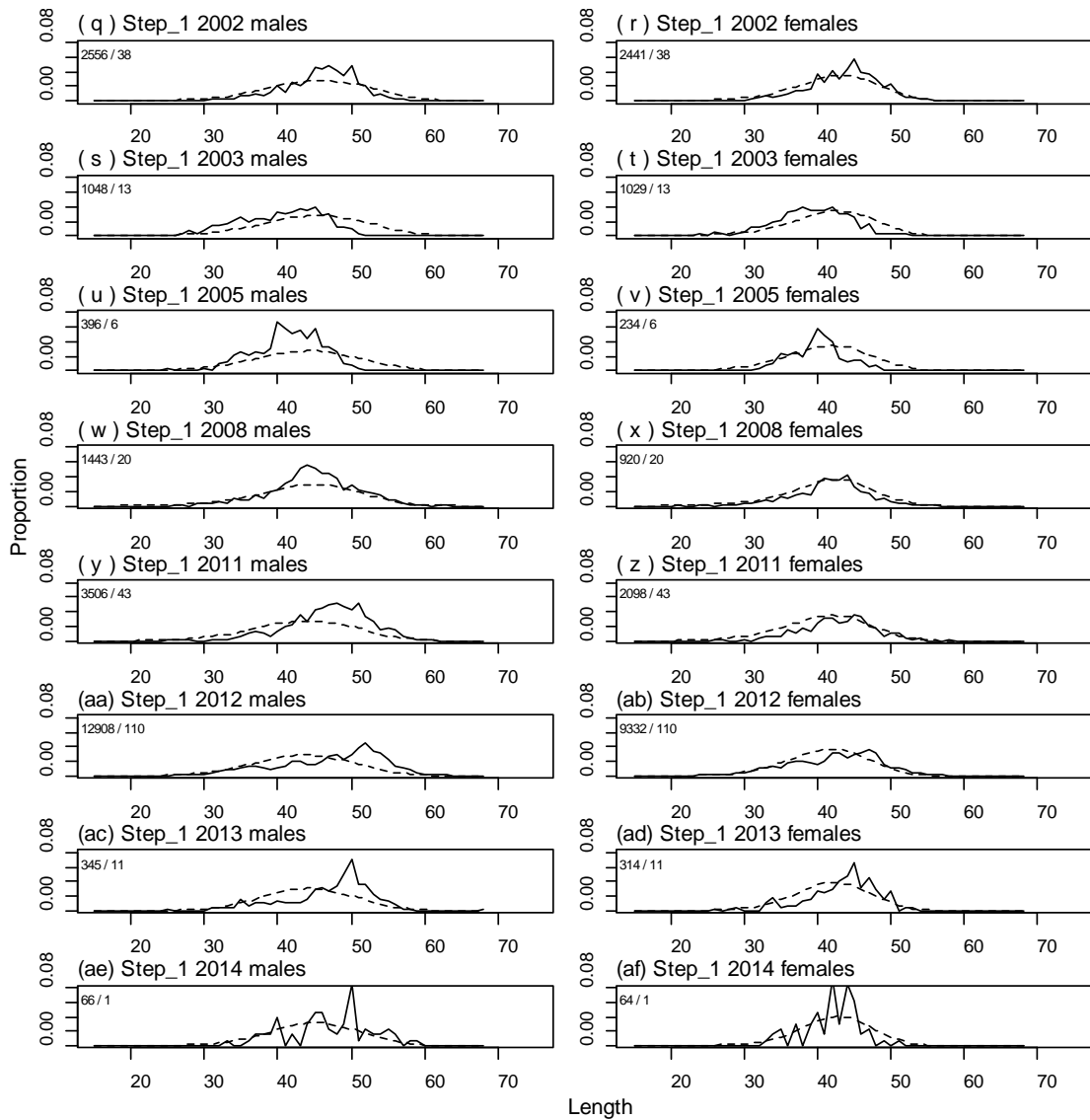
A10. 3: Fishery and survey selectivity curves for the SCI 2 M02CV25 model. Solid line – females, dotted line – males. The scampi burrow index is not sexed, and a single selectivity applies.



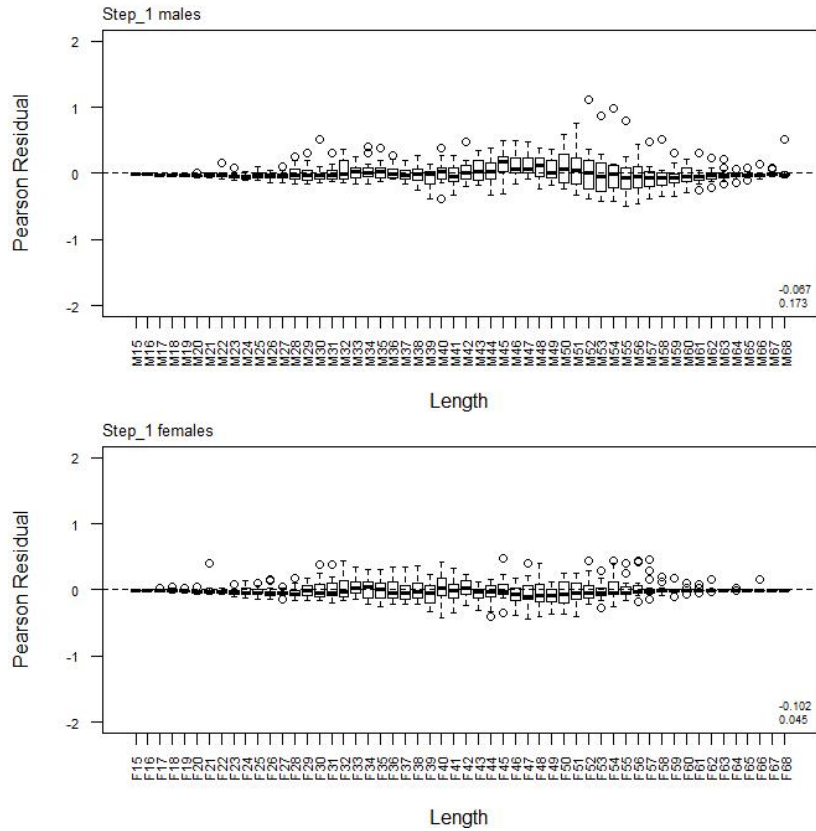
A10. 4: Catchability estimates from MPD model run, plotted in relation to prior distribution for the SCI 2 M02CV25 model.



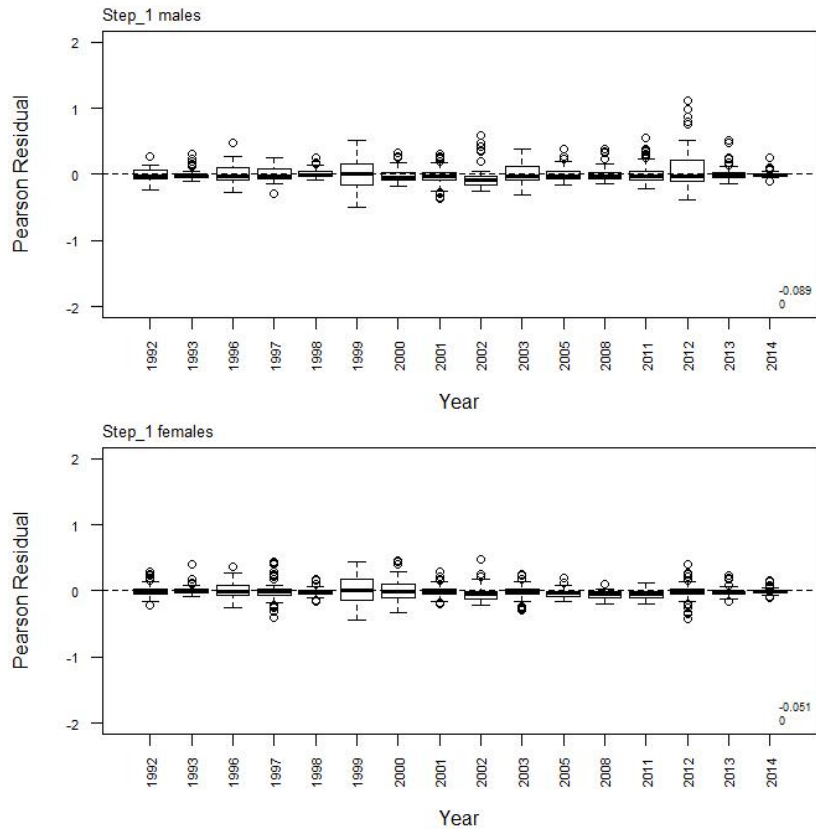
A10. 5: Observed (solid line) and fitted (dashed line) length frequency distributions from observer samples, time step 1 for SCI 2 M02CV25 model. Numbers in top left corner of each plot represent number of scampi measured / number of events sampled.



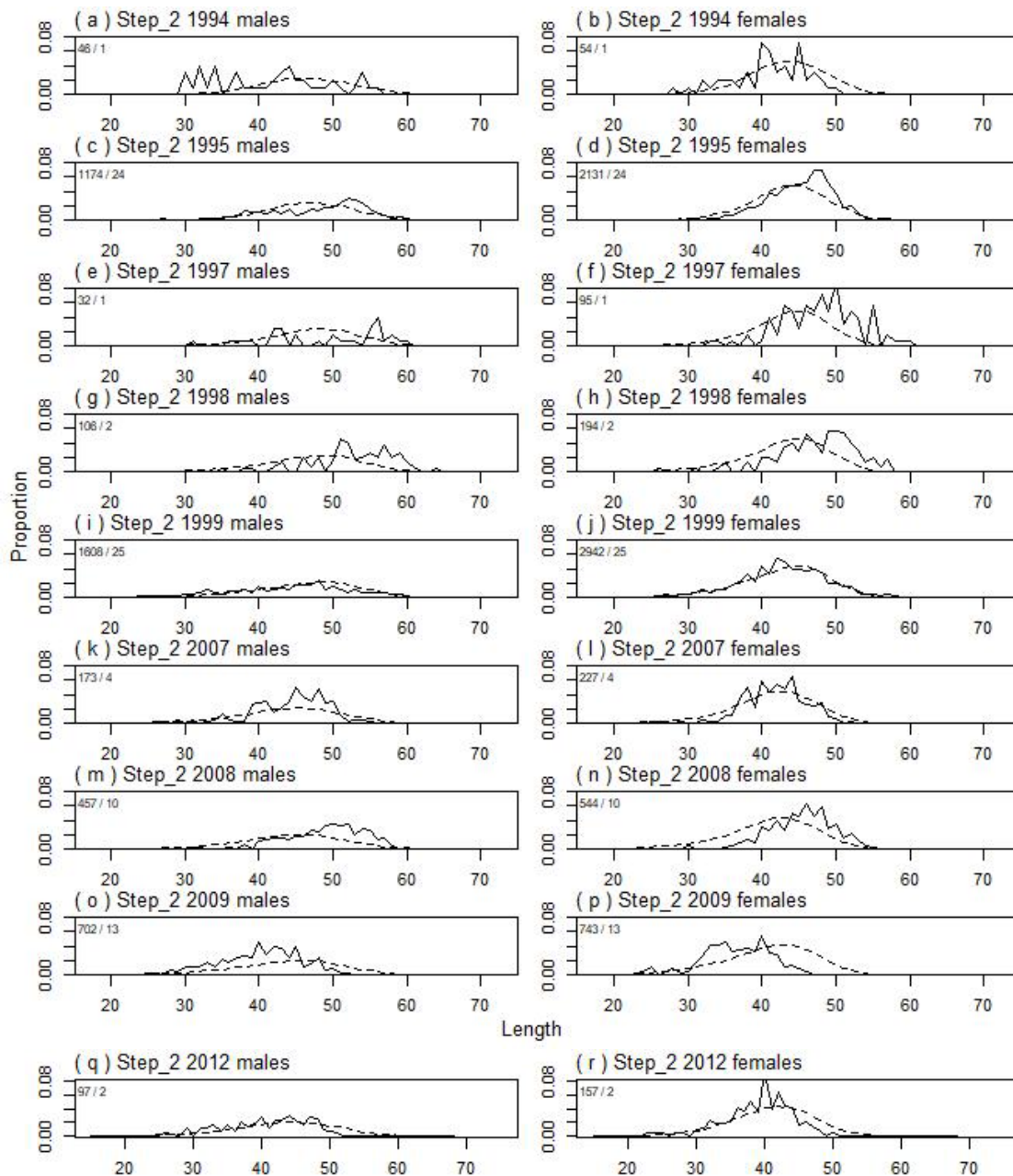
A10. 5(continued): Observed (solid line) and fitted (dashed line) length frequency distributions from observer samples, time step 1 for SCI 2 M02CV25 model. Numbers in top left corner of each plot represent number of scampi measured / number of events sampled.



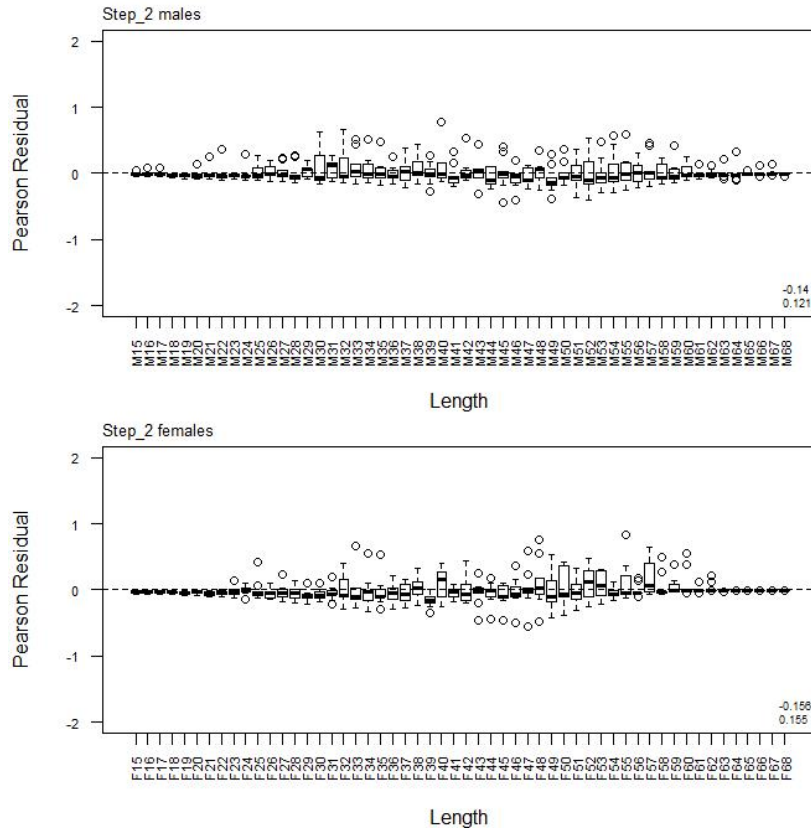
A10. 6: Box plots of Pearson residuals from the fit to length frequency distributions by length from observer sampling by sex for time step 1 for SCI 2 M02CV25 model.



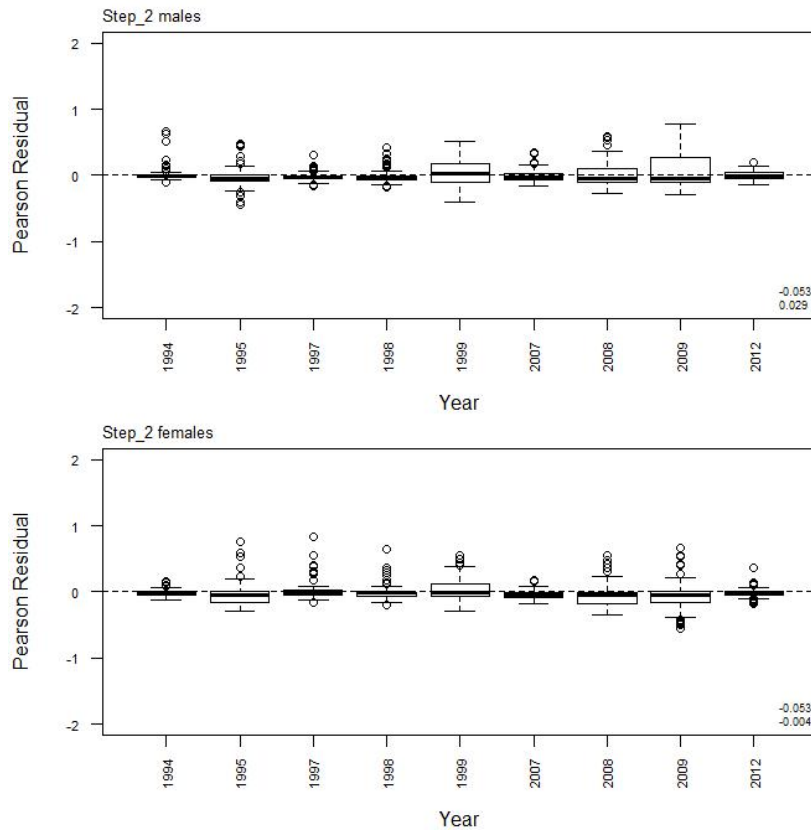
A10. 7: Box plots of Pearson residuals from the fit to length frequency distributions by year from observer sampling by sex for time step 1 for SCI 2 M02CV25 model.



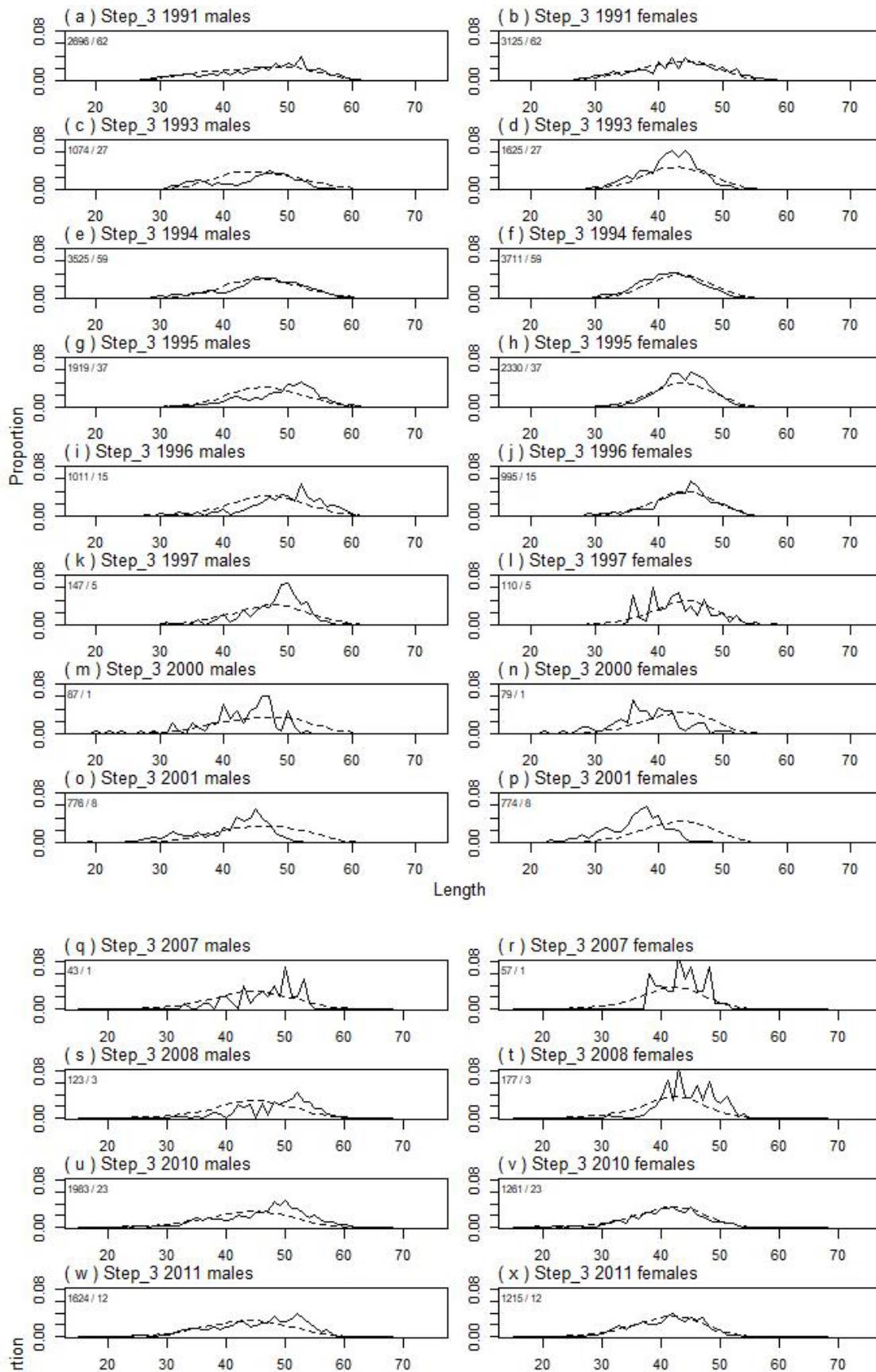
A10. 8: Observed (solid line) and fitted (dashed line) length frequency distributions from observer samples, time step 2 for SCI 2 M02CV25 model. Numbers in top left corner of each plot represent number of scampi measured / number of events sampled.



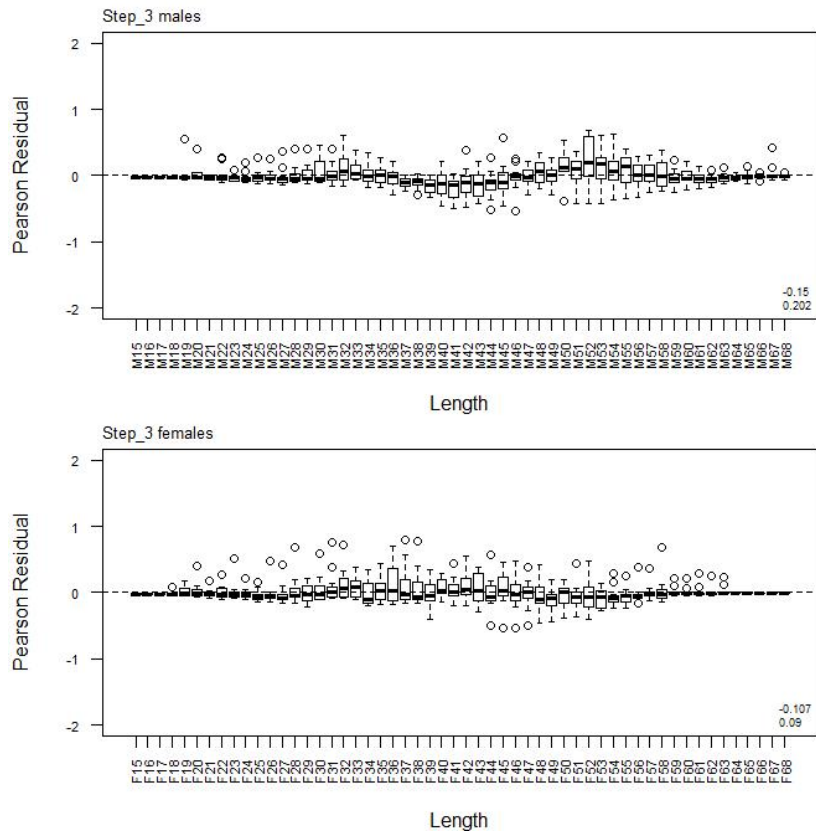
A10. 9: Box plots of Pearson residuals from the fit to length frequency distributions by length from observer sampling by sex for time step 2 for SCI 2 M02CV25 model.



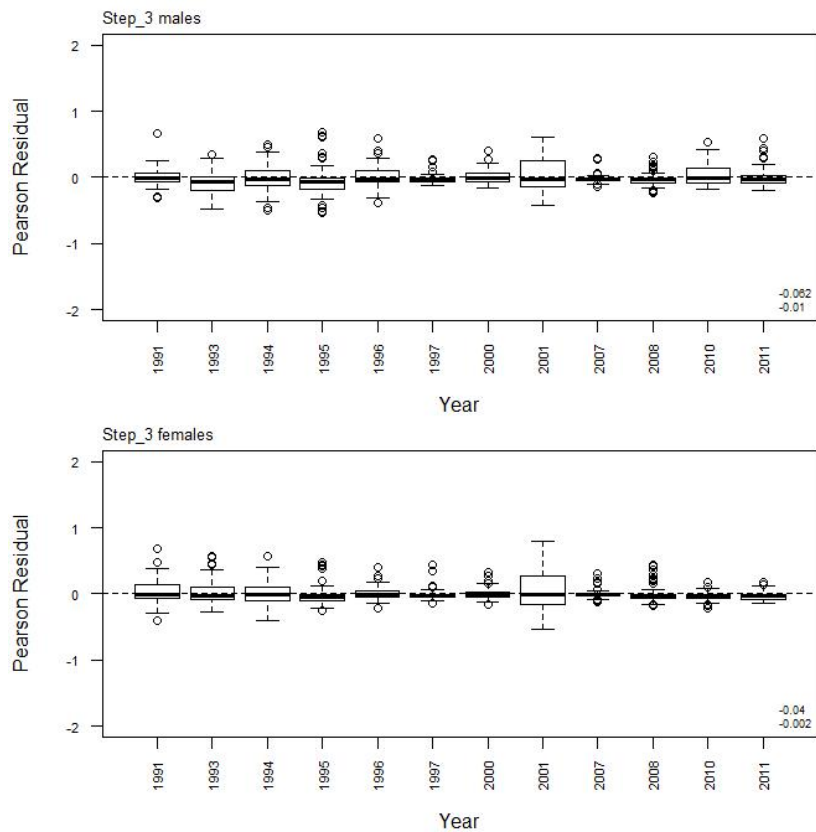
A10. 10: Box plots of Pearson residuals from the fit to length frequency distributions by year from observer sampling by sex for time step 2 for SCI 1 M02CV25 model.



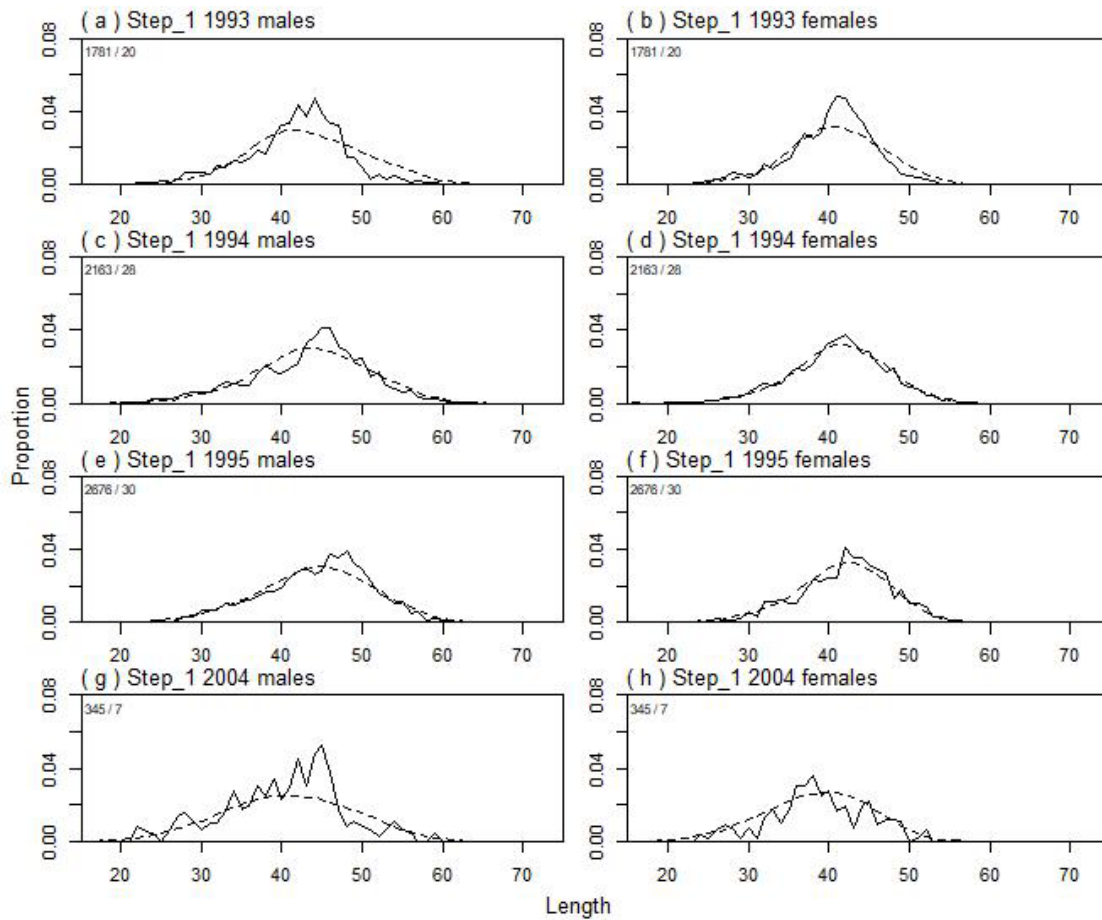
A10. 11: Observed (solid line) and fitted (dashed line) length frequency distributions from observer samples, time step 3 for SCI 2 M02CV25 model. Numbers in top left corner of each plot represent number of scampi measured / number of events sampled.



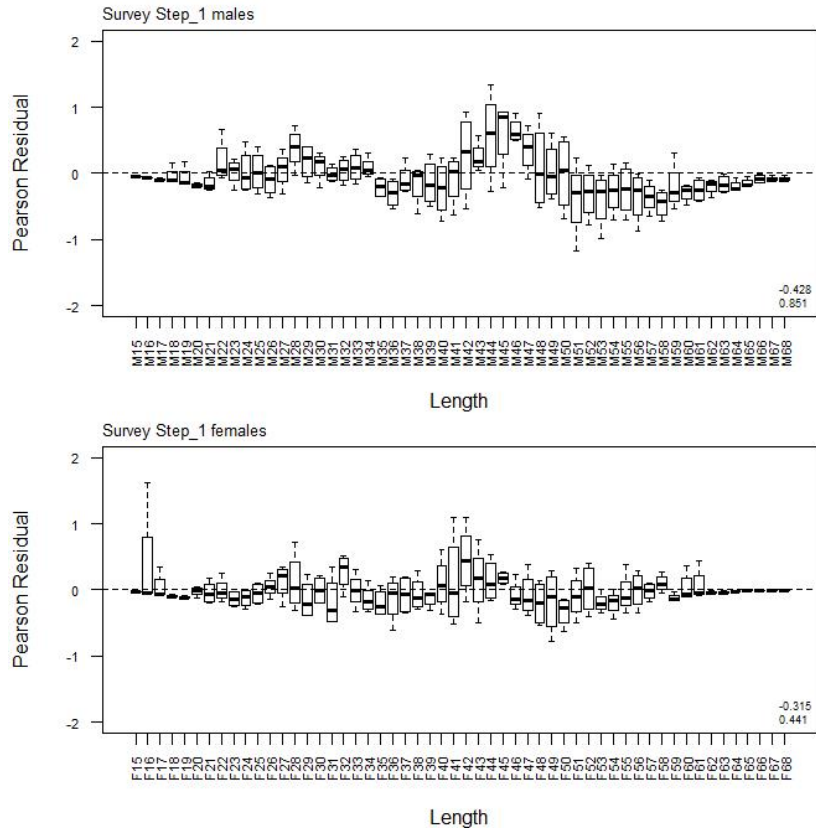
A10. 12: Box plots of Pearson residuals from the fit to length frequency distributions by length from observer sampling by sex for time step 3 for SCI 2 M02CV25 model.



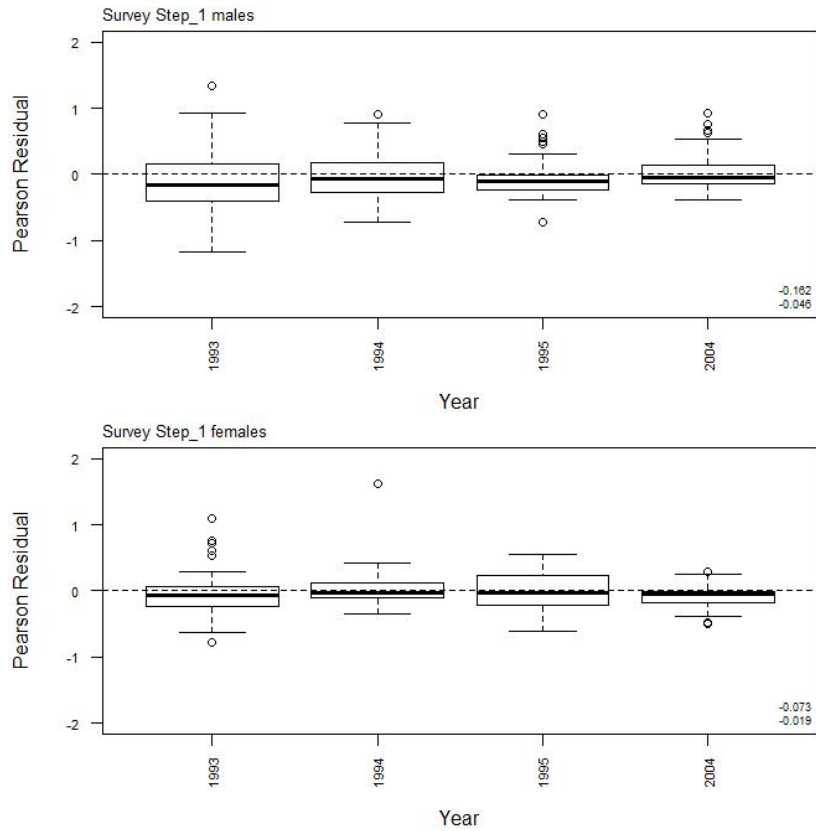
A10. 13: Box plots of Pearson residuals from the fit to length frequency distributions by year from observer sampling by sex for time step 3 for SCI 2 M02CV25 model.



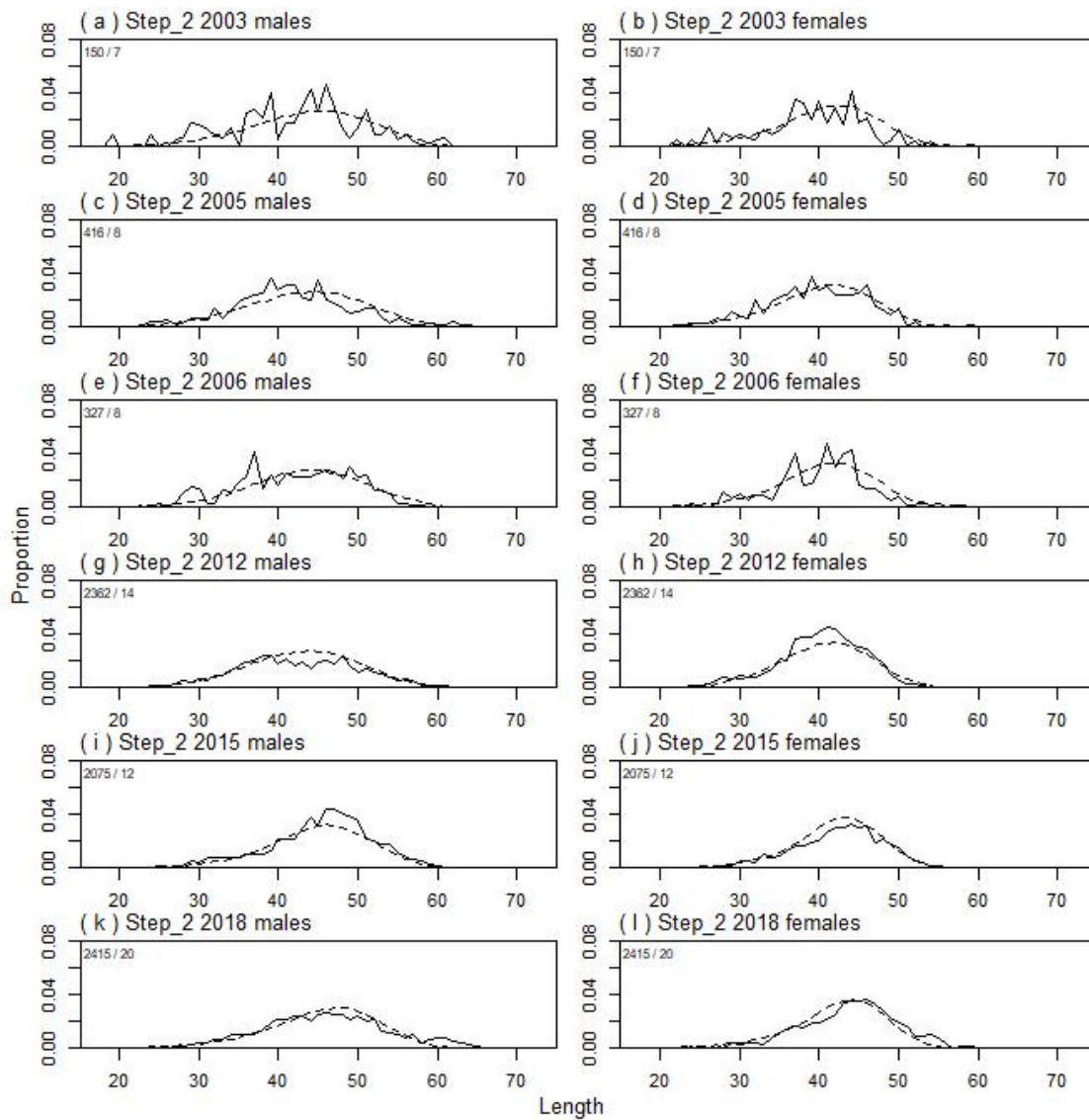
A10. 14: Observed (solid line) and fitted (dashed line) length frequency distributions from trawl survey samples for time step 1, SCI 2 M02CV25 model. Numbers in top left corner of each plot represent number of scampi measured / number of events sampled.



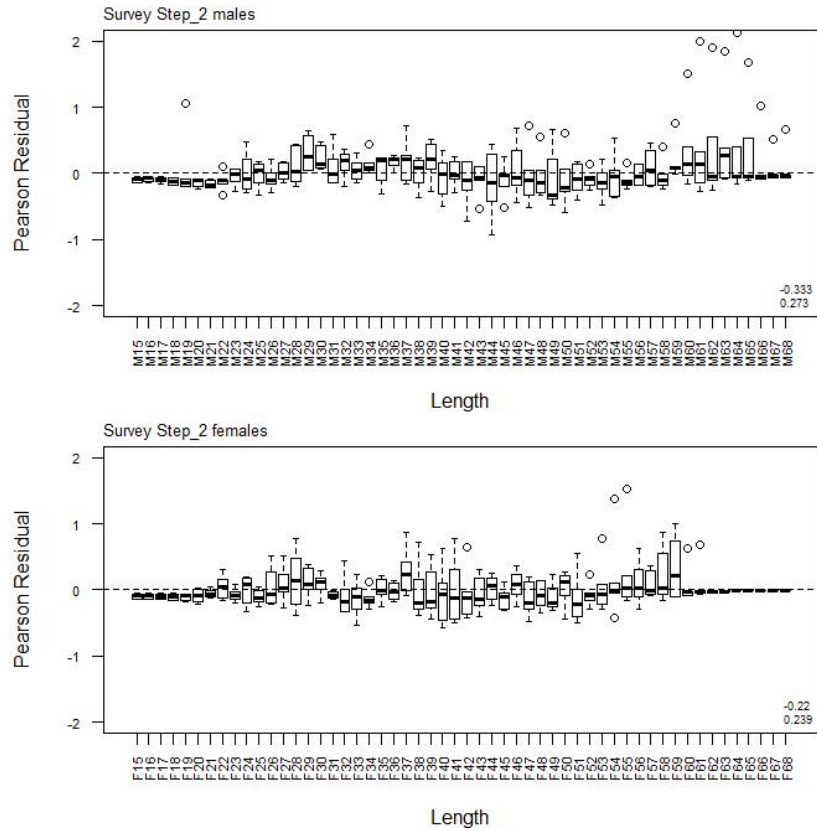
A10. 15: Box plots of Pearson residuals from the fit to length frequency distributions by length from trawl survey sampling by sex for time step 1, SCI 2 M02CV25 model.



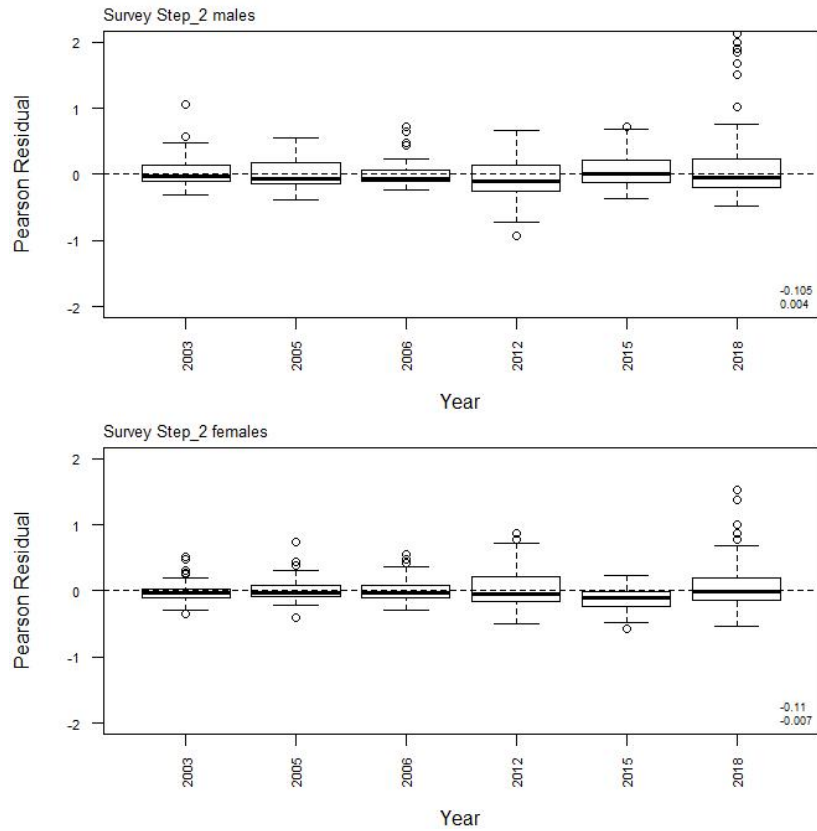
A10. 16: Box plots of Pearson residuals from the fit to length frequency distributions by year from trawl survey sampling by sex for time step 1, SCI 2 M02CV25 model.



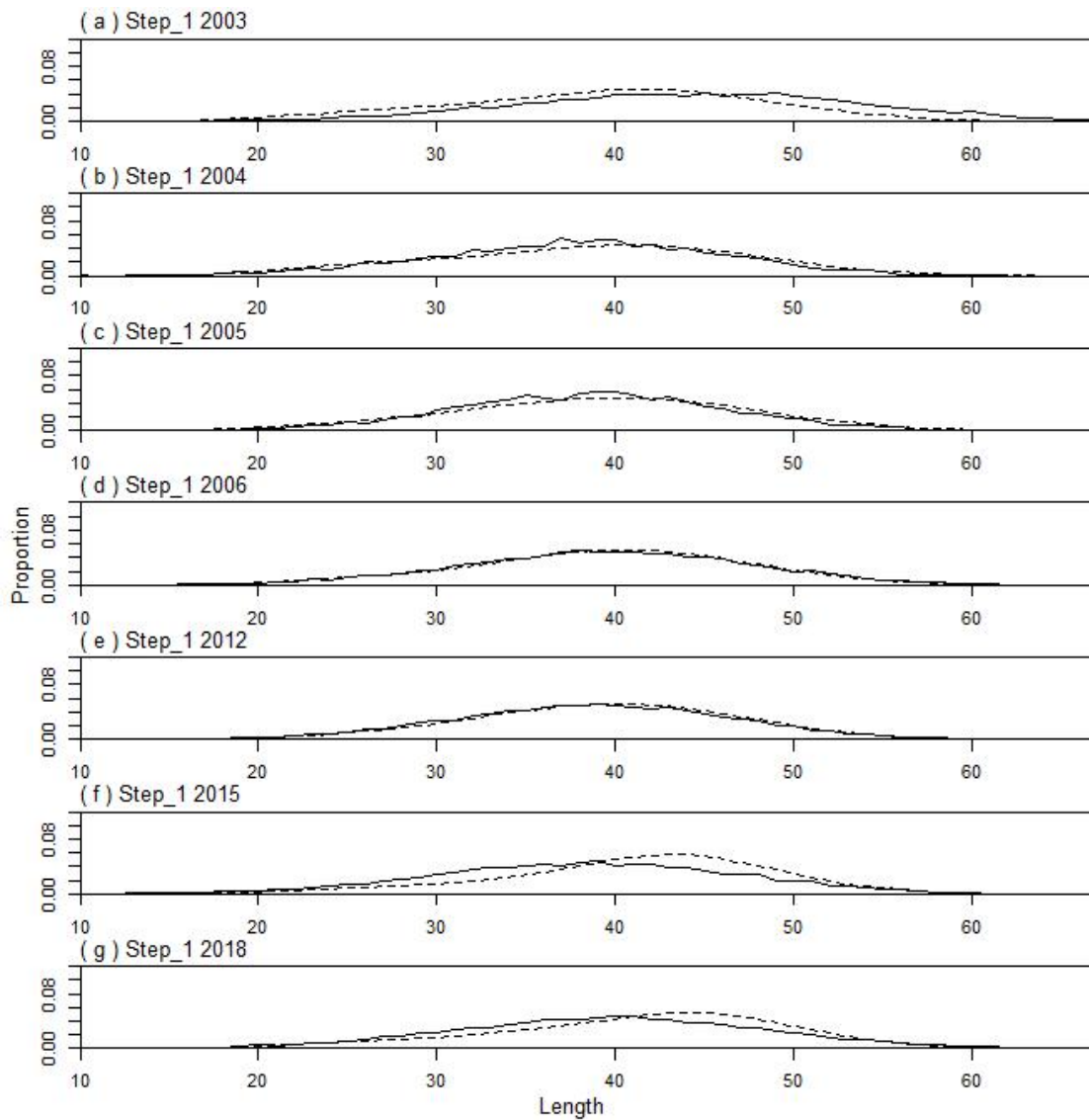
A10. 17: Observed (solid line) and fitted (dashed line) length frequency distributions from trawl survey samples for time step 2, SCI 2 M02CV25 model. Numbers in top left corner of each plot represent number of scampi measured / number of events sampled.



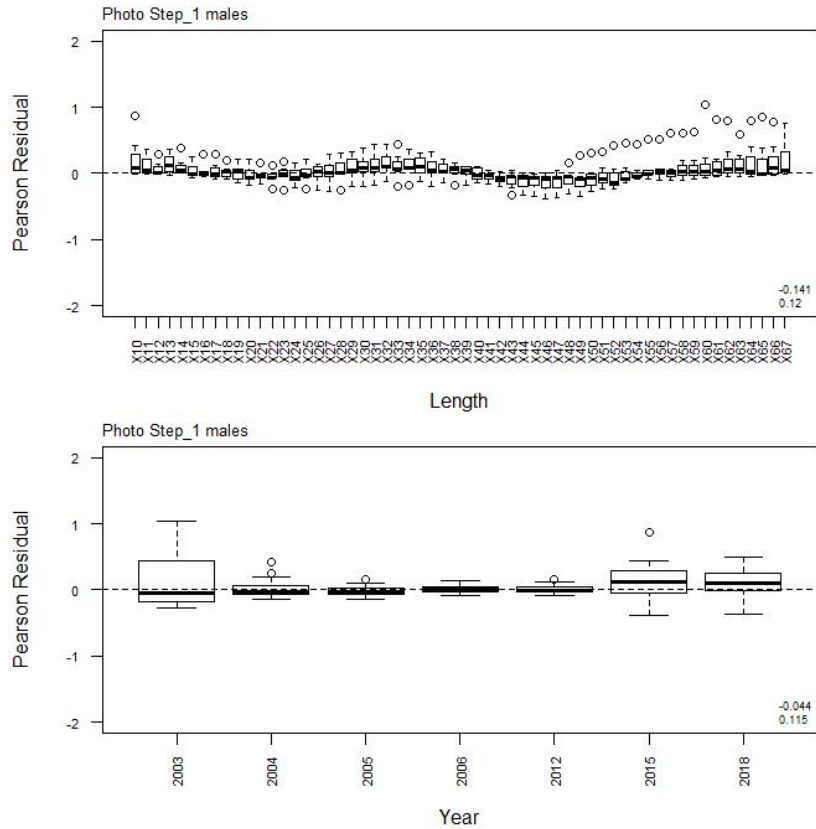
A10. 18: Box plots of Pearson residuals from the fit to length frequency distributions by length from trawl survey sampling by sex for time step 2, SCI 2 M02CV25 model.



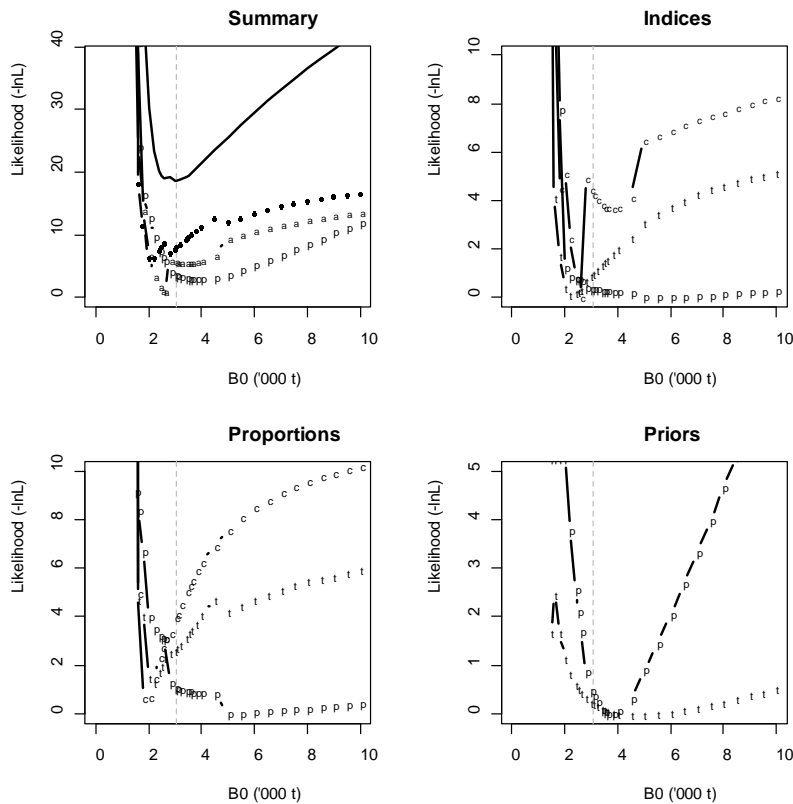
A10. 19: Box plots of Pearson residuals from the fit to length frequency distributions by year from trawl survey sampling by sex for time step 2, SCI 2 M02CV25 model.



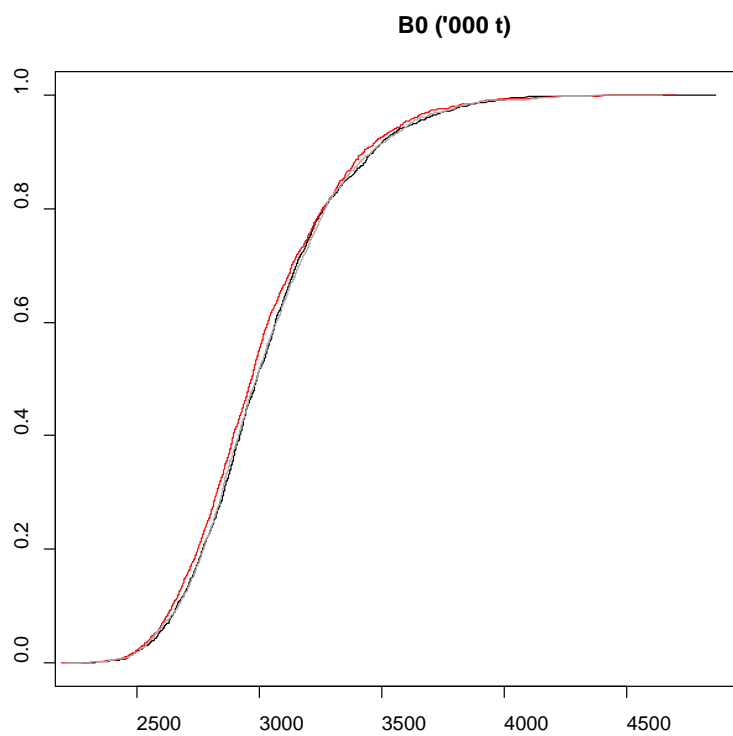
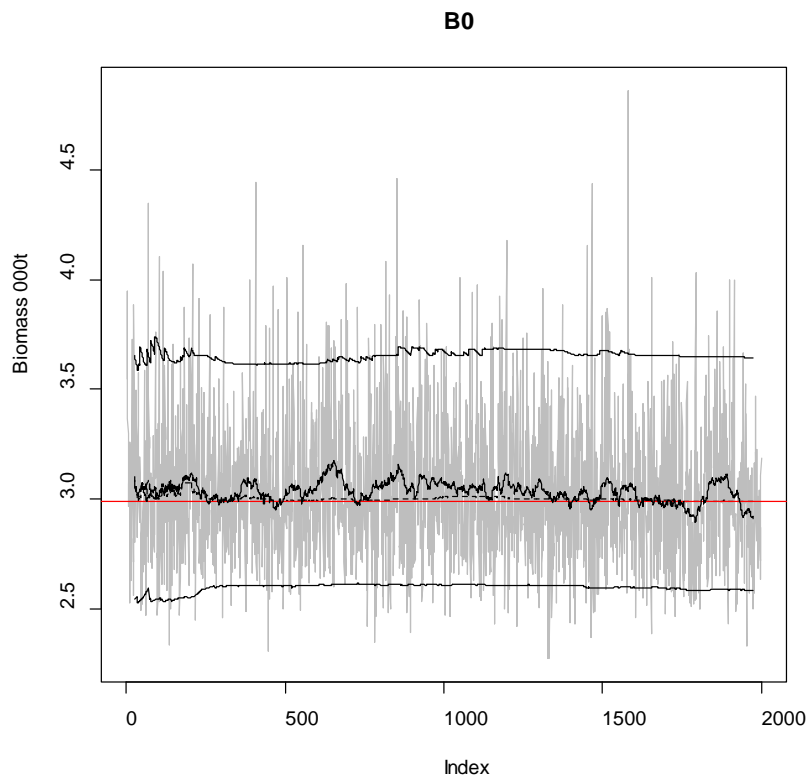
A10. 20: Observed (solid line) and fitted (dashed line) length frequency distributions from photo survey samples for SCI 2 M02CV25 model.



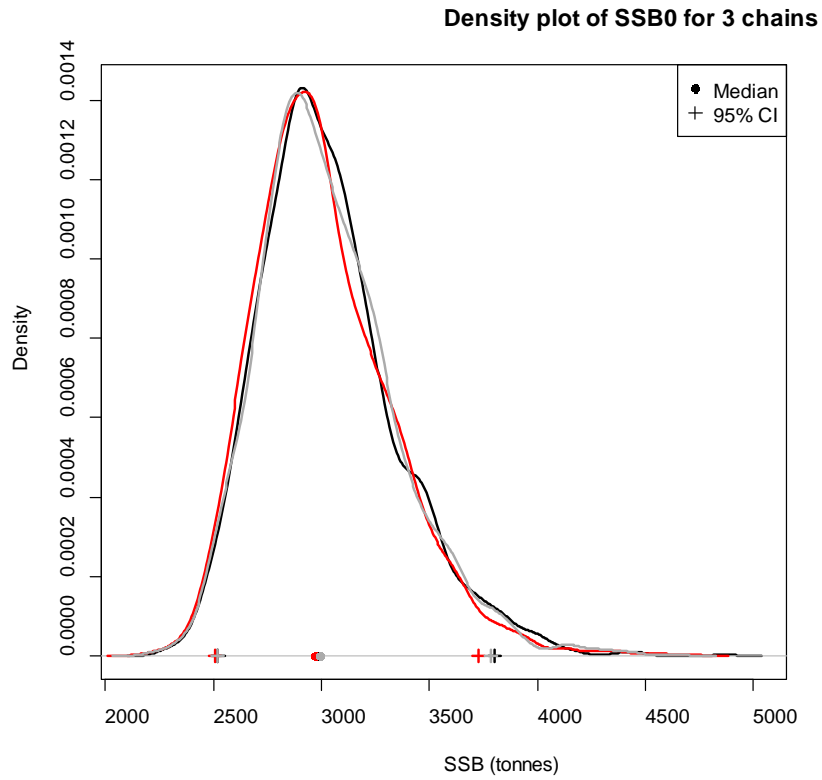
A10. 21: Box plots of Pearson residuals from the fit to length frequency distributions by length (top plot) and year (bottom plot) from photo survey sampling by sex for SCI 2 M02CV25 model.



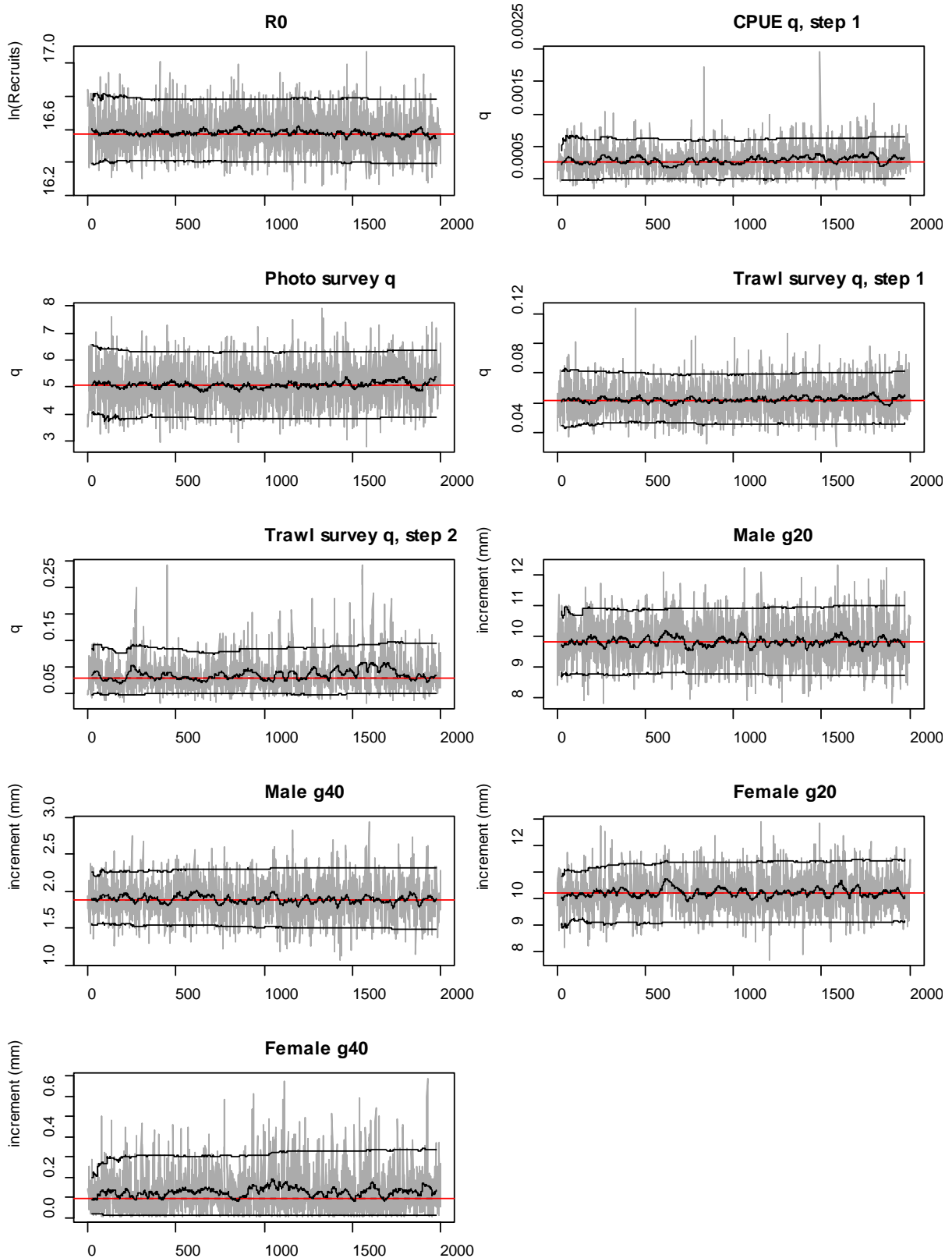
A10. 22: Likelihood profiles for model M02CV25 for SCI 2 when B_0 is fixed in the model. Figures show profiles for main priors (top left, p – priors, a – abundance indices, • – proportions at length), abundance indices (top right, t – trawl survey step, c – CPUE, p – photo survey), proportion at length data (bottom left, p-photo, t – trawl, c – observer) and priors (bottom right, p – q-Photo, t – q-Trawl).



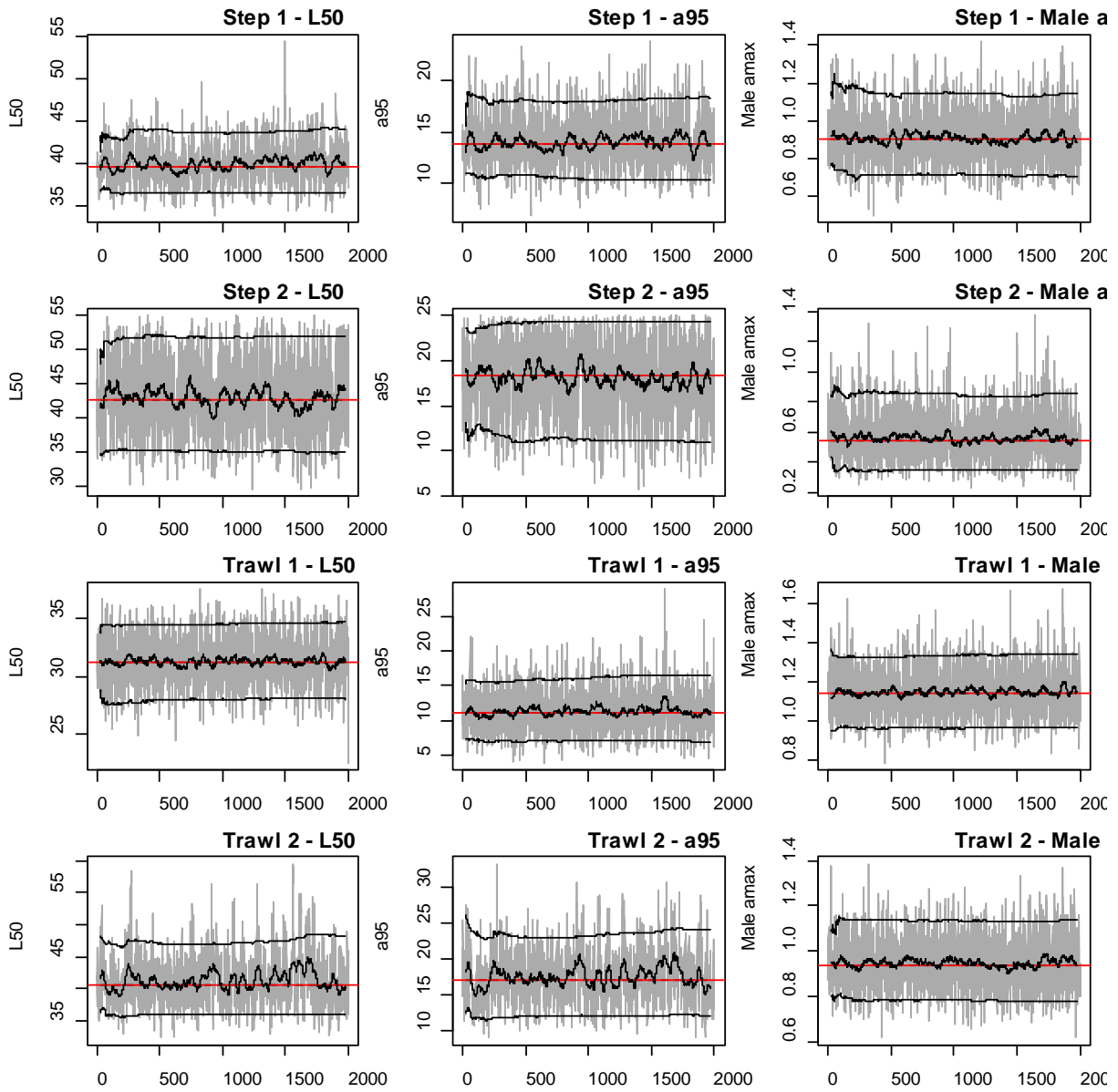
A10. 23: MCMC traces for B_0 and cumulative frequency distributions for three independent MCMC chains for the SCI 2 M02CV25 model.



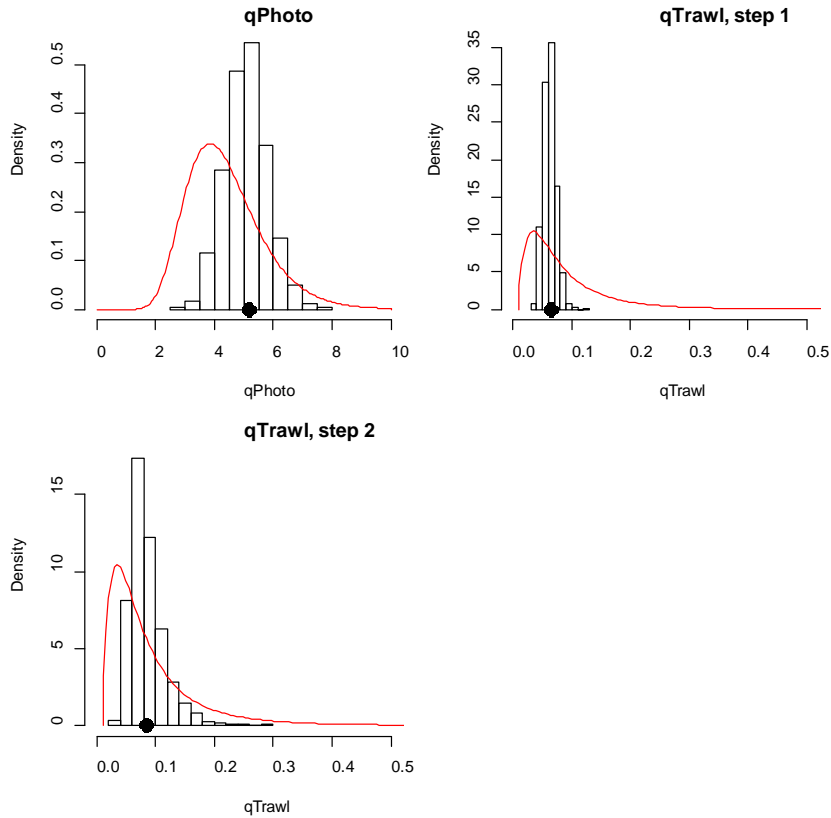
A10. 24: Density plots for B_0 for the SCI 2 M02CV25 model for three independent MCMC chains, with median and 95% confidence intervals.



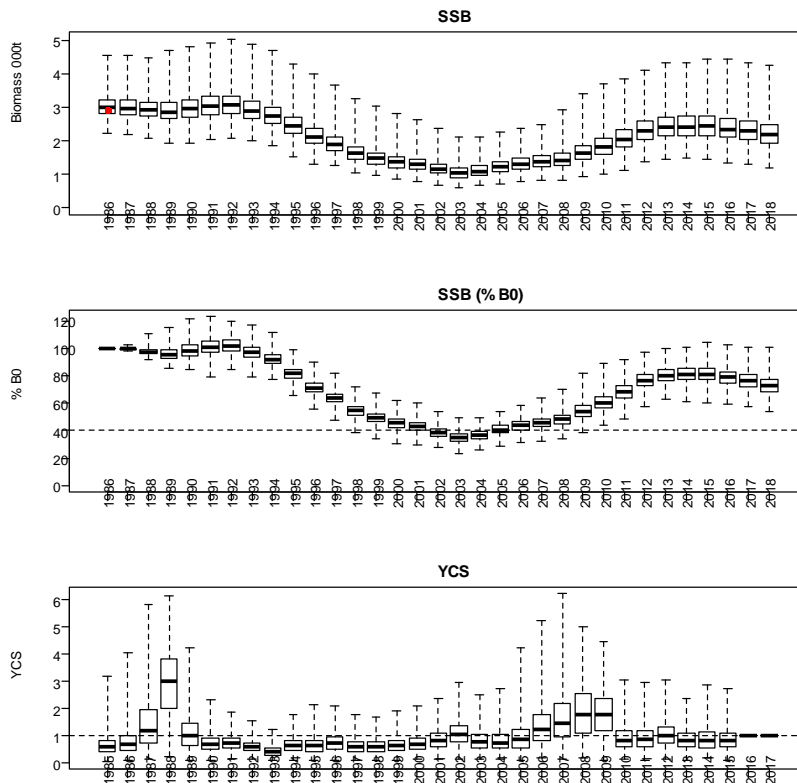
A10. 25: MCMC traces for R_0 , catchability, and growth terms for the SCI 2 M02CV25 model.



A10. 26: MCMC traces for selectivity terms for the SCI 2 M02CV25 model.

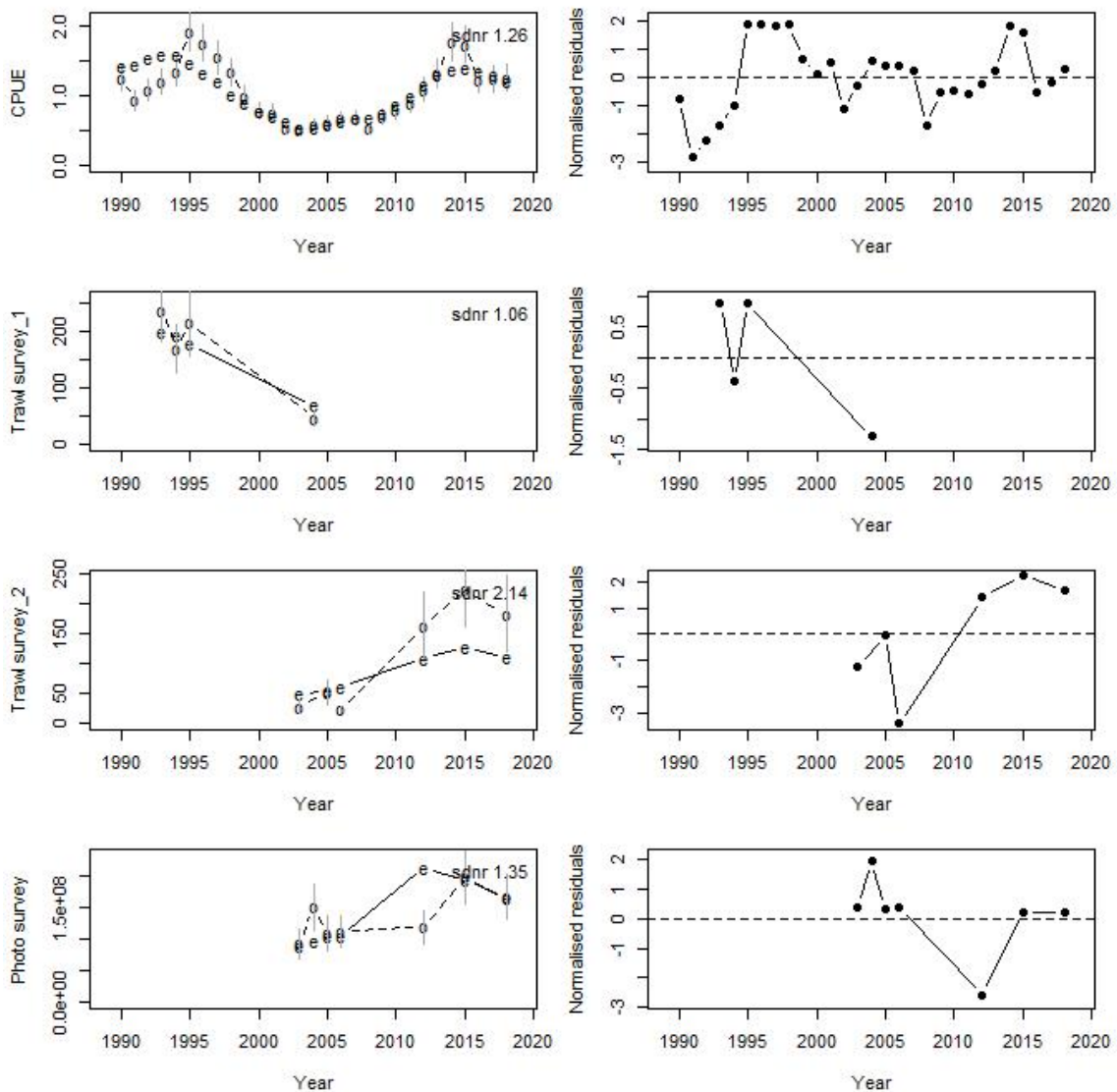


A10. 27: Marginal posterior distributions (histograms), MPD estimates (solid symbols), and distributions of priors (lines) for catchability terms for the SCI 2 M02CV25 model.

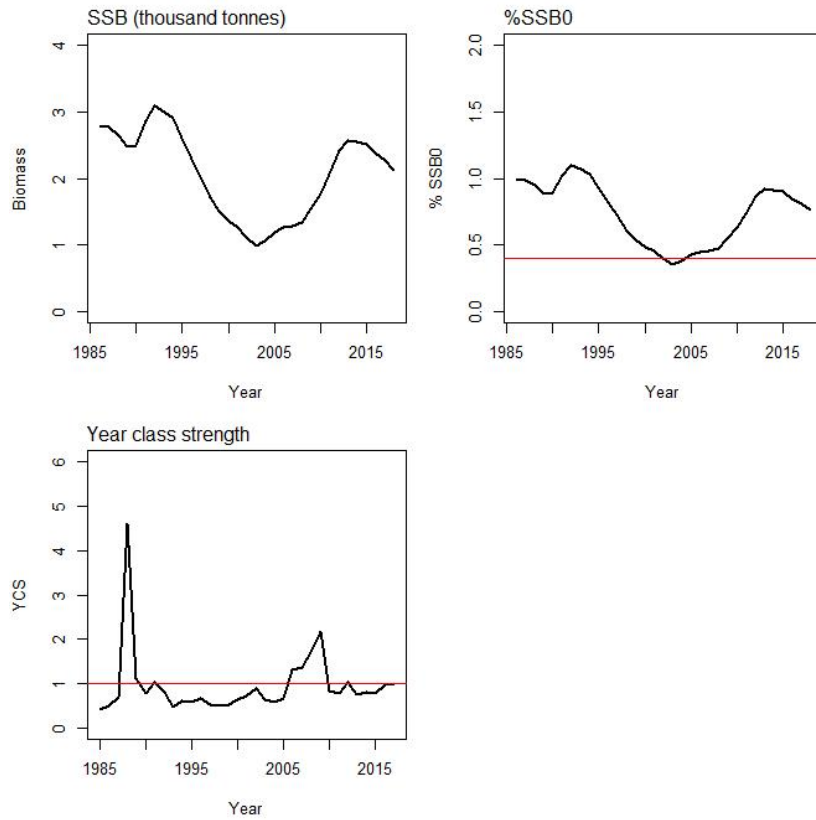


A10. 28: Posterior trajectory of SSB, SSB/SSB₀, and YCS for the SCI 2 M02CV25 model. Red dot represents MPD estimate of B₀.

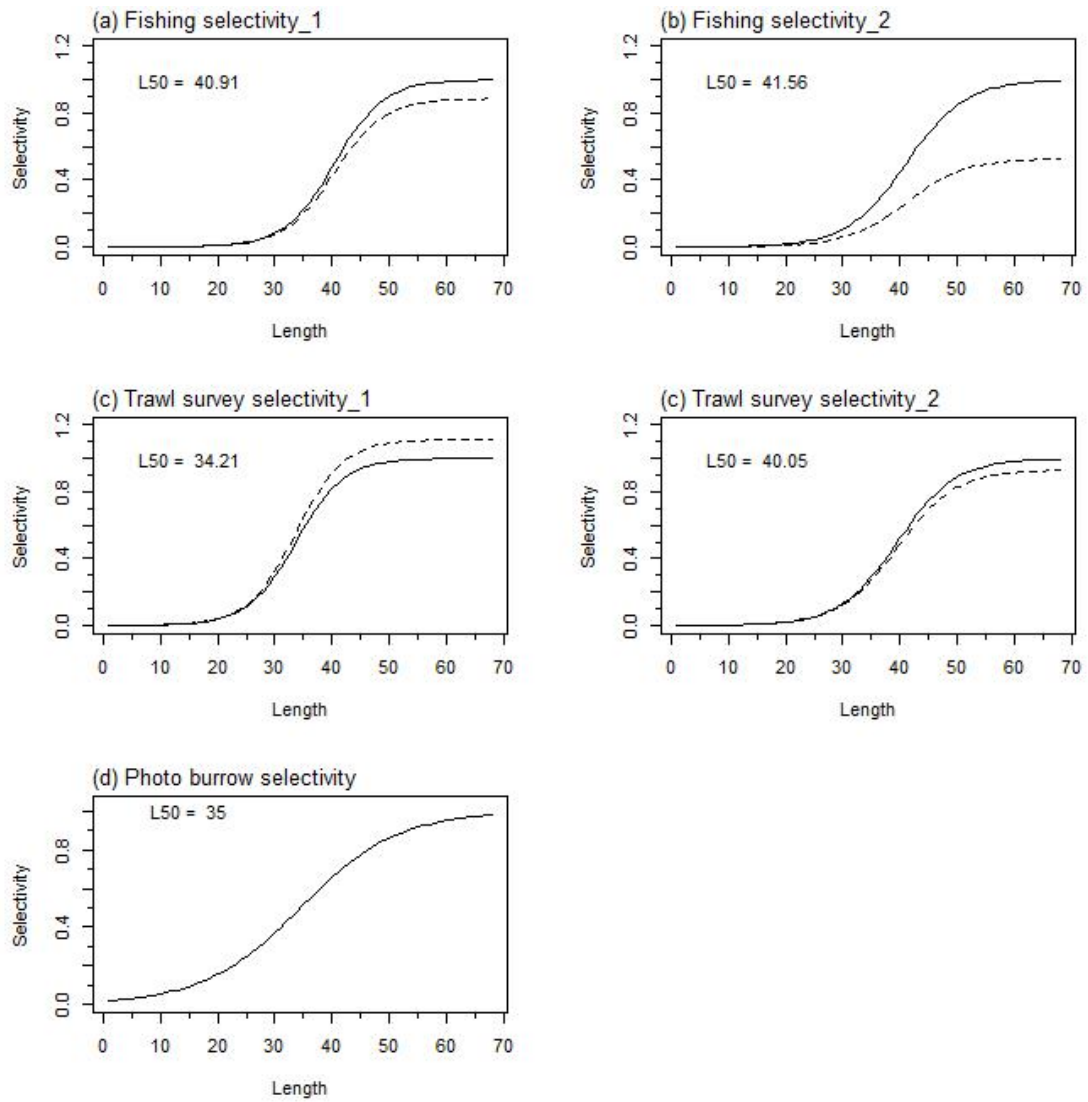
APPENDIX 11. SCI 2 M025CV15 model plots ($M=0.25$, $CV=0.15$)



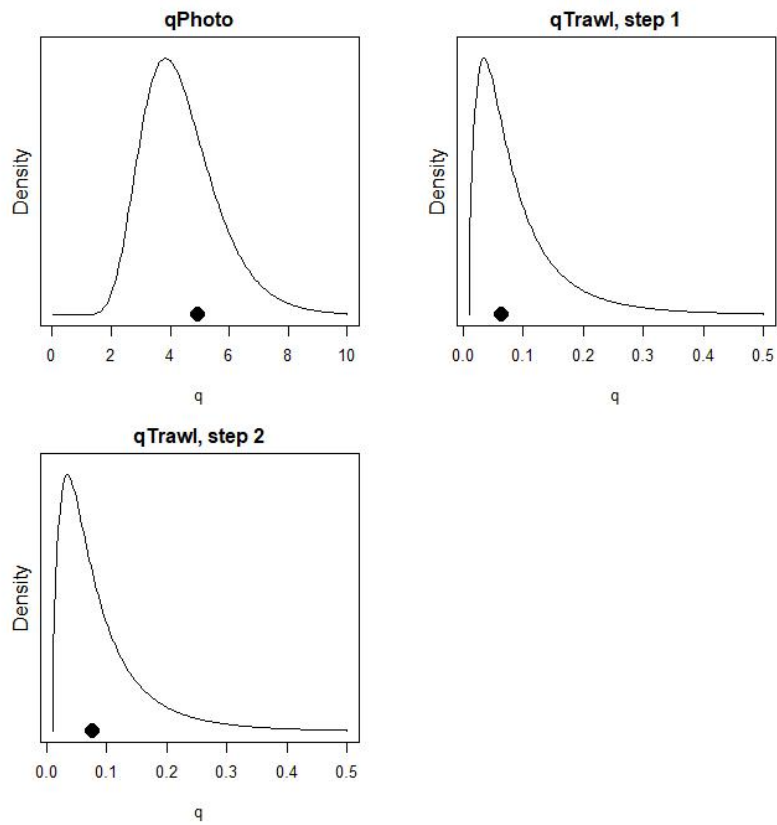
A11. 1: Fits to abundance indices (left column) and normalised residuals (right column) for standardised CPUE index (top row) trawl survey biomass index time step 1 (second row), trawl survey biomass index time step 2 (third row), and photo survey abundance index (fourth row) for the SCI 2 M025CV15 model.



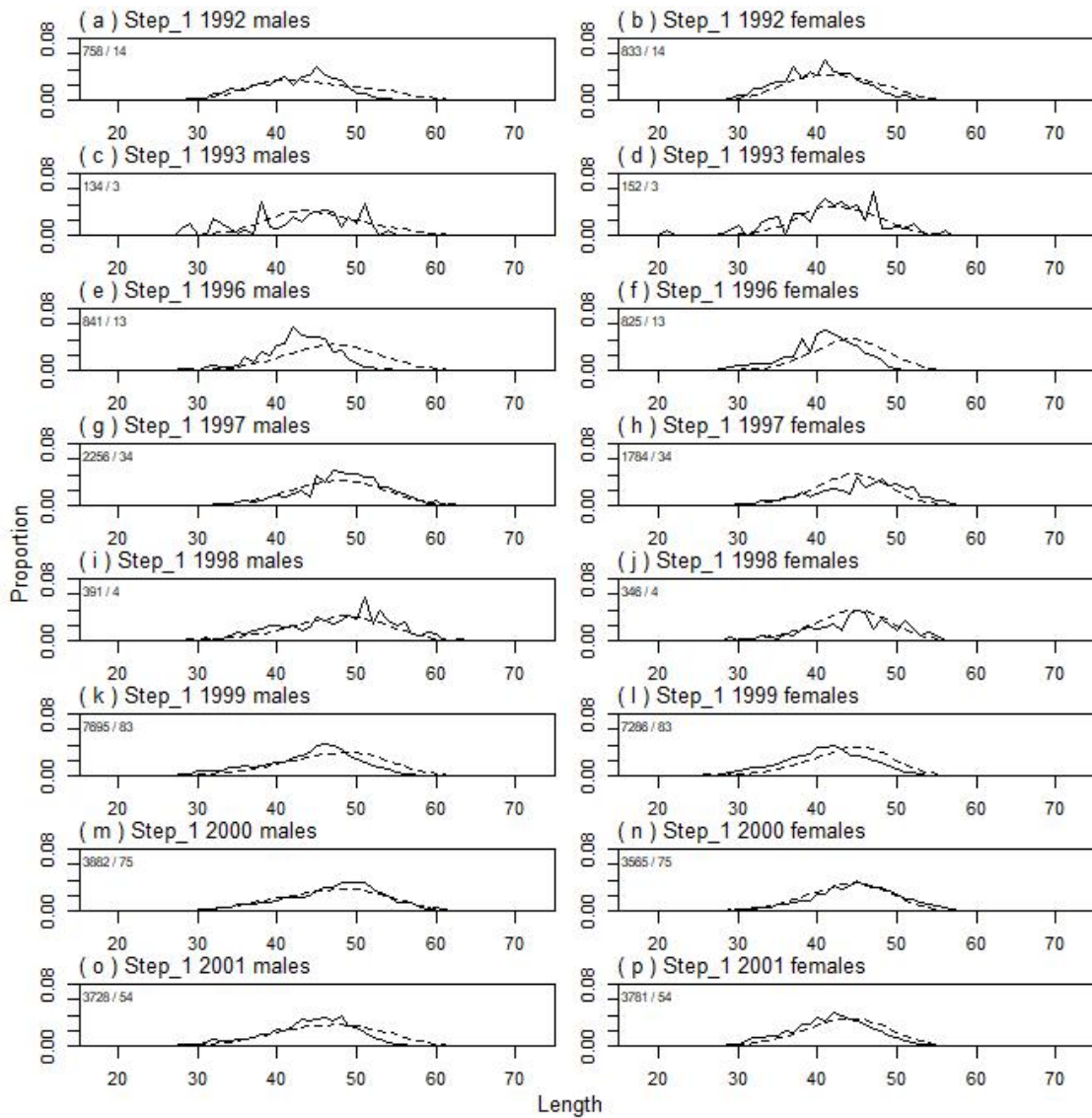
A11. 2: Spawning stock biomass trajectory (upper left), stock status (upper right), and year class strength (lower left) for the SCI 2 M025CV15 model.



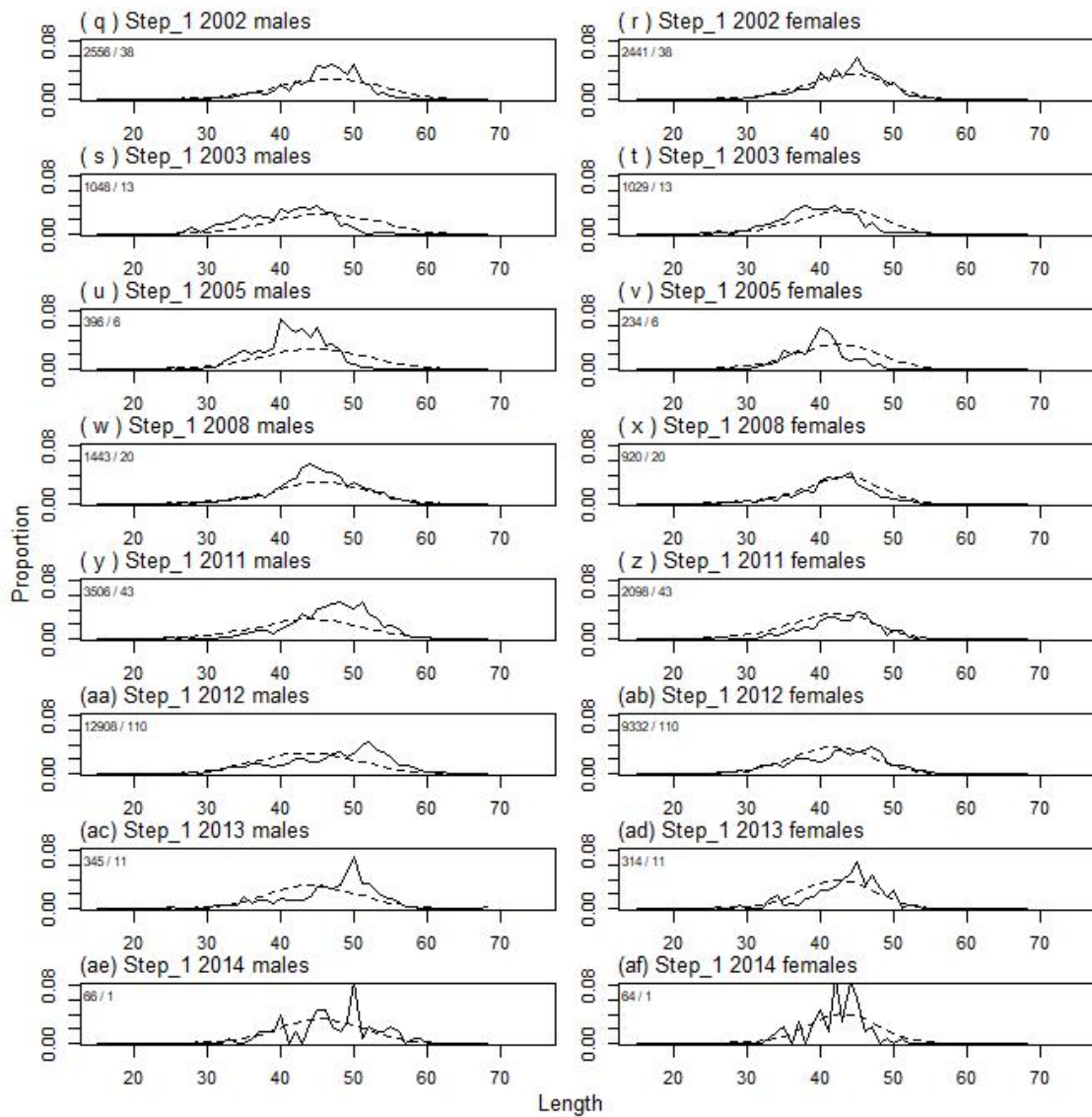
A11. 3: Fishery and survey selectivity curves for the SCI 2 M025CV15 model. Solid line – females, dotted line – males. The scampi burrow index is not sexed, and a single selectivity applies.



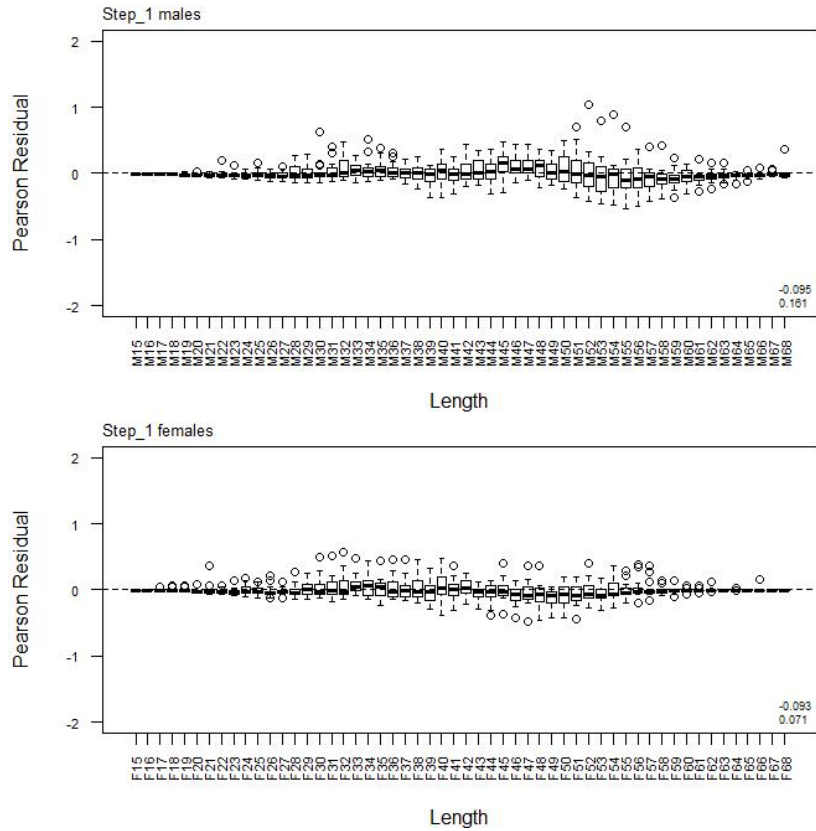
A11. 4: Catchability estimates from MPD model run, plotted in relation to prior distribution for the SCI 2 M025CV15 model.



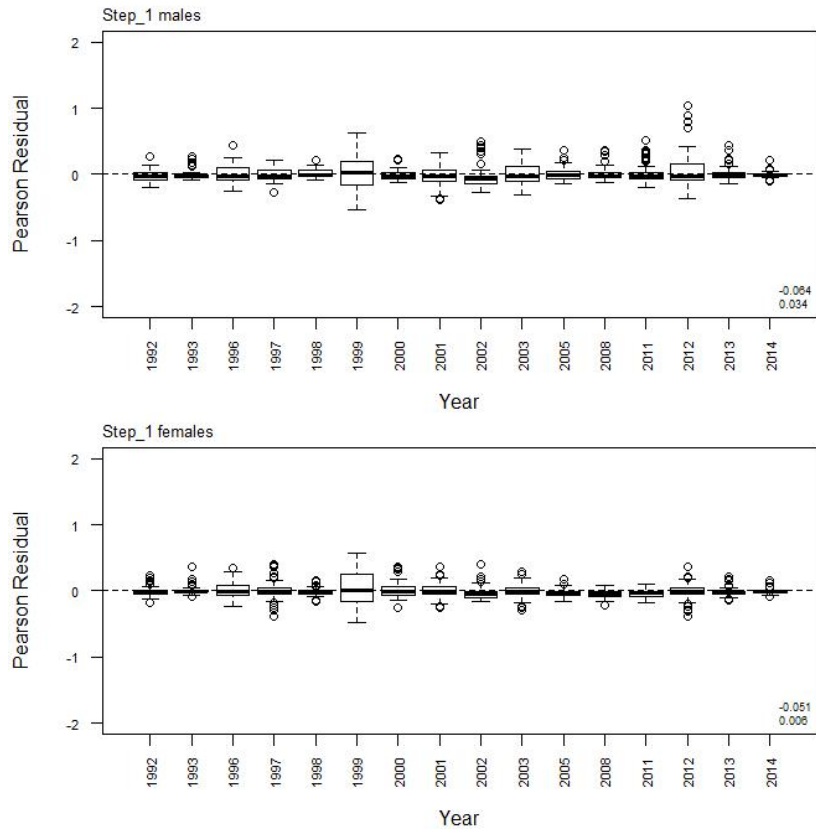
A11. 5: Observed (solid line) and fitted (dashed line) length frequency distributions from observer samples, time step 1 for SCI 2 M025CV15 model. Numbers in top left corner of each plot represent number of scampi measured / number of events sampled.



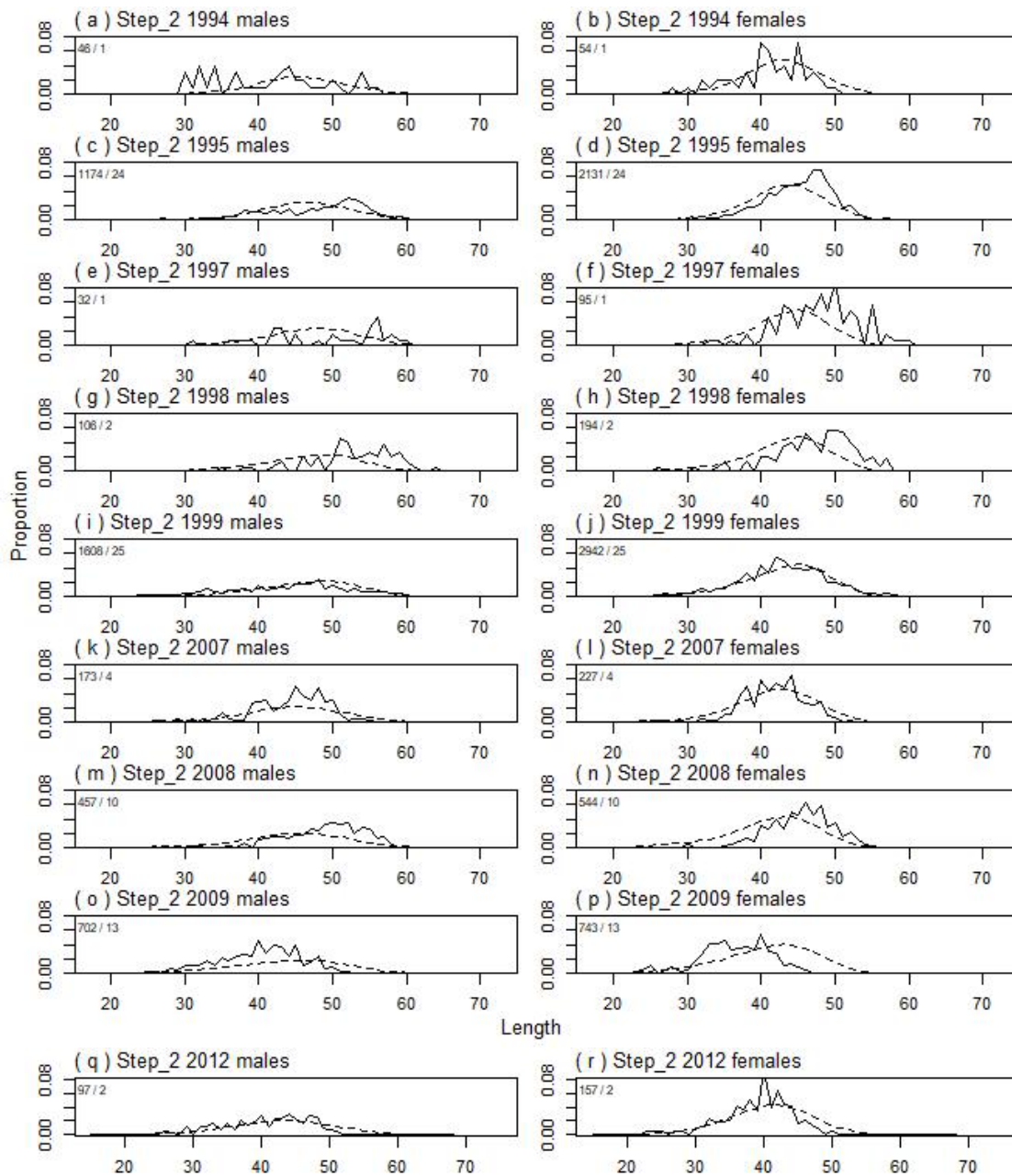
A11. 5(continued): Observed (solid line) and fitted (dashed line) length frequency distributions from observer samples, time step 1 for SCI 2 M025CV15 model. Numbers in top left corner of each plot represent number of scampi measured / number of events sampled.



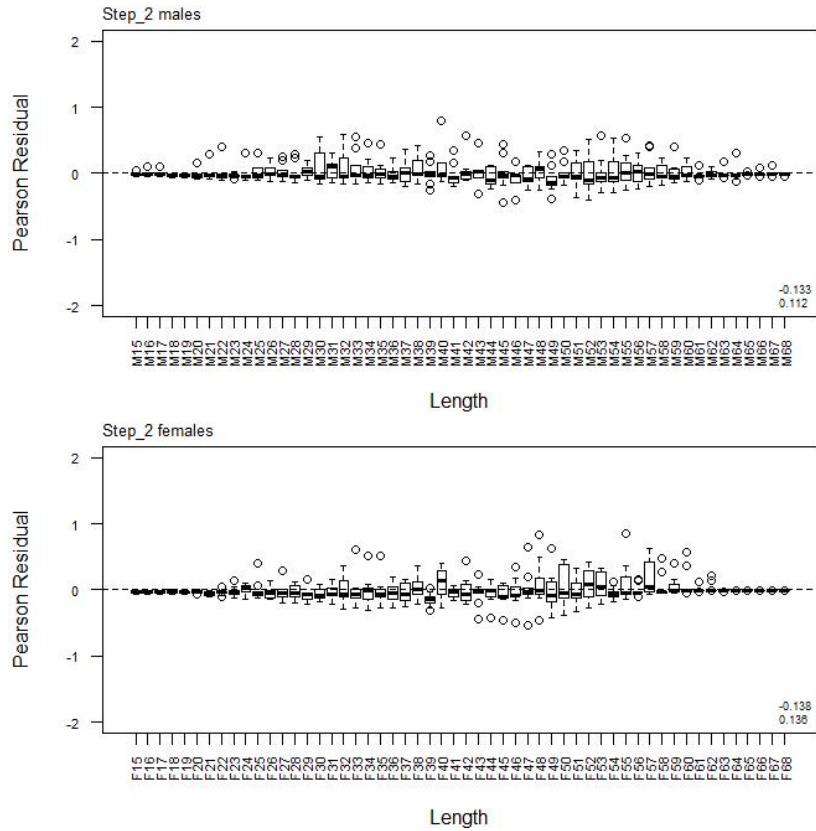
A11. 6: Box plots of Pearson residuals from the fit to length frequency distributions by length from observer sampling by sex for time step 1 for SCI 2 M025CV15 model.



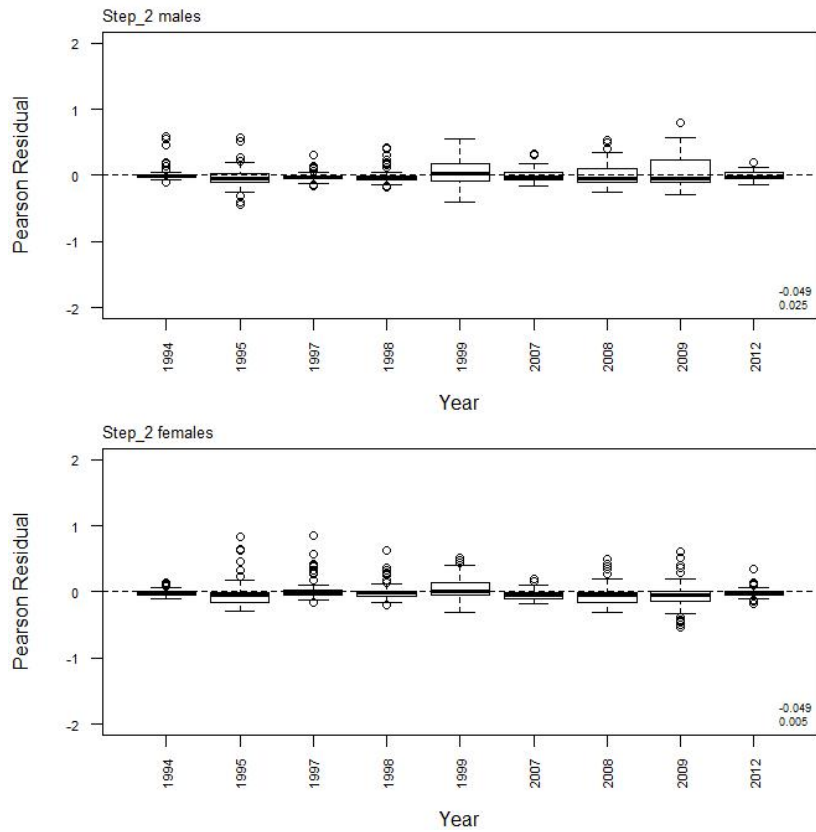
A11. 7: Box plots of Pearson residuals from the fit to length frequency distributions by year from observer sampling by sex for time step 1 for SCI 2 M025CV15 model.



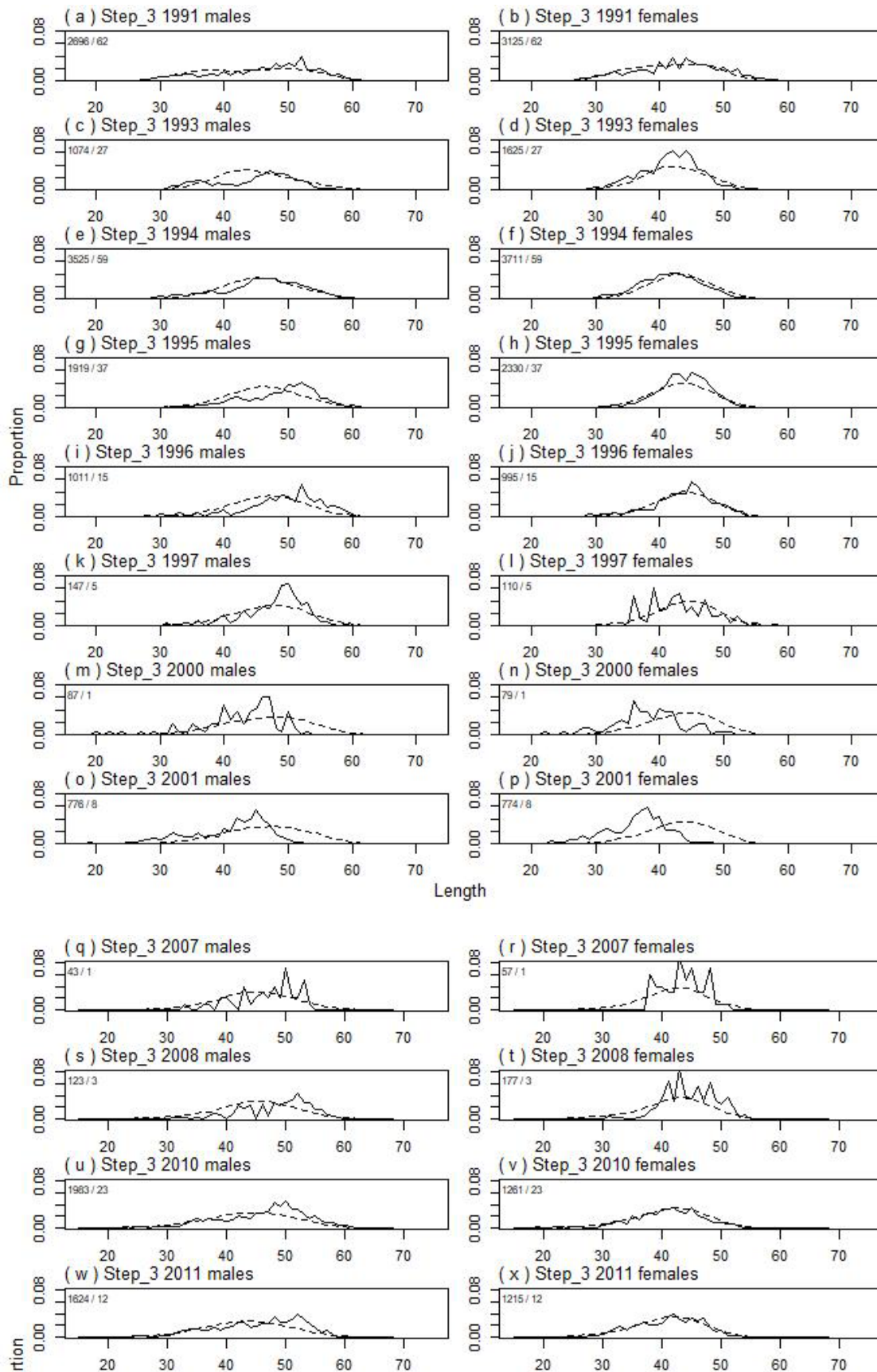
A11. 8: Observed (solid line) and fitted (dashed line) length frequency distributions from observer samples, time step 2 for SCI 2 M025CV15 model. Numbers in top left corner of each plot represent number of scampi measured / number of events sampled.



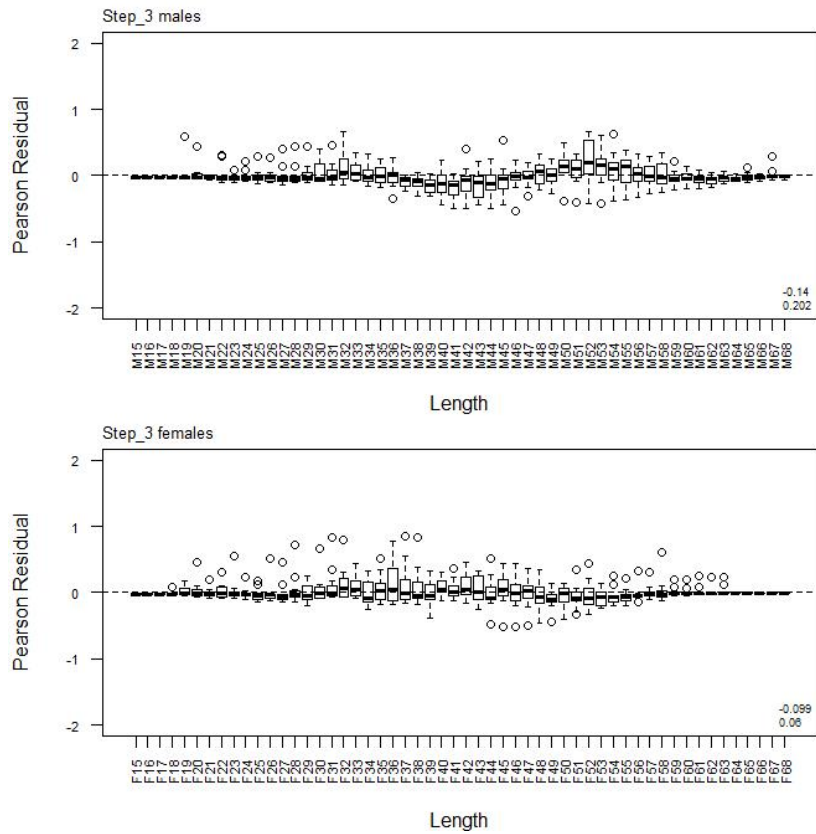
A11. 9: Box plots of Pearson residuals from the fit to length frequency distributions by length from observer sampling by sex for time step 2 for SCI 2 M025CV15 model.



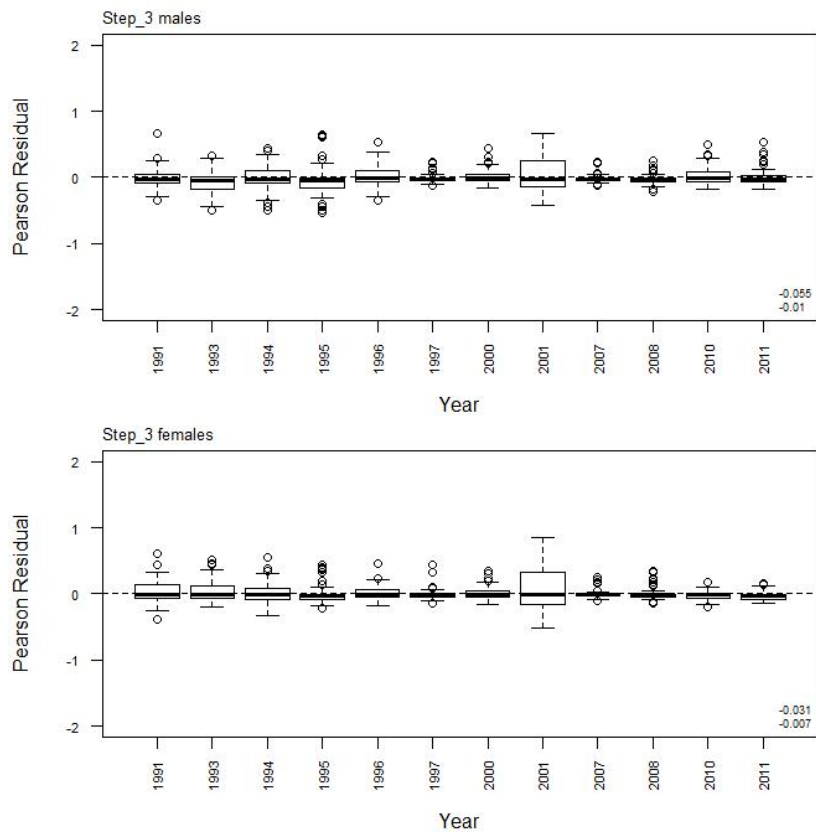
A11. 10: Box plots of Pearson residuals from the fit to length frequency distributions by year from observer sampling by sex for time step 2 for SCI 1 M025CV15 model.



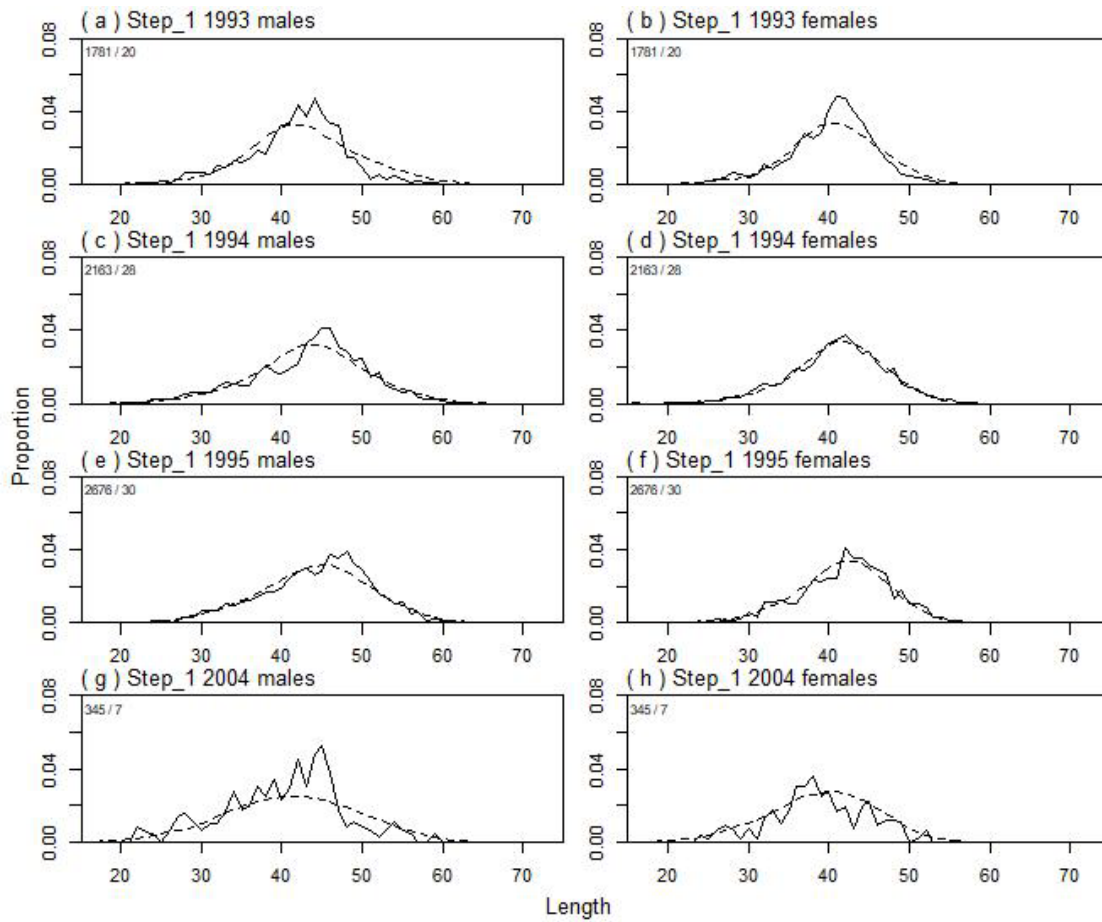
A11. 11: Observed (solid line) and fitted (dashed line) length frequency distributions from observer samples, time step 3 for SCI 2 M025CV15 model. Numbers in top left corner of each plot represent number of scampi measured / number of events sampled.



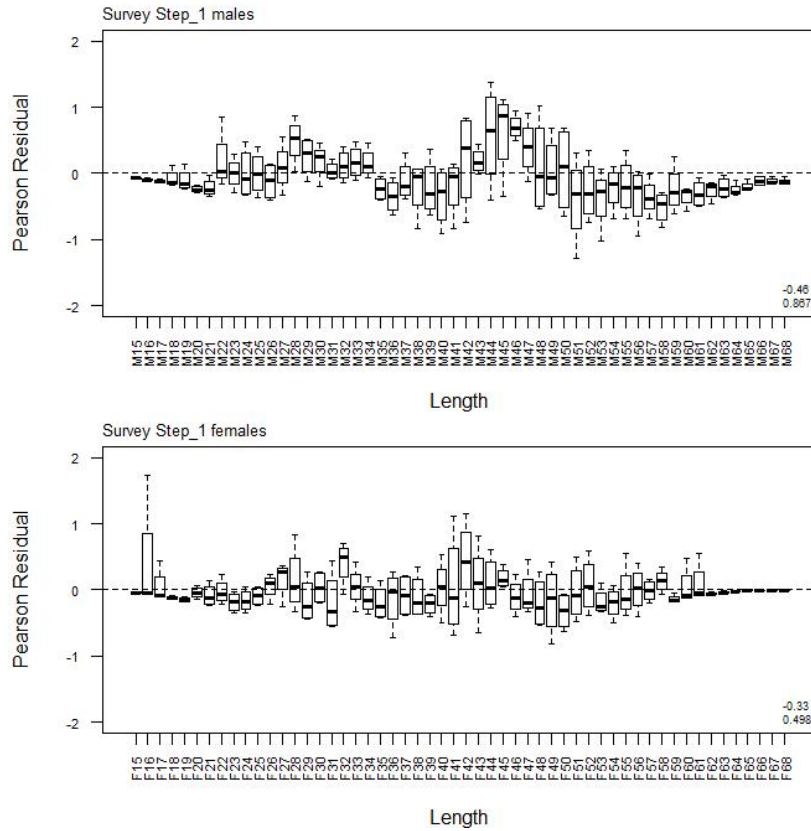
A11. 12: Box plots of Pearson residuals from the fit to length frequency distributions by length from observer sampling by sex for time step 3 for SCI 2 M025CV15 model.



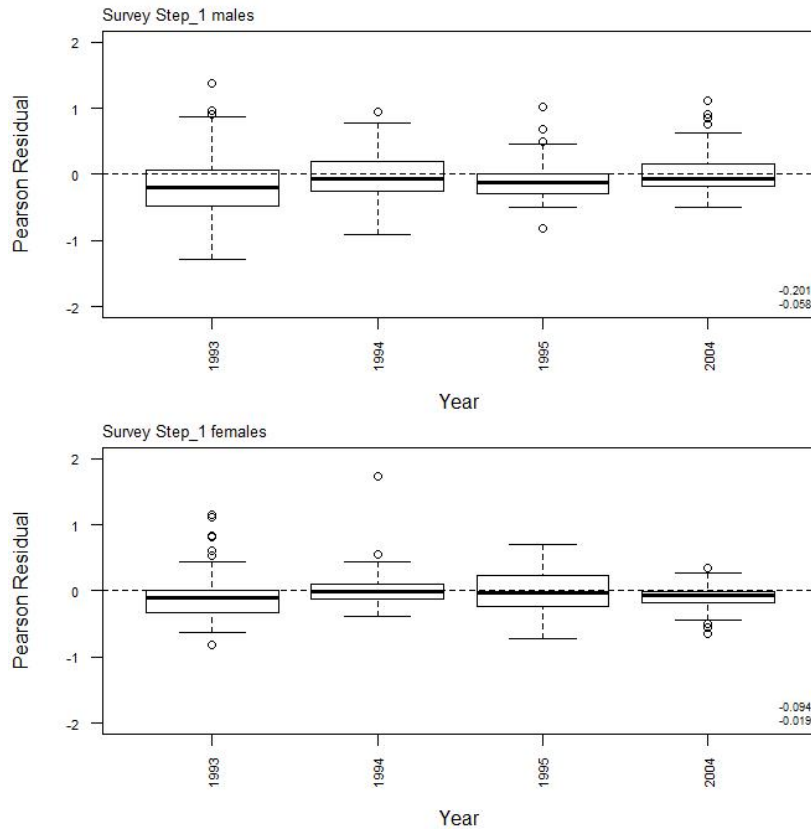
A11. 13: Box plots of Pearson residuals from the fit to length frequency distributions by year from observer sampling by sex for time step 3 for SCI 2 M025CV15 model.



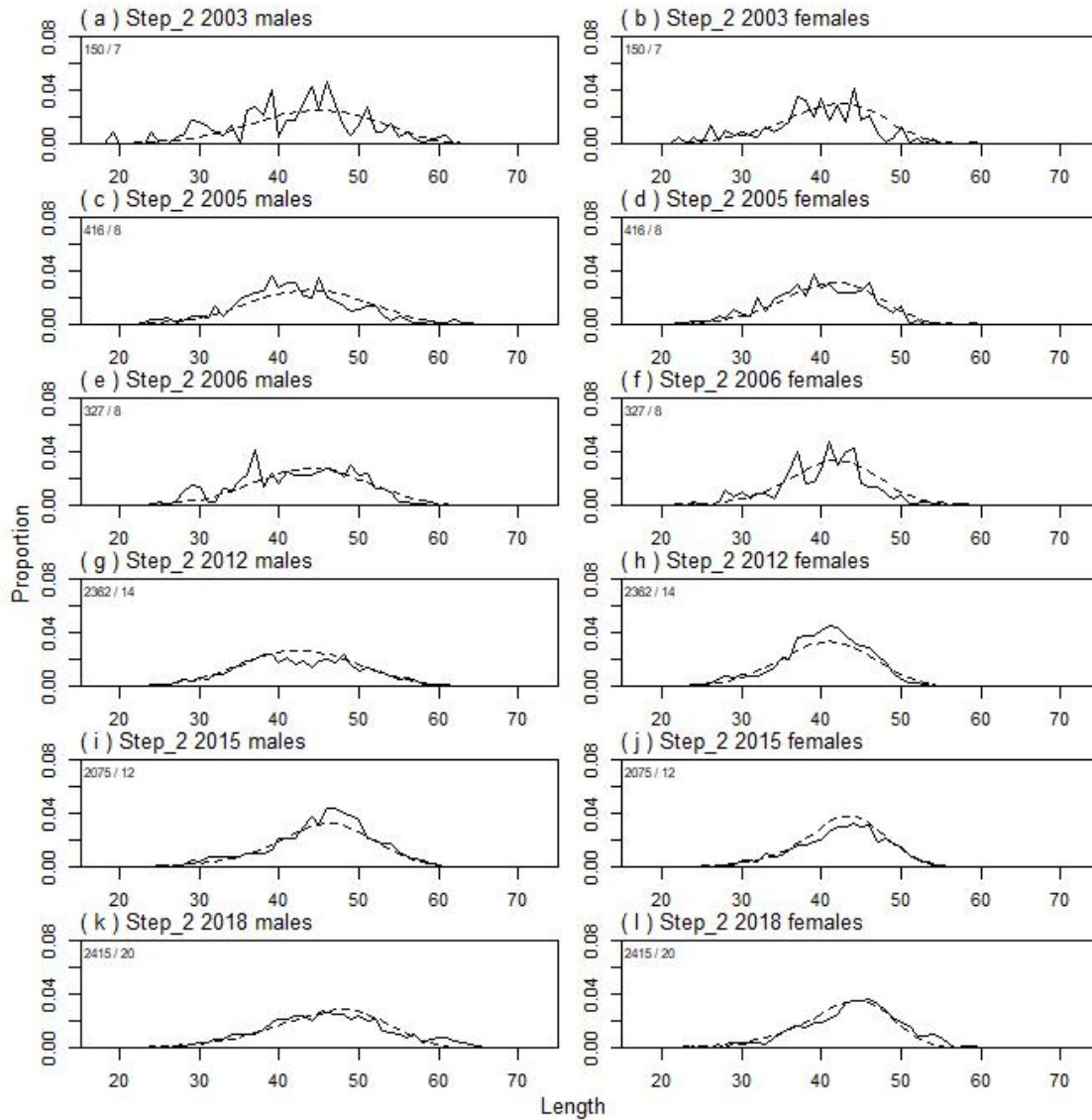
A11. 14: Observed (solid line) and fitted (dashed line) length frequency distributions from trawl survey samples for time step 1, SCI 2 M025CV15 model. Numbers in top left corner of each plot represent number of scampi measured / number of events sampled.



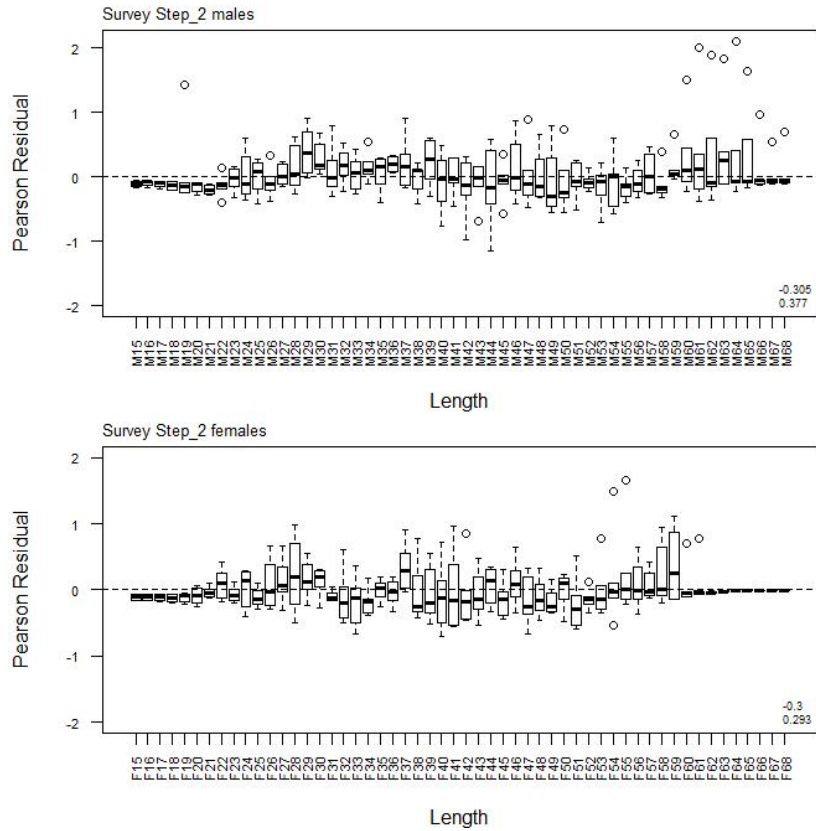
A11. 15: Box plots of Pearson residuals from the fit to length frequency distributions by length from trawl survey sampling by sex for time step 1, SCI 2 M025CV15 model.



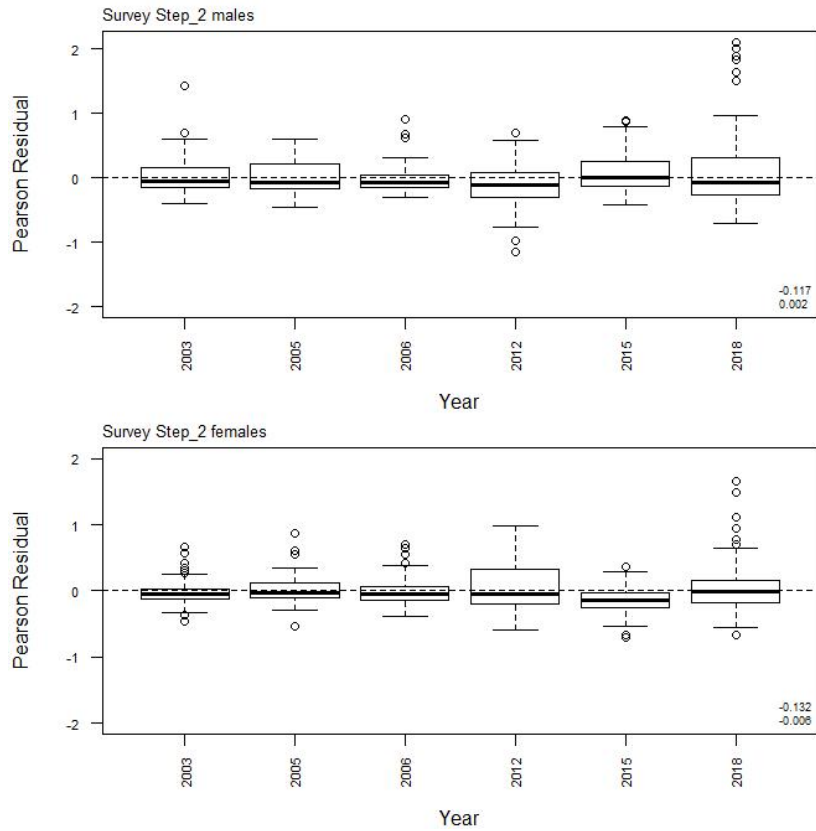
A11. 16: Box plots of Pearson residuals from the fit to length frequency distributions by year from trawl survey sampling by sex for time step 1, SCI 2 M025CV15 model.



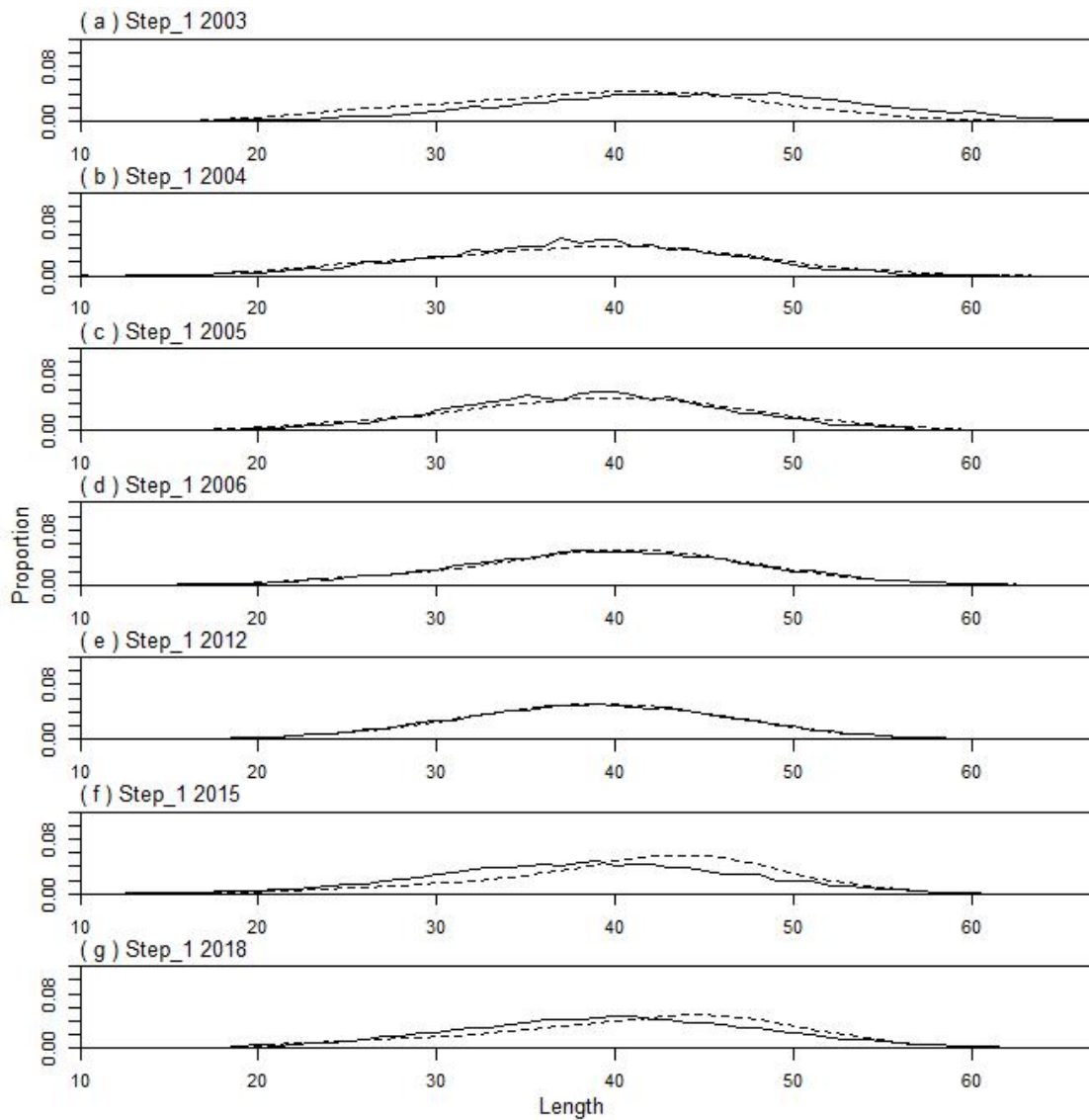
A11. 17: Observed (solid line) and fitted (dashed line) length frequency distributions from trawl survey samples for time step 2, SCI 2 M025CV15 model. Numbers in top left corner of each plot represent number of scampi measured / number of events sampled.



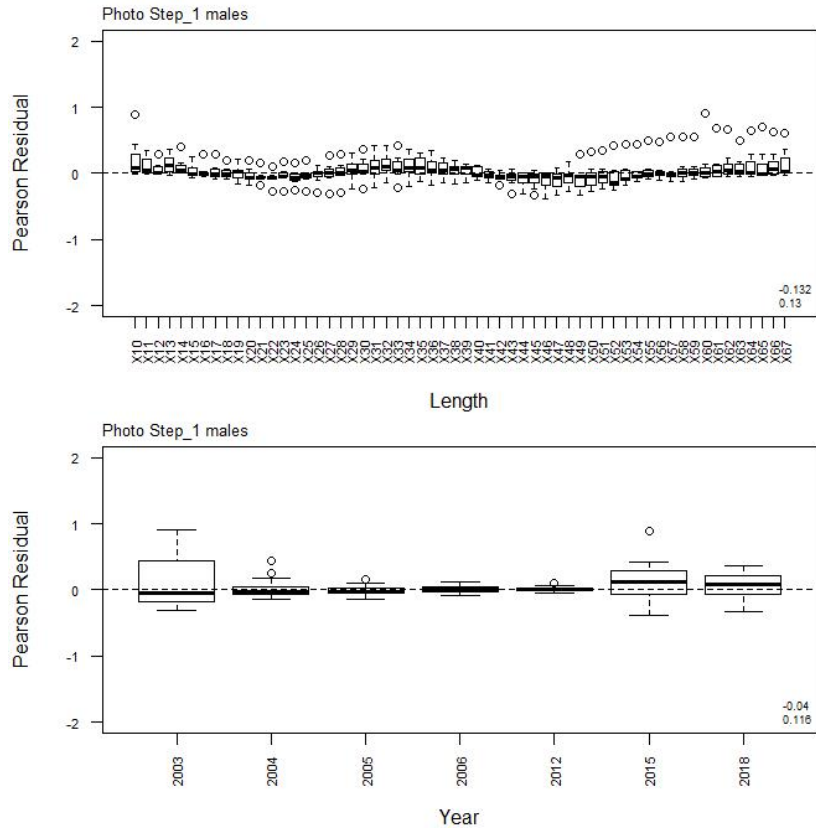
A11. 18: Box plots of Pearson residuals from the fit to length frequency distributions by length from trawl survey sampling by sex for time step 2, SCI 2 M025CV15 model.



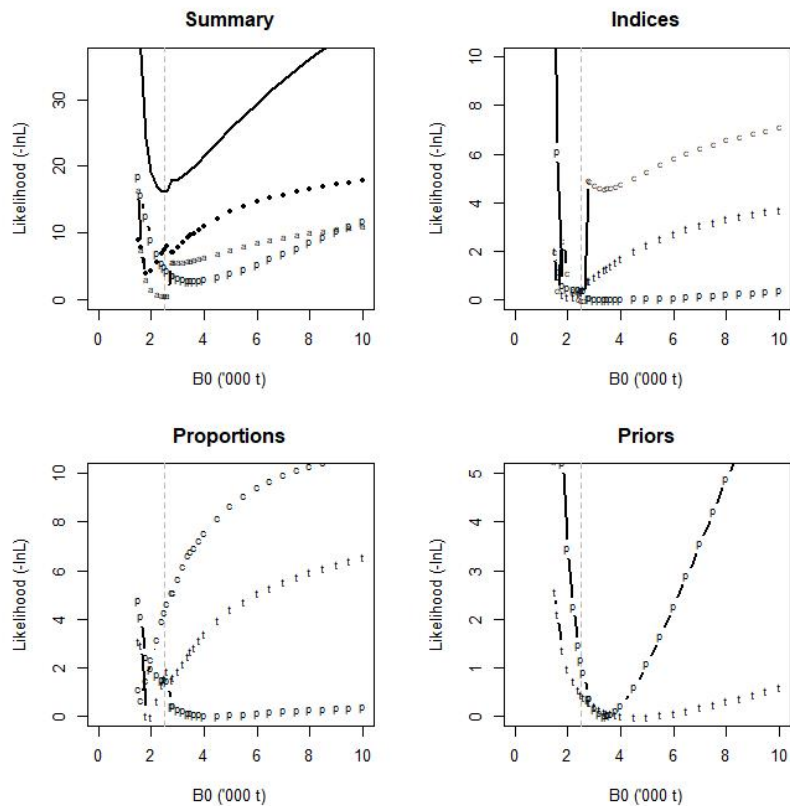
A11. 19: Box plots of Pearson residuals from the fit to length frequency distributions by year from trawl survey sampling by sex for time step 2, SCI 2 M025CV15 model.



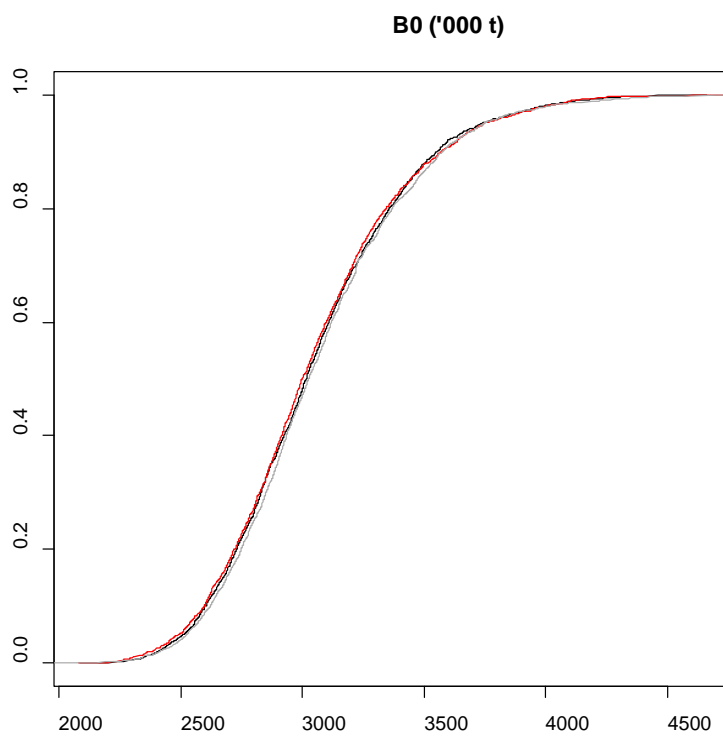
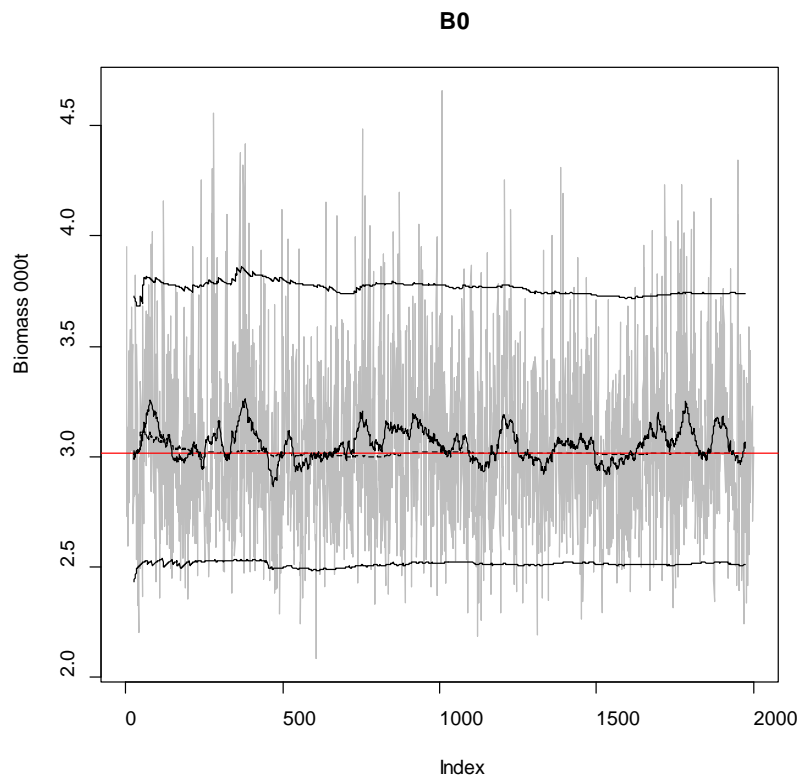
A11. 20: Observed (solid line) and fitted (dashed line) length frequency distributions from photo survey samples for SCI 2 M025CV15 model.



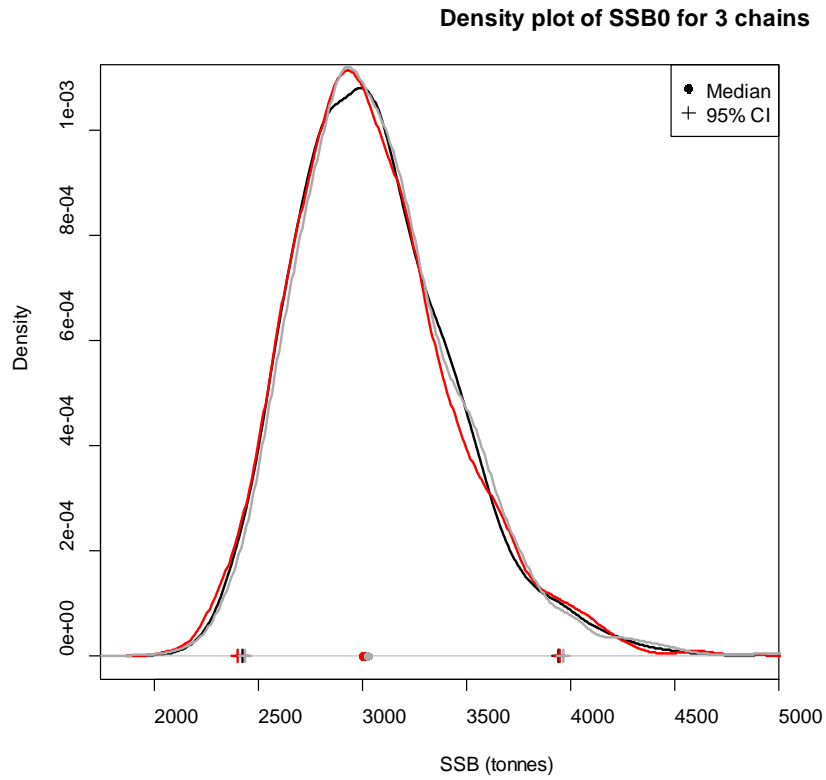
A11. 21: Box plots of Pearson residuals from the fit to length frequency distributions by length (top plot) and year (bottom plot) from photo survey sampling by sex for SCI 2 M025CV15 model.



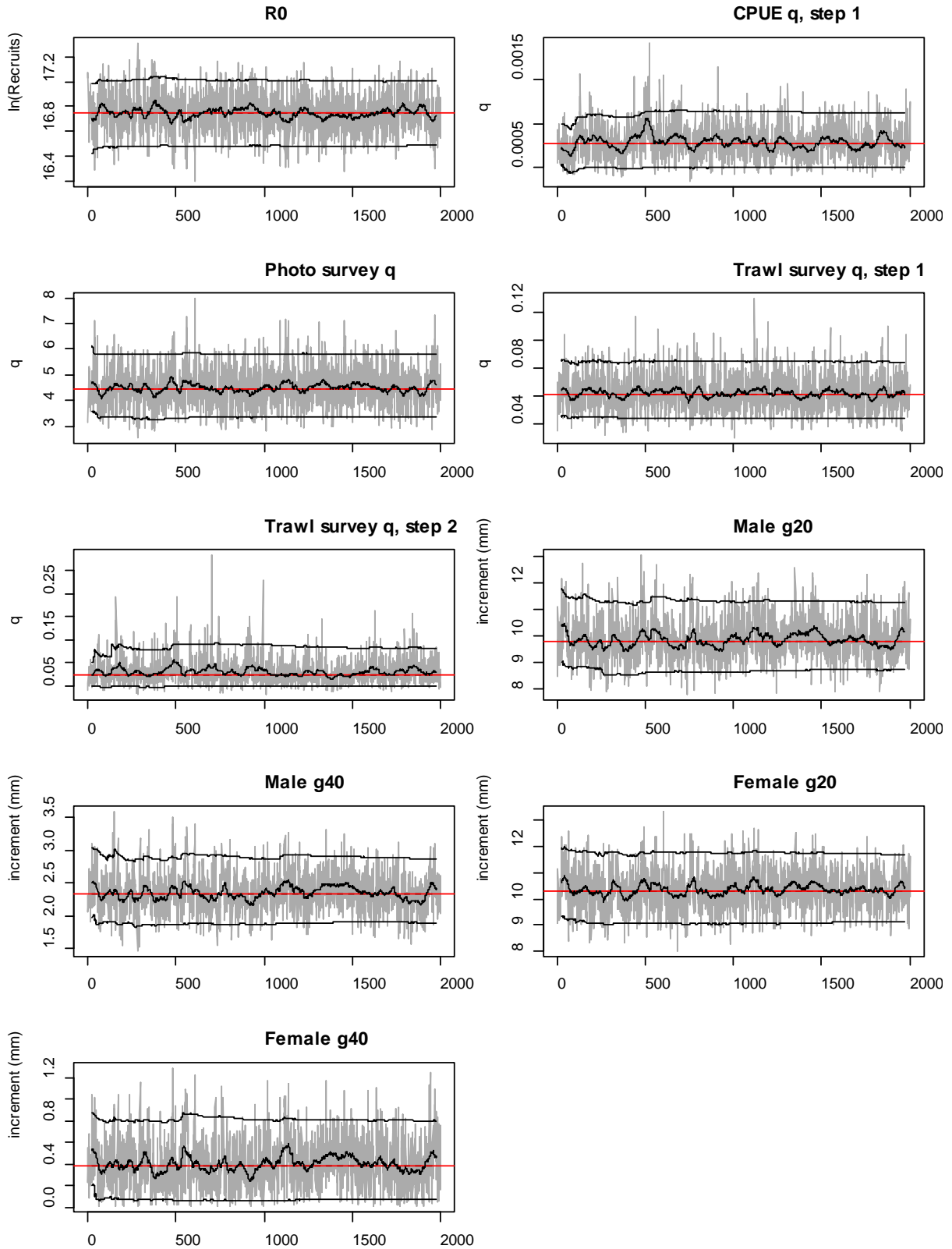
A11. 22: Likelihood profiles for model M025CV15 for SCI 2 when B_0 is fixed in the model. Figures show profiles for main priors (top left, p – priors, a – abundance indices, • – proportions at length), abundance indices (top right, t – trawl survey step, c – CPUE, p – photo survey), proportion at length data (bottom left, p – photo, t – trawl, c – observer) and priors (bottom right, p – q -Photo, t – q -Trawl).



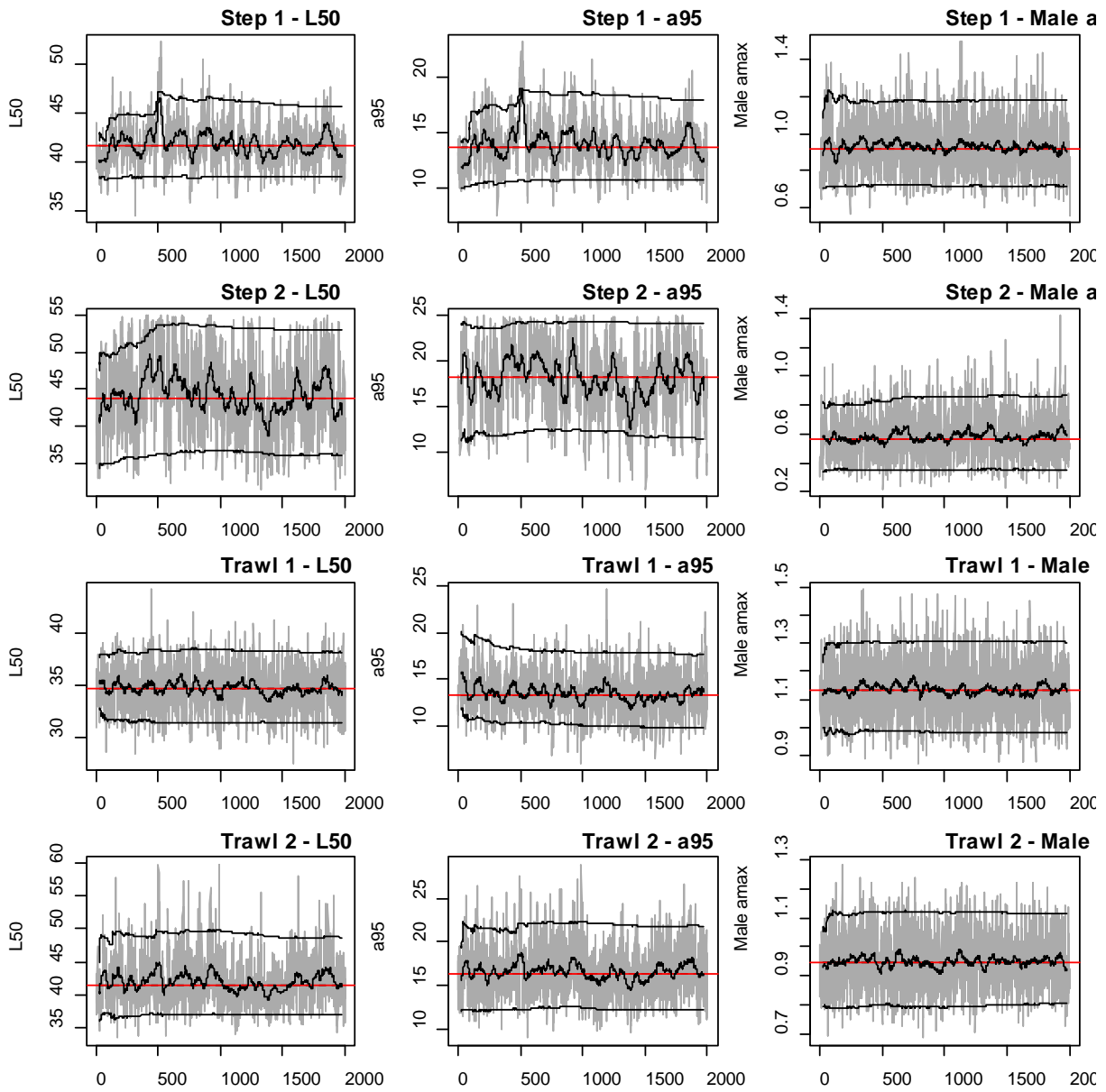
A11. 23: MCMC traces for B_0 and cumulative frequency distributions for three independent MCMC chains for the SCI 2 M025CV15 model.



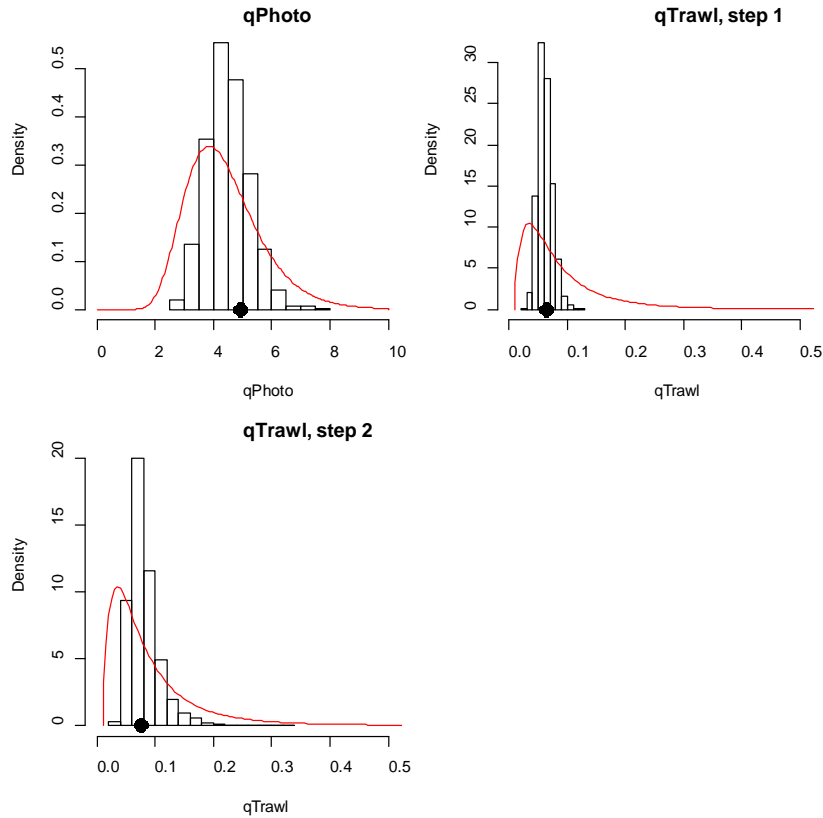
A11. 24: Density plots for B_0 for the SCI 2 M025CV15 model for three independent MCMC chains, with median and 95% confidence intervals.



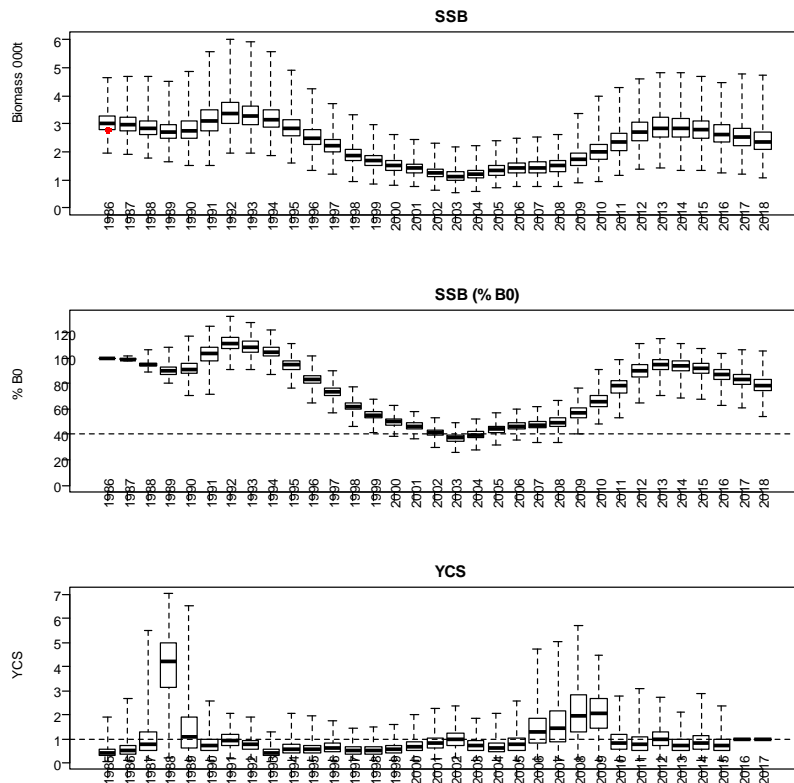
A11. 25: MCMC traces for R_0 , catchability, and growth terms for the SCI 2 M025CV15 model.



A11. 26: MCMC traces for selectivity terms for the SCI 2 M025CV15 model.

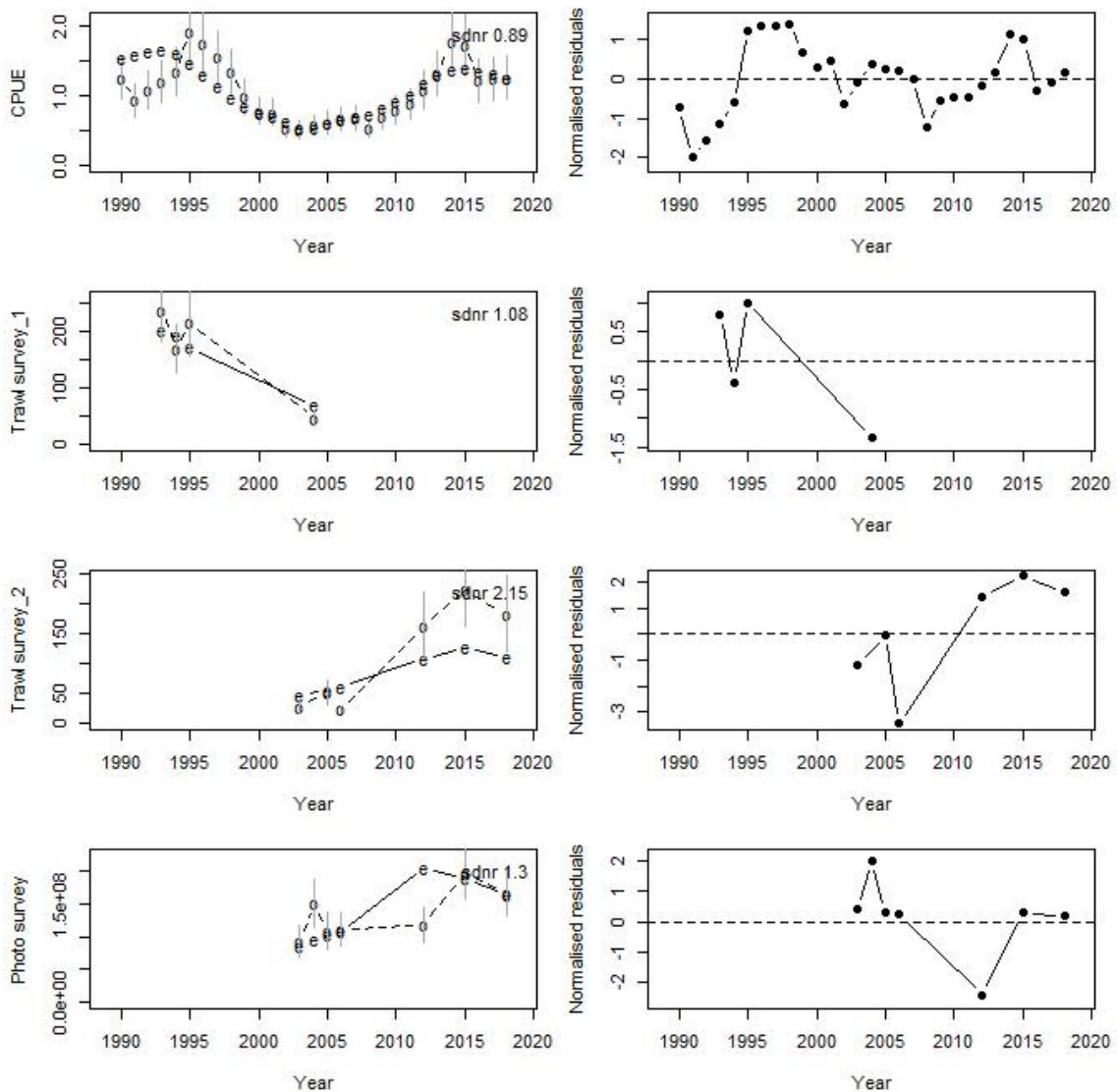


A11. 27: Marginal posterior distributions (histograms), MPD estimates (solid symbols), and distributions of priors (lines) for catchability terms for the SCI 2 M025CV15 model.

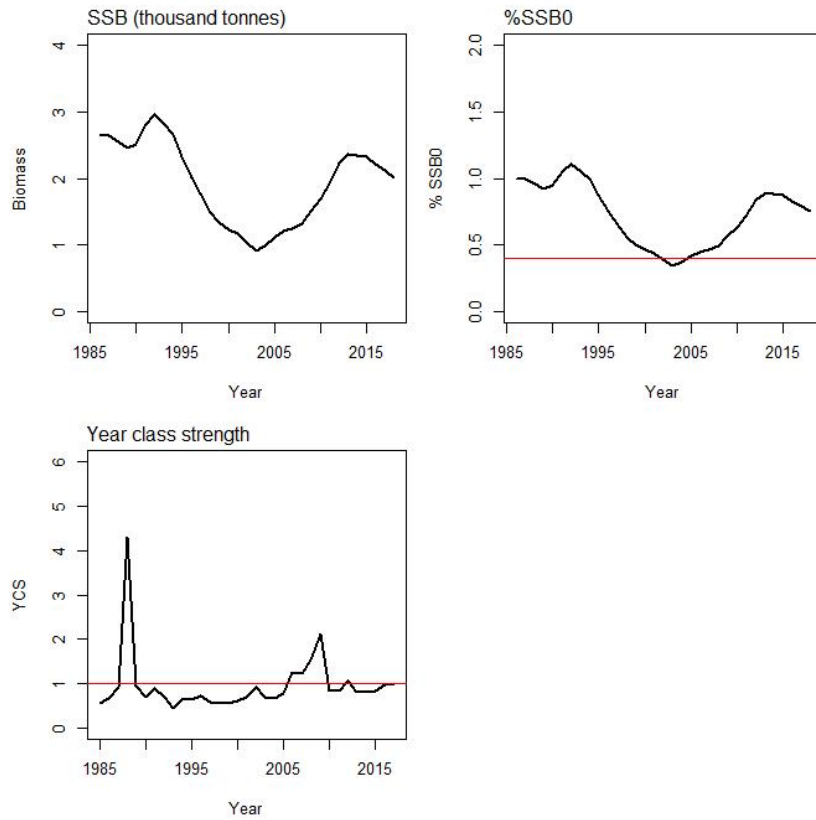


A11. 28: Posterior trajectory of SSB, SSB/SSB₀, and YCS for the SCI 2 M025CV15 model. Red dot represents MPD estimate of B₀.

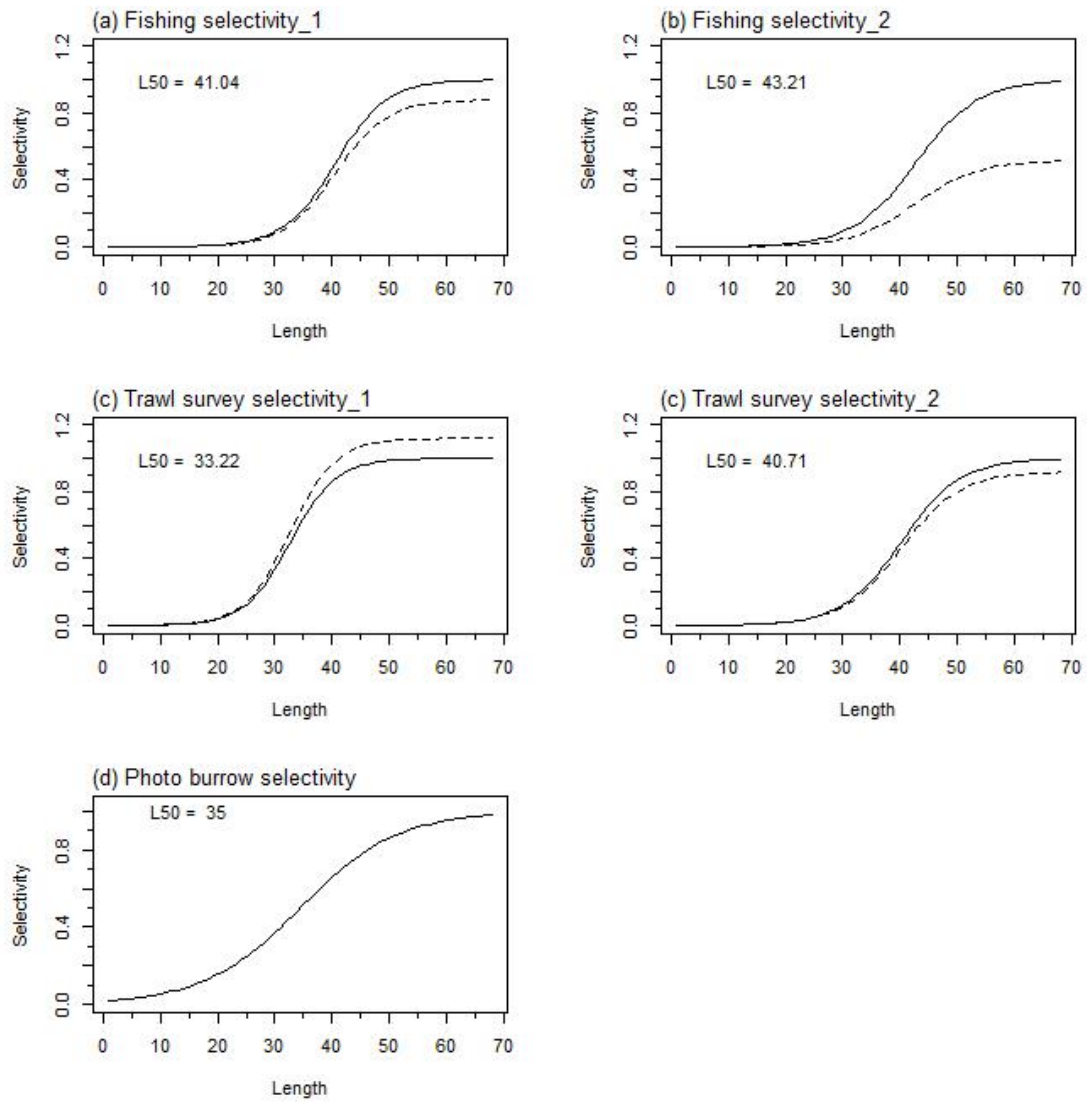
APPENDIX 12. SCI 2 M025CV25 model plots ($M=0.25$, $CV=0.25$)



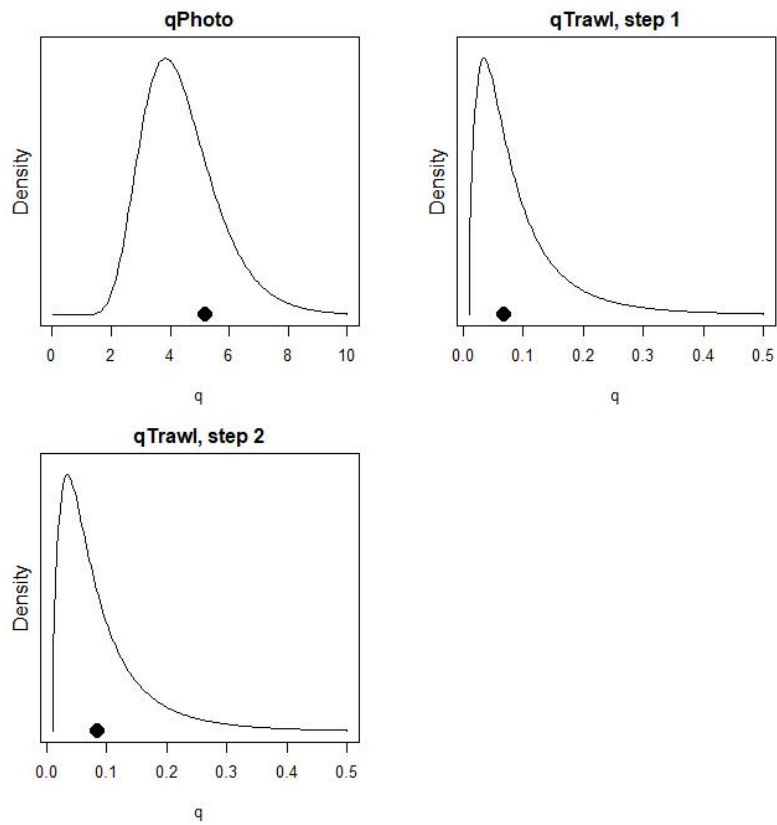
A12. 1: Fits to abundance indices (left column) and normalised residuals (right column) for standardised CPUE index (top row) trawl survey biomass index time step 1 (second row), trawl survey biomass index time step 2 (third row), and photo survey abundance index (fourth row) for the SCI 2 M025CV25 model.



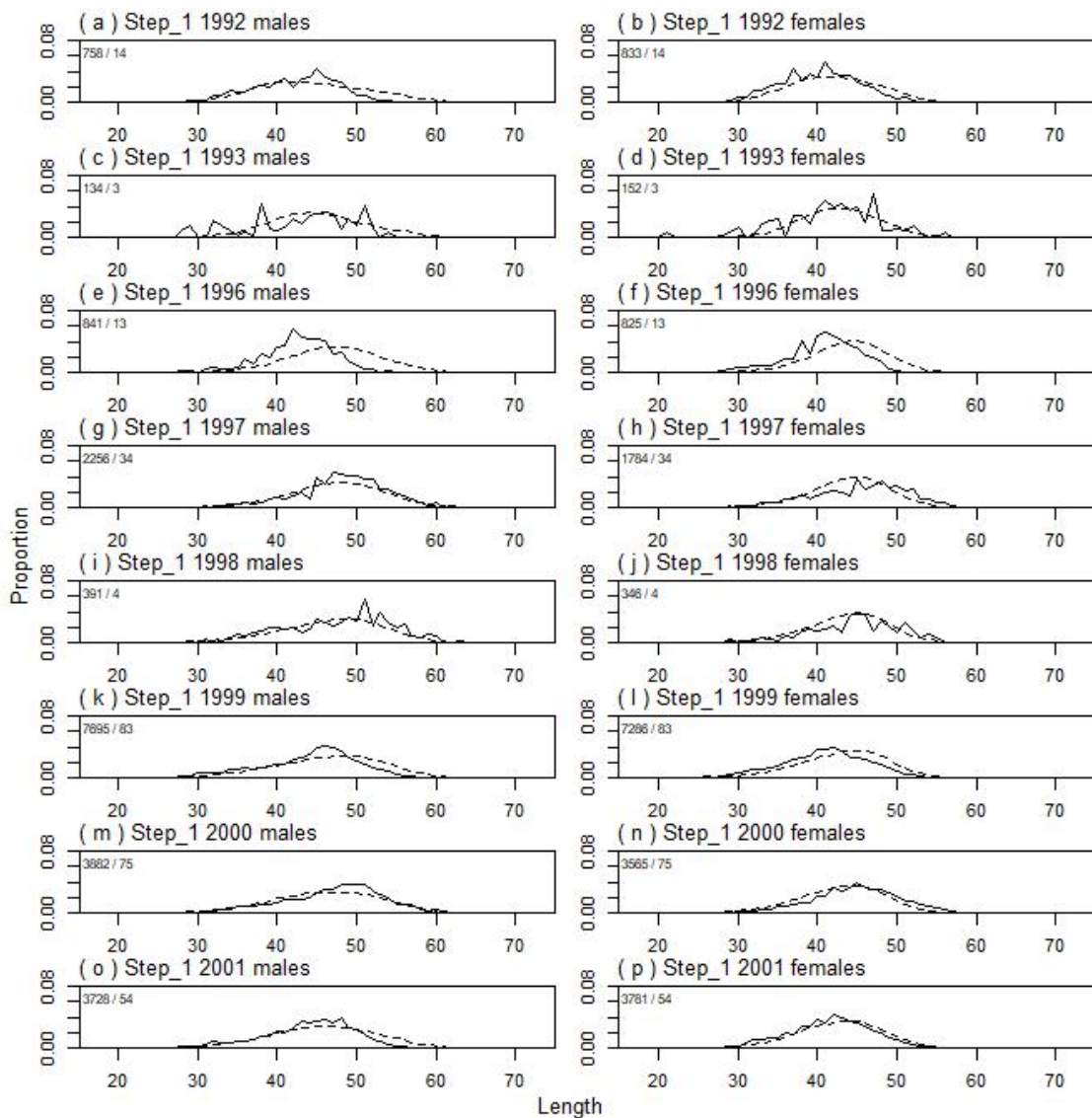
A12. 2: Spawning stock biomass trajectory (upper left), stock status (upper right), and year class strength (lower left) for the SCI 2 M025CV25 model.



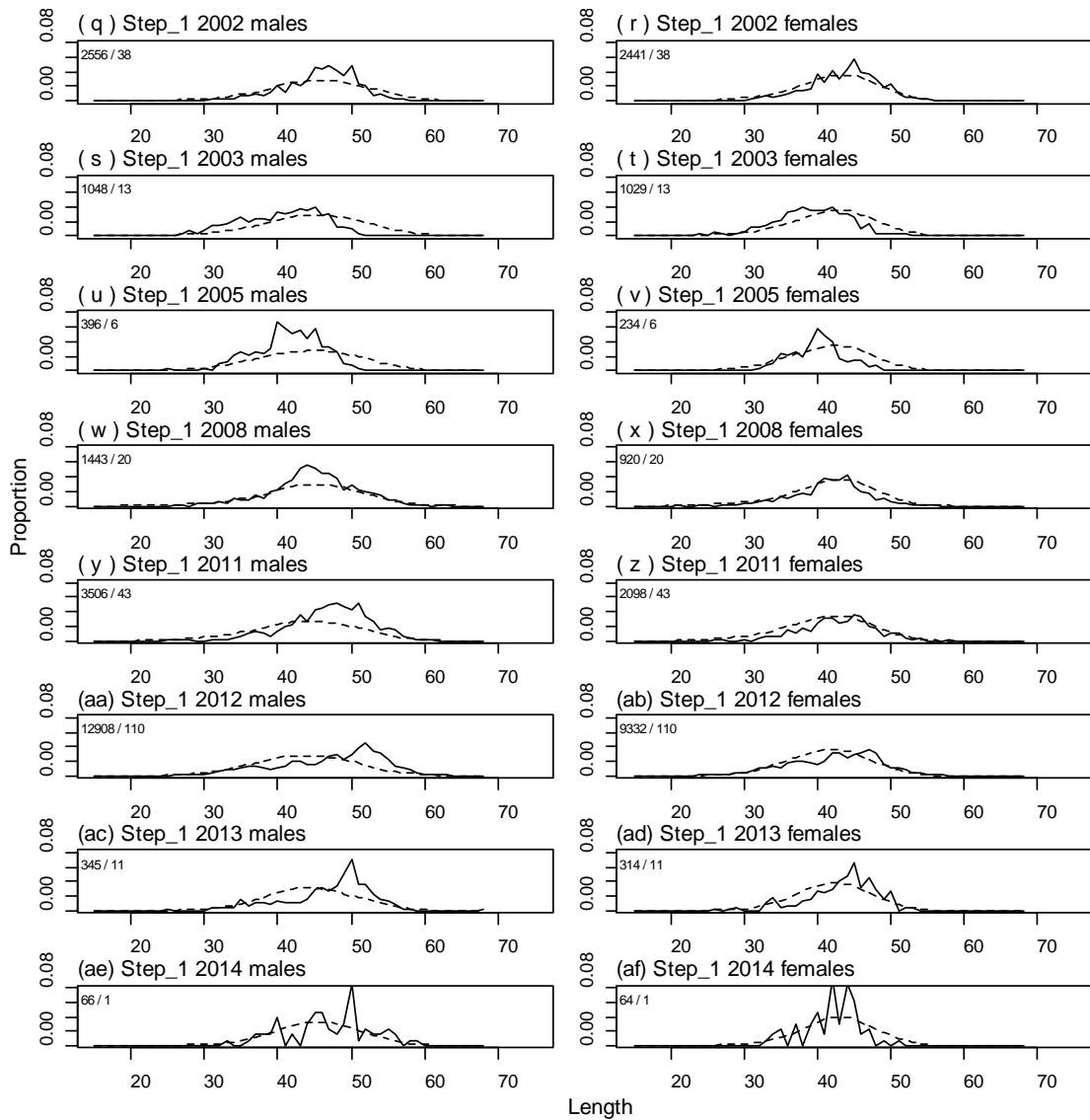
A12. 3: Fishery and survey selectivity curves for the SCI 2 M025CV25 model. Solid line – females, dotted line – males. The scampi burrow index is not sexed, and a single selectivity applies.



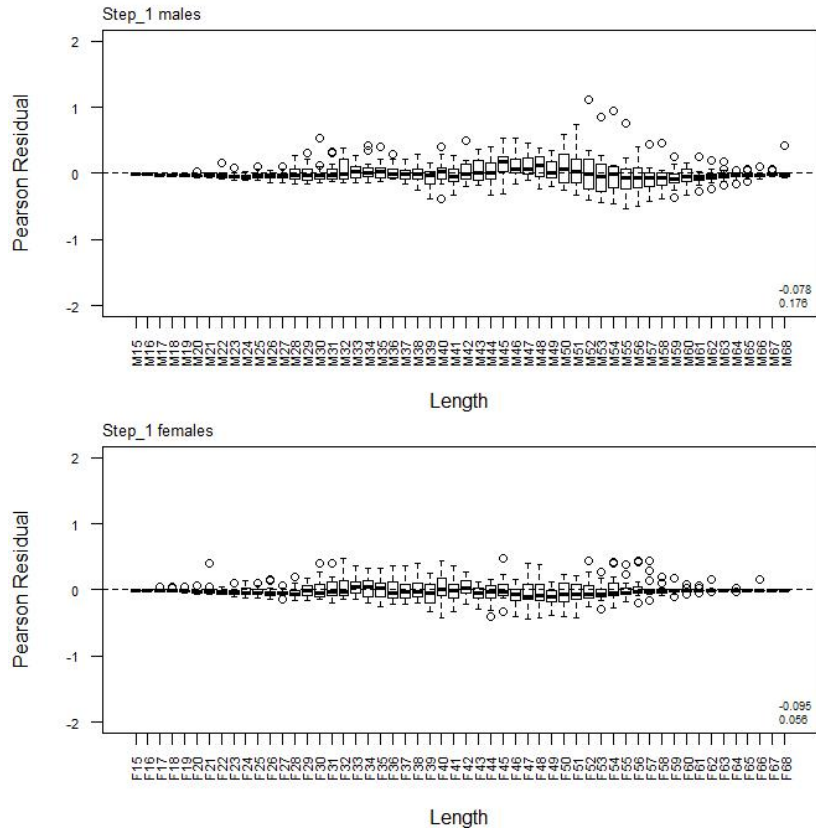
A12. 4: Catchability estimates from MPD model run, plotted in relation to prior distribution for the SCI 2 M025CV25 model.



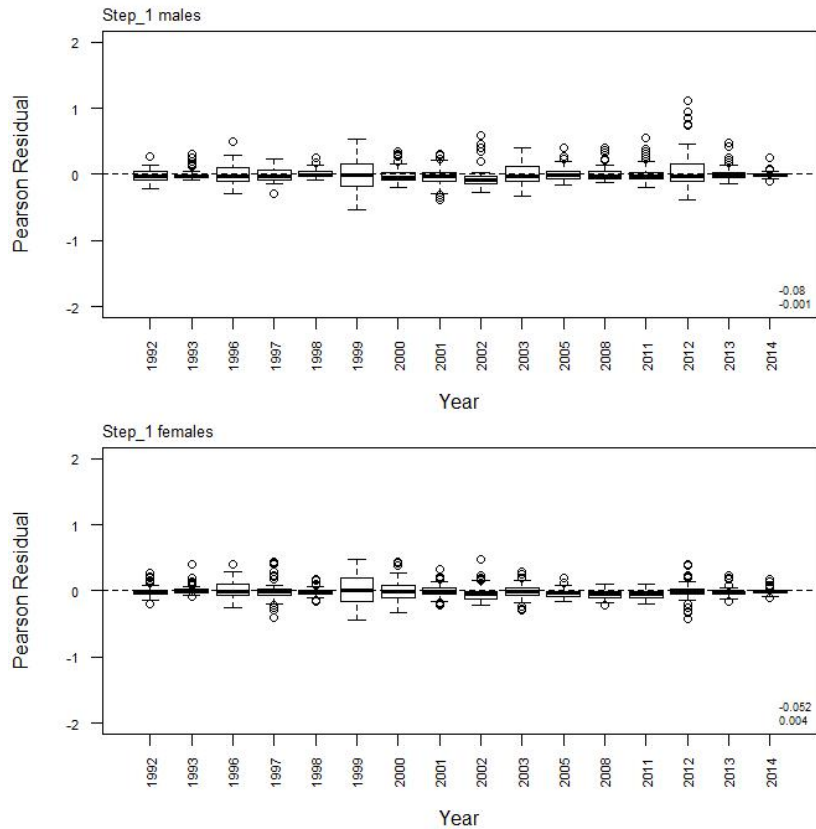
A12. 5: Observed (solid line) and fitted (dashed line) length frequency distributions from observer samples, time step 1 for SCI 2 M025CV25 model. Numbers in top left corner of each plot represent number of scampi measured / number of events sampled.



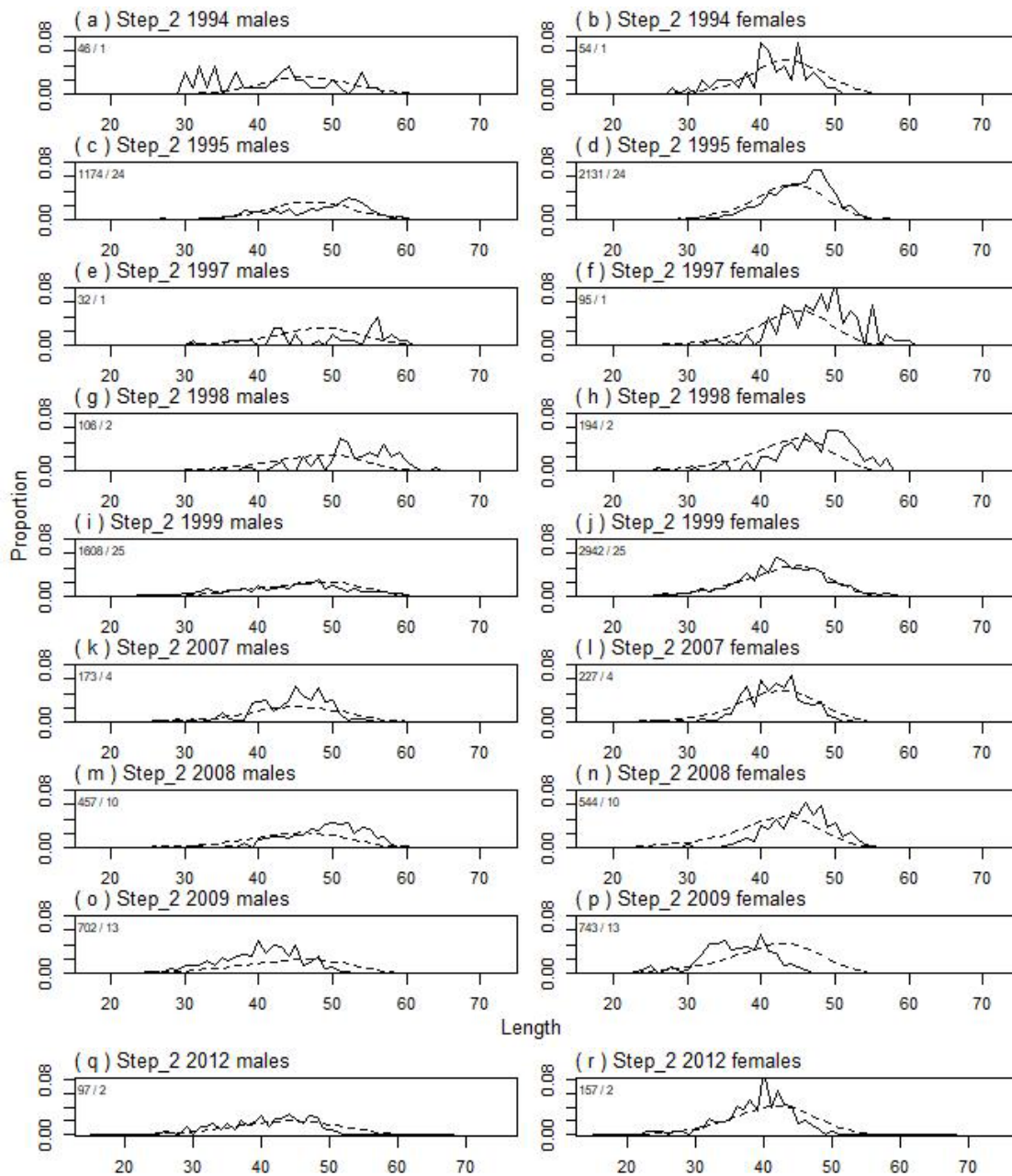
A12. 5(continued): Observed (solid line) and fitted (dashed line) length frequency distributions from observer samples, time step 1 for SCI 2 M025CV25 model. Numbers in top left corner of each plot represent number of scampi measured / number of events sampled.



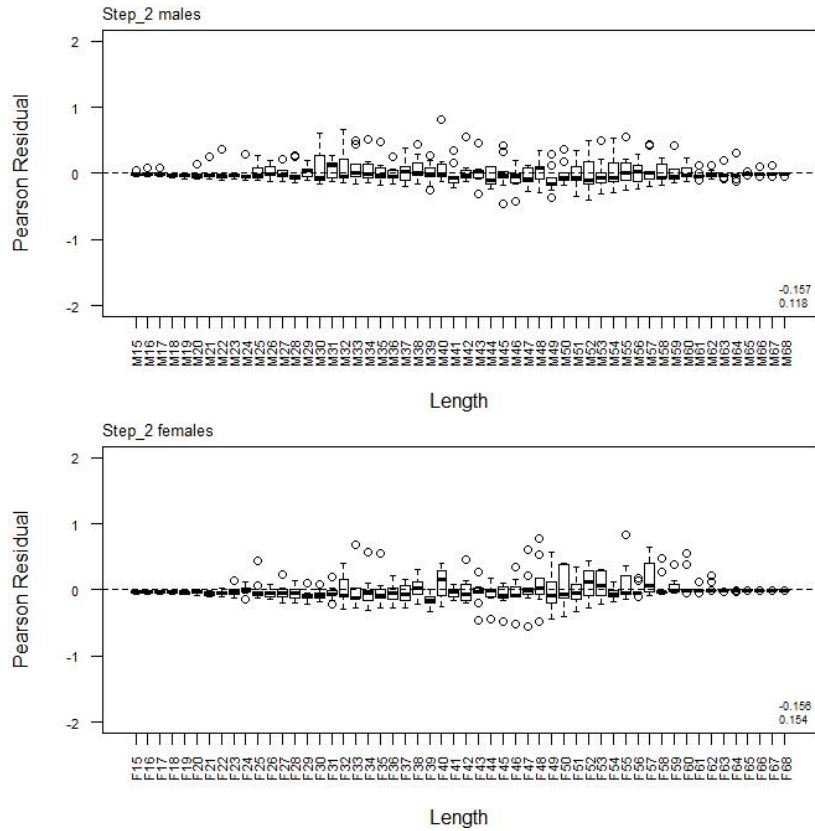
A12. 6: Box plots of Pearson residuals from the fit to length frequency distributions by length from observer sampling by sex for time step 1 for SCI 2 M025CV25 model.



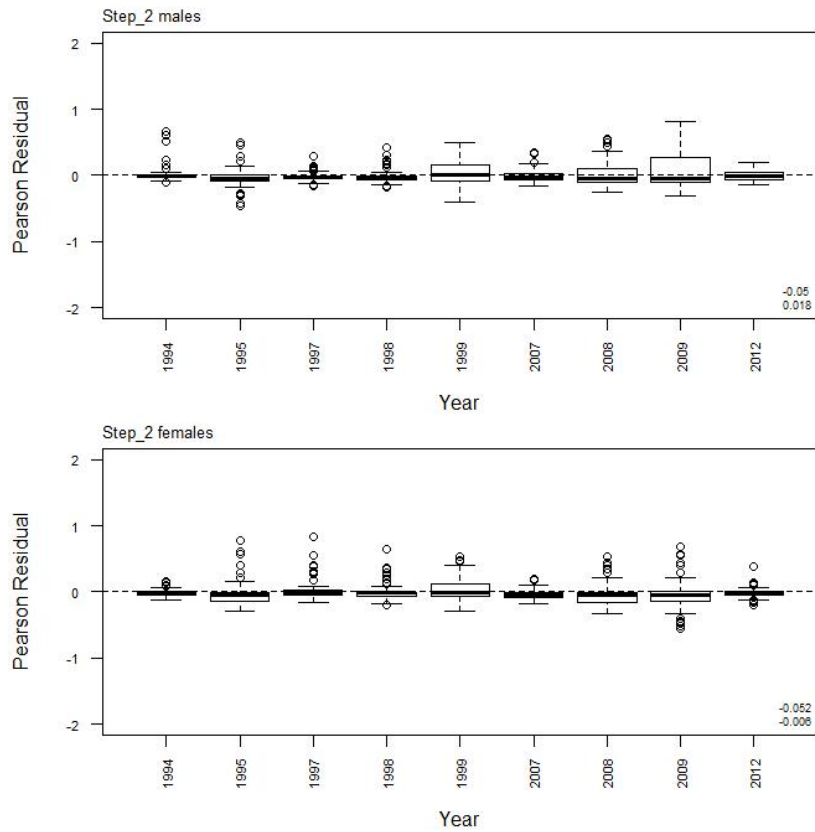
A12. 7: Box plots of Pearson residuals from the fit to length frequency distributions by year from observer sampling by sex for time step 1 for SCI 2 M025CV25 model.



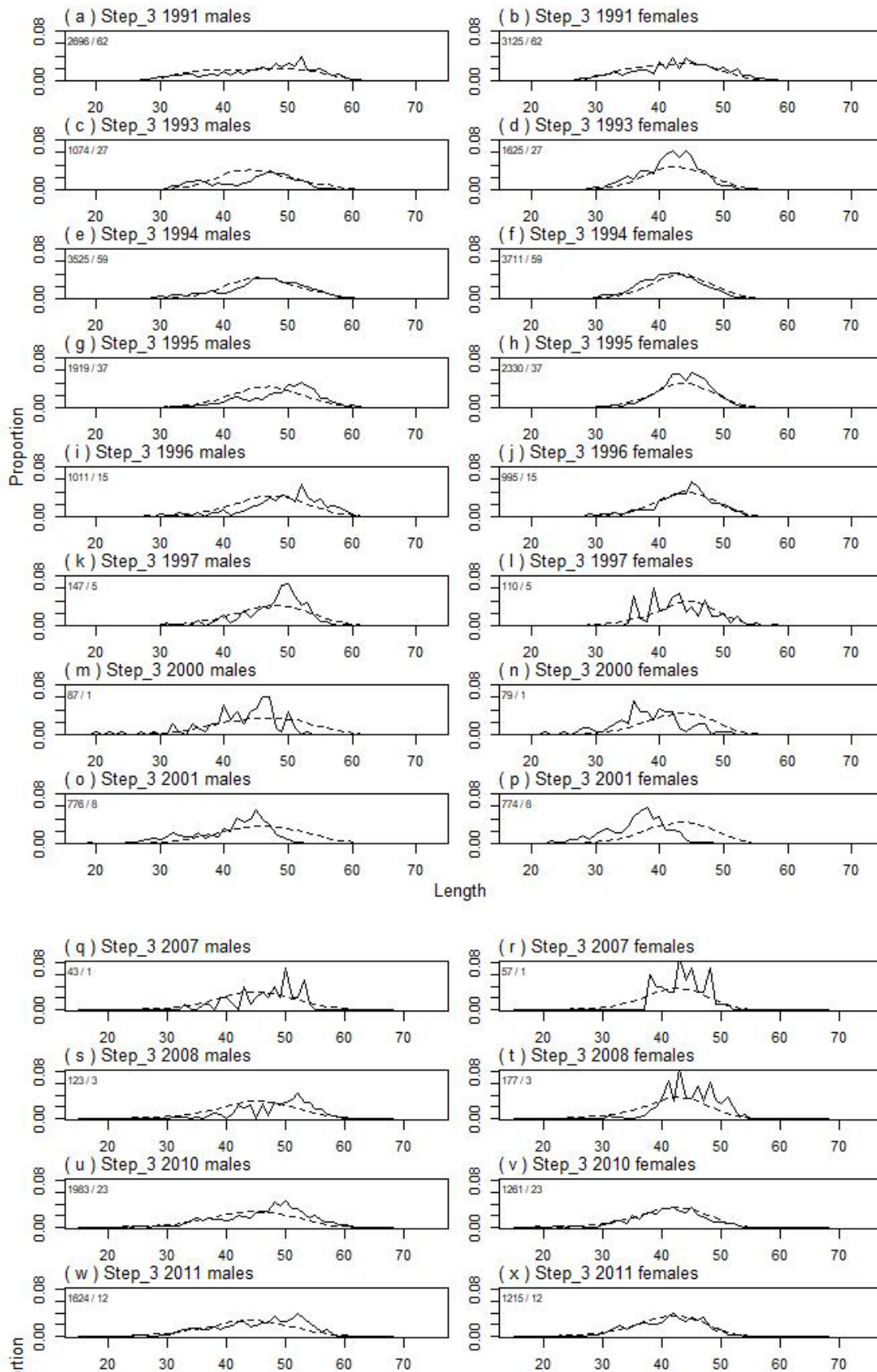
A12. 8: Observed (solid line) and fitted (dashed line) length frequency distributions from observer samples, time step 2 for SCI 2 M025CV25 model. Numbers in top left corner of each plot represent number of scampi measured / number of events sampled.



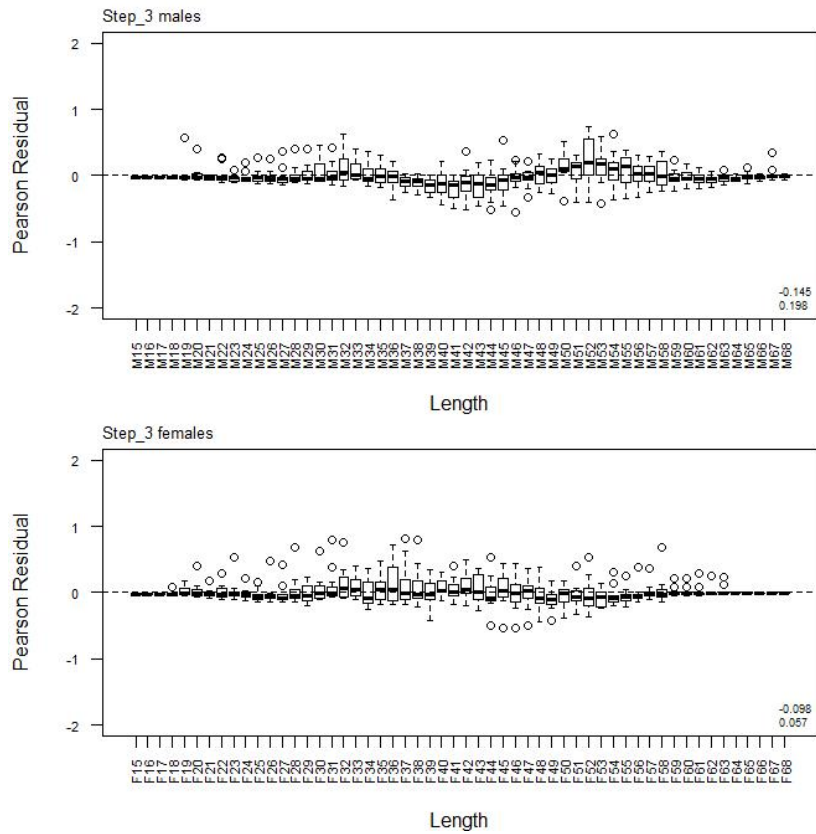
A12. 9: Box plots of Pearson residuals from the fit to length frequency distributions by length from observer sampling by sex for time step 2 for SCI 2 M025CV25 model.



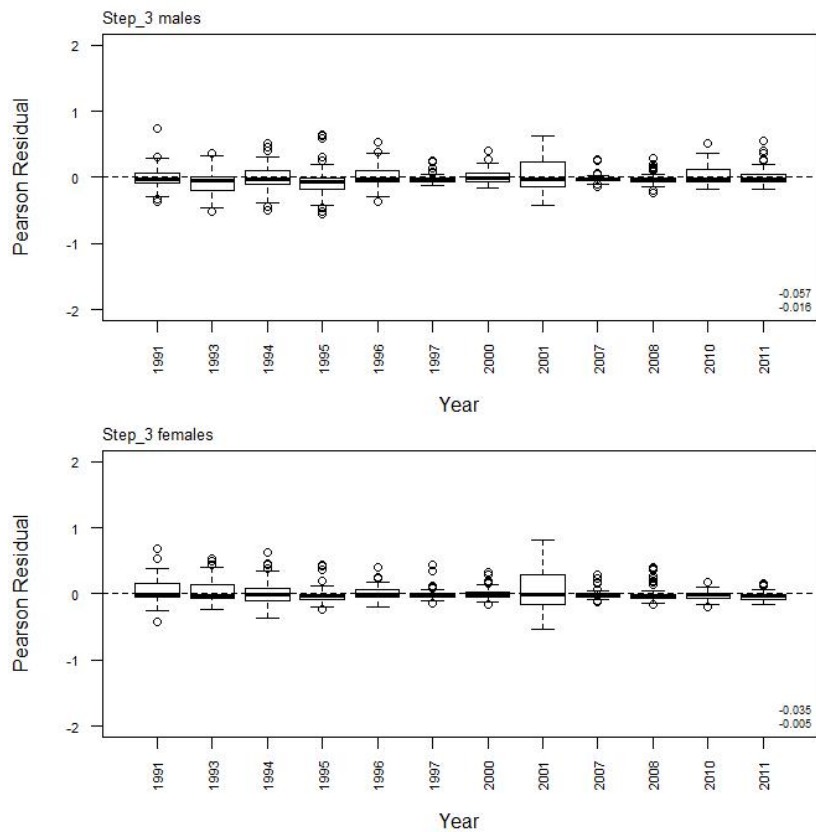
A12. 10: Box plots of Pearson residuals from the fit to length frequency distributions by year from observer sampling by sex for time step 2 for SCI 1 M025CV25 model.



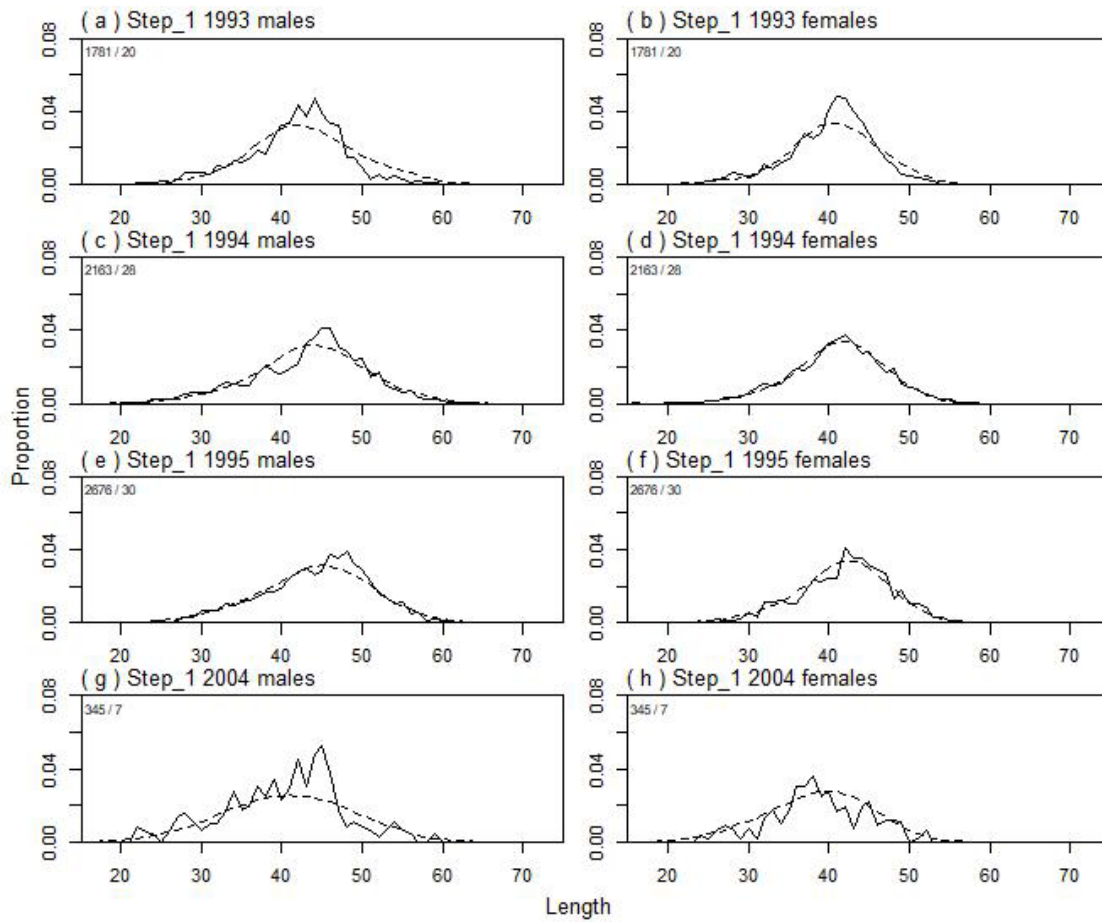
A12. 11: Observed (solid line) and fitted (dashed line) length frequency distributions from observer samples, time step 3 for SCI 2 M025CV25 model. Numbers in top left corner of each plot represent number of scampi measured / number of events sampled.



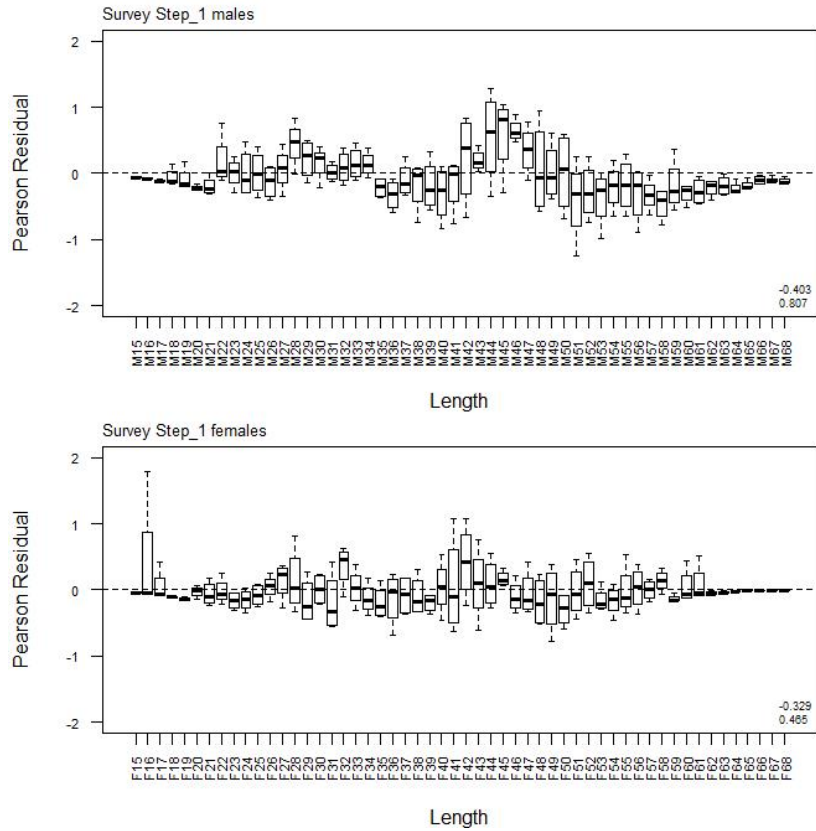
A12. 12: Box plots of Pearson residuals from the fit to length frequency distributions by length from observer sampling by sex for time step 3 for SCI 2 M025CV25 model.



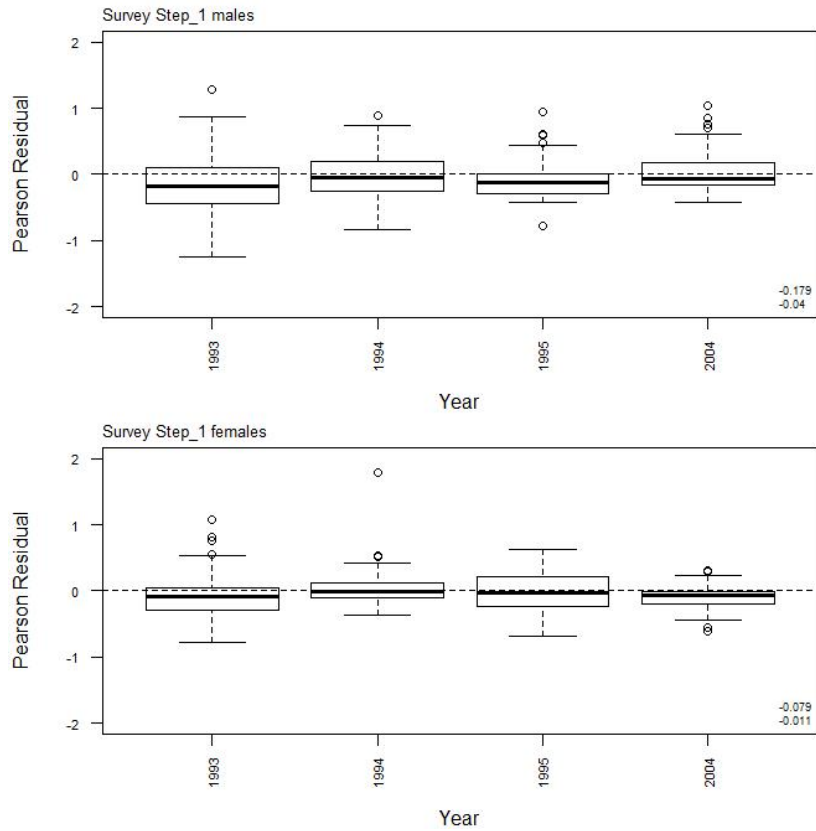
A12. 13: Box plots of Pearson residuals from the fit to length frequency distributions by year from observer sampling by sex for time step 3 for SCI 2 M025CV25 model.



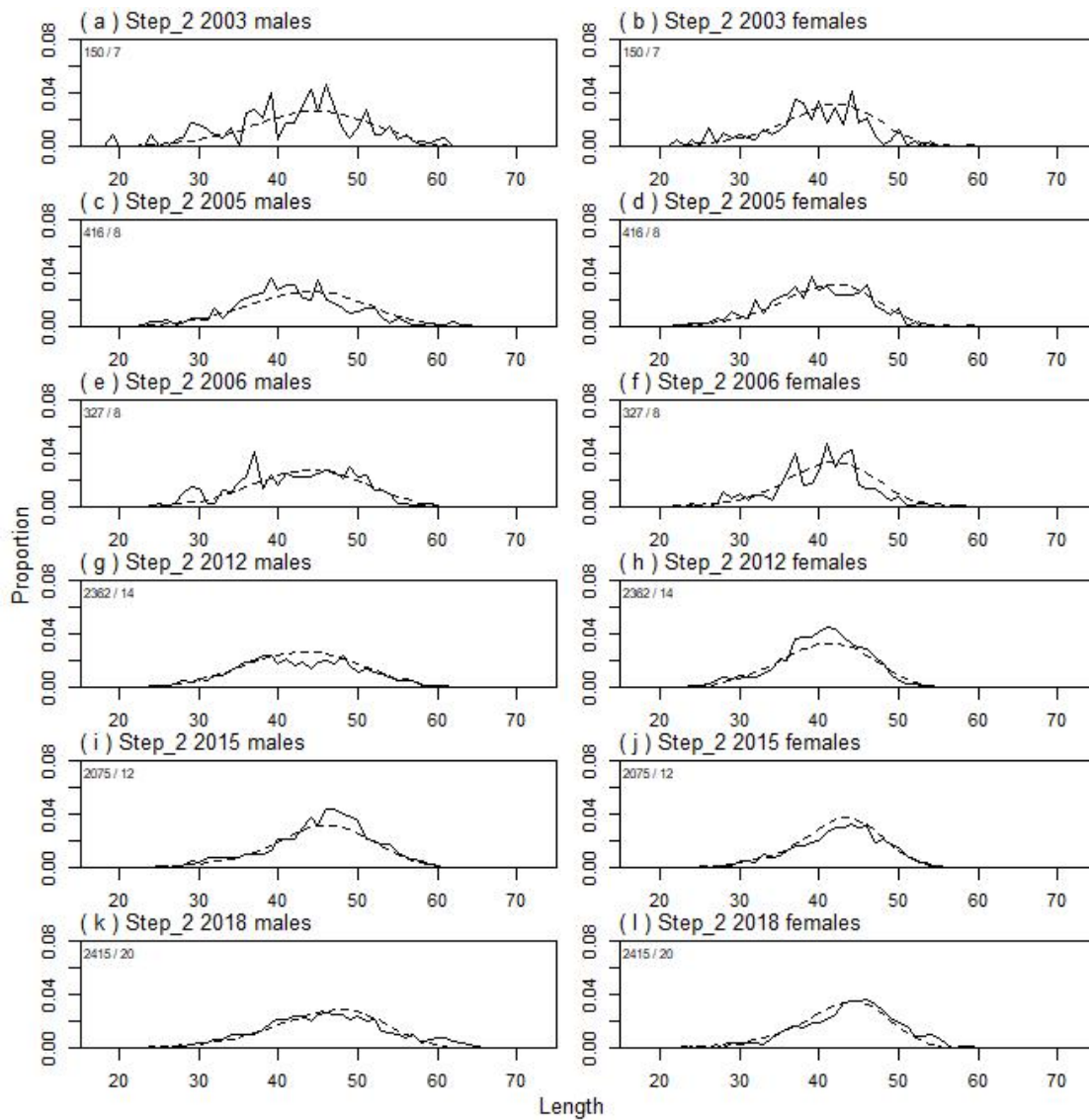
A12. 14: Observed (solid line) and fitted (dashed line) length frequency distributions from trawl survey samples for time step 1, SCI 2 M025CV25 model. Numbers in top left corner of each plot represent number of scampi measured / number of events sampled.



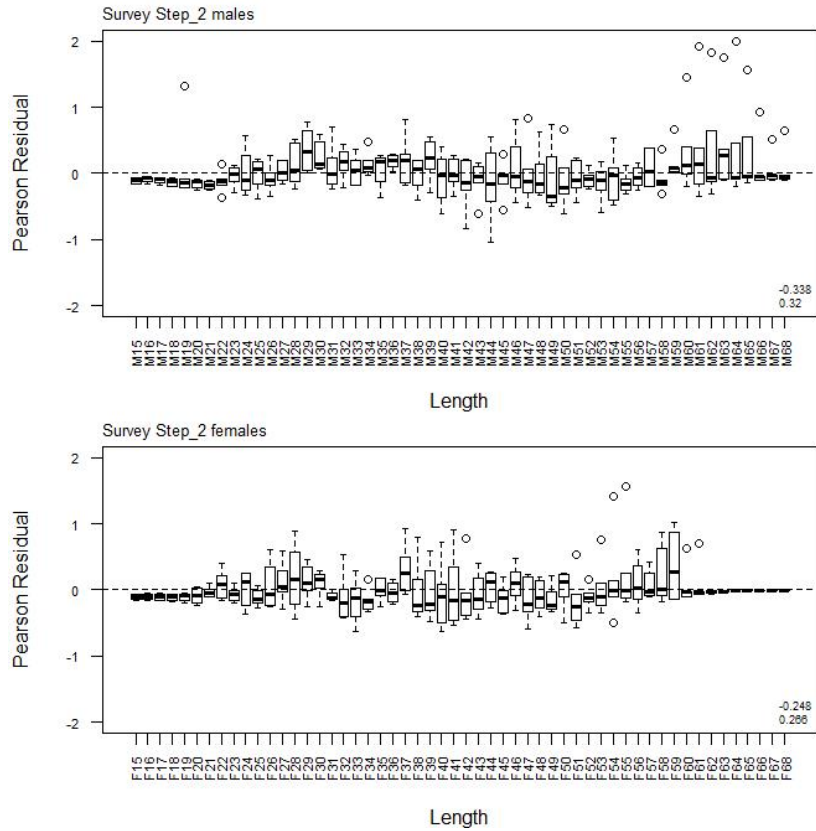
A12. 15: Box plots of Pearson residuals from the fit to length frequency distributions by length from trawl survey sampling by sex for time step 1, SCI 2 M025CV25 model.



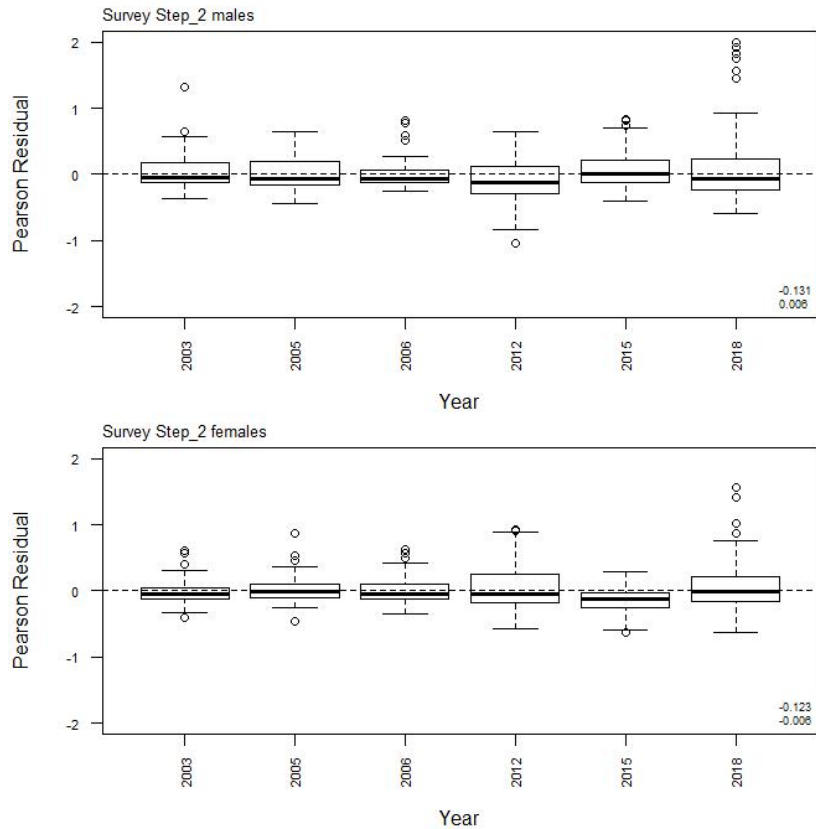
A12. 16: Box plots of Pearson residuals from the fit to length frequency distributions by year from trawl survey sampling by sex for time step 1, SCI 2 M025CV25 model.



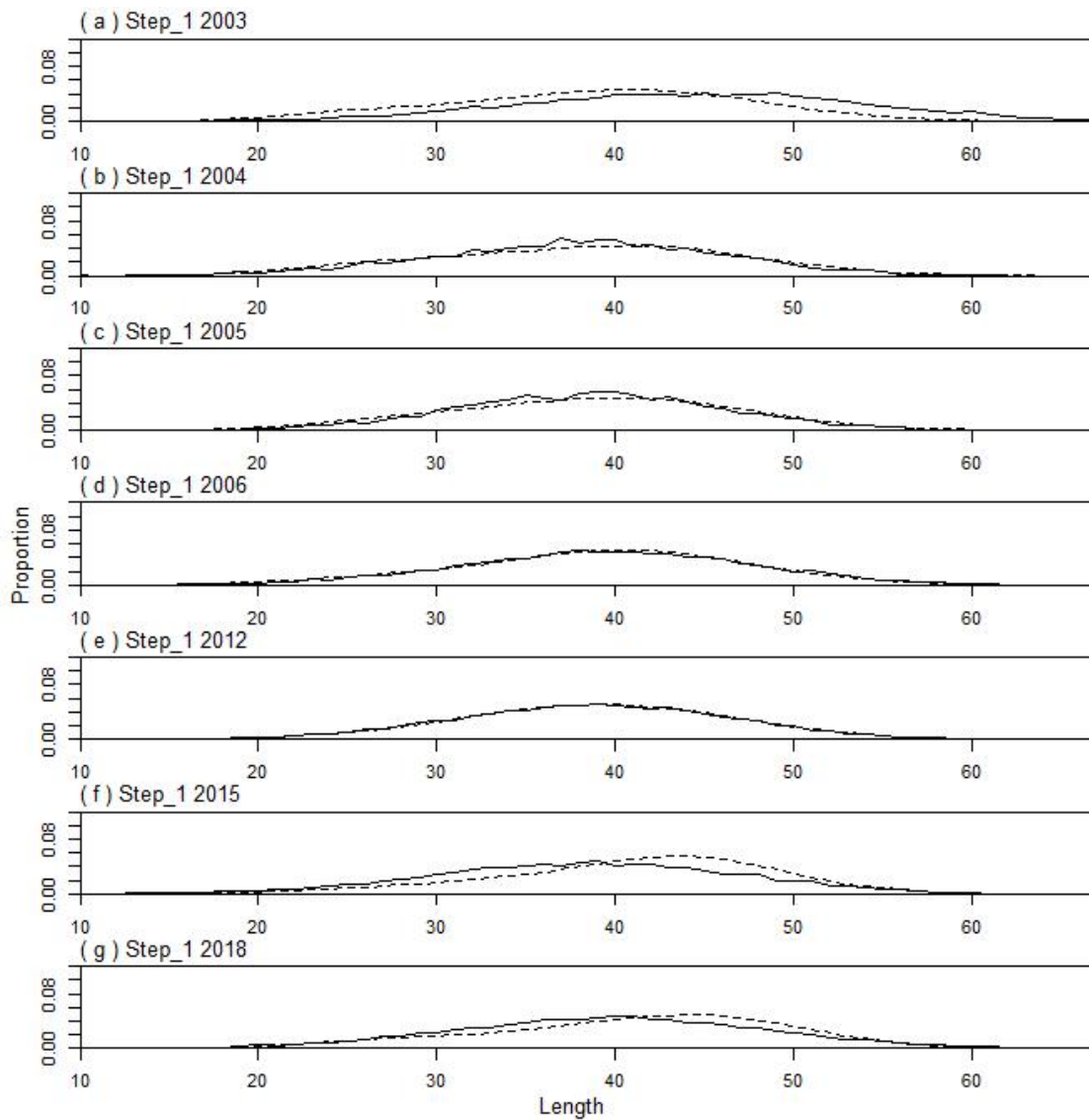
A12. 17: Observed (solid line) and fitted (dashed line) length frequency distributions from trawl survey samples for time step 2, SCI 2 M025CV25 model. Numbers in top left corner of each plot represent number of scampi measured / number of events sampled.



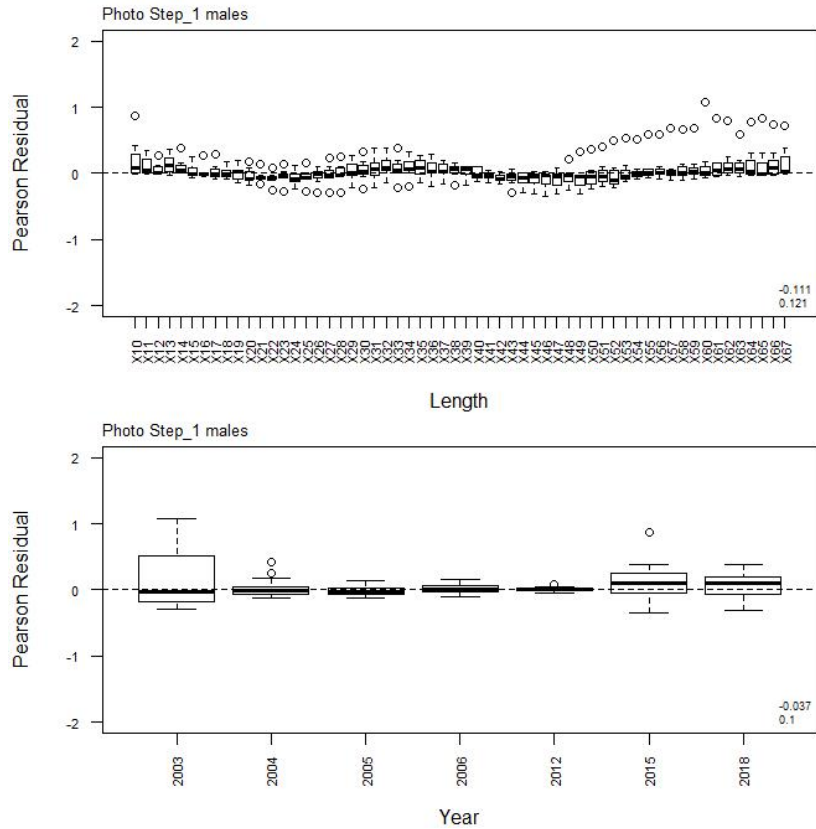
A12. 18: Box plots of Pearson residuals from the fit to length frequency distributions by length from trawl survey sampling by sex for time step 2, SCI 2 M025CV25 model.



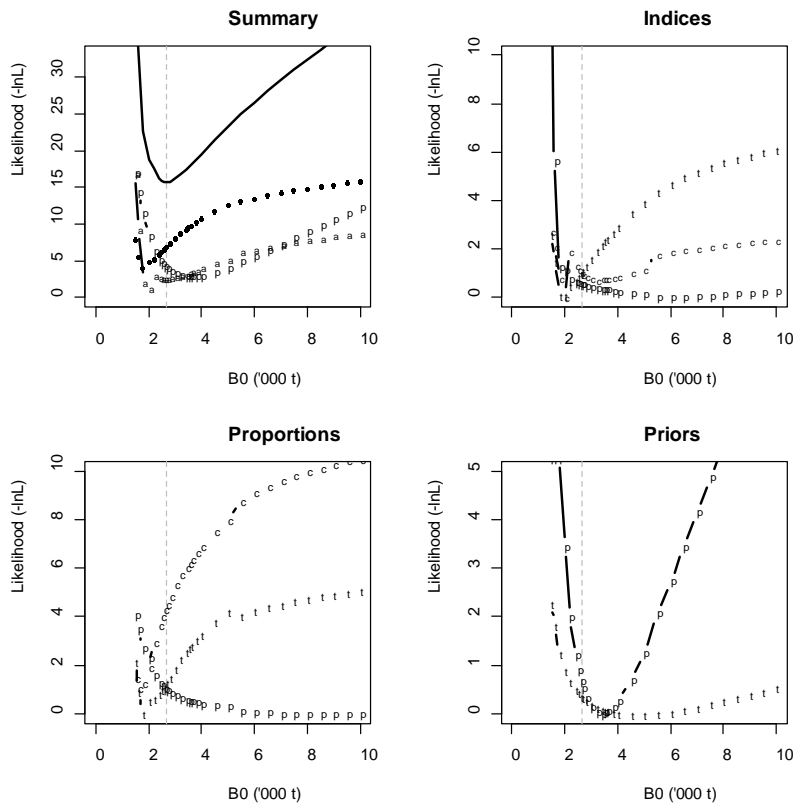
A12. 19: Box plots of Pearson residuals from the fit to length frequency distributions by year from trawl survey sampling by sex for time step 2, SCI 2 M025CV25 model.



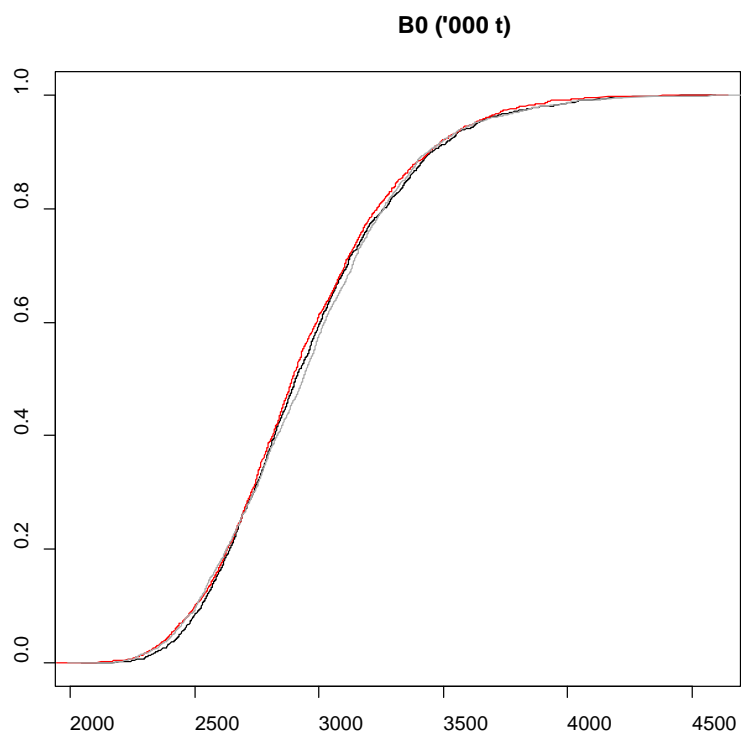
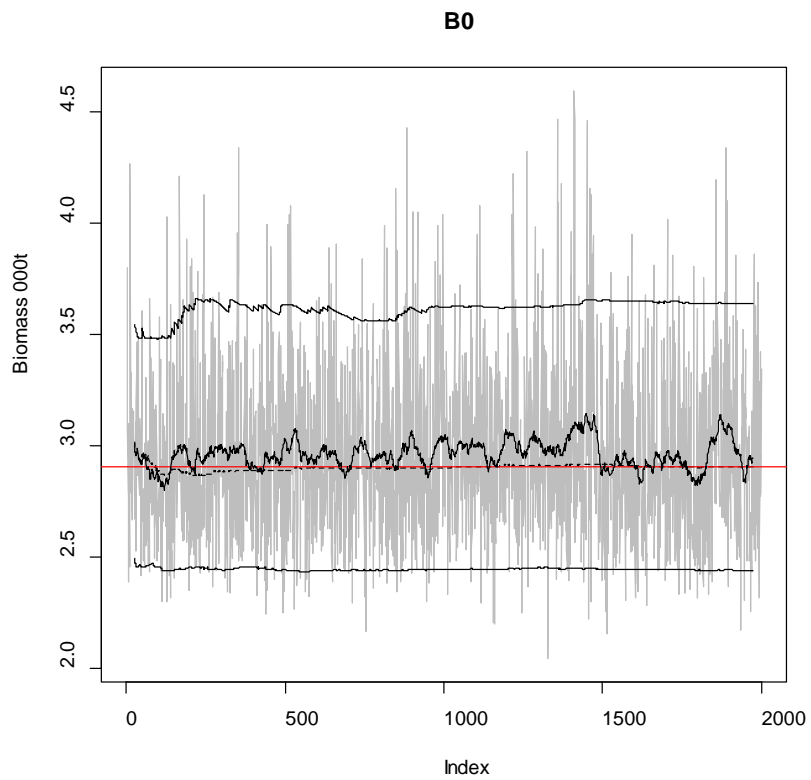
A12. 20: Observed (solid line) and fitted (dashed line) length frequency distributions from photo survey samples for SCI 2 M025CV25 model.



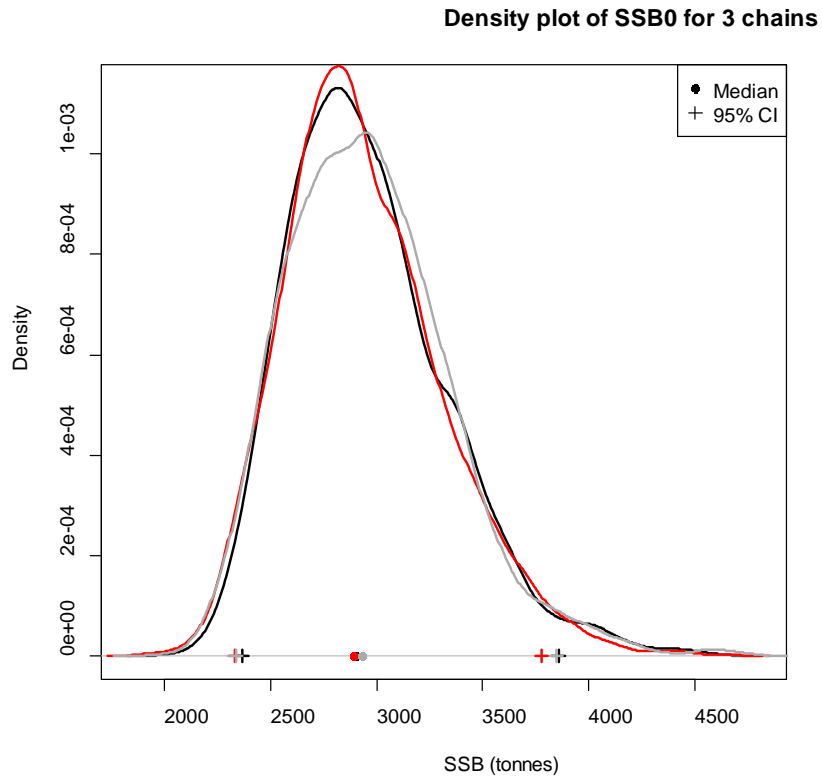
A12. 21: Box plots of Pearson residuals from the fit to length frequency distributions by length (top plot) and year (bottom plot) from photo survey sampling by sex for SCI 2 M025CV25 model.



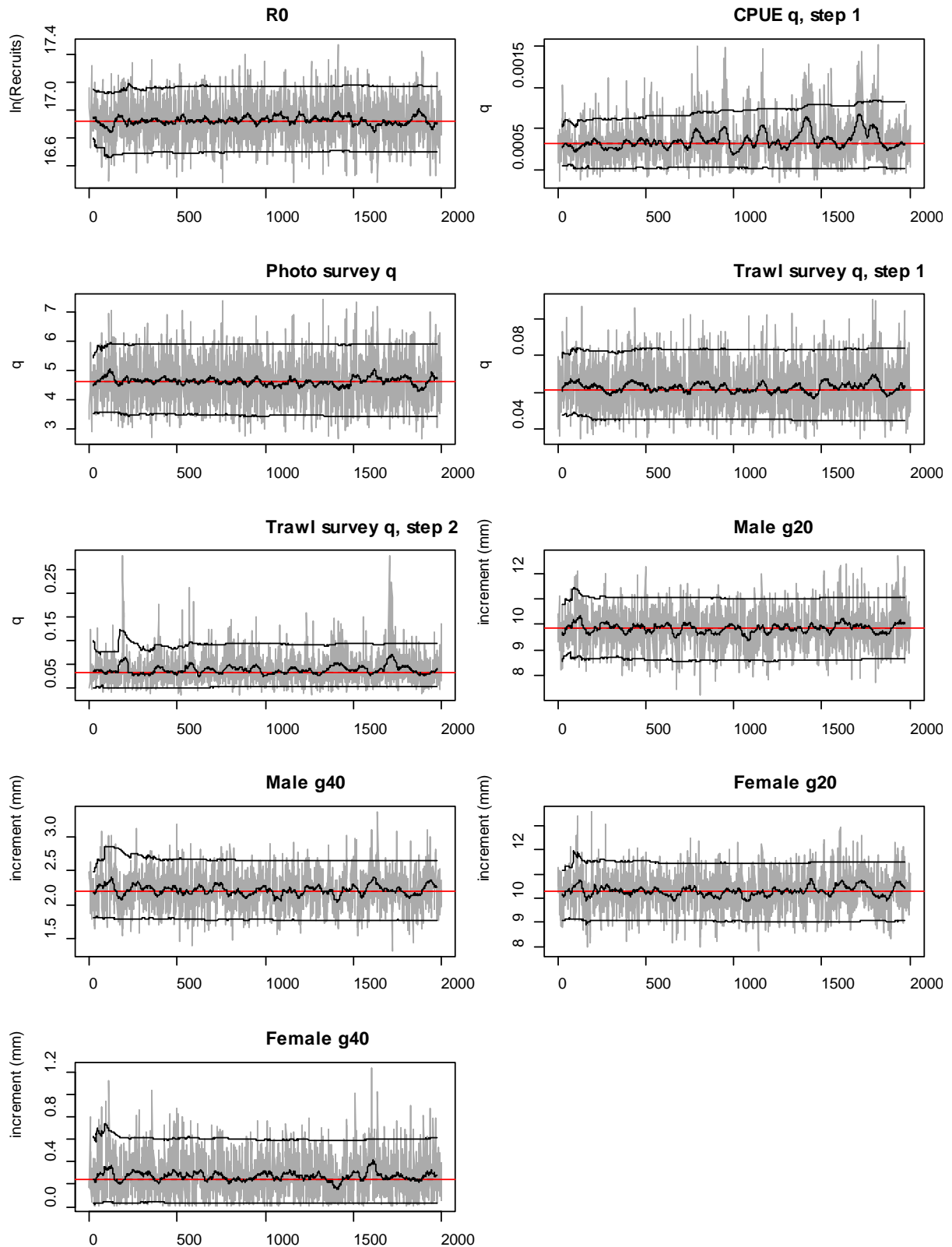
A12. 22: Likelihood profiles for model M025CV25 for SCI 2 when B_0 is fixed in the model. Figures show profiles for main priors (top left, p – priors, a – abundance indices, • – proportions at length), abundance indices (top right, t – trawl survey step, c – CPUE, p – photo survey), proportion at length data (bottom left, p – photo, t – trawl, c – observer) and priors (bottom right, p – q-Photo, t – q-Trawl).



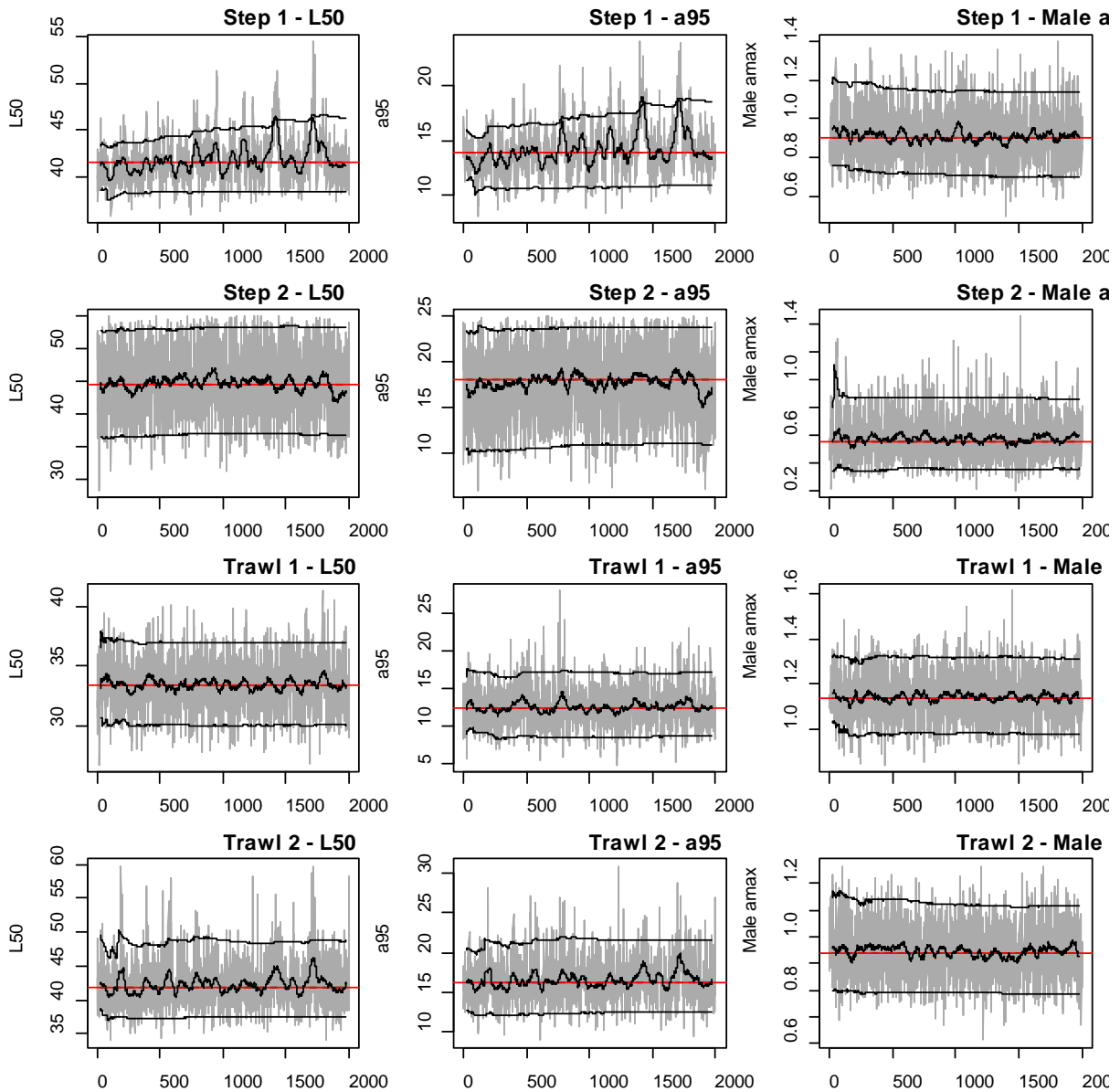
A12. 23: MCMC traces for B_0 and cumulative frequency distributions for three independent MCMC chains for the SCI 2 M025CV25 model.



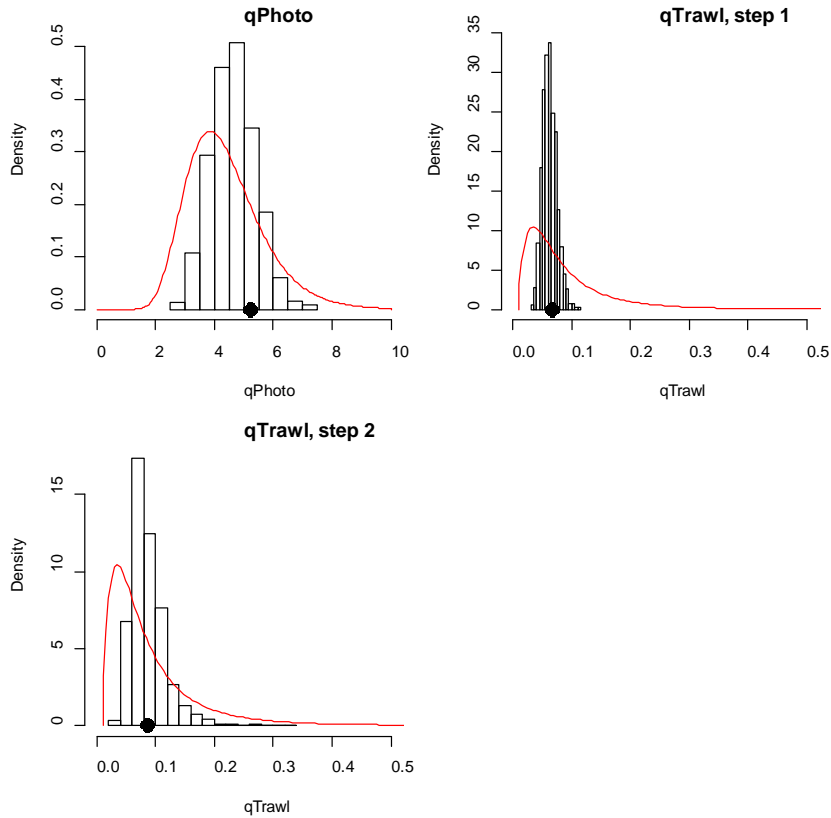
A12. 24: Density plots for B_0 for the SCI 2 M025CV25 model for three independent MCMC chains, with median and 95% confidence intervals.



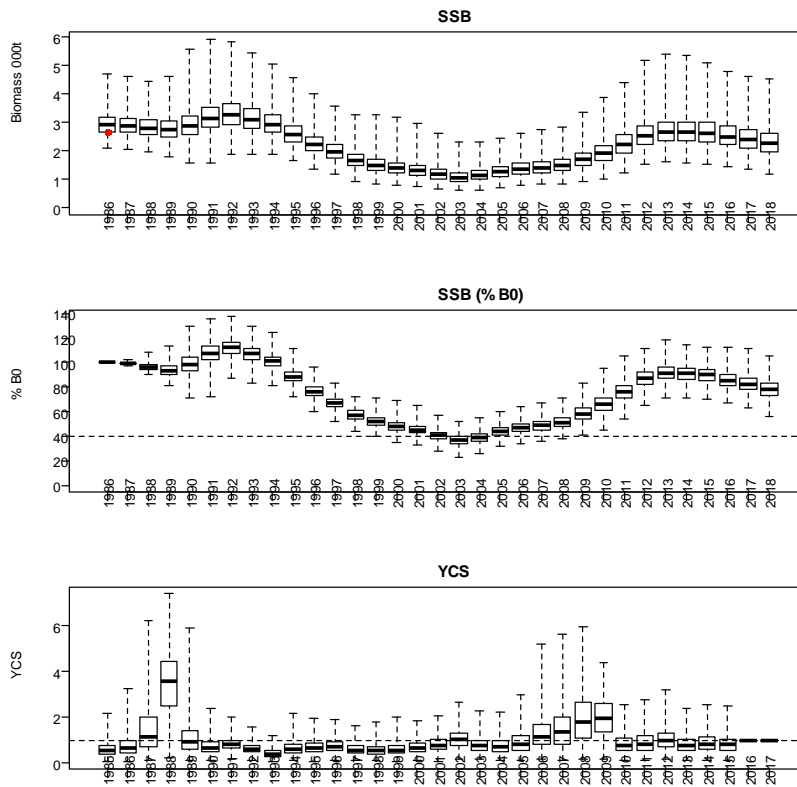
A12. 25: MCMC traces for R_0 , catchability, and growth terms for the SCI 2 M025CV25 model.



A12. 26: MCMC traces for selectivity terms for the SCI 2 M025CV25 model.

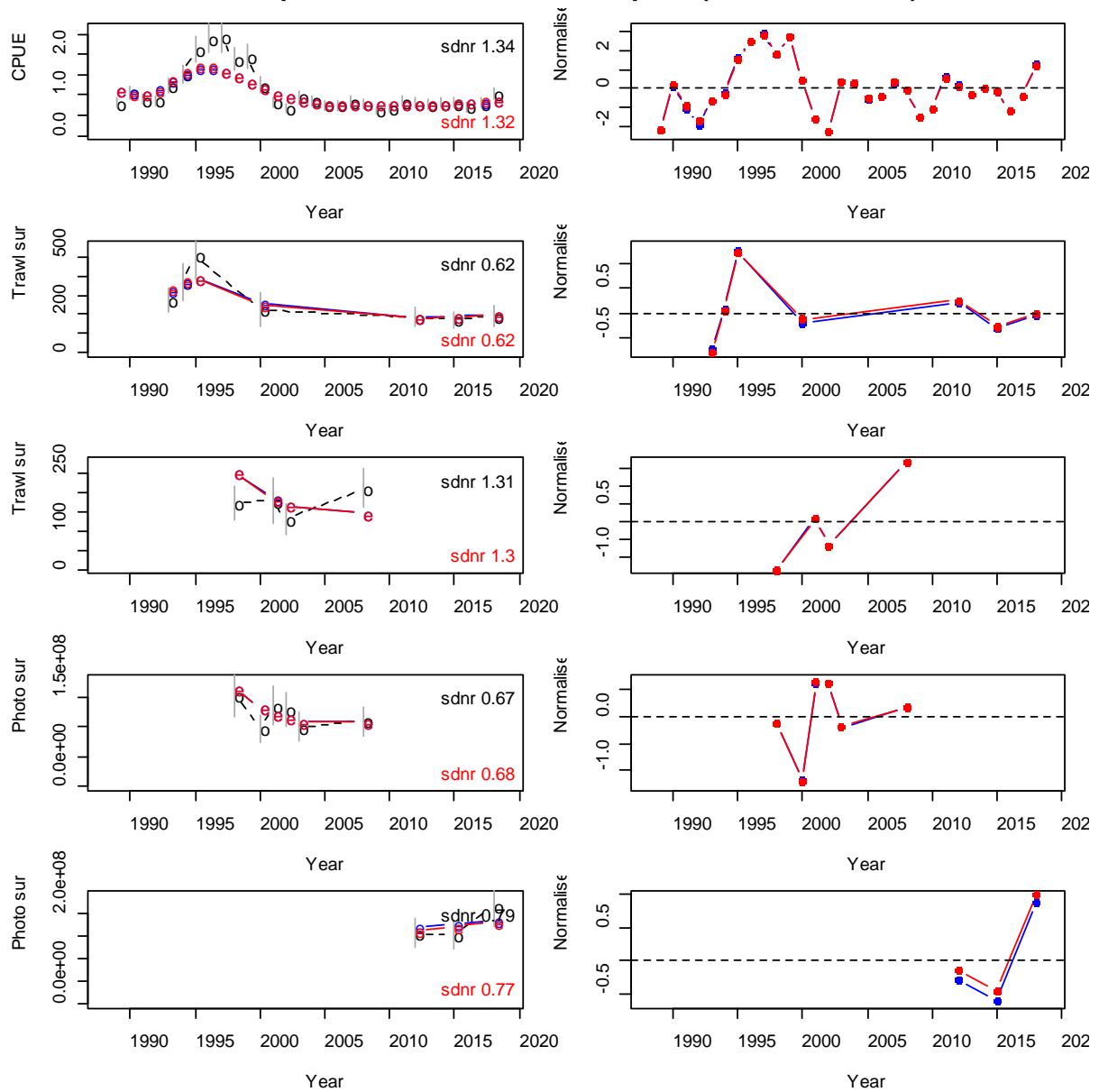


A12. 27: Marginal posterior distributions (histograms), MPD estimates (solid symbols), and distributions of priors (lines) for catchability terms for the SCI 2 M025CV25 model.

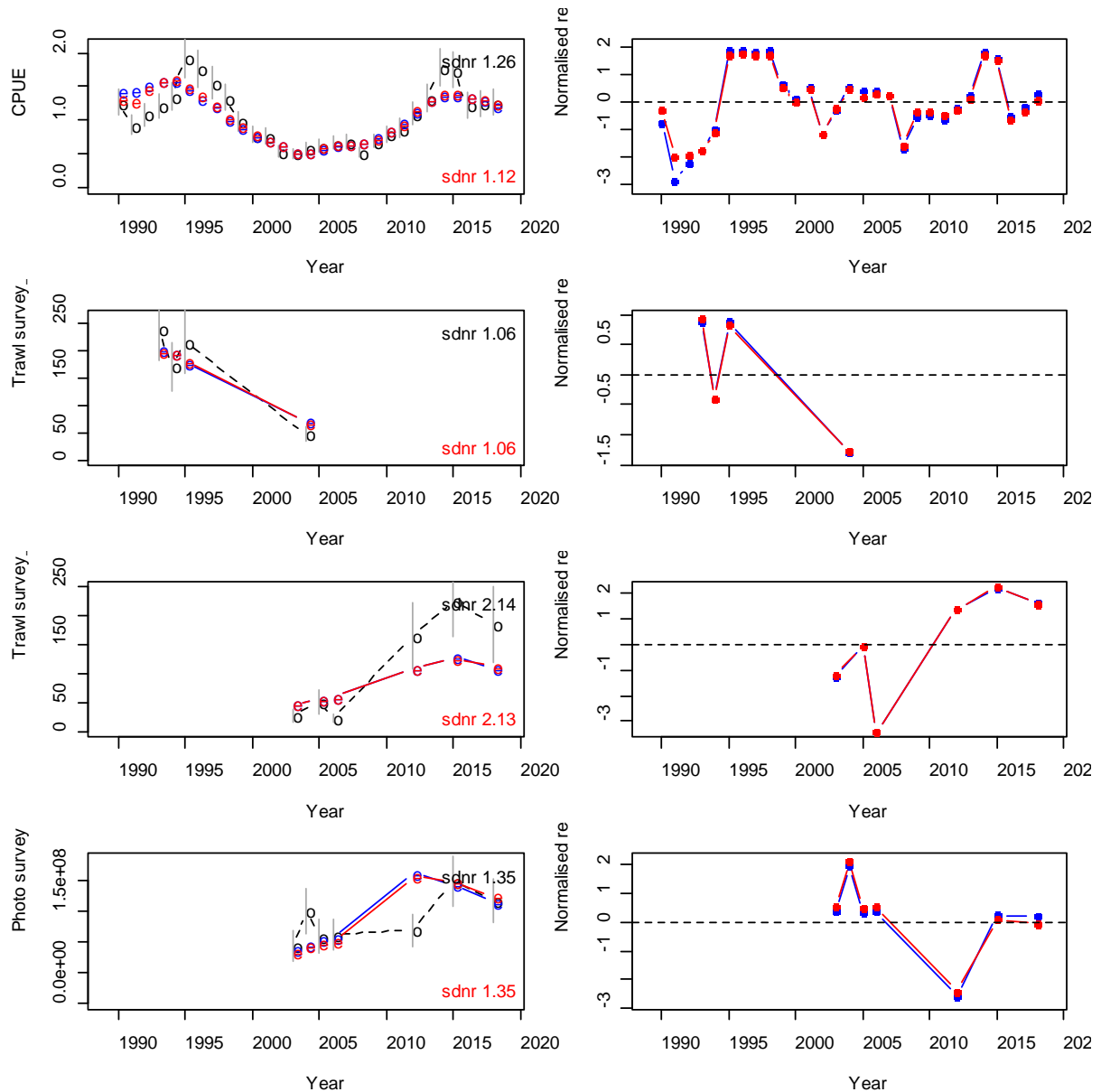


A12. 28: Posterior trajectory of SSB, SSB/SSB₀, and YCS for the SCI 2 M025CV25 model. Red dot represents MPD estimate of B₀.

APPENDIX 13. Shared parameter M025CV15 model plots ($M=0.25$, $CV=0.15$)



A13. 1: Fits to SCI 1 abundance indices (left column) and normalised residuals (right column) for standardised CPUE index (top row) trawl survey index (whole area) (second row), trawl survey index (limited area) (third row), photo survey index (limited area) (fourth row), and photo survey index (whole area) (fifth row) for the shared parameter (red) and single area M025CV15 (blue) models.



A13. 2: Fits to SCI 2 abundance indices (left column) and normalised residuals (right column) for standardised CPUE index (top row) trawl survey biomass index time step 1 (second row), trawl survey biomass index time step 2 (third row), and photo survey abundance index (fourth row) for the shared parameter (red) and single area M025CV15 (blue) models.